AD_____
(Leave blank)

Award Number: DAMD17-94-C-4069

TITLE: Services to Operate and Maintain a Microwave Research Laboratory

PRINCIPAL INVESTIGATOR: Shin-Tsu Lu, Ph.D.

CONTRACTING ORGANIZATION: McKesson BioServices Corporation
Rockville, MD 20850

REPORT DATE: May 2004

TYPE OF REPORT: Final Addendum

PREPARED FOR: U.S. Army Medical Research and Materiel Command
Fort Detrick, Maryland 21702-5012

DISTRIBUTION STATEMENT: Approved for public release;
distribution unlimited

The views, opinions and/or findings contained in this report are those of the author(s) and should not be construed as an official Department of the Army position, policy or decision unless so designated by other documentation.

Best Available Copy

20040820 014

REPORT DOCUMENTATION PAGE

Form Approved
OMB No. 074-0188

Public reporting burden for this collection of information is estimated to average 1 hour per response, including the time for reviewing instructions, searching existing data sources, gathering and maintaining the data needed, and completing and reviewing this collection of information. Send comments regarding this burden estimate or any other aspect of this collection of information, including suggestions for reducing this burden to Washington Headquarters Services, Directorate for Information Operations and Reports, 1215 Jefferson Davis Highway, Suite 1204, Arlington, VA 22202-4302, and to the Office of Management and Budget, Paperwork Reduction Project (0704-0188), Washington, DC 20503

1. Agency Use Only (Leave blank)	2. Report Date	3. Report Type and Period Covered
	May 2004	Final Addendum (21 May 2001 - 30 Apr 2004)

4. Title and Subtitle
Services to Operate and Maintain a Microwave Research Laboratory

5. Award Number
DAMD17-94-C-4069

6. Author(s)
Shin-Tsu Lu, Ph.D.

7. Performing Organization Name (Include Name, City, State, Zip Code and Email for Principal Investigator)
McKesson BioServices Corporation
Rockville, MD 20850

E-Mail: tsay7@yahoo.com

8. Performing Organization Report Number (Leave Blank)

9. Sponsoring/Monitoring Agency Name and Address
U.S. Army Medical Research and Materiel Command
Fort Detrick, Maryland 21702-5012

10. Sponsoring/Monitoring Agency Report Number (Leave Blank)

11. Supplementary Notes (i.e., report contains color photos, report contains appendix in non-print form, etc.)

12a. Distribution/Availability Statement (check one)
Approved for public release; distribution unlimited

12b. Distribution Code
(Leave Blank)

13. Abstract *(Maximum 200 Words)* *(abstract should contain no proprietary or confidential information)*

Due to growing concerns for the health and safety of military and civilian personnel exposed to radiofrequency radiation (RFR), a series of research have been performed at the U.S. Army Medical Research Detachment, Microwave Bioeffects Branch at Brooks City-Base, Texas. The research has been concentrated on neurotoxic effects of high peak power but low average power RFR, Interaction between neurotoxin and RFR on manifestation of neurotoxic effects, effects of high power RFR on hippocampus, biological hazards of ultra-wide-band (UWB) pulses on cardiovascular function and cell systems, cytotoxic effect of nanosecond high-intensity electric pulses, finite difference time domain techniques for RFR dosimetry, role of ambient temperature on manifestation of RFR induced biological effects, design fabrication and testing a circularly polarized 1.25 GHz waveguide exposure system, and formulate a research plan for body borne and helmet mounted antennas. Majority of results falls in "thermal" effect, albeit, the threshold was at lower magnitude than that previously envisioned. A model is devised to demonstrate the additive effect of RFR to thermal "stress" from ambient environment. On the other hand, some of the observed effects cannot be easily explained by the "thermal" mechanism. They were effects of UWB pulses and nanosecond high power electric pulses.

14. Subject Terms (keywords previously assigned to proposal abstract or terms which apply to this award)
high peak power pulsed microwaves, ultra-wide-band pulses, neural, Behavior, cardiovascular, cytotoxicity, neurotoxin, genotoxicity

15. Number of Pages
453

16. Price Code (Leave Blank)

17. Security Classification of Report	18. Security Classification of this Page	19. Security Classification of Abstract	20. Limitation of Abstract
Unclassified	Unclassified	Unclassified	Unlimited

Table of Contents

Cover.....1

SF 298.....2

Introduction.....4

Body.....5

Key Research Accomplishments.....6

Research on Neurotoxic Effects of High Peak Power But Low Average Power Radiofrequency Radiation (RFR) and Interaction Between Neurotoxin and RFR on Manisfestation of Neurotoxic Effects.....6

Research on Effects of High Power Radiofrequency Radiation.....10

Research on Biological Hazards of Ultra-Wide-Band Pulses on the Cardiovascular System and Other Cell Systems.....14

Cytotoxic Effects of Nanosecond High-Intensity Electric Pulses.....17

Finite Difference Time Domain Techniques and Other Techniques For Radiofrequency Radiation Dosimetry.....18

Role of Ambient Temperature on Manifestation of Radiofrequency Biological Effects.....20

Other Related Studies, Multiple Topics Reviews and Presentations.....21

Design, Fabrication, and Characterization a Circularly Polarized Waveguide Exposure System Operated at 1.25 GHz.....22

Research Plan for Body Borne and Helmet Mounted Antennas.....23

Reportable Outcomes.....32

Conclusions.....33

References.....33

Appendices.....39

INTRODUCTION

The following report summarizes the performance of McKesson BioServices Corporation (MBS) staff at the Walter Reed Army Institute of Research (WRAIR), U.S. Army Medical Research Detachment (USAMRD), Microwave Bioeffects Branch at Brooks City-Base, Texas under the contracts DAMD17-94-4069 and DAMD17-94-E-0001. MBS has nine years contract with the U.S. Army Medical Research and Acquisition Activity (USAMRAA) to operate and maintain Microwave Bioeffects Branch, a Government-owned Contractor-operated (GOCO) facility. Reports summarized the base three years (May 21, 1994 – May 20, 1997) (DTIC STINET ADA 351987, http://handle.dtic.mil/100.2/ADA351978), the first option years (May 21, 1997 – May 20, 1999) (DTIC STINET ADA367478, http://handle.dtic.mil/100.2/ADA367478) and the second options years (May 21 1999 – May 20, 2001, DTIC STINET ADA392971, http://handle.dtic.mil/100.2/ADA392971) were previously filed with the U.S. Army Medical Research and Materiel Command, Fort Detrick, Maryland in June 1997, May 1999 and May 2001. The present report covers the efforts of MBS staff during the third option years (May 21 2001 – May 20, 2003) and extensions (May 21, 2003 – May 31, 2004) of the aforementioned contract. Based on guidance provided in the contract and the guidance provided by the Contracting Officer's Representative (COR), Mr. Bruce Stuck, the research objectives are twofold:

- To operate, maintain and provide technical support for all U.S. Army Electromagnetic Bioeffects Research Program (EMBRP) Laboratories. This includes operation, maintenance and repair of high power transmitters, and all related microwave and biomedical instrumentation used in the Army EMBRP facility, and
- To furnish biomedical scientists and research assistants to plan, direct, and perform the relevant research necessary to support Army EMBRP. The protocols for research perform by MBS scientists are subjected to review/approval by the COR, the Commander, WRAIR, Institutional Animal Care and Use Committee.

Specifically, the MBS staff is to focus research in the following areas:

- Conduct research on high peak power effects from radiofrequency radiation (RFR) inherent to U.S. Army systems to assess health and safety of these systems for military personnel. Conduct a series of major studies exploring the potential neurotoxic effects of RFR exposure and interaction between known neurotoxins and RFR exposures. Complete additional matrix of rotenone and RFR effects and extend endpoints to include cellular mechanisms of alterations within the brain and activities at the University of California at Los Angeles.
- Conduct *in vitro* experiments to assess the effects of high power RFR effects on isolated hippocampus slices.
- Conduct research on the biological hazards of ultra-wide-band (UWB) pulses on the cardiovascular system and other cellular systems.
- Conduct *in vitro* experiments on cytotoxic effect of nanosecond high-intensity electrical pulses.

- Collaboration with other scientist in the area of Finite Difference Time Domain (FDTD) techniques to perform dosimetry in biological tissues for high peak power RFR and UWB radiations.
- Conduct research on thermal effects of RFR, especially, the role of ambient temperature in manifestation of radiofrequency radiation induced biological effects.
- Design, fabricate, and characterize a circularly polarized waveguide exposure system operated at 1.25 GHz to replace the irreparable FPS-7B exposure system. Perform necessary dosimetry in the circularly polarized waveguide exposure system to match peak specific absorption rate, pulse width, pulse repletion rate and whole-body average specific absorption rate as used in far-field FPS-7B exposure system.
- To develop a research plan to address biomedical issues pertinent to body borne and helmet mounted antennas.

BODY

The research efforts of MBS staff have resulted in products in form of 46 meeting abstracts, 25 publications (including 3 submitted under review, 2 in preparation) and 1 technical report. Additional manuscripts are being planned but will not be in time before the expiration of the contract and the end of Army RF bioeffects research program. A complete list and copies of abstracts, publications, manuscripts, and technical report are included in the appendices. For a small staff of 10 persons at any given period of time, productivity is exceptionally high. This contract represents a successful execution of the GOCO concept through devoted, passionate, innovative and skillful efforts of MBS staff despite an absence of financial support for equipment upgrading. Unfortunately, a decade of research effort will come to an end, while the health and safety issues of radiofrequency radiation have received unprecedented attention worldwide due to recent popularity of cellular/mobile phones. Progress in radiofrequency biological effects research efforts indeed brings out new issues in addition to old issues. These issues are addressed in the section titled "Research Plan for Body Borne and Helmet Mounted Antennas". Radiofrequency emitters are more powerful and are becoming increasingly more powerful in new systems in military than in civilian applications. In addition, multiple transmitting devices such as body borne antennas and non-lethal application of radiofrequency radiation, such as active denial system, will certainly generate new concerns in health and safety issues of newly developed systems. On the extreme, Warfighters can become the targets of RF weapons operated by opposition force. This is quite different exposure scenario from the one in the past that accidental and unavoidable exposures predominate. Long-term effects of intense radiofrequency exposure are not fully understood at the present time. The research needs and plans will also be addressed in the report.

KEY RESEARCH ACCOMPLISHMENTS

Research on Neurotoxic Effects of High Peak Power But Low Average Power Radiofrequency Radiation (RFR) and Interaction Between Neurotoxin and RFR on Manifestation of Neurotoxic Effects

- A rat model of Parkinson disease was developed in male Lewis rats by chronic intravenous and subcutaneous infusions with rotenone, a mitochondrial complex I inhibitor widely used as pesticides and may be presented in the military environments, through Azet® osmotic minipumps for 3 weeks. (Abstracts 8, 37, 38, 46; Publication 17)

    - Motor functions, locomotor activity, rearing activity, movement initiation and step test, tyrosine hydroxylase immunoreactivity in the striatum, microglial activation in the striatum, and lethality were used as endpoints.
    - Intravenous and subcutaneous dose response characteristics (0.0, 2.0, 2.5, 3.5 mg/kg/day) were assessed.
    - Lethality was dose and route dependent. Survival rates were 100, 47, 44 and 29 % for intravenous infusion, and 100, 67, 36, and 9 % respectively for subcutaneous administration of rotenone at 0.0, 2.0, 2.5, and 3.5 mg/kg/day.
    - Significant reduction in horizontal movements and distance of travel at weeks 1 for all rotenone doses, and only 3.5 mg/kg/day at weeks 3.
    - Spontaneous rearing activity was reduced at all rotenone doses and persisted throughout the 3-week observation period.
    - Subcutaneous rotenone infusion did not affect postural stability as measured by step test. Intravenous rotenone infusion yield inconsistent results on step test, significant increase at week 2 at 2.0 mg/kg/day and significant inhibition at week 3 at 3.5 mg/kg/day.
    - Rotenone administration could prolong the time to step initiation but only occur sporadically in animals subjected to subcutaneous infusion, possibly, due to large variation in the test procedure.
    - Tyrosine hydroxylase immunoreactivity (TH-IR) in the striatum decreased in a dose dependent fashion in rats received subcutaneous and intravenous infusions of rotenone.
    - Microglial activation in the striatum was parallel to TH-IR reduction.
    - Moderate chronic mitochondrial inhibition could have profound effects on motor behavior and these effects were not directly correlated with TH-IR reduction and microglial activation. Motor dysfunction could also developed in rats without histological signs of Parkinson disease induced by rotenone infusion.
    - Chronic rotenone infusion could induce loss of dopaminergic nerve terminals without neuronal loss in the striatum similar to alteration of the nigrostriatal pathway in early Parkinson disease.

- Combined effects of pulsed microwave and chronic rotenone infusion were tested in male Lewis rats received chronic rotenone infusion at 2 mg/kg/day through Azet®

osmotic minipump and subjected to L-band (1.25 GHz) microwave exposure at whole-body average specific absorption rate (SAR) of 0.4 and 4 W/kg, 6 μs pulse width and 10 Hz pulse repetition rate for 6 minutes, 4 times a week for a total of 10 exposures. (Abstracts 34, 36, 45; Publication 25)

- Exposure to pulsed microwave alone had no significant effects on any of the endpoints.
- Robust rotenone effects on increase in movement initiation time and reduction in number of rearing could be ameliorated transiently at 1 week after 2 exposures at 0.4 W/kg. Less rotenone-induced striatal TH-IR depletion was also observed in these animals 3 weeks after exposure.
- Due to irreplaceable loss of FPS-7B transmitter, two 6-minute exposures to S-band (2.8 GHz) pulses at 2 μs pulse width and 13, 20, and 200 Hz pulse repetition rates to deliver 0.04, 0.4 and 4 W/kg whole-body average SAR were performed to confirm the initial observations in L-band experiments. Rotenone-induced reduction in number of rearing and increase in movement initiation time were reconfirmed, however, amelioration of rotenone-induced behavioral effects by microwave pulses was not found.
- Additional attempt to confirm L-band ameliorative effects of rotenone-induced reduction in number of rearing and increase in movement initiation time was carried out in a circularly polarized waveguide exposure system operated at 0.4 W/kg and pulse characteristics similar to FPS-7B, i.e., 6 μs pulse width and 10 Hz pulse repetition rate. Despite of these efforts, initial observation in amelioration of rotenone-induced behavioral effects by microwave pulses was not replicated.

- Neurotoxic effects of microwave pulses and another neurotoxin, 3-nitropropionic acid (3-NP), and their interaction were studied in male Sprague-Dawley rats. Ultrastructure of caudate-putamen neurons, motor activity, and startle prepulse inhibition. Typical treatments were two doses of 10 mg/kg 3-NP i.p., and two 30-minute exposures to pulsed microwave (1.25 GHz) at 0.6 and 6 W/kg at 5.9 μs pulse width and 10 Hz pulse repetition rate in two consecutive days. (Abstracts 1, 9, 22, 23, 24; Publications 2, 10, 22; Report 1)

  - Administration of two 3-NP doses at 10 mg/kg significantly increased endoplasmic reticulum (ER) intracisternal width, ER area density and thickness of nuclear envelope but had no effect on mitochondria diameter.
  - Tranylcypromine (3 mg/kg) administered in conjunction with 10 mg/kg 3-NP increased ER intracisternal width and ER area density in a larger magnitude than 3-NP alone.
  - Exposure to microwave pulses at 6 W/kg also significantly increased ER intracisternal width, ER area density and thickness of nuclear envelope and enhanced the magnitude of changes of these endpoints caused by 10 mg/kg 3-NP alone.
  - Exposure to microwave pulses at 0.6 W/kg did not alter the ultrastructure significantly, but it reduced the effects on these endpoints caused by 10 mg/kg 3-NP.

- Motor activity was significantly reduced about 12 % 3.5-4.5 hours after two10 mg/kg administration.
- Motor activity was not affected 1.5-2.5 hours after two microwave exposures at 0.6 and 6 W/kg or these microwave exposure in combination with 10 mg/kg 3-NP.
- Startle amplitude and startle prepulse inhibition were not affected 3.5-4.5 hours after 10 mg/kg 3-NP, 1.5-2.5 hours after either 0.6 or 6 W/kg pulsed microwave, or combination of 3-NP and microwaves.
- Long term follow-up at 1, 2 and 3 weeks after treatment indicated: redction of activity over time after 0.6 W/kg pulsed microwave exposure, reduction in startle prepulse inhibition on the second day of microwave exposure by 3-NP and pulsed microwave, and lack of 3-NP induced reduction in startle prepulse inhibition 3 weeks after pulsed microwave exposure at 0.6 and 6 W/kg.

Relevant Abstracts/Publications/Report

- Brewer, P.A.; Mery, L.R.; Phelix, C.F.; and Seaman, R.L. [2001]: Monoamine oxidase inhibition enhances ultrastructural changes in rat striatal neurons after single systemic injection of 3-nitropropionic acid. In: "Abstract submitted to the 31st Annual Meeting of the Society for Neuroscience, San Diego, CA, November 10-15, 2001."

- Seaman, R.L.; Mathur, S.P.; Phinney, A.M.; and Harris, N.R. [2001]: Interaction between a neurotoxin and pulsed microwaves. In: "Abstracts of 23rd Annual Meeting of the Bioelectromagnetic Society," St. Paul, MN, June 10-14, 2001, pp. 130-131.

- Seaman, R.L.; and Phelix, C.F. [2001]: Acute changes in rat caudate-putamen neuronal ultrastructure due to 3-nitropropionic acid and microwave exposure are not reflected in behavior. In: "Abstract of the 31st Annual Meeting of the Society for Neuroscience," San Diego, CA, November 10-15, 2001.

- Seaman, R.L., and Lu, S.-T. [2002]: Neurodegeneration from microwave and neurotoxin exposure. In: "Abstracts of 24th Annual Meeting of the Bioelectromagnetic Society," Quebec City, Quebec, Canada, June 23-27, 2002, pp 91-92.

- Seaman, R.L.; Mathur, S.P.; and Phinney, A.M. [2002]: Single exposure to pulsed microwaves at 0.6 W/kg does not modify locomotor activity or acoustic startle immediately after exposure. In: "Abstracts of 24th Annual Meeting of the Bioelectromagnetic Society," Quebec City, Quebec, Canada, June 23-27, 2002, p 79.

- Seaman, R.L.; Mathur, S.P.; Phinney, A.M.; Garcia, A.S.; and Ashmore, J.L. [2002]: Rat short-term startle prepulse inhibition and some motor activities after two microwave exposures are changed by 3-NP. In: "Abstracts of the 22nd Annual Meeting of the Society for Neuroscience," Orlando, FL, November 2-7, 2002.

- Seaman, R.L.; Chesselet, M.F.; Lu, S.-T.; Mathure, S.P.; DiCarlo, C.D.; Fleming, S.M.; Zhu, C.; Mehta, A.; Carlson, B.B.; Phinney, A.M.; Garcia, A.S.; Adam, A.R.; Grado, A.R.; and Brown, A. [2003]: An animal model to test combined effects of pulsed microwave and a CNS mitochondrial toxin. In: "Abstracts of the 25th Annual Meeting of the Bioelectromagnetics Society", Maui, HI, June 22-27, 2003, p 186.

- Seaman, R.L.; Fleming, S.M.; Prosolovitch, K.; Chesselet, M.F.; Lu, S.T.; Mathur, S.P.; DiCarlo, C.D.; Garcia, A.S.; Grado, A.R.; Garza, T.H. [2003]: Effects of Exposure to Pulsed Microwaves on Movement Initiation in Rats Exposed to the Mitochondrial Toxin Rotenone. In: "Abstracts of the 6th International Congress of the European Bioelectromagnetics Assiciation", Budapest, Hungary, November 13-15, 2003, p 127.

- Zhu, C., Fleming, S.M., Mehta, A., Seaman, R.L., DiCarlo, C.D., and Chesselet, M.-F. [2003]: Chronic mitochondrial complex I inhibition induces nigrostriatal pathway dysfunction in rats. In: "Abstracts of 17th Annual Symposia on Etiology, Pathogenesis, and Treatment of Parkinson's Disease and Other Movement Disorders", San Francisco, CA, October 19, 2003.

- Zhu, C., Fleming, S.M., Mehta, A., Seaman, R.L., DiCaro, C.D., Chesselet, M.-F. [2003]: Chronic intravenous and subcutaneous rotenone infusion: survival analysis, functional assessment and microglial activation. In: "Abstracts of the Society for Neuroscience 33rd Annual Meeting", New Orleans, LA, November 8-12, 2003.

- Seaman, R.L., Chesselet, M.F., Mathur, S.P., DiCarlo, C.D., Fleming, S.M., Ashmore, J.L., Garza, T.H., Morin, J.M., Grado, A.R., and Adam, S.L. [2004]: Combined effects of pulsed microwaves and a CNS mitochondrial toxin on behavior depend on microwave-exposure parameters. In: "Abstracts of 26th Annual Meeting of the Bioelectromagnetics Society", Washington, D.C., June 20-24, 2004.

- Zhu, C., Vourc'h, P., Fernagut, P.O., Fleming, S.M., Lacan, S., DiCarlo, C.D., Seaman, R.L., and Chesselet, M.F. [2004]: Variable specificity of chronic subcutaneous administration of rotenone for the nigrostriatal pathway. Submitted to Society for Neuroscience 34th Annual Meeting.

- Seaman, R.L.; and Phelix, C.F. [2001]: Changes in ultrastructure of rat caudate-putamen neurons with a neurotoxin and exposure to pulsed microwaves. In: "Proceedings of the EBEA 2001, 5th International Congress of the European BioElectromagnetics Association" Helsinki, Finland, September 6-8, 2001, Hietanen, M., Jokela, K., and Juutilainen, J. eds., Finish Institute of Occupational Health, pp. 240-241.

- Seaman, R.L.; Mathur, S.P.; Phinney, A.M.; Garcia, A.S.; and Ashmore, J. L. [2002]: Changes in rat motor activity by pulsed microwave radiation depend on type of activity, time after exposure, and state of animal. In: "Proceedings of the Second International Workshop on Biological Effects of EMFs," Kostarakis, P. ed., (ISBN 960-86733-3-X) pp 388-394.

- Seaman, R.L.; and DeCarlo, C.D.: Effects of microwave radiation on nigrostriatal neurodegeneration in the rat. In: "Joint Medical Technology Workshop 2003, Panel F: Non-Ionizing Directed Energy Bioeffects", 10-23 October 2003, Lansdowne, VA, US Army Medical Research and Materiel Command (4 pages).

- Fleming, S.M., Zhu, C., Mehta, A., Seaman, R., and Chesselet, M.-F. [2004]: Chronic intravenous and subcutaneous rotenone infusion: survival analysis, functional assessment and microglial activation. Experimental Neurol. 187: 418-429.

- Seaman, R.L., and Phelix, C.F. [2004]: Acute effects of pulsed microwaves and 3-nitropropionic acid on neuronal ultrastructure in the rat caudate-putamen. Bioelectromagnetics (in press).

- Seaman, R.L.; Chesselet, M.-F.; Mathur, S.P.; DiCarlo, C.D.; Fleming, S.M.; Ashmore, J.L.; Garza, T.H.; and Grado, A.M. [2004]: Movement initiation in rotenone-treated rats after acute exposure to 1.25-GHz microwave pulses in circular waveguide at 0.4 W/kg. (In preparation, abstract included).

- Seaman, R.L., Mathur, S.P., and Dick, E.J. Jr. [2003]: Short-term motor activity and acoustic startle after microwave exposure and toxin-induced hypoxia. A Technical Report.

Research on Effects of High Power Radiofrequency Radiation

- A series of experiments were aimed to explore the biological effects of extremely high peak power (EHPP)/high average power microwaves. The exposure system used was a 9.3-10.6 GHz waveguide exposure system based on WR90 (22.86 × 10.16 mm) waveguide with a sapphire matching plate into a exposure chamber filled with circulating electrolyte solutions resulting in peak SAR close to GW/kg by 230-260 kW peak power transmitted into this waveguide exposure system. Due to large heat capacity and flow rate, excessive temperature rise was avoided. Biological specimens used were yeast cells, GH3 rat pituitary cells and hippocampus slices from 3-4 week old Sprague-Dawkey rats. (Abstracts 6, 7, 13, 19, 20, 21, 25, 30, 33; Publication 1, 6, 7, 15, 16, 22)

    - Calcium channel by patch clamp analysis of GH3 rat pituitary cell was not affected 5-45 minutes after 30-minute exposure to 9.6 GHz at 3.8 kW/kg as continuous wave or pulsed at 960 MW/kg peak SAR at 0.25 μs and 16 Hz, 0.5 μs and 8 Hz, or 2 μs and 2 Hz.

- Temperature dependent decrease in cell density of gel-suspended yeast cells exposed to a 9.3 GHz microwaves in a continuous gradient with average SAR from 3.2 kW/kg to 0.6 mW/kg in continuous wave (CW) or pulsed at 0.5 μs and 10 Hz for 6 hours. An equivocal difference ($p < 0.1$) between CW and pulsed microwave was noted at average SAR of 100 W/kg or higher for CW and 20 MW/kg or higher peak SAR for pulsed microwaves.
- In hippocampus slices, a brief tetanus (2 s at 50 Hz) was used to induce long term potentiation (LTP) of synaptic transmission which could be observed as increasing amplitude of population spikes, which reached a maximum in 1.5 to 2 minutes after tetanus and lasted for a minimum of 10 minutes after the maximum.
- A 2-minute EHPP (2 μs and 0.5 Hz or 0.5 μs and 2 Hz at 330 MW/kg peak SAR and 0.33 kW/kg average SAR) applied 1.5 minute before the application of tetanus for LTP did not affect the ability of neurons to develop LTP. The temperature increases in both cases were 0.5-0.6 °C.
- A graded depression of LTP was noted when hippocampus slices were exposed to EHPP at 1 μs and 360 MW/kg peak SAR for 2 minutes at 2 (0.7 kW/kg average, 1.4 °C increase), 5 (1.8 kW/kg average, 3.0 °C increase) and 10 Hz (3.6 kW/kg average, 5.8 °C increase) applied 5 min 10 s after the induction of tetanus. The microwave-induced depression of potentiated population spikes recovered shortly and completely after cessation of the exposure and the return of temperature to pre-exposure level. The results could be interpreted that "memory record" was temporarily unavailable.
- Course of the LTP development could be affected by 7-minute exposures to CW microwave or microwave pulses applied before the induction of tetanus, during LTP development and after LTP reached a maximum. Course of LTP development became more and more gradual as microwave doses increased from 0.25 kW/kg average SAR (CW or 0.5 μs and 1 Hz at 500 MW/kg peak SAR, 03-0.4 °C increase) to 1 kW/kg (CW or 2 μs and 1 Hz at 500 MW/kg peak SAR, 1.5-1.6 °C increase). Efficacy of LTP induction after exposure was not altered by any of these exposures. Furthermore, difference between CW and pulsed microwaves of equal average SAR was not found.
- Stimulation of CA3 pyramidal cells produces an evoked potential at CA1 neurons, which can be recorded as first excitatory postsynaptic potential (EPSP), population spike, and second EPSP. Pair of stimuli (conditioning and test) were applied every 15 s. The EHPP effects (9.6 GHz, 2 μs, 740 kW/kg peak SAR synchronized with various events of EPSP) on conditioning and test responses were dependent on synchronization. EHPP applied 2 ms before twin stimuli had no effect on EPSP. Conditioning EPSP decreased by EHPP when applied 3.4-4.5 ms after stimulus (during EPSP rising phase) or 14-16 ms after the stimulus (between EPSPs). Test EPSP decreased significantly when EHPP was applied 14-16 ms after the stimulus. Each EHPP pulse could increase temperature by 0.3-0.4 °C. Similar effects approximately of the same magnitude could also be induced by unsynchronized EHPP exposure at 1 Hz, which induced a 1.5-2 °C increase in temperature.
- Delayed suppression of EPSP appeared to have a threshold at 48-49 °C from a single 500 ms burst of high power microwaves. Latency of EPSP delayed

suppression was 20-50 s and could last 5-10 min to 1-2 hours. Recovery from delayed suppression usually was complete unless the heat pulse exceeded 60 °C.

- Epileptiform-type bursts, 20-40 bursts per minute, in CA3 neurons of the isolated rat hippocampus slices could be induced by superfusion with 4-aminopyridine (50-150 μM). Effects of 9.6 GHz CW or pulsed microwaves were studied. (Abstract 30, Publication 22)

  - CW exposures at 24, and 120 W/kg for 5 minutes with negligible temperature change had no effect on epileptiform burst rate induced by 50 and 100 μM 4-aminopyridine.
  - CW exposure at 600 and 3,000 W/kg with temperature increases at 0.6-0.7 and 3.5-3.7 °C had a complex effect on epileptiform burst activity induced by superfusion of 4-aminopyridine, i.e., transient cessation of burst activity coincident with on and off of the microwave exposure and followed by restart of burst activity at a higher rate. Convention heating by increasing bath temperature at 3.5-3.7 °C could also produce these effects on burst activity.
  - Transient on and off cessation effect and restarting at a higher rate of 4-aminopyridine induced burst activity could also be produced by exposure to pulsed microwave 9250 ns, 600 MW/kg peak SAR at 1, 2, 4, and 8 Hz (150, 300, 600, and 1,200 W/kg average and 0.25, 0.4, 0.9 and 1.5 °C temperature increases).

Relevant Abstracts/Publications/Report

- Pakhomov, A.G.; Doyle, J.; Mathur, S.; and Murphy, M.R. [2001]: Retaining of the long-term potentiation in hipocampal slices after high peak power microwave exposure and heating. In: "Abstracts of the Second International Symposium on Nonthermal Medical/Biological Treatments Using Electromagnetic Fields and Ionized Gases," Portsmouth, VA, May 21-23, 2001, p. 21.

- Pakhomov, A.G.; Doyle, J.; Mathur, S.; and Murphy, M.R. [2001]: Effects of extremely high power microwave pulses on the population spike and long-term potentiation in rat hippocampal slices. In: "Abstracts of the 23rd Annual Meeting of the Bioelectromagnetic Society," St. Paul, MN, June 10-14, 2001, p. 86.

- Doyle, J.; Mathur, S.; Murphy, M.R.; and Pakhomov, A.G. [2002]: Comparative effects of continuous-wave and high peak power microwave emission on the induction of long-term potentiation. In: "Abstracts of 24th Annual Meeting of the Bioelectromagnetic Society," Quebec City, Quebec, Canada, June 23-27, 2002, pp 229-230.

- Pakhomov, A.G.; Doyle, J.; Ashmore, J.; and Murphy, M.R. [2002]: Thermal limits for functional damage and recovery in brain tissue after a brief (500 ms) high-intensity microwave exposure. In: "Abstracts of 24th Annual Meeting of the Bioelectromagnetic Society," Quebec City, Quebec, Canada, June 23-27, 2002, pp 228-229.

- Pakhomov, A.G.; Doyle, J.; and Murphy, M.R. [2002]: Effect of high-power microwave pulses on synaptic transmission and plasticity in brain neurons. In: "Proceedings of the Third International Conference on Electromagnetic Fields and Human Health, Fundamental and Applied Research," Moscow-Saint Petersburg, Russia, September 17-24, 2002, p 276.

- Pakhomov, A.; Doyle, J.; and Murphy, M. [2002]: Delayed and reversible suppression of evoked activity in CA_1 area of hippocampal slices by brief heat pulses. In: "Abstracts of the 22nd Annual Meeting of the Society for Neuroscience," Orlando, FL, November 2-7, 2002.

- Doyle, J.; Murphy, M.R.; and Pakhomov, A.G. [2003]: High-power microwave pulses phased with evoked synaptic potentials may affect synaptic transmission. In: "Abstracts of the 25th Annual Meeting of the Bioelectromagnetics Society", Maui, HI, June 22-27, 2003, p 359.

- Pakhomov, A.G.; Doyle, J.; Ashmore, J.; and Murphy, M.R. [2003]: Effects of 9.6 GHz microwaves on 4-Aminopyridine-induced burst in isolated hippocampal slices. In: "Abstracts of the 25th Annual Meeting of the Bioelectromagnetics Society", Maui, HI, June 22-27, 2003, p 6.

- Pakhomov, A.G.; Mathur, S.; and Murphy, M.R. [2003]: High-resolution temperature and SAR measurement using different sensors. In: "Abstracts of the 25th Annual Meeting of the Bioelectromagnetics Society", Maui, HI, June 22-27, 2003, p 224-225.

- Pakhomov, A.; Doyle, J.; and Murphy, M. [2003]: Alteration of Synaptic Transmission by Neuron Excitation-Synchronized High-Power Microwave Pulses: A Replication Study. In: "Abstracts of the 6th International Congress of the European Bioelectromagnetics Assiciation", Budapest, Hungary, November 13-15, 2003, p 110.

- Pakhomov, A.G.; Mathur, S.; Gajsek, P.; and Murphy, M.R. [2001]: Use of gel-suspended cell cultures for analysis of dose dependence of microwave bioeffects. In: "Proceedings of the EBEA 2001, 5th International Congress of the European BioElectromagnetics Association" Helsinki, Finland, September 6-8, 2001, Hietanen, M., Jokela, K., and Juutilainen, J. eds., Finish Institute of Occupational Health, pp. 15-17.

- Pakhomov, A.G.; Gajsek, P.; Allen, L.; Stuck, B.E.; and Murphy, M.R. [2002]: Comparison of dose dependences for bioeffects of continuous-wave and high-peak power microwave emissions using gel-suspended cell cultures. Bioelectromagnetics 23: 158-167.

- Pakhomov, A.; Du, X.; Doyle, J.; Ashmore, J.; and Murphy, M.R. [2002]: Patch-clamp analysis of the effect of high-peak power and CW microwaves on calcium channels. In: "Proceedings of the Second International Workshop on Biological Effects of EMFs," Kostarakis, P. ed., (ISBN 960-86733-3-X) pp 281-288.

- Pakhomov, A.G.; Doyle, J.; Stuck, B.E.; and Murphy, M.R. [2003]: Effects of high power microwave pulses on synaptic transmission and long term potentiation in hippocampus. Bioelectromagnetics 24: 174-181.

- Pakhomov, A.G.; Stuck, B.E.; and Murphy, R. [2003]: *In vitro* model research into bioeffects of extremely high power microwave pulses. In: "Proceedings of the 3rd International EMF Seminar in China: Electromagnetic Fields and Biological Effects", pp 82-83.

- Pakhomov, A.; Doyle, J.; Morin, J.; and Murphy, M. [2004]: Extremely-high power microwave pulses (EHPP) alter 4-aminopyridine-induced bursts in isolated hippocampal slices. (In preparation, abstract included).

Research on Biological Hazards of Ultra-Wide-Band Pulses on the Cardiovascular System and Other Cell Systems

- Biological effects of ultra-wide-band (UWB) pulses were studied at 100 kV/m electrical field intensity, 1 ns pulse width, various pulse repetition rate up to 1,000 Hz and various exposure duration up to 30 minutes. Due to extremely short pulse width, the estimated SAR was below current basic limits of the DoD personnel protection guidelines. Because of the same reason, temperature increases were not observed. Therefore, thermal mechanism could not be applied. Biological endpoints studied were cardiovascular functions in rats, nitric oxide production, cell cycle progression, activation of NF-κB protein, transcription P53 target gene in cultured cells. (Abstracts 17, 18, 27, 28, 29, 35, 40, 41, 42; Publications 4, 8, 19, 20)

    - Delayed hypotension (decreased blood pressure) was noted in Wistar-Kyoto (WKY) rats exposed to UWB pulses for 6 minutes at 85-94 kV/m peak electric field intensity, 1ns pulse width, 1,000 and 500 Hz pulse repetition rates. The estimated threshold for delayed hypotension was less than 0.1 W/kg whole-body average SAR.
    - Delayed hypotension could be observed as early as 3 days after exposure, reached a maximum depression at 2 weeks after exposure, and persisted as long as 4 weeks after exposure.

- Cardiovascular effects were not found in WKY rats exposed for 6 minutes at 250 and 500 Hz.
- Delayed hypotension was confirmed in a replicated experiment in which the exposure was performed at 500 Hz.
- At 2 weeks after 6-minute exposure to 500 Hz UWB pulses, heart rate and blood pressure responses to a 47 ° head-up orthostatic stress were normal. Marginal increase in low frequency and significant increase in very low frequency components of power spectral density of short-term heart rate variability were noted at 2 weeks after exposure to 500 Hz UWB pulses. Time-domain endpoints of heart rate variability did not altered by 500 Hz UWB pulses at 2 weeks after exposure.
- PR, RT and RR intervals of the electrocardiogram in keamine-anesthetized Sprague-Dawley rats were not affected by 10 s bursts of UWB pulses at 106 kV/m peak electric field intensity, 0.78 ns pulse width and 1,000 Hz pulse repetition rate for 25 ms burstssynchronized with R- or T-wave of the electrocardiogram.
- Exposures to UWB pulses (90 minutes total, 30 minutes on and 30 minutes off for 3 times at 100 kV/m peak electric field intensity, 0.79 ns pulse width, 250 Hz pulse repetition rate) did not affect the cell cycle distributions of 244B human lymphoblastoid cells, MM6 human monocytes and HL-60 human myeloid leukemic cells at 6, 10 and 24 hours after exposure.
- NF-κB binding to DNA was increased in human Mono Mac-6 cells exposed to UWB pulses (90 minutes total, 30 minutes on and 30 minutes off for 3 times at 100 kV/m peak electric field intensity, 0.79 ns pulse width, 250 Hz pulse repetition rate) at 24 hours after exposure but not at 10 min, 0.5, 4, 8 and 48 hours after exposure.
- UWB exposure (90 minutes total, 30 minutes on and 30 minutes off for 3 times at 100 kV/m peak electric field intensity, 0.79 ns pulse width, 250 Hz pulse repetition rate) did not cause transcriptional induction of p53, or the p53 target genes p21 (cell cycle arrest), gadd45 (cell cycle arrest and DNA damage repair), PCNA (DNA damage repair) and Bax (apoptosis) in 244B cells, transactivation of p52 responsive genes in MM-6 and HL-60 cells, or loss of mitochondrial membrane potential and release of cytochrome C into cytoplasm in 244B cells.
- Nitric oxide production by RAW 264.7 macrophages stimulated by gamma interferon, lipopolysaccharide and nitrate could be enhanced by 30-minute UWB exposure at 72-95 kV/m peak electric field, 1 ns pulse width, and 600 pulse repetition rate. The estimated SAR was 0.106 W/kg.

Relevant Abstracts/Publications/Report

- Lu, S.-T. [2001]: Potential application of UWB pulses in lowering blood pressure. In: "Conference Digest of the 2001 Asia-Pacific Radio Science Conference", Tokyo, Japan, August 1-4, 2001, p. 266.

- Mathur, S.P.; Lu, S.-T.; Harris, N.; and Hurt, W.D. [2002]: Some approaches to UWB dosimetry. In: "Abstracts of the Ninth Annual Michaelson Research Conference," South Portland, ME, August 9-12, 2002.

- Meltz, M.L.; Galindo, C.; Natarajan, M.; Leach, R.; Reveles, X.; Mathur, S.; and Ashmore, J. [2002]: Investigatio of the ability of UWB RF exposure to induce translocations in human chromosomes 1, 2, or 4 using multi-color FISH technology. In: "Abstracts of the Ninth Annual Michaelson Research Conference," South Portland, ME, August 9-12, 2002.

- Natarajan, M.; Meltz, M.L.; Galindo, C.; Ashmore, J.; and Mathur, S. [2002]: Influence of UWB RF exposure on nuclear translocation of NF-κB in human MM-6 monocyte. In: "Abstracts of the Ninth Annual Michaelson Research Conference," South Portland, ME, August 9-12, 2002.

- Meltz, M.L.; Nayak, B.K.; Galindo, C.; Mathur, S.P.; and Natarajan, M. [2003]: Effects of ultrawideband radiofrequency radiation on the cell cycle progression in human cell. In: "Abstracts of the 25th Annual Meeting of the Bioelectromagnetics Society", Maui, HI, June 22-27, 2003, p 350.

- Natarajan, M.; Nayak, B.K.; Roldan, F.A.; Galindo, C.; Mathur, S.P.; and Meltz, M.L. [2003]: Genomic profiling of NF-κB-signal dependent genes in human monocytes after ultra wide band exposure. In: "Abstracts of the 25th Annual Meeting of the Bioelectromagnetics Society", Maui, HI, June 22-27, 2003, p 202.

- Nayak, B.K.; Natarajan, M.; Galindo, C.; Mathur, S.P.; and Meltz, M.L. [2003]: Transcription of p53 target genes in response to ultrawideband radiofrequency radiation. In: "Abstracts of the 25th Annual Meeting of the Bioelectromagnetics Society", Maui, HI, June 22-27, 2003, p 349.

- Seaman, R.L.; Jauchem, J.R.; Mathur, S.P.; Phinney, A.M.; and Ashmore, J.L. [2003]: Lack of change in temporal characteristics of rat ECG during exposure to ultra-wideband pulses. In: "Symposium Record Abstracts of the ElectroMed 2003 Third International Symposium on Nonthermal Medical/Biological Treatments Using Electromagnetic Fields and Ionized Gases", San Antonio, TX, June 11-13, 2003, pp 123-124.

- Lu, S.-T. [2004]: Biological Effects of ultra-wide-band pulses. In: "Abstracts of 26th Annual Meeting of the Bioelectromagnetics Society", Washington, D.C., June 20-24, 2004.

- Natarajan, M., Nayak, B.K., Mathur, S.P., Galino, C., and Meltz, M.L. [2004]: Ultrawideband electromagnetic radiation (UWB EMR) exposures and activation of an important signal transduction pathway. In: "Abstracts of 26th Annual Meeting of the Bioelectromagnetics Society", Washington, D.C., June 20-24, 2004.

- Nayak, B.K., Galindo, C., Natarajan, M., Mathur, S.P., and Meltz, M.L. [2004]: Determination of p53 protein stabilization, loss of mitochondrial membrane potential, and release of cytochrome C into the cytosol in response to UWB EMR exposure in human lymphoblastioid cells. In: "Abstracts of 26th Annual Meeting of the Bioelectromagnetics Society", Washington, D.C., June 20-24, 2004.

- Lu, S.-T.; and Mathur, S.P. [2002]: Hypotension induced by ultra-wide-band pulses: dose response, replication, orthostatic response and heart rate variability. In: "Proceedings of the Second International Workshop on Biological Effects of EMFs," Kostarakis, P. ed., (ISBN 960-86733-3-X) pp 409-418.

- Seaman, R.L.; Parker, J.E.; Kiel, J.L.; Mathure, S.P.; Grubbs, T.R.; and Prol, K. [2002]: Ultra-Wideband pulses increase nitric oxide production by RAW 264.7 macrophages incubated in nitrate. Bioelectromagnetics 23: 83-87.

- Nayak, B.K.; Natarajan, M.; Galino, C.; Mathur, S.P.; and Meltz, M.L. [2004]: Determination of p53 protein stabilization and transactivation of its target genes in response to ultrawideband electromagnetic radiation exposure in human hematopoietic cells. (Submitted).

- Naya, B.K.; Natarajan, M.; Galindo, C.; Mathur, S.P.; and Meltz, M.L. [2004]: Effect of ultrawideband electromagnetic radiation on cell cycle progression in human hematopoietic cells. (Submitted).

- Seaman, R.L., and Jauchem, J.R. [2004]: Temporal characteristics of the rat electrocardiogram during acute exposure to timed ultra-wideband pulses. (in press)

Cytotoxic Effects of Nanosecond High-Intensity Electric Pulses

- Exposure to high intensity 10 ns electrical pulses could comprise the survival of cultured U937 human histiocytic lymphoma cells and Jurkat human T-cell leukemia cells. (Abstracts 32, 43, 44; Publication 21)

    - Multiple electrical pulses at 50-174 kV/cm could produce lethality in cultured U937 cells. Lethality depended on and inverse relationship of peak electric field intensity and number of pulses, i.e., lower number of pulses needed to cause cell lethality at higher peak electric field intensity.
    - When expressed in specific absorbed dose, survival curves of U937 and Jurkat cells were similar to that of ionizing radiation, i.e., survival fraction had a significant shoulder and decreased exponentially with increasing specific absorbed dose.
    - D_0, lethal dose was 106 J/g for Jurkat cells and 266 J/g for U937 cells. The extrapolation number, n was 1.5 for Jurkat cells and 1.63 for U937 cells.

Apparently, Jurkat cells were more susceptible to lethal effect of electric pulses than U937 cells.

- Thermal effect was inadequate to explain the lethality because the bath temperature was below known lethal temperature.

Relevant Abstracts/Publications/Report

- Pakhomov, A.G.; Phinney, A.; Ashmore, J.; Kolb, J.; Kono, S.; Schoenbach, K.; and Murphy, M.R. [2003]: Quantitative analysis of cytotoxicity of ultrashort (10 ns) electrical pulses in mammalian cells. In "Symposium Record Abstract of the ElectroMed 2003 Third International Symposium on Nonthermal Medical/Biological Treatments Using Electromagnetic Fields and Ionized Gases", San Antonio, TX, June 11-13, 2003, pp 66-67.

- Pakhomov, A., Walker, K. III, Kolb, J., Schoenbach, K., and Murphy, M. [2004]: Cell killing effect of high-intensity, ultrashort electric pulses. In: "Abstracts of 22nd Annual Meeting of the Society for physical Regulation in Biology and Medicine", San Antonio, TX, January 7-9, 2004, pp. 11-12.

- Pakhomov, A., Walker, K. III, Kolb, J., Schoenbach, K., Stuck, B., and Murphy, M. [2004]: The rules of cell survival after exposure to high-intensity, ultrashort electric pulses. In: "Abstracts of 26th Annual Meeting of the Bioelectromagnetics Society", Washington, D.C., June 20-24, 2004.

- Pakhomov, A.G.; Phinney, A., Ashmore, J.; Walker, K. III; Kolb, J.; Kono S.; Schoenbach, K.H.; and Murphy, M.R. [2004]: Some Characteristics of the cytotoxic effect of nanosecond duration, high-intensity electrical pulses. IEEE Trans. Plasma Sci. (in press).

Finite Difference Time Domain Techniques and Other Techniques for Radiofrequency Radiation Dosimetry

- Finete Difference Time Domain (FDTD) techniques and other techniques for radiofrequency radiation dosimetry were performed. Due to lack of resources, FDTD simulation for dosimetry was usually in corporation and coordinated with other organization with similar interest. (Abstracts 10, 11, 12, 14, 16, 31, 39; Publication 5)

  - Thermometric dosimetric method was automated based on procedure developed in this laboratory. A LabView executive file was developed to enable user in a non-LabView platform.
  - Software tools to calculate the far-field power density from open-ended waveguide, prolate spheroid SAR, and 2D-FDTD color coder were developed.
  - Induced current in the culture flasks exposed to UWB pulses was accomplished.

- Various thermometric systems such as copper-constantan thermocouple, fiber optic probe (TP-21-MO2) and miniature fiber optic probe (FOT-HERO) were evaluated for high-resolution temperature and SAR application. HERO probe could record a clear plateau without radiofrequency pick-up artifacts.
- Extensive application of various thermometric calorimetry in tissue culture flasks, sample bottles and anesthetized animals. A recover rate of near 100 % was found in each of thermometric procedures. Therefore, thermometric calorimetry of anesthetized animals in various sizes was routinely used to determine the whole-body average absorption rate for all the experimental performed in this laboratory. Dosimetric data was also incorporated into every presentation in abstract form or in manuscript.
- Comparison between FDTD simulation and thermometric dosimetry at 16 locations in the base of brain, cortex, spinal cord and neck muscle exposed to 800 and 500 MHz microwaves. It was concluded that good agreement occurred between FDTD prediction of whole-body average SAR and that derived thermometric dosimetry data from low power transmitter but poorer agreement between FDTD and thermometric data derived from high power transmitter. Apparently, comparing model and empirical SAR data was not straightforward. Anatomical differences between model and carcasses could contribute a great portion of difficulties.
- Additional FDTD modeling of SARs (local SAR and whole-body average SAR) of a realistic rat for 1.25 and 2.8 GHz used in "rotenone" project are in progress.
- FDTD simulation of transmission of UWB pulses in the Gigahertz TEM cells was accomplished. The result indicated that pulse shape was preserved as the pulse propagated toward the load and amplitude decreased as cross-section area of the GTEM cell increased. The FDTD simulated waveforms agreed well with waveforms collected with D-dot sensor in all selected sampling points within the GTEM cell. Additional FDTD simulation of GTEM cell loaded with T-25 flasks will be conducted in the future if appropriate funding is available.

Relevant Abstracts/Publications/Report

- Ziriax, J.M.; D'Andrea, J.A.; Lu, S.-T.; Mathur, S.; and Cox, D. [2001]: Verifying electromagnetic Dosimetry. In: "Conference Digest of 2001 Asia-Pacific Radio Science Conference", Tokyo, Japan, August 1-4, 2001, p. 414.

- Ziriax, J.M.; D'Andrea, J.A.; Lu, S.-T.; Mathur, S.; Cox, D.; Henry, P.; Kosub, K.; Garay, R.; and Hurt, W. [2001]: Comparing thermometry and FDTD predictions: measurement versus theory. In: "Abstracts of 23rd Annual Meeting of the Bioelectromagnetic Society," St. Paul, MN, June 10-14, 2001, pp. 178-179.

- Cox, D.D.; Mathur, S.P.; D'Andrea, J.A.; and Lu, S.-T. [2002]: Automating the analysis of thermometric microwave-dosimetry data. In: "Abstracts of 24th Annual Meeting of the Bioelectromagnetic Society," Quebec City, Quebec, Canada, June 23-27, 2002, p 63.

- Hatcher D., Cox, D., Ziriax, J., D'Andrea, J., and Mathur, S. [2002]: Software tools to calculate the far-field for open-ended waveguide, prolate spheroid SAR, thermometric dosimetry data, and 2D-FDTD model color-coder. In: "Abstracts of 24th Annual Meeting of the Bioelectromagnetic Society," Quebec City, Quebec, Canada, June 23-27, 2002, pp 63-64.

- Ji, Z., Hagness, S.C., Brooske, J.H., Mathure, S., and Meltz, M. [2004]: Finite-Difference Time-Domain (FDTD) analysis and dosimetry of a gigahertz TEM cell. In: "Abstracts of 26th Annual Meeting of the Bioelectromagnetics Society", Washington, D.C., June 20-24, 2004.

- Mathur, S.P.; and Lu, S.-T. [2002]: Application of various thermometric calorimetry in rodent dosimetry. In: "Proceedings of the Second International Workshop on Biological Effects of EMFs," Kostarakis, P. ed., (ISBN 960-86733-3-X) pp 272-280.

Role of Ambient Temperature on Manifestation of Radiofrequency Biological Effects

- Neuroendocrine responses in rats were used as endpoints of "stress" to demonstrate the role of ambient temperature on manifestation of radiofrequency biological effects. (Abstract 26; Publication 18)

    - Typical neuroendocrine responses to microwave exposure was similar to those initiated from activation of corticotropin releasing hormone: increased serum corticosterone (CS) concentration, decreased serum growth hormone (GH) concentration, decreased thyroid stimulating hormone (TSH) concentration, and increased prolactin (PRL) concentration. Microwave-induced changes in circulating hormone concentrations were similar to "non-specific" "stress" reaction of animals.
    - Response of each hormone to microwave-induced stress varied with its own baseline and saturation of effect was frequently noted within the physiologic limits for survival.
    - Threshold and magnitude of responses for microwave-induced "stress" hormonal changes varied with experimental conditions. Notable were elevated ambient temperature, facilitated heat loss and alteration in light cycle.
    - Microwave-induced neuroendocrine changes usually accompanied by a significant change in core body temperature.
    - CS concentration changed linearly with changes in core body temperature at equilibrium and had best correlation with changes in core body temperature, the correlation coefficient frequently reached 0.90 or better. Its response ranged from normothermia to near-lethal hyperthermia approximately at 41.3-41.8 °C.

The changes in CS concentration were thus considered to be the best quantitative index of microwave-induced stress.

- Extensive studies in response of body temperature to ambient and microwave heating revealed that core body temperature increased with SAR in a curvilinear fashion while tail skin temperature assumed a linear relationship with SAR at various ambient temperature.
- Limiting factor to microwave and ambient heating in rats appeared to be tail skin temperature, which was entirely under the control of ambient temperature. Critical ambient temperature appeared to 28.5 °C ambient temperature, low end of thermoneutral temperature or 31.8 °C tail skin temperature. Once the critical temperature was reached, any elevation in ambient temperature or heat load would elevate core body temperature and tail skin temperature concurrently.
- A model was developed using current knowledge in CS and body temperature responses to microwave exposure. The model indicated that above the critical temperature, microwave energy was additive to ambient condition to alter the magnitude of change in CS concentration or "stress" level. The rate constant was 6.5 μg/dl per W/kg, approximately equaled to one tenth of full response range.

Relevant Abstracts/Publications/Report

- Lu, S.-T. [2003]: Microwave-induced responses of colonic temperature and serum corticosterone concentration in rats are susceptible to changing experimental conditions. In: "Abstracts of the 25th Annual Meeting of the Bioelectromagnetics Society", Maui, HI, June 22-27, 2003, pp 107-108.

- Lu, S.-T. [2004]: Effects of ambient temperature on microwave-induced "stress" responses (Submitted).

Other Related Studies, Multiple Topics Reviews and Presentations

Relevant Abstracts/Publications/Report

- Kiel, J.L.; Rockwell, B.A.; Thomas, R.J.; Alls, J.L.; Mathur, S.P.; Sutter, R.E.; and Morales, P.J. [2001]: Laser and microwave induced breakdown spectroscopy: basis for a new detection technique for chemical and biological agents. In: "Proceedings of IEEE International Conference of Plasma Science and IEEE International Pulsed Power Conference," Las Vagas, NV, June 17-22, 2001.

- Kiel, J.L.; Alls, J.L.; Sutter, R.E.; Mason, P.A.; Mathur, S.P.; and Morales, P.J. [2001]: Directed killing of anthrax spores by microwave induced cavitation via specific binding of organic semi-conductor. In: "Abstracts of the Second International Symposium on Nonthermal Medical/Biological Treatments Using Electromagnetic Fields and Ionized Gases", Portsmouth, VA, May 21-23, 2001.

- Lu, S.-T. [2001]: Research on biological effects of radio frequency radiation at Walter Reed Army Institute of Research. In: "Conference Digest of the 2001 Asia-Pacific Radio Science Conference", Tokyo, Japan, August 1-4, 2001, p. 270.

- Lu, S.-T. [2002]: Biological effects of radio frequency pulses. In: "Proceedings of the Third International Conference on Electromagnetic Fields and Human Health, Fundamental and Applied Research," Moscow-Saint Petersburg, Russia, September 17-24, 2002, p 285.

- Gajsek, P.; Pakhomov, A.G.; and Klauenberg, B.J. [2002]: Electromagnetic field standards in central and eastern European countries: current state and stipulations for international harmonization. Health Phys. 82: 473-483.

- Seaman, R.L. [2002]: Letter to the editor: Non-osseous sound transmission to the inner ear. Hearing Res. 166: 214-215.

- Seaman, R.L. [2002]: Transmission of microwave-induced intracranial sound to the inner ear is most likely through cranial aqueducts. In: "Proceedings of the Second International Workshop on Biological Effects of EMFs," Kostarakis, P. ed., (ISBN 960-86733-3-X) pp 942-945.

- Lu, S.-T. [2003]: Microwave bioeffects, body borne antenna and L-band. In: "Joint Medical Technology Workshop 2003, Panel F: Non-Ionizing Directed Energy Bioeffects", 10-23 October 2003, Lansdowne, VA, US Army Medical Research and Materiel Command (19 pages).

- Lu, S.-T. [2003]: Radio frequency specific effects, potential medical application. In: "Joint Medical Technology Workshop 2003, Panel F: Non-Ionizing Directed Energy Bioeffects", 10-23 October 2003, Lansdowne, VA, US Army Medical Research and Materiel Command (22 pages).

Design, Fabrication, and Characterization a Circularly Polarized Waveguide Exposure System Operated at 1.25 GHz

Two circularly polarized waveguide exposure systems have been constructed and tested for circularity and tuned to operate at 1.25 GHz. A five-power-meter method is in used to determine the whole-body average specific absorption rate (SAR) by the power loss equation and body mass of the animal. The reliability of power loss equation has been confirmed with a saline load against thermometric calorimetry, the golden standard. Thus, power loss equation was used as a transfer standard to validate the thermometric calorimetry in anesthetized animals. High degree of concordance between power loss equation and thermometric calorimetry in anesthetized animals were also obtained. Dosimetry data will be included in a manuscript being in preparation.

The system is fully operational at the present time. Due to limits set by the EPSCO transmitter (PH 40K, rated at 40 kW peak), the following exposure parameter can be achieved at 35 kW peak power, 0.4 W/kg average SAR (6.67 kW/kg peak), 6 μs pulse width, and 10 Hz pulse repetition rate. These exposure parameters matched one of two set of exposure parameters used in original L-band (1.25 GH, FPS-7B exposure system, 4 W/kg and 0.4 W/kg average, 6 μs pulse width, and 10 Hz pulse repetition rate). To operate the system at higher average, the EPSCO transmitter has to be operated at wider pulse width and/or higher pulse repetition rate. To obtain a higher peak SAR, a new transmitter with higher peak power will be needed.

Relevant Abstracts/Publications/Report

- Seaman, R.L.; Chesselet, M.-F.; Mathur, S.P.; DiCarlo, C.D.; Fleming, S.M.; Ashmore, J.L.; Garza, T.H.; and Grado, A.M. [2004]: Movement initiation in rotenone-treated rats after acute exposure to 1.25-GHz microwave pulses in circular waveguide at 0.4 W/kg. (In preparation, abstract included).

Research Plan for Body Borne and Helmet Mounted Antennas

The military operations are heavily and increasingly dependent on radiofrequency (RF) devices for command, control, communication, and intelligence. In order to defeat, or to prevent defeat by, military operations of opposition force, research engineers are developing increasingly powerful radiofrequency devices. Systems capable of delivering 100 gigawatt pulses to a transmitting antenna and establishing hundreds of kV/m electric-field intensity in the beam path are known to exist [Agee *et al.* 1995]. The development of the Active Denial System for a non-lethal alternative has actually changed the risk scenarios for warfighters from accidental exposures and "permissible" risks of operating RF devices to the intentional targets of opposition forces' devices. The increase uses of high power jamming devices, direct energy devices and EMP (electromagnetic impulse) bombs have further increased the probability of health risks. Risks of injuries have been prevented and managed through research and regulation in the past. Both in military environment and in the civilian sector, incidences of RF radiation injuries are not unheard of [Reeves 2000, Schilling 2000, Schilling 1997, Hocking *et al.* 1988, Komodin-Hedman *et al.* 1988, Marchiori *et al.* 1995, Tintinalli *et al.* 1983, Lim *et al.*], and most likely underreported.

RF overexposure, defined as exposure to RF radiation at intensities above current guidelines, in the military environment can occur as:

- Intentional exposure: targets of opposition force's devices, e.g. non-lethal weapon, EMP bombs, jamming devices and direct energy devices, etc. Unavoidable.
- Unintentional exposure: operators and personnel in the vicinity of RF devices. Overexposures are avoidable if proper testing and maintenance of devices, precautions, education, and proper training are provided.

- Accidental exposure: errors in operating of RF devices or during repair, calibration and testing. Overexposures are avoidable as in case of unintentional exposure.

Transformation to the Objective Force requires mobile forces, and command and control capability while on the move. Body borne antennas (BBA) are currently under development to facilitate communications in such a scenario. The BBA are part of future Joint Tactical Radio System (JTRS), Antennas for Communication Across the Spectrum (ACAS) and Advanced Antennas Technology Demonstration (TD) in survivability lethality analysis directorate of C4I, Command, Control, Communication, Computers, and Intelligence. The BBA are being developed to provide communication in the frequency range of 2 MHz – 44 GHz with higher gain, bandwidth, high data rate, and greater agility for on-the-move (OTM) network systems. Specific to the Army, the BBA are being developed and tested for Small Unit Situational awareness System (SUOSAS), Dismounted Battlespace Battle Laboratory (DBBL), and the Land Warrior Program. U.S. Navy also involves in the development of BBA in the frequency range of 2 – 2000 MHz through COMWIN (Combat Wear Integration) Project. Health risks of operating BBA are similar to the situations in popular mobile telephone except military devices are designed to emit higher power and to utilize more than one transmitter simultaneously. Current controversies, accelerated health effect research, and worldwide interests in resolving and assessment of mobile phone health issues can provide directions for tailoring RF health effects suitable to particular situations in military uses of RF devices. Configuration of BBA can be integrated into BDU or worn over the BDU as vest, mounted on the Man Pack or helmet or shoulder patches. Such configurations result in radiating structure sited to less than 2.5 cm from the body and partial body exposure. These configurations violates the clauses of exclusion and relaxation of limits for partial body that allow the local incident field strengths and the plane-wave equivalent power density, where applicable, to exceed the maximum permissible exposure, i.e., in compliance with personnel protection guideline, field intensity and/or specific absorption rate were to be measured and proven to be within maximum permissible exposure.

United States Army require human factor analysis (HFA) and health hazard assessment (HHA) release as per Department of Defense (DoD) Instruction 6055.11 before deployment of any RF devices. Outlines of compliance testing can be found [Kuster 2003, OET Bulletin 65]. Specific Absorption Rate (SAR) measurements in human phantom and mathematical simulation of SAR by Finite-Difference-Time-Domain (FDTD) technique are acceptable by regulatory organizations. Both local SAR and whole-body average SAR are to be measured and calculated. For a 70 kg human, radiating power less than 28 W and 5.6 W will not produce a whole-body average SAR exceeding 0.4 W/kg and 0.08 W/kg as specified in the DoD Instruction 6055.11. Additional requirements for compliance with guidelines are induced currents if the device is operating at 3 kHz to 100 MHz. Preferably, compliance assurance is to be performed by an independent laboratory following the principle of Good Laboratory Practice. Antenna design engineers usually do not have access to perform these compliance tests of their design. Example is the Navy COWIN antenna's compliance testing at Naval Health Research Center Detachment with expert input from personnel of the U.S. Army Medical Research Detachment Microwave Bioeffects Branch. Maintaining such independent

testing capability in a health research organization is essential for avoiding conflict of interest.

Health and safety issues of RF devices in the Army are covered under U.S. Army Regulation 11-9, the Army Radiation Safety Program. Regulation 11-9 requires compliance with DoDI 6055.1-1999. The DoDI is adapted from the IEEE C95.1-1999 [IEEE 1999}, a updated revision of the American National Standards Institute C95.1-1982. Federal Communications Commission [OET Bulletin 65 1987] regulates emission level of cellular (mobile) phones based on NCRP [NCRP 1986] and IEEE C95.1-1999 guidelines. Both IEEE and NCRP guidelines are very similar to ICNIRP [1998]. Only minor differences can be found among these guidelines. They all based on the acute threshold of behavioral changes such as work stoppage or decrement in work rate of ongoing behavior. Modifier was applied to the acute behavioral threshold, which was determined at 4 W/kg frequently associated with approximately 1 °C increase in core body temperature. The essence of these western guidelines is based on whole-body average SAR. A modifier of 10 is applied for the controlled environment or occupational guidelines, 0.4 W/kg and additional modifier of 5, a total of 50 to 0.08 W/kg, is applied for the uncontrolled environment or general public. For practical reason of measurement, these basic personnel restrictions are converted to electrical field intensity, magnetic field intensity, and power density if applicable. The conversion is derived from extensive knowledge on SAR derived from mathematical simulation of representative human beings across the radiofrequency spectrum. The lowest "exposure limits" or "maximum permissible exposure (MPE)" occur at "resonance absorption", are established at 1 mW/cm^2, 10 W/m^2 for the controlled environment/occupational exposure and 0.2 mW/cm^2, 2 W/m^2 for the uncontrolled environment/general public. The main concern of radiofrequency radiation between 3 kHz and 100 MHz is the induced current. These guidelines also specify the limits of induced currents to prevent shock and burn. These guidelines are established without taking variation in ambient temperature into account. It has been noted that absorption of radiofrequency radiation and ambient temperature above thermal neutral temperature were additive to each other in magnitude of hypertheria induced [Lu and Michaelson 1993]. In other words, health effects from either stressor, heat and radiofrequency radiation can compound each other. The database for these guidelines were based on experiments performed under usual laboratory environment below the thermal neutral temperature. Since Warfighters frequently operate in adverse warm environments, the compound effects of adverse environment and radiofrequency radiation should be explored.

On the other hand, Eastern European standards are derived from basic restriction to prevent effects from chronic exposure at very low intensity, which in general would not cause significant elevation of core body temperature frequently defined as "non-thermal" effects [Gajsek *et al.* 2000]. The lowest "safe" exposure limits or MPE for occupational exposure is similar to those of Western countries but limits values or MPE can be as low as 1 $\mu W/cm^2$, 10 mW/m^2. The basis of these low standards, 2 to 3 orders lower than those in Western countries, are distinct functional changes in central nervous, endocrine and immune systems [Gajsek *et al.* 2000]. Usually, the SAR concept was not incorporated during promulgation of these standards/MPE in Eastern Countries. People's

Republic of China appeared to have adapted SAR for their basic restriction in RF personnel protection standards but the basic SAR restrictions, 0.1 W/kg and 0.02 W/kg i.e., one quarter of the basic restrictions in Western Countries, were based on their own database and those available to them worldwide [Chiang and Xu 2003]. Evidence quoted were effects resulted from chronic exposure to low-intensity electromagnetic fields (EMF) including increased frequency of neuroses, liability of vegetation nervous system, electrocardiograms (ECG) and slight changes in peripheral blood, lens, and non-specific immune function. World Health Organization (WHO) has undertaken the functions of international harmonization and coordination of research efforts through the International EMF Project. Numerous international meetings have been held for these purposes. Resolutions are not forthcoming in the next few years. Part of difference in worldwide RF personnel protection guidelines/standards may also a result of difference in approach. For example, database inclusions of the IEEE guidelines tend to be those from replicable and peer-reviewed publications, and proven "adverse" health effect. The term "adverse" has not been clearly defined. On the other hand, Eastern European countries and China do not appear to bear the burden of proving a health effect is "adverse" before taking into consideration for promulgating protection guidelines/standards. WHO defines that "Health is a state of complete physical, mental and social well-being, and not merely the absence of disease or infirmity". From certain sectors of human race, IEEE, NCRP and ICNIRP guidelines are too conservative and not able to address their concerns. City of Salzburg provide an example of embracing "precautionary principle" to establish an outdoor exposure limit as low as 1 mW/m^2 (0.1 $\mu W/cm^2$) [Marsalek 2003].

Biological and/or health effects of RF radiation from body borne antennas present a unique problem because the vast majority of database used for promulgations of personnel protection guideline and standards were composed of results obtained from whole-body exposure. Guidelines, such as IEEE C95.1-1999, provide relaxation of personnel protection guidelines in partial body exposure. Factor of 20 can be applied. Therefore, basic limits in case of partial body exposure can be 8 W/kg in the controlled environment and 1.6 W/kg in the uncontrolled environment. Depending on the guidelines, the basic partial-body limits can base on an average over 1 g or 10 g of tissue. Additional relaxation of basic limits can be further relaxed if exposure time is less than the averaging time, which can be 6 or 30 minutes. The factor of 20 was based on dosimetry evaluation from whole-body exposure that ratio of local SAR to whole-body average SAR was in the range of 10 to 20. Relaxation provisions are not based on actual results of investigations on effects caused by partial body exposure. The ratio of local to whole-body average SAR can be more than hundred in a situation such as cellular phones with radiating antenna very close the human body in its normal mode of operation.

Availability of applicable database on effects of partial-body exposure is limited. Those available tend to point to partial-body exposure may induce unexpected results such as effects observed in absence of or with minimal increase in core body temperature, and occurrence of abnormal physiological responses outside of the usual thermal responses. Examples are:

- Blood-brain barrier interruption could be induced in 15 min of localized head exposure, which cause brain temperature stabilized at 43 to 48 °C but colonic temperature remained at 37.2 to 37.5 °C [Neilly and Lin 1986].
- In mice or rats, microwave pulse or pulse train of sufficient intensity can evoke whole-body movements similar "startle" reflex caused by sudden and unexpected intense visual, auditory or tactile stimuli [Brown *et al.* 1994]. The effect is dependent on specific absorption not peak SAR and local skin temperature, required a 1.2 °C minimum but reached a maximum incidence at 1.66 °C increase in skin temperature in mice, and in absence of colonic temperature changes. In rats, the effect can occur at 0.2 to 0.65 °C increase in localized skin temperature by head exposure [Raslear *et al.* 1992]. Although the pulse intensity is sufficient to cause microwave hearing, the microwave evoked whole-body movements does not depend on the integrity of cochlear [Raslear *et al.* 1992].
- Repetitive head-and-neck exposures can cause b-wave enhancement of photopic cone response and disturbing glycogen storage in photoreceptors in monkeys whose increase in rectal temperature has not rise above the pre-exposure level or actually dropped below the that sham-exposure monkeys [Lu *et al.* 2000], however, none of these functional alterations were considered to be indicative of retinal degeneration and most likely reversible.
- Decreased heart rate and decreased pulse pressure have been noted in ketamine-anesthetized rats in an exposure regimen limited to head and neck [Lu *et al.* 1992]. These cardiovascular effects began at minimal increase in colonic temperature (0.2 °C) and severity of effects co-varied with the magnitude of increases in colonic temperature to as high as 1 °C. The change temperature in the neck region was between 2 and 4 °C. It was considered to be abnormal physiologic response because physiologic functions deteriorated while physiologic demands were increasing due to hyperthermia.
- Human cutaneous pain sensation can be elicited by localized exposure. The skin temperature of the RF-induced "burning pain" occurs at 46.1 ± 1.01 °C (S.D.) at 3 GHz [Cook 1952] and 43.9 ± 0.7 °C (S.E.) at 94 GHz [Waters *et al.* 2000]. Cutaneous pain thresholds were comparable to the pain threshold induced by infrared exposure. A 10 s threshold SAR for pain sensation can be estimated as 4.2 kW/kg. Physiologically, pain sensation can be indicative of impeding injuries. Clearly, the protective mechanism of human body such as pain sensation cannot be relied upon to provide a warning.
- Human cutaneous warmth sensation can also be elicited by localized RF exposure. Updated knowledge has been part of subjects covered by a review [Lu and de Lorge 2000]. The thresholds for RF induced warmth sensation are inversely proportional to wavelength. To elicit human warmth sensation, measured and calculated increases in skin temperature are between 0.025 and 0.078 °C, values equivalent to 8.7 and 27.1 W/kg and approaching the basic partial-body limits. In fact, the cutaneous warmth sensation threshold has been determined at 4.5 ± 0.6 mW/cm^2 at 94 GHz [Blick *et al.* 1997]. This threshold is below current guidelines in Western countries.
- Microwave hearing, "auditory effect", has been reviewed [Lu and de Lorge 2000]. Microwave hearing is an audible clicking, buzzing or chirping sensation originating

from within and near the back of the head. It is caused by pulsed RF between 216 and 7,500 MHz and corresponds to recurrence rate of the RF pulses. It is caused by thermoelastic expansion of the cranial tissue launching an acoustic wave perceived by hair cells in the cochlea. The threshold is dependent on specific absorption within the pulse during the first 30 μs, 16 mJ/kg in human volunteers, 10-12 mJ/kg in cats and 0.9-1.8 mJ/kg of whole-body average specific absorption. Irrespective of underlying thermal mechanism, these threshold specific absorptions are on the order of 10^{-6} °C, hardly a quantity can be considered as thermal from the usual definition, a significant increase in core body temperature. It has been suggested that microwave hearing may cause annoyance and may be the cause of avoidance behavior in rodents.

- Acoustic startle can be inhibited or enhanced by a single 64 mJ/kg (~1.5×10^{-5} °C) microwave pulses [Seaman *et al.* 1994]. Tactile startle can also be inhibited or enhanced by a single 663 mJ/kg (~1.5×10^{-4} °C) microwave pulses [Seaman *et al.* 1994].
- Rather surprising effects from electromagnetic pulses have been reported in People's Republic of China. Typical experiments involve exposure of various species of animals to pulses operated at 60 kV/m peak electric field, 20 ns risetime, 30 μs pulse width and 5 pulses in 2 min. Reported effects included electroporation in neurons and cardiac cells [Wang *et al.* 2003], lethality, lens, corneal and retina injuries in rabbits [Jiang *et al.* 2003], temporary loss of acquired conditioned reflex, degeneration, apotosis and necrosis of hippocampus tissue in rats [Li *et al.* 2003], aptosis in peripheral lymphocytes in rhesus monkeys [Cui *et al.* 2003].

From a thermal point of view, National Institute for Occupational Safety and Health [NIOSH 1986] provides a careful and through evaluation of physiological consequences of exposure to heat and the derivation of criteria designed to the worker engaged in heavy physical labor from heat-stress related illnesses such as heat stroke, heat syncope, heat exhaustion and other disabling conditions. Deep body temperatures above 38 °C (~1 °C above normal) are considered undesirable for an average industrial workforce. However, the criteria have been challenged recently [Hancock and Vasmatzidis 1998] on the ground that change in behavioral performance efficiency is the most sensitive reflection of human response to "stress". The respective thresholds for vigilance, dual-tasks, neuro-muscular coordination tasks, simple mental performance and physiological tolerance are 0.055, 0.22, 0.88, 1.32 and 1.65 °C dynamic increases in body temperature.

In comparison to any other environmental exposure, cellular/mobile phone use has produce an unprecedented extent and magnitude of RF exposure in human population. The interest in health and safety aspects of RF radiation is well justified. Extensive database have accumulated in the past and has been the subject to frequent reviews by various guidelines/standards promulgating organizations and independent groups or individuals. Nevertheless, RF health and safety research has enjoyed increasing funding in the past decade due to explosive popularity of cellular/mobile phones, public concerns and media coverage of the topic. In general, a lot has been learned but a lot more has to be learned on this topic. At the international level,

biological effects from low-level RF exposure has been identified needing replication and further study [Repacholi 1998]. This WHO list includes:

- *In vitro* studies of cell kinetics and proliferation effects
- Effects on genes, signal transduction effects and alteration in membrane structure and function, and biophysical and biochemical mechanisms for RF field effects
- *In vivo* studies on the potential for cancer promotion, co-promotion and progression, as well as possible synergistic, genotoxic, immunological, and carcinogenic effects associated with chronic low-level RF exposure
- DNA damage, influences on central nervous system function, melatonin synthesis, permeability of blood brain barrier, reaction to neurotropic drugs
- Changes to eye structure and function
- Epidemiological studies of the use cellular/mobile phones and incidence of various cancer, heads, sleep disturbance and other subjective effects
- Studies of occupational cohorts with high RF exposure in cancer incidence, adverse pregnancy outcomes, and ocular pathology.

An updated list of WHO research agenda for radio frequency fields is available through WHO web site ("www.who.int/peh-emf/research/rf03/en/"). The updated list includes overreaching issues, ongoing, short-term or urgent needs, and long-term or future needs in epidemiology, human studies, laboratory studies: animals, laboratory studies: tissue, cells, cell free systems, and dosimetry. Short-term or urgent needs in laboratory studies are:

- Follow-up studies to immune system studies that suggest an effect of RF exposure
- Accuracy and reproducibility of published RF effects on the permeability of the blood-brain barrier and other neuropathologies (e.g., dura mater inflammation, dark neurons)
- Additional studies on the RF exposure on sleep
- Quantitative studies on the effects on the development of the central nervous system, particularly the cortex, in the embryo and fetus using morphological and functional endpoints
- Expression of stress (heat shock) proteins in mammalian cells
- Biological relevant hypothesis

Long-term or future needs in laboratory studies are:

- In cases where the results of cellular, biophysical, or theoretical studies suggest that a new type of RF signal may have a specific biological activity, this new signal should first be studied in a large scale rodent bioassays or other animal models relevant to human endpoints similar to the studies describe above.
- Further studies should be undertaken to determine the effects of prolonged and/or chronic localized heating at temperature of less than 41 °C. Emphasis should be placed on the quantitative assessment of histological damage and functional changes as well as grossly detectable injury.

- Phosphorylation profiling and other high-throughput assays characteristic of genomics, proteomics and research area.

Excluding cancer related studies, morphological and functional changes in the central nervous system (CNS) are at the top of research agenda. As indicated earlier, functional disturbances in the central nervous system in absence of morphological change is considered to be the most sensitive endpoints of RF radiation. Furthermore, behavioral endpoints as an indication of CNS disturbance have been used as the backbone of the personnel protection guidelines/standards in the Western countries. An ill-defined "neurasthenic" syndrome [Czerski and Siekierzynski 1974] was considered by Eastern European scientist to be a prominent indication of "microwave sickness" [Sadcikova 1974]. The neurasthenia is a typical set of psychological symptoms, and a somewhat variable collection of complaints that include irritability (irascibleness), headache, fatigue, lethargy, insomnia, impotence, decreased memory (mnemonic disorder), and loss of libido. Other subjective complains included heavy feeling in the head, nausea and vertigo. When persistent, this set of symptoms, in whole or in part, is not unlike that labeled the chronic depressive reaction. Only until recently, Western scientists have dismissed neurasthenic syndrome as a valid effect resulted from exposure to RF radiation. Similar complaints and incidence of neurasthenia were observed in RF worker in China in a dose-dependent manner [Chiang 1983]. A recent report [Oftedal *et al*, 2000] indicated that many people in Norway and Sweden experienced headaches, fatigue and other symptoms such as memory loss, difficulty in concentration, nausea, tingling sensation, facial warmth sensation, etc. in connection with the use mobile phone. Increased risk was observed with longer calling times and higher number of calls per day. Similar conclusion has also noted between calling time/number of calls per day and the prevalence of warmth behind/around or on the ear, headaches and fatigue and prevalence of symptoms was indepent of phone type, either digital or analogue [Sandstrom *et* al. 2001]. Self reported symptoms (visual disturbance, tingling sensation to the face, burning sensation to the ear, warm sensation behind/around the ear, unusual drowsiness/tiredness, loss of memory, difficulty in concentration, dizziness, and headache) were also studied in a community [Chia 2000]. It was concluded that the use of hand-held cellular phone was not associated with a significant increase in CNS symptoms other than headache. There is a significant increase in prevalence of headache with increasing duration of usage in minute per day. Prevalence of headache was reduced by more than 20% among those who used hand-free equipment for their cellular phone. Subsequently, the prevalence for most of the symptoms was shown to increase with higher SAR_{1g} values and longer calling time [Wilen *et al.* 2003]. In addition, the authors pointed out that specific absorption per day might be the interesting parameter for the prevalence of some of symptoms, such as dizziness, discomfort, difficulty in concentration and warmth on/behind the ear [Wilen *et al.* 2003]. Supportive evidence for headache and loss of memory in laboratory studies were impaired learning [Lai *et al.* 1994], increased blood-brain barrier leakage [Salford *et al.* 1994] and nerve cell damage [Salford *et al.* 2003], and cognitive process such as attention and short-term memory [Lass *et al.* 2002] from low intensity RF exposures. However, the impaired learning in rats was not replicated [Cobb *et al.* 2004]. Neurasthenia can progress to "autonomic vascular" changes, i.e., sweating, dermographism, and blood pressure changes, if

vagotonic, bradycardia and prolongation of intraaurical and intrventricular conductions [Sachikova 1974].

A review of neurological effects from RF radiation from 11 original case reports in human has been made [Hocking and Westerman 2003]. Peripheral neurological effects of RFR are mainly noxious sensations or dysaesthesiae. In some cases, symptoms are transitory but lasting in other. After very high exposure, nerves may be grossly injured. After lower exposures, which may result in dysaesthesia. Ordinary nerve conduction studies find no abnormality but current perception threshold studies have found abnormalities. Case Reports also point to the possibility of delayed cardiovascular disturbances from RF exposure [Williams and Webb 1980, Forman *et al.* 1982]. The existence of delayed cardiovascular disturbances is confirmed in rats exposed to ultra-wide-band pulses (a form of RF) at low average intensities [Lu and Mathur 2002].

Laboratory animals cannot verbally report symptoms as human beings do. But laboratory animals are not susceptible to suggestions perceived during interview or questionnaires. Thus, answers derived from laboratory through objective measurements are less susceptible to basis from subjective self-interpretation and selection/response biases than those in an epidemiology study. Non-invasive procedures are available for quantitative measurements of the endpoints. They can be applied in short- or long-term studies and in whole-body or local exposure scenarios. Engineering supports in compliance testing and biological experimentations are also requires. The following areas of studies are considered to be most cost-efficient, therefore, are highly recommended for future research.

- Engineering evaluation for compliance to current RF guidelines/standards
    - Perform Numerical modeling for energy deposition in human body using a realistic human model
    - Verify free-space characteristics of the antenna, if required
    - Measure local specific absorption rate (SAR) and location of the maximum SAR in full size human phantom at all frequency of interest and/or in multi-frequency environment.
    - SAR measurements in simulated field conditions if required
    - Determine the extent of surface heating of human body and antenna
    - Determine the location of RF and thermal hot spots at single and multiple frequency
    - Measure induced currents in the extremities, e.g., ankle and wrist at all frequency of interest, especially at frequency below 100 MHz.
- Engineering support for biological studies
    - Design and fabricate appropriate antenna to simulate human exposure from body borne antenna
    - Perform dosimetry to define SAR and SAR pattern

- Neurological/behavioral evaluations of RF induced neural damages

    - Sugar Preference Test: to determine the degree of anhedonia, absence of pleasure from performing acts that would ordinarily be pleasurable
    - Von Frey Test: to determine alteration in tactile sensitivity
    - Thermal Algesia Test (Hot Plate or Intense Light Beam): to determine alterations in threshold of thermal pain
    - Elevated Plus-Maze Test: to determine alterations in anxiety level
    - Rotarod Performance: to determine alterations in motor coordination if dizziness is present
    - Running Wheel Activity: to determine perturbation in circadian rhythm and degree of fatigue
    - Y-maze or Radial Arm Maze Performance: to determine alterations in memory process
    - Morris Water Maze Performance: to determine alteration in overall cognitive function
    - Heart rate, Blood Pressure and Heart Rate Variability: to determine alterations in cardiovascular functions
    - Skin Electrical Impedance Spectroscopy: to determine alterations in intracellular and/or extra cellular water content as an indication of changes in skin integrity

REPORTABLE OUTCOMES

A list of 46 meeting abstract, 25 publications and 1 technical report is included in the appendices. MBS personnel served under the present contract are:

o Dr. Shin-Tsu Lu	Principal Investigator/Project Manager/Radiation Biologist/ Veterinarian
o Dr. Andrei G. Pakhomov	Electrophysiologist
o Dr. Ronald L. Seaman	Biomedical Engineer/Physiologist
o Dr. Satnam P. Mathur	Electrical Engineer/Antenna Design
o Ms. Lori Allen	Office Manager/Safety Officer
o Mr. John Ashmore	Electronic Technician
o Ms. Joanne Doyle	Biomedical Technician
o Mr. Kerfoot P. Walker	Biomedical Technician

- Ms Amy Phinney — Biomedical Technician
- Mr. Juan Morin — Biomedical Technician
- Mr. Thomas Garza — Biomedical Technician

CONCLUSION

Tremendous amount of progress have been made by a small group of researchers. Majority of finding may still within the content of so-called "thermal" effects of radiofrequency radiation. However, the effects induced by radiofrequency radiation could occur at a lower temperature increment, 0.3-0.4 °C, a level of increase less than that (i.e., 1 °C) was usually envisioned. In addition, current personnel protection guideline/standards for radiofrequency radiation did not take into consideration of the interaction of ambient temperature. A model was developed to assess the interplay between absorption of radiofrequency radiation and ambient temperature. It was clearly indicated that absorption of radiofrequency radiation could be additive to the effect of increased ambient above a critical level which could be expressed as physiological or ambient temperature.

Some of the effects could not be classified as "thermal" easily because some types of radiofrequency exposure might not able to induce increases in body temperature or in sufficient magnitude to cause an effect as that from conventional heating. Candidates were those effects from UWB pulses, such as hypotension, increased short-term heart rate variability, increased in NF-κB binding to DNA, and enhanced nitric oxide production. Other consideration was cell lethality from 10 ns electric pulses in absence of reaching a lethal temperature.

More importantly, some of the effects observed did not occur immediately or shortly after radiofrequency radiation but delayed by days and persisted for weeks. This type long-term follow-up was not usually performed in the studies of biological effects of radiofrequency radiation.

A battery of non-invasive neurological and psychological endpoints aiming at elucidating the presence of "neurasthenia", the most prevalent symptom complex known as "microwave sickness" or "electric hypersensitivity" was proposed for future studies.

REFERENCES

- Agee FJ, Schlfield DW, Prather W, and Burger JW [1995]: Powerful untra-wide band RF emitters: status and challenges. In: "*Intense Microwave Pulses III*", Brandt HE, ed., Proc. Int. Soc. Optical Eng. 2557: 98-109.

- Blick DW, Adair ER, Hurt WD, Sherry CJ, Walters TJ, and Merritt JH [1977]: Thresholds of microwave-evoked warmth sensations in human skin. Bioelectromagnetics 18: 403-409.

- Brown DO, Lu S-T, and Elson EC [1994]: Characteristics of microwave evoked body movements in mice. Bioelectromagnetics 15: 143-161.

- Chia S-E, Chia H-P, and Tan J-S [2000]: Prevalence of headache among handheld cellular telephone users in Singapore: a community study. Environ. Health Perspect 108: 2059-1062.

- Chiang H [1983]: Assessment of health hazard and standard promulgation in China. In: "*Biological Effects and Dosimetry of Nonionizing Radiation, Radiofrequency and Microwave Energies*", Grandolfo M, Michaelson SM, and Rindi A, eds., New York, NY: Plenum Press, pp. 627-644.

- Chiang H and Xu Z [2003]: Discussion on the rationale for China EMF exposure standards. In: "3rd International EMF Seminar in China: Electromagnetic Fields and Biological Effects", Guilin, China, Oct. 13-17, 2003, pp. 56-60.

- Cobb BL, Jauchem JR, and Adair ER [2004]: Radial arm performance of rats following repeated low level microwave radiation exposure. Bioelectromagnetics 25: 49-57.

- Cook HF [1952]: The pain threshold for microwave and infra-red radiations. J. Physiol. Lond. 118: 1-11.

- Cui Y, Yang H, Gao Y, Peng R, Ying L, Zhang Y, Jiang Z, and Wang D [2003]: Effects and mechanisms of electromagnetic pulse on rhesus monkey lymphocytes. In: "3rd International EMF Seminar in China: Electromagnetic Fields and Biological Effects", Guilin, China, Oct. 13-17, 2003, p. 146.

- Czerski P, and Siekierzynski M [1974]: Analysis of occupational exposure to microwave radiation. In: "*Fundamental and Applied Aspects of non-ionizing Radiation*", Michaelson SM, Miller MW, Magin R, and Carstensen E, eds., New York, NY: Plenum Press, pp. 367-377.

- Forman C, Holmes C and McManamon V [1982]: Psychological symptoms and intermittent hypertension following acute microwave exposure. J. Occupat. Med. 24: 932-934.

- Gajsek P, Pakhomov AG, and Klauenberg BJ [2002]: Electromagnetic field standards in Central and Eastern European countries: current state and stipulations for international harmonization. Health Phys. 82: 473-483.

- Hancock PA, and Vasmatzidis I [1998]: Human occupational and performance limits under stress: the thermal environment as a prototypical example. Ergonomics 41: 1169-1191.

- Hocking B, Joyner K, and Fleming R [1988]: Health aspects of radio-frequency radiation accidents. Part I: assessment of health after a radio-frequency radiation accident. J. Microwave Power 23: 67-74.

- ICNIRP [1998]: Guidelines for limiting exposure to time-varying electric, magnetic, and electromagnetic fields (up to 300 GHz). Health Phys. 74: 494-522.

- IEEE [1999]: "*IEEE Standards for Safety Levels with Respect to Human Exposure to Radio Frequency Electromagnetic Fields, 3 kHz to 300 GHz.*" New York, NY: Institute of Electrical and Electronic Engineers.

- Jiang T, Wang DW, and Gu QY [2003]: Injuries of EMP and HPMW on rabbit optical system. In: "3rd International EMF Seminar in China: Electromagnetic Fields and Biological Effects", Guilin, China, Oct. 13-17, 2003, p. 144.

- Kolmodin-Hedman B, Mild KH, Hagberg M, Jonsson E, Andersson M-C, and Eriksson A [1988]: Health problems among operators of plastic welding machines and exposure to radiofrequency electromagnetic fields. Int. Arch. Occup. Environ. Health 60: 243-247.

- Kuster N [2003]: State-of-the-art of measurement and simulation techniques of dosimetry and localized temperature hotspots. In: "*Third International EMF Seminar in China: Electromagnetic Fields and Biological Effects*", Guilin, China, October 13-17, 2003, China Ministry of Health, pp. 35-38.

- Lai H, Horita A, and Guy AW [1994]: Microwave irradiation affects radial-arm performance in the rat. Bioelectromagnetics 15: 95-104.

- Lass J, Tuulik V, Ferenets R, Riisalo R, and Hinrikus H [2002]: Effects of 7 Hz-modulated 450 MHz electromagnetic radiation on human performance in visual memory tasks. Int. J. Radiat. Biol. 78: 937-944.

- Li Y-H, Wang D-W, Peng R-Y, Zhao M-L, Wang S-M, Gao Y-B, Chen H-Y, and Hu W-H [2003]: Preliminary studies on the effects and it's mechanisms of electromagnetic pulse on memory capability of rats. In: "3rd International EMF Seminar in China: Electromagnetic Fields and Biological Effects", Guilin, China, Oct. 13-17, 2003, pp. 144-146.

- Lim JI, Fine SL, Kues HA, and Johnson MA [1993]: Visual abnormalities associated with high-energy microwave exposure. Retina 13: 230-233.

- Lu S-T, Brown DO, Johnson CE, Mathur SP, and Elson EC [1992]: Abnormal cardiovascular responses induced by localized high power microwave exposure. IEEE Trans. Biom. Eng. 39: 484-492.

- Lu S-T, and Michaelson SM [1993]: Effect of interaction between ambient temperature and SAR on microwave-induced hyperthermia in rats. In: "*Electricity and Magnetism in Biology and Medicine.*" Blank M, ed., San Francisco, CA: San Francisco Press, Inc., pp 679-682.

- Lu S-T, and de Lorge JO [2000]: Biological effects of high peak power radio frequency pulses. In: "*Advances in Electromagnetic Fields in Living Systems, Vol. 3*", Lin JC ed., New York, NY: Kluwer Acadmic/Plenum Publishers, pp. 207-264.

- Lu S-T, Mathur SP, Stuck B, Zwick H, D'Andrea JA, Ziriax JM, Merritt JH, Lutty G, McLeod DS, and Johnson M [2000]: Effects if high peak power microwaves on the retina of the rhesus monkey. Bioelectromagnetics 21: 439-454.

- Lu S-T, and Mathur SP [2002]: Hypotension induced by ultra-wide-band pulses: dose-response, replication, orthostatic response and heart rate variability. In: "*Proceedings of the 2nd International* Workshop *Biological Effects of Electromagnetic Fields*", Oct. 7-11, Rhodes, Greece, Kostarakis P, ed., pp. 409-418.

- Marchiori PE, Silva HCA, Hirata MTA, Lina AM and Scaff M [1995]: Acute multiple mononeuropathy after accidental exposure to oven microwaves. Occup. Med. 45: 276-277.

- NCRP [1986]: *Biological Effects and Exposure Criteria for Radiofrequency Fields.*" Bethesda, MD: National Research Council on Radiation Protection and Measurements, NCRP Report 86.
- Neilly JP and Lin JC [1986]: Interaction of ethanol and microwaves on the blood-brain barrier of rats. Bioelectromagnetics 7: 405-414.

- NIOSH [1986]: Criteria for a Recommended Standar: Occupational Exposure to Hot Environments, Revised Criteria, 1986. Cincinnati, OH: National Institute for Occupational Safety and Health, DHHS (NIOSH) Publication No. 86-113.

- Marsalek E [2003]: The "round-table-consensus-model" (so called "Salzburg Model") as a possible regulatory framework for the installation of mobile-phone-base stations. In: "3rd International EMF Seminar in China: Electromagnetic Fields and Biological Effects", Guilin, China, Oct. 13-17, 2003, pp. 62-69.

- OET Bulletin 65 [1997]: "*Evaluating Compliance with FCC Guidelines for Human Exposure to Radiofrequency Electromagnetic Fields.*" Office of Engineering and Technology, Federal Communications Commission. (available through internet www.fcc.gov/oet/)

- Oftedal G, Wilen J, Sandstrom M, and Mile KH [2000]: Symptoms experienced in connection with mobile phone use. Occup. Med. 50: 237-245.

- Raslear TG, Akyel Y, Lu S-T, Swearengen JR, Varle D, DeAngelis ML, and Seaman RL [1992]: CW microwave fields evoked body movements in bilaterally cochleotomized rats. Proc. Ann. Int. Conf. IEEE-EMBS 14: 295-296.

- Reeves GI [2000]: Review of extensive workups of 34 patients overexposed to radiofrequency radiation. Aviat. Space Environ. Med. 71: 206-215.

- Repacholi MH [1998]: Low-level exposure to radiofrequency electromagnetic fields: health effects and research needs. Bioelectromagnetics 19: 1-19.

- Sachikova [1974]: Clinical manifestations of reactions to microwave radiation in various occupational groups. In: "*Biological Effects and Health Hazards of Microwave Radiation*", Czerski P, Ostrowski K, Silverman C, Shore ML, Suess MJ, and Waldeskog B, eds., Warsaw, Poland: Polish Medical Publishers, pp. 261-267.

- Salford LG, Brun A, Sturesson K, Eberhardt JL, and Persson BR [1994]: Permeability of the blood-brain barrier induced by 915 MHz electromagnetic radiation, continuous wave and modulated at 8, 16, 50 and 200 Hz. Microsc. Res. Tech. 27: 535-542.

- Salford LG, Brun AE, Eberhardt JT, Malmgren, and Persson BR [2003]: Nerve cell damage in mammalian brain after exposure to microwaves from GSM mobile phones. Environ. Health Perspect. 111: 881-883.

- Sandstrom M, Wilen J, Oftedal G, and Hasson Mild K [2001]: Mobile phone use and subjective symptoms. Comparison of symptoms experienced by users of analogue and digital mobile phones. Occup. Med. 51: 25-35.

- Schilling CJ [2000]: Effects of exposure to very high frequency radiofrequency radiation on six antenna engineers in two separate incidents. Occup. Med. 50: 49-56.

- Schilling CJ [1997]: Effects of acute exposure to ultrahigh radiofrequency radiation on three antenna engineers. Occup. Environ. Med. 54: 281-284.

- Seaman RL, Beble DA, and Raslear TG [1994]: Modification of acoustic and tactile startle by single microwave pulses. Physiol. Behav. 55: 587-595.

- Tintinalli JE, Krause G, and Gursel E [1983]: Microwave radiation injury. Ann. Emergency Med. 12: 645-647.

- Walters TJ, Blick DW, Johnson LR, Adair ER, and Foster KR [2000]: Heating and pain sensation produced in human skin by millimeter waves: comparison to a simple thermal model. Health phys. 78: 259-267.

- Wang D, Deng H, Cao X, Zhao M, Peng R, Zhan S, Wang S, Chen H, Jin H, Zhang D, Hu W, and Dong B [2003]: Study on membrane electroporation of several neurons and cells induced by EMP and HPM. In: "3rd International EMF Seminar in China: Electromagnetic Fields and Biological Effects", Guilin, China, Oct. 13-17, 2003, pp. 78-81.

- Wilen J, Sandstrom M, and Hansson Mild K [2003]: Subjective symptoms among mobile phone users – a consequence of absorption of radiofrequency fields? Bioelectromagnetics 24: 152-159.

- Williams R, and Webb T. [1980]: Exposure to radiofrequency radiation from an aircraft radar unit. Aviat. Space Environ. Med. 51: 1234-1244.

APPENDICES

LIST OF MEETING ABSTRACTS (2001-2004)

1. Brewer, P.A.; Mery, L.R.; Phelix, C.F.; and Seaman, R.L. [2001]: Monoamine oxidase inhibition enhances ultrastructural changes in rat striatal neurons after single systemic injection of 3-nitropropionic acid. In: "Abstract submitted to the 31st Annual Meeting of the Society for Neuroscience, San Diego, CA, November 10-15, 2001."

2. Kiel, J.L.; Rockwell, B.A.; Thomas, R.J.; Alls, J.L.; Mathur, S.P.; Sutter, R.E.; and Morales, P.J. [2001]: Laser and microwave induced breakdown spectroscopy: basis for a new detection technique for chemical and biological agents. In: "Proceedings of IEEE International Conference of Plasma Science and IEEE International Pulsed Power Conference," Las Vagas, NV, June 17-22, 2001.

3. Kiel, J.L.; Alls, J.L.; Sutter, R.E.; Mason, P.A.; Mathur, S.P.; and Morales, P.J. [2001]: Directed killing of anthrax spores by microwave induced cavitation via specific binding of organic semi-conductor. In: "Abstracts of the Second International Symposium on Nonthermal Medical/Biological Treatments Using Electromagnetic Fields and Ionized Gases", Portsmouth, VA, May 21-23, 2001.

4. Lu, S.-T. [2001]: Potential application of UWB pulses in lowering blood pressure. In: "Conference Digest of the 2001 Asia-Pacific Radio Science Conference", Tokyo, Japan, August 1-4, 2001, p. 266.

5. Lu, S.-T. [2001]: Research on biological effects of radio frequency radiation at Walter Reed Army Institute of Research. In: "Conference Digest of the 2001 Asia-Pacific Radio Science Conference", Tokyo, Japan, August 1-4, 2001, p. 270.

6. Pakhomov, A.G.; Doyle, J.; Mathur, S.; and Murphy, M.R. [2001]: Retaining of the long-term potentiation in hipocampal slices after high peak power microwave exposure and heating. In: "Abstracts of the Second International Symposium on Nonthermal Medical/Biological Treatments Using Electromagnetic Fields and Ionized Gases," Portsmouth, VA, May 21-23, 2001, p. 21.

7. Pakhomov, A.G.; Doyle, J.; Mathur, S.; and Murphy, M.R. [2001]: Effects of extremely high power microwave pulses on the population spike and long-term potentiation in rat hippocampal slices. In: "Abstracts of the 23rd Annual Meeting of the Bioelectromagnetic Society," St. Paul, MN, June 10-14, 2001, p. 86.

8. Seaman, R.L.; Mathur, S.P.; Phinney, A.M.; and Harris, N.R. [2001]: Interaction between a neurotoxin and pulsed microwaves. In: "Abstracts of 23rd Annual Meeting of the Bioelectromagnetic Society," St. Paul, MN, June 10-14, 2001, pp. 130-131.

9. Seaman, R.L.; and Phelix, C.F. [2001]: Acute changes in rat caudate-putamen neuronal ultrastructure due to 3-nitropropionic acid and microwave exposure are not reflected in behavior. In: "Abstract of the 31st Annual Meeting of the Society for Neuroscience," San Diego, CA, November 10-15, 2001.

10. Ziriax, J.M.; D'Andrea, J.A.; Lu, S.-T.; Mathur, S.; and Cox, D. [2001]: Verifying electromagnetic Dosimetry. In: "Conference Digest of 2001 Asia-Pacific Radio Science Conference", Tokyo, Japan, August 1-4, 2001, p. 414.

11. Ziriax, J.M.; D'Andrea, J.A.; Lu, S.-T.; Mathur, S.; Cox, D.; Henry, P.; Kosub, K.; Garay, R.; and Hurt, W. [2001]: Comparing thermometry and FDTD predictions: measurement versus theory. In: "Abstracts of 23rd Annual Meeting of the Bioelectromagnetic Society," St. Paul, MN, June 10-14, 2001, pp. 178-179.

12. Cox, D.D.; Mathur, S.P.; D'Andrea, J.A.; and Lu, S.-T. [2002]: Automating the analysis of thermometric microwave-dosimetry data. In: "Abstracts of 24th Annual Meeting of the Bioelectromagnetic Society," Quebec City, Quebec, Canada, June 23-27, 2002, p 63.

13. Doyle, J.; Mathur, S.; Murphy, M.R.; and Pakhomov, A.G. [2002]: Comparative effects of continuous-wave and high peak power microwave emission on the induction of long-term potentiation. In: "Abstracts of 24th Annual Meeting of the Bioelectromagnetic Society," Quebec City, Quebec, Canada, June 23-27, 2002, pp 229-230.

14. Hatcher D., Cox, D., Ziriax, J., D'Andrea, J., and Mathur, S. [2002]: Software tools to calculate the far-field for open-ended waveguide, prolate spheroid SAR, thermometric dosimetry data, and 2D-FDTD model color-coder. In: "Abstracts of 24th Annual Meeting of the Bioelectromagnetic Society," Quebec City, Quebec, Canada, June 23-27, 2002, pp 63-64.

15. Lu, S.-T. [2002]: Biological effects of radio frequency pulses. In: "Proceedings of the Third International Conference on Electromagnetic Fields and Human Health, Fundamental and Applied Research," Moscow-Saint Petersburg, Russia, September 17-24, 2002, p 285.

16. Mathur, S.P.; Lu, S.-T.; Harris, N.; and Hurt, W.D. [2002]: Some approaches to UWB dosimetry. In: "Abstracts of the Ninth Annual Michaelson Research Conference," South Portland, ME, August 9-12, 2002.

17. Meltz, M.L.; Galindo, C.; Natarajan, M.; Leach, R.; Reveles, X.; Mathur, S.; and Ashmore, J. [2002]: Investigatio of the ability of UWB RF exposure to induce translocations in human chromosomes 1, 2, or 4 using multi-color FISH technology. In: "Abstracts of the Ninth Annual Michaelson Research Conference," South Portland, ME, August 9-12, 2002.

18. Natarajan, M.; Meltz, M.L.; Galindo, C.; Ashmore, J.; and Mathur, S. [2002]: Influence of UWB RF exposure on nuclear translocation of NF-κB in human MM-6 monocyte. In: "Abstracts of the Ninth Annual Michaelson Research Conference," South Portland, ME, August 9-12, 2002.

19. Pakhomov, A.G.; Doyle, J.; Ashmore, J.; and Murphy, M.R. [2002]: Thermal limits for functional damage and recovery in brain tissue after a brief (500 ms) high-intensity microwave exposure. In: "Abstracts of 24th Annual Meeting of the Bioelectromagnetic Society," Quebec City, Quebec, Canada, June 23-27, 2002, pp 228-229.

20. Pakhomov, A.G.; Doyle, J.; and Murphy, M.R. [2002]: Effect of high-power microwave pulses on synaptic transmission and plasticity in brain neurons. In: "Proceedings of the Third International Conference on Electromagnetic Fields and Human Health, Fundamental and Applied Research," Moscow-Saint Petersburg, Russia, September 17-24, 2002, p 276.

21. Pakhomov, A.; Doyle, J.; and Murphy, M. [2002]: Delayed and reversible suppression of evoked activity in CA_1 area of hippocampal slices by brief heat pulses. In: "Abstracts of the 22nd Annual Meeting of the Society for Neuroscience," Orlando, FL, November 2-7, 2002.

22. Seaman, R.L., and Lu, S.-T. [2002]: Neurodegeneration from microwave and neurotoxin exposure. In: "Abstracts of 24th Annual Meeting of the Bioelectromagnetic Society," Quebec City, Quebec, Canada, June 23-27, 2002, pp 91-92.

23. Seaman, R.L.; Mathur, S.P.; and Phinney, A.M. [2002]: Single exposure to pulsed microwaves at 0.6 W/kg does not modify locomotor activity or acoustic startle immediately after exposure. In: "Abstracts of 24th Annual Meeting of the Bioelectromagnetic Society," Quebec City, Quebec, Canada, June 23-27, 2002, p 79.

24. Seaman, R.L.; Mathur, S.P.; Phinney, A.M.; Garcia, A.S.; and Ashmore, J.L. [2002]: Rat short-term startle prepulse inhibition and some motor activities after two microwave exposures are changed by 3-NP. In: "Abstracts of the 22nd Annual Meeting of the Society for Neuroscience," Orlando, FL, November 2-7, 2002.

25. Doyle, J.; Murphy, M.R.; and Pakhomov, A.G. [2003]: High-power microwave pulses phased with evoked synaptic potentials may affect synaptic transmission. In: "Abstracts of the 25th Annual Meeting of the Bioelectromagnetics Society", Maui, HI, June 22-27, 2003, p 359.

26. Lu, S.-T. [2003]: Microwave-induced responses of colonic temperature and serum corticosterone concentration in rats are susceptible to changing experimental conditions. In: "Abstracts of the 25th Annual Meeting of the Bioelectromagnetics Society", Maui, HI, June 22-27, 2003, pp 107-108.

27. Meltz, M.L.; Nayak, B.K.; Galindo, C.; Mathur, S.P.; and Natarajan, M. [2003]: Effects of ultrawideband radiofrequency radiation on the cell cycle progression in human cell. In: "Abstracts of the 25th Annual Meeting of the Bioelectromagnetics Society", Maui, HI, June 22-27, 2003, p 350.

28. Natarajan, M.; Nayak, B.K.; Roldan, F.A.; Galindo, C.; Mathur, S.P.; and Meltz, M.L. [2003]: Genomic profiling of NF-κB-signal dependent genes in human monocytes after ultra wide band exposure. In: "Abstracts of the 25th Annual Meeting of the Bioelectromagnetics Society", Maui, HI, June 22-27, 2003, p 202.

29. Nayak, B.K.; Natarajan, M.; Galindo, C.; Mathur, S.P.; and Meltz, M.L. [2003]: Transcription of p53 target genes in response to ultrawideband radiofrequency radiation. In: "Abstracts of the 25th Annual Meeting of the Bioelectromagnetics Society", Maui, HI, June 22-27, 2003, p 349.

30. Pakhomov, A.G.; Doyle, J.; Ashmore, J.; and Murphy, M.R. [2003]: Effects of 9.6 GHz microwaves on 4-Aminopyridine-induced burst in isolated hippocampal slices. In: "Abstracts of the 25th Annual Meeting of the Bioelectromagnetics Society", Maui, HI, June 22-27, 2003, p 6.

31. Pakhomov, A.G.; Mathur, S.; and Murphy, M.R. [2003]: High-resolution temperature and SAR measurement using different sensors. In: "Abstracts of the 25th Annual Meeting of the Bioelectromagnetics Society", Maui, HI, June 22-27, 2003, p 224-225.

32. Pakhomov, A.G.; Phinney, A.; Ashmore, J.; Kolb, J.; Kono, S.; Schoenbach, K.; and Murphy, M.R. [2003]: Quantitative analysis of cytotoxicity of ultrashort (10 ns) electrical pulses in mammalian cells. In "Symposium Record Abstract of the ElectroMed 2003 Third International Symposium on Nonthermal Medical/Biological Treatments Using Electromagnetic Fields and Ionized Gases", San Antonio, TX, June 11-13, 2003, pp 66-67.

33. Pakhomov, A.; Doyle, J.; and Murphy, M. [2003]: Alteration of Synaptic Transmission by Neuron Excitation-Synchronized High-Power Microwave Pulses: A Replication Study. In: "Abstracts of the 6th International Congress of the European Bioelectromagnetics Assiciation", Budapest, Hungary, November 13-15, 2003, p 110.

34. Seaman, R.L.; Chesselet, M.F.; Lu, S.-T.; Mathure, S.P.; DiCarlo, C.D.; Fleming, S.M.; Zhu, C.; Mehta, A.; Carlson, B.B.; Phinney, A.M.; Garcia, A.S.; Adam, A.R.; Grado, A.R.; and Brown, A. [2003]: An animal model to test combined effects of pulsed microwave and a CNS mitochondrial toxin. In: "Abstracts of the 25th Annual Meeting of the Bioelectromagnetics Society", Maui, HI, June 22-27, 2003, p 186.

35. Seaman, R.L.; Jauchem, J.R.; Mathur, S.P.; Phinney, A.M.; and Ashmore, J.L. [2003]: Lack of change in temporal characteristics of rat ECG during exposure to ultra-wideband pulses. In: "Symposium Record Abstracts of the ElectroMed 2003 Third International Symposium on Nonthermal Medical/Biological Treatments Using Electromagnetic Fields and Ionized Gases", San Antonio, TX, June 11-13, 2003, pp 123-124.

36. Seaman, R.L.; Fleming, S.M.; Prosolovitch, K.; Chesselet, M.F.; Lu, S.T.; Mathur, S.P.; DiCarlo, C.D.; Garcia, A.S.; Grado, A.R.; Garza, T.H. [2003]: Effects of Exposure to Pulsed Microwaves on Movement Initiation in Rats Exposed to the Mitochondrial Toxin Rotenone. In: "Abstracts of the 6th International Congress of the European Bioelectromagnetics Assiciation", Budapest, Hungary, November 13-15, 2003, p 127.

37. Zhu, C., Fleming, S.M., Mehta, A., Seaman, R.L., DiCarlo, C.D., and Chesselet, M.-F. [2003]: Chronic mitochondrial complex I inhibition induces nigrostriatal pathway dysfunction in rats. In: "Abstracts of 17th Annual Symposia on Etiology, Pathogenesis, and Treatment of Parkinson's Disease and Other Movement Disorders", San Francisco, CA, October 19, 2003.

38. Zhu, C., Fleming, S.M., Mehta, A., Seaman, R.L., DiCaro, C.D., Chesselet, M.-F. [2003]: Chronic intravenous and subcutaneous rotenone infusion: survival analysis, functional assessment and microglial activation. In: "Abstracts of the Society for Neuroscience 33rd Annual Meeting", New Orleans, LA, November 8-12, 2003.

39. Ji, Z., Hagness, S.C., Brooske, J.H., Mathure, S., and Meltz, M. [2004]: Finite-Difference Time-Domain (FDTD) analysis and dosimetry of a gigahertz TEM cell. In: "Abstracts of 26th Annual Meeting of the Bioelectromagnetics Society", Washington, D.C., June 20-24, 2004.

40. Lu, S.-T. [2004]: Biological Effects of ultra-wide-band pulses. In: "Abstracts of 26th Annual Meeting of the Bioelectromagnetics Society", Washington, D.C., June 20-24, 2004.

41. Natarajan, M., Nayak, B.K., Mathur, S.P., Galino, C., and Meltz, M.L. [2004]: Ultrawideband electromagnetic radiation (UWB EMR) exposures and activation of an important signal transduction pathway. In: "Abstracts of 26th Annual Meeting of the Bioelectromagnetics Society", Washington, D.C., June 20-24, 2004.

42. Nayak, B.K., Galindo, C., Natarajan, M., Mathur, S.P., and Meltz, M.L. [2004]: Determination of p53 protein stabilization, loss of mitochondrial membrane potential, and release of cytochrome C into the cytosol in response to UWB EMR exposure in human lymphoblastioid cells. In: "Abstracts of 26th Annual Meeting of the Bioelectromagnetics Society", Washington, D.C., June 20-24, 2004.

43. Pakhomov, A., Walker, K. III, Kolb, J., Schoenbach, K., and Murphy, M. [2004]: Cell killing effect of high-intensity, ultrashort electric pulses. In: "Abstracts of 22nd Annual Meeting of the Society for physical Regulation in Biology and Medicine", San Antonio, TX, January 7-9, 2004, pp. 11-12.

44. Pakhomov, A., Walker, K. III, Kolb, J., Schoenbach, K., Stuck, B., and Murphy, M. [2004]: The rules of cell survival after exposure to high-intensity, ultrashort electric pulses. In: "Abstracts of 26th Annual Meeting of the Bioelectromagnetics Society", Washington, D.C., June 20-24, 2004.

45. Seaman, R.L., Chesselet, M.F., Mathur, S.P., DiCarlo, C.D., Fleming, S.M., Ashmore, J.L., Garza, T.H., Morin, J.M., Grado, A.R., and Adam, S.L. [2004]: Combined effects of pulsed microwaves and a CNS mitochondrial toxin on behavior depend on microwave-exposure parameters. In: "Abstracts of 26th Annual Meeting of the Bioelectromagnetics Society", Washington, D.C., June 20-24, 2004.

46. Zhu, C., Vourc'h, P., Fernagut, P.O., Fleming, S.M., Lacan, S., DiCarlo, C.D., Seaman, R.L., and Chesselet, M.F. [2004]: Variable specificity of chronic subcutaneous administration of rotenone for the nigrostriatal pathway. Submitted to Society for Neuroscience 34th Annual Meeting.

LIST OF PUBLICATIONS (2001-2004)

1. Pakhomov, A.G.; Mathur, S.; Gajsek, P.; and Murphy, M.R. [2001]: Use of gel-suspended cell cultures for analysis of dose dependence of microwave bioeffects. In: "Proceedings of the EBEA 2001, 5th International Congress of the European BioElectromagnetics Association" Helsinki, Finland, September 6-8, 2001, Hietanen, M., Jokela, K., and Juutilainen, J. eds., Finish Institute of Occupational Health, pp. 15-17.

2. Seaman, R.L.; and Phelix, C.F. [2001]: Changes in ultrastructure of rat caudate-putamen neurons with a neurotoxin and exposure to pulsed microwaves. In: "Proceedings of the EBEA 2001, 5th International Congress of the European BioElectromagnetics Association" Helsinki, Finland, September 6-8, 2001, Hietanen, M., Jokela, K., and Juutilainen, J. eds., Finish Institute of Occupational Health, pp. 240-241.

3. Gajsek, P.; Pakhomov, A.G.; and Klauenberg, B.J. [2002]: Electromagnetic field standards in central and eastern European countries: current state and stipulations for international harmonization. Health Phys. 82: 473-483.

4. Lu, S.-T.; and Mathur, S.P. [2002]: Hypotension induced by ultra-wide-band pulses: dose response, replication, orthostatic response and heart rate variability. In: "Proceedings of the Second International Workshop on Biological Effects of EMFs," Kostarakis, P. ed., (ISBN 960-86733-3-X) pp 409-418.

5. Mathur, S.P.; and Lu, S.-T. [2002]: Application of various thermometric calorimetry in rodent dosimetry. In: "Proceedings of the Second International Workshop on Biological Effects of EMFs," Kostarakis, P. ed., (ISBN 960-86733-3-X) pp 272-280.

6. Pakhomov, A.G.; Gajsek, P.; Allen, L.; Stuck, B.E.; and Murphy, M.R. [2002]: Comparison of dose dependences for bioeffects of continuous-wave and high-peak power microwave emissions using gel-suspended cell cultures. Bioelectromagnetics 23: 158-167.

7. Pakhomov, A.; Du, X.; Doyle, J.; Ashmore, J.; and Murphy, M.R. [2002]: Patch-clamp analysis of the effect of high-peak power and CW microwaves on calcium channels. In: "Proceedings of the Second International Workshop on Biological Effects of EMFs," Kostarakis, P. ed., (ISBN 960-86733-3-X) pp 281-288.

8. Seaman, R.L.; Parker, J.E.; Kiel, J.L.; Mathure, S.P.; Grubbs, T.R.; and Prol, K. [2002]: Ultra-Wideband pulses increase nitric oxide production by RAW 264.7 macrophages incubated in nitrate. Bioelectromagnetics 23: 83-87.

9. Seaman, R.L. [2002]: Letter to the editor: Non-osseous sound transmission to the inner ear. Hearing Res. 166: 214-215.

10. Seaman, R.L.; Mathur, S.P.; Phinney, A.M.; Garcia, A.S.; and Ashmore, J. L. [2002]: Changes in rat motor activity by pulsed microwave radiation depend on type of activity, time after exposure, and state of animal. In: "Proceedings of the Second International Workshop on Biological Effects of EMFs," Kostarakis, P. ed., (ISBN 960-86733-3-X) pp 388-394.

11. Seaman, R.L. [2002]: Transmission of microwave-induced intracranial sound to the inner ear is most likely through cranial aqueducts. In: "Proceedings of the Second International Workshop on Biological Effects of EMFs," Kostarakis, P. ed., (ISBN 960-86733-3-X) pp 942-945.

12. Lu, S.-T. [2003]: Microwave bioeffects, body borne antenna and L-band. In: "Joint Medical Technology Workshop 2003, Panel F: Non-Ionizing Directed Energy Bioeffects", 10-23 October 2003, Lansdowne, VA, US Army Medical Research and Materiel Command (19 pages).

13. Lu, S.-T. [2003]: Radio frequency specific effects, potential medical application. In: "Joint Medical Technology Workshop 2003, Panel F: Non-Ionizing Directed Energy Bioeffects", 10-23 October 2003, Lansdowne, VA, US Army Medical Research and Materiel Command (22 pages).

14. Seaman, R.L.; and DeCarlo, C.D.: Effects of microwave radiation on nigrostriatal neurodegeneration in the rat. In: "Joint Medical Technology Workshop 2003, Panel F: Non-Ionizing Directed Energy Bioeffects", 10-23 October 2003, Lansdowne, VA, US Army Medical Research and Materiel Command (4 pages).

15. Pakhomov, A.G.; Doyle, J.; Stuck, B.E.; and Murphy, M.R. [2003]: Effects of high power microwave pulses on synaptic transmission and long term potentiation in hippocampus. Bioelectromagnetics 24: 174-181.

16. Pakhomov, A.G.; Stuck, B.E.; and Murphy, R. [2003]: *In vitro* model research into bioeffects of extremely high power microwave pulses. In: "Proceedings of the 3rd International EMF Seminar in China: Electromagnetic Fields and Biological Effects", pp 82-83.

17. Fleming, S.M., Zhu, C., Mehta, A., Seaman, R., and Chesselet, M.-F. [2004]: Chronic intravenous and subcutaneous rotenone infusion: survival analysis, functional assessment and microglial activation. Experimental Neurol. 187: 418-429.

18. Lu, S.-T. [2004]: Effects of ambient temperature on microwave-induced "stress" responses (In preparation).

19. Nayak, B.K.; Natarajan, M.; Galino, C.; Mathur, S.P.; and Meltz, M.L. [2004]: Determination of p53 protein stabilization and transactivation of its target genes in response to ultrawideband electromagnetic radiation exposure in human hematopoietic cells. (Submitted).

20. Naya, B.K.; Natarajan, M.; Galindo, C.; Mathur, S.P.; and Meltz, M.L. [2004]: Effect of ultrawideband electromagnetic radiation on cell cycle progression in human hematopoietic cells. (Submitted).

21. Pakhomov, A.G.; Phinney, A., Ashmore, J.; Walker, K. III; Kolb, J.; Kono S.; Schoenbach, K.H.; and Murphy, M.R. [2004]: Some Characteristics of the cytotoxic effect of nanosecond duration, high-intensity electrical pulses. IEEE Trans. Plasma Sci. (in press).

22. Pakhomov, A.; Doyle, J.; Morin, J.; and Murphy, M. [2004]: Extremely-high power microwave pulses (EHPP) alter 4-aminopyridine-induced bursts in isolated hippocampal slices. (In preparation, abstract included).

23. Seaman, R.L., and Jauchem, J.R. [2004]: Temporal characteristics of the rat electrocardiogram during acute exposure to timed ultra-wideband pulses. (in press)

24. Seaman, R.L., and Phelix, C.F. [2004]: Acute effects of pulsed microwaves and 3-nitropropionic acid on neuronal ultrastructure in the rat caudate-putamen. Bioelectromagnetics (in press).

25. Seaman, R.L.; Chesselet, M.-F.; Mathur, S.P.; DiCarlo, C.D.; Fleming, S.M.; Ashmore, J.L.; Garza, T.H.; and Grado, A.M. [2004]: Movement initiation in rotenone-treated rats after acute exposure to 1.25-GHz microwave pulses in circular waveguide at 0.4 W/kg. (In preparation, abstract included).

LIST OF REPORT (2001-2004)

1. Seaman, R.L., Mathur, S.P., and Dick, E.J. Jr. [2003]: Short-term motor activity and acoustic startle after microwave exposure and toxin-induced hypoxia. A Technical Report.

MEETING ABSTRACT 1

Abstract submitted to:
31st Annual Meeting of the Society for Neuroscience
San Diego, California, November 10-15, 2001

MONOAMINE OXIDASE INHIBITION ENHANCES ULTRASTRUCTURAL CHANGES IN RAT STRIATAL NEURONS AFTER SINGLE SYSTEMIC INJECTION OF 3-NITROPROPIONIC ACID. P.A. Brewer*[1], L.R. Mery[1], C.F. Phelix[1], R.L. Seaman[2]. 1-Div.Life Sciences, Univ. of Texas, San Antonio, TX 78249; 2-McKesson HBOC Bioservices and USAMRD Microwave Bioeffects Branch, Brooks AFB, San Antonio, TX 78235

Swelling of rough endoplasmic reticulum (RER) is an ultrastructural sign of striatal neuronal damage induced by a single 3-nitropropionic acid (3NP) treatment. Since dopamine can damage striatal neurons blockade of monoamine oxidase should modify the effect of 3NP. The objectives were first to perform a dose (0, 10, 15 mg/kg) by time (4.5 and 24 hr) study of 3NP effects and second to test if co-treatment with 3NP and tranylcypromine (3 mg/kg) enhances ultrastructural changes seen at 24 hr that occur with a single systemic injection of (10 mg/kg) 3NP. Male Sprague Dawley rats (4-6 mos) were used. Perfusion with formaldehyde - glutaraldehyde in phosphate buffered saline was performed. Coronal sections cut at 500 μm were used to punch a 3 mm diameter disk from the central dorsal striatum for transmission electron microscopic examination. Digitized images of neurons from each rat were used to measure intracisternal width of RER and 2D Stereology of area density with ImageTool UTHSCSA. A two way ANOVA showed significant dose and time effects, $p<0.001$. At 4.5 there were no significant effects but at 24 hr both doses of 3NP caused dilation of RER, $p<0.001$. Tranylcypromine plus 3NP significantly increased both RER width and area density compared with saline, $p<0.001$, and 3NP alone, $p<0.05$. This combined effect was similar to a dose of 30 mg/kg 3NP. Longer postinjection time points will have to be examined to determine if these changes are irreversible leading to neurodegeneration. Supported by HL02914 and US Army Medical Research and Materiel Command #DAMD17-94-C-4069. Views, opinions and/or findings should not be construed as an official Department of Army position, policy or decision.

MEETING ABSTRACT 2

LASER AND MICROWAVE INDUCED BREAKDOWN SPECTROSCOPY: BASIS FOR A NEW DETECTION TECHNIQUE FOR CHEMICAL AND BIOLOGICAL AGENTS

Johnathan L. Kiel[1], Benjamin A. Rockwell[1], Robert J.Thomas[2], John L. Alls[3], Satnam P. Mathur[4], Richard E. Sutter[1], and Pedro J. Morales[1]
[1]Human Effectiveness Directorate, U.S. Air Force Research Laboratory, Brooks AFB, TX 78235; [2]TASC, Inc., San Antonio, TX ; [3]Veridian, Inc., San Antonio, TX 78216; [4]McKesson BioServices, Inc., and the U.S. Army Medical Research and Material Command

Laser induced breakdown in air and solutions is a well-investigated phenomena. The emission spectra reveal the presence of atomic ionic spectra of gases from air and volatilized metallic and other ions. Microwave induced breakdown in solution is a recently observed phenomenon (Kiel et al., IEEE Transactions in Plasma Science 28: 161-167, 2000). To accomplish the latter efficiently, soluble organic semi-conductor (diazoluminomelanin) needs to be added to solutions exposed to high power microwave pulses (1.25 GHz, 10 Hz pulse rate, 6 μs pulses, 2 MW peak power). When comparable solutions are exposed to laser pulses (1 ns pulse, 540 nm wavelength), the emissions reveal not only the expected atomic spectra, but also spectra associated with the organic semi-conductor. The microwave induced breakdown spectra show similar highly resolvable emission peaks. Spectra with common and unique features were observed for the bacteria *E. coli*, anthrax spores, and chemical derivatives of the organic semi-conductor. Included in these spectral bands were peaks representative of buffer and other solution components such as sodium and chlorine. Therefore, the separate or combined use of cavitation generated by pulsed laser and/or pulsed high power microwave sources can generate analytical chemical and biological spectra for identification of these agents.
This work was sponsored in part by the U. S. Air Force Office of Scientific Research, the Joint Services Technical Base Program in Chemical and Biological Defense, and the U. S. Army Medical Research and Material Command. The views presented here are solely of the authors and do not represent the opinions or policies of the U.S. Air Force, Army, or any other agency of the Federal Government.

MEETING ABSTRACT 3

DIRECTED KILLING OF ANTHRAX SPORES BY MICROWAVE INDUCED CAVITATION VIA SPECIFIC BINDING OF ORGANIC SEMI-CONDUCTOR

Johnathan L. Kiel[1], John L. Alls[2], Richard E. Sutter[1], Patrick A. Mason[1], Satnam P. Mathur[3], and Pedro J. Morales[1]

[1]USAF Research Laboratory, Brooks AFB, TX 78235, [2]Veridian, Inc., San Antonio, TX, 78216, and [3]McKesson BioServices, Inc., and the United States Army Medical Research Command Detachment, Brooks AFB, TX 78235

We previously reported that anthrax spores could be damaged by the action of a pulsed microwave induced thermochemiluminescent response (Kiel et al, IEEE Transactions on Plasma Science 28: 161-167, 2000). They were placed into the volume of liquid that experienced the pulsed flashing effect on a bacterial filter. Therefore, the efficacy of such an approach toward decontamination of a surface contaminated with anthrax spores would be very inefficient because we could not always assure that the flashing would occur where the spores were located. To maximize the effect, we needed to attach the organic semi-conductor diazoluminomelanin (DALM) to the surface of the spores. We also needed to confirm that multiple bubble sonoluminescence and the corresponding sonochemistry were occurring on the spores. Serendipitously, we discovered that DALM biosynthesized by JM109 *E. coli* containing the plasmid pIC2ORNR$_{1.1}$ (American Type Culture Collection # 69905) specifically binds to Sterne Strain anthrax spores, but not to other species of Bacillus. The chemically synthesized form of DALM does not demonstrate this property. Therefore, the *E. coli* bacteria must generate another molecule attached to the polymer in the synthesis process that conveys the specificity. DALM does bind to magnetite particles non-specifically, and this property is maintained by both the chemically synthesized and biosynthesized DALM. Upon exposure to pulsed microwave radiation (1.25 GHz, pulse rate of 10 Hz, 6 μs pulses, peak power of 2 MW), the tagged spores demonstrated killing when flashing occurred, but not when it was absent. Examination of the light emissions demonstrated atomic gas spectra typical of air and organic components associated with the bacteria and DALM. Such spectra are typical of plasma generated by laser induced breakdown and by multiple bubble sonoluminescence. Therefore, specific directing of the binding of organic semi-conductor to target microbes may be a useful approach for selective pulsed microwave decontamination of a contaminated surface. This work was sponsored in part by the U. S. Air Force Office of Scientific Research, the Joint Services Technical Base Program in Chemical and Biological Defense, and the U. S. Army Medical Research and Material Command under Contract DAMD 17-94-C-4069. The work presented here is the opinion of the authors and does not represent official opinions or policies of the United States Air Force, Army, or any other agency of the Federal government of the United States of America.

Key Words: Diazoluminomelanin, pulsed microwaves, anthrax, and sonoluminescence

K5-03

A Treatment System Combining Interstitial Microwave Hyperthermia and Interstitial Radiation Therapy

K. Ito[1], K. Saito[1], H. Yoshimura[1], Y. Aoyagi[2], and H. Horita[2]
[1]Department of Urban Environment Systems, Faculty of Engineering, Chiba University
1-33 Yayoi-cho, Inage-ku, Chiba 263-8522, Japan
Tel: +81-43-290-3326, Fax: +81-43-290-3327, E-mail: ito@cute.te.chiba-u.ac.jp
[2]Department of Radiology, Ichikawa General Hospital, Tokyo Dental College
5-11-13 Sugano, Ichikawa 272-8513, Japan
Tel: +81-473-22-0151, Fax: +81-473-25-4456

Background

In recent years, various types of applications of electromagnetic techniques for microwave thermal therapy have been developed [1]. The authors have been studying the thin coaxial antennas for the minimally invasive microwave thermal therapy, such as interstitial microwave hyperthermia. In addition, there is also hyperthermia combined with the radiation therapy and the chemotherapy [2]. Particularly, combination of the hyperthermia and the interstitial radiation therapy is effective for treatment of radiation resistive tumor. In this study, we consider the possibility of realizing the treatment system combining the interstitial microwave hyperthermia and the interstitial radiation therapy.

Scheme of Combined Therapy

Figure 1 shows the treatment system. This treatment system is realized by using the same catheter between the interstitial hyperthermia and the interstitial radiation therapy. In this system, firstly, thin microwave antennas such as the coaxial-slot antenna with catheter heat the tumor. After heating, only the antennas are pulled out of the catheters. Then, radiation sources such as the iridium 192 are automatically inserted into the catheter by a "high dose rate afterloading system".

Fundamental Study

In this system, we must use the catheter for the interstitial radiation therapy. Therefore, in *this study, the possibility of using the catheter not* only for the interstitial radiation therapy but also for the interstitial microwave hyperthermia was examined. Firstly, we calculated the heating characteristics of the coaxial-slot antennas by using the FDTD method. Next, we confirmed the SAR distributions around the antennas by using the tissue-equivalent phantom and infrared camera. As a result, we could confirm the heating ability of the coaxial-slot antenna inside the biological tissue with the catheter for the interstitial radiation therapy.

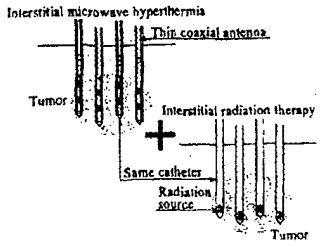


Fig. 1 Combined therapy.

References

[1] M. Hiraoka, *et al.*, "Development of RF and microwave heating equipment and clinical applications to cancer treatment in Japan," IEEE Trans. Microwave Theory Tech., vol. 48, no. 11, Nov. 2000.
[2] M. H. Seegenschmiedt *et al.* (Eds.), *"Thermoradio therapy and thermochemo therapy,"* Springer-Verlag, Berlin, 1995.

K5-04

Potential Application of UWB Pulses in Lowering Blood Pressure

S.-T. Lu
McKessonHBOC Clinical and Biological Services
U.S. Army Medical Research Detachment, Microwave Bioeffects Branch
8308 Hawks Road, Building 1168
Brooks Air Force Base Texas 78235, U.S.A.

Tel: 210-536-5596, Fax: 210-536-5382, e-mail: shin-tsu.lu@brooks.af.mil

Background

Ultra-Wide-Band radiofrequency radiation is a new modality in radar technology. Lu *et al* [1] observed that rats exposed to UWB electromagnetic pulses developed a delayed hypotension. The scope of study was expanded to include additional doses to elucidate the dose-response characteristics of this UWB induced delayed hypotension.

Material and Methods

Forty-five male Wistar-Kyoto normotensive rats, 71-89 days of age were used. They were exposed to UWB pulses in a GTEM cell for 6 minutes. They were exposed as **sham** (0 kV/m peak), or to pulses with pulse repetition rate at **125 Hz** (91 kV/m peak, 1 ns pulse width, 0.28 mW/cm^2 average power density, and 0.017 W/kg average SAR), **250 Hz** (95 kV/m peak, 1 ns pulse width, 0.61 mW/cm^2 average power density, and 0.038 W/kg average SAR), **500 Hz** (89-93 kV/m peak, 0.9 to 1.0 ns pulse width, 0.96 to 1.15 mW/cm^2 average power density, and 0.059 to 0.071 W/kg average SAR) and **1,000 Hz** (85 kV/m peak, 0.94 to 1 ns pulse width, 1.82 to 1.95 mW/cm^2 average power density and 0.11 to 0.12 W/kg average SAR). Systolic, mean and diastolic arterial blood pressures were determined by a non-invasive tail-cuff sphygmomanometry procedure using a photoelectric sensor to quantify the amplitude of arterial pulsation. Heart rate was determined from inter-pulse intervals. Baseline heart rate and arterial pressures were determined at 72 hours before exposure. Post exposure heart rate and arterial pressures were obtained within one hour, 24 hr, 72 hr, 1 week, 2 weeks, 3 weeks and 4 weeks after exposure.

Results and Discussion

Heart rate did not change significantly among five treatment groups at any sampling time point. Systolic, mean and diastolic arterial pressures in rats exposed to 500 Hz and 1,000 Hz decreased significantly from those in sham exposed rats but within normal for this specie of animal. Blood pressures in rats exposed to 125 Hz and 250 Hz did not change significantly from those in sham exposed rats at any sampling time point. The time course of delayed hypotension appeared at 1 week after exposure, reached a nadir at 2 weeks after exposure, and recovered slowly and but still significantly below those of sham at 3 and 4 weeks after exposure. Similar effect was not observed in rats 2 weeks after exposure to 2.45 GHz continuous wave microwave at 0.3, 3 and 6 W/kg whole-body average SAR for 30 minutes [2]. Although the mechanism is not clear, the potential application in treating hypertension with UWB pulses should be explored further.

Reference

[1] S.-T. Lu *et al.*, Physiol. Beh. Vol. 67, no. 3, p. 463, September 1999.
[2] S.-T. Lu *et al.* Millennium International Workshop on Biological Effects of Electromagnetic Fields Proceedings, pp. 491-496, October, 2000.

K6-2-01

Phantoms for estimation of the interaction between EM waves and a human body

K. Ito[1], H. Kawai[2], H. Yoshimura[1], Y. Koyanagi[2&3], and K. Ogawa[4]
[1]Department of Urban Environment Systems, Faculty of Engineering, Chiba University
[2]Graduate School of Science and Technology, Chiba University
1-33 Yayoi-cho, Inage-ku, Chiba 263-8522, Japan
Tel: +81-43-290-3326, Fax: +81-43-290-3327, E-mail: ito@cute.te.chiba-u.ac.jp
[3]Personal Communications Division, Matsushita Communication Industrial Co., Ltd.
4-3-1 Tsunashima-higashi, Yokohama 223-8639, Japan
[4]Device Engineering Development Center, Matsushita Electric Industrial Co., Ltd.
1006, Kadoma, Osaka 571-8501, Japan

Background

In recent years, many researches have been conducted on the interaction between electromagnetic (EM) waves radiated from an antenna and a human body. We have proposed tissue-equivalent solid phantoms, in order to estimate of such interaction at the microwave region. It has confirmed that these phantoms can be used to evaluate the SAR in the human head model at 900 MHz [1]. Furthermore, we have developed the tissue-equivalent solid phantom for the VHF band, especially at 150 MHz. In this paper, we evaluate the characteristics of an antenna close to the human body and the SAR, to confirm the phantoms can estimate such interaction at wide frequency range between the VHF and UHF band.

The tissue-equivalent solid phantom

The phantom is a material with almost the same relative permittivity and conductivity as the human tissue. In addition, the phantom has sufficiently large specific heat and small thermal conductivity. In the UHF band, we use the brain-equivalent phantom as the human head [1]. In the VHF band, it is indispensable to realize the whole body as the human model, for investigating the characteristics of the antenna that attached to the human abdomen. Figure 1 shows the structure of the whole body phantom, which is chiefly composed of the glycerin. The human is approximated by a cylindroid the dimensions of which are 0.14λ by 0.1λ in diameter and 0.65λ in height at 150 MHz. Here, the parameters of the phantom are ε_r = 42.1, σ = 0.514 S/m, ρ = 907 kg/m^3 as a mixture of all human tissues. Moreover, its ingredients are different from the phantom at 900 MHz.



Fig. 1 Whole body solid phantom at 150 MHz.

SAR measurement

In this paper, the SAR distributions of the phantoms were measured using the thermographic method and compared with the FDTD calculation at 900 MHz and 150 MHz, to confirm the validity of the phantoms as the human model. As a result, good agreements between the measured and calculated results were obtained at both frequencies. In addition, we confirmed that the phantom for 150 MHz also can estimate the characteristics of the antenna, such as the impedance and the radiation pattern, can estimate the unique phantom.

Reference

[1] Y. Okano, K. Ito, I. Ida, and M. Takahashi, "The SAR evaluation method by a combination of thermographic experiments and biological tissue-equivalent phantoms," IEEE Trans. Microwave Theo. Tech., vol. 48, no. 11, pp. 2094-2103, Nov. 2000.

K6-2-02

Research on Biological Effects of Radio Frequency Radiation at Walter Reed Army Institute of Research

S.-T. Lu
McKessonHBOC Clinical and Biological Services
U.S. Army Medical Research Detachment, Microwave Bioeffects Branch
8308 Hawks Road, Building 1168
Brooks Air Force Base Texas 78235, U.S.A.

Tel: 210-536-5596, Fax: 210-536-5382, e-mail: shin-tsu.lu@brooks.af.mil

The mission of the Microwave Bioeffects Branch of the Walter Reed Army Institute of Research is to develop bioeffects criteria and predictive models for safe exposure standards for electromagnetic radiation to assure the health and welfare of warfighters. New and increasingly complex weapons and communications systems increase the range of wavelength and pulse characteristics of electromagnetic energy to which warfighters may be exposed. Based on these facts, the mission of Microwave Bioeffects Branch is to conduct *in vivo* and *in vitro* studies to determine the effects of radio frequency fields on behavior and central nervous, ocular and cardiovascular systems. Efforts have been concentrated on biological effects of high peak but low average power pulsed microwave. Unique research topics and findings in this laboratory have been reviewed [1]. Comparison between effectiveness of CW and pulsed microwaves on lenticular cavitation, cardiovascular effects and evoked body movements were performed. TEMPO (Transformer Energized Megavolt Pulsed Output) is an unique experimental transmitter capable of delivering 3 GHz pulses at 700 MW peak power but the averaged SAR is very low (0.072 W/kg) because of the 80 ns pulse width and 0.125 Hz pulse repetition rate. Endpoints for studying biological effects of TEMPO plusses included treadmill performance, memory consolidation, time bisection, circadian rhythmicity of food consumption and despair/depression behavior. Effects of electromagnetic pulse (EMP, 100 kV/m, 7 ns rise time, 20 ns pulse duration, 6 pps) were studied in rats. Memory consolidation, general motor activity, behavioral despair and preference of EMP pulses were studied. Recently, Ultra-Wide-Band (UWB) pulses (100 kV/m peak, 1 ns pulse width, up to 1 kHz pulse repetition rate) have been used extensively. Endpoints for studies on biological effects of UWB pulses were mutation and colony formation ability in yeast cells, spontaneous activity, nociception, morphine-induced hyperactivity and analgesic effect of nitric oxide synthetase inhibition in mice; and delayed cardiovascular effects in rats. Other topics of studies were post-exposure changes in operant behavior [2] and startle modification by pulsed microwaves in rats [1], effects of mm waves on isolated nerve function and synaptic transmission in frogs [3, 4, 5], and effects of pulsed microwave on retinal function and histology of non-human primates [6]. TEMPO and UWB pulses appear to be biological active at doses below 0.4 W/kg. The effects of TEMPO and UWB pulses need to be replicated and confirmed.

Reference

[1] S.-T. Lu and J. deLorge, in "Advances in Electromagnetic Fields in Living Systems", vol. 3, J.C. Lin ed., Kluwer Academic/Plenum Press, pp207-264, 2000.
[2] Y. Akyel *et al.*, Bioelectromagnetics, vol. 12, no. 3, pp. 183-195, 1991.
[3] A.G. Pakhomov *et al.*, Electro- Magnetobiol vol. 17, no.2, pp. 115-125, 1998.
[4] A.G. Pakhomov *et al.*, Bioelectrochem. Bioenerg. vol. 43, no.1, pp. 27-33, 1997.
[5] A.G. Paknomov *et al.*, Bioelectromagnetics, vol. 18, no. 4, pp 324-334, 1997.
[6] S.-T. Lu *et al.*, Bioelectromagnetics, vol. 21, no. 6, pp. 439-454, 2000.

MEETING ABSTRACT 6

Retaining of the Long-Term Potentiation in Hippocampal Slices after High Peak Power Microwave Exposure and Heating

A.G. Pakhomov[1,2], J. Doyle[1], S. Mathur[1], and M.R. Murphy[2]
[1]McKesson BioServices, US Army Medical Research Detachment
Brooks Air Force Base, San Antonio, TX, USA
[2]Directed Energy Bioeffects Division, Human Effectiveness Directorate,
Air Force Research Laboratory, Brooks Air Force Base, San Antonio, TX, USA

The long-term potentiation (LTP) is a profound and long-lasting facilitation of neural response after a brief tetanic stimulation. This facilitation develops within minutes and may persist for hours with little or no decay. The LTP has long been thought to play a key role in memory processes and is often employed as a memory model in *in vitro* studies. The goal of the present work was to analyze if exposure to extremely-high peak power microwave pulses (EHPP) and heating may damage already developed LTP.

METHODS: The experiments were performed in sagittal hippocampal slices (350-μm thick) isolated from the brain of 4- to 6-week old male Sprague-Dawley rats. The slices were placed on a matching plate at the end of a waveguide and submerged into an artificial cerebrospinal fluid (ACSF). The exposure setup, dosimetry and thermometry were essentially the same as described earlier (Pakhomov et al., Bioelectromagnetics, 1999, V. 21, 245-254). *Stratum radiatum* area of the slice was stimulated with a bipolar tungsten electrode at 30-sec intervals, and population spikes (PS) in the CA1 area were recorded by a glass microelectrode (2-10 Mohm). Experiments began after a 30- to 90-min stabilization and lasted for 15 min. Each slice was used in a single experiment. Mean PS amplitude during the first 2 min of the experiment was considered baseline (100%) for each slice preparation. Tetanus (2 sec at 50 Hz) was applied at 2 min into the experiment. A 2-min exposure began at 7 min 45 sec, when the PS increase due to the LTP reached its maximum. A model 337X EHPP transmitter (Applied Systems Engineering, Inc.) produced 1-μs wide pulses at the peak power of 280-290 kW. At 5% reflection, the peak transmitted power was about 270 kW (1.57 MV/m), and the peak specific absorption rate (SAR) in the center of the slice reached 360 kW/g. Pulse repetition rates and time-average SAR levels were 2 Hz and 0.7 W/g (group 1), 5 Hz and 1.8W/g (group 2), and 10 Hz and 3.6 W/g (group 3). Irradiation increased the ACSF temperature from the base level of 34 °C to 35.5, 37, and 39.7 °C, respectively; initial temperature restored within 1 min after the exposure.

RESULTS: Effects of sham exposure and 3 exposure regimens were tested in 49 experiments. In all the groups, tetanization increased the PS amplitude to 150-160%. In sham exposed preparations, PS remained at this facilitated level until the end of recording. With EHPP irradiation, PS temporarily decreased, and the decrease was proportional to the time-average SAR and heating. With the maximum heating (group 3), PS dropped to its pre-LTP value (100 ± 20%). However, in all the exposed groups the PS amplitude successfully recovered soon after the restoration of temperature.

SUMMARY: Transitory PS suppression during the irradiation and briefly after it can reasonably be explained by heating. However, there was no aftereffect of the irradiation or heating on the LTP. As far as the LTP findings can be extrapolated to memory function, one can say that the EHPP and heating did not "erase" or alter the memory record. The study provided no indication of a specific bioeffect of a brief EHPP exposure, even at peak SAR and incident E-field as high as 360 kW/g and 1.57 MV/m.

ACKNOWLEDGMENTS: *The authors thank Dr. S. Alexeev (Temple Univ., Philadelphia, PA) for help with SAR calculation. The work was supported in part by the U.S. Army Medical Research and Materiel Command and the U.S. Air Force Research Laboratory (AFOSR) under U.S. Army contract DAMD17-94-C-4069 awarded to McKesson BioServices. The views expressed are those of the authors and should not be construed as reflecting the official policy or position of the Department of the Army, Department of the Air Force, or the United States Government.*

15-3

EFFECTS OF EXTREMELY HIGH POWER MICROWAVE PULSES ON THE POPULATION SPIKE AND LONG-TERM POTENTIATION IN RAT HIPPOCAMPAL SLICES. A.G. Pakhomov[1], J. Doyle*[1], S. Mathur*[1], M.R. Murphy[2]. [1]McKesson BioServices, US Army Medical Research Detachment, and [2]Directed Energy Bioeffects Division, Human Effectiveness Directorate, Air Force Research Laboratory, Brooks Air Force Base, San Antonio, TX 78235-5324, USA.

The possibility of producing specific bioeffects by extremely high power pulses (EHPP) of microwave radiation is one of the least explored areas in bioelectromagnetics. The overall number of studies where the peak specific absorption rate (SAR) in a biological specimen exceeded 10 kW/g is less than a dozen, and findings are controversial. Current safety guidelines for EHPP exposure have not been justified by any known mechanism or threshold for a specific EHPP biological effect. The present study explored whether irradiation at peak SAR as high as 330 kW/g may affect neural function, such as excitability, synaptic conduction, and long-term potentiation (LTP).

METHODS: The experiments were performed in saggital hippocampal slices (350-μm thick) isolated from the brain of 4- to 6-week old male Sprague-Dawley rats. The slices were submerged into an artificial cerebrospinal fluid (ACSF) and affixed to the bottom of an exposure bath. The design of the exposure bath, thermometry and dosimetry methods were similar to those described earlier (Pakhomov et al., *Bioelectromagnetics*, 1999, V. 21, 245-254). However, for this study we employed a more powerful EHPP transmitter (model 337X, Applied Systems Engineering, Inc., with 250-kW output). The ACSF was composed of: (in mM) glucose, 11; NaCl, 125; KCl, 3; $MgCl_2$, 1; NaH_2PO_4, 1.25; $NaHCO_3$, 26, $CaCl_2$, 2; pH 7.2-7.4. The ACSF was kept at 34 °C and was continually gassed with a 95% O_2 / 5% CO_2 mixture. *Stratum radiatum* area of the slice was stimulated with a bipolar tungsten electrode at 30-sec intervals, and population spikes (PS) in the CA1 area were recorded by a glass microelectrode (2-10 Mohm). Experiments began after a 30- to 90-min stabilization, and each slice was only used in a single experiment. Each experiment lasted for 10 min, thus including 21 PS records (every 30 sec). EHPP or sham exposure began after the 4th PS record, at 1 min 45 sec into the experiment. The exposure lasted for 2 min at 0.33 W/g average and 330 kW/g peak SAR; the pulse width was either 2 μs (0.5-Hz repetition rate) or 0.5 μs (2-Hz repetition rate). A tetanic stimulation of the *Stratum radiatum* (2 sec at 50 Hz) to induce LTP was performed after the exposure, at 5 min into the experiment. The endpoint to reveal EHPP effect was the PS amplitude, and the magnitude and the time course of the PS changes caused by the tetanus.

RESULTS: A total of 29 experiments were performed. In the sham-exposed group, the PS amplitude was stable before the tetanus. The tetanus briefly suppressed the PS, followed by the development of LTP and stable PS increase by 30-50%. Both tested exposure regimens increased the ACSF temperature by about 0.7 °C, with restoration of the original temperature within 1 min after cessation of the exposure. During the exposure and for 1-2 min after it, the PS amplitude decreased by about 10% compared with the sham control. However, the time course and magnitude of the LTP after tetanization were the same as in the control slices.

SUMMARY: A transitory PS suppression during the irradiation and briefly after it can reasonably be attributed to microwave heating. Tested regimens of EHPP exposure had no effect on the ability of hippocampal neurons to develop LTP after the irradiation. The experiments provided with no indication of any specific biological action of a brief EHPP irradiation, even at peak SAR as high as 330 kW/g.

The authors are thankful to Dr. S. Alekseev (Temple Univ., Philadelphia, PA) for calculation of SAR within brain slices. The work was supported in part by the U.S. Army Medical Research and Materiel Command and the U.S. Air Force Research Laboratory (AFOSR) under U.S. Army contract DAMD17-94-C-4069 awarded to McKesson BioServices. The views expressed are those of the authors and should not be construed as reflecting the official policy or position of the Department of the Army, Department of the Air Force, or the United States Government.

P-42

EVALUATION OF DNA DAMAGE AND APOPTOSIS IN THE IMMATURE MOUSE CEREBELLUM AFTER ACUTE EXPOSURE TO A 1 Mt, 60 Hz MAGNETIC FIELD. J.P. McNamee, P.V. Bellier, J.R. McLean*, G. Gajda, A. Thansandote. Health Canada, Radiation Protection Bureau, 775 Brookfield Rd., Ottawa, Ontario, Canada K1A 1C1.

Several recent studies have reported that whole-body exposure of rodents to power frequency magnetic fields (MF) can result in DNA single- and double-strand breaks in the brains of these animals. If MF cause DNA double-strand breaks in the rodent brain, an associated neuronal degeneration via induction of apoptosis may be observed in certain brain cell regions. The adult rodent brain is relatively resistant to apoptosis and therefore is not an ideal model to study the possible effects of MF on the induction of neuronal apoptosis. However, the external granule cell layer (EGCL) of the immature rodent cerebellum is known to undergo extensive apoptosis upon exposure to a variety of genotoxic chemicals and ionizing radiation. In addition, the immature rodent brain still has the capacity to undergo proliferation, differentiation and re-organization and more closely resembles the developing brain of a human child. Thus, the immature rodent brain may provide a sensitive and useful animal model in which to study the possible biological effects of MF.

OBJECTIVE: The current study was undertaken to investigate whether acute 2 hr exposure of a 1 mT, 60 Hz MF could elicit DNA damage, and subsequently apoptosis, in the cerebellums of immature (10-day-old) mice. METHODS: DNA single-strand breaks were quantitated at 0, 2, 4, and 24 hr after exposure using the alkaline comet assay, while apoptosis was quantitated in the external granule cell layer (EGCL) of the immature mouse cerebellum at 0 and 24 hr after exposure to MF by the TUNEL assay. Four parameters (Tail Ratio, Tail Moment, Comet Length and Tail Length) were used to assess DNA damage for each comet.

RESULTS: While increased DNA damage was detected by Tail Ratio at 2 hr and Tail Length at 24 hr after MF exposure, no supporting evidence of increased DNA damage was detected by the other parameters. In addition, no other differences were observed using the Tail Ratio or Tail Length parameters at any other post-exposure times. No increase in apoptosis was observed in the EGCL of MF exposed mice, when compared to sham mice.

CONCLUSIONS: Taken together, these results do not support the hypothesis that acute MF exposure causes DNA single-strand breaks in the cerebellums of immature mice. However, the significant differences detected in our study cannot be entirely ruled out. Thus, the only appropriate conclusion that can be derived from our DNA damage assessment data is that the results on MF-induction of DNA single-strand breaks in the immature mouse cerebellum are equivocal.

P-43

INTERACTION BETWEEN A NEUROTOXIN AND PULSED MICROWAVES. R.L. Seaman, S.P. Mathur*, A.M. Phinney*, N.R. Harris*. McKessonHBOC Clinical & Biological Services and USAMRD Microwave Bioeffects Branch, Brooks AFB, TX 78235, USA.

OBJECTIVE: Changes in rat motor activity and acoustic startle were used to assess effects of microwave exposure and mitochondrial toxin 3-nitropropionic acid (3-NP).

METHODS: Thirty male Sprague-Dawley rats weighing 569±52 g (mean±st.dev.) aged 15-23 weeks were injected intraperitoneally on two consecutive days with 10 mg/kg 3-NP or saline (0 mg/kg 3-NP). Exposure to 1.25-GHz 6- s microwave pulses at 10 Hz started 1.5 h later and lasted 30 min at specific absorption rate (SAR) of 0, 0.6, or 6 W/kg to give six 3-NP-microwave conditions. Colonic temperature was measured immediately before the animal was placed into a holder for exposure and immediately after exposure. Five animals from each experimental condition were tested at 3.5 h (week 0), 1 week, 2 weeks, and 3 weeks after the second 3-NP injection. Spontaneous motor activity was measured for 5 min in a 38.5x38.5 cm arena.

Whole-body startle response to 20-ms bursts of 120-dBA broadband noise was also measured. Prepulses 0, 3, 6, or 12 dBA above a 70-dBA background level were delivered 100 ms before the startling stimulus. Friedman two-way ANOVA by ranks and nonparametric Newman-Keuls multiple comparisons were used to test for differences between experimental conditions and week of testing with significance level of .05. **RESULTS:** Significant differences in activity ($Fr(5,23)=44.72$, $p=.0043$) consisted of decreases over the 4 weeks of testing for each experimental condition without a significant difference between experimental conditions in any week. Startle response amplitude was not significantly different between conditions or between weeks of testing ($Fr(5,23)=32.99$, $p=.08$). This was also the case for within-session habituation of response amplitude ($Fr(5,23)=30.99$, $p=.12$). Differences in percent prepulse inhibition (PPI) of startle ($Fr(5,71)=182.21$, $p<.0001$) included a number of increases for higher prepulse intensity in each week for each experimental condition. Also, at week 0 with 0 mg/kg 3-NP, PPI for the 3 dBA prepulse was larger after 6 W/kg than after 0 W/kg. At week 0 with 10 mg/kg 3-NP, PPI for both the 6 and 12 dBA prepulses was smaller after 0.6 W/kg than after 0 W/kg. PPI was smaller for 10 mg/kg 3-NP than for 0 mg/kg 3-NP for 6 dBA prepulses for 0.6 W/kg at week 0 and for 0 W/kg at week 3. Over time, PPI decreased with 10 mg/kg 3-NP for 0 W/kg but not for 0.6 and 6 W/kg and not for any condition with 0 mg/kg 3-NP. **CONCLUSIONS:** The changes seen in PPI at week 0 can be largely attributed to short-term chemical hypoxia induced by the toxin and to thermal stress (38.9-41.0°C final colonic temperature) resulting from microwave exposure at 6 W/kg. The reduction in PPI at week 0 for 0.6 W/kg occurred without thermal stress but only with the toxin, indicating possible synergistic actions of 3-NP and pulsed microwaves. The long-term reduction in PPI by 3-NP seemed to be counteracted by microwave exposure at both 0.6 and 6 W/kg, indicating a possible mitigation of some effects of the toxin by microwave exposure.
Supported by the U.S. Army Medical Research and Materiel Command under contract DAMD17-94-C-4069 awarded to McKessonHBOC BioServices. The views, opinions and/or findings contained in this report are those of the authors and should not be construed as an official Department of the Army position, policy or decision. In conducting this research, the investigator(s) adhered to the "Guide for the Care and Use of Laboratory Animals," prepared by the NRC Institute of Laboratory Animal Resources.

P-44

A SETUP FOR SMALL ANIMAL EXPOSURE TO NEAR FIELDS TO TEST A POSSIBLE PROMOTING EFFECT ON SKIN CARCINOGENESIS OF CELLULAR TELEPHONES.
J. Wang[1], O. Fujiwara*[1], K. Imaida*[2], T. Shirai*[2]. [1]Faculty of Engineering, Nagoya Institute of Technology, Gokiso-cho, Showa-ku, Nagoya 466-8555, Japan. [2]Medical School, Nagoya City University, Mizuho-ku, Nagoya 467-8601, Japan.

OBJECTIVE: An *in-vivo* experiment project has been undertaken in order to investigate a possible promoting effect of 1.5 GHz digital cellular telephones on skin carcinogenesis. The exposure target was the dorsum of CD-1 mouse. This study was conducted to develop an exposure setup for this aim. The basic requirements for the exposure setup were to realize a localized peak SAR above 2 W/kg in the superficial skin tissue and a whole-body-averaged SAR below 0.08 W/kg.
EXPOSURE SETUP: The exposure setup has two main features: one is the employment of an electrically short (1/8-wavelength) monopole antenna with a circular plate at its tip as a capacitive-loading, which supplies the ability to realize a highly localized peak SAR and a high exposure power efficiency; the other one is the use of an exposure box (21x21x29cm) with transparent absorber to allow real-time observation of both the exposure process and mouse activities during the exposure. The exposure box is made of aluminum, and its inside, except for the roof and the front door, are inlaid with planar rubber ferrite absorber having a thickness of 7 mm and a reflection loss at least 21.8 dB. The roof of the box acts as the ground for the capacitive-loading monopole antenna that is fed at the center of the roof. The front door is a new-typed transparent absorber with a thickness of 22.5 mm and is able to supply a reflection loss of 20 dB.

MEETING ABSTRACT 9

Abstract submitted to:
31st Annual Meeting of the Society for Neuroscience
San Diego, California, November 10-15, 2001

ACUTE CHANGES IN RAT CAUDATE-PUTAMEN NEURONAL ULTRASTRUCTURE DUE TO 3-NITROPROPIONIC ACID AND MICROWAVE EXPOSURE ARE NOT REFLECTED IN BEHAVIOR.

R.L. Seaman[1]* and C.F. Phelix[2]. [1]McKessonHBOC Clinical & Biological Services and USAMRD Microwave Branch, Brooks AFB, TX 78235, [2]Div. of Life Sciences, Univ. of Texas at San Antonio TX 78249.

To test for interactions between 3-nitropropionic acid (3-NP) and microwave actions, we examined neuronal ultrastructure and behavior of 66 male Sprague-Dawley rats 4-6 months old. Animals were injected with 0 or 10 mg/kg 3-NP on two consecutive days and exposed 1.5 h later each day to 6-μs, 1.25-GHz pulses at 10 Hz for 30 min at specific absorption rate of 0, 0.6, or 6 W/kg. Spontaneous activity and acoustic startle were tested 3.5-4.5 h after the second 3-NP injection and a subset of animals was perfused for electron microscopy at 4-5 h. Mitochondrion diameter in caudate-putamen neurons (N = 12-24) was not different across all conditions. Rough endoplasmic reticulum (RER) intracisternal width and nuclear envelope (NE) thickness increased for 10 mg/kg 3-NP alone, 6 W/kg alone, and their combination but unchanged for 0.6 W/kg alone. With 10 mg/kg 3-NP, the dimensions were smaller for 0.6 W/kg than for 0 or 6 W/kg. The only significant change in behavioral measures was a small but significant decrease in horizontal movement for 10 mg/kg 3-NP across microwave conditions (N = 11/group). Thus, changes in ultrastructure of caudate-putamen neurons, which were most likely GABAergic output neurons, did not correspond to changes in function.

Supported by US Army MRMC contract DAMD17-94-C-4069 (MBS) and NIH Grant HL02914 (UTSA). The investigator(s) adhered to the "Guide for the Care and Use of Laboratory Animals". Views, opinions and/or findings should not be construed as an official Department of the Army position, policy or decision.

PK7-03

Microwave Dosimetry: From Prolate Spheroids to Thermoregulatory Models

P. A. Mason[1], J. M Ziriax[2], W. D. Hurt[1], P. Gajšek[1,3,4], J. A. D'Andrea[2], M. R. Murphy[1]

[1]Air Force Research Laboratory, Directed Energy Bioeffects Division, Radio Frequency Radiation Branch, Building 1162, Brooks Air Force Base, Texas
[2] Naval Health Research Center Detachment at Brooks Air Force Base, Texas
[3]Department of Biology, Trinity University, San Antonio, Texas
[4]Institute of Health, Ljubljana 1000, Slovenia

8315 Hawks Road, Brooks Air Force Base, Texas 78235-5324,
Tel: (210) 536-2362, Fax: (210) 536-3977, e-mail: patrick.mason@brooks.af.mil

Substantial advances have been made in microwave dosimetry since the publication of the 4th edition of the Radiofrequency Radiation Dosimetry Handbook [1]. In that publication, whole-body average specific absorption rate (SAR) values were calculated using prolate spheroids. Advances in computer power and imaging techniques have recently provided the bioelectromagnetics community with digital anatomical models of man, non-human primate, and rodents. Used as input geometries to finite-difference time-domain codes, these models provide information about whole-body and localized SAR values. The whole-body SAR values are in good agreement with those produced by the prolate spheroidal models. The localized SAR data have produced numerous new questions in microwave dosimetry research. The effects of voxel size, voxel shape, sample volume size (1 vs 10 g), and permittivity values on predicted SAR values are being investigated. Inter-laboratory comparison of results is critical to develop user credibility and confidence. Likewise, there is a need to validate the results with empirical measurements, such as those obtained using e-field and temperature probes implanted in liquid simulant and multilayered phantoms. The next large advancement in microwave dosimetry will be the combination of energy absorption and thermal distribution models. With such a combination, predicted SAR values will be incorporated into thermal models (both active thermoregulation and passive thermal redistribution) to predict changes in localized and whole-body temperature during microwave exposure. The sophisticated thermoregulatory models will require mapping the blood vascular system so that heat convection by blood may be incorporated. Issues similar to those currently being addressed for the SAR modeling will need investigation, such as, the limited number of available specific heat values and the variability in these published values for a given tissue. Laboratories in the Asia-Pacific region, Europe, and United States are beginning to work together to address these important problems.

[1] C. Durney *et al., Radiofrequency Radiation Dosimetry Handbook. USAF School of Aerospace Medicine Report*, SAM-TR-85-73, Brooks AFB, TX, 1986.

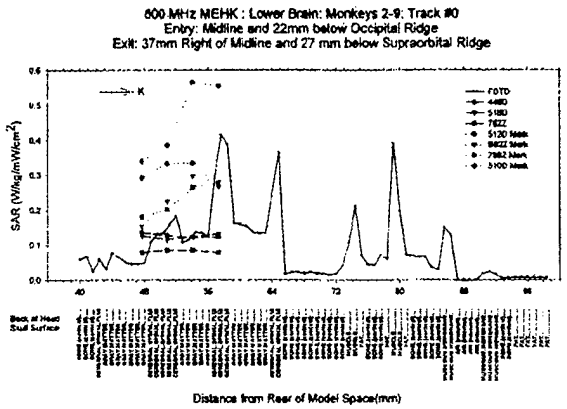
The views expressed in this article are those of the authors and do not reflect the official policy of the Department of the Air Force, Department of the Navy, Department of Defense, or the U.S. Government unless so designated by other documentation. This research was supported, in part, by Office of Naval Research Work Unit Number 61153N.MR04101.001.1603. Approved for public release; distribution unlimited.

PK7-04

VERIFYING ELECTROMAGNETIC DOSIMETRY

John M. Ziriax[1], John A. D'Andrea[1], S-T. Lu[2], S. Mathur[2], and Duane Cox[1].
[1]Naval Health Research Center Detachment, [2]McKessonHBOC BioServices
NHRC-DET, 8301 Navy Road, Brooks AFB, Texas USA 78235-5324
Tel: (210) 536-6530, Fax: (210) 536-6439, e-mail: john.ziriax@navy.brooks.af.mil

Empirical methods for characterizing biological exposures to electromagnetic radiation (EMR) have limits, require considerable expertise and are labor intensive. For this reason dosimetry modeling has become an important tool in EMR bioeffects research. We have developed several anatomically realistic data sets including rhesus monkey. Finite difference time domain (FDTD) code [1] has been adapted to use these models and output normalized specific absorption rates (SARs). The code has been parallelized and runs on a Linux cluster. Recently, the EMR source code was modularized and source modules for far field, stub, curtain, and dish antennas were created. Here we report our efforts to validate FDTD predictions using rhesus monkey carcasses. Four inline Luxtron (Santa Clara, CA) probes, a total of 16 sensors, were used to track temperature changes in the base of the brain, cortex, spinal cord and neck muscle at 800 and 500 MHz using two transmitter/horn combinations. Temperature measurements were converted to SARs [2,3]. There was a clear difference between the two transmitters (dashed vs. dotted lines); however, overall measured SARs were reasonably well approximated by FDTD predictions. FDTD results suggest the cerebral spinal fluid would experience the highest SARs.



Kunz, KS and Luebbers RJ. *"The Finite Difference Time Domain Method for Electromagnetics"*. CRC Press, Inc., Boca Raton, FL, 1993.
Gambrill, C.S. DeAngelis M.I., Lu S-T. Error analysis of a thermometric microwave-dosimetry procedure. In: Blank M, editor. *Electricity and magnetism in biology and medicine*, San Francisco: San Francisco Proess. 593-595.
Lu S-T, DeAngelis ML, Gambrill CS. Ocular microwave thermometric dosimetry and thermometry in the rabbit. In: Blank M, editor. *Electricity and magnetism in biology and medicine*. San Francisco: San Francisco Press, Inc. 675-678; 1993.

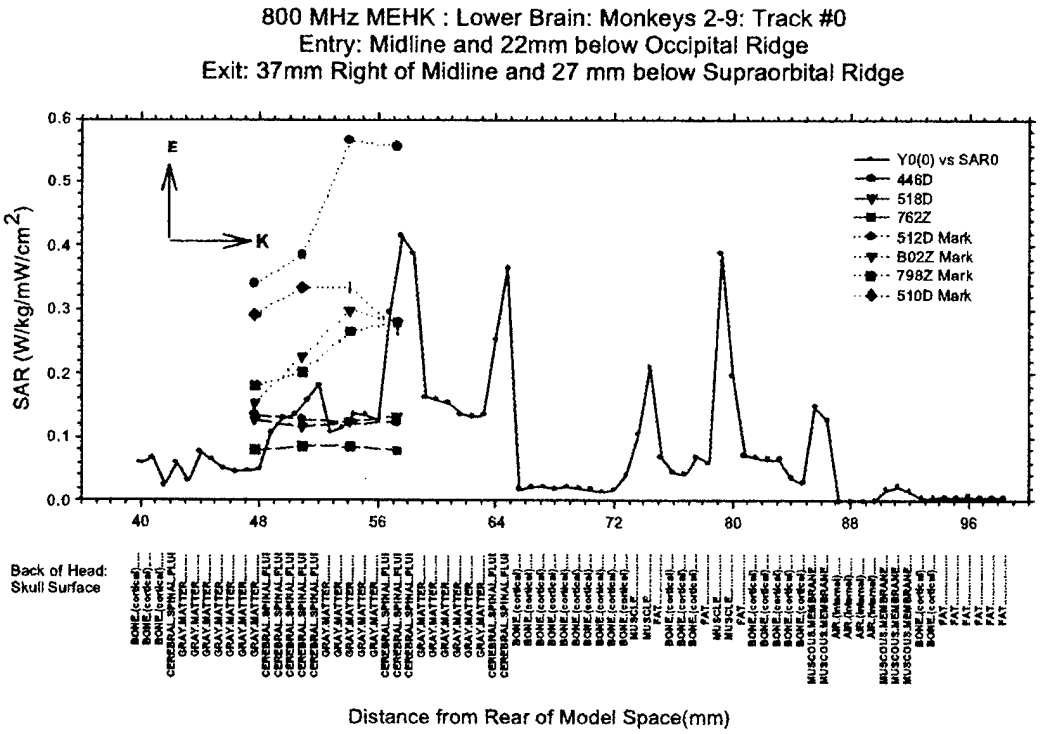
P-91

COMPARING THERMOMETRY AND FDTD PREDICTIONS: MEASUREMENT VERSUS THEORY.

J.M. Ziriax[1], J.A. D'Andrea[1], S-T. Lu[2], S. Mathur[2], D. Cox[1]*, P. Henry[1]*, K. Kosub[3]*, R. Garay[3]*, W. Hurt[4]. [1]U.S. Naval Health Research Center Detachment, Brooks AFB, TX 78235, USA. [2]McKessonHBOC BioServices, Brooks AFB, TX 78235, USA. [3]Henry M. Jackson Foundation, Inc., Brooks AFB, TX 78235, Usa. [4]U.S. Air Force Research Laboratory, Brooks AFB, TX 78235, USA.

OBJECTIVE: Verify FDTD predictions with thermometry using rhesus monkey carcasses.
BACKGROUND: U.S. Naval vessels are potentially hazardous electromagnetic environments. To further the safety of Naval personnel, the consequences of potential electromagnetic exposures must be understood. The first step in extrapolating laboratory observations to an uncontrolled exposure is accurate dosimetry. The increasing use of realistic anatomical models and RF dosimetry modeling techniques such as finite-difference time-domain (FDTD) suggests that accurate predictions of exposure can be made for complex anatomical structures. This tool would allow rapid exploration of any exposure situation. In contrast, empirical dosimetry requires expensive exposure systems, considerable expertise, animal carcasses, and substantial effort to collect data in sufficient quantities to verify even a few model predictions. However difficult, continued verification is essential to ensure model accuracy and to drive improvements in both modeling and empirical dosimetry techniques.
METHOD: FDTD computations at 500 and 800 MHz (MEHK) were used to guide the placement of 16 non-perturbing temperature probes in head and neck of 8 rhesus monkey carcasses. Probes were positioned in 4 areas predicted by the FDTD to have both relatively high and low SARs (cortex, lower brain, spinal cord and neck muscle). All probes were placed as close as possible to the midline sagittal plane. Head X-rays were used to plan sensor locations relative to anatomical landmarks. Temperature data from before, after, and during each of a series of 4 RF exposures were used to calculate SARs (Gambrill et al., 1993; Lu et al., 1993). Two RF sources were used, one having substantially higher output power (800 MHz only) than the other (800 MHz and 500MHz).
RESULTS: The figure summarizes 800 MHz data for the lower brain track of 4 temperature probes and corresponding FDTD predictions. FDTD tissue type is shown below the abscissa. There is good agreement between the predicted whole body SAR from FDTD (solid lines and small dots) and the SARs from the lower power transmitter (dashed lines), but poorer agreement with the data from the high power transmitter (dotted lines). In the final analysis, nine parallel tracks of the FDTD data rather than the single track shown in the figure will be used to approximate temperature sensor locations.
DISCUSSION: Comparing model and empirical SAR data is not entirely straightforward. Individual anatomical differences between the modeled monkey and the carcasses make it difficult is to precisely establish probe locations in the model space. In the figure, higher FDTD SARs were associated with cerebral spinal fluid, suggesting that SARs in CSF should be more closely examined. However, it may be difficult to place a probe in CSF without producing leakage into surrounding tissue. Detection of these highly localized SARs may require direct measurement of the field with a device such as a tissue implantable E-field probe. In addition, a more extensive effort to establish probe location and to identify the surrounding tissue is needed when lower power transmitters are used. The inclusion of thermal modeling in addition to electromagnetic modeling would be more useful in predicting hazards associated with EMR exposure.
Reference.
Gambrill, C.S. DeAngelis M.L., Lu S-T. Error analysis of a thermometric microwave-dosimetry procedure. In: Blank M, editor. *Electricity and magnetism in biology and medicine*, San Francisco: San Francisco Press, Inc. 593-595.
Lu S-T, DeAngelis ML, Gambrill CS. Ocular microwave thermometric dosimetry and thermometry in the rabbit. In: Blank M, editor. *Electricity and magnetism in biology and medicine.* San Francisco: San Francisco Press, Inc. 675-678; 1993.

The animals involved in this study were procured, maintained, and used in accordance with the Federal Animal Welfare Act and the "Guide for the Care and Use of Laboratory Animals," prepared by the Institute of Laboratory Animal Resources -- National Research Council." "The Air Force Research Laboratory at Brooks AFB, TX, has been fully accredited by the Association for Assessment and Accreditation of Laboratory Animal Care, International, (AAALAC) since 1967. This research was supported by Office of Naval Research Work Unit Number 61153N.MR04101.001.1603. This document is approved for public release, distribution unlimited.



P-92

SAR ANALYSIS WITH VARIETY OF THE ANTENNA STRUCTURES ON PCS HANDSET. J.D. Park[1], J.S. Kim[2], J.H. Yun[1], H.K. Kim[3], N. Kim[4]. [1]Electronics Telecommunications Research Institute, 161, Kajong-Dong, Yusong-Gu, Daejon, 305-350 Republic of Korea. [2]Songho College. [3]Aircraft Division, Aerospace Research Institute. [4]School of Electrical and Electronic Eng., Chungbuk National University, Korea.

OBJECTIVE: In this research, FDTD computer simulation is used to calculate SARs on human head caused by PCS handsets. To analyze the effect of design parameters of handset, various type of antennas are considered.

METHOD AND RESULTS: 1 g and 10 g peak averaged SARs are calculated for the type and location of antenna. The type of handset is changed and SAR distribution as depth of human head are analyzed. Among the antennas of flip type handsets, side mounted PIFA has the lowest SAR. The SARs caused by monopole antenna on folder type handset are also calculated. The handset is composed of metallic plate operating with ground, plastic case(ε_r=2.2), LCD(ε_r=2.5), button(ε_r=2.62), and antenna part. This is shown in Fig. 1.

CONCLUSION: Because the folder type handset isolates head and handset, SAR caused by folder type handset is less than that of flip type handset. SAR distributions as depth of human head of side mounted

9-6

AUTOMATING THE ANALYSIS OF THERMOMETRIC MICROWAVE-DOSIMETRY DATA FOR THE CALCULATION OF SAR. D.D. Cox[1], S.P. Mathur[2], J.A. D'Andrea[1], S-T. Lu[2]. [1]Naval Health Research Center Detachment, Brooks Air Force Base, Texas 78235 USA, McKesson HBOC BioServices, Brooks AFB, Texas, 78235 USA.

OBJECTIVE: Automate the calculations of local specific absorption rates (SARs) using the Error Analysis of a Thermometric Microwave-Dosimetry Procedure.
METHOD: Using LabVIEW version 6.1, a virtual instrument was designed to perform the Error Analysis of a Thermometric Microwave-Dosimetry Procedure developed by Gambrill, et al.(1993). This procedure is used to perfect the calculations of SAR by correcting the errors caused by the changing thermal diffusion. The process to obtain the corrected values required manual manipulation of data inside a statistical program to match the intersect points between the pre-exposure end-point and the exposure start-point and between the exposure stop-point and post-exposure start-point. This is a timely and tedious process where large amounts of data can consume several hours to complete. The automated process is able to accept existing thermometric data files with little or no modifications and to allow the user the ability to configure exposure variables. Once the data is transferred into the program it is graphed and displayed on the computer monitor. This is where the operator can manipulate the data by the point-and-click method to complete the slope-correcting phase. The automated process also enables the user to perform calculations needed to process the necessary correction factors, tissue types, and field densities to derive at normalized SAR.
SUMMARY: Normalized SAR calculations can be performed on location with the same data acquisition computer with-in moments of exposure completion. The automation of this procedure has enabled technicians to complete SAR calculations at a fraction of the time required to perform the task manually.
CONCLUSIONS: This version of the slope program is programmed as a stand-alone program that enables the user to use the program on a non-LabVIEW system. Future updates of the slope program are planned to implement this VI as an add-on to existing data collection programs. This modification would allow for real time normalized SAR calculations to be performed as data is being collected.
Supported by the Office of Naval Research Work Unit No. 601153N.M4023. This document is approved for public release; distribution is unlimited.
Reference.
Gambrill CS, DeAngelis ML, Lu S-T. 1993. Error analysis of a thermometric microwave-dosimetry procedure. In: Blank M, editor. Electricity and magnetism in biology and medicine. San Francisco: San Francisco Press. p 593-595.

9-7

SOFTWARE TOOLS TO CALCULATE THE FAR-FIELD FOR OPEN-ENDED WAVEGUIDE, PROLATE SPHERIOD SAR, THERMOMETRIC DOSIMETRY DATA, AND A 2D-FDTD MODEL COLOR-CODER. D. Hatcher[1], D. Cox[1], J. Ziriax[1], J. D'Andrea[1], S. Mathur[2]. [1]Naval Health Research Center Detachment, Brooks Air Force Base, Texas 78235 USA, [2]McKesson BioServices, Brooks Air Force Base, Texas, 78235 USA.

OBJECTIVE: A toolkit consisting of four computer programs provide the researcher with critical experimental calculations. Packaging dosimetry related programs together allows the experimenter to rapidly and accurately solve formulas that are typically required as part of a RF bioeffects experiment.
METHOD: (1) A Microsoft Excel macro (Calculations for Open-Ended Waveguide.xls) has been written to calculate the distance to the far-field when using an open-ended waveguide. Using a formula previously developed (Gandhi 1981), the macro determines the far-field distance, in meters, from the transmitted frequency, output power, distance increments and the waveguide type. The macro calculates, displays the

It is well known that heating of brain slices for a sufficient time (e.g., for 5 sec or 5 min) has an extended effect on the PS shape: the PS becomes polyphasic, which is a manifestation of hypoxia and metabolic disarray. In contrast, a 500-ms BHP never induced polyphasic PS (regardless of the temperature), indicating the prevalence of heat damage mechanisms other than hypoxia.

SUMMARY: BHP effects proved to be markedly different from those observed with a more prolonged heating. Studying the mechanisms of BHP effects in more detail will help to refine microwave exposure safety guidelines. Besides, the possibility to affect specific cell functions by BHP prompts the possibility of using it as a novel research tool in experimental biophysics and neurophysiology.

References.

1. Pakhomov et al. (2000) In: Radio Frequency Radiation Dosimetry, Kluwer Academic Publishers, Netherlands, p. 187-197.
2. 2. Pakhomov et al. (2000) *Bioelectromagnetics* 21(4), 245-254.

The work was supported by the U.S. Army Medical Research and Materiel Command and the U.S. Air Force Research Laboratory (AFOSR) under U.S. Army contract DAMD17-94-C-4069 awarded to McKesson BioServices.

P-104

COMPARATIVE EFFECTS OF CONTINUOUS-WAVE AND HIGH PEAK POWER MICROWAVE EMISSIONS ON THE INDUCTION OF LONG-TERM POTENTIATION. J. Doyle*[1], S. Mathur*[1], M.R. Murphy[2], and A.G. Pakhomov[1,2]. [1]McKesson BioServices, US Army Medical Research Detachment, and [2]Directed Energy Bioeffects Division, Human Effectiveness Directorate, Air Force Research Laboratory, Brooks Air Force Base, San Antonio, Texas, 78235-5324, USA.

INTRODUCTION: This work is a continuation of previous studies[1,2] which explored the effect of extremely-high power microwave pulses (EHPP) on the long-term potentiation (LTP) of the population spike (PS) in isolated rat hippocampal slices. Irradiation was completed shortly before induction of LTP by a brief tetanic stimulation[1]; or, conversely, the irradiation was performed when the LTP was already induced and reached its steady-state maximum[2]. In both situations, EHPP had either no effect on LTP, or produced a transient effect proportional to the temperature rise during irradiation; there was no indication of EHPP-specific ("nonthermal") effects. However, this conclusion remains incomplete without studying the effects of EHPP irradiation at the time of LTP induction and subsequent transition to the potentiated state. One can speculate that neurons may be more vulnerable during the transition, as compared to the steady-state conditions before LTP induction and after the LTP is already developed.

METHODS: The exposure, dosimetry, and physiological techniques were similar to described before[1,2]. In brief, sagittal hippocampal slices (350-μm thick) were isolated from 4- to 6-week old male Sprague-Dawley rats, fixed at the bottom of a custom-made exposure chamber, and superfused with oxygenated artificial cerebrospinal fluid at 34 °C. Refining the construction of the exposure chamber increased the efficiency of microwave absorption by about 50%, to 2 W/g per 1 W of transmitted power at 9.3 GHz. Population spikes (PS) in the CA1 neuronal area of the hippocampus were repeatedly evoked every 30 sec by stimulating *Stratum radiatum* area. LTP was induced by tetanization for 2 sec at 50 Hz.

Experiments began after a 30- to 90-min stabilization and lasted for 15 min. Each slice was used in a single experiment. In all experiments, irradiation was turned on at 1 min 45 sec, tetanization was performed at 4 min, and the radiation was turned off at 8 min 45 sec (in unexposed controls, transition to the potentiated state took about 4 min after tetanus). The main endpoints were the magnitude and time course of changes in the PS peak-to-peak amplitude after tetanization, as influenced by different regimens of microwave exposure.

The data were collected from a total of 63 successful experiments comprising 5 groups. Group 1 served as a sham-exposed control (microwaves were turned on, but routed away from the exposure chamber). Groups 2 and 3 were exposed at 0.25 W/g, groups 4 and 5 were exposed 1 W/g. This SAR was produced by a

continuous-wave (CW) radiation in the groups 2 and 4, or by EHPP in the groups 3 and 5. The EHPP pulse width was 0.5 μs in the group 3, or 2 μs in the group 5; the pulse repetition rate and peak SAR were 1 Hz and 500 kW/g in both the groups. Microwave heating reached about 0.4 °C in groups 2 and 3, and 1.6 °C the groups 4 and 5.

RESULTS: In the sham-exposed group, LTP developed within 4 min after the tetanus, and the PS amplitude stabilized at 160-170% of the initial. CW exposures slowed down the transition to the potentiated state; the effect was more pronounced in the group 4, which was exposed at the higher SAR. Potentiated amplitude of the PS after cessation of the exposure stabilized at the same level as in the sham controls. The time course of the LTP development in the EHPP-exposed groups 3 and 5 showed the same difference from the sham control group, but no difference from the CW-exposed groups. The results suggested that CW and EHPP exposures influenced LTP via some common mechanism, apparently by heating. Same as in the previous studies[1,2], we could find no indication of EHPP-specific bioeffects.

References.

1. Pakhomov et al. (2001) Abstracts of the 23rd Annual BEMS Meeting, p. 85-86
2. 2. Pakhomov et al. (2001) Record Abstracts of the 2nd ElectroMed Symposium, p. 11-12.

The work was supported by the U.S. Army Medical Research and Materiel Command and the U.S. Air Force Research Laboratory (AFOSR) under U.S. Army contract DAMD17-94-C-4069 awarded to McKesson BioServices.

P-105 Student

APOPTOSIS AND MORPHOLOGICAL CHANGES IN HIPPOCAMPUS OF RAT'S BRAIN FOLLOWING EXPOSURE TO ELECTROMAGNETIC PULSE. M.L. Zhao, X.Z. Cao, D.W. Wang* and X.M. Cuei*. Institute of Radiation Medicine, Taiping 27, Department of Pathology, Beijing 100850, China.

INTRODUCTION: Basically, electromagnetic pulse (EMP) consists of a pulse of radio-frequency waves with a nearly instantaneous rise in the electric and magnetic fields and a subsequent decline in the fields. EMP radiation may be represented as a traveling wave consisting of transverse electric and magnetic oscillating fields. An analysis of an EMP showed that it contained various frequency components extending from 0Hz to 10^9Hz. However, the pulse configuration was such that its power was mainly confined to the longer wave-lengths (<30MHz).

OBJECTIVE: EMP, an uncommon form of electromagnetic field, has been reported to cause easy fatigability, extreme irritability, aching joints and mild frontal headaches in people. Up to now, this potential hazard to man has been a matter of concern, and safety standards have not been proposed. Because that there are not enough biological data to establish firm standards. To explore the possible injury mechanism with observing the apoptosis and morphological changes on primary culture cells and Wistar rat's brain following exposure to EMP.

METHODS: EMP simulator was designed and established by National University of Defense Technology (CHINA), which provides 2.5 pulses/min with a high electric field intensity 60 KV/m, 20-nsec rise time and 25μs pulse wide. The death and apoptosis of rat hippocampal neuronal cells in primary culture following exposure to EMP were showed by MTT and flow cytometry respectively. 65 Wistar rats (weight 180±20g) were divided into exposure groups and control (sham-exposure) groups. Then the rats were killed at 1h, 6h, 12h, 24h and 48h separately. The histological sections were examined with light and electron microscopy.

RESULTS: Results show that not only happened the death of hippocampal neuron at early stage, but occurred apoptosis following exposure to EMP. MTT examine inferred EMP can promotes necrosis and apoptosis of neurons, the MTT value was significantly decreased at 0hr, 1hr and 6hrs with exposure groups (compare with control, $P<0.05$). The highest apoptosis ratio was found by flow cytometer at 6hr with hippocampus neurons. At same time, EMP could cause disturbance of center nervous system circulation,

MEETING ABSTRACT 14

9-6

AUTOMATING THE ANALYSIS OF THERMOMETRIC MICROWAVE-DOSIMETRY DATA FOR THE CALCULATION OF SAR. D.D. Cox[1], S.P. Mathur[2], J.A. D'Andrea[1], S-T. Lu[2]. [1]Naval Health Research Center Detachment, Brooks Air Force Base, Texas 78235 USA, McKesson HBOC BioServices, Brooks AFB, Texas, 78235 USA.

OBJECTIVE: Automate the calculations of local specific absorption rates (SARs) using the Error Analysis of a Thermometric Microwave-Dosimetry Procedure.
METHOD: Using LabVIEW version 6.1, a virtual instrument was designed to perform the Error Analysis of a Thermometric Microwave-Dosimetry Procedure developed by Gambrill, et al.(1993). This procedure is used to perfect the calculations of SAR by correcting the errors caused by the changing thermal diffusion. The process to obtain the corrected values required manual manipulation of data inside a statistical program to match the intersect points between the pre-exposure end-point and the exposure start-point and between the exposure stop-point and post-exposure start-point. This is a timely and tedious process where large amounts of data can consume several hours to complete. The automated process is able to accept existing thermometric data files with little or no modifications and to allow the user the ability to configure exposure variables. Once the data is transferred into the program it is graphed and displayed on the computer monitor. This is where the operator can manipulate the data by the point-and-click method to complete the slope-correcting phase. The automated process also enables the user to perform calculations needed to process the necessary correction factors, tissue types, and field densities to derive at normalized SAR.
SUMMARY: Normalized SAR calculations can be performed on location with the same data acquisition computer with-in moments of exposure completion. The automation of this procedure has enabled technicians to complete SAR calculations at a fraction of the time required to perform the task manually.
CONCLUSIONS: This version of the slope program is programmed as a stand-alone program that enables the user to use the program on a non-LabVIEW system. Future updates of the slope program are planned to implement this VI as an add-on to existing data collection programs. This modification would allow for real time normalized SAR calculations to be performed as data is being collected.
Supported by the Office of Naval Research Work Unit No. 601153N.M4023. This document is approved for public release; distribution is unlimited.
Reference.
Gambrill CS, DeAngelis ML, Lu S-T. 1993. Error analysis of a thermometric microwave-dosimetry procedure. In: Blank M, editor. Electricity and magnetism in biology and medicine. San Francisco: San Francisco Press. p 593-595.

9-7

SOFTWARE TOOLS TO CALCULATE THE FAR-FIELD FOR OPEN-ENDED WAVEGUIDE, PROLATE SPHERIOD SAR, THERMOMETRIC DOSIMETRY DATA, AND A 2D-FDTD MODEL COLOR-CODER. D. Hatcher[1], D. Cox[1], J. Ziriax[1], J. D'Andrea[1], S. Mathur[2]. [1]Naval Health Research Center Detachment, Brooks Air Force Base, Texas 78235 USA, [2]McKesson BioServices, Brooks Air Force Base, Texas, 78235 USA.

OBJECTIVE: A toolkit consisting of four computer programs provide the researcher with critical experimental calculations. Packaging dosimetry related programs together allows the experimenter to rapidly and accurately solve formulas that are typically required as part of a RF bioeffects experiment.
METHOD: (1) A Microsoft Excel macro (Calculations for Open-Ended Waveguide.xls) has been written to calculate the distance to the far-field when using an open-ended waveguide. Using a formula previously developed (Gandhi 1981), the macro determines the far-field distance, in meters, from the transmitted frequency, output power, distance increments and the waveguide type. The macro calculates, displays the

distance to far-field and draws a graph that shows the power densities (mw/cm^2) at each distance interval from the beginning of the far-field. (2) SAR.EXE calculates the SAR value for any given size prolate spheroid implementing Equation 5.10 in the Radiofrequency Radiation Dosimetry Handbook (Fourth Edition) by William D. Hurt and Luis Lozano. The program (SAR.EXE) written in Labview 6.1, simply asks the user for the height (a) and width (b) of the of the prolate spheroid (cm), the starting and ending frequency and the desired frequency intervals. The user may enter up to four different sized targets for each frequency with the peak SAR and resonant frequency displayed graphically as well as numerically. (3) Another Labview 6.1 program included in this toolkit is a procedure to automate the calculations of local SAR using the Error of Analysis of a Thermometric Microwave-Dosimetry procedure by C.S Gambrill, M.L. DeAngelis, and S. -T. Lu. This program ultimately produces normalized SAR results using the slope-correction process. The program includes features such as multiple file format acceptance, graphical representations of data, point-and-click operation and data collection for further study. (4) Also included is a procedure is to produce a color-coded display of SAR values or tissue types. A second Microsoft Excel macro (ModelCoderCoder.xls) in this toolkit will color each cell in an Excel spreadsheet according to a defined color scale for either the SAR values or tissue type data. The macro will perform several operations depending on which pull-down menu option is selected. SAR Color Coder creates a color table that will display a spectrum of colors ranging from dark purple (low SAR values) to red (high SAR values). The Tissue Type Color Coder macro creates the color table as used by (Mason et al., 1995) to create anatomical models. Each tissue type is represented by an integer and a unique color from the color table.

CONCLUSIONS: These four tools greatly reduce the time to perform frequently required calculations and will minimize human error. In the future, additional dosimetry related programs will be added as they are developed. All of these programs are available from the Naval Health Research Center Detachment upon request and are published with source code as government works.

References.
Gandhi, Om P., Microwave Engineering and Applications, Pergamon Press 1981, pp133-137
Gambrill C.S., DeAngelis M.L. and Lu, S. –T., *Error Analysis Of A Thermometric Microwave-Dosimetry Procedure*. Martin Blank, Ed Electricity and Magnetism in Biology and Medicine.

"The views expressed in this article are those of the authors and do not necessarily reflect the official policy or position of the Department of the Navy, Department of Defense, or the U.S. Government."
Supported by the Office of Naval Research Work Unit No. 601153N.M4023. This document is approved for public release; distribution is unlimited.

9-8

UMTS SIGNAL SOURCE FOR RF BIOELECTROMAGNETIC STUDIES. A. Glasmachers*, J. Streckert*, S. Gencol*, D. Rozic*, H. Ndoumbé Mbonjo Mbonjo*, A. Bitz*, V. Hansen. University of Wuppertal, Department of Electrical and Information Engineering, D-42097 Wuppertal, Germany.

INTRODUCTION: The launch of the 3rd generation universal mobile telecommunication system (UMTS) is expected for the nearest future in most European countries. With regard to the large number of additional base station antennas the public acceptance may be affected by misgivings concerning suspected adverse health effects. Being aware of this apprehensiveness and aiming at the clarification of the actual risk potential of the new UMTS features on a scientific basis a number of bioelectromagnetic experiments ('in vitro' as well as 'in vivo') have been initiated by official sponsors and by industrial associations in Germany. In order to get a set of comparable results it was decided to apply a standardized signal modulation scheme for all these investigations. Recently, the specifications of this generic UMTS test signal were defined (see References). The poster explains the implementation of the signal and the features of the developed signal generator.

OBJECTIVES: The UMTS signal to be generated differs markedly from the test signals that have been applied in experiments concerning the biological relevance of the GSM system where usually low-

BIOLOGICAL EFFECTS OF RADIO FREQUENCY PULSES

Shin-Tsu Lu

McKesson BioServices Corporation and U.S. Army Medical Research Detachment
Brooks Air Force Base, San Antonio, Texas, U.S.A.

Scientists have considered the possibility that a pulsed radio frequency radiation (RFR) can produce effects other than those by continuous-wave (CW) radiation at the same average power. Analysis of biological effects/health implications of pulsed RFR is a complicated endeavor by itself. The task is further compounded by the development of carrierless pulses that encompass a broad, risetime- and pulse duration-dependent frequency spectrum and do not produce apparent bulk heating due to a very low duty cycle.

A single RF pulse lasting from microseconds to seconds with adequate pulse energy is known to cause acute biological effects, such as brain enzyme denaturalization, stun/seizure, pain perception, decreased spontaneous activity and brain acetylcholine concentration, microwave induced whole-body movements, thermal sensation, startle modification and microwave hearing. These effects are associated with increases in tissue temperature ranging from less than 0.1 °C to more than 40 °C and pulse energy deposition from less than 10 mJ/kg to more than 57,000 J/kg in several seconds or less. The threshold for a single pulse effect appears to have a critical duration for its dependency on specific absorption.

Auditory perception of pulsed RF is the only established specific effect of pulse modulation because CW RFR is incapable of eliciting such response. Other studies on comparison between effectiveness of pulsed and CW RFRs cover a wide range of carrier frequency, modulation characteristics and biological endpoints. Differences found in these studies are usually small, disparate or not replicable. Recent provocative observations are stimulatory effect of pulsed RFR on spontaneous lymphoblastoid transformation in human lymphocytes, increased ornithine decarboxylase activity in L929 murine cells, enhanced growth rate in yeast cells and a greater increase in local skin temperature of humans exposed to pulsed RFR. Studies on carrierless pulses are rather limited at present. Nevertheless, effects in absence of overt bulk heating are delayed hypotension in rats, increased nitric oxide production in RAW 264.7 macrophages incubated in nitrate and more stress vocalizations, longer medial-to-lateral length of hippocampus and decreased mating frequency in male rats. Apparently, current knowledge regarding the effect of pulse modulation needs to be expanded. *This work is supported by a USAMRMC contract, DAMD-17-94-C-4069.*

SOME APPROACHES TO UWB DOSIMETRY

Satnam P. Mathur[1], Shin-Tsu Lu[1], Norman Harris[2], and W. D. Hurt[3], [1] McKesson BioServices, US AMRD, Brooks AFB, TX, 78235, [2] General Dynamics, Air Force Research Laboratory, HEOA, Brooks AFB, TX, 78235, [3] Air Force Research Laboratory, Brooks AFB, TX, 78235

Ultra wide band (UWB) pulses are increasingly being used in military and civilian applications. Due to the extremely high peak power and ultra-short pulse durations, validity of applying radio frequency (RF) personnel protection guidelines to such pulses is questionable. Interim guidelines for UWB exposures are based on calculation of significant sinusoid frequency to calculate free-space power density and using dosimetry handbook to calculate SAR. This procedure estimates SAR within 4% of the value calculated by FDTD simulations. Dosimetry for UWB fields to date consists of measuring fields in free-space, numerical simulations, and use of D-dot probes in liquid dielectric media. Internal fields could not be directly measured because of unavailability of small implantable E-field probes. We present some new approaches for estimating/measuring whole-body and local SAR in biological media exposed to UWB radiation. One method we have used to estimate the whole-body average SAR (WBA-SAR) is calculating the relative power spectral density of measured pulse in free-space and convolving it with the normalized WBA-SAR data from the dosimetry handbook. This yields WBA-SAR spectrum and time domain WBA-SAR waveform. For in-vitro UWB exposures, a method to measure internal E-field using simple monopole D-dot probes in liquid dielectric media has been developed. These probes allow measurement of internal UWB pulses as well as their spatial distribution with in the culture flask. Procedures are now being developed for calibrating such probes and extracting E-field waveforms from measured D-dot data. Some data from recent dosimetry study will be presented.

MEETING ABSTRACT 17

INVESTIGATION OF THE ABILITY OF UWB RF EXPOSURE TO INDUCE TRANSLOCATIONS IN HUMAN CHROMOSOMES 1, 2 OR 4 USING MULTI-COLOR FISH TECHNOLOGY. Martin L. Meltz[1], Cynthia Galindo[1], Mohan Natarajan[1], Robin Leach[2], Xavier Reveles[2], Satnam Mathur[3], and John Ashmore[3], Depts. of Radiation Oncology[1] and Cell and Structural Biology [2], Univ. of Texas Health Science Center at San Antonio, and McKesson Bioservices, USAMRD, Brooks AFB[3]

A 1 ml sample of human blood was diluted in 9 ml of pre-warmed medium with 15% HI FBS and was exposed at 37^{O} C to 90 minutes of ultrawideband RF (intermittent: repeated cycles of 30 min on, 30 min off). The exposures were begun after the cells in suspension had been allowed to settle for 30 minutes, so that they could be at the bottom of the flask where dosimetry had been performed. Immediately after the exposure, the pre-coded flasks were transported at near 37^{O} C from the GTEMS cell at Brooks AFB to the UTHSCSA. The mitogen PHA was added and the cells incubated for approximately 69 hr. Prior to the end of the incubation, colcemid was added to accumulate metaphases. Fluorescent *In Situ* Hybridization (FISH) analysis was then performed to determine if the exposure resulted in translocations between chromosomes 1, 2 and 4. The results of the first experiment will be reported.

MEETING ABSTRACT 18

INFLUENCE OF UWB RF EXPOSURE ON NUCLEAR TRANSLOCATION OF NF-*k*B IN HUMAN MM-6 MONOCYTES. Mohan Natarajan[1], Martin L. Meltz[1], Cynthia Galindo[1], John Ashmore[2], and Satnam Mathur[2], Dept. of Radiation Oncology[1], Univ. of Texas Health Science Center at San Antonio, and McKesson Bioservices, USAMRD, Brooks AFB[2]

Human monocytes (MM-6 cells) in 10 ml of pre-warmed medium with 2% HI-FBS were exposed at 37^{O} C to 90 minutes of ultrawideband RF (intermittent repeated cycles of 30 min on, 30 min off). The exposures were begun after the cells in suspension had been allowed to settle for 30 minutes, so that they would be at the bottom of the flask where dosimetry had been performed. Immediately after the exposure, the pre-coded flasks were incubated for 10 min or 3 hr, and then harvested by centrifugation and frozen. Cells to be incubated for 8 hours and 24 hr post-exposure were transported at near 37^{O} C from the GTEMS cell at Brooks AFB to the UTHSCSA. They were harvested at these times and frozen. The NF-*k*B DNA binding activity was measured by electrophoretic mobility shift analysis. The method allows for a determination of whether or not the UWB exposure could cause the translocation of the pre-existing NF-*k*B from the cytoplasm into the nucleus. The results of our initial studies will be presented. *Supported by the AFOSR.*

exposure stimulates signaling pathways that are responsible for DNA damage-induced repair mechanisms, without this being caused by DNA damage, or if RFR exposure cause alterations in the DNA that are not detected by conventional cytogenetic analysis, leading to the gene expression.
Supported by U.S. Air Force Office of Scientific Research Grant F49620-01-1-0349.

TISSUE & ORGAN – RF/ELF

P-103

THERMAL LIMITS FOR FUNCTIONAL DAMAGE AND RECOVERY IN BRAIN TISSUE AFTER A BRIEF (500 MS) HIGH-INTENSITY MICROWAVE EXPOSURE. A.G. Pakhomov[1,2], J. Doyle[*1], J. Ashmore[*1], and M.R. Murphy[2]. [1]McKesson BioServices, US Army Medical Research Detachment, and [2]Directed Energy Bioeffects Division, Human Effectiveness Directorate, Air Force Research Laboratory, Brooks Air Force Base, San Antonio, Texas, 78235-5324, USA.

OBJECTIVE: While thermal effects of microwaves have been studied intensively for decades, little is known about the bioeffects of brief (sub-second) heat pulses (BHP). This lack is explained, at least in part, by technical problems in producing and accurately measuring BHPs. In the absence of actual data, BHP effects can only be extrapolated from findings at longer exposures. However, extrapolation fails to acknowledge the possibility of triggering qualitatively different biophysical mechanisms by BHP, resulting in erroneous predictions. This study is the first attempt to analyze BHP functional effects in brain tissue *in vitro*.
METHODS: The experiments were performed in sagittal hippocampal slices (350-μm thick) isolated from the brain of 4- to 6-week old male Sprague-Dawley rats. The slices were held at the bottom of the exposure bath and superfused with an artificial cerebrospinal fluid (ACSF) at 34 °C. Nerve fibers of the *Stratum radiatum* area were stimulated at 10-sec intervals, which evoked excitatory postsynaptic potentials (EPSP) and population spikes (PS) in the CA1 area. A BHP was caused by a single 500-ms train of microwave pulses (9.6 GHz, 2-μs width, 800 kW/g peak SAR). Temperature reached maximum by the end of the train, which was exactly 10 ms prior to the next stimulus. Cooling back to 34 °C was complete within 1-2 s after the train. Temperature rise was controlled by the pulse repetition rate in the train, up to 24-28 °C at 160-200 p.p.s. Each brain slice was exposed to several BHPs, with time intervals sufficient for complete EPSP and PS recovery. Temperature in the slice was measured by a microthermocouple; the accuracy of this technique was justified earlier[1,2] and validated again by comparing with readings of a Nortech fiber optic sensor.
RESULTS AND DISCUSSION: We identified three temperature ranges that correspond to three different types of biological response: (1) Heating up to 48-49 °C caused instant PS suppression, followed by instant and complete recovery as soon as the temperature returned to pre-heating level. Even the most profound instant suppression (by 100%) showed no consequences for the function of the brain slice afterwards. BHP effects within this temperature range seem to be just a "passive" response, i.e., due to temperature-induced changes in physico-chemical properties and the rate of chemical reactions. (2) Heating to temperatures from 48-49 to 58-59 °C caused both instant and delayed PS suppression. The complete (by 100%) instant suppression was followed by a brief recovery (for some 20-50 sec) and then by a delayed suppression. Most remarkable, the magnitude and duration of the delayed suppression were exponentially dependent on the temperature reached during the exposure, and could be characterized by a Q_{10} index (which normally applies to changes **during** the period of elevated temperature, not after it). PS recovery after the delayed suppression usually was complete, even though it could take up to 1-2 hours. We interpret the delayed suppression as an "active" response (i.e., not just physico-chemical, but physiological). We observed no adaptation or sensitization to repeated BHPs. (3) Temperatures in excess of 59-61 °C caused instant and irreversible suppression of PS and EPSP. However, pre-synaptic potentials could recover even after this extreme heating.

It is well known that heating of brain slices for a sufficient time (e.g., for 5 sec or 5 min) has an extended effect on the PS shape: the PS becomes polyphasic, which is a manifestation of hypoxia and metabolic disarray. In contrast, a 500-ms BHP never induced polyphasic PS (regardless of the temperature), indicating the prevalence of heat damage mechanisms other than hypoxia.

SUMMARY: BHP effects proved to be markedly different from those observed with a more prolonged heating. Studying the mechanisms of BHP effects in more detail will help to refine microwave exposure safety guidelines. Besides, the possibility to affect specific cell functions by BHP prompts the possibility of using it as a novel research tool in experimental biophysics and neurophysiology.

References.

1. Pakhomov et al. (2000) In: Radio Frequency Radiation Dosimetry, Kluwer Academic Publishers, Netherlands, p. 187-197.
2. 2. Pakhomov et al. (2000) *Bioelectromagnetics* 21(4), 245-254.

The work was supported by the U.S. Army Medical Research and Materiel Command and the U.S. Air Force Research Laboratory (AFOSR) under U.S. Army contract DAMD17-94-C-4069 awarded to McKesson BioServices.

P-104

COMPARATIVE EFFECTS OF CONTINUOUS-WAVE AND HIGH PEAK POWER MICROWAVE EMISSIONS ON THE INDUCTION OF LONG-TERM POTENTIATION. J. Doyle[*1], S. Mathur[*1], M.R. Murphy[2], and A.G. Pakhomov[1,2]. [1]McKesson BioServices, US Army Medical Research Detachment, and [2]Directed Energy Bioeffects Division, Human Effectiveness Directorate, Air Force Research Laboratory, Brooks Air Force Base, San Antonio, Texas, 78235-5324, USA.

INTRODUCTION: This work is a continuation of previous studies[1,2] which explored the effect of extremely-high power microwave pulses (EHPP) on the long-term potentiation (LTP) of the population spike (PS) in isolated rat hippocampal slices. Irradiation was completed shortly before induction of LTP by a brief tetanic stimulation[1]; or, conversely, the irradiation was performed when the LTP was already induced and reached its steady-state maximum[2]. In both situations, EHPP had either no effect on LTP, or produced a transient effect proportional to the temperature rise during irradiation; there was no indication of EHPP-specific ("nonthermal") effects. However, this conclusion remains incomplete without studying the effects of EHPP irradiation at the time of LTP induction and subsequent transition to the potentiated state. One can speculate that neurons may be more vulnerable during the transition, as compared to the steady-state conditions before LTP induction and after the LTP is already developed.

METHODS: The exposure, dosimetry, and physiological techniques were similar to described before[1,2]. In brief, sagittal hippocampal slices (350-μm thick) were isolated from 4- to 6-week old male Sprague-Dawley rats, fixed at the bottom of a custom-made exposure chamber, and superfused with oxygenated artificial cerebrospinal fluid at 34 °C. Refining the construction of the exposure chamber increased the efficiency of microwave absorption by about 50%, to 2 W/g per 1 W of transmitted power at 9.3 GHz. Population spikes (PS) in the CA1 neuronal area of the hippocampus were repeatedly evoked every 30 sec by stimulating *Stratum radiatum* area. LTP was induced by tetanization for 2 sec at 50 Hz.

Experiments began after a 30- to 90-min stabilization and lasted for 15 min. Each slice was used in a single experiment. In all experiments, irradiation was turned on at 1 min 45 sec, tetanization was performed at 4 min, and the radiation was turned off at 8 min 45 sec (in unexposed controls, transition to the potentiated state took about 4 min after tetanus). The main endpoints were the magnitude and time course of changes in the PS peak-to-peak amplitude after tetanization, as influenced by different regimens of microwave exposure.

The data were collected from a total of 63 successful experiments comprising 5 groups. Group 1 served as a sham-exposed control (microwaves were turned on, but routed away from the exposure chamber). Groups 2 and 3 were exposed at 0.25 W/g, groups 4 and 5 were exposed 1 W/g. This SAR was produced by a

EFFECT OF HIGH-POWER MICROWAVE PULSES ON SYNAPTIC TRANSMISSION AND PLASTICITY IN BRAIN NEURONS

A.G. Pakhomov[1,2], J. Doyle[1], and M.R. Murphy[2]

[1]McKesson BioServices Corporation, US Army Medical Research Detachment
[2]Directed Energy Bioeffects Division, Human Effectiveness Directorate
Air Force Research Laboratory
Brooks Air Force Base, San Antonio, Texas, 78235-5324, USA.

Extremely high power pulses (EHPP) emitted by modern high-peak-power microwave transmitters represent a new and potentially hazardous environmental factor. We explored EHPP effects on neuronal function in isolated rat hippocampal slice model. Slices were exposed in a custom-made chamber at following parameters: carrier frequency, 9.3 or 9.6 GHz; pulse width, 0.5 to 2 μs; pulse repetition rate, 0.5 to 10 Hz; peak specific absorption rate (SAR), 330 to 780 kW/g; time-average SAR, 0.25 to 3.6 W/g; exposure duration, 2 to 30 min. Microwave heating, as measured with a miniature fiber optic probe or a microthermocouple, varied from 0.3 to 6 oC. In some experiments, effects of EHPP exposure were compared to those of a continuous-wave (CW) radiation at equal time-average SAR. Each brain slice was exposed or sham-exposed only once. Experiments with different regimens of microwave exposure and sham-exposed controls were alternated randomly. Excitatory postsynaptic potentials and population spikes (PS) in the CA1 neuronal field were recorded extracellularly with a glass micropipette following Shaffer collateral stimulation. Plasticity phenomena studied were paired-pulse facilitation (as induced by paired stimuli with a 20-ms interval) and long-term potentiation (as induced by a 2-sec, 50-Hz tetanus). In different experiments, the tetanus was applied before, during, or after irradiation.

The data were collected in more than 190 experiments, which comprised 4 independent series. The only effect observed was a transient and fully reversible decrease in the PS amplitude during irradiation. Apparently, this effect was an ordinary thermal response: it was proportional to the temperature rise but not to any specific parameter of EHPP, and it could also be induced by CW irradiation or conventional heating. The experiments did not reveal any EHPP-specific or nonthermal effects on synaptic transmission and plasticity.

The work was supported by the U.S. Army Medical Research and Materiel Command and the U.S. Air Force Research Laboratory (AFOSR) under U.S. Army contract DAMD17-94-C-4069 awarded to McKesson BioServices Corporation.

Abstract Title: DELAYED AND REVERSIBLE SUPPRESSION OF EVOKED ACTIVITY IN CA1 AREA OF HIPPOCAMPAL SLICES BY BRIEF HEAT PULSES

Contributing Authors: A. Pakhomov[1,2*]; J. Doyle[1]; M. Murphy[2]

Institutions: 1. McKesson BioServices, Brooks AFB, San Antonio, TX, USA

2. Air Force Research Laboratory, Brooks AFB, San Antonio, TX, USA

Key words: microwaves, hyperthermia, synaptic suppression

Abstract: In studying effects of temperature on brain tissue, reducing the heat exposure duration helps to prevent consequences of unbalanced metabolism, such as hypoxia. Using brief heat pulses (HP) generated by a 500-ms burst of high-power microwaves, temperatures up to 60-62 °C were reached without causing permanent damage. This allowed us to observe a new phenomenon of delayed suppression (DS) of extracellular EPSP and population spike (PS) evoked in CA1 area by Shaffer collateral stimulation. The threshold for DS induction was at 48-49 °C. At this temperature (i.e., during the HP) no EPSP or PS could be elicited, but both recovered within a few seconds as the temperature dropped back to 34 °C. DS developed with a 20-50 sec latency after the HP and could last from 5-10 min to 1-2 hours. The DS magnitude and duration were exponentially dependent on the temperature reached during the HP, and could be characterized by a Q_{10} index. Recovery from the DS usually was complete unless the HP exceeded 60 °C. PS and EHPP shapes were essentially unaffected and never changed to polyphasic (whereas a longer heating, e.g. for 5 sec, always caused polyphasic PS). DS could be repeatedly induced in the same brain slice, without signs of adaptation or sensitization. DS of the PS decreased when PS was made bigger (by rising stimulus intensity or by inducing LTP), whereas DS of the EPSP did not change. DS of the PS appears to be a secondary event, fully mediated by DS of the EPSP. This implies a transient inhibition of synapse function as most likely mechanism of DS.
Supported by: USAMRMC and AFOSR under contract DAMD17-94-C-4069 to McKesson

cells exposed for 48 hours to GSM-900 at 0.2 W/kg; lane 4: cells exposed to RF and LPS plus cytokines for 48 hours ; lane 5 sham-exposed C6 cells; lane 6 : sham-exposed C6 cells treated with LPS plus cytokines for 2 days; lane 7 : molecular weight markers. Arrow on the left stands for p^{130} NOS2

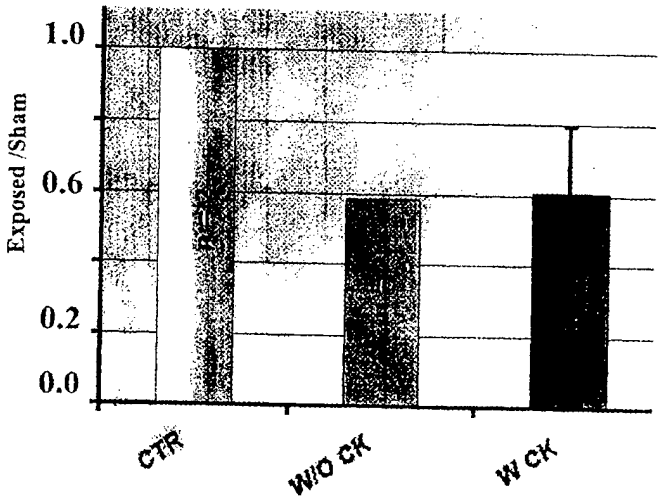


Figure 2: Effect of GSM-900 on the NOS2 expression. A 40% decrease was measured in samples exposed to GSM-900 either without (W/O CK) or with (W CK) LPS plus cytokine (CK) treatment. CTR is 100% of NOS2 expression either in sham-exposed samples or after CK treatment for the evaluation of the effect of GSM-900 alone or in combination with CK, respectively.

13-6

NEURODEGENERATION FROM MICROWAVE AND NEUROTOXIN EXPOSURE. R.L. Seaman, S.-T. Lu. McKesson Clinical Services and USAMRD Microwave Bioeffects Branch, Brooks AFB, Texas, USA.

OBJECTIVE: To investigate effects of microwave exposure on neurodegeneration in the CNS nigrostriatal system using toxin-induced degeneration in animal models. These models represent the basal ganglia and brainstem degeneration indicated in certain veterans.
METHODS: Two animal models are being studied in which mitochondrial ATP production is inhibited by specific action of neurotoxins on electron transport. In one model, 4-month old male Sprague-Dawley rats are injected intraperitoneally with 3-nitropropionic acid (3-NP). For a range of 3-NP doses, degeneration processes occur selectively in the caudate-putamen to provide a model of Huntington's disease. In the other model, male Lewis rats are implanted with osmotic pumps to deliver systemic rotenone chronically. With the proper dose of rotenone, degeneration occurs primarily in the substantia nigra and caudate-putamen to provide a model of Parkinson's disease. After animals are treated with neurotoxin in our work they are exposed to 6-μs, 1.25-GHz pulses generated by an FPS-7 radar transmitter at 10 Hz repetition frequency. Nigrostriatal function is assessed after neurotoxin and microwave treatments by testing spontaneous locomotor activity, acoustic startle, and forelimb use. Neuronal structure is assessed by means of light and electron microscopy.
RESULTS: Combined effects of microwave exposure and 3-NP have been seen in prepulse inhibition of acoustic startle and in the ultrastructure of caudate-putamen output neurons. This study is currently being

91

replicated. The rotenone model is being developed for use with microwave exposure by establishing appropriate dose and duration of delivery.

CONCLUSIONS: In the 3-NP model, combined effects of microwave exposure and 3-NP are not always synergistic as one might expect from previous reports of neuropathology after microwave exposure. Both the 3-NP and rotenone models provide the means by which combined actions of environmental chemicals, physical trauma, and/or electromagnetic fields can be studied *in vivo*. These environmental factors and their applications can be selected to simulate military occupational exposures. Use of neurotoxin-induced neurodegeneration models also allows level, duration, and sequence of simulated exposures to be controlled and studied.

Supported by the U.S. Army Medical Research and Materiel Command under contract DAMD17-94-C-4069 awarded to McKessonHBOC BioServices. The views, opinions and/or findings contained in this report are those of the authors and should not be construed as an official Department of the Army position, policy or decision. In conducting this research, the investigator(s) adhered to the "Guide for the Care and Use of Laboratory Animals," prepared by the NRC Institute of Laboratory Animal Resources.

SESSION 14: Special Symposium IVB: Presentation of REFLEX Results
Chair: Franz Adlkofer

14-1

RISK EVALUATION OF POTENTIAL ENVIRONMENTAL HAZARDS FROM LOW ENERGY ELECTROMAGNETIC FIELD EXPOSURE USING SENSITIVE IN VITRO METHODS (REFLEX) - INTRODUCTION.

F. Adlkofer[1], H. Dertinger[1], R. Tauber[2], R. Fitzner[2], K. Schlatterer[2], O. Jahn[3], H.W. Ruediger[3], E. Diem[3], S. Ivancsits[3], A.M. Wobus[4], J. Czyz[4], A. Trillo[5], A. Ubeda[5], D. Leszczynski[6], S. Joenväärä[6], R. Kuokka[6], J. Reivinen[6], H.A. Kolb[7], F. Bersani[8], C. Franceschi[8], I. Lagroye[9], B. Veyret[9], N. Kuster[10], J. Schuderer[10], F. Clementi[11], D. Fornasari[11], C. Gotti[11], C. Maercker[12]. [1]VERUM Foundation, Munich, Germany; [2]Dept. Clinical Chemistry, University Hospital Benjamin Franklin, Free University of Berlin, Germany; [3]Div. of Occupational Medicine, University of Vienna, Austria; [4]In vitro Differentiation Group, IPK, Gatersleben, Germany; [5]Insalud, Ramon y Cajal Hospital, Madrid, Spain; [6]STUK - Radiation and Nuclear Safety Authority, Helsinki, Finland; [7]Institute of Biophysics, University of Hannover, Germany; [8]Dept. of Physics, University of Bologna, Italy; [9]PIOM, Ecole National Supérieure de Chimie et de Physique, Bordeaux, France; [10]IT'IS, Swiss Federal Institute of Technology (ETH), Zurich, Switzerland, [11]Dept. of Medical Pharmacology, University of Milan, Italy, [12]Resource Center for Genome Research, Heidelberg; Germany.

INTRODUCTION: Although the biological effects of EMF exposure have been under study for the past 30-40 years, no consensus has been achieved with respect to either findings or their interpretation. The reasons for this are numerous: difficulties in measuring EMF exposure at the putative sites of action, vast differences in exposure and experimental conditions and the complete lack of agreement on biological endpoints appropriate for study. In the REFLEX project essential central elements in the function of various cell systems and in the development of disease are investigated using the most powerful molecular biological tools currently available. This will ensure a better understanding of the biological effects of EMFs, which is the prerequisite for an objective assessment of potential health hazards and perhaps also of potential therapeutic effects.

PROJECT OBJECTIVES AND STRUCTURE: Twelve research groups from all over Europe cooperate within the REFLEX project. The following five priority areas condensed in workpackages are investigated under strictly controlled conditions : 1. Direct and indirect genotoxic effects of EMFs. 2. Effects of EMFs on differentiation and function of embryonic stem cells. 3. Effects of EMFs on gene expression and protein targeting. 4. Effects of EMFs on the immune system.

MF exposure in rats. After short- term exposure a simulation effect on the immune system was observed and we could thus conclude that the response of the immune system to magnetic fields depend on the duration of exposure. More work is needed to understand the biological significance of the observed effects.

11-5

SINGLE EXPOSURE TO PULSED MICROWAVES AT 0.6 W/KG DOES NOT MODIFY LOCOMOTOR ACTIVITY OR ACOUSTIC STARTLE IMMEDIATELY AFTER EXPOSURE.

R.L. Seaman, S.P. Mathur*, and A.M. Phinney*. McKesson Clinical Services and USAMRD Microwave Bioeffects Branch, Brooks AFB, Texas 78235 USA.

OBJECTIVE: Spontaneous motor activity and acoustic startle were used to test for immediately manifested effects in rats exposed for 30-min to microwave pulses.
METHODS: Twelve male Sprague-Dawley rats weighing 508±54 g (mean±st.dev.) aged 4-5 months were used. Six animals were exposed to 1.25-GHz 6-μs microwave pulses at 10 Hz for 30 min at specific absorption rate (SAR) 0.6 W/kg. Six animals were sham exposed under otherwise identical conditions. Spontaneous motor activity was measured for 5 min in a 40.8x40.8 cm AccuScan activity monitor, starting within 6 min after exposure. Interruptions of infrared beams in the monitor were detected under computer control to provide measures of horizontal movement, vertical movement (rearing), and stereotypy (rapid, repeated movements). Immediately after activity testing, whole-body startle response to 20-ms bursts of 120-dBA broadband noise was measured. Prepulses 0, 3, 6, or 12 dBA above a 70-dBA background level were delivered to produce prepulse inhibition (PPI) of the startle response. Wilcoxon rank sum (Mann-Whitney U-test), Friedman two-way ANOVA by ranks, and nonparametric Newman-Keuls multiple comparisons were used to test for differences.
RESULTS: Colonic temperature increased on average by 0.20 and 0.52°C for sham- and microwave-exposed groups, respectively; however, the increase was not different between the groups (2-tailed t-test, p=.65). No significant difference was found between the groups for overall activity, horizontal activity (number of movements, distance), or vertical activity (number of counts, number of movements). No significant difference was found between the exposure groups for overall stereotypy activity or the number of stereotypy episodes. The total duration of stereotypical movements was different between groups (Wilcoxon p=.037) with the duration of the sham-exposed group greater than that of the microwave-exposed group (medians: 61.2 and 48.6 s, means 60.8 and 47.3 s). No significant difference between the exposure groups was found in amplitude of the startle response or its within-session habituation. Significant differences were indicated in PPI of startle (Friedman $F(6,5)$=19.43, p=.0016). The differences were all found to be in prepulse intensity and did not depend on the type of exposure.
CONCLUSIONS: Only one behavioral variable that was measured in this study was affected by the 30-min, 0.6-W/kg-microwave exposure with the pulse parameters used. This indicated that the exposure used did not affect the neural circuits underlying the majority of behaviors, or did not affect them enough to be reflected in the measures used. The reduction in duration of stereotypical movements after microwave exposure might indicate a change in the basal ganglia circuits that are involved in motor stereotypy. However, the reduction may be of minor biological significance because it was not accompanied by a significant change in two other measures of stereotypy.
Supported by the U.S. Army Medical Research and Materiel Command under contract DAMD17-94-C-4069 awarded to McKessonHBOC BioServices. The views, opinions and/or findings contained in this report are those of the authors and should not be construed as an official Department of the Army position, policy or decision. In conducting this research, the investigator(s) adhered to the "Guide for the Care and Use of Laboratory Animals," prepared by the NRC Institute of Laboratory Animal Resources.

METTING ABSTRACT 24

Abstract for 2002 Society for Neuroscience meeting

RAT SHORT-TERM STARTLE PREPULSE INHIBITION AND SOME MOTOR ACTIVITIES AFTER TWO MICROWAVE EXPOSURES ARE CHANGED BY 3-NP. R.L. Seaman*; S.P. Mathur; A.M. Phinney; A.S. Garcia; J.L. Ashmore. McKesson Clinical Services at WRAIR USAMRD, Brooks AFB, TX, USA.

Male Sprague-Dawley rats (4-6 months old, 512-613 g) were exposed on two consecutive days for 30 min to 1.25-GHz microwave pulses (5.9 μs, 10 Hz) at 0, 0.6, or 6.0 W/kg whole-body specific absorption rate. Intraperitoneal injection of 0 or 10 mg/kg 3-nitroproprionic acid (3-NP) was given 1.5 h before an exposure. Spontaneous motor activity for 10 min (N=7/condition) and acoustic startle (N=12/condition) were measured starting 1.5 h after the second microwave exposure. The main effect of 3-NP was significant for vertical (VER) and stereotypical (STR) activity variables, due to decreases after exposure at 0.6 and 6.0 W/kg when 10 mg/kg 3-NP had been given, but not for horizontal (HOR) variables. HOR, VER, and STR variables did not change after 10 mg/kg 3-NP alone or 0.6 W/kg alone and increased only slightly after 6.0 W/kg alone. Startle amplitude and within-session habituation were not different among conditions. After exposure at 0.6 or 6.0 W/kg, startle prepulse inhibition (PPI) was unchanged for 0 mg/kg 3-NP but smaller for 10 mg/kg 3-NP. As shown here, 3-NP-induced chemical hypoxia, which alone did not change activity or startle, altered the effect of microwave exposure at both 0.6 and 6.0 W/kg on VER and STR activity and startle PPI. This indicates some form of interaction that is most likely occurring in neural circuits that include the caudate-putamen. Supported by US Army MRMC contract DAMD17-94-C-4069. Investigator(s) adhered to the "Guide for the Care and Use of Laboratory Animals".

SfN 2002beh+PPIrev.doc
10/21/2002 12:52 PM

P-174-C

HIGH-POWER MICROWAVE PULSES PHASED WITH EVOKED SYNAPTIC POTENTIALS MAY AFFECT SYNAPTIC TRANSMISSION. J. Doyle*[1], M.R. Murphy[2], A.G. Pakhomov[1,2]. [1]McKesson BioServices, US Army Medical Research Detachment, [2]Directed Energy Bioeffects Division, Human Effectiveness Directorate, Air Force Research Laboratory, San Antonio, TX, 78235-5324, USA.

INTRODUCTION: Our previous studies of bioeffects of extremely high power pulses (EHPPs) in excitable tissues (isolated brain and heart slices) did not reveal any specific effects of this radiation modality [1,2]. In this study, we explored if EHPPs may cause different effects when they are applied in synchronism with membrane excitation events.

METHODS: Parasagittal hippocampal slices (350-μm thick) were isolated from 4- to 6-week old male Sprague-Dawley rats, fixed at the bottom of a custom-made exposure chamber, and superfused with oxygenated artificial cerebrospinal fluid at 34 °C. Excitatory postsynaptic potentials (EPSPs) in CA1 field were evoked by twin pulse stimulation of Schaffer collateral (20 ms interpulse interval, 1 pair/15 sec) and recorded extracellularly with a glass micropipette (2-8 Mohm). In each experiment, EPSPs were recorded for 5 min prior to exposure (baseline, taken as 100%), for 5 min during exposure or sham exposure, and for 5 more min after irradiation. All exposures were performed at 9.6 GHz, using 2-μs pulses at 740 kW/g. EHPPs were synchronized with the 1st electrical stimulus in the pair, to come either 2 ms prior to the stimulus (regimen A), or after it with a delay of 1, 3.5-4.5, or 14-15 ms (regimens B, C, and D, respectively). These delays corresponded to the action potential propagation through neuronal terminals to synapses (B), EPSP rising phase (C), and a "silent" interval between the conditioning and test EPSPs (D). Each EHPP pulse briefly raised the temperature by 0.3-0.4 °C; however, 15-sec intervals between EHPPs allowed more than enough time for heat dissipation and the overall heating was negligible. In addition to these regimens, we tested the effect of EHPPs applied at a 1-Hz rate independent from stimulation; this exposure increased the temperature by 2 °C and was primarily intended to serve as a positive control (regimen P). Each successful preparation was used in several experiments; the sequence of regimens was determined by rolling a die. Amplitudes of the conditioning and test EPSPs throughout the experiment were measured automatically, with a help of an MP100 data acquisition system (BIOPAC), and normalized to their average pre-exposure value.

RESULTS: Each exposure regimen was tested in 13-14 brain slice preparations. In sham-, A-, B-, and D-experiments, the amplitude of both EPSPs stayed within ±10% of the baseline level. Some EPSP changes in the above groups remarkably coincided in time with the onset and the cessation of exposure; however, these changes were not statistically significant. In contrast, C-regimen caused a profound suppression of the conditioning EPSP, which developed gradually during the first 2-3 min of exposure. During the last minute of exposure, EPSP was at 81±7% (sham, at 107.5±5%, $p<0.01$, 2-tailed *t*-test) and showed only a minor, if any, recovery by the end of the experiment (84±7% versus 104.8±4.2% in sham control, $p<0.02$). Moreover, this dynamics of changes was different from the positive control group, in which the EPSP also fell to about 80% during exposure, but effectively recovered to over 100% afterwards. Changes in the amplitude of the test EPSP (the 2nd in the pair) in C-group were less pronounced, but also indicative of the exposure effect.

DISCUSSION: EPSP decrease during exposure in the C group can, at least in part, be explained by distortion of the EPSP signal by EHPP interference, which might affect the accuracy of measurements (although every effort was made to minimize the distortion). However, continued suppression of EPSP after the exposure, or suppression of the test EPSP cannot be easily explained at this time. Replicative experiments will need to be performed to validate the suspected EHPP effect and to explore its underlying mechanisms

References:

1. Pakhomov et al., Bioelectromagnetics 2000, 21(4), 245-254. 2. Pakhomov et al., Bioelectromagnetics 2003 (in press).

The work was supported by the U.S. Army Medical Research and Materiel Command and the U.S. Air Force Research Laboratory under U.S. Army contract DAMD17-94-C-4069 awarded to McKesson BioServices.

© The Bioelectromagnetics Society

MEETING ABSTRACT 26

11-2

MICROWAVE-INDUCED RESPONSES OF COLONIC TEMPERATURE AND SERUM CORTICOSTERONE CONCENTRATION IN RATS ARE SUSCEPTIBLE TO CHANGING EXPERIMENTAL CONDITIONS. S.T. Lu, McKesson BioServices Corporation/U.S. Army Medical Research Detachment, Microwave Bioeffects Branch, Brooks City-Base Texas 78235, USA.

INTRODUCTION: Microwave exposure of significant intensity and duration can induce increases in colonic temperature and serum coritcosterone concentration in rats [1,2] and in the monkey [3]. In well-controlled experiments, adrenocorticcal activation was not observed in absence of a significant hyperthermia. Thermal dependency of microwave-induced adrenocortical activation has not been evaluated in various experimental conditions that can alter the thermal response and subsequently the degree of adrenocortical activation.

OBJECTIVE: The objective of this study is to evaluate the thermal dependency of microwave-induced adrenocortical activation by changing experimental conditions to achieve decreased hyperthermic response through facilitated heat loss (hair removal) and enhanced hyperthermic response by increasing ambient temperature above normally used in the laboratory. In addition, microwave-induced hyperthermia and adrenocortical activation in rats during quiescent (diurnal) and active (nocturnal) phases of circadian rhythm were also compared.

METHOD: Male Long-Evans rats (Charles River Breeding Laboratories, Inc., Wilmington, Mass) were used. They were maintained at 12-h light-dark cycle (light: 0800 to 2000 h), 24 ± 1 °C, feed and water *ad libitum*. Animals were acclimated to experimental procedures including 2 weeks of handling and 3 simulated exposures. After acclimation, animals were subjected to sham or microwave exposures for 2 hours (1200-1400 h) after a three-hour equilibration period between 0900 and 1200 h. Microwave exposures were performed in an anechoic chamber. The microwave was 2.45 GHz and 120 Hz amplitude modulated at 0, 1 (0.21 W/kg), 10 (2.1 W/kg), 20 (4.2 W/kg), 30 (6.3 W/kg), 40 (8.4 W/kg) and 50 mW/cm^2 (10.5 W/kg). Colonic temperature (Tco) was measured immediately after exposure. Serum obtained after decapitation was frozen until assay for corticosterone concentration (CS) by a competitive protein-binding assay. Exposure conditions were: (1). 24 °C diurnal exposure, (2). Facilitated heat loss (by hair removal 24 h prior to exposure under barbiturate anesthesia, additional group was exposed at 12.6 W/kg) and 24 °C diurnal exposure, (3). 24 °C diurnal exposure in an anechoic chamber within an environmental chamber, (4). 28 °C diurnal exposure in an anechoic chamber within an environmental chamber, and (5). 24 °C nocturnal exposure in animal acclimated to reversed light-dark cycle (light on: 2000 to 0800 h) for 4 weeks. A minimum of 8 animals was used in each treatment.

RESULTS: Facilitated heat loss increased thresholds for microwave-induced hyperthermia from 2.1 W/kg to 6.3 W/kg and microwave-induced elevation in CS from 6.3 W/kg to 8.4 W/kg (Fig. 1).

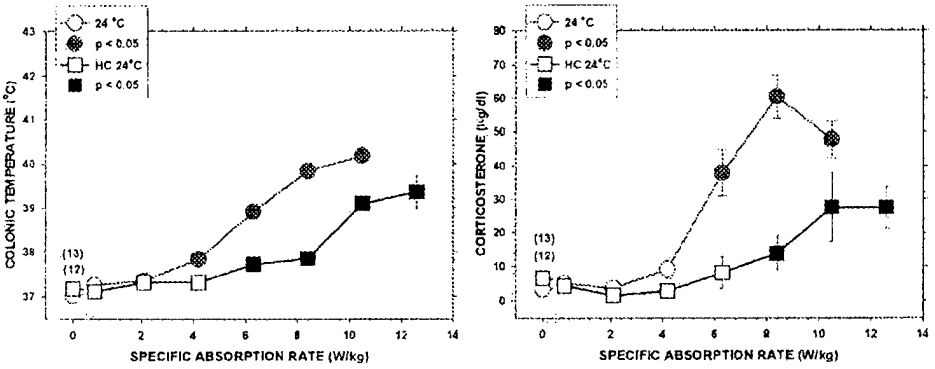


Figure 1. Effects of facilitated loss on microwave-induced hyperthermia and elevation in serum corticosterone concentration.

Elevated ambient temperature from 24 °C to 28 °C in an environmental chamber decreased both thresholds for microwave-induced hyperthermia and microwave-induced CS elevation from 6.3 W/kg to 4.2 W/kg (Fig. 2). Rats could not tolerate a 2-hour exposure at 10.5 W/kg (lethality= 4/8) at 28 °C. Spontaneous activity increases during the light off period. Increased spontaneous activities were evident by the elevations in Tco also in CS in nocturnally sham-exposed animals (Fig. 3). Threshold for alteration in Tco was not changed when microwave exposure was

© The Bioelectromagnetics Society

11-2 (Cont'd)

performed during light off. However, Tco decreased from sham-exposure baseline in animal nocturnally exposed at 2.1 and 4.2 W/kg. Hyperthermia induced by diurnal and nocturnal microwave exposures at 6.3 W/kg or higher did not vary from each other. Intolerance was also found in rats exposed nocturnally at 10.5 W/kg (lethality= 3/15). Due to an elevated baseline CS, threshold for increased CS raised from 6.3 to 8.4 W/kg.

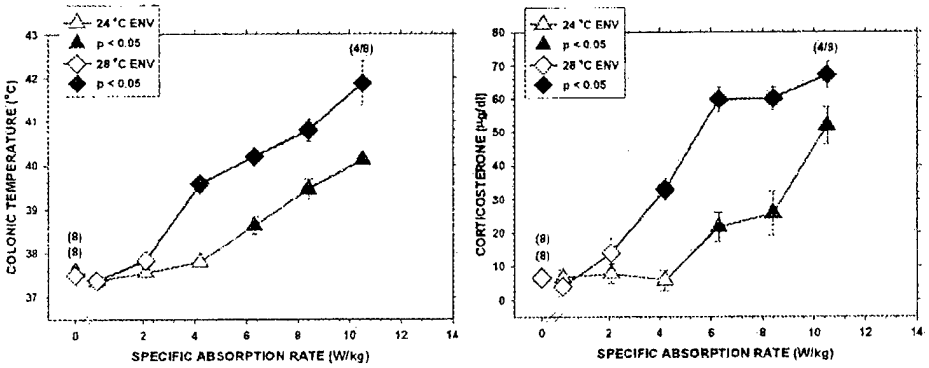


Figure 2. Effects of increased ambient temperature on microwave-induced hyperthermia and elevation of serum corticosterone concentration.

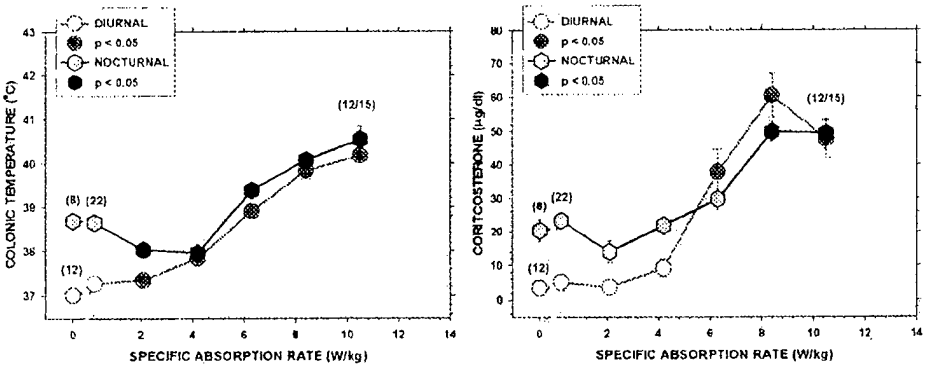


Figure 3. Comparison between nocturnal and diurnal exposures on microwave-induced changes in colonic temperature and elevation of serum corticosterone concentration.

CONCLUSION: Adrenocortical activation during microwave exposure is clearly a thermal effect dependent on the magnitude of induced hyperthermia. Environmental conditions that modify effective heat storage, i.e., core body temperature, can therefore alter the magnitude of adrenocortical activation as indicated by elevation in serum corticosterone concentration in rats.

References.

W.G. Lotz and S.M. Michaelson. Temperature and corticosterone relationships in microwave-exposed rat. J. Appl. Physiol. 44: 438-445, 1978.

S.T. Lu, S. Pettit, S.J. Lu and S.M. Michaelson. Effects of microwaves on the adrenal cortex. Radiat. Res. 107: 235-249, 1986.

W.G. Lotz and R.P. Podgorski. Temperature and adrenocorticcal responses in Rhesus monkeys exposed to microwave. J. Appl. Physiol. 53: 1565-1571, 1982.

This work is supported by U.S. Army Medical Research and Materiel Command under contract DAMD17-94-4069 with McKesson BioServices and PHS Grant ES 03330. Technical assistances by S. Pettit and S.-J. Lu are acknowledged. Use of laboratory animals adhered to the "Guide for the Care and Use of Laboratory Animals." The views, opinions and/or findings are those of author and should not be construed as an official Department of the Army position, policy, or decision unless so designated by other documentation.

© The Bioelectromagnetics Society

MEETING ABSTRACT 27

P-167-B

EFFECTS OF ULTRAWIDEBAND RADIOFREQUENCY RADIATION ON THE CELL CYCLE PROGRESSION IN HUMAN CELLS. M.L. Meltz, B.K. Nayak*, C. Galindo*, S.P. Mathur[1]*, M. Natarajan. Department of Radiation Oncology, University of Texas Health Science Center at San Antonio, 7703 Floyd Curl Drive, San Antonio, Texas 78229, USA. [1]McKesson BioServices, US Army Medical Research Detachment, Brooks Air Force Base, San Antonio, Texas 78235, USA.

INTRODUCTION: The debate over whether or not there are measurable biological responses after exposure of mammalian cells to radiofrequency radiation (RF), where heating is not involved, has been ongoing. Two studies reported alterations in the cell cycle in response to microwave radiation, although the experimental analysis is questionable. There is no information about any such alterations of the cell cycle after ultrawideband (UWB) RF exposure.

OBJECTIVE: The objective of the present study was to analyze the effect of UWB radiofrequency radiation on the cell cycle.

METHODS: In the present study, cell lines with different p53 status were analyzed. The 244B human lymphoblastoid cells with wild-type p53, a human monocyte cell line (MM6) with a compromised p53, and a human myeloid leukemic cell line (HL60) with p53-null status were exposed to UWB pulses intermittently for a period of 90 minutes (30 minute on and 30 minute off, repeated three times) at a pulse repetition rate of 250 pulses per second. The pulse duration was less than 1 ns. The peak E-field was maintained as close to 100 KV/m as possible. The E-field spectrum ranged from DC to a few GHz. The rise time ranged from 150 to 250 ps. The temperature in the sham and RFR-exposed flasks was monitored and maintained at 37°C through out the exposure period. As a positive control, cells were exposed to ionizing gamma radiation (2 to 5 Gy). Cells were processed for cell cycle analysis at 6, 10, and 24 hr post-exposure. Cells fixed in 70% ethanol were stained with propidium iodide and cell cycle analysis was performed by flow cytometry.

RESULTS: There was no effect of UWB-RF on the cell cycle distribution in 244B cells, as indicated from the percentage of cells in different phases of the cell cycle in sham-exposed and RF-exposed cells. There was also no effect of UWB-RF on the cell cycle in p53-compromised MM6 cells and p53-null HL60 cells. The 244B cells exposed to gamma radiation as a positive control showed an expected accumulation of cells in both the G1 and G2/M phases of the cell cycle indicating a cell cycle arrest.

CONCLUSION: The study shows that UWB-RF has no effect on the cell cycle in p53-positive, p53-compromised, and p53-null human cells. Further, it indicates that UWB-RF might not induce DNA damage, since activation of the p53 gene after such damage would lead to a cell cycle alteration.

© The Bioelectromagnetics Society

P-38-B

GENOMIC PROFILING OF NF-Kb SIGNAL DEPENDENT GENES IN HUMAN MONOCYTES AFTER ULTRA WIDE BAND EXPOSURE. M. Natarajan[1], B.K. Nayak[1], F.A. Roldan[1], C. Galindo[1], S.P. Mathur[2], M.L. Meltz[1]. [1]Department of Radiation Oncology, University of Texas Health Science Center, San Antonio, Texas 78229, USA. [2]McKesson BioServices, US Army Medical Research Detachment, Brooks Air Force Base, Building 1168, 8355 Hawks Road, San Antonio, Texas 78235, USA.

INTRODUCTION: Only a limited number of studies are available describing biological responses after ultrawideband (UWB) pulsed microwave radiation. Little is known about the molecular responses that could occur after such exposure. Since activation of one of the *Rel* protein family member, NF–κB, by other extracellular stimuli is implicated in the modulation of a multitude of cell functions, the activation of this critical cell signaling mediator and its downstream effect in response to UWB have been investigated.

OBJECTIVES: To study whether the exposure of normal human monocytes to pulsed ultrawideband triggers NF–κB-dependent transcriptional regulation and induces the expression of downstream target gene.

METHODS: Human Mono Mac-6 cells were exposed intermittently to UWB pulses for a period of 90 minutes (three recurring exposures of 30 minute on and 30 minute off). The pulse width was less than 1 ns and the pulse repetition rate was 250pps. The temperature of the medium was maintained at 37°C in both sham and RFR-exposed flasks. Immediately after exposure the cells were transferred to 37°C Air/CO_2 incubator and harvested after 10 min, 0.5 h, 4 h, 8 h, 24 h, and 48 h. Nuclear extracts were analyzed for NF–κB DNA-binding activity by EMSA analysis. Second, cells transiently transfected either with NF–κB-luciferase reporter vector or control vector were exposed as described above and harvested after 16 h for transcriptional activation of NF–κB by luciferase reporter assay. Third, differential expression of NF–κB dependent genes was screened at 8 and 24 h after UWB exposure by NF–κB super array.

RESULTS: The nuclear extracts analyzed by electrophoretic mobility shift assay showed a detectable level of NF–κB DNA-binding activity in the untreated incubator control cells. Compared to incubator controls, the mock-irradiated cells showed only a very slight increase in the NF–κB DNA binding activity. Similarly, no difference in the levels of NF–κB activation was observed in cells exposed to UWB and harvested after 10 min, 30 min, 4h and 8h. However, cells exposed to UWB and incubated for 24 h post-irradiation showed a marked increase in the NF–κB DNA-binding activity compared to mock-irradiated controls. The level was again decreased to the basal level at 48 h. Competition experiments with cold NF–κB-specific oligonucleotides confirmed the specificity of the DNA binding activity. To determine whether the activation of NF–κB after UWB exposure is functionally active, Mercury Pathway™ constructs containing 4X NF–κB binding sites associated with luciferase reporter system are transiently transfected and examined for NF–κB driven luciferase activity. Since activation of NF–κB has been observed, the possibility of the transcriptional regulation of kB-dependent target gene expression in response to UWB was investigated by signal-specific gene array. The gene expression profile is discussed

DISCUSSION: The results provide evidence that UWB can initiate NF–κB-dependent cell signaling pathway. The cell signaling response after UWB exposure appears to be a delayed effect, since, unlike UWB, Mono Mac cells exposed to 2.5 and 8.2 GHz microwave radiation, showed the activation of NF–κB at much earlier time point (4 and 8 h).

© The Bioelectromagnetics Society

MEETING ABSTRACT 29

P-166-A

TRANSCRIPTION OF P53 TARGET GENES IN RESPONSE TO ULTRAWIDEBAND RADIO-FREQUENCY RADIATION. B.K. Nayak*, M. Natarajan, C. Galindo*, S.P. Mathur[1°], M.L. Meltz. Department of Radiation Oncology, University of Texas Health Science Center at San Antonio. San Antonio, Texas 78229, USA. [1]McKesson BioServices, US Army Medical Research Detachment, Brooks Air Force Base, San Antonio, Texas 78235, USA.

INTRODUCTION: There has been a great deal of controversy over whether or not RFR has any biological effect, let alone an adverse biological effect. A large number of studies reporting the presence or absence of effects of radiofrequency radiation (RFR) have been performed at the cellular, cytogenetic and organism levels. There are a much smaller number of studies at the molecular response level. Almost no information is available at this level after ultrawideband (UWB) RF exposures. The p53 tumor suppressor gene is activated in response to a variety of stress signals, and in turn p53 activates a number of target genes, including those that can elicit cell growth arrest and/or apoptosis.

OBJECTIVE: The present study was undertaken to examine the effect of ultrawideband radiofrequency radiation on the transcription of p53 target genes involved in mammalian cell growth arrest and apoptosis.

METHODS: The cells used in this study were the 244B human lymphoblastoid cell line, the human MM6 monocyte cell line, and the human HL-60 myeloid leukemic cell line. The cells were exposed to UWB pulses intermittently for a total period of 90 minutes (30 minute on and 30 minute off, repeated three times) at a pulse repetition rate of 250 pulses per second. The pulse duration was less than 1 ns. The peak E-field was maintained as close to 100 KV/m as possible. The E-field spectrum ranged from DC to a few GHz. The rise time ranged from 150 to 250 ps. The temperature in the sham and RFR-exposed flasks was monitored and maintained at 37°C throughout the exposure period. Cells were exposed to ionizing gamma radiation (2 to 5 Gy) as a positive control. Total RNA was isolated at 2, 6, and 24 hr post-exposure. Transcription of p53 target genes was analyzed by RNase Protection Assay (RPA) using a human multi-probe template set consisting of p53 and p53 target genes p21, PCNA, gadd45, and bax. Housekeeping genes L32 and GAPDH were used as internal controls.

RESULTS: The transcription of p53 and p53 target genes involved in DNA damage repair (PCNA, gadd45), cell cycle arrest (p21, gadd45), and apoptosis (bax) was examined. There was no evidence of transcriptional induction of p53, or the p53 target genes p21, gadd45, PCNA, and bax as a result of the UWB radiofrequency radiation exposure. In the positive control cells (244B) exposed to ionizing radiation, there was an induction of the p53 target genes p21 and bax, indicating the onset of cell cycle arrest and apoptosis after this type of irradiation.

CONCLUSION: Lack of transcriptional activation of p53 target genes in response to UWB radiofrequency radiation exposure suggests that pulsed RF exposure does not induce DNA damage, and that the UWB exposure might not be a stress factor/agent to the cells.

MEETING ABSTRACT 30

1-3

EFFECT OF 9.6 GHZ MICROWAVES ON 4-AMINOPYRIDINE-INDUCED BURSTS IN ISOLATED HIPPOCAMPAL SLICES. A.G. Pakhomov[1,2], J. Doyle*[1], J. Ashmore*, and M.R. Murphy[2]. [1]McKesson BioServices, US Army Medical Research Detachment, and [2]Directed Energy Bioeffects Division, Human Effectiveness Directorate, Air Force Research Laboratory, San Antonio, Texas, 78235-5324, USA.

INTRODUCTION: Tattersall et al. reported recently that exposure to low-intensity CW microwaves (700 MHz) could have a profound effect on epileptiform bursting activity, induced in isolated hippocampal slices by superfusion with 4-aminopyridine (4-AP) [1]. This effect occurred at a threshold field intensity as low as 50 V/m (less than 5 μW/g) in 36% of microwave-exposed slices, but never in the controls.

OBJECTIVE: The present study attempted to utilize the same functional test to reveal possible nonthermal effect of CW microwaves at a different frequency, 9.6 GHz.

METHODS: Parasagittal hippocampal slices (350-μm thick) were isolated from 4- to 6-week old male Sprague-Dawley rats, fixed at the bottom of a custom-made exposure chamber, and superfused with oxygenated artificial cerebrospinal fluid at 34 °C. An extracellular recording micropipette (2-8 Mohm) was positioned in the neuronal layer of the CA3 area; the location was verified by stimulation of mossy fibers prior to the experiment. The drug concentrations tested were 50 and 100 μM (Series 1), and 150 μM (Series 2). In Series 1, the exposure intensity was ramped up every 5 min (same procedure as described in [1]). The steps were at zero power (sham), then 0.024, 0.12, 0.6, and 3 W/g, followed by no exposure and drug wash for 20 min. The two highest SAR increased the temperature by 0.6-0.7 and 3.5-3.7 °C, respectively; otherwise microwave heating was negligible. In Series 2, exposures also lasted 5 min each, but were separated by 10-min periods of no exposure. Each 15-min data recording interval, including 5 min before, during, and after the exposure, was processed as a separate experiment. Exposures were performed at the same SAR as in Series 1; in addition, we tested the effect of a 5-min conventional heating, which imitated the thermal effect of exposure at 3 W/g. Each brain slice underwent from 2 to 8 exposures; in most cases, the sequence of exposures was chosen by rolling a die.

RESULTS: In Series 1, we performed experiments in 8 brain slices and did not observe any obvious effect. To explore the possibility of more subtle effects, we switched to Series 2, which had a more stringent protocol. Over 100 treatments (counting exposures, sham exposures, and conventional heat treatments) were performed in 26 brain slice preparations; some data were later discarded, based on unstable activity before the treatment or various technical problems. The data from 76 treatments were rendered acceptable and used for statistical analysis. Typical rate of the bursting activity varied from 20 to 40 bursts/min in different brain slices, so the data were normalized for each experiment; the average bursting rate for a 5-min period prior to each exposure was taken as 100%. In the sham control group, as well as in the groups exposed at 0.024 and 0.12 W/g, the bursting rate stayed unchanged at about 100% throughout the experiment. Exposure at 3 W/g, as well as the equivalent conventional heating (+3.5-37 °C), produced complex changes in the bursting activity. These changes included a transient response while the temperature was rising or decreasing (typically, the activity briefly ceased and restarted at a higher pace), and a steady-state response while the temperature was maintained at a constant elevated level (the activity gradually decreased by some 10% per minute). There was no significant difference in responses to microwave and conventional heating. Exposure at the intermediate SAR of 0.6 W/g caused qualitatively similar effects as 3 W/g, but far less profound.

CONCLUSIONS: In our experimental conditions. 5-min exposure to 9.6 GHz microwaves at 0.024 and 0.12 W/g did not alter the spontaneous bursting activity caused in hippocampal slices by superfusion with 4-AP. Exposure at higher intensities of 0.6 and 3 W/g induced bursting rate changes that were similar to the effect of conventional heating.

References.

1. Tattersall et al., Brain Research (2001), 904:43-53.

The work was supported by the U.S. Army Medical Research and Materiel Command and the U.S. Air Force Research Laboratory (AFOSR) under U.S. Army contract DAMD17-94-C-4069 awarded to McKesson BioServices.

© The Bioelectromagnetics Society

MEETING ABSTRACT 31

P-54-C

HIGH-RESOLUTION TEMPERATURE AND SAR MEASUREMENT USING DIFFERENT SENSORS.
A.G. Pakhomov[1,2], S.P. Mathur[1*], and M.R. Murphy[2]. [1]McKesson BioServices, US Army Medical Research Detachment, and [2]Directed Energy Bioeffects Division, Human Effectiveness Directorate, Air Force Research Laboratory, San Antonio, Texas, 78235-5324, USA.

INTRODUCTION: Measurement of the local temperature and specific absorption rate (SAR) in microwave-exposed specimens is crucial in a variety of bioelectromagnetic studies. Predictions of these values by numerical modeling, including finite-difference time-domain technique, suffer errors due to approximations of the spatial and dielectric characteristics of exposed objects. Whenever possible, the accuracy of numerical predictions must be verified by direct measurements with appropriate temperature and E-field probes. However, selection of the right probe is a serious problem. Traditionally, temperature probes that are immune to EMF pick-up are regarded as "artifact-free"; these probes are widely used in various applications, without appreciation of the fact that the probe itself can distort the field and affect SAR and temperature. On the other hand, some artifact-prone probes, like microthermocouples (MTCs), have proven to be highly accurate and reliable in some dosimetry applications [1,2].
OBJECTIVE: The purpose of this study was to compare the performance of three different temperature probes under rather demanding conditions of a high-intensity, high-gradient, pulsed microwave exposure.
METHODS: The probes tested were the following:
(1) A copper-constantan MTC, made of 25-μm wires (Omega), and plugged via a cold junction compensator (Omega) into a DAM50 DC amplifier (WPI). As of today, MTC is probably the smallest and the fastest of temperature probes; it is inexpensive, combines negligible heat capacity, high sensitivity, and virtually instant response, but is prone to EMF pick-up.
(2) A "typical" fiber optic probe, TP-21-MO2 with a REFLEX thermometer (Nortech Fibronics, Canada). This probe is completely immune to EMF, has good sensitivity and stability; it is moderately priced and easy to operate. However, the probe is relatively bulky (~ 0.8 mm) and slow.
(3) A new-type miniature fiber optic sensor, FOT-HERO with a VELOCE signal conditioner (FISO Technologies, Canada). Based on a Fabry-Pérot interferometer, this probe measures thermal expansion of a tiny optical cavity placed at the tip of the fiber. Being immune to EMF, this probe also features unmatched sensitivity and exceptionally fast response. These unique properties make HERO most promising and universal for high-resolution thermometry and dosimetry. However, the probe is costly and, in our experience, troublesome to operate, including sensitivity to movements of the fiber optic cable and drifts of calibration values.
Voltage outputs of the probes were scaled and continually recorded with a help of an MP100 data acquisition system. The probes were positioned together in an exposure chamber using micromanipulators, under a visual control via a microscope. For maximum accuracy, the probes were calibrated against each other after being positioned in the chamber. Within the interval of interest (20-50°C), all the probes had a linear response to temperature. The exposure chamber was mounted atop a waveguide flange and filled with saline; the waveguide opening was sealed with a sapphire matching plate, flush with the flange [2]. Exposures were performed at 9.6 GHz, using either "regular" pulses (peak SAR 5 to 50 W/g) or extremely-high power pulses (EHPP, peak SAR 0.3-0.8 MW/g). Duty cycle and exposure duration were varied widely.
RESULTS: (1) MTC and HERO probes read similar amplitude and dynamics of temperature changes under exposure to "regular" microwave pulses. HERO readings often were slightly (5-10%) higher than those of the MTC; the reason for such behavior has not been understood yet. Withdrawal of either probe from the exposure chamber had no significant effect on the readings of the remaining probe. (2) However, the readings of both MTC and HERO changed significantly (increased) if the 3rd probe (TP-21) was brought close to them. (3) The TP-21 probe, despite being immune to microwaves, might read a drastically higher temperature rise than two other probes (Figure 1). Apparently, insertion of this probe caused profound field distortion and additional local heating. (4) With EHPP exposure (HERO and MTC together, TP-21 removed), MTC readings included transitory artifacts due to EMF pick-up. Under tested conditions, the amplitude of the artifacts was under 0.5 °C, and they lasted 20-40 ms after a single EHPP or an EHPP train; thereafter, MTC and HERO readings stayed the same. (5) An important feature of MTC is its ability to record a short-lived temperature plateau that occurs in a uniform lossy medium after a brief (e.g., 0.1-50 ms) microwave heating. This feature allowed for accurate, high-resolution measurement of local SAR [1,2]. The post-exposure plateau cannot be detected by most artifact-free probes, which are a lot slower than MTC. However, HERO probe was an exception: it routinely recorded a clear plateau of the same amplitude as MTC, and, even better, this plateau was not contaminated by EMF pick-up artifacts.

© The Bioelectromagnetics Society

P-54-C (Cont'd)

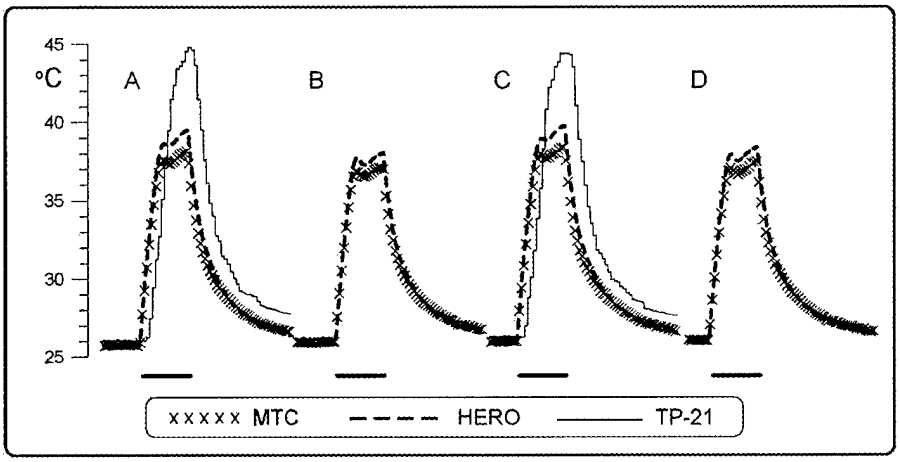


Figure 1. Repetitive local heating of saline by 5-sec trains of microwave pulses (shown by horizontal bars), as recorded by three different temperature probes (MTC, HERO, and TP-21). Fragments A-D are cutouts of a continuous temperature record. In fragments A and C, all three probes are positioned together in the exposed chamber. In fragments B and D, TP-21 probe is withdrawn without disturbing two other probes. Note that TP-21 probe not only reports much higher heating, but also, just by its presence, increases temperature readings by HERO and MTC. The probes have been calibrated against each other and responded equally to conventional heating.

SUMMARY: HERO probe performed well under all exposure conditions. Both HERO and MTC probes unequivocally detected a temperature plateau after a brief irradiation and therefore could be used for high-resolution local SAR measurement. Readings of MTC could be contaminated by EMF pick-up, but, under most conditions, the artifacts had little or no effect on the accuracy of thermo- and dosimetry. In contrast, a larger probe (TP-21), despite being immune to EMF interference, could produce markedly erroneous readings because of local field distortion. Likewise, other presumably "artifact-free" temperature probes (e.g., Luxtron) should be used with caution, since the errors caused by field distortion by the probe can be significant.

References.

1. Pakhomov et al. (2000) In: Radio Frequency Radiation Dosimetry, Kluwer Academic Publishers, Netherlands, p. 187-197.

2. Pakhomov et al. (2000) Bioelectromagnetics 21(4), 245-254.

The work was supported by the U.S. Army Medical Research and Materiel Command and the U.S. Air Force Research Laboratory (AFOSR) under U.S. Army contract DAMD17-94-C-4069 awarded to McKesson BioServices. The authors appreciate continual help of MengChe Looi of FISO Technologies, Canada.

© The Bioelectromagnetics Society

Quantitative Analysis Of Cytotoxicity Of Ultrashort (10 ns) Electrical Pulses In Mammalian Cells

A. Pakhomov[1,2], A. Phinney[1], J. Ashmore[1], J. Kolb[3],
S. Kono[3], K. Schoenbach[3], and M. Murphy[2].
[1] McKesson BioServices Corporation, US Army Medical Research Detachment,
Brooks City Base, San Antonio, TX, USA
[2] Directed Energy Bioeffects Division, Human Effectiveness Directorate,
Air Force Research Laboratory, Brooks City Base, San Antonio, TX, USA
[3] Dept. of Electrical and Computer Engineering,
Old Dominion Univ., Norfolk, VA, USA

Objective:

It has recently been reported that ultrashort electrical pulses (UEP) can induce apoptotic cell death. However, no systematic research has been performed yet to quantify the dependence of the UEP cytotoxic effect on exposure parameters such as the E-field voltage, absorbed dose, the number of applied pulses, or the pulse repetition rate.

Methods:

Experiments were performed in cultured human histiocytic lymphoma cells U937 obtained from ATCC. Cells were grown in ATCC-modified RPMI 1640 medium supplemented with 10% fetal bovine serum, at 37 oC with 5% CO2 in air. Cells were exposed in the growth medium at 0.2 x 106 cells/ml in gene transfer cuvettes (BIORAD) with 1- or 2-mm gap between the electrodes. The resistance of filled cuvettes was 8-9 Ohm. The samples were exposed to 10-ns UEP using a Blumlein line generator manufactured at the Old Dominion University. UEP shape and voltage were monitored on a 500-MHz TDS3052B Tektronix oscilloscope using a custom-made high-voltage probe. The pulses were nearly rectangular, and their amplitude could be varied from 10 to about 40 kV by changing SF6 gas pressure in the switch chamber of the generator. The pulse rate was set at 0.1, 0.4, or 1 Hz by changing or interrupting the charging current from a high-voltage power supply. Aliquots of exposed samples were placed in the incubator until analysis, for up to 50 hr post exposure. Sham exposed

samples were treated in exactly the same manner (excluding only the UEP exposure), in parallel with actual exposures. Cell culture growth and survival were assessed directly, by counting live and dead cells in a hemocytometer (live cells were identified by exclusion of Tryphan blue), or indirectly, from conversion of an MTS tetrazolium compound into a soluble formazan product by actively metabolizing cells (CellTiter 96 One Solution Cell Proliferation Assay, Promega). Possible apoptosis induction by exposures was examined by Western blot from cleavage of poly(ADP-ribose) polymerase (PARP).

Results:

The data were collected and analyzed from several sets of experiments totaling nearly 500 samples. In sham-exposed controls, the density of live cells doubled about every 24 hr, and the fraction of dead cells remained stably low (1-5%). UEP exposure could cause up to 25-30% reduction of the live cells density (compared to concurrent control values), along with up to a 6-fold increase in the fraction of dead cells ($p<0.01$). The threshold exposure parameters to reduce the live cells density were 10-20 pulses at 54 kV/cm and 0.1 Hz, or 1-5 pulses at a higher voltage (110 kV/cm). Surprisingly, this effect was not substantially modified by applying higher voltages (160, 230 or 350 kV/cm), by varying the number of pulses per train at these voltages (1, 5, 10, 15, or 20), or by delivering the pulses at higher rates (0.25 and 1 Hz). In contrast, the other observed effect (increase of the dead cells fraction) was proportional to both the number of pulses per train and their voltage, albeit the increase was rather gradual (e.g., by 2% per 100 kV/cm). This effect also clearly increased with increasing the specific absorbed dose, which ranged from 0.1 to 300 J/g. At present, we could not establish unambiguously if the cell death was due to necrosis or apoptosis; these experiments will be continued.

Summary:

U937 cells showed remarkably high resistance to 10-ns UEP. At such extreme exposure parameters as the E-field in excess of 350 kV/cm, SAR over 1 GW/g, and SA up to 300 J/g, only a minor fraction of the cell population was lethally damaged, whereas most of the exposed cells appeared unaffected. Further experiments will explore if this high resistance is a unique property of the employed cell line, and will analyze the role of other factors that can affect UEP cytotoxicity (e.g., medium conductivity and composition, cell density during exposure).

Acknowledgements:

The work was supported by the U.S. Army Medical Research and Materiel Command and the U.S. Air Force Research Laboratory (AFOSR) under U.S. Army contract DAMD17-94-C-4069 awarded to McKesson BioServices Corporation.

MEETING ABSTRACT 33

6th International Congress of the European Bioelectromagnetics Association
13–15 November 2003 Budapest, Hungary

O-9-06

ALTERATION OF SYNAPTIC TRANSMISSION BY NEURON EXCITATION-SYNCHRONIZED HIGH-POWER MICROWAVE PULSES: A REPLICATION STUDY

ANDREI PAKHOMOV[1,2], JOANNE DOYLE*[1], AND MICHAEL MURPHY[2]

[1]*McKesson BioServices Corporation, US Army Medical Research Detachment*
[2]*Directed Energy Bioeffects Division, Human Effectiveness Directorate, Air Force Research Laboratory*
Brooks City-Base, San Antonio, Texas, 78235-5324, USA

BACKGROUND:
Our previous studies in diverse objects (yeast and mammalian cells, isolated brain and heart slices) exposed to extremely high power microwave pulses (EHPP) did not reveal any bioeffects other than thermal [1,2]. However, recent experiments with EHPP applied in synchrony with evoked postsynaptic potentials indicated that the latter could be suppressed without appreciable microwave heating [3]. The present study attempted to replicate this observation under more stringent experimental conditions.

METHODS:
Excitatory postsynaptic potentials (EPSPs) in CA1 field of isolated rat hippocampal slices were continually evoked by twin pulse stimulation of Schaffer collateral (20 ms interpulse interval, 1 pair/15 sec). The EPSPs were recorded extracellularly with a glass micropipette (2-8 Mohm) for 5 min before EHPP or sham exposure, for 10 min during it, and for 10 min after. EHPPs (9.6 GHz, 2-μs, 740 kW/g) were triggered once every 15 sec: 2 ms prior to the 1st electrical stimulus (A); or 3.5-4.5 ms after the stimulus, during EPSP rising phase (B); or 14-16 ms after the stimulus, between the EPSPs (C); or at 1-Hz rate independently from the stimuli (D). In A, B, and C, EHPP briefly raised the temperature by 0.3-0.4 °C, but with 15-sec interval between them, gross heating was negligible. In D (positive control), the temperature increased by 1.5-2 °C. Each brain slice was used in a single experiment and then discarded.

RESULTS:
The data were collected from 63 experiments (10-14 per group). In sham-exposed slices and in "A" exposed group, EPSP showed no significant changes. In the other 3 groups, EPSP decreased to almost equal extent (by about 20%, $p<0.05$), and the onset of this change coincided with the beginning of exposure. Test EPSP (the 2nd in each pair) decreased significantly in "C" and "D" groups. These effects were similar to those reported earlier [3] or even more profound. Except for the positive control "D" group, the effects are unlikely to be explained by heating. However, the possibility of artifact readings due to interference with EHPP needs further investigation.

REFERENCES:
[1] *Pakhomov et al., Bioelectromagnetics 2000, 21(4), 245-254.*
[2] *Pakhomov et al., Bioelectromagnetics 2003, 24(3), 174-181.* [3] *Doyle et al., Abstracts of the 25th Annual BEMS Meeting, in press.*

ACKNOWLEDGEMENTS:
The work was supported by the U.S. Army Medical Research and Materiel Command and the U.S. Air Force Research Laboratory under U.S. Army contract DAMD17-94-C-4069 awarded to McKesson BioServices Corporation.

MEETING ABSTRACT 34

P-24-C

AN ANIMAL MODEL TO TEST COMBINED EFFECTS OF PULSED MICROWAVE AND A CNS MITOCHONDRIAL TOXIN. R. Seaman, M.F. Chesselet[*2], S.T. Lu[1], S.P. Mathur[*1], C.D. DiCarlo[*3], S.M. Fleming[*2], C. Zhu[*2], A. Mehta[*2], B.B. Carlson[*2], A.M. Phinney[*1], A.S. Garcia[*1], S.L. Adam[*3], A.R. Grado[*3], A. Brown[*3]. [1]McKesson BioServices at US Army Medical Research Detachment, Brooks City Base, Texas 78235; [2]Dept. Of Neurology, UCLA School of Medicine, Los Angeles, CA 90095; [3]US Army Medical Research Detachment, Brooks City Base, Texas 78235, USA.
82

OBJECTIVE: To define behavioral and histological endpoints to study effects of exposure to pulsed microwave radiation in an animal model of toxin-induced mitochondrial dysfunction.
METHODS: An animal model of Parkinson's disease using rotenone to inhibit mitochondrial energy production in the male Lewis rat [1] was evaluated. Different doses of rotenone in dimethylsulfoxide/polyethylene glycol were delivered from 2ML4 Alzet® osmotic minipumps (DURECT Corp., Cupertino, CA) with Teflon® flow modulators implanted using aseptic technique. In approximately one-half of the animals, the minipump was implanted subcutaneously for subcutaneous (SC) delivery of rotenone. In the other half, the minipump was implanted subcutaneously and was connected to a catheter inserted into the jugular vein for intravenous (IV) delivery of rotenone. Initiation and level of motor activity were measured weekly in four tests: forced step, step initiation, spontaneous vertical activity (rearing) in a dark cylinder, and spontaneous motor activity in a dark arena. Injury to the substantia nigra and caudate-putamen in the brain was assessed by immunostaining for tyrosine hydroxylase (TH), the enzyme of dopamine synthesis. Microwave exposure to radar-like 6-μs pulses of 1.25-GHz microwaves at 10 Hz will be delivered in later experiments by an open-ended WR650 waveguide. Thermometry-based dosimetry was used to obtain whole-body and local specific absorption rate (SAR) in animals with and without implanted osmotic pumps [2].
RESULTS: Step initiation time and rearing activity were most sensitive to rotenone, with larger changes for higher doses. Reproducible increases in step initiation time and decreases in rearing were observed after SC administration of rotenone at 2.0 mg/kg/day for 3 weeks. Number of forced steps and spontaneous motor activity were not affected by rotenone, indicating that the effects were not due to gross motor anomalies. Although a subset of animals showed either moderate or marked decrease in caudate-putamen TH, the level of TH depletion was not correlated with behavioral anomalies, suggesting that these were likely related to nigrostriatal dysfunction rather than to neuronal loss. Microwave dosimetry showed that 0.4 and 4 W/kg whole-body SAR could be accomplished concurrently during microwave exposure in two animals at different locations. The implanted minipump had no measurable effect on whole-body SAR. Because temperature change at the minipump during microwave exposure was less than 0.2°C in magnitude, minipump performance would not be affected by the exposure.
CONCLUSIONS: Based on survival rate, rotenone-induced brain injury, and behavioral endpoints, a rotenone dose of 2.0 mg/kg/day delivered for 3 weeks was selected for future use. The effects of these conditions left room for either an increase or a decrease in endpoints by microwave exposure in later experiments. The SC rotenone delivery was chosen for use because endpoint changes were more consistent with SC delivery then with IV delivery and because of easier implementation and less surgical trauma of the SC delivery. This model is the first to use chronic delivery of a toxin to study effects of microwave exposure on *in vivo* cellular neurodegenerative processes. The model will provide information on brain injury and changes in behavior resulting from combinations of rotenone-induced toxicity and microwave exposure. Results of studies using the model will provide information on combined effects of stressors that can occur in military occupational situations.
References.
Betarbet R. et al. 2000. Chronic systemic pesticide exposure reproduces features of Parkinson's disease. Nature Neuroscience 3:1301-1306.
Mathur SP, Lu ST. 2002. Application of various thermometric calorimetry in rodent dosimetry. Proc. Second International Workshop on Biological Effects of Electromagnetic Fields 2:272-280.

Supported by US Army MRMC contract DAMD17-94-C-4069. Investigator(s) adhered to the "Guide for the Care and Use of Laboratory Animals". The views, opinions and/or findings contained in this report are those of the author(s) and should not be construed as an official Department of the Army position, policy or decision.

© The Bioelectromagnetics Society

Lack Of Change In Temporal Characteristics Of The Rat ECG During Exposure To Ultra-Wideband Pulses

Ronald L. Seaman[1], James R. Jauchem[2],
Satnam P. Mathur[1], Amy M. Phinney[1], John L. Ashmore[1].
[1]McKesson BioServices Corporation at WRAIR US Army Medical Research Detachment, Brooks City-Base, Texas USA. 2US Air Force Research Laboratory, Directed Energy Bioeffects Division, Radio Frequency Radiation Branch, Brooks City-Base, Texas USA.

Objective:

An experiment was conducted to determine whether changes occurred in the cardiac cycle of an anesthetized rat during exposure to brief bursts of ultra-wideband (UWB) pulses for 10 s using the electrocardiogram (ECG) to monitor cardiac electrical activity.

Methods:

The carotid artery of 10 male Sprague-Dawley rats (330-397 g) was cannulated under ketamine anesthesia, which was maintained throughout testing. For UWB exposure, the animal was placed ventral recumbent on 2.5 cm thick Styrofoam on a horizontal ground plane in a giga transverse electromagnetic (GTEM) cell. The animal was centrally located with its head toward the source end of the GTEM cell, and thus along the direction of UWB propagation, or in k-polarization orientation. The cannula was extended through a small hole in the wall of the GTEM cell and connected to a blood pressure transducer. Carbon-loaded Teflon leads attached subcutaneously at each limb also passed through the hole and were connected to a shielded ECG cable. Pressure transducer and ECG cables were connected to standard Gould Pressure Processor and ECG/Biotach units outside the electrically shielded room containing the GTEM cell. UWB pulses with 106±5 kV/m peak amplitude, 0.79±0.02 ns duration, and 186±17 ps rise time at animal thorax were applied in 25 ms bursts at 1 kHz repetition frequency, or 25 pulses per burst. Nine 10 μs UWB exposures were applied in pseudorandom sequence to each animal: 3 exposures with no pulses (sham control exposure), 3 exposures with a burst starting at each R-wave, and 3 exposures with a burst

during each T-wave. Individual exposures were separated by an average of 23.8 s (end-to-start). Lead II ECG and blood pressure were recorded artifact-free continuously and stored using a BioPac/AcqKnowledge system. Intervals in the ECG were measured from 10 s before to 10 s after each exposure using AcqKnowledge software. Interval values were computed for 100 ms time increments using cubic interpolation in QuattroPro spreadsheets and averaged for like exposures for each animal. An averaged interval record for each type of exposure represented an animal in combined data. Here we report on R-R interval, between start of R-wave and start of next R-wave, and P-R interval, between start of P-wave and R-wave. Analysis of other ECG parameters and blood pressure are in progress.

Results:

No difference was seen in R-R or P-R interval for any part of the 10μs UWB exposures when compared to respective values for sham exposure and pre-exposure values.

Conclusions: UWB pulses as applied in the GTEM cell for 10 s do not change R R interval or P-R interval of the rat ECG during exposure. This is consistent with our previous findings of no immediate effect of UWB pulses on average heart rate and blood pressure during 2 min exposures. Any change that might have occurred was considerably smaller than background variability in the variables

Keywords:

UWB radiation, Sprague-Dawley rat, electrocardiogram, R-R interval, P-R interval

This work is supported by the U.S. Army Medical Research and Materiel Command under contract DAMD17-94-C-4069 awarded to McKesson BioServices Corporation. The views, opinions and/or findings contained in this report are those of the author(s) and should not be construed as *an official Department of the Army or Department of the Air Force position*, policy or decision unless so designated by other documentation. In conducting research using animals, the investigator(s) adhered to the "Guide for the Care and Use of Laboratory Animals" prepared by the Institute of Laboratory Animal Resources, National Research Council (Washington, DC: National Academy Press, 1996).

MEETING ABSTRACT 36

6th International Congress of the European Bioelectromagnetics Association
13–15 November 2003 Budapest, Hungary

P-005

EFFECTS OF EXPOSURE TO PULSED MICROWAVES ON MOVEMENT INITIATION IN RATS EXPOSED TO THE MITOCHONDRIAL TOXIN ROTENONE

R.L. SEAMAN[1], S.M. FLEMING [2], K. PROSOLOVITCH[2], M.F. CHESSELET[2], S.T. LU[1], S.P. MATHUR[1], C.D. DICARLO[3], A.S. GARCIA[1], A.R. GRADO[3], T.H. GARZA[1]

[1]McKesson BioServices at USAMRD, Brooks City-Base, Texas 78235 USA
[2]Dept. of Neurology, UCLA School of Medicine, Los Angeles, California 90095 USA
[3]US Army Medical Research Detachment, Brooks City-Base, Texas 78235 USA

OBJECTIVE:
To evaluate the effect of microwave exposure on an animal model of mitochondrial toxicity using rotenone in the male Lewis rat.

METHODS:
Rotenone was delivered at 2.0 mg/kg/day in a dimethylsulfoxide-polyethylene glycol vehicle by means of 2MLA Alzet® osmotic minipumps (DURECT Corp., Cupertino, CA, USA) fitted with Teflon® flow modulators implanted subcutaneously using aseptic technique under isoflurane anesthesia (rotenone animals). Vehicle-control animals were identical except no rotenone was included (vehicle animals). Animals weighed 292±33 g at surgery. They were exposed without physical or chemical restraint to microwaves consisting of 1.25-GHz L-band radiation delivered as 6-μs pulses at 10 Hz with whole-body specific absorption rate of 0 (sham), 0.4, or 4 W/kg. Implanted minipumps did not significantly change whole-body averaged SAR. Time to initiate movement toward home-cage litter was measured 6 days after surgery in 9-12 animals per condition after two microwave or sham exposures, one on each of post-op days 4 and 5, for each animal. Results were tested using ANOVA and post-hoc Newman-Keuls test for differences using GB-STAT software (v5.4, Dynamic Microsystems, Silver Spring, MD, USA).

RESULTS:
Mean times for movement initiation (MI) of cage-control animals (no minipump or exposure) and sham-exposed vehicle animals were 7.3 and 6.1 s, respectively, which were not different (2-sided t-test). ANOVA of MI times for rotenone-microwave conditions showed a significant rotenone-microwave interaction [$F(2,57) = 3.94$, $p = 0.02$] with the main effect of rotenone approaching significance [$F(1,57) = 3.57$, $p = 0.06$] but without a main effect of microwaves [$F(2,57) = 1.91$, $p = 0.16$]. MI times of vehicle animals and rotenone animals exposed at either 0.4 or 4 W/kg were 5.7-10.0 s and were not different among these conditions or from cage-control and sham-exposed MI times. However, the MI time of 16.6 s for sham-exposed rotenone animals was significantly longer by 1.5-2.5 times than MI times for other conditions.

CONCLUSIONS:
Results indicated that microwave exposure at 0.4 or 4 W/kg alone did not change MI time from control values. On the other hand, initiation of movement was slowed significantly by the rotenone treatment, by an amount consistent with previous observations in our laboratory. However, rotenone-treated animals that had also been exposed twice to pulsed microwaves at 0.4 or 4 W/kg did not exhibit slower times in the MI test. This difference in MI times between non-exposed and exposed rotenone animals indicated a possible interaction of rotenone and microwave actions on parts of the central nervous system responsible for movement initiation.

Supported by US Army MRMC contract DAMD17-94-C-4069. Investigator(s) adhered to NIH "Guide for the Care and Use of Laboratory Animals". The views, opinions and/or findings contained in this report are those of the author(s) and should not be construed as an official Department of the Army position, policy or decision.

MEETING ABSTRACT 37

Chronic Mitochondrial Complex I inhibition Induces Nigrostriatal Pathway Dysfunction in Rats

C. Zhu[1], S.M. Fleming[1], A. Mehta[1], R.L. Seaman[2], C.D. DiCarlo[3], M.-F. Chesselet[1]
[1]Department of Neurology and Neurobiology, Geffen School of Medicine, UCLA, Los Angeles, CA 90095, [2]McKesson BioServices at USAMRD, [3]USAMRD, Brooks City-Base, Texas 78235.

Mitochondrial complex I is one of the most important sites of intracellular reactive oxygen species (ROS) formation. Moderate inhibition of mitochondria complex I is sufficient to induce significant ROS generation in vitro. Oxidative damage due to excess production of ROS has been implicated in pathogenesis of neurodegenerative diseases such as Parkinson's disease, Huntington's disease and Alzheimer's disease. Rotenone is a naturally occurring, classic mitochondria complex I inhibitor and is commonly used as a pesticide. In this study, Lewis rats were infused with rotenone at different doses (0.0, 2.0, 2.5, 3.5 mg/kg/day) subcutaneously or intravenously for three weeks. Motor function was assessed with a battery of behavioral tests sensitive to varying degrees of dopamine loss in the striatum and substantia nigra. In addition, microglial activation and tyrosine hydroxylase immunoreactivity (TH-IR) in the striatum were analyzed. A dose dependent increase in mortality was observed in both iv and sc infusion groups. Animals treated with sc rotenone infusion showed more consistent behavioral deficits across the three weeks. Motor dysfunction observed in these animals is typically associated with dysfunction in the nigrostriatal dopaminergic pathway. A variable decrease of TH-IR in the striatum was observed in both iv and sc rotenone treated animals and was not correlated with behavioral deficits. Microglial activation was detected in the striatum showing TH-IR reduction. The results of the present study indicates that moderate chronic mitochondrial inhibition in the rat has profound effects on motor behavior and these effects were not directly correlated with TH-IR reduction and microglial activation.

MEETING ABSTRACT 38

Abstract submitted to 2003 Society for Neuroscience meeting

CHRONIC INTRAVENOUS AND SUBCUTANEOUS ROTENONE INFUSION: SURVIVAL ANALYSIS, FUNCTIONAL ASSESSMENT AND MICROGLIAL ACTIVATION. C. Zhu[1], S.M. Fleming[1], A. Mehta[1], R.L. Seaman[2], C.D. DiCarlo[3], M.-F. Chesselet[1]
[1]Department of Neurology and Neurobiology, Geffen School of Medicine, Los Angeles, CA 90095, [2]McKesson BioServices at USAMRD, [3]USAMRD, Brooks City-Base, Texas 78235.

Impairment of mitochondrial function in neurons can lead to a decrease in ATP synthesis and an increase in the production of free radicals. Mitochondrial impairment can occur as a result of exposure to mitochondrial toxins, and administration of the mitochondrial inhibitor rotenone has been shown to induce Parkinson-like alterations in dopaminergic nigrostriatal neurons. However, the behavioral effects of rotenone administration and their relationship to dopamine depletion have not been characterized in detail. The aim of the present study was to compare the chronic effects of rotenone administered intravenously (iv) or subcutaneously (sc) at different doses (0.0, 2.0, 2.5, 3.5 mg/kg/day) on motor behavior, tyrosine hydroxylase (rate-limiting enzyme in dopamine biosynthesis) immunoreactivity (TH-IR) and microglial activation in the striatum. Survival analysis indicated a dose dependent decrease in survival rates with both iv and sc administration routes. Behaviorally, animals receiving sc rotenone showed a consistent decrease in spontaneous rearing and increased movement initiation times over three weeks, whereas, a more variable behavioral response was observed in animals receiving iv rotenone, perhaps due to patency of the cannula. Variable decreases in TH-IR in the striatum were observed in iv and sc animals but were not correlated with motor behavior. Microglial activation was observed in the striatum when there was a concomitant reduction in TH-IR. These results demonstrate that low doses of rotenone induce motor abnormalities that are compatible with a dysfunction of the nigrostriatal pathway but do not directly correlate with reduced TH-IR and microglial activation in the striatum.

Key words: mitochondria complex 1, motor function, tyrosine hydroxylase
Supported by: US Army MRMC contract DAMD17-94-C-4069.

Theme G: Neurological and Psychiatric Conditions
1. Neurodegenerative Disorders
h. Parkinson's Disease: Models

sfnChunni1 McK B&W.doc
5/25/2004

MEETING ABSTRACT 39

FINITE-DIFFERENCE TIME-DOMAIN (FDTD) ANALYSIS AND DOSIMETRY OF A GIGAHERTZ TEM CELL. Z. Ji*, S. C. Hagness, J. H. Booske*, S. Mathur*,[1] and M. Meltz,[2] Department of Electrical and Computer Engineering, University of Wisconsin-Madison, 1415 Engineering Drive, Madison, Wisconsin 53706, [1]McKesson BioServices, 8355 Hawks Road, Building 1168, Brooks City-Base, Texas 78235, and [2] Department of Radiation Oncology, University of Texas Health Science Center at San Antonio, San Antonio, Texas 78229.

INTRODUCTION: A Gigahertz TEM (GTEM) cell has been designed and adopted for ultrawideband (UWB) baseband electromagnetic pulse (EMP) exposure studies of biological specimens. The objective of the experiments are to expose biological cells to ~ 1 ns, intense EMPs by loading the GTEM cell with T-25 flasks containing cells suspended in culture media. Important information about the spatial uniformity and temporal transients of electromagnetic fields within the media in the flasks is very difficult to obtain experimentally. FDTD simulations are regarded as a practical means of acquiring the required dosimetry information. While FDTD models of a few unloaded GTEM cells have been previously reported [1,2], recent advances in computing power and FDTD algorithms [3] permit the modeling of UWB EMP propagation in GTEM cells with increased accuracy.
OBJECTIVE: The ultimate objective of this study is to obtain transient dosimetry information in a GTEM cell loaded with T-25 flasks containing cell culture media. The objective of the first phase of this study is to develop a realistic three-dimensional simulation model of the unloaded GTEM cell and to validate the simulation results by comparison with experimental measurements of the electric field pulses at several points within the GTEM cell.
METHOD: The FDTD method is used to simulate the GTEM cell. The load end of the GTEM cell is terminated with Perfectly Matched Layer absorbing boundary conditions. The source end of the modeled GTEM cell is extended beyond the experimental source plane to form an apex similar to that of Refs. [1, 2]. This choice permits accurate excitations of UWB pulses without having to model the complex feed structure of the actual experimental assembly. The experimentally generated waveform is approximated using a double exponential pulse with a width of ~ 1 ns, excited between the septum and the outer ground plane of the GTEM cell. This source waveform is plotted in Fig. 1a. The FDTD grid is comprised of a uniform lattice of cubic grid cells ($\Delta = 2.5$ mm). This grid resolution corresponds to 120 points per free-space wavelength at 1 GHz, and is therefore fine enough to accommodate accurate staircasing of the flared metal surfaces as well as the later inclusion of cell culture media. The GTEM walls and septum are modeled as Perfect Electrical Conductors.
RESULTS: Figure 1a shows the FDTD-computed time-domain vertical electric fields recorded at three sampling points along the horizontal floor of the empty GTEM cell. These results illustrate that the pulse shape is preserved as the pulse propagates towards the load. (The amplitude, and thus the power density, decreases as the cross-sectional area of the GTEM cell increases.) The slight fluctuations in the pulse tails were established to be the result of the staircase approximation of smooth tapered walls, particularly at the source end. Figure 1b compares the simulated and measured vertical electric field at a common observation point. The experimental waveform was measured using a Tektronix SCD 5000 transient digitizer and an asymptotic conical dipole D-dot sensor [4]. The FDTD-computed waveforms agree well with the waveforms collected in measurements at all selected sample points. Ongoing computational studies of the GTEM cell loaded with T-25 flasks are being conducted to evaluate field distributions in space and time, as well as SAR distributions, inside the cell culture medium.

References:
[1] T.E. Harrington, "GTEM Fields FDTD Modeling," IEEE International Symposium on Electromagnetic Compatibility, pp. 614 – 619, 1997.
[2] W.A. Radasky, K.S. Smith, D. Hansen, and D. Ristau, "Calculations and Measurements of Fast EM Pulses in the GTEM Cell," IEEE International Symposium on Electromagnetic Compatibility, pp. 52 – 57 1996.
[3] Allen Taflove and Susan C. Hagness, *Computational Electrodynamics: The Finite-Difference Time-Domain Method, 2nd ed.*, Norwood, MA: Artech House, 2000.
[4] J.-Z. Bao, "Picosecond domain electromagnetic pulse measurement in an exposure facility: An error compensation routine using deconvolution techniques," *Rev. Sci. Instrum.*, vol. 68, pp. 2221 – 2227, 1997.

This study was funded by the Air Force Office of Scientific Research (grant no. F49620-01-1-0349). Two of the authors (SCH, JHB) were supported in part by the US Department of Defense under its FY01 "RF Bioeffects" MURI program, through a consortium grant with Old Dominion University and managed by the Air Force Office of Scientific Research.

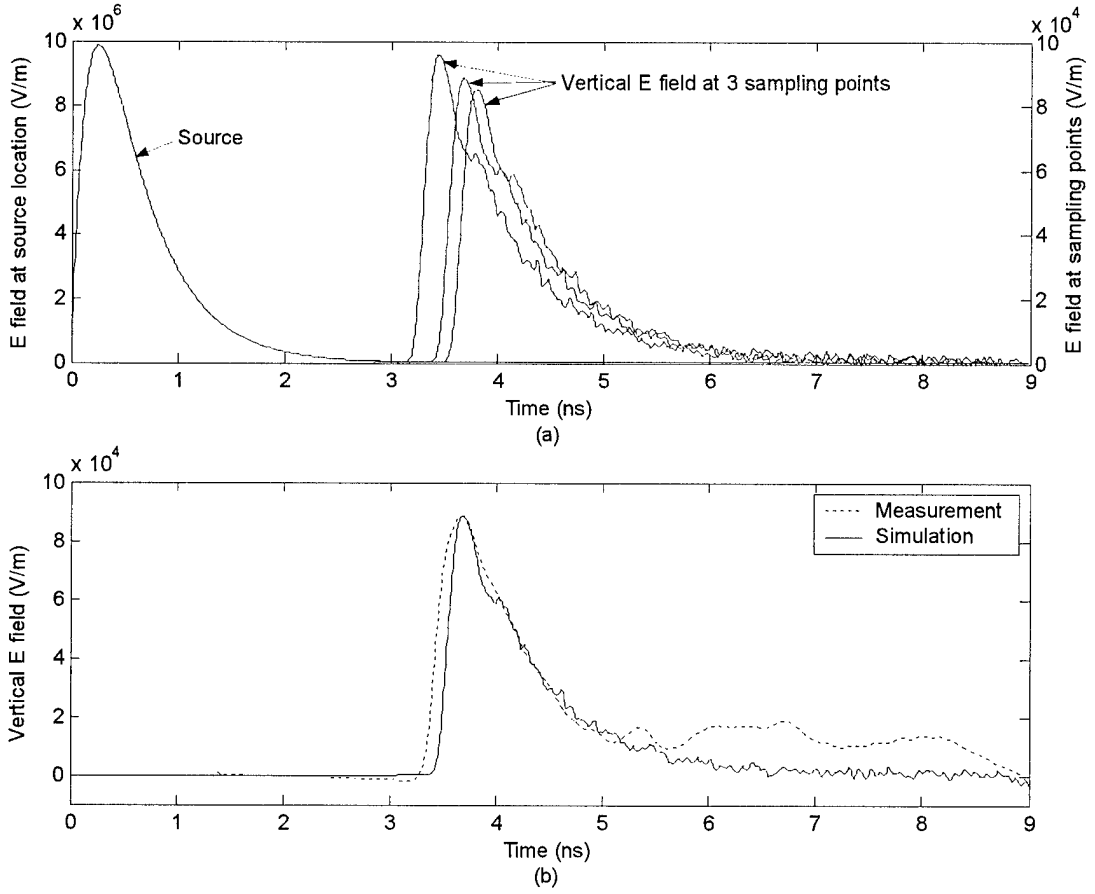


Figure 1: (a) Simulated UWB source waveform (far left) and radiated vertical electric fields computed along the horizontal floor of the GTEM cell. (b) Simulated and measured vertical electric field recorded at a common sampling point.

MEETING ABSTRACT 40

BIOLOGICAL EFFECTS OF ULTRA-WIDE-BAND PULSES. S.-T. Lu. McKesson BioServices, U.S. Army Medical Research Detachment, Microwave Bioeffects Branch, Brooks City-Base, Texas 78235, U.S.A.

INTRODUCTION: Ultra-Wide-Band (UWB) technology and device are known since 1960. The UWB device is used to transmit and receive an extremely short duration pulse of radio frequency energy, typically a few tens of picoseconds to a few nanoseconds. In addition to military application, UWB device has been used in imaging, vehicular radar, communication, and measurement systems. Newly developed UWB sources are capable of generating hundreds of gigawatts peak power and establishing hundreds of kV/m peak electric field. Safety aspects of high peak power of ultrashort electromagnetic pulses have been questioned and debated. Earliest report on this topic appeared in 1993. Biological database is limited that hinder a judicious promulgation of personnel protection guidelines/standards. Due to ultrashort pulse duration that results in very low duty factor, specific absorption rate and specific absorption, thermal mechanism cannot be used adequately to interpret a few biological effects observed.
OBJECTIVE: The objective of this presentation is to update the current progress in studies of biological effects of UWB pulses that was included in a previous publication [1].
RESULTS: UWB pulses have been used *in vitro* and *in vivo* to elucidate potential biological effects of UWB pulses. Peak e-field intensity ranged from 55 kV/m to 250 kV/m with duty factor between 4.5×10^{-7} to 1.2×10^{-5}. Estimated specific absorption rates ranged between 3.7 mW/kg and 300 mW/kg *in vivo*. Duration of exposure ranged from 25 ms to 30 minutes. Endpoints studied were mutagenesis, UV-induced mutagenesis and recombination, cell cycle progression, p53 target gene transcription, NF-κB DNA binding activity, endpoints in functional observation battery, swimming performance, brain c-fos protein expression, metrozol-induced seizure, pentylenetetrazol-induced seizure, nociception, morphine-induced analgesia, morphine-induced hyperactivity, L-NAME (N^G-nitro-L-arginine methyl ester) - induced hyperactivity, L-NAME-induced analgesia, nitric oxide production, blood pressure, heart rate, time-domain and frequency-domain heart rate variability, posture-induced alterations in heart rate and blood pressures, development of mammary tumor, and neural and behavioral teratologies. Biological effects were not found when exposure duration was less than 2 minutes. Biological effects observed were: blocking of the L-NAME induced hyperactivity [2], delayed hypotension and increased VLF power spectrum density of the frequency-domain heart variability [3], enhanced nitric oxide production in γ-interferone and lypopolysaccharide stimulated murine macrophages, increased NF-κB binding activity in human cells [4], more stress vocalization in rat pups, longer medial-to-lateral length in hippocampus and decreased mating frequency [5].
CONCLUSION: Biological effects were observed in cells and animals exposed to UWB pulses at peak e-field around 100 kV/m or less. Additional studies are needed.

[1] Lu S-T, de Lorge JO (1999) In: "Advances in Electromagnetic Fields in Living Systems", vol. 3, Lin JC ed., Kluwer Academic/Plenum Publishers, NY, NY, pp 207-264.
[2] Seaman RL, Belt ML, Doyle JM, Mathure SP (1999) Bioelectromagnetics 20: 431-439.
[3] Lu S-T, Mathur SP (2002) In: "Proceedings of the 2nd International Workshop on Biological Effects of Electromagnetic Fields", Kostarakis P ed., pp 409-418.
[4] Natarajan M, Vijayalaxmi, Szilagyi M, Roldan FN, Meltz ML (2003) 25th Annual Meetings of Bioelectromagnetics Society, Maui, HI, USA, June 22-27, p 202.
[5] Cobb BL, Jauchem JR, Mason PA, Dooley MP, Miller SA, Ziriax JM, Murphy MR (2002) Bioelectromagnetics 21: 524-537.

This work is supported by the U.S. Army Medical Research and Materiel Command under contract DAMD17-94-4069 with McKesson BioServices. The views, opinions and/or findings are those of author and should not be construed as an official Department of the Army position, policy, or decision unless so designated by other documents.

MEETING ABSTRACT 41

ULTRAWIDEBAND ELECTROMAGNETIC RADIATION (UWB EMR) EXPOSURES AND ACTIVATION OF AN IMPORTANT SIGNAL TRANSDUCTION PATHWAY. M. Natarajan[1], B.K. Nayak[1]*, S.P. Mathur[2], C. Galindo[1]*, M.L. Meltz[1]. [1]Department of Radiation Oncology, University of Texas Health Science Center at San Antonio, [2]McKesson BioServices, US Army Medical Research Detachment, Brooks City-Base, San Antonio, Texas 78235 USA.

Introduction: The study of cell signaling mechanisms continues to move forward at a prodigious rate. Signal transduction is a fundamental process that cells and organisms use to respond to external stimuli, and thereby attempt to maintain normal function and homeostasis. Since a subtle change in the environment can initiate and transduce signals, it has immense value for (a) estimating an agent's biological activity, (b) defining an agent's mode of action and (c) establishing an agent's antagonism or synergism with other agents. In an attempt to identify and understand the biological effects initiated by electromagnetic radiation exposure of mammalian cells, our focus is directed towards examining the activation of signaling mechanisms. In this presentation we will review the studies on signaling mechanisms induced/inhibited by ultrawideband EMR exposures. We will also discuss studies currently underway in our laboratory on cell signaling after UWB EMR exposure of human cells.

Methods: Human monocytes were exposed intermittently to UWB EMR pulses for a total of 90 minutes (three recurring exposures of 30 minute on and 30 minute off). The pulse width was 0.8 ns, pulse rise time was between 258 to 273 ps, average peak pulse E-field was 100 kV/m, and the pulse repetition rate was 250pps. The temperature of the medium was maintained at 37°C in both sham and RFR-exposed flasks. Immediately after exposure, the cells were transferred to a 37°C Air/CO_2 incubator and harvested after 10 min, 0.5 h, 4 h, 8 h, 24 h, and 48 h. Initiation of the NF-κB signaling pathway was analyzed by EMSA analysis. To examine the downstream effect of the NF-κB signaling pathway, cells transiently transfected with either an NF-κB-luciferase reporter vector or a control vector were exposed as described above, and harvested after 16 h of additional incubation. The whole-cell extract was examined for NF-κB-dependent transcriptional activation of downstream genes by luciferase reporter assay. The differential expression of NF-κB dependent genes was screened at 8 and 24 h after UWB EMR exposure by NF-κB super array.

Results: Cells exposed to UWB and incubated for 24 h post-irradiation showed a marked increase in the NF-κB DNA-binding activity compared to mock-irradiated controls. The results provide evidence that UWB EMR can initiate the NF-κB-dependent cell signaling pathway. The cell signaling response after UWB EMR exposure appears to be a delayed effect, since, unlike after UWB EMR exposure, Mono Mac cells exposed to 2.5 and 8.2 GHz microwave radiation, showed the activation of NF-κB at much earlier time points (4 and 8 h). Cells transiently transfected with Mercury Pathway™ constructs containing 4X NF-κB binding sites associated with luciferase reporter system did not induce NF-*k*B driven luciferase activity, indicating that the activation of NF-κB after UWB exposure is functionally inactive. Similarly, the transcriptional regulation of κB-dependent target gene expression in response to UWB EMR, investigated by Human TranSignal™ NF-κB target gene array, revealed no difference in the gene expression profile. This further confirms that the UWB EMR -induced NF-κB is only a transient response, with minimal or no downstream effect. This work was supported by the AFOSR Grant No. F49620-01-1-0349

MEETING ABSTRACT 42

DETERMINATION OF P53 PROTEIN STABILIZATION, LOSS OF MITOCHONDRIAL MEMBRANE POTENTIAL, AND RELEASE OF CYTOCHROME C INTO THE CYTOSOL IN RESPONSE TO UWB EMR EXPOSURE IN HUMAN LYMPHOBLASTOID CELLS. B.K. Nayak, C. Galindo*, M. Natarajan, S.P. Mathur[1]*, M.L. Meltz. Department of Radiation Oncology, University of Texas Health Science Center at San Antonio, 7703 Floyd Curl Drive, San Antonio, Texas 78229, USA. [1]McKesson BioServices, US Army Medical Research Detachment, Brooks Air Force Base, 8355 Hawks Road, Building 1168, San Antonio, Texas 78235, USA.

Objective: The aim of the study was to determine the effect of ultrawideband electromagnetic radiation (UWB EMR) exposure on p53 protein stabilization, loss in mitochondrial membrane potential, and the release of cytochrome C into the cytoplasm, which are molecular alterations associated either with induction of apoptosis or inhibition of cell cycle progression when DNA is damaged.
Methods: The studies were performed in 244B human lymphoblastoid cells. The cells were exposed to UWB EMR pulses intermittently for a total of 90 minutes (30 min on, 30 min off). The UWB EMR pulses had an average peak amplitude of 100 kV/m, an average pulse width of 0.80 ns, an average rise time of 200 ps, and a pulse repetition frequency of 250 pps. The frequencies ranged from D.C. to ~2 GHz. The stabilization of p53 protein was examined by western blot analysis. The transactivation of p53 target genes (p21, gadd45, Bax) was analyzed using the RNase protection assay. Further, evidence of the induction of apoptosis in response to UWB EMR exposure was determined by measuring a change in mitochondrial membrane potential using JC1 staining, and by detecting the release of cytochrome C into the cytoplasm (western blot analysis).
Results: The p53 protein was not stabilized after the UWB EMR exposure of the 244B cells, i.e., there was no increase in the p53 protein level as compared to the sham and incubator control. There was no evidence of transcriptional induction of the p53 responsive genes p21, gadd45, and Bax after the UWB EMR exposure. In the positive control cells exposed to ionizing radiation, the p53 protein level was increased and there was an induction of the p53 target genes p21 and Bax. These are molecular responses associated with cell cycle arrest and apoptosis after this type of irradiation.
There was no loss of mitochondrial membrane potential and there was no release of cytochrome C into the cytoplasm in response to UWB EMR exposures (suggesting that apoptosis was not occurring), while in the positive control cells treated with staurosporine (1 μg/ml), there was a loss of mitochondrial membrane potential accompanied with the release of cytochrome C into the cytosol, indicating the onset of apoptosis.
Conclusion: The analysis of several different molecular parameters, such as p53 protein stabilization, loss of mitochondrial membrane potential, and cytochrome C release into the cytosol, indicates that after this type of UWB EMR exposure, induction of apoptosis and effects on cell cycle progression in human lymphoblastoid cells do not occur. The evidence is not supportive of the hypothesis that this type of exposure induces DNA strand breaks.
This work was supported by AFOSR Grant No. F49620-01-1-0349.

MEETING ABSTRACT 43

CELL KILLING EFFECT OF HIGH-INTENSITY, ULTRASHORT ELECTRICAL PULSES. A. Pakhomov[1,2], K. Walker III[1], J. Kolb[3], K.H. Schoenbach[3], and M. Murphy[2]. [1]McKesson BioServices Corporation, US Army Medical Research Detachment, Brooks City Base, San Antonio, TX, USA. [2]Directed Energy Bioeffects Division, Human Effectiveness Directorate, Air Force Research Laboratory, Brooks City Base, San Antonio, TX, USA. [3]Center for Bioelectrics, Old Dominion Univ., Norfolk, VA, USA

OBJECTIVE: The study explored time- and dose-dependences of the cytotoxic effect of 10-ns electrical pulses (EP), and analyzed potential involvement of different physical and physiological mechanisms.

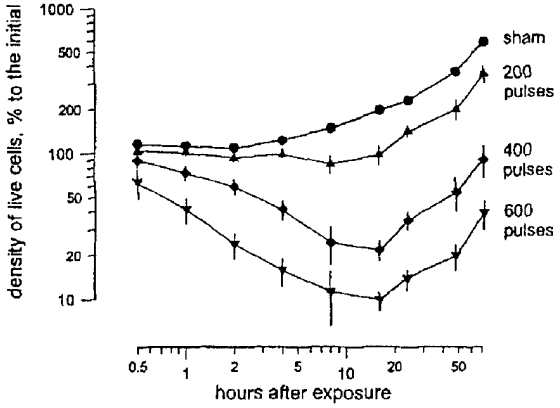


Figure 1. U937 cell survival as a function of time after EP exposure. 10-ns pulses of 110-140 kV/cm were applied at 2 Hz in trains of 200, 400, or 600 pulses. Each point is the mean ± s.e. for 10-17 experiments. A log-log scale was used for better resolution of early timepoints.

METHODS: Human histiocytic lymphoma cells U937 were obtained from ATCC and grown at 37 °C with 5% CO_2 in air in ATCC-modified RPMI 1640 medium with 10% fetal bovine serum. Cells were exposed in the growth medium at 0.2 x 10^6 cells/ml in gene transfer cuvettes (BIORAD) with 1- or 2-mm gap between the electrodes. High-intensity 10-ns pulses were applied using a Blumlein line generator manufactured at the Old Dominion University. Pulse shape and amplitude were monitored with a 500-MHz TDS3052B Tektronix digital oscilloscope using a custom-made high-voltage probe. Pulses of 50 to 300 kV/cm were applied at 0.1-2 Hz, from 1 to 2000 pulses per train. Live and dead cell densities were counted in a hemocytometer at intervals from 0.5 to 72 hours post exposure; live cells were identified by exclusion of the Trypan blue stain. The induction of apoptosis by EP was evaluated by the specific cleavage of poly(ADP-ribose) polymerase (PARP) using Western blot, and by internucleosomal DNA fragmentation using agarose gel electrophoresis. Cells forced into apoptosis by a moderate heat shock or by an exposure to 9% alcohol served as positive controls. In some experiments, the growth medium was exchanged immediately after EP exposure, to check if the cell death might be caused by incubation in the EP-treated medium. In some other experiments, a potent free radical scavenger (500-mM DMSO) was added into the medium prior to EP exposure, to check if the free radical formation is involved in cell killing.

RESULTS: (1) Brief EP trains (e.g., 100 pulses at 100 kV/cm, or 200 pulses at 75 kV/cm) had little, if any cytotoxic effect in U937 cells. (2) Longer EP trains caused profound cell killing, proportional both to the pulse voltage and to the number of pulses applied. (3) Some cells died immediately after the EP exposure; however, the cell survival reached minimum much later, at 8-16 hours after the exposure (Fig. 1). This delay was uniform across a wide range of EP voltages and train durations. (4) The cells that survived the EP treatment proliferated at a regular pace. (5) Initially, tests for apoptosis were performed at scattered time intervals (1-24 hours) after varied EP exposures; only weak or no signs of apoptosis were detected. Recently, the completion of studies of the dose and time dependences in EP-induced cell death made it

possible to identify optimum exposure parameters and specific delays for apoptosis induction and detection, e.g., 4-8 hours after 400-600 EP at 110-140 kV/cm. Indeed, this treatment caused profound apoptosis, as evidenced by both PARP cleavage and DNA ladder assays. (6) During exposures, the temperature of samples was increased by Joule heating. However, direct measurements of temperature in exposed samples with a miniature fiber optic probe established that in all cases the temperature remained far below potentially lethal levels. (7) Replacement of the growth medium after EP exposure with a fresh medium had no effect on cell survival. (8) The presence of DMSO in the medium during EP exposure had no effect on cell survival.

SUMMARY: The study established that trains of 10-ns EP may induce apoptosis in U937 cells. Temperature rise, electrochemical changes in the medium, or free radical formation do not appear to be involved in the EP-induced cell death.

The work was supported by the U.S. Army Medical Research and Materiel Command and the U.S. Air Force Research Laboratory under U.S. Army contract DAMD17-94-C-4069 awarded to McKesson BioServices Corporation, and by an AFOSR/DOD MURI grant on Subcellular Responses to Narrowband and Wideband Radiofrequency Radiation, administered through Old Dominion University.

NANOSECOND PULSED ELECTRIC FIELDS (NSPEF) INDUCE APOPTOSIS IN A p53 INDEPENDENT MANNER IN HUMAN COLON CARCINOMA CELLS. E.H. Hall[1,3,4], P.M. Fox[4], K.H. Schoenbach[3], and S.J. Beebe[2,3,4]. [1]Biomedical Sciences Program, Eastern Virginia Medical School and Old Dominion University, Norfolk, VA [2]Department of Physiological Sciences, Eastern Virginia Medical School, Norfolk, VA [3]Center for Bioelectrics, Old Dominion University, Norfolk, VA [4]Center for Pediatric Research, Eastern Virginia Medical School and Children's Hospital of the Kings Daughters, Norfolk, VA 23510 USA

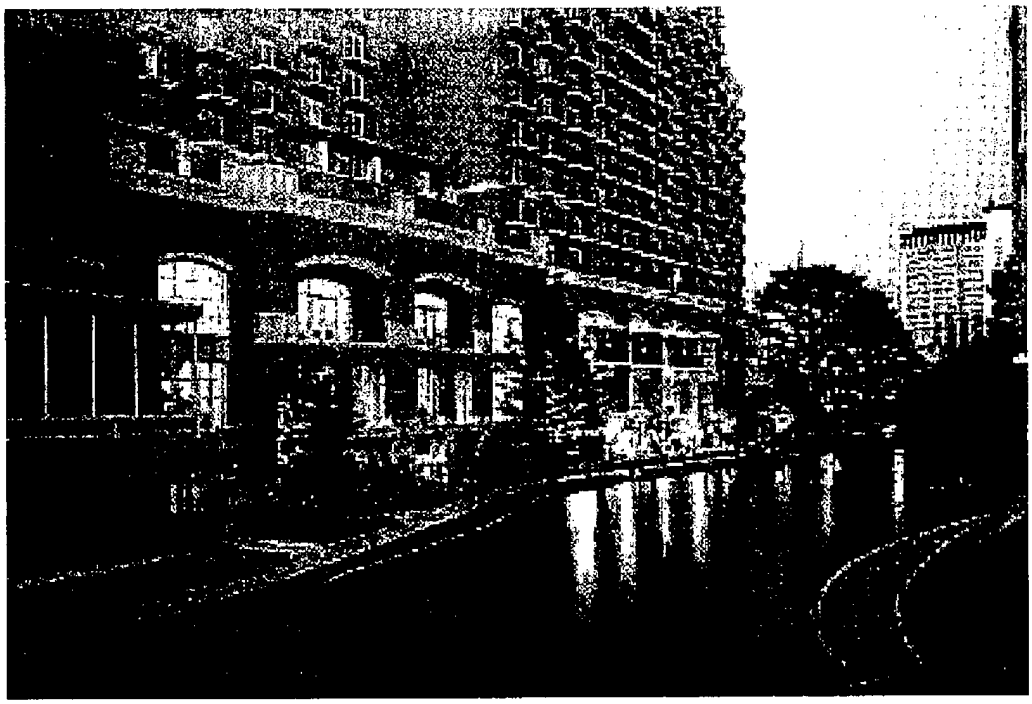
OBJECTIVES: Apoptosis, programmed cell death, can be induced through a variety of extra- and intra-cellular stimuli. Apoptosis has been extensively studied when induced by natural ligands, γ-irradiation, ultraviolet light and chemical stimuli. Cells undergoing apoptosis exhibit a distinctive phenotype characterized by maintenance of membrane integrity, phosphotidylserine (PS) externalization at the plasma membrane and activation of caspase proteases. P53, an important regulator of apoptosis, functions to modulate the cell cycle by arresting cells in the G_1 and G_2 phases to repair DNA damage, and/or to induce apoptosis. In this study we examine the mechanism of p53 in apoptosis when human colon carcinoma cells are stimulated by nanosecond pulsed electric fields (nsPEF).

METHODS: Human colon carcinoma cells, HCT116, which are homozygous for P53 (p53+/+), and p53 null (p53-/-) were grown in RPMI 1640 supplemented with 10% fetal calf serum, 100 U/ml penicillin, 100 µg/ml streptomycin and 2mM L-glutamine. Cells were maintained at 37° C under 5% CO_2. $1x10^6$ cells were placed in 0.1cm electrogap Gene Pulser cuvettes. Cells were pulsed at a common energy density of 1.7J/cc for 1, 3, or 5 times at 60ns 60 kV/cm or 300ns 40kV/cm. nsPEF was delivered to the load, a cuvette containing cell suspensions, by means of a cable pulse generator. The generator consists of a pulse-forming network (PFN), - five 50Ω cables in parallel - and a spark gap in atmospheric air as nanosecond closing switch. The resulting PFN impedance of 10 Ω is matched to the resistance of the load to generate a square wave electric field pulse in the suspension. The pulse duration for the matched system is twice the cable length divided by the speed of light in the dielectric material between inner and outer cable conductor. For a 60 ns pulse generator the length of the cables, which serve as PFN, is 6 m; for a 300 ns pulse generator, the length is 30 m. Cells were removed from the cuvettes and analyzed for a number of apoptotic markers: Ethidium Homodimer-1, a membrane impermeable DNA stain, is a marker for membrane integrity; Annexin-V-FITC binds to phosphatidylserine that is externalized during apoptosis, identifying the cell for phagocytosis *in vivo*; and FITC-VAD-FMK (CaspACE-FITC), a cell permeable, irreversible caspase inhibitor, shows caspase activation in intact cells. Cells were analyzed on a BD FacsCalibur Flow Cytometer. Acquisition and data analysis was done with CellQuest software.

The Society for Physical Regulation in Biology and Medicine

22nd Annual Meeting

January 7-9, 2004



Westin Riverwalk Hotel

San Antonio, Texas, USA

MEETING ABSTRACT 44

THE RULES OF CELL SURVIVAL AFTER EXPOSURE TO HIGH-INTENSITY, ULTRASHORT ELECTRICAL PULSES. Andrei Pakhomov[1,3], Kerfoot Walker III[1], Juergen Kolb[3], Karl Schoenbach[3], [2]Bruce Stuck, and Michael Murphy[4]. [1]McKesson BioServices Corporation, [1,2]US Army Medical Research Detachment, Brooks City-Base, San Antonio, TX, USA; [3]Center for Bioelectrics, Old Dominion Univ., Norfolk, VA, USA; [4]Directed Energy Bioeffects Division, Human Effectiveness Directorate, Air Force Research Laboratory, Brooks City-Base, San Antonio, TX, USA.

OBJECTIVES: The study was aimed to: (1) analyze the dependence of cytotoxic effect of 10-ns electrical pulses (EP) on their voltage, number, and repetition rate, (2) characterize the time dynamics and general mechanisms of cell death, and (3) develop quantitative criteria of sensitivity of different cell lines to 10-ns EP.

METHODS: Experiments were performed in two cell lines, U937 (human histiocytic lymphoma) and Jurkat (human T-cell leukemia). Cells were grown at 37 °C with 5% CO_2 in air in ATCC-modified RPMI 1640 medium with 10% fetal bovine serum. Cells were exposed in the growth medium at 0.2 x 10^6 cells/ml in gene transfer cuvettes (BIORAD) with 1- or 2-mm gap between the electrodes. High-intensity 10-ns EP were applied using a Blumlein line generator manufactured at the Old Dominion University. Pulse shape and amplitude were monitored with a 500-MHz TDS3052B Tektronix digital oscilloscope using a custom-made high-voltage probe. All exposures were performed at a room temperature of 24-25 °C, and even under the most intensive EP treatment the temperature of exposed samples did not exceed 37 °C. Live and dead cell densities were determined by hemocytometer cell counts after Trypan blue staining, at intervals from 0.5 to 72 hr post exposure. The induction of apoptosis by EP was evaluated by the specific cleavage of poly(ADP-ribose) polymerase (PARP) using Western blot, and by internucleosomal DNA fragmentation using agarose gel electrophoresis.

RESULTS: In U937 cells, exposure to brief pulse trains (e.g., 100 pulses at 100 kV/cm, or 200 pulses at 75 kV/cm) killed only few cells, if any. Longer pulse trains and/or higher voltages caused both immediate (necrotic) and delayed (at least partially apoptotic) cell death. Live cell density reached its minimum at 8-16 hr after the exposure; afterwards, surviving cells proliferated at a regular pace. Jurkat cells showed the same immediate and delayed types of cell death, but were far more sensitive to the same EP treatment than U937. Jurkat survivors failed to restore normal proliferation rate within 72 hr of post-exposure observation.

Analysis of the cytotoxic efficiency of varied EP treatments (different E-field values, numbers of pulses, and pulse repetition rates) established that, in most cases, same values of the specific absorbed dose (D, J/g) caused the same decrease in cell survival. For both tested cell lines, the survival decreased exponentially with increasing D, with an initial shoulder at lower doses (Fig.1). However, at survival rates under 10%, the

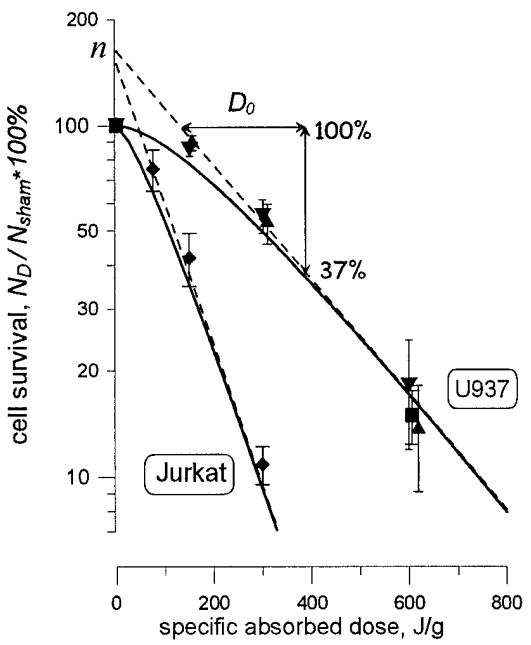


Figure 1. Survival of Jurkat (left) and U937 cells as a function of the specific absorbed dose. Different symbols for U937 cells correspond to mean survival values (±s.e.) for different voltages (87, 125, and 174 kV/cm). Datapoints at doses producing average survival under 10% have not been included. Dashed and solid lines are the best fits approximations using equations (1) and (2), respectively (see text). Calculation of D_0 is illustrated for U937 cells only. See text for more detail.

mean survival values often were situated above the exponential fit line, either due to the presence of a resistant cell fraction in the population, or because of nonuiniform exposure of samples. The survival curves such as shown in Fig. 1 closely resemble well-known types of dose response for bioeffects of ionizing radiation, and can be conveniently descried in the same terms. Disregarding the initial shoulder, the surviving cell fraction $N_{(D)}/N_{(sham)}$ can be calculated as:

$$N_{(D)}/N_{(sham)} = e^{(-\frac{D}{D_0})} \qquad (1),$$

where D_0 is the dose that decreases the survival to 37%. The initial shoulder can be taken into account using the function:

$$N_{(D)}/N_{(sham)} = 1-(1-e^{(-\frac{D}{D_0})})^n \qquad (2),$$

where n is the extrapolated intercept of the exponential portion of the curve with the ordinate axis. (See Fig. 1 for illustration of procedures employed to calculate n and D_0.)

SUMMARY: The indices D_0 and n can be used for quantitative comparison of EP sensitivity of different cell lines. Their respective values in our study were 108 J/g and 1.5 for Jurkat cells, and 266 J/g and 1.63 for U937. Cellular mechanisms responsible for so different sensitivity of these cell lines to EP have yet to be understood. It is important to note, however, that, even at the highest tested doses, heating of samples was not the cause of cell death. The similarity of the dose-response curves with those of the ionizing radiation effect may be pointing to common interaction principles and/or cell killing mechanisms. The possibility of selective killing of certain cell types with little impact on other cells may have potential applications in biotechnology and medicine.

The work was supported by the U.S. Army Medical Research and Materiel Command and the U.S. Air Force Research Laboratory under U.S. Army contract DAMD17-94-C-4069 awarded to McKesson BioServices Corporation, and by an AFOSR/DOD MURI grant on Subcellular Responses to Narrowband and Wideband Radiofrequency Radiation, administered through Old Dominion University.

COMBINED EFFECTS OF PULSED MICROWAVES AND A CNS MITOCHONDRIAL TOXIN ON BEHAVIOR DEPEND ON MICROWAVE-EXPOSURE PARAMETERS. R.L. Seaman[1], M.F. Chesselet*[2], S.P. Mathur*[1], C.D. DiCarlo*[3], S.M. Fleming*[2], J.L. Ashmore*[1], T.H. Garza*[1], J.M. Morin*[1], A.R. Grado*[3], S.L. Adam*[1,3]. [1]McKesson BioServices at US Army Medical Research Detachment, Brooks City-Base, Texas 78235; [2]Dept. of Neurology, UCLA School of Medicine, Los Angeles, CA 90095; [3]US Army Medical Research Detachment, Brooks City-Base, Texas 78235.

OBJECTIVE: To test effects of different microwave pulse parameters typical of military applications on rotenone-induced changes in behavior.

METHODS: *Male Lewis rats (216-293 g) were implanted subcutaneously with 2ML4 Alzet® osmotic minipumps (DURECT Corp.) with Teflon® flow modulators using aseptic surgical technique. The minipumps delivered 0 or 2 mg/kg/day rotenone in dimethylsulfoxide/polyethylene glycol as an animal model of CNS changes in Parkinson's disease [1]. In three different experiments, animals (10-13 per condition in each experiment) were exposed for 6 min on post-op days 4 and 5 to 2.8-GHz microwaves applied as 2-μs pulses at 13, 20, or 200 Hz with respective specific absorption rates (SARs) of 0.4, 0.4, or 4 W/kg or sham-exposed. On post-op day 6, rotenone-induced deficits were quantified by (1) measuring the delay between placement of a forepaw firmly on a flat surface and first movement in a movement-initiation (MI) test and (2) counting the vertical rears made in 5 min in a darkened upright plastic cylinder [2]. The cylinder test was also performed on the day before surgery. Data were tested using ANOVA with rotenone dose and microwave exposure as factors.*

RESULTS: No significant change in colonic temperature occurred during any type of exposure. Across experiments, MI time was generally longer and number of cylinder rears smaller with rotenone, but both variables were unchanged by microwave exposure. The main effects of rotenone on MI time and cylinder rears were significant at the .01 level in each experiment, with the exception of the 13-Hz MI time (p=.5). The main effect of microwave exposure and the rotenone dose-microwave exposure interaction were not significant in any experiment.

CONCLUSIONS: Rotenone had strong, robust effects to increase MI time and reduce number of rears in the cylinder, as expected from our previous work [2]. The lack of effect of exposure to pulsed 2.8-GHz microwaves on rotenone-induced changes, however, contrasted with results of a similar experiment using 1.25-GHz microwaves applied as 6-μs pulses at 10 Hz [3]. Exposure of rotenone-treated animals at 0.4 W/kg in the earlier experiment significantly reduced the longer MI time and tended to increase the smaller number of cylinder rears, both effects in the direction of the respective values without rotenone. Exposure at 4 W/kg in the earlier experiment tended to reduce the rotenone-induced increase in MI time. Differences in results between the current experiments and the earlier experiment may be due to differences in microwave frequency, pulse duration, pulse repetition frequency, exposure setup, or some combination of these factors. Identification of critical microwave exposure parameters for the previously observed effects will be essential in optimizing them for reversal of effects of mitochondrial toxins.

1. *Betarbet R. et al. 2000. Chronic systemic pesticide exposure reproduces features of Parkinson's disease. Nature Neuroscience 3:1301-1306.*
2. *Zhu C et al. 2003. Chronic intravenous and subcutaneous rotenone infusion: Survival analysis, functional assessment and microglial activation." Society for Neuroscience 23rd Annual Meeting, Program No. 95.1.*
3. *Seaman RL et al. 2003. Effects of exposure to pulsed microwaves on movement initiation in rats exposed to the mitochondrial toxin rotenone. 6th Congress of the European Bioelectromagnetics Association (EBEA). Abstracts, p 27.*

Supported by US Army MRMC contract DAMD17-94-C-4069. Investigator(s) adhered to the "Guide for the Care and Use of Laboratory Animals". The views, opinions and/or findings contained in this report are those of the author(s) and should not be construed as an official Department of the Army position, policy or decision.

MEETING ABSTRACT 46

Variable specificity of chronic subcutaneous administration of rotenone for the nigrostriatal pathway.

C. Zhu[1*]; P. Vourc'h[1]; P.O. Fernagut[1]; S.M. Fleming[1]; S. Lacan[1]; C.D. DiCarlo[3]; R.L. Seaman[2]; M.F. Chesselet[1]

[1]Dept Neurol. & Neurobiol., UCLA, LA, CA USA, [2]McKesson BioServices, San Antonio, TX, USA, [3]USAMRD, Brooks City-Base, TX, USA.

Rotenone, a mitochondrial complex I inhibitor, induces neurodegeneration of the nigrostriatal pathway as observed in Parkinson's disease (PD) after systemic infusion in rats (Betarbet et al. '00). However, the specificity of rotenone neurotoxicity remains controversial. We have examined the effects of rotenone in the substantia nigra and the striatum of rats after infusion of rotenone s.c. (2 mg/kg/d) for 21 days. Three patterns of striatal tyrosine hydroxylase immunoreactivity (TH-IR) were observed after rotenone infusion: 46% of animals showed no reduction in TH-IR, 46% of animals showed diffuse reduction in TH-IR, and one animal presented distinct, focal circumscribed loss of TH-IR in the center of the striatum. Confocal microscopy showed that the vesicular monoamine transporter (VMAT2) was decreased in parallel with TH-IR, strongly suggesting a loss of DA nerve terminals in the striatum (rather than a decrease in TH expression) in rats with diffuse or central loss of TH-IR. No TH-IR neuronal loss was detected by stereology in the substantia nigra of rotenone treated rats. Nissl staining, NeuN and DARPP-32 immunoreactivity in the striatum showed an absence of striatal neuronal loss in animals with either preserved striatal TH-IR or diffused TH-IR reduction. However, in the rat with focal TH-IR loss, severe striatal neuronal loss was evident in the center and periphery of the striatum, with central microglial activation. The results indicate that chronic low doses of rotenone rarely induce significant striatal neuronal loss, even when diffuse loss of striatal TH-IR nerve terminals indicates an alteration of the nigrostriatal pathway similar to that seen in early PD. Suppt by USAMRMC DAMD 17-94-C-4069 and PHS ES PHS U54 ES12078.
Keywords: mitochondrial complex I, tyrosine hydroxylase, vesicular monoamine transporter, stereology

Theme G: Neurological and Psychiatric Conditions

Topic: 1. Neurodegenerative Disorders

i. Parkinson's disease: Models

Use of gel-suspended cell cultures for analysis of dose dependence of microwave bioeffects

Pakhomov AG [1,2], *Mathur S* [1], *Gajšek P* [2,3], *Murphy MR* [2]
[1] McKesson BioServices, US Army Medical Research Detachment, Brooks Air Force Base, San Antonio, Texas, USA
[2] Directed Energy Bioeffects Division, Human Effectiveness Directorate, Air Force Research Laboratory, Brooks Air Force Base, San Antonio, Texas, USA
[3] National Institute of Public Health, Ljubljana, Slovenia

Introduction

Exploring the dependence of a microwave bioeffect upon the specific absorption rate (SAR) usually is a laborious process. Numerous experiments are needed to collect biological data after exposures at different SAR levels. We propose a new technique that enables to characterize the effects of a wide range of SAR levels in just a single experiment. For this, small biological specimens (e.g., cells) are exposed to microwaves within a lossy gel (e.g., a cell culture medium solidified with agar). SAR in such a gel decreases exponentially with the distance from the microwave-exposed surface. For example, at 10 GHz, the SAR falls about 2-fold per 1 mm; then, just at 20 mm into the gel, the SAR decreases more than millionfold (by 2^{20}). Consequently, cells suspended within the gel are also exposed at SAR levels ranging more than millionfold. After the exposure, the dependence of a microwave effect on the SAR in these cells can be revealed by customary biological assays.

We employed this technique to compare the effect of continuous-wave (CW) microwaves and extremely high power pulses (EHPP) on the growth rate of yeast cells. The objective of this work was to reveal possible specific effect of EHPP radiation and to establish its SAR threshold.

Methods

Square microwave pulses (9.3 GHz, 0.5-μs width, 10 Hz, 250–270 kW peak) were produced by a model 337X magnetron transmitter (Applied Systems Engineering, Inc.) into a WR90 waveguide (22.86 x 10.16 mm). The peak E-field in the waveguide reached 1.57 MV/m. CW radiation at 9.3 GHz was produced into the same waveguide by means of an HP 8690A sweep oscillator and Hughes 8020H amplifier. The transmitted power was about 1.3 W for both EHPP and CW, with reflection under 3%.

The waveguide terminated via a sapphire matching plate into a custom-made exposure chamber [1]. A similar chamber was used to hold a parallel control sample. The chambers had a common water jacket and were stabilized at 25 °C by a water flow from a circulating bath. This only set the initial temperature, but did not (and was not intended to) compensate for microwave heating in the exposed chamber.

Agarose gels containing yeasts (*Saccharomyces cerevisiae* BY4741) at 2 x 10^6 cells/ml in YPD medium were prepared in two plastic cuvettes (10 x 10 x 35 mm). The cuvettes were put in the exposure and control chambers and submerged into YPD broth. The exposed cuvette axis was aligned with the waveguide axis, and its open bottom was placed directly on the sapphire matching plate. Thus, cells at the bottom of this cuvette were exposed at the highest SAR, which gradually decreased father in the gel.

Local SAR values were calculated by an analytical formula [2], by an FDTD numerical simulation, and also were measured directly using a microthermocouple technique [1–2]. All three methods produced similar results, though the direct measurement data were regarded as the most reliable. Local temperatures in the gel were measured with a Northec fluoroptic thermometer equipped with a PMDE probe (0.55-mm diameter).

The measurements established identical SAR and heating patterns for the CW and EHPP exposures. Along the gel axis, the time-average SAR and peak SAR (EHPP) decreased exponentially from 2 W/g and 390 kW/g at 1 mm from the matching plate to 1 μW/g and 0.25 W/g at 23 mm. Irradiation increased the temperature in the entire gel, with the high at 40.7 °C and the low at 27.5 °C, for the same spots as above. After a 6-hour irradiation, the exposed and control gels were sliced into 2-mm thick pieces in a plane perpendicular to the gel axis. The cell density in the slices was measured by nephelometry and expressed as the optical density (OD) at 600 nm.

Results

Cell density was measured in 24 slices (12 exposed + 12 control) in 16 experiments (8 CW + 8 EHPP). OD of the control gel slices showed only minimal variations which reflected the imprecision of the experimental procedures. The average OD of the control slices was used as a reference level (100%) for each experiment. Slices from both CW- and EHPP-exposed gels showed a profound OD change with the distance from the matching plate. In the vicinity of the plate, the OD steeply increased, from 95–110% in the slice touching the plate to 200–210% in the 4th slice. In the next 4 slices, the OD gradually decreased to 160% and showed only minor fluctuations thereafter. These data correlated well with the temperature profile in the gels: The temperature was optimum for yeast growth (34–35 °C) in the 4th slice, which therefore achieved the highest OD. Slower growth at both higher and lower temperatures resulted in lower OD numbers both closer to the matching plate and father from it. The temperature fell most steeply near the matching plate, and the OD in adjacent slices differed 1.2-1.5 times; there was little temperature gradient in 15–23 mm from the plate, and slice OD values varied by less than 10%.

Obviously, the temperature had major effect on the cell growth rate. While EHPP and CW exposures produced exactly the same heating patterns, their biological effects appeared somewhat different. For example, the OD in the 1st slice (the highest SAR) was 110.2±3.3% after EHPP irradiation, but 96.1±7.6% after CW (mean±s.e.). Most remarkable, the EHPP and CW data differed in the first three slices, but in no one of the other nine slices that were exposed at lower SAR, father away from the exposed gel

surface. Though not statistically significant ($p<0.1$), this trend may manifest a specific effect of EHPP on the cell growth rate, with a threshold at 20–30 kW/g.

Summary

Irradiation of gel-suspended cell cultures proved to be a reliable and highly efficient technique. Combining this technique with color assays and digital image analysis can further its sensitivity and informativeness. The first results are indicative of a specific effect of EHPP at peak SAR over 20–30 kW/g, but the data need confirmation.

Acknowledgements

The authors are thankful to Dr. S. Avery for the yeast strain and to Dr. O. Pakhomova for valuable consultations during this project. The work was supported in part by the U.S. Army Medical Research and Materiel Command and the U.S. Air Force Research Laboratory (AFOSR) under U.S. Army contract DAMD17-94-C-4069 awarded to McKesson BioServices. The views expressed are those of the authors and should not be construed as reflecting the official policy or position of the Department of the Army, Department of the Air Force, or the United States Government.

References

1. Pakhomov A, Mathur S, Doyle J, Stuck B, Kiel J, Murphy M. Comparative effects of extremely high power microwave pulses and a brief CW irradiation on pacemaker function in isolated frog heart slices. Bioelectromagnetics, 2000, 21:245–254.
2. Pakhomov A, Mathur S, Akyel Y, Kiel J, Murphy M. High-resolution microwave dosimetry in lossy media. In: Radio Frequency Radiation Dosimetry (B. J. Klauenberg and D. Miklavcic, eds.), Kluwer Academic Publishers, Netherlands, 2000, 187–197.

Proceedings of the EBEA 2001 5th International Congress of the European BioElectromagnetics Association

6–8 September 2001
Marina Congress Center, Helsinki, Finland

Organizers
European BioElectromagnetics Association (EBEA)
in collaboration with
International Commission on Non-Ionizing Radiation Protection (ICNIRP)
World Health Organization (WHO)

National Organizers
Finnish Institute of Occupational Health
Radiation and Nuclear Safety Authority (STUK)
University of Kuopio
Helsinki Energy

Editors
Maila Hietanen, Kari Jokela and Jukka Juutilainen

Finnish Institute of Occupational Health
Helsinki 2001

Changes in ultrastructure of rat caudate-putamen neurons with a neurotoxin and exposure to pulsed microwaves

Seaman RL [1], *Phelix CF* [2]
[1] McKessonHBOC Clinical & Biological Services and USAMRD Microwave Bioeffects Branch, Brooks AFB, USA
[2] Division of Life Sciences, University of Texas at San Antonio, San Antonio, USA

Objective

Ultrastructure of rat caudate-putamen neurons was assessed after administration of 3-nitropropionic acid (3-NP) and exposure to pulsed microwaves to study possible interaction at the neuronal level. Changes in neuron ultrastructure have previously been reported in the rat after microwave exposure [1] and 3-NP dosing [2] as well as in thermal stress [3] and hypoglycemia [4].

Materials and methods

Eighteen male Sprague-Dawley rats weighing 569±52 g (mean±st.dev.) aged 15–23 weeks were injected intraperitoneally on two consecutive days with 10 mg/kg 3-NP or saline (0 mg/kg 3-NP). Exposure to 1.25-GHz 6-μs microwave pulses at 10 Hz with 0, 0.6, or 6 W/kg whole-body specific absorption rate (SAR) started 1.5 h later and lasted 30 min, giving a total of six experimental conditions. Colonic temperature was measured before and after exposure. Animals were transcardially perfused under deep anesthesia after 3-NP dosing, microwave exposure, and behavioral testing on the second day. The brain was removed and a sample of dorsolateral caudate-putamen of the striatum was taken. Digitized transmission electron microscope images of neuronal somata were taken from randomly selected fields in ultrathin sections. Qualitative analysis of imaged neurons was done by assessing the integrity of cytoplasm, mitochondria, rough endoplasmic reticulum (RER), Golgi apparatus, nucleus, and membranes. Computerized quantitative image analysis of the neurons was done using UTHSCSA Image Tool (University of Texas Health Science Center, San Antonio) to measure mitochondrion diameter, RER intracisternal width, and nuclear envelope (NE) thickness. Assessments and measurements were done by an investigator blind to the experimental conditions.

Results

Percent of examined caudate-putamen neurons (12–24 per condition) that exhibited qualitative abnormalities was, for 0, 0.6, and 6 W/kg, respectively, 15, 43, and 71% for 0 mg/kg 3-NP and 93, 33, and 100% for 10 mg/kg 3-NP. Mitochondrion diameter was not significantly different from control for any microwave, 3-NP, or microwave-3-NP condition. Without 3-NP, RER and NE dimensions for 6 W/kg were approximately

twice their respective values for 0 and 0.6 W/kg. With 10 mg/kg 3-NP, RER and NE dimensions for 0 and 6 W/kg were similar to or larger than the respective value for 6 W/kg without 3-NP. The RER and NE dimensions with 10 mg/kg 3-NP for 0.6 W/kg (2 animals) were smaller than for 0 and 6 W/kg and approximated values for 0 and 0.6 W/kg with 0 mg/kg 3-NP.

Conclusions

Two doses of 10 mg/kg 3-NP and two exposures to pulsed microwaves at 6 W/kg each increased RER and NE dimensions of striatal neurons. The effect of 3-NP and microwaves at this SAR seemed to be additive for RER. Microwave exposure at 0.6 W/kg alone did not change any measure but seemed to lessen the effect of 10 mg/kg on RER and NE. Although sampled at an early point in any neurodegeneration process that might have been initiated, the observed changes in ultrastructure had many characteristics of changes reported after other microwave exposures and 3-NP dosings [1–2] as well as in thermal stress [3] and energy depletion [4]. No change seen here indicated ensuing cell death. Chemical hypoxia induced by 3-NP and thermal stress (38.9-41.0°C colonic temperature) caused by 6 W/kg SAR were most likely responsible for the ultrastructural changes seen here.

Acknowledgement

Supported by the U.S. Army Medical Research and Materiel Command under contract DAMD17-94-C-4069 awarded to McKessonHBOC BioServices and by NIH Grant HL02914. The views, opinions and/or findings contained in this report are those of the authors and should not be construed as an official Department of the Army position, policy or decision. In conducting this research, the investigator(s) adhered to the "Guide for the Care and Use of Laboratory Animals," prepared by the NRC Institute of Laboratory Animal Resources. Image Tool is available at maxrad6.uthscsa.edu.

References

1. Albert EN, DeSantis M. Do microwaves alter nervous system structure? Ann NY Acad Sci 1975, 247:87–100.
2. Hamilton BF, Gould DH. Nature and distribution of brain lesions in rats intoxicated with 3-nitropropionic acid: A type of hypoxic (energy deficient) brain damage. Acta Neuropathol (Berl) 1987, 72:286–297.
3. Sharma HS, Westman J, Nyberg F. Pathophysiology of brain edema and cell changes following hyperthermic brain injury. Prog Brain Res 1998, 115:351–412.
4. Kalimo H, Auer RN, Siesjö BK. The temporal evolution of hypoglycemic brain damage. III. Light and electron microscopic findings in the rat caudoputamen. Acta Neuropathol (Berl) 1985, 67:37–50.

Proceedings of the EBEA 2001 5th International Congress of the European BioElectromagnetics Association

6–8 September 2001
Marina Congress Center, Helsinki, Finland

Organizers
European BioElectromagnetics Association (EBEA)
in collaboration with
International Commission on Non-Ionizing Radiation Protection (ICNIRP)
World Health Organization (WHO)

National Organizers
Finnish Institute of Occupational Health
Radiation and Nuclear Safety Authority (STUK)
University of Kuopio
Helsinki Energy

Editors
Maila Hietanen, Kari Jokela and Jukka Juutilainen

Finnish Institute of Occupational Health
Helsinki 2001

Paper

ELECTROMAGNETIC FIELD STANDARDS IN CENTRAL AND EASTERN EUROPEAN COUNTRIES: CURRENT STATE AND STIPULATIONS FOR INTERNATIONAL HARMONIZATION

P. Gajšek,*† A. G. Pakhomov,*‡ B. J. Klauenberg*

Abstract—**Electromagnetic field standards in the West are based on well-established acute biological effects that could be considered as signaling a potentially adverse health effect. The specific absorption rate, which is proportional to the tissue heating (thermal effects), represents the basic restriction of exposure to Radio-Frequency (RF) fields. On the other hand, Eastern European standards are designed to protect from potential non-thermal effects that might be caused by chronic exposure to very low intensities, where a so-called "power load" (a product of field intensity and duration of exposure) represents the basic limitation. Thus, electromagnetic field standards in Eastern European countries differ considerably from those which are proposed by the International Commission of Non-ionizing Radiation Protection and the Standards Coordinating Committee 28 of the Institute of Electrical and Electronics Engineers, Inc. In the present paper, the strategies for development of exposure limit values in electromagnetic fields standards currently in force in Eastern and Central European countries are discussed. Some differences as well as similarities of the national health and safety standards and the main obstacles to harmonization of these standards with those being established by Western national and international organizations and agencies are presented.**
Health Phys. 82(4):473–483; 2002

Key words: radiation, nonionizing; safety standards; electromagnetic fields; radiation protection

INTRODUCTION

GLOBALIZATION AND the rapid growth of mobile telecommunications world-wide have focused attention on the large differences existing in standards limiting exposure to electromagnetic fields (EMF). Differences in the exposure limit values in EMF standards among some Eastern European (EE) and those of Western countries are over two orders of magnitude. These differences have raised concerns about the lack of uniformity and have led to public concern and distrust about EMF exposures from the increased use of various EMF sources in the living and working environment (Gajšek 2000). It has become evident since the first standards and guidelines began to be discussed in the late 1950's, that different approaches were being taken by various national and international authorities and agencies in the drafting of standards and guidelines.

Differences in Western standards have recently been reviewed. Erdreich and Klauenberg (2001) identified sources of differences in exposure limits by evaluating eight standards that were selected using the following criteria: 1) derived by a scientific or technical organization from an examination of scientific data rather than an adaptation of or adoption of another standard; 2) included some description of their approach; 3) included the general population instead of solely workers as the group to be protected; and 4) available in English. Comparisons were made by examining the scope of the underlying database and the various rationales for safety factors. They reported that each of the standards evaluated in the energy-deposition range (0.1 MHz to 10.0 GHz) was found to use the same basic restriction (0.4 W kg^{-1}), based on biological data and a 10-fold safety factor, although the actual interpretations of the underlying biological data differed. In the surface-heating range (10–300 GHz), variability in exposure limits and approaches to time averaging and frequency dependence were seen. They noted that often explanations were insufficient to account for differences among the standards. The largest measure of difference was that of how safety factors were incorporated into the standards and the basis for the safety factors. They concluded that the standards reviewed were based on threshold-acting effects with additional safety factors. This is generally consistent with the methods for non-cancer risk assessment used by major scientific organizations worldwide and with the view that risk assessment procedures should facilitate harmonization of RF standards.

In contrast, the lack of published data from EE research groups in peer reviewed journals including unknown scientific criteria for establishment of the health hazards makes validation of the rationale used in EE standards very difficult. An effort to analyze the available research data, which were used as a basis for EE standards, is underway (see Conclusion).

In collaboration with many countries worldwide, which are now considering new EMF standards, the

* Air Force Research Laboratory, Directed Energy Bioeffects Division, Brooks AFB, TX 78235; † National Institute of Public Health, Ljubljana 1000, Slovenia; ‡ McKesson BioServices, Brooks AFB, San Antonio, TX 78235.

For correspondence or reprints contact: Peter Gajšek, Institute of Public Health, Trubarjeva 2, 1000 Ljubljana, Slovenia, or email at Peter.Gajsek@IVZ-RS.si.

(*Manuscript received* 1 *November* 2000; *revised manuscript received* 22 *August* 2001, *accepted* 26 *November* 2001)

0017-9078/02/0

Copyright © 2002 Health Physics Society

World Health Organization (WHO) has launched a project for establishing internationally-acceptable EMF standards. In order to facilitate the harmonization of EMF standards, many scientific meetings have been held worldwide (Russia 1998, Slovenia 1998, Croatia 1998, China 1999, Italy 1999, Germany 2000, China 2000, USA 2000, Bulgaria 2001).

BASIS FOR EE STANDARDS

Currently there is a large body of literature available from East and West illustrating the great variety of reactions of the organism (including human) to exposure to EMFs. If there was an agreement among scientists in the interpretation of what an adverse health effect[§] is and the reasons for that effect, then bioeffects in the form of functional changes of one or another biological system might not be interpreted differently. Some authors (Paltsev and Suvorov 1998; Nikitina 1998) consider any change in reaction of the organism (including human) in response to EMF exposure as unfavorable. These differences in the interpretation of the human organism's reactions to the effects of EMFs are the most important factor since the final exposure limit values in "Hygienic Standards" depend on interpretation.

Basic questions about the biological effects in Western as well as in EE countries concern the possibility of effects of prolonged exposure to low level EMF, in addition to the heating or thermal effects. While Western experts do not consider such effects established, and thus not suitable for basing standards upon, this premise has strongly shifted the research focus and influenced the rationale for standards setting in EE.

Much of the key experimental research that had represented the background for very low limit values in EE standards investigated the effects of chronic microwave radiation exposure on different organisms including humans in the former USSR. The length of one exposure is usually indirectly proportional to the intensity of the field in order to avoid acute manifestation of the heating effect. In principle, long term irradiation of relatively low intensities was applied (power density from 1 up to 1,000 μWcm^{-2}; irradiation from several minutes to 7 h daily or 5 d/wk, for a total duration of up to several months). Some results of the experimental research have shown distinct dependence of microwave bioeffects on the intensity and duration of exposure (Lokhmatova 1994; Tomashevskaya and Dumansky 1988; Marha 1963). A variety of techniques was employed to analyze the organism response to irradiation, including such endpoints as the body weight, temperature, heart rate, blood pressure, behavior, electrical activity of the brain, hormone production, immune function, blood and tissue composition, fertility, and the estrus cycle (Pakhomov and Murphy 2000; Marha 1971). In many experiments in EE, long term irradiation of comparatively low intensities provoked distinctive functional changes in the central nervous and endocrine systems, including immunity (Grigoriev 1998; Nikitina 1998; Pakhomov and Murphy 2000).

While some studies were flawed, or were poorly presented in publications, still many other good quality studies have convincingly demonstrated bioeffects of low level RF (see for review Pakhomov and Murphy 2000). Most reported bioeffects of low-intensity RF were just subtle functional changes, not exceeding the range of normal physiological variation and only detectable by sensitive tests (Nikitina 1998). However, some studies did report clearly pathogenic effects, and an independent confirmation of these findings would be of principal importance for understanding of the health hazards from RF exposure and development of safety standards (Pakhomov and Murphy 2000). Replication seems to be a very difficult task due to methodological deficiencies that could be found in many EE publications (lack of statistical and dosimetric data, poorly developed extrapolation of experimental data from animals to humans, and results obtained in experiments with high EMF intensities to low intensities).

The experimental research necessary to establish a threshold for a harmful effect encounters a series of challenges that are difficult to resolve. Research results depend on the adequacy and sensitivity of the methods used, on the species and body dimensions of the laboratory animals, on the quality of the applied dosimetric techniques, on the qualifications of the researcher, and many other considerations. Therefore, it is not always possible to replicate and compare the results of experiments carried out by different researchers.

Several studies, which were used as basis for standards settings in EE,** are illustrated here.

Vinogradov and Naumenko (1986) found that prolonged microwave irradiation of rats disrupted the antigenic properties of brain tissue and suggested that this action could provoke an autoimmune response. Wistar rats were exposed in an anechoic chamber to 2,375 MHz microwaves at 50 or 500 μWcm^{-2} for 7 h daily over a 30-d period. Experimental results revealed that exposure at 500 μWcm^{-2} evoked a pronounced autoimmune response in comparison with sham-exposed animals: auto-antibody levels rose 2.5 times, the basophil degranulation index increased from 4.8% to 26.3%, and the percent of plaque-forming cells rose from 0.6% to 5.9%. The lower radiation intensity had essentially the same but less pronounced effects. The authors' further experiments demonstrated that the autoimmune response at 500 μWcm^{-2}, in contrast to changes caused at 50 μWcm^{-2}, can be regarded as an autoimmune disorder. They also suggested that the detected

[§] Biological effects producing consequences outside the body's normal range of physiological compensation and are detrimental to health or well-being. WHO defines health as a state of complete physical, mental and social well-being, and not merely the absence of disease or infirmity. WHO's definition of health requires that effects such as headaches, sleep disturbance, irritability or other effects that compromise well-being must be taken into account.

** Personal communication, Y. Grigoriev, 2000.

autoimmune alterations could result from damage to the blood-brain barrier caused by chronic microwave exposure.

Perhaps the most pronounced and unambiguously adverse effects of low-intensity microwave radiation were reported by Lokhmatova (1994). Effects on reproductive organs of a 4-mo exposure for 2 h per day (3 GHz, 250 μWcm^{-2}) were studied in 22 adult male rats. The experiments revealed explicit morphofunctional disorders in RF exposed animals. Most of these disorders showed only a subtle or lack of trend to recovery in 4 mo after the end of exposures. The author concluded that the changes evoked by the prolonged microwave exposure are likely to result in stable impairments of production and balance of steroid hormones and premature loss of reproductive function.

Navakatikyan et al. (1990) reported on the influence of RF on the thyroid gland. Multiple irradiation of rats with continuous-wave (CW) RF (2,450 MHz, 1 $mWcm^{-2}$) increased the functional activity of the thyroid gland, while a pulsed RF (3,000 MHz, 0.1 to 1 $mWcm^{-2}$) had the opposite effect; no changes were found in the triiodothyronine and thyroxin levels in blood serum.

In a different study (Navakatikyan 1990), albino rats were exposed at 2,375 MHz, 1, 5, 50, or 500 μWcm^{-2}, 7 h per day, 5 days a week for 1 to 3 mo. Inhibition of the activity during open field tests and diminution of consolidation of the defensive conditioned reflexes in a chamber occurred during RF treatment (5 to 500 μWcm^{-2}) while general activity increased and reflex consolidation gradually normalized during the post-irradiation period.

Tomashevskaya and Dumansky (1988) exposed adult white rats to 400-Hz microwave pulses for 16 h per day for 4 months using various carrier frequencies, intermittence regimens, and field intensities: (1) 2,750 MHz, 50, 100, or 500 $mWcm^{-2}$, (2) 1,310 MHz, 20 or 100 $mWcm^{-2}$, and (3) 850 MHz, 20, 100, or 500 $mWcm^{-2}$. The experiments established that exposures at 100 and 500 $mWcm^{-2}$ could cause statistically significant changes in the activity of several marker enzymes (cholinesterase, cytochrome oxidase, succinate dehydrogenase, and ceruloplasmin); the magnitude of changes in different tissues varied depending on the particular irradiation regimen. Exposures at 20 and 50 $mWcm^{-2}$ produced no statistically significant effects compared to sham-exposed controls.

Navakatikyan et al. (1991) studied the animals' exploratory activity in a maze and conditioned avoidance reflex in a shuttle box during 3 GHz pulsed radiation exposure to 0.1, 0.5, and 2.5 $mWcm^{-2}$ of duration of 2 mo. Most of the exposure regimens slightly stimulated the locomotor activity (except at 0.5 and 2.5 $mWcm^{-2}$). Performance in the shuttle-box after exposures was characterized by decreased latency of responses and increased number of correct responses. Overall, the changes were interpreted as a prolonged and moderately expressed activation of the central nervous system.

Navakatikyan and Tomashevskaya (1994) reported on suppression of the central nervous system during 2,450 MHz CW irradiation to 0.01–1 $mWcm^{-2}$ of duration of 2 mo, in contrast to weak activation under pulsed irradiation. Pulsed microwaves consistently and reproducibly decreased blood levels of insulin and testosterone, while CW exposure had no effect. The authors have speculated that inhibition of behavior was a direct effect of irradiation on the nervous system, whereas activation might be mediated by hormonal changes.

In the scientific community, there are different opinions and interpretations on the background of EE standards. Most Western experts argue that EE standards are based on unconvincing research evidence and, thus, much less reliable than those founded on the concept of specific absorption rate (SAR[††]). Since unknown scientific evaluation criteria have been used to establish thresholds for unfavorable effects or even a no-effects level, it is not clear how the EE standards were derived. It could be presumed that lower exposure limits in the EE standards are largely based on possible negative health outcomes at levels of RF, which can not be explained by thermal mechanisms (Sliney et al. 1985). Grigoriev (1998) reported that EE countries set standards based on the position that EMF exposure should not affect homeostasis or activate protective and adaptation-compensatory mechanisms either acutely or in the long term.

It is well established that the existence of biological responses to low level EMF is a normal phenomenon for humans and need not be accompanied by negative health consequences. In spite of all that, this approach has been taken as a rationale for permissible EMF levels and is shared by the majority of experts in EE countries. Based on the data illustrated above and other experimental studies, as well as on clinical research in exposed workers, the following exposure restrictions were set (Grigoriev 1998; Savin 1988; Nikonova 1998):

- 100 μWcm^{-2} = duration of exposure up to 2 h;
- 1,000 μWcm^{-2} = exposure duration up to 20 min for a full work day; and
- For a working day a dose ([power density ($mWcm^{-2}$) multiplied by the duration of exposure (h)] may be 200 $\mu Wcm^{-2}h$.

This early concept, that was introduced in former USSR (Federal Standard of the USSR 1984), was strongly supported and adopted with some changes by the EE countries that were member states of the Warsaw Pact. Limit values for occupational exposure ("power load"–power density vs. duration of exposure) in the frequency range 0.3–300 GHz according to EE standards are presented in the Fig. 1.

CURRENT STATUS OF EMF STANDARDS IN EASTERN AND SOME CENTRAL EUROPEAN COUNTRIES

In the process of the integration into the European Union, many Central and Eastern European countries

[††] To find the total rate of energy absorbed by an object, the rate of absorbed energy must be calculated at each point inside the body and summed (integrated) over the entire volume of the body. SAR (W/kg) is defined, at a point in the absorber, as the time rate of change of energy transferred to an infinitesimal volume at that point, divided by the mass of the infinitesimal volume. In Western standards, the SAR is a measure of the dose rate, but is usually referred to as dose.

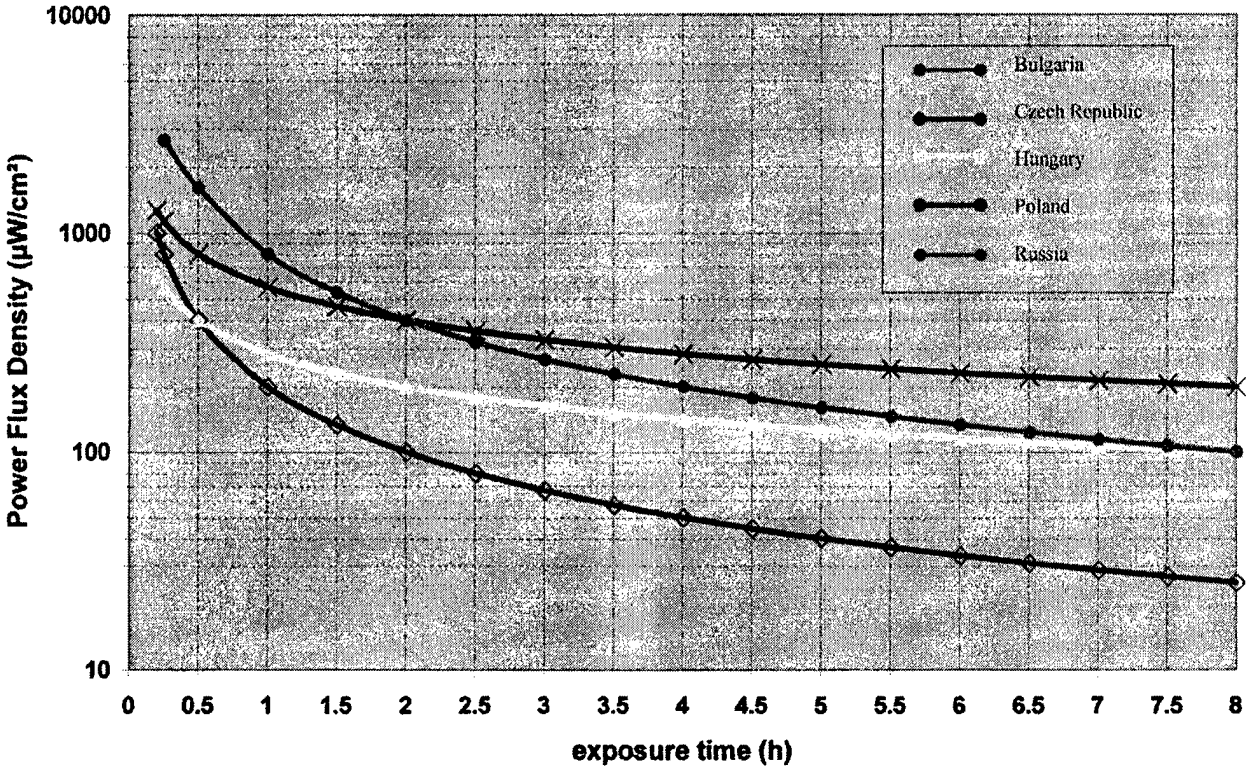


Fig. 1. Limit values (power load) for occupational exposure (power density vs. duration of exposure) in the frequency range 0.3–300 GHz according to Bulgarian (BG), Czech (CZ), Hungarian (H), Polish (PL), and Russian (RUS) standards.

have implemented European legislation and standards. In 1995, the European Committee for Electrotechnical Standardization (CENELEC) released the pre-standard on human exposure to EMF (CENELEC 1995). Some CE and EE countries have adopted that European pre-standard. In the meantime, CENELEC did not get a mandate to adopt the pre-standard. The main tasks of CENELEC-Technical Committee (TC 211) for the future will be related to developing procedures and technical norms for implementation of the recommended exposure limits rather than to promulgate standards related to protection of human health. In 1998, the European Council has introduced a Recommendation on EMF in order for the Member States of the European Union to adopt a harmonized policy, which should avoid concerns of the public and increase the trust in the authorities. In particular, Member States are recommended to enforce a unique safety standard, which conforms to the recent guidelines of the International Commission for Non Ionizing Radiation Protection (ICNIRP 1998).

Some EE countries have a long tradition in setting RF health and safety standards. The first "Hygienic Standards" for EMF were established in the former Soviet Union (USSR) in the mid-1950's, where the exposure limits were adopted for an occupational exposure standard in the frequency range 100 kHz to 300 MHz. In 1958, temporary standards for centimeter waves were adopted and later extended also to decimeter and millimeter ranges. Current EMF standards in EE countries [Bulgaria (BG), Czech Republic (CS), Hungary (H), Poland (PL), Romania (RO), Russia (RUS), and Slovakia (SK)] show some differences, but a comparison of exposure limits reveals certain elements that are common to all and which differentiate them from Western standards:

1. A "dose"‡‡ concept of EMF occupational exposure (time limitation in duration of exposure in stronger EMF fields-measure of cumulative exposure) with high EMF intensity allowed for a short-term (few minutes) exposure and low EMF intensity for a full workday (8–10 h daily) exposure;
2. Very low limit values for public unlimited exposure to RF radiation. Some EE countries have also implemented a "dose" concept in exposure limits for the general public;
3. Limit values for pulsed vs. continuous RF fields at frequencies 0.3–300 GHz are higher by a factor of 10; and
4. Standards in some EE countries divide the area below the restricted area into numerous (usually 3–5) zones with different time and/or dwelling limitations.

‡‡ This is not really a dose absorbed in the body, but rather the quantity that represents the environmental levels of incident power flux intensity of field strengths and duration of the exposure (cumulative exposure). EE standards are implementing this term with an aim to calculate the time dependent occupational or residential exposure.

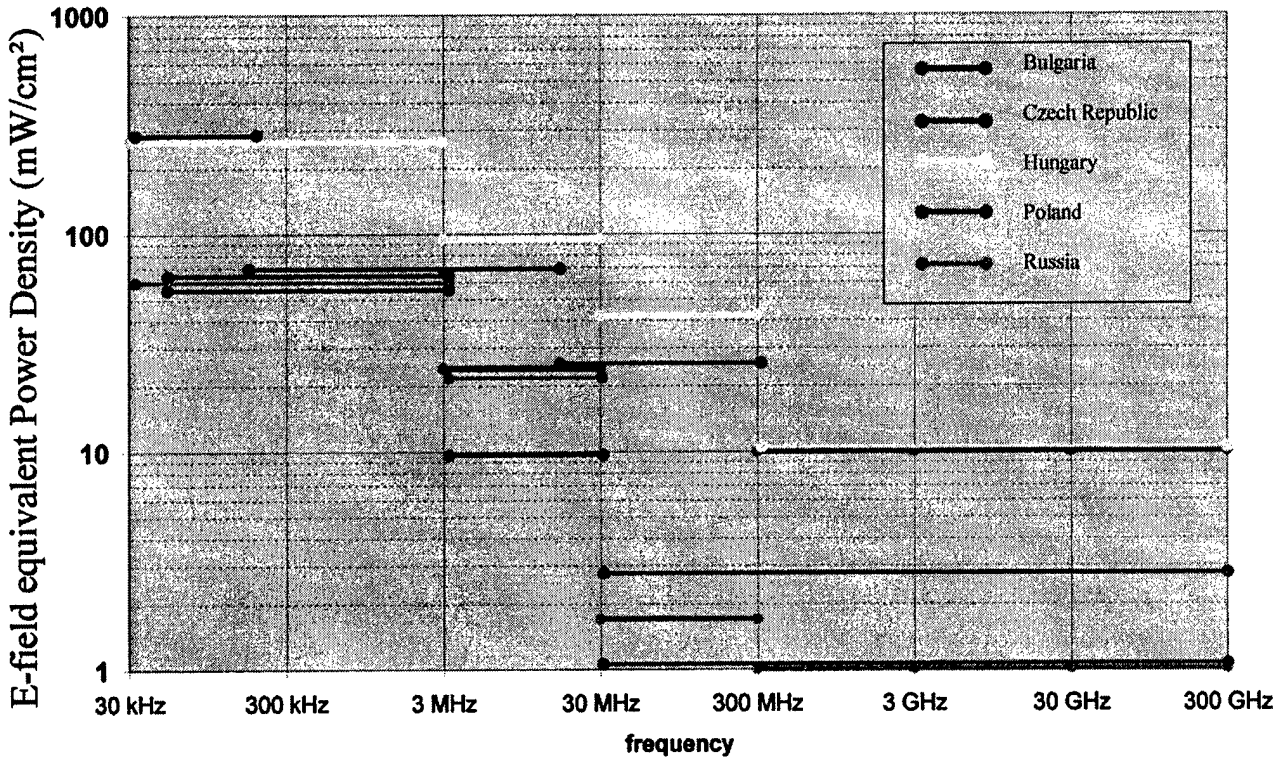


Fig. 2. Limit values for maximal permissible occupational exposure (not allowed any time) in the frequency range 30 kHz–300 GHz according to Bulgarian (BG), Czech (CZ), Hungarian (H), Polish (PL), and Russian (RUS) standards.

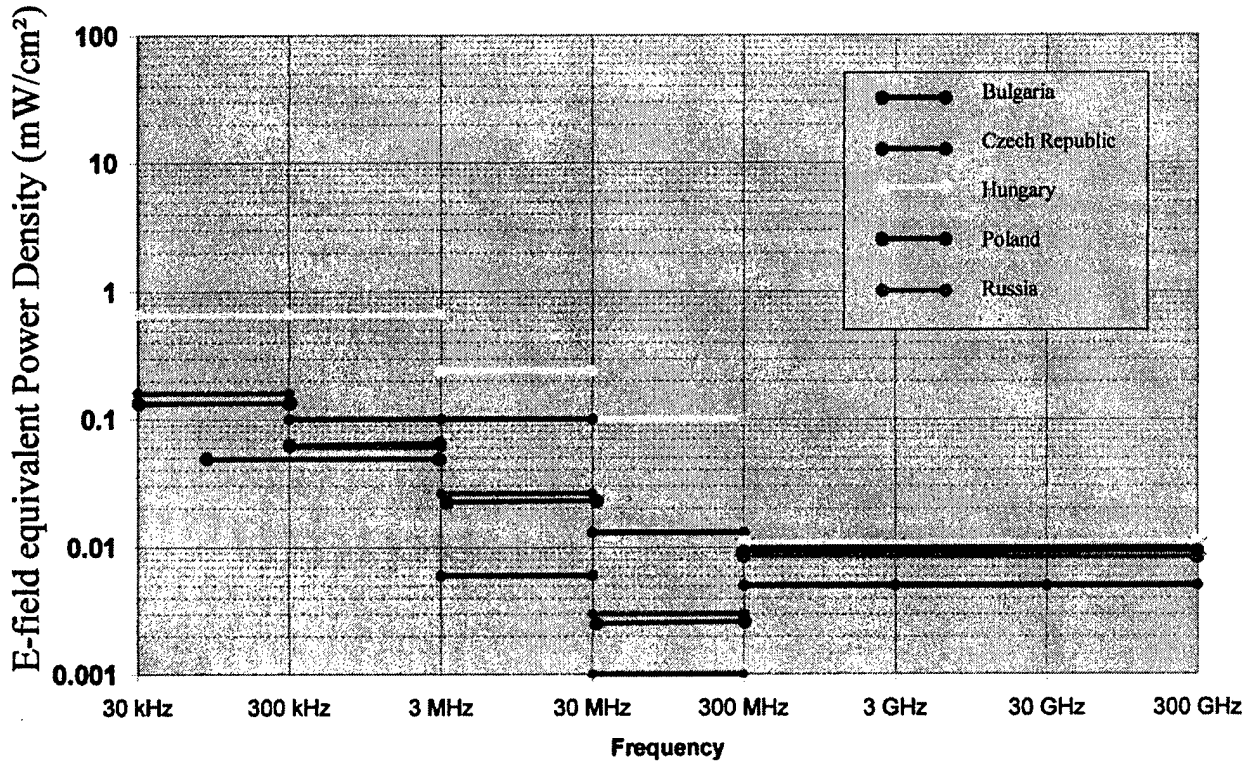


Fig. 3. Limit values for unlimited public exposure in the frequency range 30 kHz–300 GHz according to Bulgarian (BG), Czech (CZ), Hungarian (H), Polish (PL), and Russian (RUS) standards.

Table 1. Limit values for occupational and public exposure to RF EMF in Bulgaria.

	Occupational exposure						Public exposure	
f (MHz)	E_{max} (Vm^{-1})[a]	H_{max} (Am^{-1})[a]	S_{max} (μWcm^{-2})[a]	W_E ($V^2\ m^{-2}\ h$)[b]	W_H ($A^2\ m^{-2}\ h$)[b]	W_S ($\mu Wcm^{-2}\ h$)[b]	E_m (Vm^{-1})[c]	S_m (μWcm^{-2})[c]
0.03–0.06							25	
0.06–0.3	500	50		20,000	200		25	
>0.3–3	500	50		20,000	200		15	
3–30	200	50		3,200	200		10	
30–300	60			800			3	
300–30,000			1,000			200		10

[a] E_{max}—maximal electric field strength; H_{max}—maximal magnetic field strength; S_{max}—maximal power density.
[b] W_E—maximal permissible exposure parameter (power load) expressed in electric field (E) and duration of exposure in hours (h); W_H—maximal permissible exposure parameter (power load) expressed in magnetic field (H) and duration of exposure in hours (h); W_S—maximal permissible exposure parameter (power load) expressed in power density (S) and duration of exposure in hours (h).
[c] E_m—maximal electric field strength allowed for unlimited exposure; S_m—maximal power density allowed for unlimited exposure.

Table 2. Limit values for occupational and public exposure to RF EMF in Hungary.[a]

		Occupational exposure Duration of exposure			Public exposure
f (MHz)	Intensity	$t = 8$ (controlled)	$0.8 < t < 8$ (restricted time)	(not allowed)	Unlimited exposure
0.03–3	E (Vm^{-1})	≤120	$960/t$	>1,000	50
3–30	E (Vm^{-1})	≤60	$480/t$	>600	<30
30–300	E (Vm^{-1})	≤40	$320/t$	>400	<20
300–300,000	S ($mWcm^{-2}$)	≤0.1	$\sqrt{0.08/t}$	>10	<0.01

[a] Notes: t = duration of exposure in hours.

The currently effective EE safety standards are reviewed in more detail below and presented in Figs. 1, 2, and 3.

Bulgaria

In Bulgaria, there are several ordinances (obligatory) and national standards (voluntary) dealing with EMFs in the frequency range 60 kHz–300 GHz for occupational exposure and in the frequency range 30 kHz–30 GHz for general public exposure (BNS 1990a, b). The current RF EMF standards are in close conformity with the Russian standards for occupational and public exposures which are based on two parameters: intensity and duration of exposure (Table 1). There are also other ordinances and standards that cover static and low frequency EMF. Standard setting authorities in Bulgaria are in the process of updating the existing standards and thereby harmonizing them with other newly updated EU standards. Since the Bulgarian government has started negotiations with EU for associate membership, most of the laws and regulations in the country are based on European Directives and Standards. In 1999, the European pre-standard (CENELEC 1995) was translated and accepted as a non-obligatory national standard.

Hungary

In 1985, the Hungarian Standard Institution (HSI) released a standard (Hungarian National Standards 1986) relevant to electromagnetic fields and human exposure in the frequency range of 30 kHz–300 GHz (Table 2). The standard had separate permissible levels for general public and workers, defined as controlled and uncontrolled areas. A third area was also defined in which access is allowed only with safety-shielded clothes. In the range of 30 kHz–300 MHz, the standard defines a fourth tier called a harmless area where a flat limit value of 3 Vm^{-1} is introduced. The values of permissible levels are close to those of other Eastern European countries. Below 30 kHz there is no national standard relevant to human exposure. There is a National Standard (MSZ 151/5-86) dealing with power frequency electric field only. In practice, the ICNIRP guidelines for the frequency range below 30 kHz are used. According to the general policy of the Hungarian Government, all EU confirmed standards are considered as Hungarian National Standards. In May 1997, the HSI released the European Prestandard (CENELEC 1995) as the Hungarian Prestandard.

The Czech Republic and Slovakia

In the Czech Republic, the ordinance on human health protection from the adverse effects of electromagnetic radiation was implemented in 1990 (Czech Republic 1990). The ordinance determines the values of the maximum permissible irradiation and field ceiling levels for both occupational exposure and general population in the frequency range between 60 kHz and 300 GHz (Czech Republic 1993). The values of permissible levels are close to the reference levels of other Eastern European countries, but are very conservative. The time factor together with the field level for occupational and public exposure are shown in Table 3. Identical standards and legislation are used in Slovakia.

Table 3. Limit values for occupational and public exposure to RF EMF in the Czech Republic and Slovakia.

	Occupational exposure						Public exposure		
f (MHz)	E_{max} (Vm^{-1})[a]	H_{max} (Am^{-1})[a]	S_{max} (μWcm^{-2})[a]	W_{E_2} ($V^2\ m^{-2}\ h$)[b]	W_{H_2} ($A^2\ m^{-2}\ h$)[b]	W_S ($\mu Wcm^{-2}\ h$)[b]	W_{E_2} ($V^2\ m^{-2}\ h$)[b]	W_{H_2} ($A^2\ m^{-2}\ h$)[b]	W_S ($\mu Wcm^{-2}\ h$)[b]
0.06–3	500	50		50,000	200		5,000	20	
3–30	300			7,000			700		
30–300	100			800			100		
>300			2,560			800 K_1[c]			120 K_2[c]

[a] E_{max}—maximal electric field strength; H_{max}—maximal magnetic field strength; S_{max}—maximal power density.
[b] W_E—maximal permissible exposure parameter (power load) expressed in electric field (E) and duration of exposure in hours (h); W_H—maximal permissible exposure parameter (power load) expressed in magnetic field (H) and duration of exposure in hours (h); W_S—maximal permissible exposure parameter (power load) expressed in power density (S) and duration of exposure in hours (h).
[c] K_1—multiplication factor for stationary (K = 1) or rotating antennas (K = 2.5–120); K_2—multiplication factor for stationary (K = 1) or rotating antennas (K = 5–360).

Table 4. Limit values for occupational and public exposure to RF EMF fields in Poland.[a]

		Occupational exposure Duration of exposure			
f (MHz)	Intensity	t = 8 (safety zone)	0.08 < t < 8 (intermediate zone)	t = 0 (dangerous zone)	Public exposure Unlimited exposure
0.001–0.1	E (Vm^{-1})	≤100	$100/(\sqrt{t/8})$	>1,000	—
	H (Am^{-1})	≤10	$10/(\sqrt{t/8})$	>100	—
0.1–10	E (Vm^{-1})	≤70	$560/t$	>560	<5
	H (Am^{-1})	≤10	$80/t$	>250	—
10–300	E (Vm^{-1})	≤20	$20/(\sqrt{t/8})$	>300	<2
	H (Am^{-1})	—	—	—	—
300–3,000,000	S (Wm^{-2})	≤2	$2/(\sqrt{t/8})$	>100	<0.025

[a] Notes: t = duration of exposure in hours.

As a part of integration into the EU, the Czech Republic is discussing the implementation of the ICNIRP guidelines.

Poland

The Polish standard gives the limit values in the frequency range 0.1–300 GHz in close agreement with reference levels of other Eastern European countries (Table 4). Limit values for occupational exposure (for 8-h working shift) are one order of magnitude lower than comparable Western standards (Szmigielski 1999). New limit values for general public were issued in August 1998 and were set lower than Western standards for the same frequency range (0.1 Hz to 300 GHz). This is due to the fact that the earlier Polish standard was set at extremely low levels and it would be difficult to increase the limit values for public exposure in the future. It seems rather questionable that Poland will accept the proposed Western limit values. In the future a complex of occupational and public exposure standards covering the whole frequency range from 0 Hz to 300 GHz is planned.

Romania

Romania does not have a national standard for exposure to RF fields. Although a draft version was published in 1995, no final version has been accepted yet. In the meantime the directions Romania follow are those of European Prestandard (CENELEC 1995). Internal regulations are those directed by the Romanian Work and Social Protection Department and by the Health Department. Exposure limitations to RF fields are connected to the average SAR value maximum limit of 0.4 W kg^{-1} for any interval of 6 min (for f > 10 MHz). For occupational exposure of durations longer than 6 min, plane wave equivalent power density maximum limits are shown in Table 5. So far, only occupational exposure is under evaluation in Romania. No special attention is being paid to general public exposure.

Russia

In 1958, the first EMF standard in the range of 300 MHz–300 GHz was authorized in the USSR. This standard has remained essentially unchanged for the past 40 y. In Russia, the system of the standards on electromagnetic safety consists of State Standards (GOST) and Sanitary Norms and rules (SanPiN). These interconnected documents are mandatory. In the low RF frequency range, the permitted levels of occupational exposure are time-dependent and have been the same since 1976. The SanPiN (1996) standard establishes separate maximum permissible exposure levels (MPEL) for occupational exposure and for the general public for frequencies from 30 kHz to 300 GHz. For occupational exposure, the MPEL is determined by a so-called "maximum exposure energy" (MEE). For the 30 kHz to 300 MHz range, MEE is defined as a product of a square of the electric or magnetic field strength (in Vm^{-1} and Am^{-1}, respectively) and the duration of exposure during a day in hours (Table 6). For 300 MHz to 300 GHz range, the MEE is defined as a product of the incident power density (in μWcm^{-2}) and the duration of exposure

Table 5. Limit values for occupational exposure to RF EMF in Romania.

		Duration of exposure					
f (MHz)	Intensity	6 min	12 min	1 h	2 h	4 h	8 h
100–400	S ($mWcm^{-2}$)	1	0.5	0.1	0.05	0.025	0.0125
400–300,000	S ($mWcm^{-2}$)	5	2.5	0.5	0.25	0.125	0.0625

Table 6. Maximum permissible levels of RF EMF for occupational and public exposure in Russia.

	Occupational exposure						Public exposure	
f (MHz)	E_{max} (Vm^{-1})[a]	H_{max} (Am^{-1})[a]	S_{max} (μWcm^{-2})[a]	W_{E_2} (V^2 m^{-2} h)[b]	W_{H_2} (A^2 m^{-2} h)[b]	W_S (μWcm^{-2} h)[b]	E_m (Vm^{-1})[c]	S_m (μWcm^{-2})[c]
0.03–0.3	500	50		20,000			25	
0.3–3	500	50		20,000	200		15	
3–30	296	50		7,000			10	
30–50	80	3		800	0.72		3	
50–300	80			800			3	
300–30,000			1,000			200		10

[a] E_{max}—maximal electric field strength; H_{max}—maximal magnetic field strength; S_{max}—maximal power density.
[b] W_E—maximal permissible exposure parameter (power load) expressed in electric field (E) and duration of exposure in hours (h); W_H—maximal permissible exposure parameter (power load) expressed in magnetic field (H) and duration of exposure in hours (h); W_S—maximal permissible exposure parameter (power load) expressed in power density (S) and duration of exposure in hours (h).
[c] E_m—maximal electric field strength allowed for unlimited exposure; S_m—maximal power density allowed for unlimited exposure.

during a day, in hours (SanPin 1996; Federal Standard of the USSR 1984). For general public (i.e., for residential and recreation areas, inside and outside buildings, schools, hospitals, etc., and at work places of persons under 18 and pregnant women), the MPEL is not dependent on the exposure duration.

Central European countries

In some central European countries (Slovenia, Croatia), the EE concepts for EMF exposure limits have never been applied. Since these countries are involved in the admission processes for the EU membership, their legislation will have to be harmonized with the directives of the European Union and the recommendations of the international institutions (WHO, ICNIRP). Furthermore, regulations based on a precautionary principle[§§] have been enforced in Slovenia and Croatia as well as in some other West European countries (Italy, Switzerland).

In 1996, Slovenia implemented an Ordinance based on ICNIRP guidelines that clearly defines the highest level of EMF exposure allowed and appropriate protective measures. As a result of the concern about the potential health effects of electromagnetic fields, the government judges that the state of the science in the field of bioelectromagnetics justifies the application of protective measures in the form of environmental protection. For new systems and installations of EMF sources in the environment, an additional safety factor of 10 across the whole frequency spectrum was introduced to the current limit values. Apparently, this represents a political decision, which does not rely on specific scientific knowledge (Gajšek 1995).

Since 1999, Croatia has a Non-Ionizing Radiation Law under the Ministry of Health. An ordinance related to protection from EMF (0–300 GHz) is under development. The ordinance has two-tier limits (for general population and for sensitive part of general population, e.g., children in kindergartens, people in hospitals). The general population limits are based on ICNIRP levels. The second group, so-called sensitive population, has limits with a safety factor of 10 for the whole RF part of the frequency spectrum.

Both of these NATO Partners for Peace countries, as well as others and the new NATO members (PL, CZ, H), will need to consider harmonization to the NATO military standard (STANAG) for purposes of interoperability in multinational military operations.

COMPARISON BETWEEN WESTERN AND EE STANDARDS

Because of the lack of detailed methodological description in published work on which this rationale can be based, it is very difficult to scientifically validate the limit values used in EE standards or replicate some of the experimental studies. This makes comparison of EE to Western standards difficult, if not impossible (Paltsev and Nikonova 1996).

The development of health based EMF standards requires a critical in-depth evaluation of the established scientific literature. Using established scientific literature allows exposure restrictions to be determined with a higher degree of confidence about their protective value.

[§§] Because of health concerns by the public, governments are increasingly called on to adopt precautionary approaches to regulating EMF exposure. A wide variety of such policies is possible. They can be either regulatory (mandatory) or non-regulatory (voluntary), or supplement or replace health-based exposure guidelines for EMF (Foster et al. 2000). In Europe, precautionary policies are generally framed in terms of the Precautionary Principle, where the Treaty on European Union is the basis of European environmental policies. To avoid arbitrary application of the Precautionary Principle, the European Commission issued guidelines for its use in the European Union (EC 2000).

Copyright © Health Physics Society. Unauthorized reproduction of this article is prohibited.

Literature for review should have been published in scientific peer review journals. Additional review is necessary to evaluate study design, conduct and analysis of each report, and to compare them with the results of other studies. Detailed guidelines on the conduct of high quality laboratory research can be found in FDA (1993) and Repacholi and Stolwijk (1991). Criteria that have been widely accepted when evaluating epidemiological studies have been recently summarized by Repacholi and Cardis (1997). Under these criteria, strength and consistency of the association between EMF exposure and biological effects, evidence of a dose-response relationship, evidence provided by laboratory studies, and plausibility that biological systems exposed to EMF fields manifest biological effects are all examined.

The Western standards in the RF range are primarily based on the concept of a thermal mechanism and protect only against "thermal" effects. Indeed, the current consensus among Western scientists is that only thermal RF effects could be harmful, but this certainly does not mean that studies reporting possible non-thermal effects were ignored (IEEE 1999). A brief review of some Western RF safety standards, such as the International Commission of Non-ionizing Radiation Protection (ICNIRP) and Institute of Electrical and Electronics Engineers, Inc. (IEEE) standards (ICNIRP 1998; IEEE 1999) reveals that they include consideration of frequency dependent absorption in human body. In addition, special restrictions on localized exposure including methods for volume averaging are introduced. For the purpose of determining compliance with the standard, appropriate time period (averaging time) is introduced.

In contrast to the Western approach, the "Hygienic Standards" of EMF in EE countries are plainly based not only on thermal effects, but also on numerous reactions (which do not necessarily lead to adverse health effects) of the organism without a temperature increase following prolonged exposure. EE standards are based on a "dose" approach (high intensity EMF allowed for a short time, lower levels allowed for long term exposure), which refers to whole body exposure only. The concept of "complete prevention of health risks" is based on the establishment of limit values for chronic exposure to RF fields depending on the evaluation of the minimal intensities (about 10 μW cm^{-2}) provoking a response from the central nervous system (Zhavoronkov and Petin 1998).

The general opinion is that the EE standards are set at considerably lower levels, although this is only partially true. In fact, frequently the EE standards allow considerably higher EMF levels at certain frequencies, although for a shorter period of time, than is permitted for workers in Western standards.

Overall, existing differences in EE and Western safety standards could be attributed to dissimilarities in all stages of the standard setting process: from methodology employed in experimental studies to different philosophies for standards development and the scientific data used as basis for standards including risk perception and risk acceptance.

STIPULATIONS FOR POSSIBLE INTERNATIONAL HARMONIZATION OF EMF STANDARDS

In the last 10 years, new political and economic situations in Central and East European countries (BG, CRO, CZ, H, PL, ROM, SK, SLO, RUS) have dramatically changed international relations and the geopolitical map in this part of the world. In most countries, new, democratically-elected authorities decided to join the European Union (EU) and NATO and adapt their regulations and standards. Therefore, both standards and existing legislation in the field of EMF in many CE and EE countries are a subject for harmonization with EU legislation for civilian and NATO standardization for military purposes.

This is, no doubt, the first step in a long process of the global harmonization of the EMF standards. The next step calls for a coordinated program of work, based on an international consensus of what needs to be done. Thus, the scientific criteria for evaluation of the literature reporting on biological effects of the EMF and requirements for a scientific rationale to support limits have been established (Bernhardt 1998).

Another important step has been made with foundation of a group of leading experts from Eastern European countries that will carry out an analysis of the all available research data which were used as a basis for EE standards.*** The main goal of this expert group is to address questions such as

- are biological effects induced by low intensity EMF exposure scientifically valid?
- are biological effects of chronic exposure based on sound scientific criteria?
- what is the rationale for EE standards?

This evaluation process is one of the major actions in the near term towards standards harmonization. Harmonization should cover the issues of differentiating stationary and rotating EMF sources, pulse-modulated vs. continuous EMF, and the "dose concept" in occupational exposure. Another issue concerns the protection of residents against secondary coupling of EMFs (0.1–3 MHz) and effect of currents induced on ungrounded metallic objects in relatively weak EMFs (spark discharges). Harmonization of EMF standards should also consider the different interests of all parties in trying to address numerous questions. Some of these issues have recently been discussed (Erderich and Klauenberg 2001). Should standards be one or two tiered (public vs. occupational) and should one standard cover the whole frequency range from 0 to 300 GHz? What about safety factors? Do they or should they address scientific uncertainties in fundamental research or imprecisions in the techniques used for exposure assessment? A paramount issue will be the development of commonality in research methodology. Should gaps in knowledge be considered?

*** Personal communication, M. R. Murphy, 2001.

There are some questions regarding the most appropriate model for developing standards and accurate methods for determining compliance. Other important questions are how and to what degree of confidence can results be extrapolated to other frequencies or intensities. There are some common areas among the criteria chosen for evaluating the science, models, and safety factors.

One of the chief concerns about differences in EMF standards is interpretation of data from animal studies. Can the effects observed in animals exposed to EMFs be used to set human exposure standards? Which effects are important for human safety and which are not? In applying safety standards the issue of how to measure EMF absorption in the body is not easily solved. Typically, what is specified in the safety standard are field strength or power density that should not be exceeded. These limits are designed to prevent excessively high specific absorption rates in the human body. Thus, better dosimetry methods are needed to properly measure EMF absorption and extrapolate or relate effects observed in animals to those expected to be found in people. The resulting data could lead to modification of existing safety standards or establishment of new safety standards.

However, what about risk perception/risk acceptance? Should these concepts be a part of the framework for standards or kept aside to be included with social and economic considerations? The latter have implications with regard to differences in the processes that take place within the various countries. Problems and questions arising from "action," "reference," or "investigation" levels need to be resolved. Furthermore, close attention must be paid to the practical implementation of the guidelines not only from the point of view of levels and quantities measured but also looseness or lack of clarity in wording.

A serious obstacle to the harmonization of health and safety standards is insufficient knowledge of EMF biological effects, in particular the dependence of biological effects on physical parameters of exposure, and interaction mechanisms of EMF of various frequency ranges with biological tissue. Especially the role of modulation seems to be underestimated (Grigoriev 1996; Choy et al. 1986). These problems call for fundamental investigations.

CONCLUSION

The EMF standards now in force in EE countries use much lower exposure levels than those in the West. Most EE experts are aware that their standards are based on unconvincing research evidence that requires more precise specifications, improvements, and the implementation of the concept of frequency dependent absorption (Nikonova 1998).

Limit values reflect the level of contemporary knowledge about biological effects and methodological approaches in their establishment. EMF standards are more or less based on theoretical estimates and extrapolations and judgments about what the experimental data (laboratory animals) imply for human exposure. It is precisely this aspect that leads to the so-called "controversy" among scientists, and the understandable, but unfounded, demands for absolute assurances and proof of safety from workers and the public. For this reason there will always be uncertainties in exposure guidelines. Nevertheless, while the thresholds and values in current Western standards seem well supported, the rationale for these standards remains influenced by arbitrary safety factors. Critics of this approach believe that postulated and unconfirmed effects at lower levels have not been taken into account in setting the standards. This may be true, although it is equally true that any conceivable health impact of exposure is widely believed to be prevented by the magnitude of the safety factors.

Protecting populations against potentially hazardous agents is part of the political process so there is no reason to expect that all jurisdictions will choose exactly the same level of protection. It is accepted and expected that different countries, and even different jurisdictions within a single country, may sometimes choose to provide different levels of protection against environmental hazards, responding to their citizens' wishes and not solely based upon scientific risk assessment.

Most experts agree that data gaps exist and, thus, experiments conducted in the West as well as complementary experiments from EE countries are needed for better understanding of the possible bioeffects of EMF.

It is hoped that the harmonization process will benefit from ongoing research and health risk assessment such as those expected from WHO and International Agency for Research on Cancer. Thus, the next generation of standards would be able to incorporate the latest information on health risks within the same harmonized standards framework.

REFERENCES

Bernhardt JH. The new ICNIRP guidelines—scientific background and basic steps for international harmonization. In: Gajsek P, Miklavcic D, eds. Proceedings of the International Seminar on Global Harmonization of the EMF Standards. Ljubljana: Institute of Public Health; 1998: 25–29.

Bulgarian National Standards. 14525–90. Radiofrequency electromagnetic fields, permissible levels and control requirements for RF fields in the frequency range 60 kHz to 300 MHz. Sofia: National Standards Institute; 1990a.

Bulgarian National Standards. 17137–90. Microwave electromagnetic fields, permissible levels and control requirements for exposures to microwave radiation (300 MHz-300 GHz). Sofia: National Standards Institute; 1990b.

Choy R, Monro J, Smith C. Electrical sensitivities in allergy patients. Clinical Ecol 4:93–98; 1986.

Czech Republic. Ordinance concerning the protection of health from the adverse effects of electromagnetic radiation. No. 408. Praha: Ministry of Health of the Czech Republic; 1990.

Czech Republic. Checking compliance with maximum admissible values of general population's irradiation in the vicinity of AM, FM, TV and radar stations and radio relay systems, methodological guideline of the Chief Hygienic Officer of the Czech Republic to Supplement of Order No. 408. Praha: Ministry of Health of the Czech Republic; AHEM, edit. NIPH Praha, Suppl No 3; 1993.

Erdreich LS, Klauenberg BJ. Radio frequency radiation exposure standards: considerations for harmonization. Health Phys 80:430–439; 2001.

European Committee for Electrotechnical Standardization (CENELEC). Human exposure to electromagnetic fields (0–300 GHz). Brussels: CENELEC; Pre-ENV 50166; 1995.

European Commission. Communication on the precautionary principle. Available at http://europa.eu.int/comm/off/com/health_consumer/precaution.htm; accessed 15 May 2000.

Federal Standard of the USSR (GOST). Occupational safety standards system—Permissible levels at work places and requirements for control. Moscow: Federal Standard; 12.1.006–84; 1984: 120–125 (in Russian).

Food and Drug Adminitsration. Good laboratory practice for non-clinical laboratory studies. Washington, DC: U.S. Department of Health and Human Services; Fed Reg 21 CFR Ch 1 (4–1-93 Edition), Part 58:245–258; 1993.

Foster KR, Vecchia P, Repacholi MH. Science and the precautionary principle. Science 288:979–980; 2000.

Gajšek P. Prudence in Slovenia. In: Proceedings of Seventeenth Annual Meeting of Bioelectromagnetics Society. Boston, MA: BEMS; 1995: 132.

Gajšek P. Radiofrequency measurements and sources. In: Klauenberg BJ, Miklavcic D, eds. Radio frequency radiation dosimetry and its relationship to the biological effects of electromagnetic fields. Dordrecht, The Netherlands: Kluwer Academic Publishers; 2000: 309–320.

Grigoriev Y. The role of modulation in a biological influence of an electromagnetic radiation. Radiat Biol Ecol 36:659–670; 1996.

Grigoriev Y. The Russian Standardization and the opinion about international harmonization of the electromagnetic standards, In: Gajsek P, Miklavcic D, eds. Proceedings of the International Seminar on Global Harmonization of the EMF Standards. Ljubljana: IVZ; 1998: 33–38.

Hungarian National Standards. 16260-86. Safety levels of high frequency electromagnetic fields in the frequency range 30 kHz-300 GHz. Budapest: National Standards Institute; 1986 (in Hungarian).

Institute of Electrical and Electronics Engineers, Inc. Standard for safety levels with respect to human exposure to radio frequency electromagnetic fields, 3 kHz to 300 GHz. New York: Institute of Electrical and Electronics Engineers; 1999.

International Commission of Non-ionizing Radiation. Guidelines for limiting exposure to time-varying electric, magnetic and electromagnetic fields (up to 300 GHz). Health Phys 74:494–522; 1998.

Lokhmatova SA. The effect of low-intensity prolonged impulse electromagnetic irradiation in the uhf range on the testes and the appendages of the testis in rats. Radiat Biol Radioecol 34:279–285; 1994 (in Russian).

Marha K. Bioloski ucinki elektromagnetickych vln o vysoke frekvenci. Pract Lek Vol 15:238–241; 1963 (in Czech).

Marha K. Microwave radiation safety standards in Eastern Europe. IEEE trans Microwave Theory Tech 19:165–168; 1971.

Navakatikyan MA. Changes in the activity and conditioned reflexes of Albino rats during and after chronic microwave irradiation. J Radiobiol (Academy of Science) 30:120–125; 1990 (in Russian).

Navakatikyan MA, Tomashevskaya LA. Phasic behavioral and endocrine effects of microwaves of non-thermal intensity. In: Carpenter DO, Ayrapetyan S, eds. Biological effects of electric and magnetic fields, Vol 1: Sources and mechanisms. San Diego: Academic Press; 1994: 333–342.

Navakatikyan MA, Gordienko VM, Slavnov VN. The influence of microwave radiation on the thyroid gland. J Radiobiol (Academy of Science of the USSR) 30:679–684; 1990 (in Russian).

Navakatikian MA, Soldatchenkov VN, Bitkin SV, Zotov SV. The status of the higher nervous activity in animals exposed to microwaves in conditions simulating the intermittent work of radiolocators. Gig Sanit 7:57–61; 1991 (in Russian).

Nikitina VN. Long term effects of radiofrequency range EMF exposure. In: Repacholi MH, Robutsova NM, Muc AM, eds. Proceedings of the International Meeting Biological Effects and Hygienic Standardization. Moscow: WHO; 1998: 343–349.

Nikonova KV. Status and implementation of Russian Hygienic Radiofrequency Standards. In: Repacholi MH, Robutsova NM, Muc AM, eds. Proceedings of the International Meeting Biological Effects and Hygienic Standardization, Moscow. Geneva: World Health Organization; 1998: 477–483.

Pakhomov AG, Murphy MR. A comprehensive review of the research on biological effects of pulsed radiofrequency radiation in Russia and the former Soviet Union. In: Lin J, ed. Advances in electromagnetic fields in living systems. Dordrecht: Plenum Press; 2000: 116–135.

Paltsev Y, Nikonova KV. General trends in the development of national hygienic standards for EMR in the radiofrequency region. Problems in electromagnetic hazards for humans. In: Proceedings of an International Conference. Moscow: WHO; 1996: 88–89.

Paltsev YP, Suvorov GA. Hygienic standardization methodology for EMF and the evaluation of their harmful effects on the human organism. In: Repacholi MH, Robutsova NM, Muc AM, eds. Proceedings of the International Meeting Biological Effects and Hygienic Standardization, Moscow. Geneva: World Health Organization; 1998: 9–18.

Repacholi MH, Stolwijk JA. Criteria for evaluating scientific literature and developing exposure limits. Radiat Prot Australia 9:97–84; 1991.

Repacholi MH, Cardis E. Criteria for EMF health risk assessment. Radiat Prot Dosim 72:305–312; 1997.

Sanitary Rules and Norms. Radiofrequency electromagnetic radiation. Moscow: National Standards Office; SanPin 2.2.4/2.1.8.055–96; 1996 (in Russian).

Savin BM. The contemporary state and perspectives in the area of hygienic standards setting for radiofrequency electromagnetic radiation. The biological effects and hygienic standards setting for EMF in the KV Region. Monograph. SRI OH GT and PZ AMS USSR, Moscow; 36:8–32; 1988 (in Russian).

Sliney DH, Wolbarsht ML, Muc AM. Differing radiofrequency standards in the microwave region—Implications for future Research. Health Phys 49:677–683; 1985.

Szmigielski S. EMF standards for occupational and environmental exposure in Eastern European countries. In: Bersani F, ed. Electricity and magnetism in biology and medicine. Dordrecht: Kluwer Academic Plenum Publishers; 1999: 69–72.

Tomashevskaya LA, Dumansky YD. Hygiene estimation of exposure impulse EMF 850–2750 MHz. J Hygiene and Sanitation 8:22–24; 1988 (in Russian).

Vinogradov GI, Naumenko GM. Experimental simulation of autoimmune reactions by exposure to non-ionizing microwave radiation. Monograph. A. N. Marzeev Research Institute of Common and Communal Hygiene, Kiev, Radiobiologiia 26:705–708; 1986 (in Russian).

Zhavoronkov LP, Petin VG. The dose-power approach in hygienic standardization of microwaves: The concept, biophysical modeling, and experimental estimation. In: Repacholi MH, Robutsova NM, Muc AM, eds. Proceedings of the International Meeting Biological Effects and Hygienic Standardization, Moscow. Geneva: World Health Organization; 1998: 457–466.

■ ■

Copyright © Taylor & Francis Ltd. Reproduction forbidden. Unauthorized distribution of this article is prohibited.

BIOLOGICAL EFFECTS of EMFs

2nd INTERNATIONAL WORKSHOP

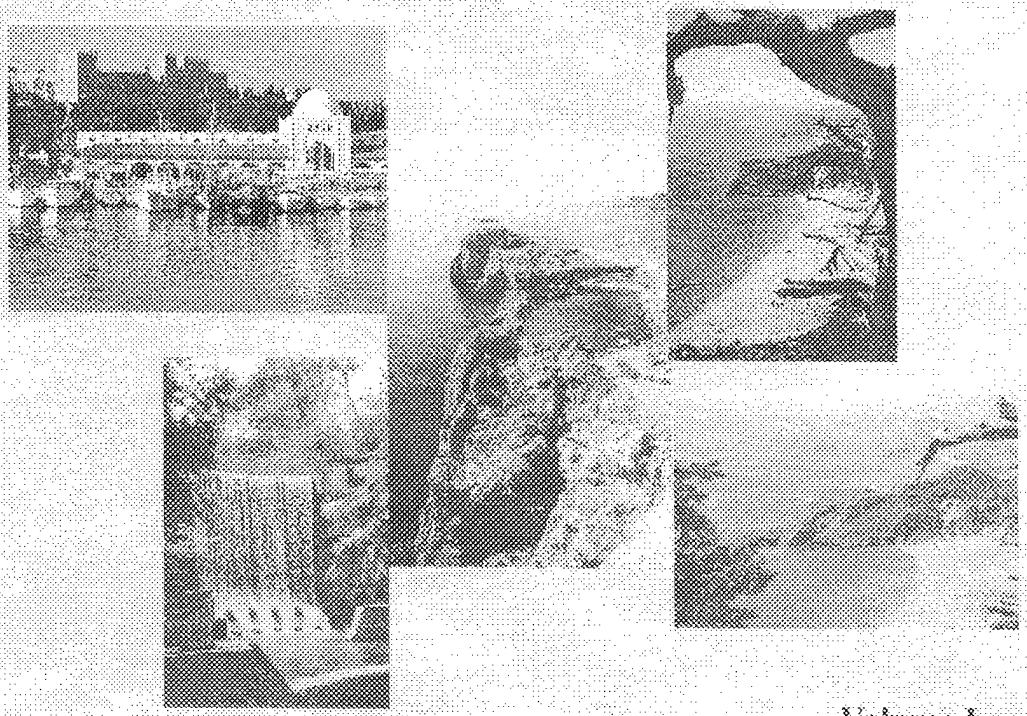




Electronics - Telecom &
Applications Laboratory
Physics Department
University of Ioannina

Institute of Informatics &
Telecommunications
N.C.S.R. "Demokritos"

Proceedings



Volume I

Rhodes, Greece, 7 -11 October, 2002

UWB-INDUCED HYPOTENSION

HYPOTENSION INDUCED BY ULTRA-WIDE-BAND PULSES: DOSE RESPONSE, REPLICATION, ORTHOSTATIC RESPONSE AND HEART RATE VARIABILITY

SHIN-TSU LU and SATNAM P. MATHUR

MCKESSON BIOSERVICES CORPORATION
U.S. ARMY MEDICAL RESEARCH DETACHMENT
8308 HAWKS ROAD, BUILDING 1168
BROOKS AIR FORCE BASE, SAN ANTONIO, TEXAS 78235-5322, U.S.A.

ABSTRACT

Six-minute exposure to 85-94 kV/m, 1 ns Ultra-Wide-Band (UWB) pulses caused delayed hypotension in male Wistar-Kyoto rats. Effective exposures were 1,000 and 500 Hz pulse repetition rates while 250 and 125 Hz pulses were ineffective. The hypotensive effect was delayed by 3-7 days, reached a maximum at two weeks and persisted as long as four weeks after exposure. The whole-body average specific absorption rate was estimated to be less than 0.1 W/kg equivalent to less than 0.01 cal/g in 6 minutes. In a replication study, decreased systolic pressure was noted at 0.3 hours and two weeks after 6-minute exposure to 500 Hz UWB pulses. Cardiovascular responses to a 47° head-up tilt orthostatic stress were normal in these animals at 2 weeks after exposure. Fifteen days after exposure, short-term heart rate variability was determined by time- and frequency- domain methods in 512 consecutive heart cycles. Marginal increase in low frequency and significant increase in very low frequency components of power spectral density were noted. Therefore, alterations in autonomic function cannot be proven nor dismissed entirely.

INTRODUCTION

The ultra-wide-band (UWB) radio frequency (RF) radiation is a new modality in radar technology and electronic warfare. Some of these sources can produce repetitive nanosecond (ns) pulses with sub-nanosecond rise time and peak electric field intensity in several hundred kV/m [1]. At much lower power, an example of forthcoming civilian UWB radar application is in the automobile device for obstacle avoidance. Because the primary military purpose of high peak power UWB pulses is to damage or destroy electronic equipment [2], the laymen's concern of health effect is multiplied by the apparent high field intensity that may be encountered in its operation. Due to a lack of exposure apparatus for biological experimentation, studies on biological effects of UWB pulses are primarily limited to research institutes affiliated with military organizations. Only a handful research papers in the United States have been published due to the novelty of the technology.

Erwin and Hurt [3] presented probably the first summary of various studies on biological effects of UWB pulses performed under a collaborative program between Phillips Laboratory and Armstrong Laboratory. Endpoints were cardiovascular functions, performance scores of the "Function Observation Battery" (29 physiological and behavioral measures), serum enzymes, plasma electrolyte and hemoglobin concentrations, brain C-fos protein activation, and metrazole seizure activity in rats, and equilibrium task performance in monkeys. Other than metrazole-induced seizure activity that was replaced by pentylenetetrazol-induced seizure [4], experimental results were subsequently published [5,6]. The exposure duration was 2 minutes or less in these experiments. Two different UWB pulses were used. The "H-2" bipolar pulses were 250 kV/m (166 MW/m^2) peak electric field intensity, 318-377 ps rise time and 5-10 ns pulse duration, 60 pulses per second (pps) or "sweep" pulse repetition starting at 1 pps to 400 pps to a total of 12,000 pulses in 1 min. A "Kentech PBG3" device produce pulses at 40 kV/m (4.24 MW/m^2) peak electric field intensity, 1.92 ns pulse duration, 176 ps rise time and 1,000 pps. The estimated whole-body average specific absorption rate (SAR) was 20 mW/kg in rats and 300 mW/kg in monkeys for "H-2", and 16 mW/kg in rats for the "Kentech" pulses. None of these endpoints were affected by UWB exposures.

Pakhomova *et al.* [7,8] studied the mutagenic effects of UWB pulses in yeast, Saccharomyces cerevisiae, strain D7 with or without 254 nm ultraviolet pretreatment. The pulses were generated by a "Sandia" source into a GTEM cell at 16 pps, 104 kV/m (28.7 MW/m^2) peak, 165 ps rise time, and 1 ns pulse duration or at 600 pps, 102 kV/m (27.6 MW/m^2) peak, 165 ps rise time, and 1 ns pulse duration. The SAR was not estimated or measured. Results indicated that UWB pulses did not cause mutagenesis and gene recombination nor alter UV-induced mutagenesis and gene recombination. Exposure to similar "Sandia" pulses at different repetition rates (60 and 600 pps) did not affect the nociception and morphine-induced analgesia in CF-1 and C57BL/6 mice nor the spontaneous activity and morphine-induced hyperactivity in C57BL/6 mice [9]. The exposure duration was 30 minutes and estimated whole-body average SARs were 3.7 mW/kg (60 pps) and 37 mW/kg (600 pps). However, exposure for 30 minutes to the 600 pps "Sandia" pulses blocked the hyperactivity but not the nociception effect of the N^G-nitro-L-arginine methyl ester (L-NAME), a nitric oxide synthase inhibitor in mice [10]. The effect was probably through blocking the inhibition of nitric oxide production. In supporting this hypothesis, Seaman *et al.* [11] found a 41 % enhancement of nitrite (a stable product of nitric oxide decomposition) production in stimulated murine macrophases, RAW 264.7, exposed to UWB pulses (72-95 kV/m peak, 198-216 ps rise time, and 1.01-1.07 ns pulse duration) for 30 minutes and incubated with potassium nitrate in the culture medium.

Cobb *et al.* [12] evaluated the neural and behavioral teratologies in rats exposed *in utero* and postnatally to UWB pulses. The "Kentech" UWB pulses were 55 kV/m (8.02 MW/m^2) peak, 300 ps rise time, 1.8 ns pulse width, and 1,000 Hz for 2 minutes per day. The estimated SAR for dams was 45 mW/kg. Exposures were performed on gestation days 3-18 and postnatal days 1-10. Offspring were examined for litter size, sex ratio, weight, coat appearance, tooth eruption, eye-opening, air-righting, and ultrasonic stress vocalization in pubs. Locomotor, water-maze learning, and fertilization performances were tested in male pups. Hippocampal morphology and operant behavior were examined in postnatally exposed pups. Sham exposure and positive controls (2 mg/ml lead acid in drinking water) were used. Behavioral, functional and morphological endpoints were unremarkable. However, three significant changes were noted, i.e., UWB-exposed pups emitted more stress vocalization, had longer medial-to-lateral length in hippocampus and mated less frequently than the sham-exposed pups. Jauchem *et al.* [12] did not find any effects of "Kentech" UWB pulses on the development of mammary tumor in mammary tumor-prone C3H/HeA mice in incidence, latency, and growth rate of the mammary tumor, body weight, survival rate and tumor incidence in all tissue. The UWB pulses were 40 kV/m (4.24 MW/m^2) peak electric filed, 1.9 ns pulse duration, 176 ps rise time, 3.5 ns fall time, and 1,000 pps. Estimated whole-body average SAR was 9.8 mW/kg. Exposure duration was 2 minutes once a week for 12 weeks.

Jauchem *et al.* [3,14,15] found no UWB effect on cardiovascular endpoints (heart rate and blood pressure) in ketamine-anesthetized cannulated rats exposed to UWB pulses. Typically, 2-minute exposure was used. UWB pulses were: a). "H-2 " pulses at 250 kV/m (166 MW/m^2) peak, 318-377 ps rise time, 5-10 ns pulse duration, 60 pps, 20 W/kg estimated whole-body average SAR, b). "Bournlea" pulses, 10-21 kV/m^2 (0.96 MW/m^2) peak, 327 ps rise time, 6 ns pulse duration, 2,000 pps on for 0.5 s off for 5 s or 1,000 pps on for 2 s off for 2 s, 28 mW/kg estimated whole-body average SAR, c). "Sandia" pulses, 104 kV/m (28.7 MW/m^2) peak, 174 ps rise time, 0.97 ns pulse duration, 50 pps, 7.4 mW/kg estimated whole-body average SAR, d). "Sandia" pulses, 102 kV/m (27.6 MW/m^2) peak, 174 ps rise time, 0.97 ps pulse duration, 500 pps, 71 mW/kg estimated whole-body average SAR, and e). "Sandia" pulses, 87 kV/m (20 MW/m^2) peak, 218 ps rise time, 0.99 ns pulse duration, 1,000 pps, 114 mW/kg estimated whole-body average SAR.

Based on the reported delayed effects [16,17], Lu *et al.* [18] studied the cardiovascular function non-invasively in non-anesthetized and conscious Wistar Kyoto rats exposed to "Sandia" UWB pulses from pre-exposure baseline to 4 weeks after exposure. Decreased blood pressure (hypotension) in absence of changes in heart rate was found. This study was extended to cover dose response characteristics, replication of the observation, orthostatic responses and heart rate variability.

MATERIAL AND METHODS

Seventy-three male Wistar-Kyoto (WKY) rats aged between 71 and 89 days were used at the beginning of the experiment. They were obtained at 56 days of age from a commercial source (Charles River, Portage MI). They were in the vivarium at 21-23 °C ambient temperature, 100% conditioned fresh air for more than 10 exchanges per hour, and a 12L-12D (lights on 0600-1800 h) light cycle. Tap water and feed (Purina Rodent Diet 5008, Ralston Purina Co., St. Louis, MO) were available *ad lib*. After a 10-day quarantine period, they were

acclimated to a test holder (model 81, IITC Life Science, Woodland Hills, CA) 1 hour daily for 3 days. Pre-exposure baseline of the heart rate and arterial pressures (systolic, mean and diastolic) were determined 1-2 days after the holder acclimation. Three to 4 days later, they were individually subjected to sham exposure, or UWB exposure for 6 minutes in a GTEM cell between 0900 and 1000 h [18]. On the exposure day, average body weight was 250 ± 4 g (mean ± S.E.). Heart rate and blood pressures were again measured 20-45 min, 24 h, 72 h, 1, 2, 3, and 4 weeks after exposure. Four to 6 measurements were obtained. Four series of experiments were performed with their concurrent sham-exposed animals served as controls. Experiment Series I-III were for dose-response characteristics and Experiment Series IV for replication. Details of UWB pulses were shown in Table 1. In the replication study (Experiment Series IV), double blind design was incorporated. The code was revealed only after completion of the study.

Table 1. Characteristics of UWB Pulses

Exp	Peak E Field (kV/m)	Rise Time (ps)	Pulse Duration (ps)	Repetition Rate (Hz)	Average P.D. (mW/cm^2)	Average SAR (W/kg)	Heating Potential* (10^{-2} °C)
	0.0	N.A.	N.A.	N.A.	0.00	0.000	0.00
I	93.0	170	1.00	500	1.15	0.071	0.74
	84.6	200	1.03	1,000	1.95	0.120	1.25
	0.0	N.A.	N.A.	N.A.	0.00	0.000	0.00
II	91.3	156	1.02	125	0.28	0.017	0.18
	94.9	168	1.02	250	0.61	0.038	0.39
	0.0	N.A.	N.A.	N.A.	0.00	0.000	0.00
III	89.3	160	0.91	500	0.96	0.059	0.61
	85.4	167	0.94	1,000	1.82	0.112	1.17
	0	N.A.	N.A.	N.A.	0.00	0.000	0.00
IV	101.6	172	0.82	500	1.12	0.069	0.72

** Heating potential (thermal energy deposition) was calculated from averaged power density (mW/cm^2), SAR (61.7 mW/kg per mW/cm^2), duration of exposure (360 s) and specific heat (3470 J/°C-kg). The value was 6.4 × 10^{-3} °C per 1 mW/cm^2 average power density.*

During the replication study, data for heart rate and blood pressures were collected as pre-exposure baseline and 10-30 min, 24 h and 2 week after exposure. In addition, orthostatic tilt response (47 ° head-up) was performed for each individual animal immediately after the 2-week determinations served as pre-tilt baseline. Data collected were 1, 5, and 10 min after tilt. Endpoints were changes in heart rate and arterial pressures (systolic, mean, and diastolic) from pre-tilt baseline in each individual animal. One day later, data on heart rate variability was collected in these animals.

A commercial indirect tail-cuff arterial pressure measurement system (IITC Life Science, Woodland Hills, CA) with a photoelectric sensor was used throughout these experiments. The measurement system composed of animal holder (model 81), pulse amplifier (model 29), tail cuff-photoelectric sensor assembly (model B-60, 5/8" cuff) and small-bore tubing (Tygon, 1.66 mm i.d., 0.8 mm wall thickness) for connecting tail-cuff, pressure amplifier, pressurizing bulb and pressure gauge. Analog outputs of pulse amplifier, pulse amplitude and cuff pressure were displayed on a digital oscilloscope for viewing and digitized and recorded at 50 Hz data acquisition rate. The recorded data were processed offline with a graphic program (SigmaPlot, SPSS, Inc. San Rafael, CA). To maintain a constant temperature during cardiovascular function determination, a microenvironment chamber with circulating water from a precision circulator water bath was used. In general, the ambient temperature within the microenvironment chamber was maintained between 27-29 °C [18].

For measurement cardiovascular endpoints, rats were transported from the vivarium to the laboratory in the morning. They were allowed to sit quietly in their own cages for at least 30 min before being transferred to the test holder. The rat and test holder were than inserted into the microenvironment chamber. After passing the tail through the tail-cuff/photoelectric sensor assembly, the apparatus was attached to the test holder. After 10-20 minutes, characteristic tail pulses could be detected if cuff was inflated to 40-60 mm Hg. When the presence of tail pulses was ascertained, tail cuff was quickly inflated to 200-220 mm Hg until tail pulses disappeared. The tail cuff was then deflated immediately at approximately 2 mm Hg per heartbeat for 25.6 s. Systolic pressure (*Ps*) was determined during the deflation cycle as the corresponding cuff pressure at reappearance of the tail

pulse while mean pressure (*Pm*) was the cuff pressure when amplitude of the tail pulse reached a maximum. Diastolic pressure (*Pd*) was calculated by $Pd = (Pm \times 3 - Ps) \div 2$. Heart rate was determined from the average pulse-to-pulse intervals for at least 60 heartbeats.

For heart rate variability (HRV), the recommendations by the Task Force of the European Society of Cardiology and the North American Society of Pacing and Electrophysiology [19] were used. At 15 days after exposure, cuff pressure was maintained approximately at the *Pm* after the appearance of tail pulses. Tail pulses were recorded with a data acquisition system (MP 100, Biopac System, Inc., Santa Barbara, CA) at 500 Hz data acquisition rate for two minutes. Data were analyzed with the aid of a software package (Acknowledge, Biopac System, Inc., Santa Barbara, CA). Heart rate was determined from peak-to-peak of individual tail pulse. A total of 512 consecutive heart beat intervals were determined from tail pulses. Fast Fourier Transform was used to determine the power spectrum density of the sequential heart beat intervals for frequency-dependent heart rate variability. Endpoints of frequency-dependent HRV were power spectrum density of very low frequency (VLF, >0.004 to 0.04 Hz), low frequency (LF, >0.04 to 0.14 Hz), high frequency (HF, >0.14 to 0.40 Hz), total (=VLF+LF+HF), and LF/HF ratio. Standard deviation of 512 heartbeats was used to evaluate the time-dependent heart rate variability.

RESULTS

Results of the first three series of experiments were analyzed individually. Differences among sham-exposed animals in the first three series of experiments were not significant. Differences between data obtained from animals exposed to 500 and 1,000 Hz in series I and III were not significant either. Therefore, data from these series of experiments were combined according to original research plan for constructing the dose-response curve according to treatments, i.e., sham-exposure, 125, 250, 500 and 1,000 Hz groups. Figures 1 through 4 show these results. Analysis of variance (ANOVA) was used at eight different sampling times. The F values were included in each chart immediately under the upper abscissa. *Post hoc* Dunnett's test was used at each sampling time point when result of the ANOVA indicated a significant difference.

Apparently, six-minute exposure to 85-102 kV/m, 1 ns UWB pulses could cause delayed hypotension in male Wistar-Kyoto rats. Effective exposures were 1,000 and 500 Hz pulse repletion rates while 250 and 125 Hz pulses were ineffective. The systolic hypotension, decreased systolic pressure, was delayed by 1 week, reached a maximum at 2 weeks and persisted as long as 4 weeks after exposure (Fig.1). Similar time course was noted in the manifestation of decreased mean arterial and diastolic pressures (Fig. 2 and 3). Decreased mean and diastolic pressures appeared as early as 3 days after 500 and/or 1,000 Hz exposures. The maximum decrease in mean arterial blood pressure occurred at 1 (1,000 Hz) or 2 weeks (500 Hz) after exposure while maximum diastolic hypotension appeared at 1 week after exposure in both cases. In contrast to these findings, UWB exposures did not alter heart rates significantly (Fig. 4). Absence of UWB effects on the heart rate was clearly evident by insignificant F values at all sampling time points.

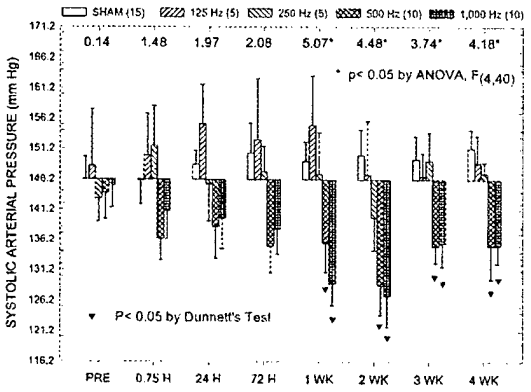


Figure 1. Effects of UWB Exposures on Systolic Pressure

UWB-INDUCED HYPOTENSION

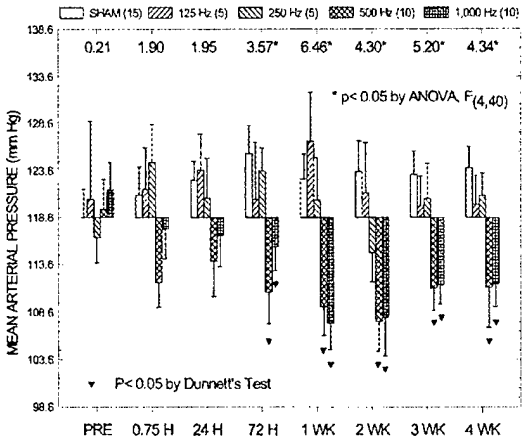


Figure 2. Effects of UWB Exposures on Mean Arterial Blood Pressure

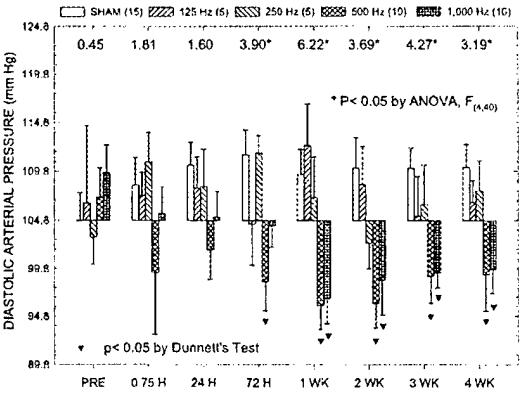


Figure 3. Effects of UWB Exposures on Diastolic Pressure

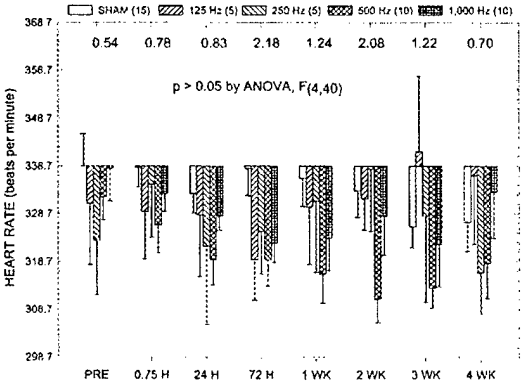


Figure 4. Effects of UWB Exposures on Heart Rate

In the double blind replication study (Experiment Series IV), baseline systolic pressures were higher than those of the sham exposure rats in the original study (Experiment Series I, II and III). Due to baseline changes, a decreasing trend toward baseline of the original study was noted in the sham-exposed animals (Fig. 5). Most likely, the baseline drift was caused by inadequate acclimation and/or inadequate equilibration during the cardiovascular testing. Results of a two-way ANOVA indicated significant main effects, UWB-treatment and time and insignificant interaction between main effects. In comparison to systolic pressures of sham-exposed rats, decreases occurred in rats exposed to 500 Hz UWB pulses at 0.3 hours ($t = 2.08$, $p < 0.05$, one tail) and 2 weeks ($t = 1.99$, $p < 0.05$, one tail) after exposure. Furthermore, the systolic pressure at 2 weeks after exposure was lower than the corresponding baselines in 500 Hz exposed rats but not in sham-exposed rats by a paired t-test.

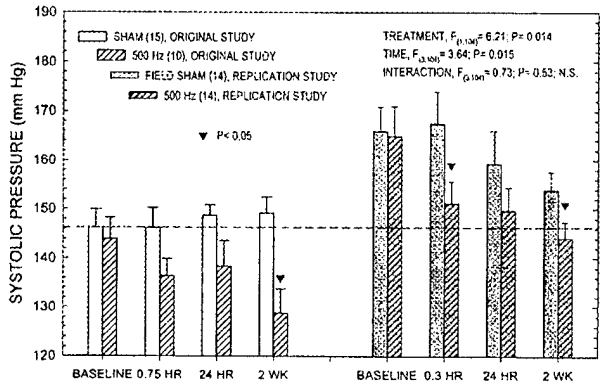


Figure 5. UWB-induced Systolic Hypotension in a Replication Study

Graded postural (orthostatic) stress such as head-up tilt is a known to cause graded increases in heart rate, arterial pressure and sympathetic activity in human beings [20,21]. Graded cardiac response to postural stress was seen in two groups of rats subjected to 22° and 47° head-up tilt (Fig. 6) but the changes in arterial pressures (systolic, mean and diastolic) were not. Apparently, two weeks after a 500 Hz UWB exposure, the cardiovascular responses to a 47° head-up tilt (Fig. 7) were not altered.

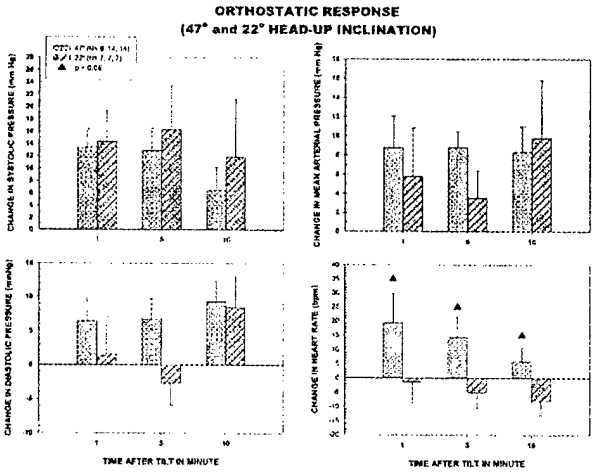


Figure 6. Cardiovascular Responses to Postural Stress in Rats

UWB-INDUCED HYPOTENSION

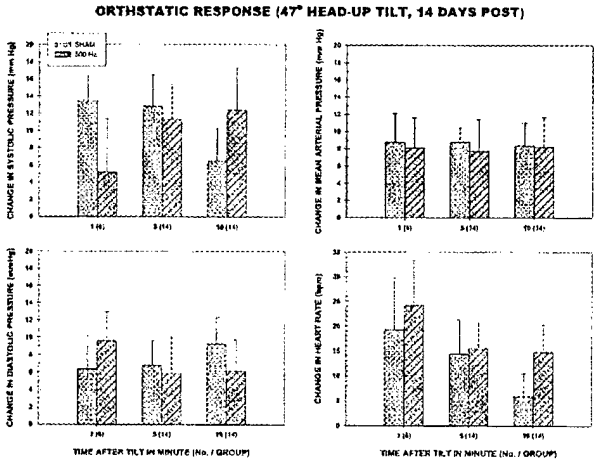


Figure 7. Absence of UWB Effects on Cardiovascular Responses to Postural Stress

The same postural stress (47° head-up tilt) was also used to identify markers for sympathetic excitation and alteration in heart rate variability. In rats, LF (low frequency) and HF (high frequency) were inversely correlated with heart rate increases to head-up tilt, while LF/HF ratio increased proportionally with the heart rate induced by the 47° head-up tilt (Fig. 8). The LF/HF ratio reliably indexed the sympathetic dominance of the cardiac response to postural stress with the highest degree of concordance.

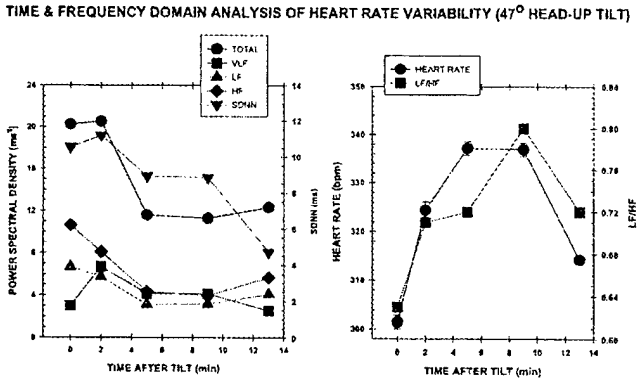


Figure 8. Heart Rate Variability Elicited by Postural Stress

Fifteen days after exposure to 500 Hz UWB, absolute power spectral density of the VLF component increased significantly and marginally so in the LF component (Fig. 9). Other HRV frequency- and time-domain indices, such as HF component and total power spectral densities, standard deviation of beat-to-beat intervals and heart beat intervals were not altered significantly.

DISCUSSION

The observation of a delayed, robust, and persistent decrease in arterial pressure (delayed hypotention) without changes in the heart rate in rats subjected to an acute UWB exposure is uncommon (Figs. 1-4, Experiment Series I-III). The anticipated UWB cardiovascular effects were hypothesized to be hypertension as

part of "atypical post-traumatic syndrome" observed in case reports [16,17]. Heart rate is known to co-vary or to be more susceptible than blood pressure to RF perturbation in *in vivo* experiments [22]. Reports of RF-induced hypotension were published in formal Soviet Union in rats repeatedly exposed to microwaves for various durations and in human beings in clinical studies [22]. Since similar exposure for two minutes failed to alter cardiovascular function during and immediately after exposure in ketamine-anesthetized rats [3,14,15], a minimum exposure duration and period of delay appear to be required for the manifestation of UWB-induced hypotension. In addition, minimum repetition rate or average exposure intensity is also required for the induction of delayed hypotension.

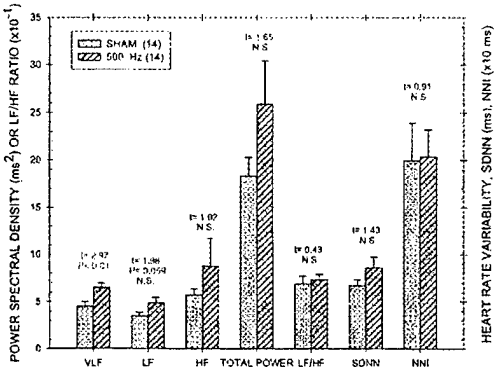


Figure 9. Effects of UWB Pulses on Heart Rate Variability

The effective UWB exposure for inducing hypotension appeared to have a threshold at low average intensity (1.12 mW/cm^2), low estimated whole-body average SAR (0.069 W/kg) and very low heating potential (0.0072 °C) (Table 1). Because of this low heating potential, the thermal consideration does not apply. Specificity of the UWB-induced delayed hypotension observed in the present experiment cannot be evaluated because majority of RF research on cardiovascular function involved exposures at much higher intensities that induced significant increases in body temperature and changes in cardiovascular functions. Due to lack of information, dependency of the delayed hypotension on peak exposure intensity cannot be evaluated either.

Indirect blood pressure measurement in un-anesthetized rats is preferable method recommended by the Committee on Care and Use of Spontaneous Hypertensive Rats of the Institute of Laboratory Resources [23]. However, restraint and acclimation are necessary for the successful use of the technique for blood pressure measurement. Inadequate acclimation and equilibration could result in tachycardia (increased heart rate) and hypertension (increased blood pressure) through sympathetic arousal and increased endpoint variation in animals [24-26]. Inadequate acclimation and equilibration might contribute to the elevated baseline blood pressure in rats in Experiment Series IV and subsequent decreases in blood pressures in sham-exposed rats. Nevertheless, the 500 Hz UWB exposure did cause additional decreases in systolic blood pressures (Fig. 5) although the magnitude was smaller when comparison was made in respective to those of sham-exposed rats in Experiment Series I-III at two weeks after exposure (9.80 versus 20.27 mm Hg, Fig. 5). Instead of 2 weeks after exposure in Experiment I-III, the maximum UWB effect in the Experiment Series IV (16.24 mm Hg) was noted at 0.3 hours. On the other hand, the magnitude of changes in systolic pressure from the initial pre-exposure baseline in Experiment Series IV (20.82 mm Hg) was more than that in Experiment Series I-III (15.20 mm Hg).

The physiological mechanisms of UWB-induced hypotension are not clear at present. Current results indicated that UWB-induced hypotension was not caused by lack of responses in cardiovascular system to postural stress (Fig. 7). Significant increase in VLF and marginal increase in LF components of frequency domain heart rate variability in absence of changes in heart rate were interesting. The physiological significance of VLF is not clear at present [18]. However, increased LF component in absence of LF/HF ratio may point to a disturbance (decrease in sympathetic tonicity rather than increase in vagal tonicity) in cardiac autonomic control. Due to inadequate acclimation, additional studies will be required to derive solid conclusions on cardiac autonomic tonicity and other mechanism such as baroreceptor responses.

ACKNOWLEDGEMENT: This research was supported by the U.S. Army Medical Research and Materiel Command under contract No. DAMD 17-94-4069 with McKesson BioServices. The authors wished to acknowledge the technical assistance provided by Jian-Zhong Bao, Pamela J. Henry, D. Duane Cox, and Jonathan C. Lee. The animals used in this study were procured, maintained, and used in accordance with Federal Animal Welfare Act and the "Guide for the Care and Use of Laboratory Animals," prepared by the Institute of Laboratory Animal Resources-National Research Council.

DISCLAIMER: The views, opinions and/or finding contained in this report are those of the authors and should not be construed as an official Department of the Army position, policy or decision unless so designated by other documentation. This article is a U.S. Government work and, as such, is in the public domain in the United States of America.

REFERENCES

[1] F.J. Agee, D.W. Schlfield, W. Prather, and J.W. Burger, "Powerful ultra-wide band RF emitters: status and challenges," in *Intense Microwave Pulses III*, Proceeding of the Int. Soc. Optical Eng., H.E. Brandt, ed. 1995, vol 2557, pp 98-109.

[2] D. Fuerer, "Electronic countermeasures in wideband spectrum systems," in *Propagation Limitations for Systems Using Band Spreading*, Advisory Group for Aerospace Research and Development, AGARD-LS-172, 1991, pp 1-11.

[3] D.N. Erwin, and W. Hurt, "Biological effects of ultrawideband emissions," in *EMP Human Health effects Science Review Panel Proceedings*, J. de Lorge and W. Mick, eds, Washington, D.C.: U.S. Navy Theater Nuclear Warfare Program and Operational Medicine and Fleet Support, 1993, pp 91-95.

[4] S.A. Miller, M.E. Bronson, and M.R. Murphy, "Ultrawideband radiation and pentylenetetrazol-induced convulsions in rats," Bioelectromagnetics 20(5): 327-329, 1999.

[5] C.J. Sherry, D.W. Blick, T.J. Walters, G.C. Brown, and M.R. Murphy, "Lack of behavioral effects in non-human primates after exposure to ultrawideband electromagnetic radiation in the microwave frequency range," Radiat. Res. 143(1): 93-97, 1995.

[6] T.J. Walters, P.A. Mason, C.J. Sherry, C. Steffen, and J.H. Merritt, "No detectable bioeffects following acute exposure to high peak power ultra-wide band electromagnetic radiation in rats," Aviat. Space Environ. Med. 66(6): 562-567, 1995.

[7] O.N. Pakhomova, M.L. Belt, S.P. Mathur, J.C. Lee, and Y. Akyel, "Lack of genetic effects of ultrawide-band electromagnetic radiation in yeast," Electro-Magnetobiol. 16(3): 195-201, 1997.

[8] O.N. Pakhomova, M.L. Belt, S.P. Mathur, J.C. Lee, and Y. Akyel, "Ultra-wide band electromagnetic radiation does not affect UV-induced recombination and mutagenesis in yeast," Bioelectromagnetics 19(2): 128-130, 1998.

[9] R.L. Seaman, M.L. Belt, J.M. Doyle, and S.P. Mathur, "Ultra-wideband Electromagnetic pulses and morphine-induced changes in nociception and activity in mice," Physiol. Beh. 65(2): 263-270, 1998.

[10] R.L. Seaman, M.L. Belt, J.M. Doyle, and S.P. Mathur, "Hyperactivity caused by a nitric oxide synthase inhibitor is countered by ultra-wideband pulses," Bioelectromagnetics 20(7): 431-439, 1999.

[11] R.L. Seaman, J.E. Parker, J.L. Kiel, S.P. Mathur, T.R. Grubbs, and H.K. Prol, "Ultra-wideband pulses increase nitric oxide production by RAW 264.7 macrophages incubated in nitrate," Bioelectromagnetics 23(1): 83-87, 2002.

[12] B.L. Cobb, J.R. Jauchem, P.A. Mason, M.P. Dooley, S.A. Miller, J.M. Ziriax, and M.R. Murphy, "Neural and behavioral teratological evaluation of rats exposed to ultra-wideband electromagnetic fields," Bioelectromagnetics 21(7): 524-537, 2000.

[13] J.R. Jauchem, K.L. Ryan, M.R. Frei, S.J. Dusch, M. Lehnert, and R.M/ Kovatch, "Repeated exposure of C3H/HeJ mice to ultra-wideband electromagnetic pulses: lack of effect on mammary tumors," Radiat. Res. 155: 369-377, 2001.

[14] J.R. Jauchem, R.L. Seaman, H.M. Lehnert, S.P. Mathur, K.L. Ryan, M.R. Frei, and W.D. Hurt, "Ultra-wideband electromagnetic pulses: lack of effects on heart rate and blood pressure during two-minute exposures of rats," Bioelectromagnetics 19(5): 330-333, 1998.

[15] J.R. Jauchem, M.R. Frei, K.L. Ryan, J.H. Merritt, and M.R. Murphy, "Lack of effects on heart rate and blood pressure in ketamine-anesthetized rats briefly exposed to ultra-wideband electromagnetic pulses," IEEE Trans. Biomed. Eng. 46(1): 117-120, 1999.

[16] C. Forman, C. Holmes, and V. McManamon, "Psychological symptoms and intermittent hypertension following acute microwave exposure," J. Occupat. Med. 24(1): 932-934, 1982.

[17] R. Williams, and T. Webb, "Exposure to radiofrequency radiation from an aircraft radar unit," Aviat. Space Environ. Med. 51(11): 1243-1244, 1980.

[18] S.-T. Lu, S.P. Mathur, Y. Akyel, and J.C. Lee, "Erratum "Ultrawide-band electromagnetic pulses inducedhypotension in rats,"" Physiol. Beh. 67(3): 463; 65(4/5): 753-761, 1999.

[19] Task Force of the European Society of Cardiology and the North American Society of Pacing and Electrophysiology, "Heart rate variability, standards of measurement, physiological interpretation, and clinical use," Circulation 93(5): 1043-1065, 1996.

[20] D.L. Jardine, I.C. Melton, I.G. Crozier, S. English, S.I. Bennet, C.M. Frampton, and H. Ikram, "Decrease in cardiac output and muscle sympathetic activity during vasovagal syncope," Am. J. Physiol. Heart Circulatory Physiol. 282(5): H1804-H1809, 2002.

[21] J.K. Shoemaker, C.S. Hogeman, M. Khan, D.S. Kimmerly, and L.I. Sinoway, "Gender affects sympathetic and hemodynamic response postural stress," Am. J. Physiol.: Heart Circulatory Physiol. 281(5): H2028-2035, 2001.

[22] S.M. Michaelson, and J.C. Lin, "Cardiovascular effects," in: *Biological Effects and Health Implications of Radiofrequency Radiation*, New York, N.Y.: Plenum Press, 1987, Ch. 13, pp. 451-488.

[23] Institute of Laboratory Resources: Committee on Care and Use of Spontaneously Hypertensive Rats, "Spontaneously hypertensive (SHR) rats: guidelines for breeding care and use," ILAR News 19: G1-G20, 1976.

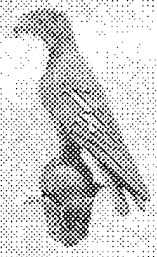
[24] B.A. Barron, and G.R. Van Loon, "Role of sympathoadrenomedullary system in cardiovascular response to stress in rats," J. Autonomi. Ner. Syst. 28(2): 179-188, 1989.

[25] A. Sagakuchi, J.E. LeDoux, and D.J. Reis, "Sympathetic nerves and adrenal medulla: contribution to cardiovascular-conditioned emotional responses in spontaneous hypertensive rats," Hypertension 5(5): 728-738, 1983.

[26] A.U. Ferrari, A. Daffonchio, V. McManamon, and W. Wedding, "Inverse relationship between heart rate and blood variabilities in rats," Hypertension 10(5): 533-537, 1987.

BIOLOGICAL EFFECTS of EMFs

2nd INTERNATIONAL WORKSHOP

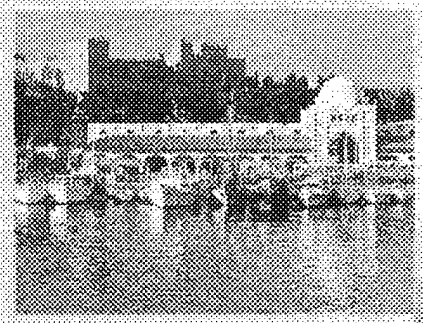




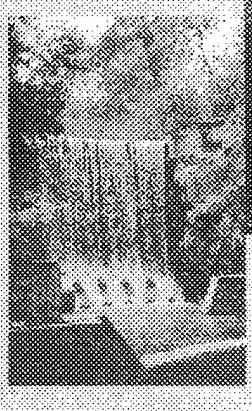
Electronics - Telecom & Applications Laboratory
Physics Department
University of Ioannina

Institute of Informatics & Telecommunications
N.C.S.R. "Demokritos"

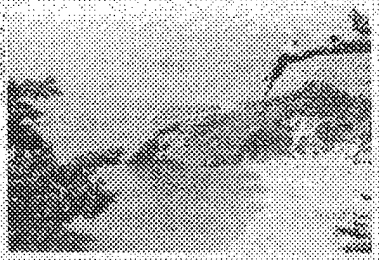
Proceedings











Volume I

Rhodes, Greece, 7 -11 October, 2002

APPLICATION OF VARIOUS THERMOMETRIC CALORIMETRY IN RODENT DOSIMETRY

SATNAM P. MATHUR
SHIN-TSU LU

McKesson BioServices Corporation and U.S. Army Medical Research Detachment
Brooks Air Force Base, San Antonio, Texas, 78235-5460 U.S.A.

ABSTRACT

Thermometric calorimetry is defined as a method for determining changes in the heat content of a specimen through changes in specimen temperatures. Inexpensive and accurate temperature measurement devices with fast and miniaturized probes can be used for radio frequency dosimetry in animals. The accuracy of the thermometric dosimetry has been determined with a T-75 flask filled with water tested in a circularly polarized waveguide exposure system in which power deposition can be determined continuously with power meters. A recovery rate of 100 % has been found. Several variations of thermometric calorimetry have been used routinely in this laboratory. They are whole-body average (WBA) specific absorption (SAR) in cylindrical liquid phantoms, local SARs in animal carcasses, and whole-body average SAR in anesthetized animals. These methods allow us to identify a multibody effect on WBA SAR between cylindrical liquid phantoms, mass dependencies of WBA SAR in cylindrical liquid phantoms and anesthetized rats, and alterations of local SARs but not the WBA SAR caused by an implanted osmotic pump in animal carcass. The thermometric calorimetry methods can be powerful tools in determining SAR.

INTRODUCTION

Determination of the dose and/or dose rate administered in radio frequency (RF)/microwave bioeffects research is an integral of the research protocol. The absorbed dose in the animal is expressed as the local and whole-body average specific absorption rate (WBA SAR). The dosimetry data is the basis for comparisons among laboratories that employ different animal exposure methods, and the basis of current safety standards. Local SAR is defined at a point in the absorbing body. Measurement of SAR distribution in an absorbing body is the measurement of local SAR at various points in the body, and is necessary to investigate the location and magnitude of RF absorption hot spots as a result of inhomogeneity of the absorbing body and/or as a result of implanted devices such as an osmotic pump. SAR is determined by measuring either the internal electric field at a point or by measuring the rate of temperature rises within the object. The temperature rise may be characterized by a calorimetric measurement (WBA measurement), a point measurement (thermometer implanted at a point in the body being exposed), or a thermographic camera analysis of bisected phantom models that have been exposed to RF fields [1]. In this paper we use simple and accurate thermometric microwave dosimetry procedures to calculate WBA SAR in a simple cylindrical model of rat and compare it to WBA SAR measured in rat cadavers and anesthetized rats.

Early theoretical calculations of whole-body absorption in human and animal were based on planar, cylindrical, spherical, ellipsoidal and homogeneous prolate spheroidal models [2-3]. The calculated SARs of cylindrical models of standard man and rats of three different body masses, along with those of prolate spheroid models, show that cylindrical models can be useful for calculation of WBA SAR from 400 MHz to 10 GHz for electric and magnetic polarizations. SAR can be measured in animal cadavers; but measuring SAR in phantoms is more convenient, more reproducible, and almost as accurate as in cadavers. Prolate spherical (PS) models filled with saline have been used to measure WBA SAR and data has been correlated to WBA SAR measured in anesthetized rats of different body masses. [5]. Kim [6] measured the WBA SAR with twin-well calorimeters, for simultaneous free-space exposure a group of mice of varying body mass and exposure geometry. Kim's results indicated that measured SARs in multi-animal exposures were significantly different from the SARs predicted by a single-body model.

In this paper, we describe a thermometric dosimetry technique to measure WBA SAR in cylindrical liquid phantoms. The accuracy of the thermometric calorimetry is verified by the WBA SAR determination in a

T-75 flask filled with water, placed in a Styrofoam box and tested in a cylindrical circular waveguide, using the power equation method [7]. SAR calculated from thermometric calorimetry and power equation method showed excellent correlation, with 3.7 % discrepancy between the two methods. Thermometric method tends to overestimate the SAR as compared to the power equation method. Thus, cylindrical liquid phantoms can be used for accurate measurement of WBA SAR in a well-defined, enclosed exposure system. The thermometric calorimetry method has been applied to measure WBA SAR for free-space L-Band exposures (1.25 GHz, 1.0 MW peak power, 6.0 μs pulse duration) of rats in E-polarization, and to verify the measured data against theoretical calculations based on prolate spheroid models of rats. We correlate the WBA SAR in cylindrical liquid phantoms to those measured using rat carcasses and anesthetized rats of varying body mass. Use of cylindrical liquid phantoms in a multi-body free-space exposure scenario is explored and uncertainties in such measurements are quantified.

MATERIALS AND METHODS

A. Water Bottle Thermometry

In the thermometry procedure we measure average initial and final temperatures in the cylindrical liquid phantom for the sham and microwave exposures using a thermistor thermometer (Cole-Parmer model 8502-16) and a thermistor probe (Yellow Spring Instruments, YSI-427). The duration of exposure and average power of the transmitter is adjusted to yield an approximately 1 – 1.5 °C temperature rise. The liquid phantom was placed in a 2" Styrofoam box during the exposures to reduce heat loss to the environment during exposure. The water bottle was thoroughly shaken by inversion by hand at least 120 times before making the temperature measurements to ensure uniformity of the temperature in the bottle/flask. The net temperature rise was calculated by subtracting the temperature rise during sham exposure from that during microwave exposure. WBA SAR is then calculated by multiplying the net temperature rise by the specific heat capacity of the liquid phantom. We have used a T-75 flask filled with 200 g of water for the in-waveguide dosimetry, and two cylindrical polyethylene bottles (Nalgene, HDPE IP2 bottles) of 250 and 500 ml capacity, filled with 240 g and 325 g of 0.9% saline solution for the L-Band free-space exposures in the anechoic chamber. The 500 ml bottle also contained 118 g of paraffin wax to fill up the large volume. We have ignored the wax heat capacity in calculating SAR for the 325 g phantom load because it is a poor RF absorber and has low thermal conductivity. Each determination was replicated six times, in pairs of sham and microwave exposures and WBA SAR was then calculated as mean of six replications to minimize experimental errors. The free-space exposures for single and two liquid phantom loads were performed in an L-Band anechoic chamber at bore-sight and three off bore- sight locations as described below.

B. Thermometry in anesthetized rats and rat cadavers

Each rat was anesthetized by Xylazine (80 mg/kg) and Ketamnine (5 mg/kg) administered IP prior to the exposures. Supplemental Ketamine injections (30 mg/kg) were administered as needed during the experimental run. A Luxtron (Model 3000) fiber optic thermometer and linear array type of fiber optic, non-perturbing probes (MAM-05) containing four sensors at 5 mm spacing, are used to measure temperature rise at various locations in the rats. In the case of anesthetized rats one MAM-05 probe is inserted 5.5 cm into the rectal orifice, with sensor A located 5 cm from the orifice. Sensors B, C, and D are located 4.5, 4.0 and 3.5 cm from the orifice. The rat is placed in a 2" Styrofoam box with a breathing hole, 30 cm in front of an WR-650 open-ended waveguide antenna on the bore-sight and exposed for 5 minutes to microwave pulsed radiation of 1.0 MW peak power, 6 μs pulses, and 21 or 25 Hz pulse repetition rate at 1.25 GHz from an FPS-7B, L-Band transmitter, in E-polarization (horizontal polarization). Temperature data was collected for 5 minutes prior to microwave exposure, 5 minutes during the microwave exposure, and for 5 minutes after the microwave exposure. WBA SAR was calculated using a procedure described by Gambrill et al [8], which compensates for errors caused by changing thermal diffusion and minimum detectable SAR as limited by the sensitivity of the measuring equipment. Mean WBA SAR from "r" replications, averaged over "j" locations is calculated as:

$$\text{WBA SAR} = \sum_{j} \{ \sum_{r} \text{SAR}_r \}_j \qquad (1)$$

We are using the thermal mixing of the circulatory system of the anesthetized rat and thermal insulation to measure WBA SAR by changes in core temperatures. To quantify the variation in WBA SAR with body mass, rats from 240 to 330 g in body mass were used. For comparison, the length, L (=2a), and chest circumference (=2 π b) of the rats were also measured to calculate WBA SAR from equivalent (PS) model.

Four rats of varying body mass were euthanized using CO_2 just prior to the experiment and their body mass, length, and torso circumference was measured. Rat cadavers were implanted with two MAM-05 probes in two different locations, for a total of sixteen different points in the cadaver. Two thermometric experiments were conducted, one with an osmotic pump (Azet, model 2ML4, 5.1 cm long, 1.4 cm dia., 5.1 g, made of styrene acrylonitrile body, ploye thylene cap, and a teflon tube) filled with saline, installed at the back, and the other with the osmotic pump removed. Selected fiber optic probe locations were chosen to measure local SAR enhancement or reduction in the vicinity of the osmotic pump. Other sensor locations were chosen to measure the subcutaneous temperature rise on the "lit" and the "shadow" side and in colonic region. Each experiment was replicated four times and WBA SAR was calculated as an average over four replications at sixteen locations.

C. Exposure systems

An in-waveguide exposure system consisting of a 918 MHz wire-mesh, cylindrical circular waveguide retrofitted with 2450- MHz circular waveguide with built in circular polarizer; two probes attached to a 50-ohm terminations. The waveguide supports TE_{11} and TM_{11} modes and a circularly polarized propagating wave at 2450 MHz. As described in [8], this system provides a relatively constant and easily quantifiable coupling of fields to the animal/phantom load. When an animal or a phantom load is placed in the waveguide around the midway point between the input port and the termination port and exposed to the two propagating waves, the power absorbed by the animal/load is given by the equation (2):

$$P_a = P_{in} - P_{rr} - P_{rl} - P_{ta} - P_{tb} \qquad (2)$$

Where, P_{in} is the input power, P_{rr} and P_{rl} are powers reflected of both the right-hand and left-hand circularly polarized waves respectively that couples back at the probes in the feed section for the 2450 MHz waveguide, and P_{ta} and P_{tb} are the powers measured at the termination terminals. WBA SAR is then calculated as

$$SAR = (P_a - P_{ac}) / w \qquad (3)$$

Where, P_a is the power absorbed when the phantom load is in the waveguide, $P_{ac,}$ is the power loss measured in the empty waveguide, and w is the mass of the phantom load.

The free-space exposure system consists of an L-Band, FPS-7B transmitter connected to an open-ended WR650 waveguide antenna radiating a horizontal E-Field. The far zone of this antenna is 28 cm at 1250 MHz. All exposures were performed at 1250 MHz, at the bore-sight location, 30 cm from the antenna along the bore-sight line. The liquid phantoms or animals were placed such that exposures were in E-polarization. In multi-body experiments, two loads were placed one (rat or saline bottle) at the bore-sight location and the other load (saline bottle) at 40, 50, or 60 cm horizontal offsets from the bore-sight location. The intention was to determine the WBA SAR at off bore-sight location and the change in WBA SAR at bore sight location due to the presence of the off bore-sight load. A 10 dB lower dose at the off-bore sight location as compared to that at the bore sight location was desired.

RESULTS AND DISCUSSION

A. Validation of thermometry procedure

A 200 g water load was placed in a 2" Styrofoam box in the center of the waveguide and exposed for either 120 or 150 s at input power of 15 to 25 W, resulting in temperature rises of 1 to 1.5 ° C. WBA SAR calculated from equation (2) is denoted as SAR_p and that calculated from thermometry procedure is denoted as SAR_t. Figure 1 shows the correlation between SAR_p and SAR_t. WBA SAR calculated from the power equation and the thermometric method shows excellent correlation; a recovery rate of 96 % is indicated by the slope obtained by a least square data-fitting algorithm. The thermometric procedure slightly overestimates the SAR calculated from the power equation method. This shows that our thermometric procedure has successfully reduced the heat loss to the environment thorough the use of Styrofoam box, liquid phantom load heats up slightly during the temperature measurement.

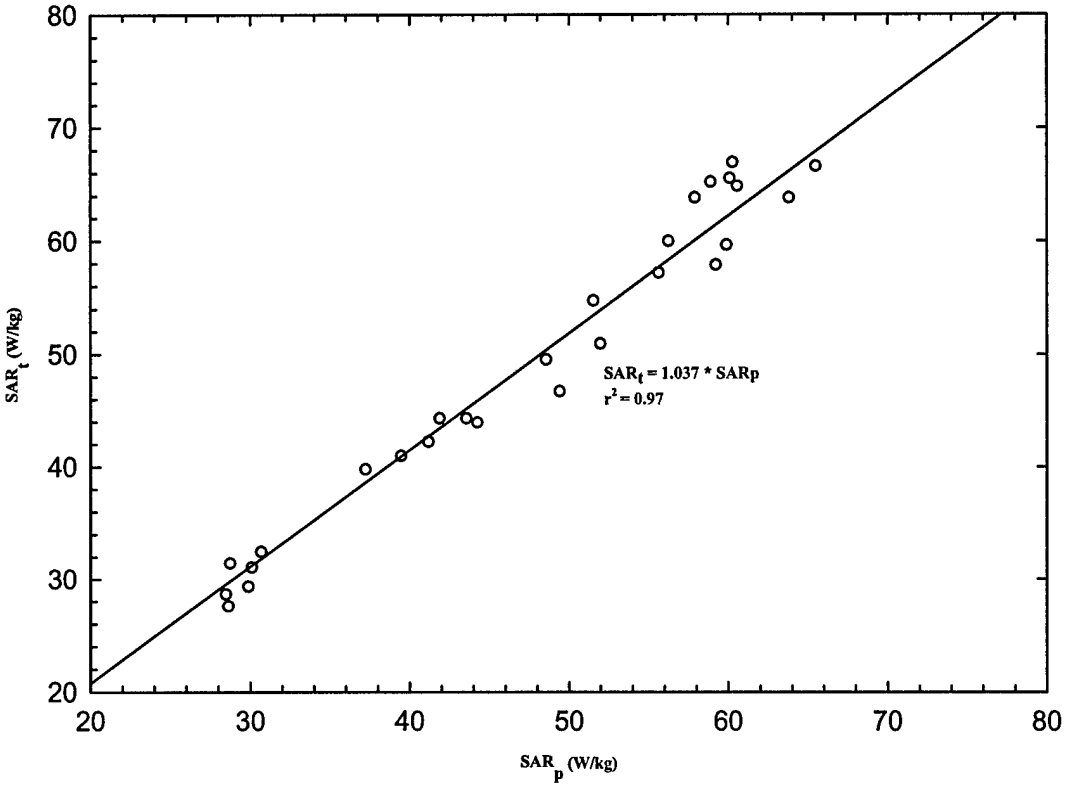


Figure 1. SAR Correlation between power equation and calorimetry method.

B. Saline filled cylindrical phantom thermometric Calorimetry in free-space

As part of the dosimetry study for a protocol that calls for exposing two rats simultaneously to two WBA SAR levels in the ratio of 10:1, we conducted SAR measurements on a single cylindrical phantom load as well as two loads at the two different locations. One phantom load receiving the higher SAR was placed 30 cm in front of a WR-650 open-ended waveguide antenna along the bore sight line while 40, 50 or 60 cm in the horizontal direction offset the other load. All WBA SARs are normalized to the average power density incident on a rectangular area passing vertically through the center of the bottle. Since the rats to be used in the protocol will vary in body mass from 240 to 325 g, we have selected two liquid phantoms of 240 and 325 g respectively to bracket the WBA SAR at the two ends, to investigate the effects of the second load at off bore-sight locations on the one at the bore-sight location, and to determine the ratio of the WBA SAR at the two locations. In the anesthetized rat and rat cadaver thermometric calorimetry, the cylindrical liquid phantom load will represent one of the animals. Thus, it is necessary to ascertain how well a cylindrical liquid phantom simulates a rat. Table I shows the results of single liquid phantom (cylindrical bottle) placed at bore-sight location as compared to the SAR predicted by the prolate spheroid (PS) model of equivalent mass; the length of the bottle is taken as the major axis of the prolate spheroid, while the minor axis of the prolate spheroid was calculated from the expression $W = (2/3).\pi .b^2. L. \rho$, where ρ is the average mass density and W is the body mass.

Table I. WBA SAR for single phantom loads at bore sight

Phantom mass (g)	Phantom size (length, L, and diameter, d, cm)	PS model (2a, 2b, cm)	Measured SAR (W/kg/mW/cm^2)	PS SAR (W/kg/mW/cm^2)
240	L = 11.5, d = 6.2	11.5, 6.31	0.26	0.32
325	L = 16.0, d = 7.2	16.0, 6.23	0.25	0.31

The difference in SARs measured by thermometric calorimetry method and that predicted by the PS model is about 19 % for both the loads. This is expected as a cylindrical phantom load exposed in E-polarization behaves differently than a prolate spheroid exposed to E-polarization due to end effects. If the cylindrical models were of infinite length the magnitude of the internal electrical fields in the cylinder will be same as the incident field

causing a strong coupling, and the resulting SAR will be higher than that for the equivalent PS model. Our cylindrical loads are of finite length, and have the same volumes and cross-sectional areas, i.e., the largest cross-sectional area is normal to the direction of propagation vector of the incident wave, as the corresponding PS models. A 4 % difference in energy absorption by the cylindrical and PS models, filled with lower dielectric constant materials, has been reported for E - polarization and frequencies lower than 500 MHz [4]. In our case however, the cylindrical loads are filled with saline, which is a high dielectric constant material, and measurements were made at a higher frequency of 1.25 GHz. Thus, a 19 % difference between cylindrical loads and PS model may be explained by these factors.

Next, we measure the effect on WBA SAR measured at bore-sight location when a second phantom load is present at an off bore-sight location; three off bore-sight locations at 40, 50, and 60 cm horizontal offset were considered, and WBA SAR at off bore-sight locations were measured as well. For measurements of SAR at off bore-sight locations peak power was raised to 3.0 MW, and pulse repetition frequency was raised to 25.83 Hz. This allowed us to work with a temperature rise of about 0.5 ° C in 5 minutes, as opposed to a temperature rise of 0.7 – 0.8 ° C in 5 minutes at a lower average power for the bore-sight measurements. Figures 2a through 2d show the effect on WBA SAR at bore sight location due to another load at an off-bore sight location and WBA SAR at off bore-sight locations for 240 and 325 g phantom loads. The presence of another load at any off bore-sight location for 240 g loads; show a significant difference in WBA SAR at bore-sight location as compared to the single load at bore-sight (t-test at $p < 0.05$ level) for off bore-sight load at 40 cm and 60 cm but not at 50 cm. However, there is no difference in bore-sight WBA SARs for a single 325 g load or with two loads at the three off bore-sight locations. The off bore-sight WBA SAR decreases linearly from that at bore- sight as shown in figures 2b and 2d for 240 g and 325 g loads respectively. A 10 dB drop off in WBA SAR occurs at approximately 60 cm separation between the loads. Note, also that the bore-sight WBA SAR increases from that of a single load case for both 240 and 325 g loads, when another load is present at 60 cm horizontal offset; increases is 14.5 % for 240 g load and 6.1 % for 325 g load. This could be due to constructive interference of the fields at bore-sight due to the load at the off bore-sight location.

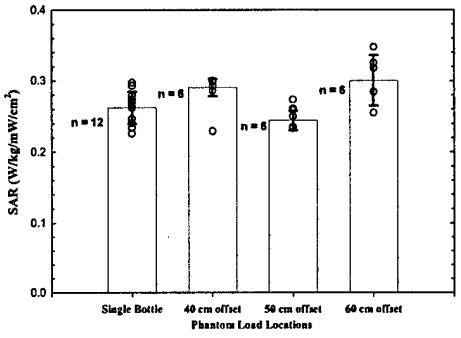


Figure 2a. WBA SAR at bore sight for 240 g phantom load

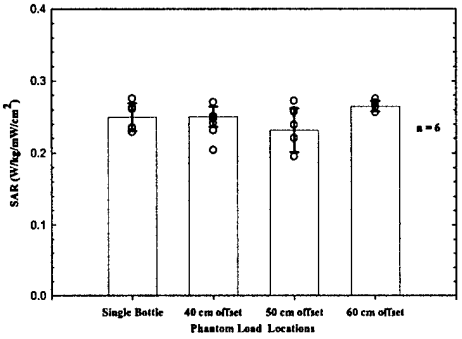


Figure 2c. WBA SAR for 325 g phntom loads at bore sight

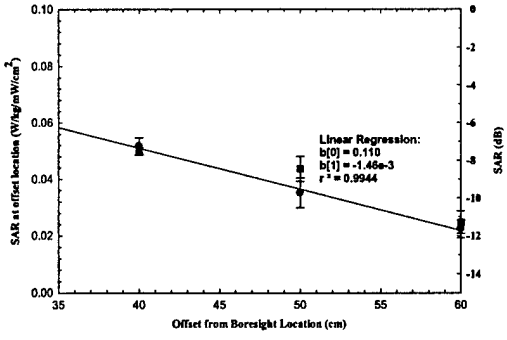


Figure 2b. WBA SAR at off bore-sight locations for 240 g load.

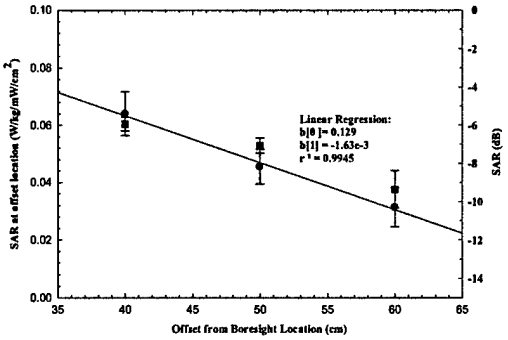


Figure 2d. WBA SAR at off bore-sight locations for 325 g load.

C. Whole-body thermometric calorimetry for anesthetized rats

Figure 3 shows the results of bore sight WBA SAR measured for anesthetized rats as compared to WBA SAR predicted by equivalent PS model and those by liquid phantom models. The WBA SAR for anesthetized rats was calculated from SAR at individual locations from Equation (1), where r= 4 and j = 4 in this case. All measurements were made with rat at bore-sight and a liquid phantom load located at horizontally 60 cm off bore-sight. Note, that PS model does not predict correct WBA SAR as measured in anesthetized rats and rat cadavers. This is as expected because PS model is only valid for single body exposures. The presence of other lossy loads in the exposure area cause complicated field interference at the bore sight location. The liquid phantoms, PS model, and rat cadavers shows a decreasing SAR with increasing body mass whereas the SAR for anesthetized rats increases slightly with increasing body mass. It is not clear why this behavior is seen but the rates of increase or decrease of SAR are very small (-0.0009 per g for PS model; -0.0004 per g for liquid phantoms, 0.00075 per g for anesthetized rats, and –0.0002 per g for rat cadavers). However, the difference can be as much as 0.09 W/kg/mW/cm^2 when body mass increases from 240 g to 340 g.

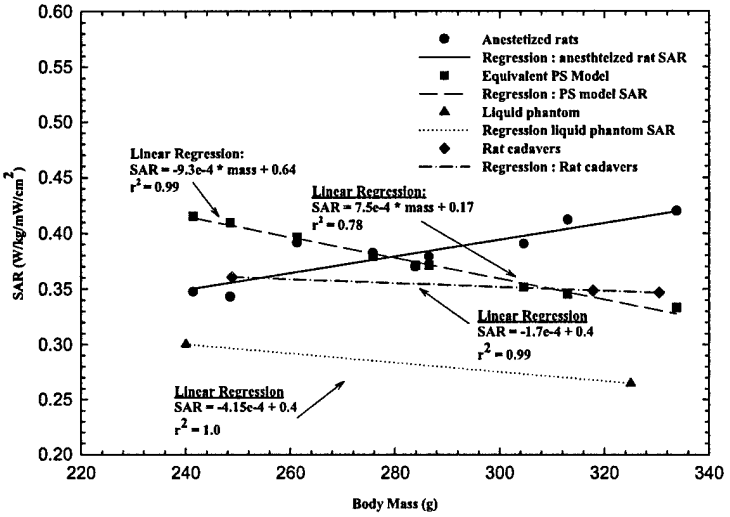


Figure 3. WBA SAR for anesthetized rats compared to liquid phantom loads and PS Model SAR

D. Local SAR distribution in rat cadavers

Four rat cadavers, A17, A15, A20, and A24 were implanted with Azet osmotic pumps and local SAR was measured with Luxtron fiber optic thermometer with two MAM-05 fiber optic probes. Each probe has four sensors A, B, C, and D arranged in an array fashion. Figures 4 through 8 show changes in local SAR at various locations in the rat cadaver measured when implanted with Azet osmotic pump and with the pump removed. Figures 4 - 8, plot (SAR_{wp} - SAR_{wop}), where SAR_{wp} is the SAR measured with the pump implanted and SAR_{wop} is the SAR measured without the pump for each of the sensors locations. All measurements were performed with rat cadaver at the bore-sight location and a liquid phantom load at 60 cm horizontally off bore-sight location.

As seen in Figures 4a – 4d, there is a large change in local SARs due to the presence of the pump for sensors on the "lit" or the incident field side as well as on the "shadow" side of the cadaver. There is no definite trend; in some animal cadavers, the change is positive whereas in the others it is negative. The magnitude the change in SAR can be as high as 50 % on either side, positive or negative, depending on the rat cadaver and probe locations. Animal to animal variability may be better characterized if a larger number of experiments on different rat cadavers are done. However, largest changes are seen in locations next to the implanted Azet pump, on the "lit" side (the incident field side), while ten fold smaller changes are seen on the "shadow" side. Changes in SAR measured at the core locations is at least two times smaller than those seen in locations on the "lit" side.

The presence of Azet pump consistently decreases local SARs at the "shadow" side (Figure 4c) across animals and probe locations.

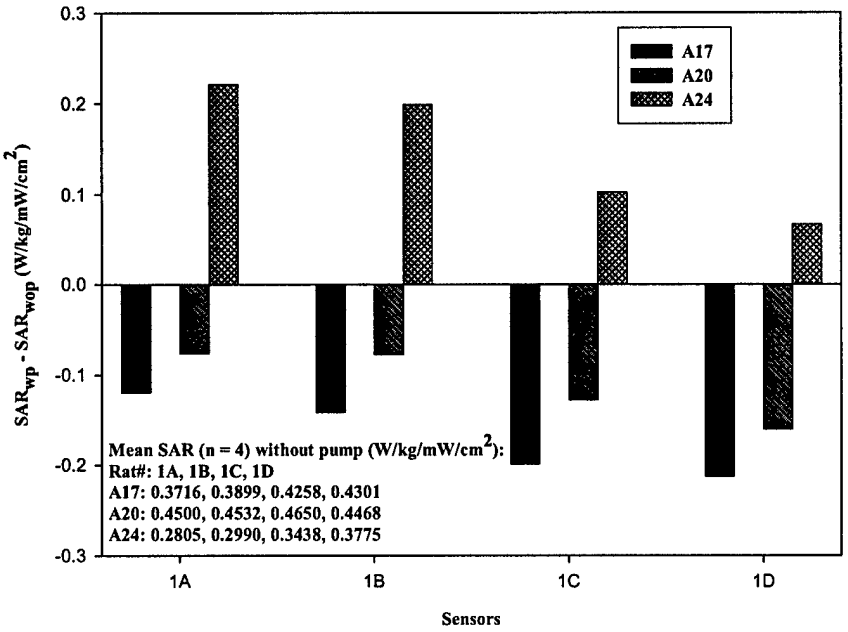


Figure 4a. Change in SAR with & without pump. Probe Location #1, Luxtron Probe #1 (MAM-05). Dorsal subcutaneous on the incident field side, in contact with Azet pump, sensor A is 12 mm from the tip which is at the cranial end of the pump.

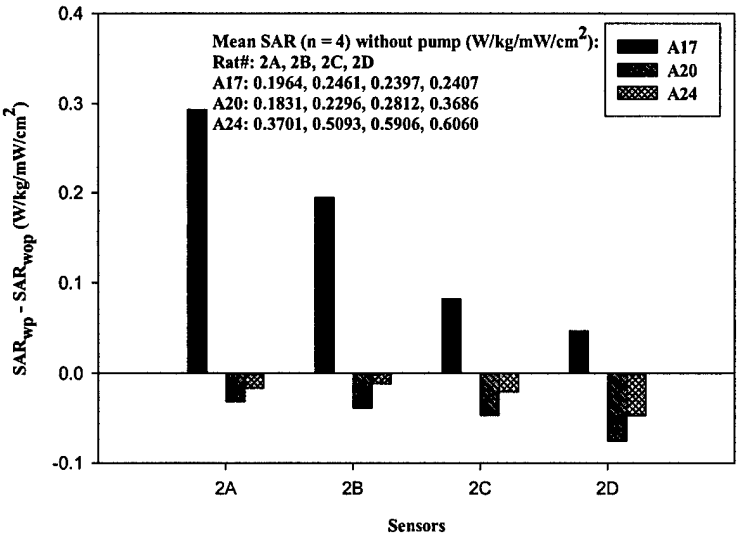


Figure 4b. Change in SAR with & without pump. Probe Location #1, Luxtron Probe #2 (MAM-05). Sensor A is 5 mm from probe tip. Subcutaneous on the incident field side, and 1.6 to 3.0 cm ventral to the probe #1at lateral summit of the chest, on the incident field side. Tip of the probe is vertically aligned with tip of probe #1.

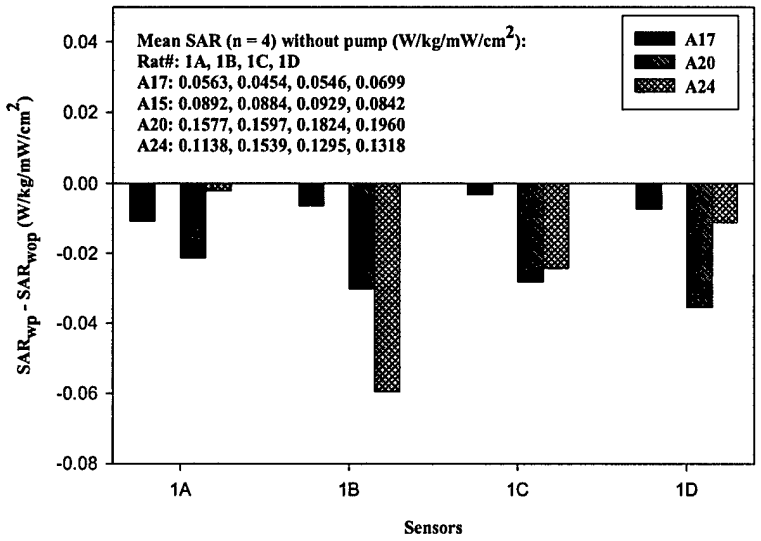


Figure 4c. Change in SAR with & without pump. Probe Location #2, Luxtron Probe #1 (MAM-05). On the shadow side, subcutaneous at crest of chest vertically 2.0 - 2.5 cm from the base of the pump. Probe tip is approximately at the cranial end of the pump. Sensor A is 12 mm from the tip of the probe.

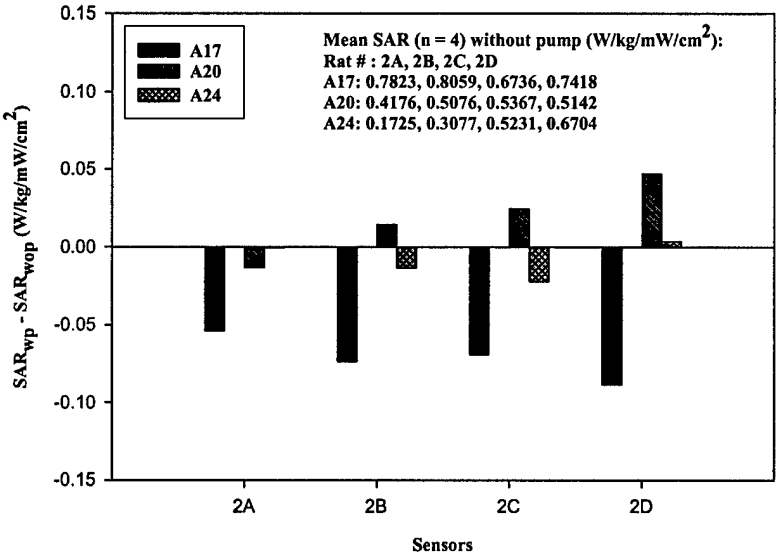


Figure 4d. Change in SAR with & without pump. Probe Location #2, Luxtron Probe #2 (MAM-05). Sensor A is 5 mm from probe tip. Rectal probe. Tip of the probe inserted to 5.5 cm through the orifice.

SUMMARY

We have presented a thermometric calorimetry method, which uses simple liquid phantom loads to estimate WBA SAR in rodents, both in a single-body and multi-body environments. The thermometric method has been verified comparing it to WBA SAR measured using the reliable, accurate, and reproducible power equation method. The thermometric method tends to overestimate the WBA SAR by 3.7 %. Thermometric method yields results for single-body exposures in free-space that are within 19 % of the theoretically predicted results from equivalent prolate spheroid model calculations. Use of liquid phantoms is however limited in predicting WBA SARs for multi-body exposures; only relative WBA SAR can be reliably measured. For more accurate determination of WBA SAR in a multi-body exposure situation, a twin-well or gradient layer calorimetry should be used. The simple thermometric calorimetry is useful in determining the effects of implanted devices such as an osmotic pump on local SAR distribution.

ACKNOWLEDGMENTS

This work is supported by the U. S. Army Medical Research and Materiel Command under contract DAMD17-94-C-4069 awarded to McKesson BioServices corporation. The views, opinions and/or findings contained in this report are those of the author(s) and should not be construed as an official Department of the Army position, policy, or decision unless so designated by other documentation. In conducting research using animals, the investigator(s) adhered to the "Guide for the Care and Use of Laboratory Animals" prepared by the Institute of Laboratory Animal Resources, National Research Council (Washington, DC: National Academy Press, 1996). This article is a US Government work and, as such, is in the public domain in the United States of America. WRAIR is the Walter Reed Army Institute of research in Washington, DC USA.

REFERENCES

[1] Hurt, W. D., "Absorption characteristics and measurement concepts" in *Radio frequency radiation Dosimetry and its relationship to the biological effects of electromagnetic fields.*, B. J. Klaunberg and D. Miklavčič (eds.), 2000, pp. 39-52.

[2] Rowlandson, G. I., and P.W. Barber, "Absorption of higher-frequency RF energy by biological models based on geometrical optics", *Radio Science*, Nov. Dec. 1979, vol. 14, Number 6S, pp. 43-50.

[3] Massoudi H., C. H. Durney, and C. C. Johnson, " Comparison of the average specific absorption rate in the ellipsoidal conductor and dielectric models of humans and monkeys at radio frequencies" *Radio Science*, Nov. Dec. 1977, vol. 12, Number 6S, pp. 65-72.

[4] Massoudi, H., C. H. Durney, and C. C. Johnson, "A geometrical-optics and an exact solution for internal fields in and energy absorption by a cylindrical model of man irradiated by an electromagnetic plane wave", *Radio Science*, Nov. Dec. 1979, vol. 14, Number 6S, pp. 35-42.

[5] Gandhi, O. P., "Frequency and orientation effects on whole animal absorption of electromagnetic waves", *IEEE Trans. on Biomedical Engineering,* Nov. 1975, vol. BME-22, pp. 536-542.

[6] Kim, J. B., "Whole-body dosimetry of microwave radiation in small animals: The effect of body mass and exposure geometry", *Radio Science*, Nov. Dec. 1977, vol. 12, Number 6S, pp. 61-64.

[7] Guy, A. W., J. Wallace, and J. A. McDougall, "Circularly polarized 2450-MHz waveguide system for chronic exposure of small animals to microwaves", *Radio Science*, Nov. Dec. 1979, vol. 14, Number 6S, pp. 63-74.

[8] Gambrill, C. S.., M. L. DeAngelis, and S. –T. Lu, "Error analysis of a thermometric microwave-dosimetry procedure", in *Electricity and Magnetism in Biology and Medicine*, Martin Blank (ed.), 1993, San Francisco: San Francisco Press, Inc. pp. 593-595.

Bioelectromagnetics 23:158–167 (2002)
DOI 10.1002/bem.108

Comparison of Dose Dependences for Bioeffects of Continuous-Wave and High-Peak Power Microwave Emissions Using Gel-Suspended Cell Cultures

Andrei G. Pakhomov,[1,3]* Peter Gajšek,[3,4] Lori Allen,[1] Bruce E. Stuck,[2] and Michael R. Murphy[3]

[1]*McKesson BioServices, Brooks Air Force Base, San Antonio, Texas*
[2]*US Army Medical Research Detachment of the Walter Reed Army Institute of Research, Brooks Air Force Base, San Antonio, Texas*
[3]*Directed Energy Bioeffects Division, Human Effectiveness Directorate, Air Force Research Laboratory, Brooks Air Force Base, San Antonio, Texas*
[4]*National Institute of Public Health, Ljubljana, Slovenia*

The study compared bioeffects of continuous wave (CW) microwaves and short, extremely high power pulses (EHPP) at the same carrier frequency (9.3 GHz) and average power (1.25 W). The peak transmitted power for EHPP was 250 kW (0.5-μs pulse width, 10 p.p.s.), producing the E field of 1.57 MV/m in the waveguide. A biological endpoint was the density of yeast cells, achieved after a 6 h growth period in a solid nutrient medium (agarose gel) during EHPP or CW exposure. Owing to power losses in the medium, the specific absorption rate (SAR) ranged from 3.2 kW/kg at the exposed surface of the sample to 0.6 mW/kg at 24 mm depth. Absorption and penetration of EHPP was identical to CW, producing peak SAR values 200 000 times higher than the average SAR, as high as 650 MW/kg at the surface. CW and EHPP exposures produced highly nonuniform but identical heating patterns in exposed samples. Following the exposure, the samples were sliced in a plane perpendicular to the wave propagation, in order to separate cell masses exposed at different SAR levels. Cell density in the slices was determined by nephelometry and compared to unexposed parallel control samples. Cell density was strongly affected by irradiation, and the changes correlated well with the local temperature rise. However, the data revealed no statistically significant difference between CW and EHPP samples across the entire studied range of SAR levels (over six orders of magnitude). A trend ($P < 0.1$) for such a difference was observed in slices that were exposed at a time average SAR of 100 W/kg and higher, which corresponded to peak SAR above 20 MW/kg for the EHPP condition. These numbers could be indicative of a threshold for a specific (not merely thermal) exposure effect if the trend is confirmed by future studies. Bioelectromagnetics 23:158–167, 2002. Published 2002 Wiley-Liss, Inc.†

Key words: high power microwave pulses; specific effects; yeast; growth rate; nonthermal; thermal effects

INTRODUCTION

One recognized difficulty in studying bioeffects of pulsed microwaves is the large number of radiation parameters which hypothetically may determine the exposure effectiveness. Even in the simplest cases, the parameters to consider include the exposure duration, the carrier frequency, the time average and peak specific absorption rate (SAR), pulse shape and width, and pulse repetition rate or the duty cycle. Thermal effects of the radiation usually can be adequately described by the exposure duration and the time average SAR, but the situation with possible "specific" effects is far more complicated.

Perhaps the only specific effect that has been known in good detail is a microwave auditory effect

Contract grant sponsor: US Army Medical Research and Material Command; Contract grant sponsor: US Air Force Research Laboratory (AFOSR) (to McKesson BioServices); Contract grant number: DAMD17-94-C-4069.

*Correspondence to: Andrei G. Pakhomov, McKesson BioServices, 8308 Hawks Road, Building 1168, Brooks Air Force Base, San Antonio, TX 78235-5324.
E-mail: andrei.pakhomov@brooks.af.mil

Received for review 10 May 2001; Final revision received 12 July 2001

Published 2002 Wiley-Liss, Inc.
†This article is a US Government work and, as such, is in the public domain in the United States of America.

[Guy et al., 1975; Lin, 1978; Chou et al., 1982; Lin, 1989]. Knowledge about other claimed specific effects is largely empirical, and existing hypotheses about their mechanism do not have enough predictive power to explain problems with reproducibility of these effects in different laboratories. Meanwhile, if a theory does not explain which exposure parameters are critical, the experimental search for effective parameters may be excessively laborious, especially with so-called "window effect" phenomena.

The essence of window effects is that they occur only within a limited range of exposure parameters, i.e., an effectiveness window. Studies in various biological subjects have demonstrated effectiveness windows for the carrier frequency [Grundler and Kaiser, 1992; Kataev et al., 1993; Belyaev et al., 1996], the average radiation intensity or the average SAR [Dutta et al., 1992; Lukianova, 1999], and peak intensity [Semin et al., 1995a]. To add more complications, some specific effects required a precise combination of different exposure parameters, e.g., the carrier frequency and pulse repetition rate [Gapeev et al., 1994; Semin et al., 1995b] or the modulation frequency and the radiation intensity [Blackman et al., 1980; Adey, 1988; Dutta et al., 1989; Schwartz et al., 1990]. Since the windows often are very narrow, the experimental search for unique combinations of different exposure parameters among the innumerable possibilities is problematic, and it is no wonder that many attempts to reveal the effectiveness windows by probing various combinations of exposure parameters resulted in negative findings [Chou and Guy, 1978; Bush et al., 1981; Liu et al., 1982; Pakhomov et al., 1992, 1995]. More information and discussion of window phenomena can be found in specialized reviews on pulsed microwave bioeffects [Blackwell and Saunders, 1986; Postow and Swicord, 1986; Pakhomov and Murphy, 2000].

Obviously, exploring specific microwave bioeffects, as well as the search for effectiveness windows, could be expedited greatly if a wide range of values of a certain exposure parameter could be probed in a single exposed sample during a single exposure. In the present study, we tested a simple technique which makes it possible to characterize a bioeffect across a wide range of values of SAR using a single exposure of an in vitro sample. The technique allows one to develop a complete dose-effect dependence and identify possible "power windows" from a single experiment.

For this purpose, small biological specimens, e.g., cells, are exposed to microwaves within a lossy gel, e.g., a cell culture medium solidified with agar. Microwave absorptive properties of the gel are chosen to be similar to those of living tissue. SAR in such a gel decreases exponentially with the distance from the microwave exposed surface. For example, at 10 GHz, the SAR falls about twofold per millimeter; just 20 mm into the gel, the SAR decreases more than a millionfold (by 2^{20}). Consequently, cells suspended within the gel are also exposed at SAR levels ranging over more than a millionfold. After the exposure, the cells or cell masses exposed at different SAR levels can be mechanically separated, and the dependence of a microwave effect on the SAR in these cells can be revealed by ordinary biological assays.

We employed this technique to compare the effect of continuous wave (CW) microwaves and extremely high power pulses (EHPP) on the proliferation rate of yeast cells. While the proliferation rate has no specific link to human disease or health hazards, it is a convenient integrative index that has been widely used in microwave studies [Anderstam et al., 1983; Grundler and Kaiser, 1992; Gos et al., 1997]. Published data regarding EHPP bioeffects were recently summarized and discussed [Pakhomov et al., 2000b; see also Pakhomov and Murphy, 2000].

In short, current knowledge about EHPP bioeffects and potential health hazards is very limited. The few studies that have explored EHPP bioeffects at peak SAR levels over 1 MW/kg have produced isolated, sometimes contradictory, and generally inconclusive data. Intuitively, it is understandable that at a certain — perhaps, very high — peak SAR, bioeffects of EHPP will become different from CW and that specific effects of EHPP may be hazardous. This dictates the need to identify the peak SAR threshold for specific EHPP bioeffects, a task that has not been accomplished yet. Therefore, our present study attempted to find this threshold by comparing CW and EHPP bioeffects across a wide range of SAR levels. It is worth mentioning that the maximum peak SAR achieved in this study, 650 MW/kg, was higher than ever reported before in biological research.

Concurrently, this study intended to test the usefulness of the proposed technique of using gel-suspended cell cultures for dose-effect analysis and for identification of possible "power windows".

MATERIALS AND METHODS

Biological Methods

Main experiment and general procedures. The experiments employed yeast *Saccharomyces cerevisiae*, strain BY4741, kindly supplied by Dr. S. Avery (University of Nottingham, U.K.). To prepare a stock, cells were propagated in a YPD nutrient broth (Sigma,

USA) at 30°C to a density of 3×10^7 cells/ml. After addition of glycerol (10% by volume), 0.4 ml samples were dispensed into individual tubes and frozen at −70°C. On the eve of an experiment, one tube was taken from the stock; the medium was thawed and diluted 1000–5000 fold with YPD broth. Cultures were left overnight at 30°C on a shaker (150–200 rpm).

Next morning, the exact cell density was counted using a hemacytometer and/or measured as an optical density (OD) at 600 nm with a spectrophotometer (Milton Roy Spectronic 1001 plus). The cell suspension was diluted by appropriate amounts of YPD broth and melted YPD + 2% agarose gel to produce a final concentration of 2×10^6 cells/ml in YPD + 1% agarose medium. The use of an agarose with a low gel point (type VII-A; Sigma) made it possible to perform the dilution at a low temperature of 35°C, avoiding any heat shock to the cells. Diluted and carefully mixed cell samples were dispensed into two 4.5 ml rectangular cuvettes, flush with the edges. We used standard size ($10 \times 10 \times 45$ mm) methacrylate spectrophotometer cuvettes (Fisher, USA); the plastic bottom of the cuvette was removed beforehand and replaced with a cap, to ease gel removal after the exposure. The dispensed samples gelled within few minutes, preventing cell sedimentation or redistribution.

The cuvettes, later referred to as the "exposed" and "control" ones, were placed upside down in the exposure and control compartments of the exposure chamber, leaving no gap between the gel and the bottom of the chamber (Fig. 1). Custom holders provided for exactly the same position of the cuvettes in the compartments. The axis of the exposed cuvette coincided with the axis of the waveguide. The rest of the volume of the compartments was filled with YPD broth. The compartments had a common water jacket filled with circulating water at 25°C; however, the exposed cuvette was strongly heated by microwaves (Fig. 2). More details are provided below in the "Exposure System" section.

With the cuvettes already installed in the position, a die was rolled to choose whether CW or EHPP exposure will be performed. Then, the exposure was turned on and continued for 6 h. Exposure parameters and temperature were checked at least hourly and adjusted if necessary.

After the exposure, the exposed and control cuvettes were placed into a +5°C refrigerator for at least 5 min. Then, the gel columns were pushed out of the cuvettes and sliced into 2-mm thick squares by pressing the gel against an array of uniformly spaced razor blades. A total of 12 slices were collected from the exposed gel, starting with the gel surface that was

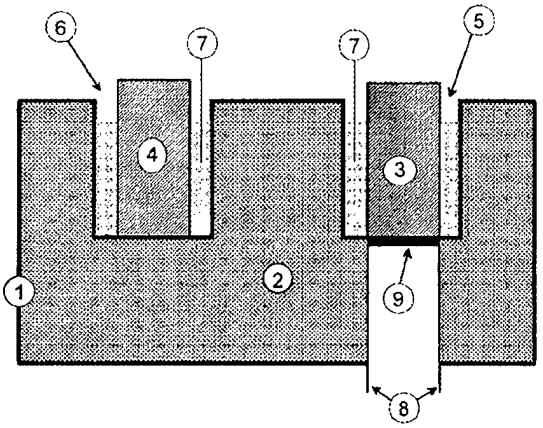


Fig. 1. A sketch of the exposure chamber (side view of a slice through the center plane, not to scale). The outer water jacket made of Plexiglas (1) is filled with circulating water at 25°C (2). Cuvettes with exposed and control samples (3 and 4) are positioned in the exposure and control compartments (5 and 6). The rest of the volume in the compartments is filled with YPD broth (7). Waveguide (8) terminates into the exposure compartment (5) via a sapphire matching plate (9).

facing the irradiator and ending at 24 mm deep into the gel; the rest of the sample was discarded. Thus, each slice included cell masses that were exposed at different SAR and temperature ranges. The control gel was sliced in precisely the same manner, though the entire control gel column was kept at the uniform temperature (25°C) and without exposure. Without a temperature or SAR gradient in the parallel control gel,

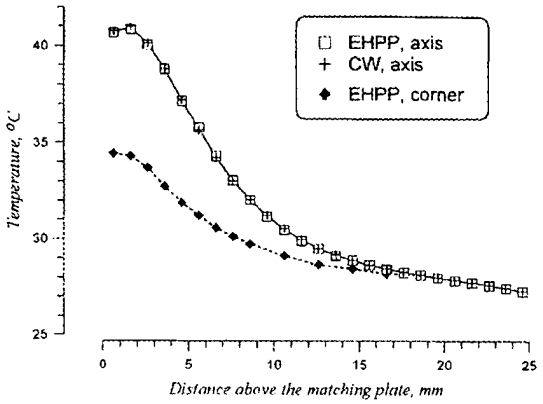


Fig. 2. Steady-state temperature profile in gels exposed to EHPP or CW radiation at the same time-average transmitted power (1.25 W). Each datapoint in the upper graphs is the mean ± SE for three separate runs; however, the error bars in all cases are smaller than the central symbol.

the data variabiliy between its slices was just a control for the accuracy of slicing and other manipulations.

The slices were transferred into individual semi-micro (1.5 ml) methacrylate spectrophotometer cuvettes (Fisher) and thawed on a water bath for 2 min at 71°C. An amount of 0.6 ml of melted YPD + 1% agarose medium at 35°C was added to each cuvette and carefully mixed with its contents. This procedure was necessary to bring the volume in each cuvette to 0.8 ml, the minimum needed for reliable OD measurement in semi-micro cuvettes. The samples gelled in 3–4 min and were allowed an additional 12–15 min for equilibration to room temperature and gel stabilization. Finally, the cell density in each cuvette was determined from light absorbance (i.e., the OD) at 600 nm, as compared to light absorbance by the same gelled medium containing no cells (see "OD control" below).

Temperature and OD controls. Aside from the exposed and control cuvettes, the diluted cell suspension before the experiment was dispensed into three more cuvettes that were used as "temperature controls". These cuvettes were filled to about 80% of the volume, capped to prevent drying, and left for incubation at 30, 35, and 40°C concurrently with the exposed and control cuvettes. The purpose of conducting the temperature control was to determine the effect of temperature alone, i.e., without microwaves, on the cell density change after a 6-h incubation.

One more cuvette was filled with the same medium as all the others (YPD + 1% agarose), but no yeast cells were added. This cuvette was held at 30°C for 6 h and later on was used as an "OD control", i.e., the reference for the light absorbance by the culture medium itself.

After the experiment, gels from these cuvettes were sliced and processed in the same way as the exposed and control samples. However, there was no need to use and analyze all 12 slices. Therefore, measurement data were averaged from three slices randomly picked up from each sliced gel, and the other nine slices were discarded.

Culture growth controls. The culture growth control experiments were focused on the time dynamics of the yeast culture propagation in anaerobic conditions within the gelled medium and the effect of temperature on the growth rate. Some of these experiments were performed prior to the main series, in order to optimize such conditions as the initial cell density and experiment duration.

Yeast cells in melted YPD + 1% agarose medium were dispensed into four semi-micro cuvettes, and four more cuvettes were filled with the same medium without cells, to be used as respective OD controls. All the cuvettes were allowed to solidify, then were capped and transferred in pairs into 25, 30, 35, and 40°C environments. OD attained in this cuvettes was measured hourly for 6 h or longer, then the samples were discarded.

Exposure System, Thermometry and Dosimetry

The exposure set-up was essentially the same as described earlier [Pakhomov et al., 2000b], with some upgrades and modifications.

EHPP were generated by a model 337X magnetron transmitter (Applied Systems Engineering, Inc., USA) with the peak output of 260–270 kW. The peak E field in the waveguide (WR90, 22.86×10.16 mm) reached 1.57 MV/m. CW radiation was produced into the same waveguide by means of an HP 8690A sweep oscillator and Hughes 1277H amplifier.

Both transmitters were tuned to 9.3 GHz using an HP 8566B spectrum analyzer. Incident and reflected powers in the waveguide were measured via directional couplers by an HP 438A power meter with HP 8481A power sensors. The reflection in the waveguide was under 3%; the average transmitted power, i.e., the incident power minus reflected, for EHPP and CW was set equal at about 1.25 W. EHPP shape was monitored via an HP 432 detector on a TEK 2430A digital oscilloscope. The pulses were nearly rectangular, their width was set at 0.5 μs, and the repetition rate was 10 Hz.

Comparison of the frequency spectra of the CW and EHPP emissions revealed a number of additional harmonics in the EHPP signal. Apparently, these were introduced by the rise and fall of pulses. The additional harmonics were concentrated within the 9.2–9.4 GHz range and were 15–45 dB weaker than the main peak at the carrier frequency (9.3 GHz). The presence of the additional harmonics had no detectable impact on SAR or temperature distribution in exposed samples.

The exposure chamber (Fig. 1) had two compartments, one for exposed sample and one for parallel control. The waveguide terminated via a sapphire matching plate into the exposure compartment. The compartments had a common water jacket and were stabilized at 25°C by flow from a circulating bath. This only set the base level temperature, but did not and was not intended to compensate for microwave heating in the exposed compartment.

Local temperatures in the gel were measured by a Reflex fiber optic thermometer (Nortech Fibronic, Canada). The thermometer was equipped with a PMDE probe, which was the smallest commercially available artifact-free temperature sensor (0.5-mm height, 0.55-mm diameter). A micromanipulator with

0.1 mm resolution was used to position and move the probe within the microwave-exposed gel.

As expected, heating of gel samples during irradiation was highly nonuniform (Fig. 2). Steady temperature conditions were reached after about 20 min of exposure. Local heating was determined in a complex way by the microwave absorption (i.e., local SAR) and by conductive heat flows to and from other locations. Higher temperatures were reached on the axis of the cuvette, where SAR was higher and heat dissipation was poorer than in the corners. The highest SAR was reached at the gel surface adjacent to the matching plate; however, since the plate itself was an efficient heat sink, the highest temperature (40.9°C) was measured 1.5 mm deeper into the gel. At distances over 5–6 mm from the plate, local SAR decreased to such an extent that microwave absorption could not account for any considerable heating; nonetheless, the temperature increased markedly due to heat conduction.

Most important EHPP and CW exposures produced identical temperature distributions, so their thermal effects on the cell growth at the same locations within the gel should have been indentical as well. Therefore, a difference in EHPP and CW effects, if observed, will be an indication of some specific (nonthermal) biological effect.

Local SAR values were measured directly using a microthermocouple technique [Pakhomov et al., 2000a,b]. The measurements were additionally confirmed by calculation using an analytical solution for a waveguide filled with a lossy medium [Chou and Guy, 1978] and by a numerical simulation using an XFDTD software (REMCOM Corporation, USA, version 4.04). Although both these theoretical methods assumed somewhat simplified spatial geometry, they produced SAR values within less than 3 dB from the microthermocouple measurements.

Measured distribution of local SAR values along the axis of the cuvette (K vector), as well as in E and H vector directions, is shown in Figure 3. CW and EHPP exposures produced the same local SAR values, which decreased exponentially with increasing the distance from the matching plate (Fig. 3A). Field intensity distribution in a plane perpendicular to the propagation vector was bell-shaped, with SAR dropping about twofold at 5 mm from the axis (Fig. 3B).

For a uniform lossy medium, SAR decrease along the propagation vector is strictly exponential, and knowing SAR for any two locations is sufficient to plot the entire curve. Therefore, a best fit exponential curve through microthermocouple measurements (Fig. 3A) could be reliably extrapolated to locations where SAR was too small for instrumental measurements (Fig. 3C, dashed line).

However, the irradiation produced a significant temperature gradient (Fig. 2), so the medium during actual exposure experiments could not be regarded uniform. The dependence of the linear loss coefficient on the temperature, as well as the dependence of the temperature on the distance were used to adjust the exponential line to a "corrected SAR" curve (Fig. 3C, solid line).

This curve gradually gets steeper as the medium gets cooler and microwave absorption per unit of distance increases. Within the studied ranged of 24 mm from the matching plate, SAR changed by more than six orders of magnitude. For the employed transmitted powers of 1.25 W (average) and 250 kW (peak), the studied SAR ranges were from 3.2 kW/kg to 0.6 mW/kg (average) and from 650 MW/kg and 130 W/kg (peak).

Obviously, when such a wide range of SAR values is "covered" by 12 specimens, i.e., by 12 slices of the gel, there is an appreciable SAR and temperature gradient within each slice. Consequently, yeast cells at different locations within one slice could be exposed at SAR levels differing up to sixfold. In what follows, we will use the local SAR and temperature values for the geometrical center of each gel slice.

RESULTS

Measurements in the culture growth controls established that the growth was exponential during the first 6 h at all studied temperatures (Fig. 4). A longer incubation, e.g., for one or two extra hours, could initiate fermentation with production of gas bubbles into the medium, and therefore had to be avoided. The growth rate was maximum at about 35°C and decreased at both higher and lower temperatures. Hence, in case of a merely thermal effect in the main series of experiments, one could anticipate the maximum cell density at the distance of about 6 mm above the matching plate, where the temperature during the exposure was 35°C.

Indeed, the highest cell density in the exposed samples was typically achieved in the fourth slice, the center of which was at 7 mm from the irradiator (Fig. 5). Cell density in the slices fell sharply toward the irradiator and more gradually away from it, just as expected from the temperature distribution curve. The data for the parallel control slices showed only minor variability, reflecting the degree of imprecision of slicing, dilution, and OD measurement.

The fact that the cell growth rate in the exposed gel was predominantly, if not exclusively, determined by the temperature is supported by the possibility of using OD measurements as a thermometer. An

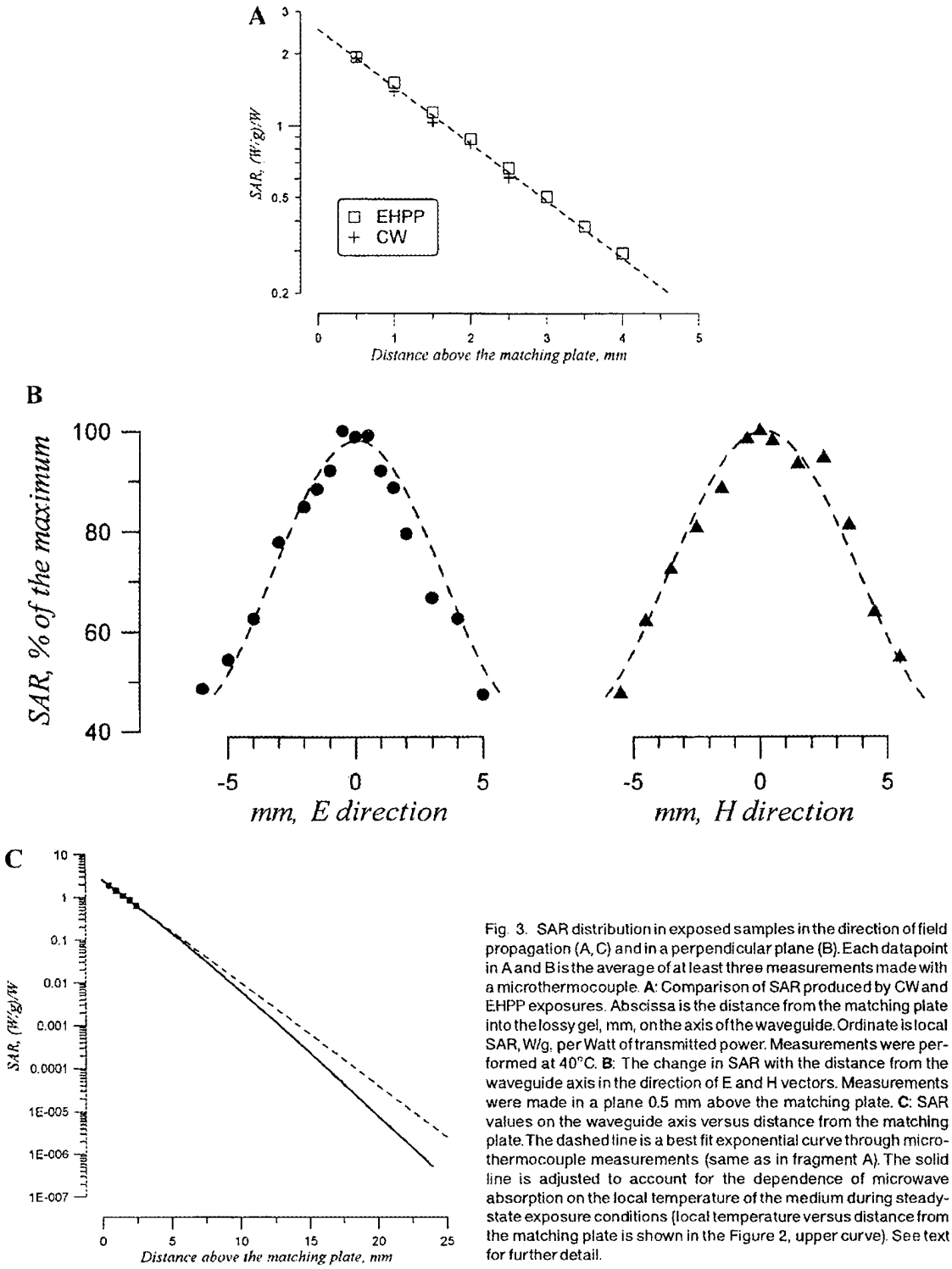


Fig. 3. SAR distribution in exposed samples in the direction of field propagation (A, C) and in a perpendicular plane (B). Each datapoint in A and B is the average of at least three measurements made with a microthermocouple. **A**: Comparison of SAR produced by CW and EHPP exposures. Abscissa is the distance from the matching plate into the lossy gel, mm, on the axis of the waveguide. Ordinate is local SAR, W/g, per Watt of transmitted power. Measurements were performed at 40°C. **B**: The change in SAR with the distance from the waveguide axis in the direction of E and H vectors. Measurements were made in a plane 0.5 mm above the matching plate. **C**: SAR values on the waveguide axis versus distance from the matching plate. The dashed line is a best fit exponential curve through microthermocouple measurements (same as in fragment A). The solid line is adjusted to account for the dependence of microwave absorption on the local temperature of the medium during steady-state exposure conditions (local temperature versus distance from the matching plate is shown in the Figure 2, upper curve). See text for further detail.

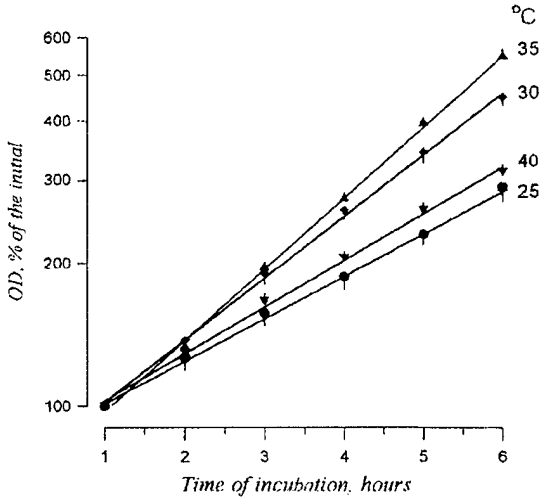


Fig. 4. Yeast culture growth within gelled nutrient medium at different temperatures. Cell density is measured by nephelometry; the value at 1 h of incubation is taken as 100%. Each data point is a mean ± SE from nine independent experiments.

example of a reverse calculation of local temperature from the OD data is illustrated in Figure 5 by dashed lines. To find a temperature for an arbitrary location in the exposed gel (in this case, 14 mm), we draw a vertical line from the abscissa, until it hits the OD graph. From that point, the line is continued horizontally, until it hits the OD graph for temperature controls. From there, the line goes downwards to read the temperature at this location (29.5°C). This reading matches well the actual temperature measured at this spot with the fiber optic probe (29.1°C, Fig. 2).

This method works well for locations in gel father than 6–10 mm from the plate, but becomes increasingly inaccurate for closer locations. This obviously results from a greater difference in temperatures within the slice, which is maximal in the first slice and then gradually smoothes down, see Figure 2, making the temperature in the slice center a less reliable indicator of the average cell growth rate. Besides, there is a possibility of a specific effect of microwaves, which is superimposed on the thermal effect.

To identify possible specific effects, we compared the average OD data for slices from CW and EHPP exposed gels (Fig. 6). The average OD of the parallel control slices was used as a reference level (100%) for each experiment. Obviously, the temperature had major effect on the cell density in all cases, but the data might be indicative of a specific effect as well. While EHPP and CW exposures produced exactly the same heating patterns, their biological effects were somewhat different in the first three slices. For example, the OD in the first slice (the highest SAR) was $110.2 \pm 3.3\%$ after EHPP irradiation, but $96.1 \pm 7.6\%$ after CW (mean ± SE, $n = 8$). While

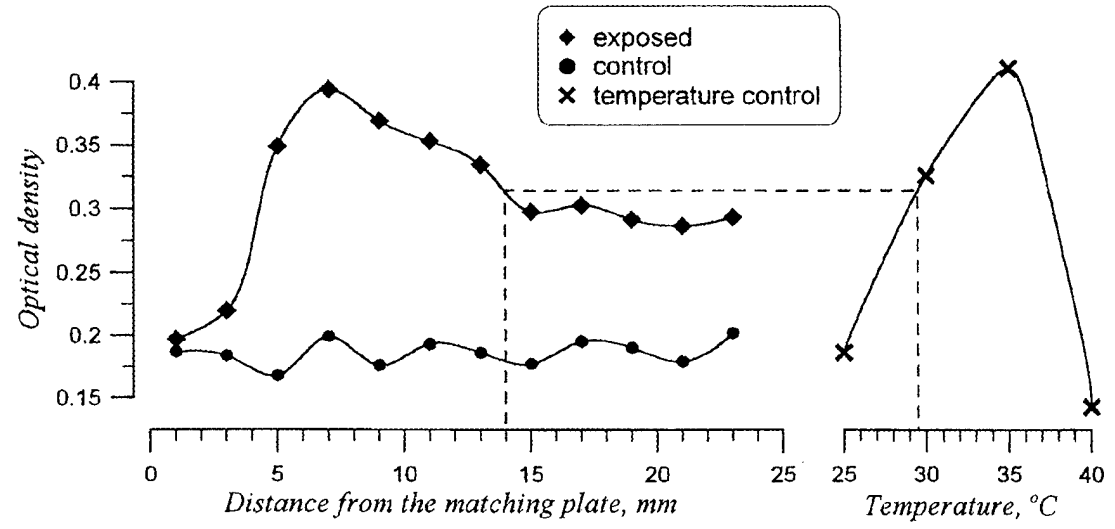


Fig. 5. Effect of microwave irradiation and temperature on the cell density (sample data from a selected experiment with CW irradiation). Left graphs, the OD of slices from exposed (above) and parallel control (below) gels as a function of the distance from the irradiator. Right, the OD attained by "temperature controls" as a function of the incubation temperature (except for the 25°C datapoint, which is a mean of the parallel control measurements). Dashed line illustrates calculation of the local temperature from the OD achieved after microwave exposure. See text for more explanation.

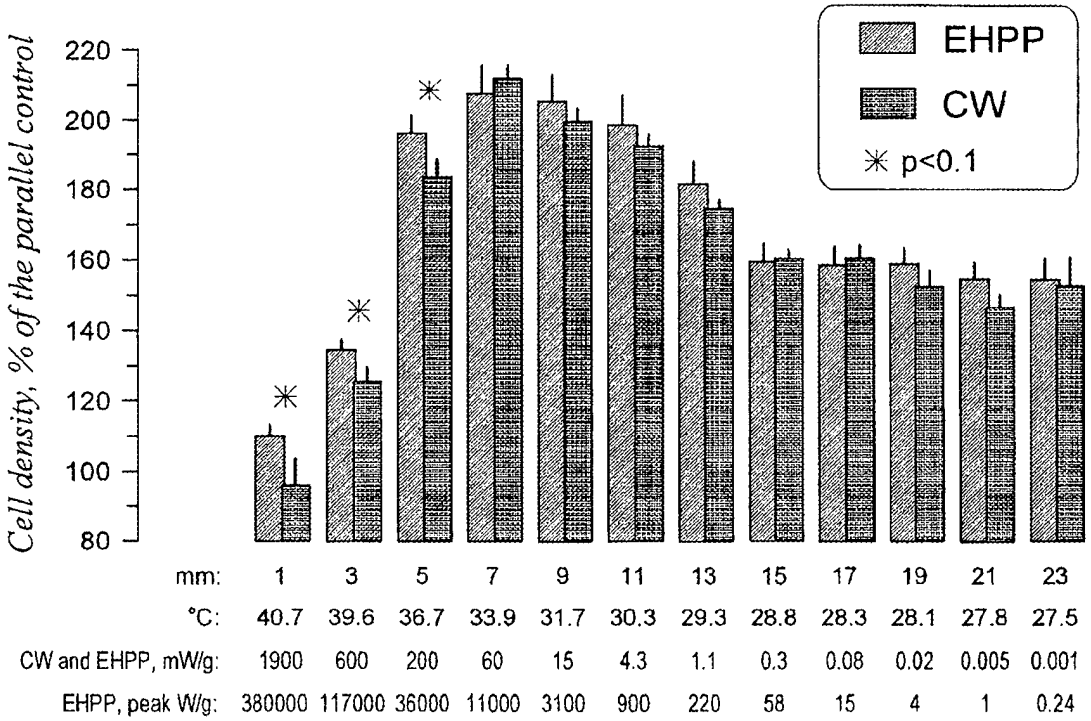


Fig. 6. Comparison of the effects of a CW and EHPP exposures on the cell density. Each bar is a mean ± SE for eight independent experiments. Shown under the bars are the distance from the irradiator to the center of the slice (mm), temperature (°C), time average SAR (mW/g), and peak SAR (EHPP, W/g) in the center of each slice. See text for more detail.

formally this difference was not statistically significant ($P < 0.1$, Student's paired t-test), the following facts should have also been taken into consideration: (1) in the other nine pairs of slices the difference did not reach $P < 0.1$ level, (2) the slices with the alleged specific effect were all situated together, i.e., not dispersed among others, and were exposed at the highest peak and average SAR, and (3) there were no statistically significant differences between the parallel controls to CW and to EHPP exposures, nor were there any between the respective "temperature controls" (results not shown). The importance of these circumstances is difficult to estimate by a statistical test; however, taken together, they indicate an appreciable possibility of EHPP-specific effect on cell growth, with a threshold at peak SAR of 20–30 MW/kg. This possibility has to be tested in forthcoming studies.

DISCUSSION

Regardless of the observed trend, the formal conclusion of this study is that EHPP irradiation of yeast cells for 6 h at peak SAR up to as high as 650 MW/kg (local maximum at the exposed gel surface) did not produce specific bioeffects, as compared to a CW exposure at the same average SAR. Perhaps this conclusion is not final and may be "adjusted" in future by using more sophisticated and accurate techniques (just like any other conclusion of any other research). Nonetheless, an important implication of this study is that the specific EHPP effect on the cell growth is minuscule, even if it proves real. The maximum cell density change due to the suspected specific effect, as seen in the first slice, is only 16% after a 6-h exposure; the same change may be caused by just a 1°C decrease of the incubation temperature, e.g., from 37 to 36°C.

The peak SAR, peak E-field in the incident wave, and the exposure duration in this study exceeded by far the respective values found in various safety standards [SanPin 2.2.4/2.1.8.055-96, 1996; ICNIRP Guidelines, 1998; IEEE Std C95. 1, 1999], and our present findings do not support the existing restrictions. Of course, one still cannot exclude the possibility of hazardous EHPP-specific bioeffects via mechanisms that are not

involved in cell division and were not explored in the present work; this warrants the necessity for more research into EHPP bioeffects using various biological criteria and endpoints.

The proposed new approach of using gel-suspended cell cultures to analyze how microwave bioeffects depend on SAR proved to be convenient and highly efficient. The main deficiency of the technique noted so far was averaging of the data for all cells within each slice, despite the fact that these cells might be exposed at quite different temperatures and SAR. This puts a limit on the accuracy of the method and its ability to resolve possible "power windows". At a first glance, the accuracy could be improved by cutting thinner gel slices, as well as by using cells from only the center of each slice and discarding the rest of it. In reality, however, the quantity of cells in some slices at the end of the experiment, e.g., in parallel control slices, was only marginally adequate for nephelometry. Further reduction in the slice size would have reduced the number of cells per slice, thus increasing the error of OD measurements and rendering them unreliable.

Instead, our preferred approach would be to try various histochemical staining assays that are used to quantify cell growth rate, metabolism, etc., in order to select assays that can work for gel-embedded cells. In-gel cell staining will make it possible to avoid cutting numerous slices and measuring their OD. Instead, it will be sufficient to prepare a single slice through the central line of the gel, which will contain areas exposed at all tested SAR, from maximum to minimum. After staining, this slice can be scanned into a computer, and its OD within a narrow stripe along the central line, i.e., along the SAR gradient, can be quantified by image analysis software. The cell populations included in the analysis will be much more uniform, and the spatial resolution to separate the areas exposed at different SAR will improve to 0.2–0.5 mm. The increased accuracy of measurements and the possibility of probing various cell functions by different histochemical assays make this approach quite promising for dose-effect analyses, as well as for searches for possible "power windows".

ACKNOWLEDGMENTS

The authors are thankful to Dr. S. Avery for the yeast strain and to Dr. O. Pakhomova for valuable consultations during this project. The views expressed are those of the authors and should not be construed as reflecting the official policy or position of the Department of the Army, Department of the Air Force, or the United States government.

REFERENCES

Adey WR. 1988. Biological effects of radio frequency electromagnetic radiation. In: Lin JC, editor. Interaction of Electromagnetic Waves With Biological Systems. New York: Plenum Press. pp 1–33.

Anderstam B, Hamnerius Y, Hussain S, Ehrenberg L. 1983. Studies of possible genetic effects in bacteria of high-frequency electromagnetic-fields. Hereditas 98:11–32.

Belyaev IY, Shcheglov VS, Alipov YD, Polunin VA. 1996. Resonance effect of millimeter waves in the power range from 10^{-19} to 3×10^{-3} W/cm^{2}on *Escherichia coli* cells at different concentrations. Bioelectromagnetics 17:312–321.

Blackman CF, Benane SG, Elder JA, House DE, Lampe JA, Faulk JM. 1980. Induction of calciumion efflux from brain tissue by radiofrequency radiation: effect of sample number and modulation frequency on the power density window. Bioelectromagnetics 1:35–43.

Blackwell RP, Saunders RD. 1986. The effects of low-level radiofrequency and microwave radiation on brain tissue and animal behavior. Int J Radiat Biol 50:761–787.

Bush LG, Hill DW, Riazi A, Stensaas LJ, Partlow LM, Gandhi OP. 1981. Effects of millimeter-wave radiation on monolayer cell cultures. III. A search for frequency-specific athermal biological effects on protein synthesis. Bioelectromagnetics 2(2):151–159.

Chou CK, Guy AW. 1978. Effects of electromagnetic fields on isolated nerve and muscle preparations. IEEE Transact Microwave Theory Techniq MTT 26:141–147.

Chou CK, Guy AW, Galambos R. 1982. Auditory perception of radio-frequency electromagnetic fields. J Acoust Soc Am 71(6):1321–1334.

Dutta SK, Gosh B, Blackman CF. 1989. Radiofrequency radiation-induced calcium ion efflux enhancement from human and other neuroblastoma cells in culture. Bioelectromagnetics 10:197–202.

Dutta SK, Das K, Ghosh B, Blackman CF. 1992. Dose dependence of acetylcholinesterase activity in neuroblastoma cells exposed to modulated radio-frequency electromagnetic radiation. Bioelectromagnetics 13:317–322.

Gapeev AB, Chemeris NK, Fesenko EE, Khramov RN. 1994. Resonance effects of a low-intensity modulated EHF field. Alteration of the locomotor activity of the protozoa *Paramecium caudatum*. Biofizika 39:74–82.

Gos P, Eicher B, Kohli J, Heyer W-D. 1997. Extremely high frequency electromagnetic fields at low power density do not affect the division of exponential phase *Saccharomyces cerevisiae* cells. Bioelectromagnetics 18:142–155.

Grundler W, Kaiser F. 1992. Experimental evidence for coherent excitations correlated with growth. Nanobiology 1:163–176.

Guy AW, Chou CK, Lin JC. 1975. Microwave-induced acoustic effects in mammalian auditory systems and physical materials. Ann NY Acad Sci 247:194–218.

ICNIRP Guidelines. 1998. Guidelines for limiting exposure to time-varying electric, magnetic, and electromagnetic fields up to 300 GHz. Health Phys 74:494–522.

IEEE Std C95.1, 1999. IEEE Standard For Safety Levels With Respect to Human Exposure to Radio Frequency Electromagnetic Fields, 3 kHz To 300 GHz. 1999 edition. New York: Inst. of Electrical and Electronics Engineers, Inc. 73 p.

Kataev AA, Alexandrov AA, Tikhonova LL, Berestovsky GN. 1993. Frequency-dependent effects of the electromagnetic

millimeter waves on the ion currents in the cell membrane of Nitellopsis: nonthermal action. Biofizika 38:446–462.

Lin JC. 1978. Microwave Auditory Effects And Applications. Springfield, Illinois: Charles C. Thomas. 227 p.

Lin JC. 1989. Pulsed radiofrequency field effects in biological systems. In: Lin JC, editor. Electromagnetic Interaction with Biological Systems. New York: Plenum Press. pp 165–177.

Liu LM, Garber F, Cleary SF. 1982. Investigation of the effects of continuous-wave, pulse- and amplitude-modulated microwaves on single excitable cells of Chara corallina. Bioelectromagnetics 3:203–212.

Lukianova SN. 1999. Reaction of the central nervous system to low-level and short-term microwave irradiation. In: Repacholi MH, Rubtsov NB, Muc AM, editors. Electromagnetic Fields: Biological Effects and Hygienic Standardization. Geneva, Switzerlland: World Health Organization. pp 381–387.

Pakhomov AG, Murphy MR. 2000. A comprehensive review of the research on biological effects of pulsed radiofrequency radiation in Russia and the former Soviet Union. In: Lin JC, editor. Advances in Electromagnetic Fields in Living Systems. V. 3. New York: Kluwer Academic/Plenum Publishers. pp 265–290.

Pakhomov AG, Dubovick BV, Kolupayev VE, Pronkevich AN. 1992. Absence of nonthermal microwave effects on the function of giant nerve fibers. J. Bioelectricity 10:185–203.

Pakhomov AG, Dubovick BV, Degtyariov IG, Pronkevich AN. 1995. Microwave influence on the isolated heart function: I. effect of modulation. Bioelectromagnetics 16(4):241–249.

Pakhomov AG, Mathur SP, Akyel Y, Kiel JL, Murphy MR. 2000a. High-resolution microwave dosimetry in lossy media. In: Klauenberg BJ, Miklavcic D, editors. Radio Frequency Radiation Dosimetry. Netherlands: Kluwer: Academic Publishers. pp 187–197.

Pakhomov AG, Mathur SP, Doyle J, Stuck BE, Kiel JL, Murphy MR. 2000b. Comparative effects of extremely high power microwave pulses and a brief CW irradiation on pacemaker function in isolated frog heart slices. Bioelectromagnetics 21:245–254.

Postow E, Swicord ML. 1986. Modulated fields and "window" effects. In: Polk C, Postow E, editors. Handbook of Biological Effects of Electromagnetic Fields. Boca Raton, FL: CRC Press, Inc. pp 425–460.

SanPin 2.2.4/2.1.8.055-96. 1996. Sanitary Rules and Norms Radiofrequency electromagnetic radiations (2.2.4. Physical factors of industrial surroundings. 2.1.8. Physical factors of the environment). Goskomsanepidanadzor of Russia, 28 p.

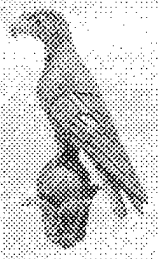
Schwartz JL, House DE, Mealing GAR. 1990. Exposure of frog hearts to CW or amplitude-modulated VHF fields: selective efflux of calcium ions at 16 Hz. Bioelectromagnetics 11:349–358.

Semin IuA, Shvartsburg LK, Dubovik BV. 1995a. Changes in the secondary structure of DNA under the influence of an external low-intensity electromagnetic field. Radiats Biol Radioecol 35:36–41.

Semin YuA, Shwarzburg LK, Dubovick BV. 1995b. Electromagnetic field interaction with DNA in solution. Boston, MA: 17th Annual Meeting of the Bioelectromagnetics Society, June 1995. 196 p.

BIOLOGICAL EFFECTS of EMFs

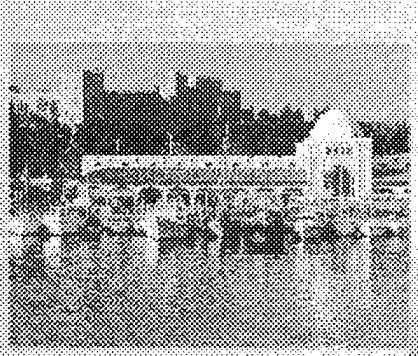
2nd INTERNATIONAL WORKSHOP



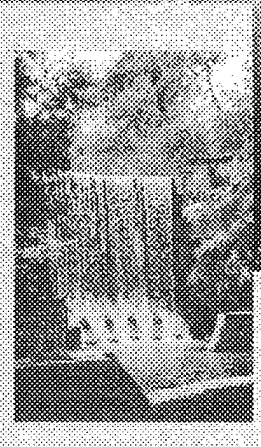
Electronics - Telecom &
Applications Laboratory
Physics Department
University of Ioannina

Institute of Informatics &
Telecommunications
N.C.S.R. "Demokritos"

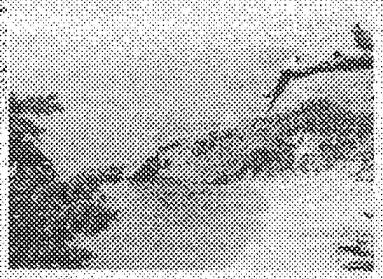
Proceedings











Volume I

Rhodes, Greece, 7 -11 October, 2002

HIGH POWER MICROWAVES AND CA^{2+} CHANNELS

PATCH-CLAMP ANALYSIS OF THE EFFECT OF HIGH-PEAK POWER AND CW MICROWAVES ON CALCIUM CHANNELS

A. PAKHOMOV[1,2], X. DU[1], J. DOYLE[1],
J. ASHMORE[1], and M.R. MURPHY[2]

[1]McKesson BioServices Corporation, US Army Medical Research Detachment
[2]Directed Energy Bioeffects Division, Human Effectiveness Directorate,
Air Force Research Laboratory
Brooks Air Force Base, San Antonio, Texas, 78235-5324, USA.
E-mail: andrei.pakhomov@brooks.af.mil

Abstract

Calcium channel currents in cultured rat pituitary tumor cells (GH_3) were recorded using a whole-cell patch clamp technique at 5- to 45-min intervals after a 10-min microwave exposure. Peak transmembrane current as carried by Ba^{2+} (10 mM) was measured during 200-ms steps from holding potential (-80 mV or -40 mV) to different test potentials (from –70 to +70 mV, with 10 mV increments). All irradiations were performed at 10.6 GHz and 3.8 W/g, either continuous-wave (CW) or pulsed (0.25-μs pulses at 16 Hz repetition rate; 0.5-μs pulses at 8 Hz; and 2-μs pulses at 2 Hz). Incident E-field during microwave pulses was 1.57 MV/m, producing peak absorption rate as high as 960 kW/g. Temperature rise during the exposure was the same for all regimens, about 0.8 °C. The data were collected from over 180 individual cells, comprising 10 groups in 3 independent series of experiments. Analysis of current-voltage curves established that microwaves, even at extremely high peak power, produced no detectable effect on calcium channel function.

Introduction

This paper continues the series of our studies into bioeffects of extremely-high power microwave pulses (EHPP). The first studies (1, 2) attempted to reveal EHPP-specific effects in isolated, spontaneously beating frog heart slices. The slices were exposed to brief EHPP trains (4-ms to 10-sec long, 9.2 or 9.5 GHz, 1-μs pulse width, 10- to 100-Hz repetition rate, 250 to 350 kW/g peak and 3 to 30 W/g time-average SAR). These exposures immediately shortened the inter-beat interval, and the magnitude of changes was proportional to the total absorbed energy and to the temperature rise. When an EHPP exposure produced the same temperature change as a CW irradiation, their bioeffects were also the same. These effects were consistent with the thermal paradigm and provided no indication of other interaction mechanisms.

Another study (3) explored EHPP effects on the growth rate of yeasts. Use of a gel-suspended cell culture technique greatly facilitated data analysis for a wide range of SAR and peak SAR levels (from 0.6 μW/g to 3.2 W/g, and from 1.2 W/g to 650 kW/g, respectively). The carrier frequency was 9.3 GHz, and EHPP pulse width and repetition rate were 0.5 μs and 10 Hz, EHPP and CW exposures created complex but identical temperature profiles in exposed gels. The local cell density in gels after exposure closely followed the local temperature, but the data for EHPP and CW exposures showed no statistically significant difference. Hence, the data suggested solely thermal effect of EHPP within the entire studied range of peak and time-average SAR levels.

Further EHPP studies employed isolated rat hippocampal slices to model characteristic functions of a neural circuitry (4-7). The endpoints studied under a variety of EHPP and CW exposure regimens were the synaptic transmission from Schaffer collateral fibers to CA1 area neurons and excitability of these neurons (as judged from the induction of excitatory postsynaptic potentials, EPSP, and population spikes, PS), as well as synaptic plasticity phenomena (paired-pulse facilitation and long-term potentiation, LTP). Tested carrier frequencies were 9.3 and 9.6 GHz; the pulse width ranged from 0.5 to 2 μs at pulse repetition rates from less than 1 Hz to 100-200 Hz. The peak SAR reached up to 780 kW/g. Depending on the task of a particular experiment, the exposure duration was from 0.5 sec to 30 min, and the time-average microwave heating varied from negligible to 20-25 °C (over the base temperature of 34 °C). To explore EHPP effect on LTP, the LTP

condition was induced by a brief tetanus of the Schaffer collateral. In different sets of experiments, this tetanization was performed before, during, or after irradiation. Overall, the data collected in more than 300 individual brain slices revealed no sign of microwave-specific bioeffects. CW and EHPP exposures produced either no effect (when microwave heating was negligible), or produced the same effect (when CW and EHPP caused the same heating). In the latter situation, the effect was transient, proportional to the temperature rise, and similar to the effect of ordinary (non-microwave) heating.

These negative results were contradictory to alleged findings of EHPP-specific bioeffects on alga growth rate and oxygen evolution (8); on tumor cells survival in culture and tumor growth in animals (9,10); on the growth rate of a Fusarium fungus and on ontogenesis and developmental aberrations in Drosophila flies (11). However, these "positive-effect" studies could have suffered various flaws, both in biological experiment protocols and dosimetry (12). In the present study, we attempted to reveal possible EHPP-specific bioeffects on the function of Ca^{2+} channels of the cell membrane. The peak SAR level tested in this work was 960 kW/g, higher than in our previous studies and higher than ever reported by other authors.

Methods

Cell culture

GH_3 cells, derived from a rat pituitary tumor, were purchased from American Type Culture Collection (ATCC). Cells were cultured in 60-mm polystyrene culture dishes at 37°C in a 5% CO_2 environment. The culture medium was Kaighn's modification of Ham's F12 medium (F12K) with 2 mM L-glutamine, modified by ATCC to contain 1.5 g/l sodium bicarbonate and supplemented with 15% horse serum and 2.5% fetal bovine serum. Cells were plated on 10-mm glass cover slips and used for experiments after growing for 3-5 days.

Solutions

To perform an experiment, a cover slip with cells was transferred from the growth medium into the exposure cell and submerged into a potassium-containing solution of the following composition (mM): 144 NaCl, 5.4 KCl, 10 Hepes-NaOH (PH 7.4), 1.8 $CaCl_2$, 1 $MgCl_2$, and 5.5 Glucose. In approximately 16 min (comprised of 5 min before, 10 min during, and 1 min after the exposure), the cover slip was transferred into a patch-clamp recording chamber. The solutions for patch-clamp recording were formulated to measure current via voltage-gated Ca^{2+} channels using Ba^{2+} ions as a charge carrier. The bath solution contained (mM): 120 NaCl, 10 CsCl, 10 $BaCl_2$, 2 $MgCl_2$, 10 tetraethyl-ammonium (TEA), 10 *N*-2-hydroxyethylpiperazine-*N'*-2-ethanesulfonic acid (HEPES), 5.5 glucose and 500 nM of tetrodotoxin (TTX). The pipette solution consisted of (mM): 120 CsCl, 1.5 $MgCl_2$, 20 TEA, 5 Mg-ATP, 5 EGTA, and 10 HEPES. The pH of both solutions was adjusted to 7.2 with CsOH. In the patch clamp recording condition, potassium channels were blocked with extracellular TEA and intracellular TEA and Cs^+, and sodium channels were blocked with extracellular TTX.

Whole-cell patch clamp

Patch pipettes were pulled from 1.2-mm o.d., 0.6-mm i.d. borosilicate glass (Sutter Instruments, USA) and lightly firepolished. Initial electrode resistance ranged from 3 to 6 MOhm when filled with the pipette solution. Whole cell currents were recorded with a PC-505B patch clamp amplifier (Warner Instrument, Hamden, CT, USA) with a low-pass filter set at 10 kHz. Voltage protocols were generated with pCLAMP software (version 8.1, Axon Instruments, CA) running on a Pentium II computer. Membrane current signal was digitized at 10 kHz by a Digidata 1322A analog-to-digital converter (Axon Instruments) and processed by the pCLAMP software.

Under slight positive pressure, the electrode tip was lowered to the cover slip shortly after the slip had been transferred from exposure to the patch clamp recording chamber. A cell to be patched was selected within a 1-1.5 mm radius from the center of the slip. Once the electrode touched the cell, a small negative pressure was applied to form a seal of at least 1 GOhm. After seal formation, the membrane within the pipette was ruptured by applying additional negative pressure. Series resistance (generally 7-15 MOhm after breaking the cell membrane) was monitored over the course of the experiment and cells were rejected if large increases were detected. All recordings were performed at the room temperature of 23-24 °C.

Membrane currents were recorded in about 2 min after the whole cell configuration had been established. The membrane was clamped to a holding potential of –80 mV, and inward Ba^{2+} current was assessed by application of a series of 200-ms test pulses, with 10-mV increments, from the holding potential to

+ 70 mV. The peak values of this current, as measured in about 5 ms after the onset of each test pulse, were used to plot current-voltage curves for the whole cell current, which, in GH_3 cells, is comprised of the currents through low-threshold (T-type) and high-threshold (L-type) calcium channels (13). Current through the high-threshold channels was isolated by raising the holding potential to –40 mV and repeating the step voltage protocol. Then, the current through the low-threshold channels could be identified, too, by subtracting the high-threshold current from the total current at each testing potentials. However, the total current was a sufficiently good index to identify the presence or absence of exposure effect, so a separate analysis for low- and high-threshold channels was in most cases redundant.

Patch-clamp measurements were performed at different time intervals after the exposure, from 5 to 45 min (see Table 1). To minimize the run-down effect, a separate cell was patched for each timepoint. The cells had different size and, obviously, larger currents were measured in larger cells which had more membrane surface. The variability in the cell size was accounted for in a standard manner, by normalizing the transmembrane current to the cell capacitance (the capacitance is proportional to the cell membrane surface). Thus, the current values were expressed in pA/pF and averaged for similarly exposed cells for each timepoint after the exposure. Differences between the groups were then assessed by a two-sided Student's t-test.

The junction potential between the pipette and bath solution, as calculated using Clampex 8.1 software (Axon Instruments, CA), was about –6 mV. Results shown in this paper were not corrected for the junction potential.

Table 1. Exposure regimens and timepoints tested in three sequential series of experiments.

time post exposure	Series 1	Series 2	Series 3
5 min	sham 0.5 µs / 8 Hz 2.0 µs / 2 Hz CW		
15 min	sham 0.5 µs / 8 Hz 2.0 µs / 2 Hz CW		
25 min	sham 0.5 µs / 8 Hz 2.0 µs / 2 Hz CW	sham 0.5 µs / 8 Hz	sham 0.5 µs / 8 Hz 0.25 µs / 16 Hz
35 min		sham 0.5 µs / 8 Hz	
45 min		sham 0.5 µs / 8 Hz	

SHAM:
10 min

EHPP:
10.6 GHz
10 min
3.8 W/g
+ 0.8 °C
960 kW/g

CW:
10.6 GHz
10 min
3.8 W/g
+ 0.8 °C

Exposure Setup

The exposure chamber design was essentially the same as described before (4-7). The chamber was mounted atop a vertical waveguide section, which was sealed with a sapphire matching plate flush with the waveguide flange. Additional layer of glass (0.08-mm thick) was glued over the entire flange and the matching plate. This glass served as a bottom of the exposure chamber and protected the waveguide from solution in the chamber. Thin glass layer had no measurable impact on the matching plate performance.

The cover slip with cells was placed directly on the bottom of the exposure chamber, cells facing up. Small barriers were glued to the glass bottom in such a way that to center the cover slip over the waveguide axis, where the field intensity was maximum. The chamber was filled with the potassium-containing solution to the depth of about 20 mm. This solution was kept at 37 °C and circulated at about 10 ml/min, to reduce microwave heating of cell samples and improve heating uniformity.

EHPP were generated by a model 337X magnetron transmitter (Applied Systems Engineering, Inc.) with the peak output of up to 260 kW. The peak E-field in the waveguide (WR90, 22.86 x 10.16 mm) reached 1.57 MV/m. CW radiation was produced into the same waveguide by means of an HP 8690A sweep oscillator and Hughes 8020H amplifier. Both the transmitters were tuned to 9.6 GHz using an HP 8566B spectrum

analyzer. Incident and reflected powers in the waveguide were measured via directional couplers by an HP 438A power meter with HP 8481A power sensors. Reflection from the exposure chamber into the waveguide was less than 3%. EHPP shape was nearly rectangular, as monitored via an HP 432 detector on a TEK 2430A digital oscilloscope.

For a sham exposure, all procedures were the same, but microwaves were re-directed from the exposure chamber to a matching load in a different leg of the waveguide. Different regimens of EHPP and CW exposure, as defined in Table 1, and sham exposures were alternated in random manner. EHPP and CW regimens were designed to produce the same time-average SAR and equal heating of the samples (by about 0.8 °C). A decision on applying a particular exposure regimen was made by rolling a die, after the cover slip with cells had already been positioned in the exposure chamber. The person who performed patch-clamp measurements had no information about the exposure regimen, i.e., these measurements were performed in a "blind" manner.

Dosimetry and Thermometry

A method of high-resolution microwave dosimetry was described in detail and justified in our previous publications (2,14). Local SAR values in the exposure chamber filled with the potassium-containing solution were measured using a microthermocouple driven by a hydraulic micromanipulator (model MX 6500, Siskiyou Design Instruments, USA). Along the axis of the waveguide, SAR fell exponentially with increasing the height above the cover slip with cells (Figure 1, A). These measurements also proved that all local SAR values were identical for EHPP and CW exposures. Because of small size of cells, for dosimetry purposes they were considered as situated at the zero height above the cover slip; however, instrumental SAR measurements could be reliably performed only for the heights of 0.2 mm and more. Therefore, SAR for the position of cells was obtained by extrapolation of the exponential fit curve to zero height, producing a value of 4.25 W/g per 1 W of power transmitted to the exposure chamber. With EHPP peak power output at the employed frequency of 9.6 GHz being 225-230 kW, the peak SAR in exposed cells reached 960 kW/g.

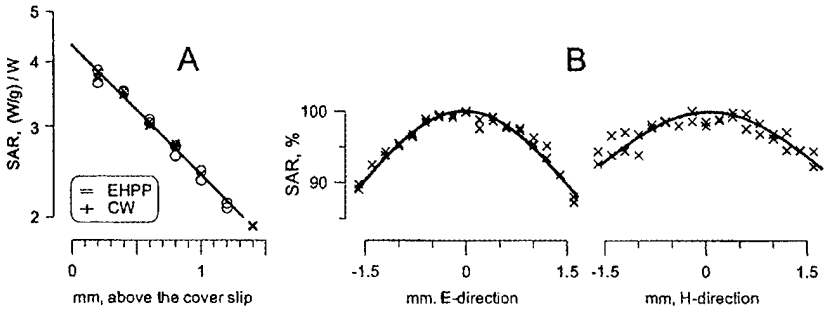


Figure 1. Local SAR distribution in the exposure chamber filled with the potassium-containing solution. **A**, changes in local SAR with the height above the cover slip with attached cells. SAR values are expressed in W/g per 1 W of power transmitted into the waveguide. Exposed cells are considered to be at zero height, where SAR is 4.25 (W/g)/W. Note the sameness of absorption and losses for CW and EHPP emissions. **B**, SAR distribution in the horizontal plane (parallel to the cover slip surface) in the direction of E- and H-vectors. Measurements were performed at 0.2-mm height above the slip. Zero distance is the central axis of the waveguide

SAR distribution in the horizontal plane, parallel to E and H vectors, was measured at 0.2 mm above the cover slip (Figure 1, B). In a center circle with a diameter of 3 mm, SAR varied within just ± 5%, which practically constitutes a uniform exposure.

Temperature during experiments was continually monitored with a Reflex fiber optic thermometer (Nortech Fibronic, Canada). The sensor was placed directly on the cover slip, 3-4 mm away from its center. The temperature increased by about 0.8 °C during CW and EHPP exposures, and stayed unchanged at 37 °C during sham exposures.

HIGH POWER MICROWAVES AND CA^{2+} CHANNELS

Results

Examples of the transmembrane current induced by stepping the membrane potential from -80 mV to test potentials are shown in Figure 2. The inward current reached its maximum at the membrane potential of about –10 mV; further increase of the potential reduced the current, partly because of inactivation of the calcium channels, and partly because of the decreased driving force for Ba^{2+} ions.

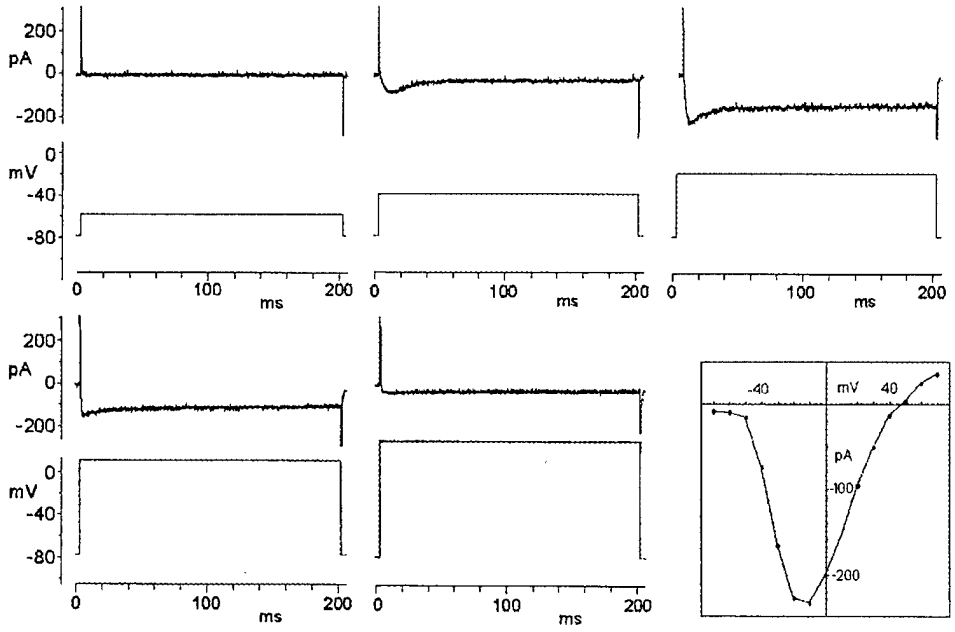


Figure 2. Sample records of the whole cell current (pA) evoked by 200-ms command voltage pulses, stepped from the holding potential (-80 mV) to various test potentials. Current-voltage relationship for peak current amplitudes is shown on the low right panel.

In the first series of experiments, technically satisfactory data with the holding potential of –80 mV were obtained from 106 individual cells. The current-voltage curves for various exposure regimens and timepoints showed no statistically significant difference, with one exception: At 25 min after 0.5-μs, 8-Hz EHPP exposure, the inward current at the membrane potentials of -20, -10, and 0 mV was decreased by 25-30% of the respective sham control values ($p<0.05$, Figure 3). This change could indicate a delayed suppression of calcium channels' function by EHPP exposure, but could also be just a "statistical glitch". To distinguish between one and another, the data had to be replicated in a separate experiment.

This replication was attempted in Series 2 and 3 (see Table 1 for detail). In Series 2, the variety of exposure regimens was reduced to just two (sham exposure and potentially-effective EHPP exposure, i.e., 0.5-μs pulses at 8 Hz). In addition, we included 35- and 45-min timepoints, to test the possibility if the delayed suppression of the calcium channels might become more profound at longer intervals after the exposure. Series 3 was launched after the completion of the Series 2, and included just a single timepoint, 25 min after the exposure. Sham and 0.5 μs/8 Hz EHPP exposures were tested once again, plus we tried an EHPP exposure with still shorter pulses but the same peak and time-average SAR (0.25 μs/16 Hz).

The results of the replication studies are shown in Figures 4 and 5. Satisfactory data were recorded from 53 and 23 individual cells, respectively (7-10 cells per a timepoint for each exposure regimen). The data demonstrated no statistically significant differences, and the alleged effect from the Series 1 could not be confirmed.

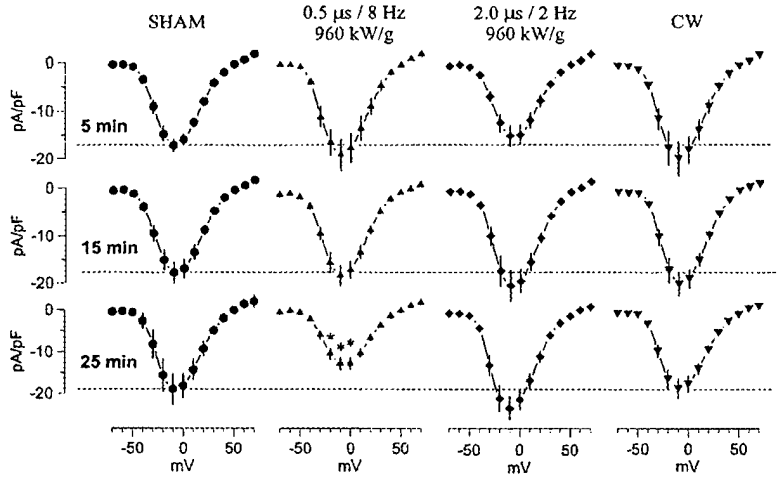


Figure 3. Current-voltage curves for Series 1 experiments. Transmembrane current, normalized to the cell capacitance, is plotted against the membrane potential. The data were collected from sham-exposed samples (column 1), EHPP-exposed samples (columns 2 and 3), and CW-exposed samples (column 4) at 5, 15, and 25 min after the cessation of exposure. Each datapoint is the mean ± s.e., n=6÷12. Dashed im current in the sham-exposed group.

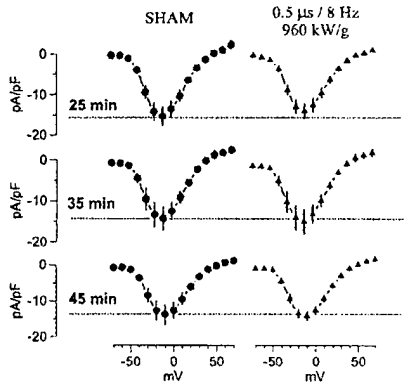


Figure 4. Current-voltage curves for Series 2. Designations are the same as in Figure 2

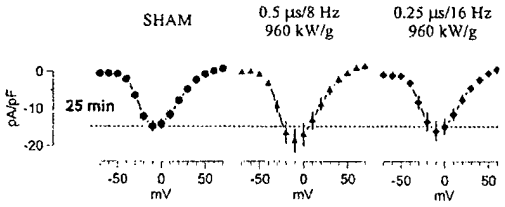


Figure 5. Current-voltage curves for Series 3. Designations are the same as in Figure 2

Since all three series were performed in the same manner, randomized, and double-blind, it was possible to pool together all the data for sham and 0.5 μs/8 Hz EHPP exposures for the 25-min timepoint. Each of the resulting two large groups was further analyzed to separate the high- and low-threshold components of the transmembrane current (Figure 6). These analyses demonstrated the identity of calcium channels' function in both the groups, and confirmed the absence of exposure effect.

Discussion

In experimental studies with electromagnetic fields, observations of a statistically significant difference between exposed and control populations are often interpreted as the effect of exposure. This presumption, however, is not accurate, even for studies punctiliously designed to take care of all potentially biasing factors (i.e., sham-controlled, randomized, blind, etc.). By the nature of statistics, the statistical significance is not equal to the effect but is only a measure of its probability. For example, conventionally used 95% significance level means that there is a 5% chance that the result is not true. Therefore, on average 1 out of 20 comparisons will be a "false positive", i.e., a statistically significant difference will be found when no effect is present. Biological studies often employ far more than 20 comparisons, such as between multiple groups, multiple variables, and multiple timepoints, and relying solely on statistical significance in such studies can be very misleading. In some cases, simple techniques such as a "split halves" test may help to distinguish between false positives and real effects; however, in practice the reproducibility of changes remains the only reliable criterion. In other words, any alleged biological effect must be tested in replication experiments.

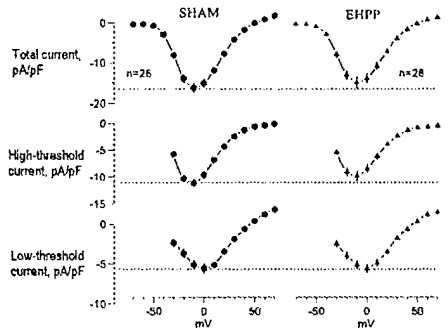


Figure 6. Lack of the effect of 0.5 μs/8 Hz EHPP (10.6 GHz, 3.8 W/g, 960 kW/g peak) on high- and low-threshold calcium channels. Combined data from Series 1, 2, and 3, at 25 min after the exposure; n is the number of cells in each group. See text and Figure 2 for more explanation.

In our study, observation of a statistically in Series 1 necessitated the replication Series 2 and 3. Whereas these replication experiments have not been originally planned, there was no other way to establish if a real effect of exposure was found. Based on the analysis of all three series, we can unambiguously state that CW and EHPP exposures, within the studied range of parameters, had no detectable effect on the function of calcium channels of cell membrane.

This finding is consistent with our prior observations of the lack of specific bioeffects of EHPP in such diverse objects as isolated frog heart (1, 2), yeast cells (3), and isolated rat hippocampus (4-7). The peak SAR reached in this study was the highest (960 kW/g), but obviously still below the threshold for hypothetical EHPP-specific bioeffects. One can speculate that all the tested biological objects just happened to be insensitive to EHPP; however, there is no guidance or indications that some other objects or processes might be more vulnerable. As of the up-to-date knowledge, EHPP appear to be a no more dangerous modality than CW emissions, and the safety standards based on general microwave heating of tissues should be just as applicable to EHPP as to "regular" microwave radiations.

Acknowledgements

The authors are thankful to Dr. V. Moiseenko (LRCC, London, Ontario, Canada) for valuable advice and discussions. The work was supported in part by the U.S. Army Medical Research and Materiel Command and the U.S. Air Force Research Laboratory under U.S. Army contract DAMD17-94-C-4069 awarded to McKesson BioServices Corporation. The views expressed are those of the authors and should not be construed as reflecting the official policy or position of the Department of the Army, Department of the Air Force, or the United States Government.

References

1. Pakhomov A.G., Mathur S.P., Belt M, Murphy M.R. Dose dependencies in bioeffects of extremely high peak power microwave pulses. *In: "Electromagnetic Fields: Biological Effects and Hygienic Standardization" (M.H. Repacholi, N. B. Rubtsova, and A. M. Muc, eds.), Proceedings of the International Meeting (18-22 May 1998, Moscow, Russia), World Health Organization, Geneva, Switzerland, 1999, p. 325-334*

2. Pakhomov A.G., Mathur S.P., Doyle J., Stuck B.E., Kiel J. L., Murphy M.R. Comparative effects of extremely high power microwave pulses and a brief CW irradiation on pacemaker function in isolated frog heart slices. *Bioelectromagnetics, 2000, 21(4), 245-254.*
3. Pakhomov A.G., Gajšek P., Allen L., Stuck B.E., Murphy M.R. Comparison of dose dependences for bioeffects of continuous-wave and high-peak power microwave emissions using gel-suspended cell cultures. *Bioelectromagnetics, 2002, 23(2), 158-167.*
4. Pakhomov A.G., Doyle J., Mathur S.P., and Murphy M.R. Retaining of the long-term potentiation in hippocampal slices after high peak power microwave exposure and heating. *ElectroMed 2001, Second International Symposium on Nonthermal Medical/Biological Treatments Using Electromagnetic Fields and Ionized Gases (20-23 May, 2001, Portsmouth, Virginia). Symposium Record Abstracts, 2001, p. 11-12.*
5. Pakhomov A.G., Doyle J., Mathur S.P., and Murphy M.R. Effects of extremely high power microwave pulses on the population spike and long-term potentiation in rat hippocampal slices. *Abstracts of the 23rd Annual Meeting of the Bioelectromagnetics Society (June 10-14, St. Paul, Minnesota), 2001, 85-86.*
6. Doyle J., Mathur S.P., Murphy M.R., and Pakhomov A.G. Comparative effects of continuous-wave and high peak power microwave emissions on the induction of long-term potentiation. *Abstracts of the 24th Annual Meeting of the Bioelectromagnetics Society (June 23-27, 2002, Quebec, Canada), 2002, p. 228-229.*
7. Pakhomov A.G., Doyle J., Stuck B.E., Murphy M.R. Effects of high-power microwave pulses on synaptic transmission and long-term potentiation in hippocampus. *Bioelectromagnetics, 2002 (in press).*
8. Tambiev, A. Kh., Kirikova, N. N., Lapshin, O. M., Betzkii, O. V., Novskova, T. A., Nechaev, V. M., and Petrov, I. Yu., 1989, The combined effect of exposure to EMF of millimeter and centimeter wavelength ranges on productivity of microalgae. In: *Millimeter Waves in Medicine and Biology*, N. D. Devyatkov, ed., Radioelectronica, Moscow, p. 183-188.
9. Deviatkov, N. D., Betskii, O. V., Kabisov, R. K., Morozova, N. B., Pletnev, S. D., Faikin, V. V., and Chernov, Z. S., 1998, Effect of low-energy pulsed EHF and microwave radiation with nanosecond pulse duration and high peak power on biological structures (malignant neoplasms). Biomedicinskaya Radioelectronica, 1, 56-62.
10. Deviatkov, N. D., Pletnev, S. D., Chernov, Z. S., Faikin, V. V., Bernashevskii, G. A., and Shchitkov, K. G., 1994, Effect of low-energy pulses of EHF and SHF-radiation of nanosecond duration with a high peak intensity on biological structures (malignant neoplasms). Dokladi Akademii Nauk, 336, 6, 826-828.
11. Bolshakov, M. A., Bugaev, S. P., Goncharik, A. O., Gunin, A. V., Evdokimov, E. V., Klimov, A. I., Korovin, S. D., Pegel', I. V., and Rostov, V. V., 2000, Effects of intense microwave radiation of nanosecond duration on some biological objects. Dokladi Akademii Nauk, 2000, 371, 691-695.
12. Pakhomov A.G. and Murphy M.R. A comprehensive review of the research on biological effects of pulsed radiofrequency radiation in Russia and the former Soviet Union. *In: Advances in Electromagnetic Fields in Living Systems, V. 3 (J. C. Lin, ed.), Kluwer Academic /Plenum Publishers, New York, 2000, 265-290.*
13. Rosen A.D. Temperature modulation of calcium channel function in GH_3 cells. Am J Physiol, 1996, 271, 863-868.
14. Pakhomov A.G., Mathur S. P., Akyel Y., Kiel J. L., and Murphy M. R. High-resolution microwave dosimetry in lossy media. In: Radio Frequency Radiation Dosimetry. B. J. Klauenberg and D. Miklavcic, eds., Kluwer Academic Publishers, Netherlands, 2000, p. 187-197.

Bioelectromagnetics 23:83–87 (2002)

Brief Communication

Ultra-Wideband Pulses Increase Nitric Oxide Production by RAW 264.7 Macrophages Incubated in Nitrate

Ronald L. Seaman,[1]* Jill E. Parker,[2] Johnathan L. Kiel,[2] Satnam P. Mathur,[1] Teri R. Grubbs,[2] and H. Kenneth Prol[1]

[1]*McKessonHBOC Clinical and Biological Services and, Microwave Bioeffects Branch, U.S. Army Medical Research Detachment, Brooks AFB, Texas, USA*
[2]*Directed Energy Bioeffects Division, U.S. Air Force Research Laboratory, Brooks AFB, Texas, USA*

The possible effects of ultra-wideband (UWB) pulses on cellular nitric oxide production were tested by measuring nitrite in the medium bathing UWB exposed RAW 264.7 macrophages. A 30 min exposure to 1 ns UWB pulses, repeated at 600 Hz with an estimated SAR of 0.106 W/kg, did not change nitric oxide production by RAW 264.7 cells, with or without stimulation by gamma interferon and lipopolysaccharide. However, when nitrate was added to the medium of stimulated cells, nitric oxide production increased after UWB exposure, indicating a possible action of UWB pulses on induced nitric oxide synthase under certain conditions. Bioelectromagnetics 23:83–87, 2002. Published 2002 Wiley-Liss, Inc.†

Key words: gamma interferon; lipopolysaccharide; nitric oxide synthase; GTEM cell

Use of ultra-wideband (UWB) electromagnetic pulses is increasing in various military and civilian applications [Agee et al., 1998]. The extremely short pulses have durations of a few nanoseconds, rise times of 100–500 ps, and broad frequency spectra typically ranging from 0 Hz to microwave frequencies. Because of concern for health and safety issues related to UWB pulses, studies of their possible biological effects are needed to develop guidelines for human exposure. Potential mechanisms for biological effects of UWB pulses as well as other types of electromagnetic fields include action on free radicals and enzymes [Grissom, 1995; Walleczek, 1995; Brocklehurst and McLauchlan, 1996; Mohtat et al., 1998].

Nitric oxide (NO), a free radical, and L-citrulline are produced by oxidation of L-arginine by nitric oxide synthase (NOS) enzymes in many types of tissue [Andrew and Mayer, 1999; Bredt, 1999; Rao, 2000]. Neuronal NOS and endothelial NOS are constitutive enzymes which produce NO for signaling in the nervous and cardiovascular systems. In addition, cytokines stimulate NO production in various types of cells by inducing NOS (iNOS) through transcription and translation processes. In macrophages, iNOS produces large amounts of NO for immunological defense.

A number of changes have been reported in macrophages exposed to electromagnetic fields. Phagocytosis by murine peritoneal macrophages has been reported to change with exposure to pulsed and CW 2.45 GHz microwaves [Mayers and Habeshaw, 1973; Zafra et al., 1988] as well as with exposure to static magnetic fields [Flipo et al., 1998]. Cultured P338D1 cells are stimulated by 150 MHz magnetic fields [Gamaley et al., 1995]. These changes, all in stimulated cells, have been reported to occur without heating by the applied fields. We report here results of

---

The views, opinions and/or findings contained in this report are those of the authors and should not be construed as an official Department of the Army or Department of the Air Force position, policy or decision unless so designated by other documentation.

Contract grant sponsor: U.S. Army Medical Research and Materiel Command; Contract grant number: DAMD17-94-C-4069; Contract grant sponsor: U.S. Air Force Office of Scientific Research.

*Correspondence to: Ronald L. Seaman, McKessonHBOC Clinical and Biological Services, P.O. Box 35460, Brooks AFB, TX 78235-5460. E-mail: ronald.seaman@brooks.af.mil

Received for review 3 April 2001; Final revision received 6 August 2001

Published 2002 Wiley-Liss, Inc.
†This article is a US Government work and, as such is in the public domain in the United States of America.
DOI 10.1002/bem.100

experiments on the effects of UWB pulses on NO production by iNOS in the murine macrophage cell line RAW 264.7.

RAW 264.7 cells (ATCC TIB 71) were subcultured for 5 days in T75 culture flasks at 37°C to approximately 80% confluency in RPMI 1640 growth medium that included fetal bovine serum (10%), penicillin (10 U/ml), streptomycin (10 μg/ml), and sodium bicarbonate buffer (2.7 g/l) (fetal bovine serum from Hyclone, Logan, UT; all others from Sigma Chemicals, St. Louis, MO). Table 1 summarizes the three culture treatments and three incubation periods in the experiment. Cells were plated from a single cell suspension using equal amounts for each flask and incubated for 24 h, during which gamma interferon (IFN-γ, 10 U/ml) and lipopolysaccharide (LPS, 5 ng/ml) were used to stimulate NO production in two of the treatments (GLO and GLN). After washing with phosphate buffered saline (PBS), unstimulated cells in treatment OOO and stimulated cells in treatment GLO were incubated another 24 h in RPMI 1640 while stimulated cells in treatment GLN were incubated in RPMI 1640 plus 39 mM KNO_3 for 24 h. After sham or UWB exposure, cells were incubated until the next day in RPMI 1640 (OOO and GLO) or in RPMI 1640 with 39 mM KNO_3 (GLN). Phenol red was not added to media after exposure to avoid interference with the nitrite assay. Individual flasks contained 10 ml of medium before exposure and 5 ml after exposure.

Cells were exposed at room temperature (20–25°C) to UWB pulses in a custom built giga transverse electromagnetic (GTEM) cell, a tapered two conductor transmission line with a square cross section. The UWB exposure system, including the GTEM cell, has been described previously [Lu et al., 1999; Seaman et al., 1999]. The UWB pulses were triggered by an external pulse generator at 600 Hz for UWB exposure and were not triggered for sham exposure. Both types of exposure lasted 30 min. Cells were washed in the coded flask and covered with 235 ml PBS at room temperature before the flask was placed in the GTEM cell. Pairs of flasks were stood on end on the horizontal ground plane in the region where a pure TEM wave propagated. The flat growth surface of each flask faced the source end of the GTEM cell. That is, the growth surface was vertical, parallel to the electric field, and orthogonal to the direction of pulse propagation. Flasks were positioned symmetrically on either side of the midline of the GTEM cell to have the same incident fields on both flasks. Cells exposed in different flasks at the same time were not necessarily from the same culture treatment. After exposure, PBS was poured off, 5 ml of respective medium added, and the flask incubated horizontally until the next day. Six flasks were tested for each of six conditions: three culture treatments (OOO, GLO, and GLN) by two exposure types (sham and UWB). The UWB pulses used in this experiment had peak amplitude of 103 ± 7 kV/m, duration of 0.98 ± 0.03 ns, and rise time of 162 ± 9 ps (mean $\pm$ SD) at the GTEM cell midline in the plane of flask growth surfaces.

After exposure and subsequent incubation for 21–26 h, a sample of medium was removed, coded, and frozen for later analysis. The concentration of nitrite, a stable product of NO decomposition and an indicator of cumulative NO production, was measured using fluorescence intensity of 2,3-diaminonaphthalene [Misko et al., 1993]. Samples of culture media were tested in duplicate. Nitrite was not detectable in RPMI 1640 medium or the medium plus KNO_3. The coded results were not identified with experimental conditions until necessary for statistical analysis, which was performed using GB-STAT software (Dynamic Microsystems, Silver Spring, MD) with $P < .05$ considered significant.

As expected, stimulation of RAW 264.7 murine macrophages by IFN-γ and LPS resulted in increased nitrite concentration in the medium (treatment GLO versus treatment OOO in Fig. 1). The presence of 39 mM KNO_3 after stimulation (treatment GLN) increased nitrite concentration further. Two-way analysis of variance (ANOVA) indicated significant main effects of culture treatment ($F(2,30) = 126.3$, $P < .0001$) and exposure ($F(1,30) = 5.91$, $P = .021$) as

TABLE 1. Culture Treatments for RAW 264.7 Cells

	Incubation period		
Culture treatment	First	Second	Third
OOO	RPMI	RPMI	RPMI
GLO	RPMI + IFN-γ + LPS	RPMI	RPMI
GLN	RPMI + IFN-γ + LPS	RPMI + NO_3	RPMI + NO_3

RPMI: RPMI 1640 growth medium; NO_3: 39 mM KNO_3; IFN-γ: gamma interferon (100 U/ml); LPS, lipopolysaccharide (5 ng/ml).
Phenol red was present during the first and second incubation periods. Sham or UWB exposure occurred between the second and third incubation periods.

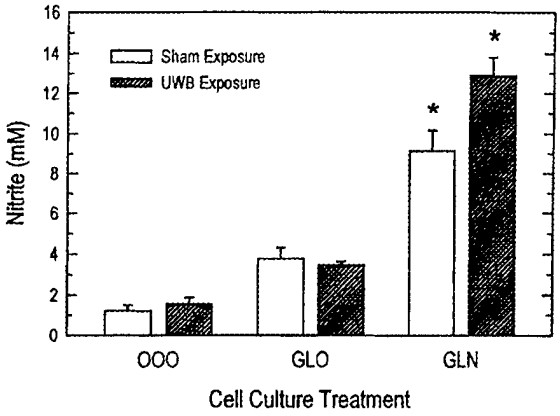


Fig. 1. Nitrite concentration (mean ± SEM, N = 6) measured in medium bathing RAW 264.7 cells 1 day after 30 min sham or UWB exposure. Cell culture treatments are OOO, unstimulated; GLO, stimulated with IFN-γ and LPS; GLN, stimulated with IFN-γ and LPS and incubated with nitrate. *$P < 0.01$ compared to each other and to other culture treatment-UWB conditions.

well as significant interaction between culture treatment and exposure ($F(2,30) = 5.92$, $P = .0068$). Newman–Keuls testing showed that the nitrite concentrations for sham and UWB exposures for treatment GLN were each significantly different from all other conditions, including each other. Nitrite concentration for UWB exposure in treatment GLO was significantly greater than for both sham and UWB exposures in treatment OOO, while nitrite concentration for sham exposure in treatment GLO was significantly greater than only nitrite concentration for sham exposure in treatment OOO. In treatments OOO and GLO, Newman–Keuls testing showed no difference in nitrite concentration between sham and UWB exposures. Thus, the differences in nitrite concentration were between culture conditions and between sham and UWB exposures for treatment GLN, the latter difference indicating an effect of UWB pulses on NO production.

Unfortunately, no method is yet available to measure electric and magnetic fields in biological preparations exposed to UWB pulses in the GTEM cell. Also, specific absorption rate (SAR) in the preparations is too small to produce a measurable temperature increase. Estimates of electric field and SAR at the cells in the flasks can be calculated using a transmission line model with an electric field pulse incident on an infinite lossy dielectric. For a UWB pulse with duration of 0.98 ns and rise time of 162 ps the median frequency is 0.51 GHz and the principal frequency components are between 0.0844 and 3.08 GHz [Foster, 1995]. The relative dielectric constant ε_r of 75.4 and conductivity of 1.6 S/m at the median frequency for PBS at 20°C are similar to respective values across the calculated frequency band and measured room temperatures [Stogryn, 1971]. The corresponding skin depth is 3.1 cm. The electric field just inside the PBS is calculated as the transmission coefficient, $2/(1+\varepsilon_r^{1/2})$, times the incident field. We have estimated that the peak electric field at the PBS surface was 10.6 kV/m for an incident peak field of 103 kV/m. At a depth of 10 μm, the approximate diameter of RAW 264.7 cells, the electric field decayed less than 0.1% and little pulse distortion was expected. The SAR at the cells was calculated as 0.106 W/kg, the product of PBS conductivity and the squared rms transmitted electric field divided by PBS mass density, taken as 1 g/cm^3. The maximum rate of temperature increase calculated using this SAR is 2.52×10^{-5}°C/s. This corresponds to a maximum possible temperature increase during a 30-min exposure of only 0.045 °C, found by assuming no heat loss.

The peak magnetic field of the UWB pulses in the GTEM cell has been estimated to be 0.33 mT [Seaman et al., 1999], which is in the range of 0.1–10 mT of static and ELF magnetic fields capable of changing radical pair chemistry [Grissom, 1995; Walleczek, 1995; Brocklehurst and McLauchlan, 1996]. The time averaged magnetic field was, of course, much smaller, about 0.2 nT, because of the small duty cycle of 5.88×10^{-7}. Thus, the change in NO production in treatment GLN with UWB exposure, as reflected by nitrite levels, was more likely due to action of UWB electromagnetic fields than to a change in temperature. The increase in NO production is consistent with the previously reported changes in macrophages exposed to electromagnetic fields, which also occurred without gross heating.

Because NO produced without nitrate after stimulation in treatment GLO was not changed by UWB exposure, the effect of UWB may depend on presence of nitrate, greater NO production with nitrate, or some combination of these. Because 48 h incubation with 39 mM KNO_3 does not increase NO production by unstimulated RAW 264.7 cells [Kiel, 1995, p 151–153] the UWB action might require the combination of stimulation by IFN-γ and LPS and the presence of nitrate.

The most likely actions of nitrate and UWB pulses to increase nitrite concentration in the medium would seem to be directly on iNOS and its production of NO. However, action on other effectors generated concurrently with NO by stimulated RAW 264.7 cells cannot be ruled out. The other effectors include superoxide radicals and prostaglandin as well as the cytokines tumor necrosis factor (TNF) and

interleukin-1β (IL-1β) [Riese et al., 1994; Brüne et al., 1997; Held et al., 1999; Eu et al., 2000]. Changes in production of superoxide radicals or in their interaction with nitric oxide caused by nitrate and UWB pulses could have been reflected in nitrite concentration in the medium. Added nitrate increases TNF production in murine P338D1 macrophages [Kiel, 1995, p 151–153] and magnetic fields pulsed at 50 Hz increase TNF and IL-1β production in stimulated human peripheral blood mononuclear cells in culture [Pessina and Aldinucci, 1998]. If production of TNF or IL-1β was affected similarly by nitrate and/or UWB pulses, then production of NO and superoxide radicals could change due to autocrine functions of the cytokines. For these changes, the action of UWB pulses with nitrate present would involve effector enzymes and/or free radical chemistry. An effect of UWB pulses on iNOS could also indicate possible direct or indirect effects of UWB pulses on iNOS and effectors in other cell types and on constitutive isozymes of iNOS in endothelial cells and neurons.

We would have liked to investigate further the change in NO production by RAW 264.7 cells by varying one UWB variable at a time, i.e., performing a dose response study. However, to our knowledge, capabilities do not exist to do this, and they were certainly not available in our exposure system. Pulse amplitude, shape, duration, and repetition frequency are the UWB exposure parameters to be varied for dose-response experiments. Pulse amplitude can be changed in our system by moving objects from the TEM region to another location in our GTEM cell. Pulse amplitude and repetition frequency are the only variables that can be changed in our system without substantial hardware modification. However, both of these manipulations also change other pulse parameters, especially when changed to a degree appropriate for dose-response. Hardware modifications have since been found also to change multiple pulse parameters. Thus, we were not able to perform a dose response study on any pulse parameter.

ACKNOWLEDGMENTS

We are grateful to M. Belt, D. Cox, and J. Lee for continuous operation of the UWB exposure system and assistance with field measurements. We also thank Dr. S-T Lu for his careful reading of the manuscript.

REFERENCES

Agee FJ, Baum CE, Prather WD, Lehr JM, O'Loughlin JP, Burger JW, Schoenberg JSH, Scholfield DW, Torres RJ, Hull JP, Gaudet JA. 1998. Ultra-wideband transmitter research. IEEE Trans Plasma Sci 26:860–873.

Andrew PJ, Mayer B. 1999. Enzymatic function of nitric oxide synthases. Cardiovasc Res 43:521–531.

Bredt DS. 1999. Endogenous nitric oxide synthesis: biological functions and pathophysiology. Free Rad Res 31:577–596.

Brocklehurst B, McLauchlan KA. 1996. Free radical mechanism for the effects of environmental electromagnetic fields on biological systems. Int J Radiat Biol 69:3–24.

Brüne B, Götz C, Meßmer UK, Sandau K, Hirvonen MR, Lapetina EG. 1997. Superoxide formation and macrophage resistance to nitric oxide-mediated apoptosis. J Biol Chem 272:7253–7258.

Eu JP, Liu L, Zeng M, Stamler JS. 2000. An apoptotic model for nitrosative stress. Biochemistry 39:1040–1047.

Flipo D, Fournier M, Benquet C, Roux P, Le Boulaire C, Pinsky C, LaBella FS, Krzystyniak K. 1998. Increased apoptosis, changes in intracellular Ca^{2+}, and functional alterations in lymphocytes and macrophages after in vitro exposure to static magnetic field. J Toxicol Environ Health A 54: 63–76.

Foster PR. 1995. Antennas and UWB signals. In: Taylor JD, editor. Introduction to ultra-wideband radar systems. Boca Raton: CRC Press. p 147–216.

Gamaley I, Augsten K, Berg H. 1995. Electrostimulation of macrophage NADPH oxidase by modulated high-frequency electromagnetic fields. Bioelectrochem Bioenerg 38:415–418.

Grissom CB. 1995. Magnetic field effects in biology: A survey of possible mechanisms with emphasis on radical-pair recombination. Chem Rev 95:3–24.

Held TK, Weihua X, Yuan L, Kalvakolanu DV, Cross AS. 1999. Gamma interferon augments macrophage activation by lipopolysaccharide by two distinct mechanisms, at the signal transduction level and via an autocrine mechanism involving tumor necrosis factor alpha and interleukin-1. Infect Immun 67:206–212.

Kiel JL. 1995. Type-b Cytochromes: sensors and switches. Boca Raton: CRC Press. 220 p.

Lu S-T, Mathur SP, Akyel Y, Lee JC. 1999. Ultrawide-band electromagnetic pulses induced hypotension in rats. Physiol Behav 65:753–761.

Mayers CP, Habeshaw JA. 1973. Depression of phagocytosis: A non-thermal effect of microwave radiation as a potential hazard to health. Int J Radiat Biol 24:449–461.

Misko TP, Schilling RJ, Salvemini D, Moore WM, Currie MG. 1993. A fluorometric assay for measurement of nitrite in biological samples. Anal Biochem 214:11–16.

Mohtat N, Cozens FL, Hancock-Chen T, Scaiano JC, McLean J, Kim J. 1998. Magnetic field effects on the behavior of radicals in protein and DNA environments. Photochem Photobiol 67:111–118.

Pessina GP, Aldinucci C. 1998. Pulsed electromagnetic fields enhance the induction of cytokines by peripheral blood mononuclear cells challenged with phytohemagglutinin. Bioelectromagnetics 19:445–451.

Rao KMK. 2000. Molecular mechanisms regulating iNOS expression in various cell types. J Toxicol Environ Health B 3:27–58.

Riese J, Hoff T, Nordhoff A, DeWitt DL, Resch K, Kaever V. 1994. Transient expression of prostaglandin endoperoxide synthase-2 during mouse macrophage activation. J Leukoc Biol 55:476–482.

Seaman RL, Belt ML, Doyle JM, Mathur SP. 1999. Hyperactivity caused by a nitric oxide synthase inhibitor is countered by ultra-wideband pulses. Bioelectromagnetics 20:431–439.

Stogryn A. 1971. Equations for calculating the dielectric constant of saline water. IEEE Trans Microwave Theory Tech 19:733–736.

Walleczek J. 1995. Magnetokinetic effects on radical pairs: A paradigm for magnetic field interactions with biological systems at lower than thermal energy. In: Blank M, editor. Electromagnetic Fields: Biological Interactions and Mechanisms, Advances in Chemistry Series, No. 250. Washington, DC: American Chemical Society. p 395–420.

Zafra C, Peña J, de la Fuente M. 1988. Effect of microwaves on the activity of murine macrophages in vitro. Int Archs Allergy Appl Immun 85:478–482.

ELSEVIER

Hearing Research 166 (2002) 214–215

HEARING RESEARCH

www.elsevier.com/locate/heares

Letter to the editor

Non-osseous sound transmission to the inner ear

Ronald L. Seaman *

McKesson HBOC Clinical Services and Biological Services and US Army Medical Research Detachment, 8308 Hawks Road, Building 1168, Brooks AFB, TX 78235, USA

Received 5 November 2001

Recent reports of non-osseous transmission of intracranial sound to the inner ear (Freeman et al., 2000; Sohmer et al., 2000) are very interesting. Convincing evidence from three different rodents and humans is given to show that this pathway is a major mechanism in bone conduction. Results consistent with these findings have been obtained in an amphibian and a preliminary report made (Seaman and Rasbury, 1991).

The evoked potential of the left eighth-nerve was recorded to detect inner ear stimulation in the anesthetized bullfrog (*Rana catesbeiana*) (Seaman, 1991). A hole was made in the frontoparietal bone to expose dura over the dorsal midbrain. An Etymotic ER-3A earphone and ER-10B low-noise microphone were supported by a micromanipulator. They were acoustically coupled to the left tympanum using an Etymotic 15-mm impedance tip with inverted flange and a seal made with vacuum grease. Output of the ER-10B microphone and amplified evoked potential (X1000, 10-ms and 100-μs filter settings, Grass P16 preamplifier) were displayed and averaged by a Tektronix 2430A digital oscilloscope triggered by respective stimulus signals. Averaged waveforms of 128 or 256 responses were saved to computer data files.

Mechanical stimuli were applied to bone or exposed dura by means of a custom-made apparatus consisting of a plastic probe attached to the moving coil of a permanent magnet speaker. The speaker and probe were supported by a micromanipulator used to position the probe tip accurately onto dura through the hole in bone or on bone near the hole. Mechanical stimuli were generated by applying 5-V, 1- or 5-ms pulses from a Grass S44 stimulator to the speaker coil. All stimuli were delivered at 1.2–3.4 Hz.

Fig. 1 presents results from one animal that are representative of those obtained in five animals. The top panel is the response evoked with the probe tip touching the dura. The middle panel is the response evoked with the probe touching bone. These waveforms are qualitatively similar with an initial positive peak followed by two negative peaks, the latter possibly with an intervening positive peak. The response in the bottom panel, recorded when the probe was not touching the animal, is much smaller than responses obtained when the probe touched dura or bone. This non-contact response can be attributed to seismic stimulation by substrate vibration caused by movement of the speaker coil (Koyama et al., 1982; Lewis et al., 1985). For contact stimuli, latency to the first peak was 3.55 ± 0.10 ms (mean ± S.D.) for contact with dura and 2.54 ± 0.14 ms for contact with bone. These contact latencies were significantly different (two-tailed paired t-test, $P < 0.05$). The latency to response peak for click stimuli applied through the ER-3A earphone was 2.47 ± 0.12 ms, which by t-test was different from dura-contact latency but not different from bone-contact latency.

Results from the bullfrog lead to conclusions similar to the ones based on the experiments in mammals (Freeman et al., 2000; Sohmer et al., 2000). The principal, common conclusion is that intracranial pressure changes can be transmitted to the inner ear and stimulate sensory receptors there. In mammals, this was shown to occur without detectable motion of bone and may well be the major transmission pathway. Intermediate transmission through bone was not ruled out completely in the bullfrog but seemed unlikely because of the small surface displacements and the acoustic impedance mismatch between brain/cerebrospinal fluid (CSF) and bone. Because the cranium interior and the inner ear are connected similarly in vertebrates through ducts in the cranium (Lewis et al., 1985; Donaldson and Duckert, 1991), we can expect similar sound transmission in mammals and amphibians.

In these tests of sound transmission, pressure of in-

* Tel.: +1 (210) 536 5595: Fax: +1 (210) 536 5382.
E-mail address: ronald.seaman@brooks.af.mil (R.L. Seaman).

0378-5955/02/$ – see front matter © 2002 Elsevier Science B.V. All rights reserved.
PII: S0378-5955(02)00282-4

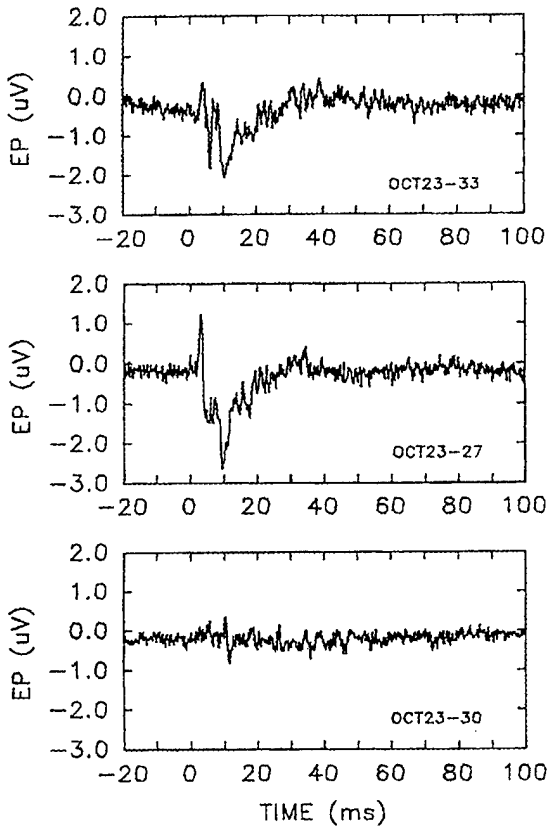


Fig. 1. Evoked potential (EP) response of the bullfrog eighth-nerve to pulsatile mechanical stimuli applied with a probe. Top: probe tip on dura, middle: probe tip on frontoparietal bone, and bottom: probe tip above animal.

tracranial contents was changed at auditory frequencies by applying mechanical stimuli to exposed dura. The sound generated undoubtedly propagated throughout the enclosed CSF and brain. We can well expect that sound generated within CSF and brain by volume energy absorption would likewise be transmitted to the inner ear. Possible examples of this type of auditory stimulation have been reported for ultrasound pulses applied to dura in cats (Foster and Wiederhold, 1978) and directed to basilar artery in humans (Magee and Davies, 1993). Possible examples for microwave pulses have been reported in numerous investigations of 'microwave hearing' in animals and humans (e.g. Chou et al., 1982; Seaman and Lebovitz, 1987).

Applying the methods used in the recent reports will lead to a better understanding of bone conduction and auditory phenomena resulting from other forms of energy. Because this type of sound transmission depends on physical dimensions of the ducts connecting the intracranial cavity with the inner ear, we can expect that duct anatomy will influence auditory perception of intracranial sound. This means that perception will likely be different for different animals and for different ducts within a species. For example, taking the intracranial cavity as a pressure source that is connected to a closed cavity through a duct results in a frequency-dependent transfer function that exhibits resonance in the auditory range (Seaman and Barron, 1991). Such a frequency characteristic might prove useful in future study and application of this type of auditory stimulation.

References

Chou, C.K., Guy, A.W., Galambos, R., 1982. Auditory perception of radio frequency electromagnetic fields. J. Acoust. Soc. Am. 71, 1321–1334.

Donaldson, J.A., Duckert, L.G., 1991. Anatomy of the ear. In: Paparella, M.M., Shumrick, D.A., Gluckman, J.L., Meyerhoff, W.L. (Eds.), Otolaryngology, 3rd edn. W.B. Saunders, Philadelphia, PA, pp. 23–58.

Foster, K.R., Wiederhold, M.L., 1978. Auditory responses in cats produced by pulsed ultrasound. J. Acoust. Soc. Am. 63, 1199–1205.

Freeman, S., Sichel, J.Y., Sohmer, H., 2000. Bone conduction experiments in animals: evidence for a non-osseous mechanism. Hear. Res. 146, 72–80.

Koyama, H., Lewis, E.R., Leverenz, E.L., Baird, R.A., 1982. Acute seismic sensitivity in the bullfrog ear. Brain Res. 250, 168–172.

Lewis, E.R., Leverenz, E.L., Bialek, W.S., 1985. The Vertebrate Inner Ear. CRC Press, Boca Raton, FL.

Magee, T.R., Davies, A.H., 1993. Auditory phenomena during transcranial Doppler insonation of the basilar artery. J. Ultrasound Med. 12, 747–750.

Seaman, R.L., 1991. Method to record evoked potentials from the frog eighth nerve. Hear. Res. 51, 301–306.

Seaman, R.L., Barron, R.F., 1991. Resonant pressure transmission to the inner ear. Proc. Annu. Int. Conf. IEEE Eng. Med. Biol. Soc. 13, pp. 1873–1874.

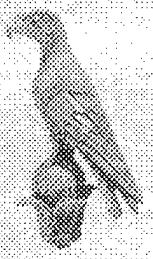
Seaman, R.L., Lebovitz, R.M., 1987. Auditory unit responses to single-pulse and twin-pulse microwave stimuli. Hear. Res. 26, 105–116.

Seaman, R.L., Rasbury, J.A., 1991. Transient intracranial pressure evokes eighth nerve potentials in frog. Soc. Neurosci. Abstr. 17, 1213.

Sohmer, H., Freeman, S., Geal-Dor, M., Adelman, C., Savion, I., 2000. Bone conduction experiments in humans: a fluid pathway from bone to ear. Hear. Res. 146, 81–88.

BIOLOGICAL EFFECTS of EMFs

2nd INTERNATIONAL WORKSHOP

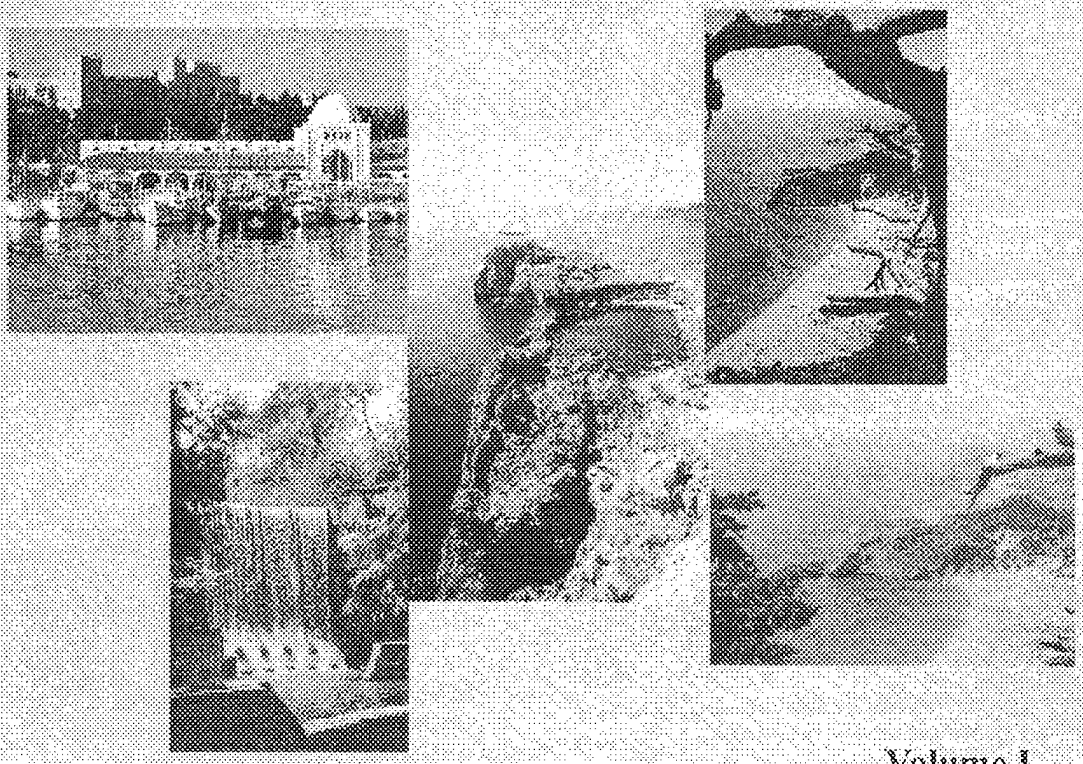




Electronics - Telecom & Applications Laboratory
Physics Department
University of Ioannina

Institute of Informatics & Telecommunications
N.C.S.R. "Demokritos"

Proceedings



Volume I

Rhodes, Greece, 7 -11 October, 2002

MOTOR ACTIVITY FACTORS

CHANGES IN RAT MOTOR ACTIVITY BY PULSED MICROWAVE RADIATION DEPEND ON TYPE OF ACTIVITY, TIME AFTER EXPOSURE, AND STATE OF ANIMAL

RONALD L. SEAMAN, SATNAM P. MATHUR, AMY M. PHINNEY, ADRIAN S. GARCIA, JOHN L. ASHMORE
MCKESSON BIOSERVICES CORPORATION
AT WRAIR US ARMY MEDICAL RESEARCH DETACHMENT
8308 HAWKS ROAD, BUILDING 1168, BROOKS AIR FORCE BASE, TEXAS 78235 USA

Abstract

Spontaneous motor activity of male Sprague-Dawley rats (4-6 months old, 512-613 g) was measured at different times after two daily 30-min whole-body exposures to 1.25-GHz microwave pulses (5.9 μs, 10 Hz) at 0 (sham), 0.6, or 6.0 W/kg whole-body specific absorption rate. Intraperitoneal injection of some animals with 10 mg/kg 3-nitroproprionic acid (3-NP) given 1.5 h before each exposure induced a generalized chemical hypoxia. At 1.5 h after the second microwave exposure, a significant main effect of 3-NP was found in ANOVA (N=7/condition) for vertical (rearing) and stereotypical (rapid) activities but not for horizontal activity. One stereotypy variable also had a significant interaction between 3-NP and microwave exposure. One week later, a significant main effect of microwave exposure was found in ANOVA for horizontal and stereotypical activities but not for vertical activity. At 2 weeks after the treatments, no significant effect was found for any activity variable. These results indicate that effects of pulsed microwave radiation on activity depend on type of activity measured, when the activity is measured, and the physiological state of the animal during exposure. These points may explain some of the differences in reported effects on activity and be relevant in assessment of effects on other types of behavior.

Introduction

Background

One experimental approach to testing for effects of exposure to microwave radiation on the nervous system is to observe and measure changes in animal behavior either during or after exposure [1-3]. Changes in neurotransmitters and their receptors in the central nervous system (CNS) have been found during and after microwave exposure [2-7]. However, changes in spontaneous and learned behavior that might be affected by changes in neurotransmission are found after microwave exposure in some studies but not in others [8-11]. Among the factors that might affect behavior are, of course, those associated with the exposure itself such as microwave frequency, modulation, peak power, average power, and specific absorption rate (SAR) as well as the duration of exposure and environmental conditions in the exposure chamber. For a given type of behavior and the same type of microwave exposure, we might expect that behavior, as well as neurotransmitters, could be changed differently at different times after exposure [2,12,13].

In research to study effects of exposure to pulsed microwaves on neurodegenerative processes we have observed that changes in rat spontaneous motor activity depend on a number of factors. This report summarizes changes in three types of activity – horizontal, vertical, and stereotypical movements – three times after the second of two exposures – 1.5 h, 1 week, and 2 weeks – at 0.6 or 6.0 W/kg for 30 min. The measures were obtained from animals exposed only to microwaves and from animals in a state of chemical hypoxia when exposed after injection with the neurotoxin 3-nitropropionic acid (3-NP). Systemic administration of 3-NP causes a hypoxic state through its inhibition of succinate dehydrogenase and this can initiate processes of neurodegeneration with sufficient dosing [14,15]. The use of two treatment days had been indicated by results from a pilot experiment with 3-NP.

MOTOR ACTIVITY FACTORS

Animals

Male Sprague-Dawley rats (Charles River Labs, Portage, Michigan) weighing 512-613 g and 4-6 months of age were used. Animals of this age were used in order to have a more uniform effect of 3-NP. After quarantine, animals were housed individually with a 12/12 light/dark cycle and provided Purina rodent chow and tap water ad libitum.

Microwave exposure and dosimetry

Microwave exposure was accomplished with an antenna consisting of the open end of a WR-650 rectangular waveguide that provided a horizontal electric field within a microwave anechoic chamber. Air temperature inside the chamber, monitored using a YSI 401 temperature probe placed behind the antenna, was 22.51±0.70°C (mean±SD) over all exposures. The maximum temperature elevation in the animal holder, described below, during exposure of an animal was estimated to be about 1.2°C.

A General Electric FPS-7B radar transmitter produced 5.9-μs, 1.25-GHz (L-band) pulses at 10 Hz. Forward and reflected microwave pulses were sampled with crystal detectors at calibrated waveguide couplers and displayed on a Tektronix 2430A digital oscilloscope. The transmitter high voltage was switched on to start a microwave exposure and quickly adjusted manually to attain the desired pulse peak power, which was adjusted during exposure if necessary to maintain average power. The high voltage was switched off to terminate an exposure.

For microwave exposure, an animal was placed in a nonrestricting, well-ventilated plastic holder made from a hollow clear cylinder 19.5 cm long with 17.1-cm inside diameter, 0.32-cm thick walls, closed ends, and a 19.5x14.7 cm floor made of plastic rods. The horizontal axis of the animal holder was orthogonal to the horizontal antenna bore sight and parallel to the propagating electric field vector. An animal in the center of the holder was on the bore sight and its body axis tended to be aligned with the holder axis and thus the electric field (E polarization). The SAR was set to E-polarization value of 6 or 0.6 W/kg by placing the animal holder so that its center was 30 or 85 cm, respectively, from the antenna and setting the peak power of transmitted microwave pulses for the required net average power.

Activity measurement

Spontaneous motor activity was tested by placing an animal in a clean DigiScan (AccuScan, Columbus, Ohio USA) square arena (40.8x40.8 cm with 30.5-cm walls) for 10 min with room lights off. Interruptions of infrared beams at 3.6 cm and 14.7 cm above the floor were detected under control of DigiPro (AccuScan, Columbus, Ohio USA) software and used to derive measures of horizontal, vertical (rearing), and stereotypical animal movements. Stereotypical movements were animal movements causing repetitive interruptions of the same horizontal beam occurring with less than 1 s between interruptions. Measures of horizontal movement were number of lower level horizontal-sensor beam interruptions (HACTV), distance moved in cm (TOTDIST), number of horizontal movement episodes (MOVNO), and time spent moving (MOVTIME). Measures of vertical movement were number of upper level vertical-sensor beam interuptions (VACTV), number of vertical movement episodes (VMOVNO), and time spent in vertical movement (VTIME). Measures of stereotypy were number of repetitive rapid beam interruptions (STRCNT), number of stereotypy episodes (STRNO), and time spent in stereotypy (STRTIME). Other measures were also obtained and are mentioned below when they were found significantly different between experimental conditions..

Procedure

Animals were assigned in sequence to one of six experimental 3-NP-microwave (mg/kg-W/kg) conditions: 0-0, 0-0.6, 0-6, 10-0, 10-0.6, and 10-6, each consisting of injections on two consecutive days with an exposure after each injection. Conditions were applied in random sequence within a group of six animals. All conditions in a group were completed before the next group was started. The seven groups of animals tested thus provided 7 animals per condition.

On the day before its first injection and exposure, an animal was familiarized with procedures by being in the animal holder in the anechoic chamber for 20-30 min and having its colonic temperature measured with a YSI 423 temperature probe. Motor activity was then tested to insure an acceptable level of spontaneous activity.

Experimental treatments were delivered to animals on two consecutive days. The first post-treatment test of activity was on the second day. At 3-5.5 h after lights on in the animal room on the first day, an animal was injected intraperitoneally with sterile 0.9% saline (0 mg/kg) or 10 mg/kg 3-NP (Sigma-Aldrich, St. Louis, USA) in sterile water with pH adjusted to 7.4. One hour 25 min after injection, colonic temperature was measured, the animal was placed into the animal holder, and the holder was placed in front of the open-ended waveguide at 30 or 85 cm. After 5 min, exposure at 0 (sham), 0.6, or 6 W/kg SAR was started. When exposure was terminated 30 min later, the animal was removed from the animal holder, colonic temperature was measured, and the animal was returned to its home cage.

MOTOR ACTIVITY FACTORS

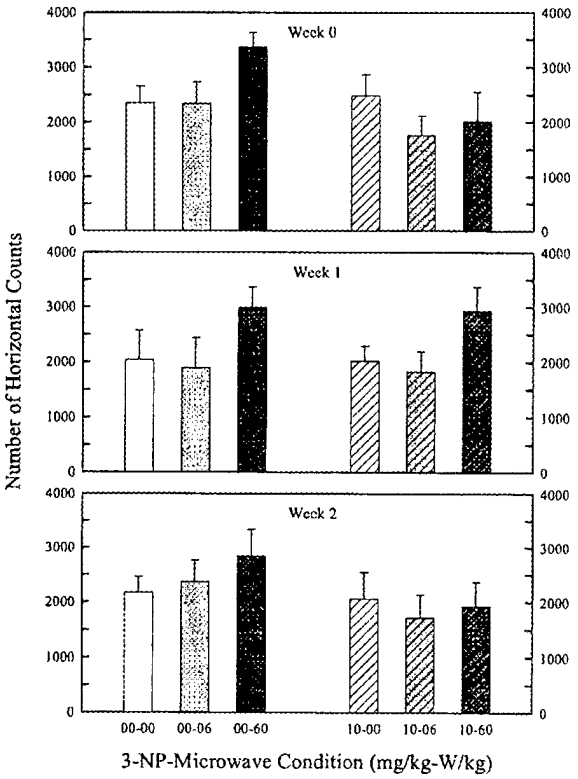


Figure 1. Horizontal activity counts (mean and s.e.m.) for the six experimental conditions over three weeks of testing.

On the second day of treatment, the same procedure was repeated with the same 3-NP dose and microwave SAR for a particular animal. In addition, motor activity was tested 1.5 h after exposure, or 3.5 h after 3-NP injection, referred to as week 0. Microwave exposures occurred 4.5-8 h after lights on; activity testing, 6-9 h after lights on. Activity was also tested at the same time of day 1 week and 2 weeks later.

Data analysis

Experimental conditions were designated by 3-NP dose and microwave SAR described above as 00-00, 00-06, 00-60, 10-00, 10-06, and 10-60. Times of testing after exposure refer to time elapsed from the end of the second microwave exposure – 1.5 h, 1 week, and 2 weeks, but are actually 1.5 h and 25.5 h; 1 week and 1 week plus 1 day; and 2 weeks plus 1 day after the second and first exposures, respectively. Differences in activity measures were tested with analysis of variance (ANOVA) and post-hoc Newman-Keuls pair-wise tests. These parametric tests were used after data were tested with the Shapiro-Wilk test of normality. Differences in colonic temperature were tested with nonparametric Friedman two-way ANOVA by ranks, Fr(cases,df); Newman-Keuls pair-wise multiple comparisons test; and Wilcoxon one-sample signed rank test. Statistical testing was done with GB-STAT software (v5.4, Dynamic Microsystems, Silver Spring, MD) with a (two-tailed) significance level of 0.05 in all tests.

Results

Colonic temperature increased with microwave exposure at 6 W/kg by 1.9-2.3 C° on average, with immediate post-exposure temperatures of 37.3-40.3°C, similar to those found previously for exposure at this SAR for 30 min [16]. With the exception of a mean decrease of 0.7C° on the second day of saline injection and sham exposure, temperature change for exposures at 0 and 0.6 W/kg was not different from 0 (Wilcoxon test). Multiple comparisons after Friedman ANOVA ($Fr(7,11)=56.53$, $p<.0001$) showed that the four increases at 6 W/kg were each significantly different from all changes at 0 and 0.6 W/kg. The four increases were also not different from each other, indicating that 3-NP and day of exposure had no effect on colonic temperature change.

Motor activity for each week is illustrated in Fig. 1 with HACTV, a measure which reflected general patterns of activity for the respective weeks. At 1.5 h after the second sham or microwave exposure (week 0), HACTV was greatest for condition 00-60. However, as listed in Table 1 for HACTV, the main effects of both 3-NP and microwave exposure as well as their interaction were not significant. This was also the case for other measures of horizontal activity except that 3-NP-microwave interaction was significant for MOVNO. The interaction was reflected in post-hoc pair-wise testing by a significant difference between conditions 00-60 and 10-60, similar to the difference in HACTV in Fig. 1, which did not reach significance.

At week 0, vertical and stereotypical activity appeared to be more affected by 3-NP than did horizontal activity (Table 1). The main effect of 3-NP was significant for vertical activity measures VACTV, VMOVNO, and VTIME and stereotypy measures STRCNT, STRNO, and STRTIME. This was due to activity for

MOTOR ACTIVITY FACTORS

Table 1. ANOVA Results.

Time Point	3-NP		Microwave		Interaction	
MEASURE	*F*	*p*	*F*	*p*	*F*	*p*
Week 0						
HACTV	3.73	n.s.	1.46	n.s.	1.92	n.s.
TOTDIST	1.83	n.s.	1.75	n.s.	1.15	n.s.
MOVNO	3.95	n.s.	1.77	n.s.	3.30	.0482
MOVTIME	2.22	n.s.	1.59	n.s.	2.04	n.s.
VACTV	6.45	.0155	1.20	n.s.	2.00	n.s.
VMOVNO	4.37	.0438	<1	n.s.	1.30	n.s.
VTIME	4.46	.0418	<1	n.s.	<1	n.s.
STRCNT	4.72	.0365	<1	n.s.	2.02	n.s.
STRNO	8.39	.0064	2.79	n.s.	3.97	.0276
STRTIME	9.20	.0045	<1	n.s.	2.72	n.s.
Week 1						
HACTV	<1	n.s.	3.76	.0329	<1	n.s.
TOTDIST	<1	n.s.	3.91	.0291	<1	n.s.
MOVNO	<1	n.s.	2.85	n.s.	<1	n.s.
MOVTIME	<1	n.s.	3.00	n.s.	<1	n.s.
All Vertical	<1	n.s.	1.3-1.8	n.s.	<1	n.s.
STRCNT	<1	n.s.	3.88	.0297	<1	n.s.
STRNO	<1	n.s.	3.94	.0282	<1	n.s.
STRTIME	<1	n.s.	3.14	n.s.	<1	n.s.
Week 2						
HACTV	2.56	n.s.	<1	n.s.	<1	n.s.
All Horizontal	1.6-3.5	n.s.	<1	n.s.	<1	n.s.
All Vertical	<1-1.8	n.s.	<1	n.s.	<1	n.s.
All Stereotypy	<1-2.3	n.s.	<1	n.s.	<1	n.s.

conditions with 3-NP -- 10-00, 10-06, and 10-60 – to be at a similar or lower level relative to conditions without 3-NP – 00-00, 00-06, and 00-60 – and not due to a significant difference between a pair of conditions. In addition, 3-NP-microwave interaction was significant for STRNO. The interaction for STRNO was due primarily to a significant difference between conditions 00-60 and 10-60. Overall, the differences reflected the tendency for values in condition 00-60 to be larger than respective control values (condition 00-00), values in condition 10-06 and/or 10-60 to be smaller than respective control values, and values in condition 10-60 to be smaller than respective values in conditon 00-60.

At week 1, the main effect of 3-NP and the effect of 3-NP-microwave interaction were not significant for any horizontal, vertical, or stereotypical activity measure (Table 1). The main effect of microwave exposure was significant for horizontal activity in HACTV and TOTDIST and for stereotypical activity in STRCNT and STRNO (Table 1). The main effect of microwave exposure, however, was not significant for any measure of vertical activity. The main effect of microwave exposure in horizontal and stereotypical activities was due to increased activity for conditions 00-60 and 10-60, that is, for SAR of 6 W/kg regardless of 3-NP dose, a pattern which is evident in Fig. 1 for HACTV. Interestingly, the main effect of microwave exposure was also significant for horizontal distance traveled within 5-6 cm of arena walls (margin distance, MRGDIST) with a similar pattern among conditions.

At week 2, the main effect of 3-NP, the main effect of microwave exposure, and the effect of 3-NP-microwave interaction were not significant for any horizontal, vertical, or stereotypical activity measure (Table 1). The main effect of 3-NP approached significance for horizontal activity measures TOTDIST and MOVTIME, reflecting the tendency of slightly less activity for conditions with 3-NP -- 10-00, 10-06, and 10-60 – relative to conditions without 3-NP – 00-00, 00-06, and 00-60 – as shown for HACTV in Fig. 1.

Summary

No difference was found in ANOVA between experimental groups in pre-treatment baseline measures of any activity. Thus, changes in activity after 3-NP-microwave treatment can be expected to be due to treatment rather than to differences between groups. Some of the observed changes occurred for different types of

spontaneous activity at different times after treatment. The 3-NP-induced chemical hypoxia seemed to affect activity by reducing or eliminating changes associated with microwave exposure.

We can summarize changes in rat activity after microwave exposure by the following:

- Horizontal activity does not change at 1.5 h and 2 weeks after exposure.
- Significant change in horizontal activity can be detected at 1 week after exposure.
- Vertical activity does not change at 1.5 h, 1 week, and 2 weeks after exposure.
- Stereotypical activity does not change at 1.5 h and 2 weeks after exposure, similar to horizontal activity.
- Significant change in stereotypical activity can be detected at 1 week after exposure, also similar to horizontal activity.
- Microwave exposure and 3-NP-induced hypoxia interact at 1.5 h after exposure for horizontal activity and stereotypical activity but not for vertical activity. The effect of 3-NP is to reduce a change seen with microwave exposure.
- No interaction occurs between microwave exposure and 3-NP-induced hypoxia for any activity at 1 week and 2 weeks after exposure.

Of course, replication is needed through additional research to confirm the above patterns. In addition, the noted changes might only be for the types of microwave exposure used, i.e., for the SARs of 0.6 and 6 W/kg of pulsed microwave radiation for 30 min. We note that significant changes in behavior associated with microwave exposure were primarily due to exposure at 6 W/kg, which caused a significant increase in colonic temperature. The increased temperature would have explained changes in activity at 1.5 h while the animal could still be recovering from the increased temperature, but only weak indications of change with microwave exposure were found at this time point. The somewhat surprising changes with microwave exposure at 1 week after exposure, however, might be due to some sort of delayed effect of the increased temperature, perhaps reflecting changes in the central nervous system initiated by microwave exposure.

We can summarize changes in rat activity after 3-NP injection by the following:

- Horizontal activity does not change at 3.5 h, 1 week, and 2 weeks after injection.
- Changes in vertical activity and stereotypical activity can be detected 3.5 h after injection.
- Vertical activity and stereotypical activity are not different from respective controls at 1 week and 2 weeks after injection.

Of course, replication of the 3-NP results would confirm the above patterns.

Measures of horizontal movement (locomotion) here are most like measures of locomotion made by counting line crossings on an open-field grid. The lack of change in locomotion here at 1.5 h (and 25.5 h) after whole-body microwave exposure is consistent with the lack of change seen immediately after exposure and at 24 h for rats after microwave exposure of the head [4,5]. Based on results here, measurements of horizontal activity, as well as stereotypical activity, at 1 week after exposure might be more sensitive to change occurring in the central nervous system and thus more useful in detecting effects of microwave exposure. Of course, changes might not peak at exactly 1 week so that a delay a little longer or a little shorter might be even more sensitive.

The spontaneous horizontal and vertical motor activities measured here involve exploration of the environment. The stereotypical activity here is associated with rapid, repetitive movements such as might occur in grooming. These motor activities are among those that are initiated and coordinated by neural pathways that include basal ganglia and cerebellum [17-20], sites at which changes in neurotransmitter receptors have been found after microwave exposure [4,5]. If changes in receptors lead to changes in activity 1 week later, as seems to be indicated here, then long-term changes in the involved neural circuits might be occurring.

A key observation here is that different results can be obtained for activity at different times after exposure. Dependency on time has been noted for other types of behavior after various microwave exposures [13]. Although results here are for two 30-min exposures to pulsed microwaves, they might well apply in general to other exposure schedules, including single 30-min exposures as well as chronic exposures. Indeed, results seen after chronic exposure could possibly be due to delayed effects of the first 30 min, or so, of exposure and not to cumulative effects of prolonged exposure.

Acknowledgments

MOTOR ACTIVITY FACTORS

This work is supported by the U.S. Army Medical Research and Materiel Command under contract DAMD17-94-C-4069 awarded to McKesson BioServices Corporation. The views, opinions and/or findings contained in this report are those of the author(s) and should not be construed as an official Department of the Army position, policy or decision unless so designated by other documentation. In conducting research using animals, the investigator(s) adhered to the "Guide for the Care and Use of Laboratory Animals" prepared by the Institute of Laboratory Animal Resources, National Research Council (Washington, DC: National Academy Press, 1996). This article is a US Government work and, as such, is in the public domain in the United States of America. WRAIR is the Walter Reed Army Institute of Research in Washington, DC USA. The FPS-7B radar transmitter was used through an agreement with the U.S. Naval Health Research Center Detachment, Brooks AFB.

MOTOR ACTIVITY FACTORS

References

[1] D'Andrea JA. 1999. Behavioral evaluation of microwave irradiation. Bioelectromagnetics 20(Suppl. 4):64-74.

[2] Lai H. 1994. Neurological effects of radiofrequency electromagnetic radiation. In Lin JC (ed): Advances in Electromagnetic Fields in Living Systems, Vol. 1. New York: Plenum Press. pp 27-80.

[3] Lai H. 1992. Research on the neurological effects of nonionizing radiation at the University of Washington. Bioelectromagnetics 13(6):513-526.

[4] Mausset AL, de Seze R, Montpeyroux F, Privat A. 2001. Effects of radiofrequency exposure on the GABAergic system in the rat cerebellum: Clues from semi-quantitative immunohistochemistry. Brain Res 912(1):33-46.

[5] Mausset AL, Hirbec H, Vignon J, Privat, De Seze R. 2002. Effects of high power 900 MHz microwaves on neurotransmission in the rat brain. Bioelectromagnetics Society Annual Meeting Abstracts 24:115-116.

[6] Testylier G, Tonduli L, Malabiau R, Debouzy JC. 2002. Effects of exposure to low level radiofrequency fields on acetylcholine release in hippocampus of freely moving rats. Bioelectromagnetics 23(4):249-255.

[7] Testylier G, Hugon M, Debouzy JC. 2002. Acetylcholine release in hippocampus of free moving rats exposed to low energy 915 MHz radiofrequency fields: Effect of low frequency amplitude modulation. Bioelectromagnetics Society Annual Meeting Abstracts 24:243-244.

[8] Lai H, Horita A, Guy AW. 1994. Microwave irradiation affects radial-arm maze performance in the rat. Bioelectromagnetics 15(2):95-104.

[9] Wang B, Lai H. 2000. Acute exposure to pulsed 2450-MHz microwaves affects water-maze performance of rats. Bioelectromagnetics 21(1):52-56.

[10] Dubreuil D, Jay T, Edeline JM. 2002. Does head-only exposure to GSM-900 electromagnetic fields affect the performance of rats in spatial learning tasks? Behav Brain Res 129(1-2):203-210.

[11] Cobb BL, Adair ER. 2002. Radial-arm maze performance in rats following repeated low level microwave (MW) radiation. Bioelectromagnetics Society Annual Meeting Abstracts 24:23-24.

[12] Lai H, Carino MA, Horita A, Guy AW. 1992. Single vs. repeated microwave exposrue: Effects on benzodiazepine receptors in the brain of the rat. Bioelectromagnetics 13(1):57-66.

[13] Navakatikian MA, Tomashevskaya LA. 1994. Phasic bahavioral and endocrine effects of microwaves of nonthernal intensity. In Carpenter DO, Ayrapetyan S (eds): Biological Effects of Electric and magnetic fields, Vol. 1. San Diego: Academic Press. pp 333-342.

[14] Alexi T, Hughes PE, Knusel B, Tobin AJ. 1998. Metabolic compromise with systemic 3-nitropropionic acid produces striatal apoptosis in Sprague-Dawley rats but not in BALB/c ByJ mice. Exp Neurol 153(1):74-93.

[15] Guyot MC, Hantraye P, Dolan R, Palfi S, Maziére M, Brouillet E. 1997. Quantifiable bradykinesia, gait abnormalities and Huntington's disease-like striatal lesions in rats chronically treated with 3-nitropropionic acid. Neuroscience 79(1):45-56.

[16] Seaman RL, Mathur SP, Dick EJ, Jr, Gonzalez MY. 2000. Effects of microwave exposure and 3-nitropropionic acid on rat activity, acoustic startle, and brain histology. Bioelectromagnetics Society Annual Meeting Abstracts 22:285-286.

[17] Hauber W. 1998. Involvement of basal ganglia transmitter systems in movement initiation. Prog Neurobiol 56:507-540.

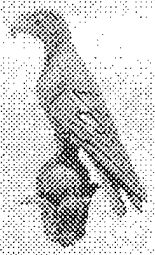
[18] Canales JJ, Graybiel. 2000. A measure of striatal function predicts motor stereotypy. Nature Neurosci 3(4):377-383.

[19] Middleton FA, StrickPL. 2000. Basal ganglia and cerebellar loops: Motor and cognitive circuits. Brain Res Rev 31(2-3):236-250.

[20] Thompson RF, Kim JJ. 1996. Memory systems in the brain and localization of a memory. Proc Natl Acad Sci U S A 93(24):13438-13444.

BIOLOGICAL EFFECTS of EMFs

2nd INTERNATIONAL WORKSHOP

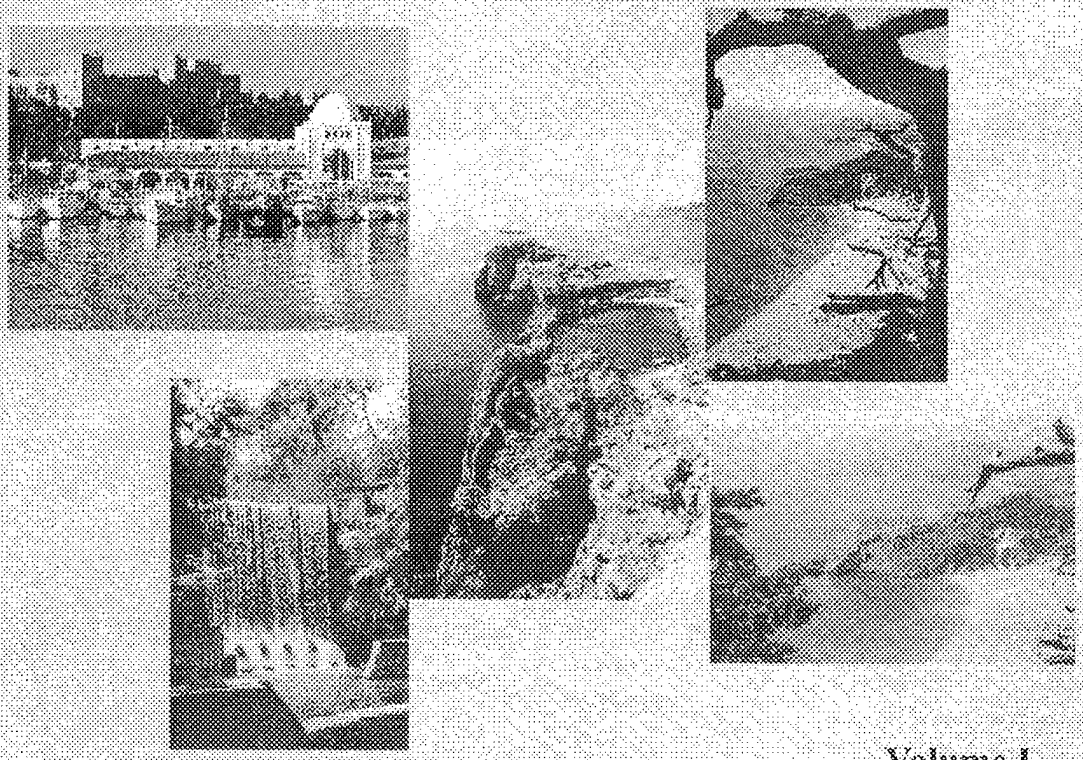




Electronics - Telecom & Applications Laboratory
Physics Department
University of Ioannina

Institute of Informatics & Telecommunications
N.C.S.R. "Demokritos"

Proceedings



Volume I

Rhodes, Greece, 7 -11 October, 2002

MICROWAVE HEARING PATHWAY

TRANSMISSION OF MICROWAVE-INDUCED INTRACRANIAL SOUND TO THE INNER EAR IS MOST LIKELY THROUGH CRANIAL AQUEDUCTS

RONALD L. SEAMAN
MCKESSON BIOSERVICES CORPORATION
AT WRAIR US ARMY MEDICAL RESEARCH DETACHMENT
8308 HAWKS ROAD, BUILDING 1168, BROOKS AIR FORCE BASE, TEXAS 78235 USA

Abstract

The most frequently cited sequence of events used to explain auditory sensations resulting from microwave pulses, or "microwave hearing", starts with transduction of microwave energy to sound in the head. In this explanation, the sound is then transmitted through cranial bones, i.e., by bone conduction, to stimulate hair cells in the inner ear. Recently reported experiments with animals and humans indicate that sound conduction through bone itself is not necessary in bone-conduction hearing. Instead, sound generated inside the cranium is most efficiently transmitted through holes in the cranium that form channels to the inner ear: vestibular aqueduct, cochlear aqueduct, and/or perivascular and perineural spaces. The short latency of cochlear microphonics reported for microwave hearing and the oscillation of the microphonics at the calculated brain resonant frequency are consistent with transmission through the channels. Thus, the channels are the most likely pathway for transmission of sound to the inner ear in microwave hearing. Consideration of this transmission pathway may be useful in reconciling results from various microwave hearing experiments.

Introduction

Microwave hearing is the auditory perception of microwave pulses impinging on the head, which has been reviewed in the literature [1-3]. The chain of events described in these reviews starts with generation of acoustic energy (sound) in the head. The sound produced is transmitted by bone conduction to the inner ear where it stimulates auditory receptors in the cochlea. The resulting neural signal is then processed normally by the auditory nervous system. Understanding processes involved in microwave hearing is important because of the use of microwave hearing thresholds in setting limits for human exposure to microwave pulses [4].

Fig. 1 shows principal components of the mammalian inner ear for reference and locations of the components within the temporal bone. The figure is adapted from images created by Alec N. Salt, Washington University [http://oto.wustl.edu/cochlea/intro1.htm].

Fig. 2 emphasizes acoustic pathways in a schematic diagram of the inner ear and nearby tissues. The cochlear aqueduct connection with the cochlea is much closer to the middle ear than depicted in this figure. Cranial contents are represented by brain tissue and cerebral spinal fluid (CSF) in Fig. 2. Distance between CSF and the temporal bone is exaggerated in both figures for clarity.

The most likely mechanism for transduction of a pulse of microwave energy to sound in tissue is thermoelastic expansion during the pulse [1-3,5-7]. Mathematical models of thermoelastic expansion in spherical heads having the dielectric properties of brain tissue predict that the generated sound has a fundamental resonant frequency determined only by head size [3,6]. Characteristics of sound measured in spherical tissue models and animal heads of different sizes are consistent with the prediction [7-9]. In addition, the round-window cochlear microphonic, which represents the acoustic waveform in the cochlea, recorded in animals in response to a microwave pulse oscillates near the calculated resonant frequency for the head being exposed [2,3,10,11].

Reports of and reviews on microwave hearing that mention bone conduction of sound to the inner ear [1-3,5,12] do not distinguish among the several known mechanisms of bone conduction. Stimulation of auditory receptors in the cochlea by bone conduction, differentiated from stimulation by air condution through the external meatus, was previously thought to occur through the following three pathways: (1) relative motion of inner ear contents due to inertial lag, (2) relative motion of inner ear contents due to distortion of the bony cochlear shell, and (3) coupling of energy to air in the external meatus [13,14]. These pathways, all of which depend on sound transmission in bone, are depicted in Fig. 2 by two curved arrows originating near the bone stimulator, a device commonly used to elicit auditory responses by bone conduction. The solid arrow directed to the cochlea represents the first two pathways. The dashed arrow directed to the external meatus-middle ear region is dashed to indicate the minor contribution of the third pathway to bone-conduction hearing unless the

MICROWAVE HEARING PATHWAY

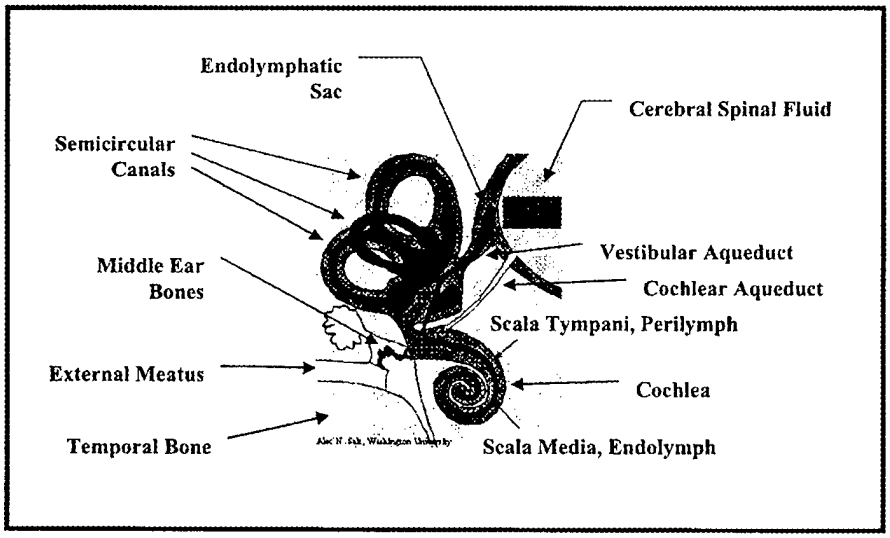


Figure 1. A diagram of the mammalian inner ear.

external meatus is blocked. Because microwave hearing literature sites work on bone-conduction hearing tested with a bone stimulator [15], a pathway through bone of the type represented by the solid arrow from the bone stimulator and to the cochlea in Fig. 2 was probably intended. Of course, when the source of sound is inside the cranium, the pathway through bone originates at the interior surface of temporal bone rather than the exterior.

An additional pathway for sound transmission to the inner ear by bone conduction has recently been discovered in experiments on rodents and humans [14,16]. This pathway is not through bone tissue itself but through channels that connect cranial contents with the inner ear. This pathway is shown in Fig. 2 as a curved

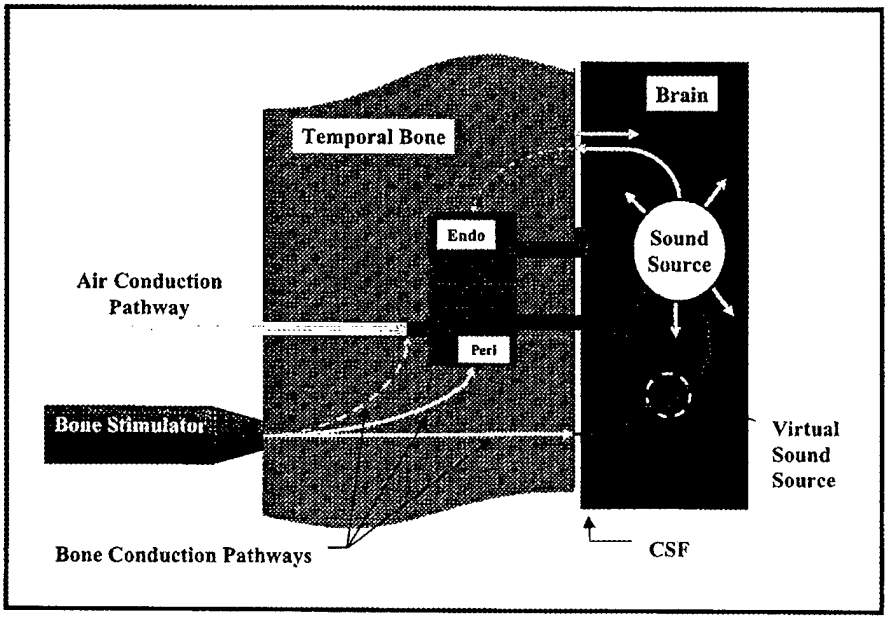


Figure 2. Sound pathways in air- and bone-conduction hearing.

arrow originating near the bone stimulator, passing as two branches (one partially obscured) into cranial contents, and then through channels in the bone into the inner ear. The channels likely contributing most to transmission in this pathway are the vestibular and cochlear aqueducts, as shown Fig. 2. Channels through which nerves and blood vessels travel provide additional possible paths for sound transmission in parallel with the aqueducts. Together these channnels constitute a "non-osseous" pathway that accounts for most of the sound transmitted to the cochlea in bone-conduction hearing [14,16].

An experimental finding in the recent bone-conduction experiments is that sound in cranial contents capable of stimulating the inner ear does not produce detectable vibration of bone [14,16]. This was tested in a number of ways that included placing a bone stimulator directly on the dura mater, which covers the CSF. Stimulation of the amphibian inner ear has also been observed by tapping exposed dura [17]. We can expect that sound generated by absorption of microwave pulses inside the cranium travels to the inner ear by the same pathway. Sound generation within the cranial contents, say, by microwave absorption, is represented in Fig. 2 by a sound source located in the brain. The pathway to the inner ear is shown by curved arrows originating at the sound source and passing through the aqueducts. An arrow from the sound source to bone is shown to represent generated sound that is transmitted into bone. Because of the difference in acoustic impedance at the CSF-bone interface [14], most of the sound is reflected back into intracranial soft tissues (straight arrow) and very little is transmitted into bone (dashed curved arrow).

At least two observations in microwave hearing research provide support for the proposed direct pathway for sound transmission. One is the correspondence between the frequency of cochlear microphonic oscillations and the calculated resonant frequency of the brain [2,3,11]. If sound generated intracranially were to couple to bones of the skull we would expect resonant vibration of the skull to be reflected in the cochlear microphonic. The resonant frequency of the adult human skull is 1-2 kHz [18-20]. This is about one-tenth of the predicted brain resonant frequency of 11 kHz for microwave hearing in adults [3]. In the absence of data on animal skulls, we might expect a similar ratio between resonant frequencies of brain and skull for other mammals. However, only the higher frequency of brain resonance is observed in cochlear microphonic oscillations. Lack of skull vibration is consistent with vibration not being detected with exposure to microwave pulses [21].

Another relevant observation is the short delay of less than 40 μs between onset of microwave pulse and start of cochlear microphonic in animals [2,10,11]. Auditory responses to bone stimulation can be expected to be delayed 0.1-0.5 ms (100-500 μs) from stimulus onset, depending on type of animal, location of stimulus, and other factors [22-23]. We might also expect a delay due to mass inertia of the skull and the relatively low resonant frequency of the skull. Propagation delays of sound travelling between points on the skull and low-pass filtering by the skull have been measured with bone stimulation [23]. One might suggest that a later, slower component of the microwave cochlear microphonic might have been overlooked in microwave hearing experiments because of the short time window used to study the high-frequency cochlear microphonic at the round window. However, one would expect that a microphonic component of comparable or larger amplitude, as well as being less impacted by the early microwave-pulse-induced artifact, would be easily identified before detailed observations of the high-frequency component were made. The short latency of the only or, perhaps, the most dominant microwave cochlear microphonic is inconsistent with forms of bone conduction that involve vibration of the bone.

Summary

Based on a number of considerations, we can reasonably conclude that the pathway for transmission of sound from intracranial tissues to the inner ear in microwave hearing is through various channels in bone that connect to the intracranial space to the inner ear. This pathway appears to dominate over other pathways in bone-conduction hearing and can be driven by bone-conducted sound, but the pathway through bone does not require that sound actually travel in the bone itself. The previously proposed pathway for sound transmission to the cochlea in microwave hearing that includes bone vibration is most likely not the pathway. This observation should be useful in reconciling results from various experiments on microwave hearing. Results from future microwave hearing experiments to test for non-osseous bone conduction can be considered in setting exposure limits for microwave pulses.

Acknowledgments

This work is supported by U.S. Army Medical Research and Materiel Command contract DAMD17-94-C-4069 awarded to McKesson BioServices Corporation. The views, opinions and/or findings contained in this report are those of the author(s) and should not be construed as an official Department of the Army position, policy or decision unless so designated by other documentation. This article is a US Government work and, as such, is in the public domain in the United States of America. WRAIR is the Walter Reed Army Institute of Research in Washington, DC USA. The author is grateful to Dr. Clifford Sherry for various stimulating discussions on microwave hearing topics.

References

[1] Lin JC. 1980. The microwave auditory phenomenon. Proc IEEE 68(1):67-73.

[2] Chou CK, Guy AW, Galambos R. 1982. Auditory perception of radio frequency electromagnetic fields. J Acoust Soc Am 71(6):1321-1334.

[3] Lin JC. 1990. Auditory perception of pulsed microwave radiation. In Gandhi OP (ed): Biological Effects and Medical Applications of Electromagnetic Fields. New York: Prentice-Hall, pp 277-318.

[4] International Commission on Non-Ionizing Radiation Protection. 1998. Guidelines for limiting exposure to time-varying electric, magnetic, and electromagnetic fields (up to 300 GHz). Health Phys 74(4):494-522.

[5] Foster KR, Finch ED. 1974. Microwave hearing: Evidence for thermoacoustic auditory stimulation by pulsed microwaves. Science185(147):256-258.

[6] Lin JC. 1978. Microwave Auditory Effects and Applications. Springfield,Illinois: Charles C. Thomas.

[7] Lin JC, Su JL, Wang Y. 1988. Microwave-induced thermoelastic pressure wave propagation in the cat brain. Bioelectromagnetics 9(2):141-147.

[8] Olsen RG, Lin JC. 1981. Microwave pulse-induced acoustic resonances in spherical head models. IEEE Trans Microwave Theory and Tech 29(10):1114-1117.

[9] Olsen RG, Lin JC. 1983. Microwave-induced pressure waves in mammalian brains. IEEE Trans Biomed Eng 30(5):289-294.

[10] Chou CK, Galambos R, Guy AW, Lovely RH. 1975. Cochlear microphonics generated by microwave pulses. J Microwave Power 10(4):361-367.

[11] Chou CK, Guy AW, Galambos R. 1977. Characteristics of microwave-induced cochlear microphonics. Radio Sci 12(6S):221-227.

[12] Chou CK, Galambos R. 1979. Middle-ear structures contribute little to auditory perception of microwaves. J Microwave Power 14(4):321-326.

[13] Tonndorf J. 1972. Bone conduction. In Tobias JV (ed): Foundations of Modern Auditory Theory. New York: Academic Press, pp 197-237.

[14] Freeman S, Sichel JY, Sohmer H. 2000. Bone conduction experiments in animals: Evidence for a non-osseous mechanism. Hear Res 146(1-2):72-80.

[15] Corso JF. 1963. Bone-conduction thresholds for sonic and ultrasonic frequencies. J Acoust Society Am 35(11):1738-1743.

[16] Sohmer H, Freeman S, Geal-Dor J, Adelman C, Savion I. 2000. Bone conduction experiments in humans: A fluid pathway from bone to ear. Hear Res 146(1-2):81-88.

[17] Seaman RL. 2002. Non-osseous sound transmission to the inner ear (letter). Hear Res 166(1-2):218-219.

[18] Håkansson B, Carlsson P, Tjellström A. 1986. The mechanical point impedance of the human head, with and without skin penetration. J Acoust Soc Am 80(4):1065-1075.

[19] Kosugi Y, Ikebe J, Hara S, Takakura K. 1987. Detection and analysis of cranial bruit. IEEE Trans Biomed Eng 34(3):185-191.

[20] Stenfelt S, Håkansson B, Tjellström A. 2000. Vibration characteristics of bone conducted sound *in vitro*. J Acoust Soc Am 107(1):422-431.

[21] Frey AH, Coren E. 1979. Holographic assessment of a hypothesized microwave hearing mechanism. Science 206(4415):232-234.

[22] Sohmer H, Freeman S. 2001. The latency of auditory nerve brainstem evoked responses to air- and bone-conducted stimuli. Hear Res 160(1-2):111-113.

[23] Durrant JD, Hyre R. 1993. Observations on temporal aspects of bone-conduction clicks: Real head measurements. J Am Acad Audiol 4(3):213-219.

Microwave Bioeffects
Body Borne Antennas and L-Band

Presentation to the USAMRMC Medical
Technology Review Panel F

By

Shin-Tsu Lu, BVM, Ph.D., Project Manager
McKesson BioServices / USAMRD Microwave Bioeffects Branch
Brooks City-Base, TX 78235-5323

October 20 – 22, 2003

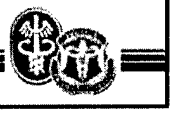
McKESSON
Empowering Healthcare

USAMRD - WRAIR, BROOKS CITY-BASE, TX, U.S.A.



BODY BORNE ANTENNAS[1]

- Army's transformation to the Objective Force requires mobile forces and command and control capability while on the move. Body Borne Antennas facilitate communications in such a scenario.
- Body Borne antennas are part of Antennas for communication Across the Spectrum (ACAS) and Advanced Antennas Technology Demonstration (TD) in survivability lethality analysis directorate of C4I (Command, Control, Communication, Computers, and Intelligence).
- Body Borne antennas are being developed to provide communication in the frequency range of 2 MHz - 44 GHz, with higher gain, bandwidth, high data-rate, and greater agility for on-the-move (OTM) networked systems.
- Body Borne Antennas are being developed and tested for Small Unit Situational awareness System (SUOSAS), Dismounted Battlespace Battle Laboratory (DBBL), and the Land Warrior program.



BODY BORNE ANTENNAS[2]

- Body Borne Antennas are part of the future Joint Tactical Radio System (JTRS) and ACAS TD.
- Advanced Antenna TD (2000 – 2006) aims to develop a family of efficient, practical, cost-effective antennas that reduces co site and control problems; provide greater agility for OTM operations and lower profiles, reduces platform, and visual signatures. Body Borne Antennas fit the requirements.
- Navy's COMWIN (Combat Wear Integration) project includes development of several body borne antennas in the frequency range of 2 – 2000 MHz.
- Communication at several frequencies simultaneously is envisaged

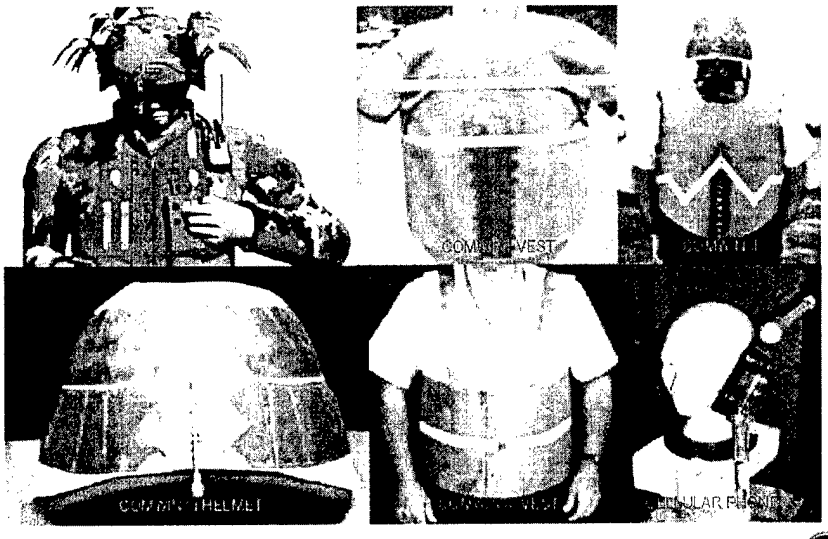


BODY BORNE ANTENNA[3]

- Body Borne (or Body Worn) antennas can be:
  - Integrated into the BDU or worn over the BDU as vest.
  - Mounted on the Man Pack carried by the soldier.
  - Mounted on the helmet.
  - Mounted as shoulder patches on the soldier.
- Non-Military Applications of Body Borne (or Body Worn) antennas can be:
  - Body Area Networks: Personal, mobile LANs where human body is used as a network node.
  - Body Worn Antennas for Tactical Video Systems used in:
    - Remote Surveillance
    - SWAT Operations
    - Emergency Response
    - Training
  - Embedded or body worn antennas in medical telemetry systems.

McKESSON Empowering Healthcare — USAMRD - WRAIR, BROOKS CITY-BASE, TX, U.S.A.

EXAMPLES OF BODY BORNE ANTENNAS



McKESSON Empowering Healthcare — USAMRD - WRAIR, BROOKS CITY-BASE, TX, U.S.A.

BODY BORNE ANTENNAS
ISSUES IN HEALTH HAZARD ASSESSMENT (HHA)[1]

- US Army requires human factors analysis (HFA) & HHA safety release as per DoD Instruction Number 6055.11, before deploying body borne antennas. Body borne antennas do not fall under the low power device exception since they are mounted within less than 2.5 cm from the body.
- HFA includes calculations of impact of body losses and RF exposure of human body to antenna performance, i.e., gain and radiation pattern.
- HHA includes calculation and/or measurement of RF energy deposited in the human body from Body Borne antennas and its potential health impacts on Soldiers.
- There is complex interaction between RFR and complex biological system (human body), possibly in a multi-frequency environment.

McKESSON *Empowering Healthcare* USAMRD - WRAIR, BROOKS CITY-BASE, TX, U.S.A.



BODY BORNE ANTENNAS
ISSUES FOR HEALTH HAZARD ASSESSMENT (HHA)[2]

- Current knowledge base is insufficient to address health and safety issues raised by the RFR exposure from the deployment of the body borne antennas especially, partial body and multiple frequency RFR exposures. Biological database on multiple frequency RFR exposures is virtually none. Current practice is by limiting the sum of ratio to maximum permissible exposure incurred within each contributing frequency interval to less than unity. Guidelines for multiple frequency partial body exposure are not available.

McKESSON *Empowering Healthcare* USAMRD - WRAIR, BROOKS CITY-BASE, TX, U.S.A.



APPLICABLE PERSONNEL PROTECTION GUIDELINES/STANDARDS[1]

- ARMY REGULATION 11-9, THE ARYMY RADIATION SAFETY PROGRAM: referring to DoDI 6055.11
- DEPARTMENT OF DEFENSE INSTRUCTION DoDI 6055.11-1999, PROTECTION OF DoD PERSONNEL FROM EXPOSURE TO RADIO FREQUENCY RADIATION: adapting from IEEE C95.1-1999, an revision of the IEEE C95.1-1991, an revision of American National Standards Institute C95.1-1982
- INSTITUTE OF ELECTRICAL AND ELECTRONICS ENGINEERS, INC IEEE Std C95.1-1999, IEEE STANDARD FOR SAFETY LEVELS WITH RESPECT TO HUMAN EXPOSURE TO RADIO FREQUENCY ELECTROMAGNETIC FIELDS, 3 kHz TO 300 GHz

McKESSON Empowering Healthcare — USAMRD - WRAIR, BROOKS CITY-BASE, TX, U.S.A.

APPLICABLE PERSONNEL PROTECTION GUIDELINES/STANDARDS[2]

- FEDERAL COMMUNICATIONS COMMISSION OET65, EVALUATING COMPLIANCE WITH FCC GUIDELINES FOR HUMAN EXPOSURE TO RADIOFREQUENCY ELECTROMAGNETIC FIELDS: adapting from National Council on Radiation Protection and Measurements Report 86 and American National Standards Institute ANSI C95.1-1982
- INTERNATIONAL COMMISSION ON NON-IONIZING RADIATION PROTECTION, GUIDELINES FOR LIMITING EXPOSURE TO TIME-VARYING ELECTRIC, MAGNETIC, AND ELECTROMAGNETIC FIELDS (UP TO 300 GHz)

McKESSON Empowering Healthcare — USAMRD - WRAIR, BROOKS CITY-BASE, TX, U.S.A.

QUANTITY AND UNIT IN PERSONNNEL PROTECTION AGAINST RADIO FREQUENCY RADIATION

- POWER DENSITY (S): W/m² (in U.S. mW/cm² = 10 W/m²)

$$S = E \times H = \frac{E^2}{377} = 377\,H^2$$

  - ELECTRIC FIELD STRENGTH (E): V/m $\quad E = \frac{F}{q}$
  - MAGNETIC FIELD STRENGTH (H): A/m $\quad H = \frac{B}{\mu}$
  - MAGNETIC FLUX DENSITY (B): T (Wb/m²) $\quad \frac{F}{q} = (v \times B)$

- SPECIFIC ABSORPTION RATE (SAR): W/kg

$$SAR = \frac{d}{dt}\left(\frac{dW}{dm}\right) = \frac{d}{dt}\left(\frac{dW}{\rho\, dV}\right) = \frac{\sigma\, E^2}{\rho}$$

- SPECIFIC ABSORPTION (SA): J/kg $\quad SA = \frac{dW}{dm} = \frac{dW}{\rho\, dV}$

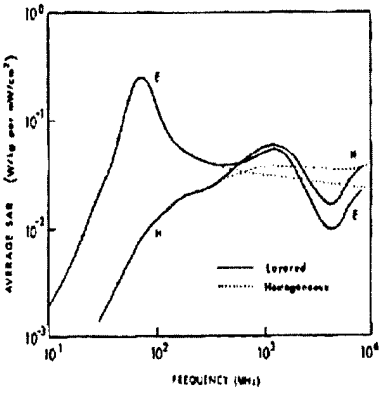
McKESSON Empowering Healthcare — USAMRD - WRAIR, BROOKS CITY-BASE, TX, U.S.A.

FACTORS THAT AFFECT ABSORPTION OF RADIO FREQUENCY RADIATION

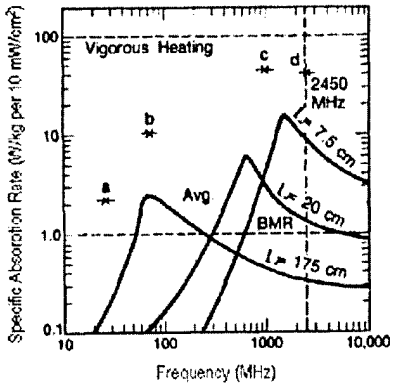
- Physical parameters of the electromagnetic source
  - Frequency
  - Polarization
  - Modulation (AM, FM, pulse, CW)
  - Field pattern (near, intermediate, or far field: uniformity)
  - Measuring technique
  - Calibration technique
  - Power
  - Transmitting and radiating equipment
  - Environment (e.g., surrounding material and dimensions)
- Biological Parameters
  - Tissue dielectric properties
  - Size and geometry
  - Relation to polarization
  - Spatial relations of objects (e.g. humans, animals)
- Artifacts
  - Ground or conductor plate
  - Container for experimental animals (material, size)
  - Metallic implants
  - Shielding materials
  - Metallic or nonmetallic objects in the field

McKESSON Empowering Healthcare — USAMRD - WRAIR, BROOKS CITY-BASE, TX, U.S.A.

EXAMPLES OF ORIENTATION AND SIZE-DEPENDENT ABSORPTION OF RADIO FREQUENCY RADIATION

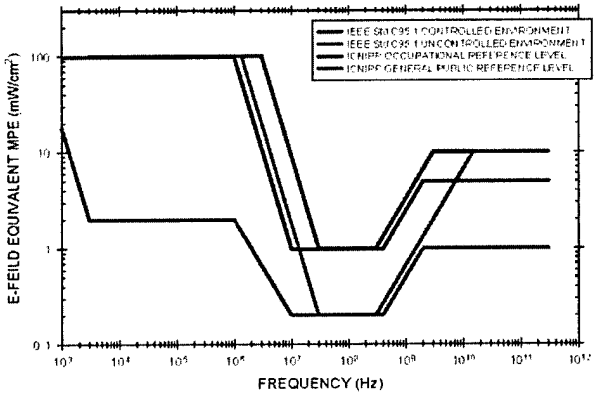


*Absorption of radio frequency is highly dependent on the orientation of object to field polarization.



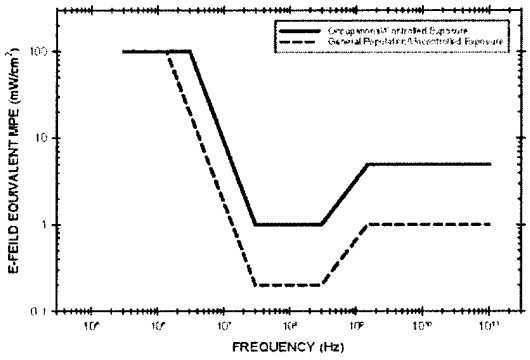
*Prolate spheroids of various length. a and b: models of human beings, c: rats d: mice.

IEEE C95.1-1999 AND ICNIRP GUIDELINES



- Both of these guidelines adapt two-tier standards for occupational (controlled environment) and general population (uncontrolled environment) exposures. They were derived from approximately the same database, and the same threshold whole-body average SAR of 4 W/kg (work stoppage or decrement in operant behavior). Modifiers (safety factors) of 10 (0.4 W/kg) and 50 (0.08 W/kg) were then applied to obtain the reference SAR. MPE and Reference Level were derived from these reference SARs by taking into the consideration of frequency dependent absorption of various size of human being from infant to adult.

FCC (NCRP) LIMITS FOR MAXIMUM PERMISSIBLE EXPOSURE (MPE) PLANE-WAVE EQUIVALENT POWER DENSITY

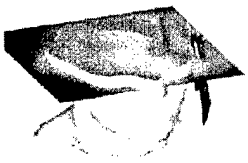


- FCC regulates the transmitter output power through licensing Cellular phones are within FCC's regulatory authority. Again, the FCC's MPEs were adaptation of an older version of guidelines proposed by NCRP (1986). The two-tier MPEs were derived from the same reference SAR as IEEE and ICNIRP. The lowest MPE for occupational/controlled exposure (1 mW/cm^2) and general population/uncontrolled exposure (0.2 mW/cm^2) are also the same as IEEE and ICNIRP.

COMPLIANCE OF BODY BORNE ANTENNAS TO CURRENT REGULATION/INSTRUCTION/GUIDELINES/STANDARDS

- Similar to cellular phones, radiating elements of body borne antennas are within less than 2.5 cm from the body. Instead of whole-body exposure, partial-body exposure is anticipated.





  - Field measurements do not apply. Whole-body average SAR and local SARs are to be calculated or measured to be in compliance with personnel protection guidelines or standards. The reference local SARs are 20 times of the reference whole-body average SARs (0.4 and 0.08 W/kg), i.e., 8 W/kg for the controlled (occupational) exposure and 1.6 W/kg for the uncontrolled (general population) exposure. For a 70 kg human, radiating power less than 28 W and 5.6 W will not produce a whole-body average SAR exceeding 0.4 W/kg and 0.08 W/kg.

RF INDUCED CURRENT CONSIDERATIONS OF BODY BORNE ANTENNAS IN COMPLIANCE WITH DoDI 6055.11

- Body borne antennas are to be operated at frequency below 100 MHz. Radio frequency induced current and contact current restrictions are applicable.

	Frequency Range (MHz)	Maximum Current Through Both Feet (mA)	Maximum Current Through Each Foot (mA)	Contact Current (mA)
Controlled Environment	0.003 – 0.1	2000 f*	1000 f*	1000 f*
	0.1 – 100	200**	100**	100**
Uncontrolled Environment	0.003 – 0.1	900 f*	450 f*	450 f*
	0.1 – 100	90***	45***	45***

* Average rms induced current (mA) over any 1 second period.
** Average rms induced current (mA) over any 6 minute period subject to a ceiling limit of 500 mA (for an averaging time of 1/25 of the normal averaging time).
*** Average rms induced current (mA) over any 6 minute period subject to a ceiling limit of 220 mA (for an averaging time of 1/25 of normal averaging time).

OTHER CONCERNS[1]

- Lack of uniformity and differences in the permissible exposure levels internationally
  - o In selected frequency band, Eastern European PELs can be two or more orders of magnitude (1 – 10 $\mu W/cm^2$) lower than those of Western countries.
  - o PELs of Western countries base on threshold of adverse effects (hazard) on a "SAR" base while Eastern European countries base on effects on a "dose" and effects approach.
  - o Internal harmonization is ongoing but differences have not been resolved.
- Controversies in biological effects of radio frequency radiation continue, e.g., the recent results of genotoxicity studies perform by the EU-funded REFLEX (Risk Evaluation of Potential Environmental Hazards From Low Energy Electromagnetic Field Exposure Using Sensitive *In Vitro* Method).

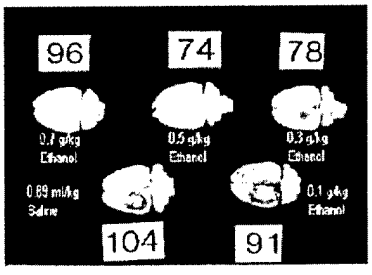
OTHER CONCERNS[2]

- Unsettled carcinogenicity potential and experiments are still in progress or being planned.
- Limited database of applicable partial-body exposure on biological systems is available and those available point to partial-body RF exposure may induce unexpected results.
  - o Biological effects induced by partial-body exposure can be observed in absence of or with minimal increase in core body temperature.
  - o Abnormal physiological responses can occur by partial-body RF exposure.

McKESSON Empowering Healthcare — USAMRD - WRAIR, BROOKS CITY-BASE, TX, U.S.A.

LOCALIZED EFFECT OF RF ON BLOOD-BRAIN BARRIER

- Blood-brain barrier interruption indicated by permeation of Evans blue dye could be induced in barbiturate-anesthetized male Wistar rats using an Elmed dielectric loaded 12 mm applicator locally on the surface of skull at 3.15 GHz, 3.0 W/cm^2 for 15 minutes.

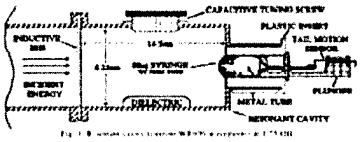


- Depending on ethanol does, brain temperature increased during the first 4–5 min and stabilized at 43 to 48 °C for the remainder of the exposure period.
- Colonic temperature was not affected and remained at 37.2 to 37.5 °C.
- Blood-brain barrier interruption depended on ethanol doses: enhanced at 0.1 g/kg, reduced with graded doses of ethanol and disappeared entirely at 0.7 g/kg.
- Ethanol interaction on RF-induced blood-brain barrier appeared to associate with the effect of ethanol on brain temperatures.

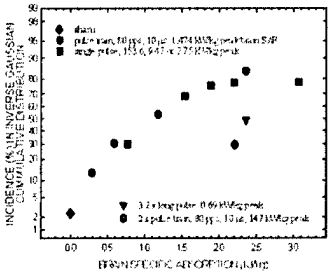
McKESSON Empowering Healthcare — USAMRD - WRAIR, BROOKS CITY-BASE, TX, U.S.A.

MICROWAVE EVOKED WHOLE-BODY MOVEMENTS (L-band)

- In mice and rats, microwave pulse or pulse train of sufficient intensity can evoke whole-body movements similar to "startle" reflex caused by sudden and unexpected intense visual, auditory or tactile stimuli.



- The effect is independent of pulse modulation or peak SAR and the probability of occurrence is dependent on SA but not on peak SAR.
- Evoked body movements occur in absence of changes in T_{core} but highly dependent on change in local T_{sk}.

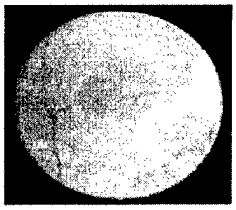


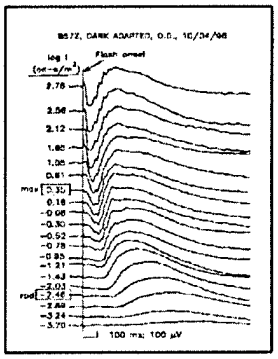
- Absolute threshold T_{sk} is estimated at 1.2 °C in mice. Incidence reaches a maximum at 1.66 °C (78% incidence). A lower Tsk was noted (15% at 0.2 °C and 80% at 0.65 °C) in rats irrespective of similar brain SAs.
- Microwave evoked body movements do not require an intact hearing and pulse duration longer than 1 s is less effective.

McKESSON *Empowering Healthcare* — USAMRD - WRAIR, BROOKS CITY-BASE, TX, U.S.A.

RETINAL STUDY (L-BAND USAMRD)

- 17 Rhesus monkeys (Mcacaca mulatto, 6 males, 11 females), 4 to 9.5 year old, 4.3 to 8.8 kg free of physical defect, tuberculosis and B virus, clinically healthy and free of ocular defects
- Localized facial exposures at 1.25 GHz, 1.30 MW/kg peak, 5.59 μs pulse width from FPS-7 transmitter; average ocular SAR of 0, 4.3, 8.4 and 20.2 W/kg achieved by 0, 0.59, 1.18 and 2.79 Hz pulse repetition rate; 4 hrs / day, 3 days / wk for 3 wks



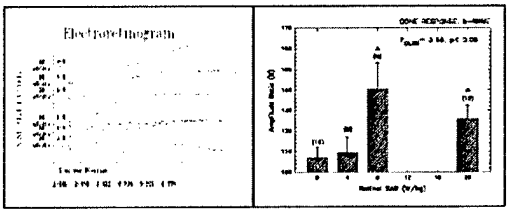


- Ocular endpoints
  - Pre- and post-exposure fundus photography
  - Pre- and post-exposure fluroscein and indocyanine angiography
  - Pre- and post-exposure electroretinogram: scotopic intensity response curve (rod b-wave amplitude and implicit time, combined a-wave and b-wave amplitude and implicit time, Naka-Rushton constants), scotopic 30 Hz flicker response (oscillatory potential) and photopic cone response (a-wave and b-wave amplitude and implicit time)
  - Post-exposure retinal histopathlogy

McKESSON *Empowering Healthcare* — USAMRD - WRAIR, BROOKS CITY-BASE, TX, U.S.A.

RESULTS OF THE RETINAL STUDY (L-BAND USAMRD)[1]

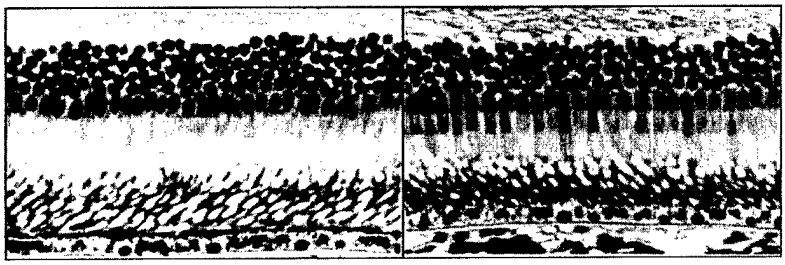
- Facial exposure up to 20 W/kg ocular average SAR could increase facial surface temperature by 4 to 5 °C but never exceeded 34.5 °C.
- Rectal temperature did not increase above the pre-exposure level. Comparing to those of sham-exposed animal, a higher rectal temperature at the end of each exposure was noted in monkeys exposed at 4 and 8 W/kg but not at 20 W/kg.
- No visible changes in clinical morphology, such as fundus pictures and angiographies were found.



- Post-exposure b-wave enhancement of photopic cone response was noted in monkeys exposed at 8 and 20 W/kg ocular average SAR.

RESULTS OF THE RETINAL STUDY (L-BAND USAMRD)[2]

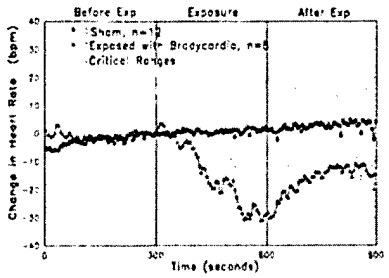
- Increased cone photoreceptor glycogen storage indicated by enhanced uptake of PAS (Periodic Acid Schiff's) stain was found in all the monkeys exposed at 8.4 W/kg (3/3), evenly distributed between sham (2/5) and 20.2 W/kg monkeys (2/5) but none in 4.3 W/kg monkeys (0/4).



- ERG enhancement and alterations in photoreceptor glycogen receptors were not indicative of retinal degeneration. These functional alterations were most likely reversible.

ABNORMAL CARDIOVASCULAR RESPONSES INDUCED BY LOCALIZED MICROWAVE EXPOSURE (L-BAND WRAIR)[1]

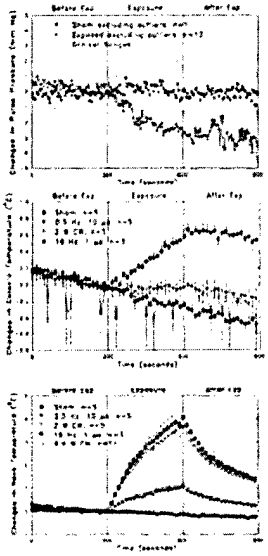
- Ketamine-anesthetized cannulated rat model (350 g), head and neck exposure to pulsed (400 kW, 2 and 6.4 W average) and CW (2 and 6.4 W) of equal SARs for 5 min
- Whole-body average SARs were 0 W/kg, < 5.7 W/kg and < 18.3 W/kg.
- Brain SARs were 0 W/kg, 9.5 W/kg (1.9 MW/kg peak, 10 μs, 0.5 Hz) and 30.4 W/kg (1.9 MW/kg peak, 1 μs, 16 Hz).
- Neck SARs (at carotid bifurcation) were 0 W/kg, 34.3 W/kg (6.86 MW/kg peak, 10 μs, 0.5 Hz) and 109.8 W/kg (6.86 MW/kg peak, 1 μs, 16 Hz).



- Bradycardia developed at 1.5 min into exposure, worsened with duration of exposure and gradually recovered after exposure. Incidence was SAR dependent, 0/12 in shams, 5/23 in low SAR and 13/23 in high SAR groups. CW exposure appeared to cause a severer bradycardia but incidence between CW and pulsed exposures were not distinguishable.

McKESSON Empowering Healthcare — USAMRD - WRAIR, BROOKS CITY-BASE, TX, U.S.A.

ABNORMAL CARDIOVASCULAR RESPONSES INDUCED BY LOCALIZED MICROWAVE EXPOSURE (L-BAND WRAIR)[2]



- Respiration rate and mean arterial pressure were not altered in any exposure groups.
- Decreased pulse pressure, possible indication of decreased stroke volume, was noted in the high SAR groups only and independent on type of radiation (CW vs pulsed).
- In the high SAR group, bradycardia onset occurred at a minimal colonic temperature increase (0.2 °C) and co-varied with gradual increase in colonic temperature to 1.0 °C. The neck temperature at onset of bradycardia and end of exposure were 2 and 4 °C.
- Normal responses of animals to hyperthermia or increased body temperature are to increase heart rate with variable changes in blood pressure and to increase cardiac output to meet the challenge of increased metabolic demand. Bradycardia and decreased pulse pressure were physiologically abnormal responses.

McKESSON Empowering Healthcare — USAMRD - WRAIR, BROOKS CITY-BASE, TX, U.S.A.

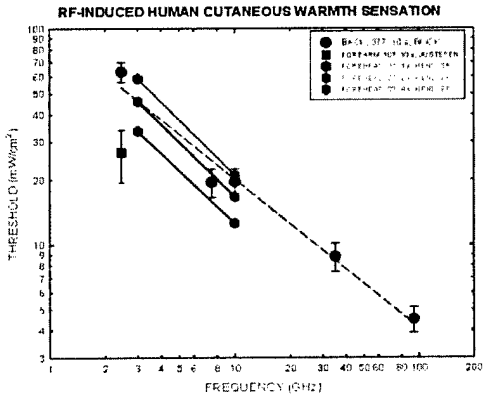
RF-INDUCED HUMAN CUTANEOUS PAIN SENSATION

- Human cutaneous pain sensation can be elicited by localized RF exposure.
- Skin temperature of the RF-induced "burning pain" occurred at 46.1 ± 1.01 °C (S.D.) at 3 GHz and 43.9 ± 0.2 °C (S.E.) at 94 GHz.
- Depending on location, skin temperature of the Infrared-induced "pricking pain" occurred at 42.2 ± 1.4 °C (S.D.) at the back, 44,4 ± 1.01 °C ± 1.6 °C (S.D.) at the forearm, 45.1 ± 1.7 °C (S.D.) at the palm, 45.7 ± 1.01 °C at the forehead and 53.7 ± 2.2 °C at the heel.
- Thermode-induced cutaneous pain sensation had a much lower threshold at 40.2 ± 4.2 °C (S.D.).
- Assuming a 30 °C skin temperature, SA required to elicit cutaneous pain sensation is in the range 42 kJ/kg. For a 10 s threshold, the SAR is 4.2 kW/kg.

McKESSON Empowering Healthcare — USAMRD - WRAIR, BROOKS CITY-BASE, TX, U.S.A.

RF-INDUCED HUMAN CUTANEOUS WARMTH SENSATION

- Human cutaneous warmth sensation can be elicited by localized RF exposure. The RF-induced warmth sensation is dependent on specific absorption, and depth of penetration or wavelength. Measured and calculated increase in skin temperature at threshold is between 0.025 and 0.078 °C, equivalent to 87-271 J/kg effective SA. For a 10 s exposure time, the local SAR is 8.7 to 27.1 W/kg. Other factors are location of skin and possible size of exposure field.



McKESSON Empowering Healthcare — USAMRD - WRAIR, BROOKS CITY-BASE, TX, U.S.A.

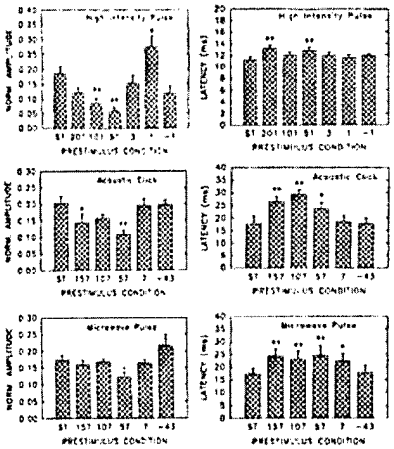
AUDITORY EFFECT – MICROWAVE HEARING

- An audible clicking, buzzing or chirping sensation originating from within and near the back of the head
- Caused by pulsed RF only
- Effective carrier frequency: 216 – 7,500 MHz
- Corresponding to the recurrence rate of microwave pulses
- Thermoelastic expansion of cranial tissue launching an acoustic wave perceived by hair cells in the cochlea
- Dependent on SA per pulse during the first 30 μs of the pulse, 16 mJ/kg in human volunteers, 10 – 12 mJ/kg in cats and 0.9 – 1.8 mJ/kg (WBA-SA) in rats
- Threshold SA on the order of 10^{-6} °C
- Possible annoyance and cause of avoidance behavior in rodent

McKESSON Empowering Healthcare — USAMRD - WRAIR, BROOKS CITY-BASE, TX, U.S.A.

STARTLE MODIFICATION (WRAIR)

- Male Long-Evans rats, 260 – 280 g BW, head-and-neck 1.25 GHz pulsed microwave served as a brief sensory but non-startle-evoking stimulus to modify acoustic, tactile or (photic) startle



- Acoustic startle (50 ms, 106 dB SPL, 100 – 40 KHz) was inhibited (101 and 51 ms) or enhanced (1 ms) by a single 64 mJ/kg microwave pulse (0.96 μs, 64 kW/kg peak) but not by 26.3 mJ/kg (0.96 μs, 21.2 KW/kg peak) Caused by pulsed RF only
- Acoustic click (8 μs, 94 dB SPL) inhibited tactile startle (air burst 48 – 52 psi)
- 663 mJ/kg microwave pulse (7.9 μs, 77 kW/kg peak) inhibited (57 ms) and enhanced (45 ms after tactile startle stimulus) startle amplitude

McKESSON Empowering Healthcare — USAMRD - WRAIR, BROOKS CITY-BASE, TX, U.S.A.

RESEARCH APPROACH (ENGINEERING)

- Engineering evaluation is required to test body borne antennas for compliance to current RFR safety standards:
  - Perform numerical modeling of the energy deposition in the human body using realistic human model.
  - Verify free-space characteristics of the antenna, if required.
  - Determine the extent of surface heating of human body and antennas.
  - Measure local specific absorption rate (SAR) and location of the maximum SAR in full size human phantom at all frequencies of interest and/or in multi-frequency environment. The SAR measurements in simulated field conditions will also be considered if required.
  - Determine the location of any RF and thermal hot spots at single and multiple frequencies.
  - Measure induced currents in the extremities like ankle and wrist, at all frequencies of interest, especially at frequency below 100 kHz.
- Engineering support for biological evaluation:
  - Design and fabricate appropriate antennas to simulate human exposure from body borne antennas.
  - Perform dosimetry to define SAR and SAR pattern for defining dose-response characteristics of biological effects resulted from partial body exposure using various body borne antennas.

RESEARCH APPROACH (BIOLOGY)[1]

- Target organs for effects of RF radiations have not been clearly defined. Virtually, all biological processes and/or systems can be affected by RF radiation.
- Given sufficient field strength, there is no question that a range of effects will be produced. The problem is not whether effects exist (They surely do) but to understand the nature and anticipate the exposure conditions that will elicit them.
- Functional disturbance in the central nervous system (CNS) in absence of morphological change is considered to be most sensitive endpoints of the biological effects of radio frequency radiation. The threshold CNS functional disturbance such as behavior endpoints has been used as the basis in promulgation of personnel protection guidelines/standards in Western countries.
- An ill-defined "neurasthenia" syndrome was considered by Eastern European Scientist to be a prominent indication of "microwave sickness". Western scientists frequently dismissed RF radiation as a possible cause of "neurasthenia".

RESEARCH APPROACH (BIOLOGY)[2]

- Symptoms of neurasthenia include feeling of "heaviness of head" (vague pain), tiredness, irritability, sleep disturbance, memory loss, decreased libido, and constipation, etc. Neurasthenia can progress to "autonomic vascular" changes, i.e., sweating, dermographism, and blood pressure changes, and if vagotonic, bradycardia and prolongation of intraaurical and intraventricular conduction.
- Most of these symptoms also appeared in case reports that dealt with the health effects of overexposure to RF radiation. In addition, dysaesthesia (burning, tingling and numbness sensations) and delayed hypertension appeared in various case reports. These neurological symptoms could persist long time after accidental overexposure to RF radiation.
- A recent report (2003) suggested that among cellular phone users prevalence of subjective symptoms increased with higher SAR (>0.5 W/kg), especially discomfort and dizziness. The user who reported subjective symptoms such as dizziness, discomfort, difficulties in concentration and warmth sensation appeared to have received a higher SAD (specific absorption per day). The latter finding was interpreted as possible evidence of a cumulative effect.

RESEARCH APPROACH (BIOLOGY)[3]

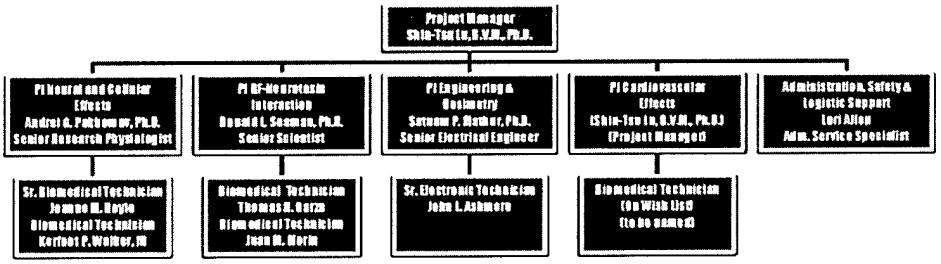
- Neurasthenia, the weakness or debility of nerve shares some resemblance to chronic depression which includes symptoms such as anhedonia (reduced responsiveness to pleasurable stimuli), difficulty sleeping, appetite change, fatigue, altered endocrine functions, increased basal heart rate, reduced heart rate variability and exaggerated reactivity to stressors.
- Although non-invasive neurological and psychological methods are currently available to quantify the severity of individual symptoms listed under neurasthenia/depression syndrome individually, the application of these techniques appears to be lacking at the present time.
- If care is taken, non-invasive neurological and psychological methods can be used repetitively for long term follow up to detect the presence of delayed and/or cumulative alterations in neurological and psychological functions and injuries.

RESEARCH APPROACH (BIOLOGY)[4]

- Available non-invasive methods for quantitative evaluation of RF-induced neurological/psychological changes and skin integrity are:

1. Sucrose Preference Test: to determine the degree of anhedonia
2. Von Frey Test: to determine alterations in tactile sensitivity
3. Thermal Algesia Test (Hot Plate, Intense Light Beam): to determine alterations in thermal pain threshold
4. Elevated Plus-Maze Test: to determine alterations in anxiety level
5. Rotarod Performance: to determine alterations in motor coordination if dizziness is present
6. Running Wheel Activity: to determine alteration in circadian rhythm and long-term disturbance of locomotor activity
7. Heart Rate, Blood Pressures and Heart Rate variability: to determine alterations in cardiovascular function
8. Y-maze or Radial Arm Maze performance: to determine alterations in memory process
9. Skin Electrical Impedance Spectroscopy: to determine alterations in intracellular and/or extracellular water content as an indication of changes in skin integrity.

U.S. ARMY MEDICAL RESEARCH DETACHMENT
MICROWAVE BIOEFFECTS BRANCH / MCKESSON BIOSERVICES



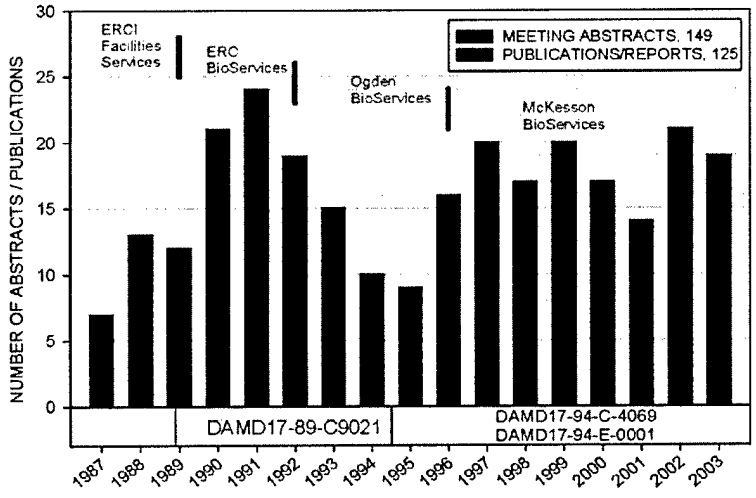
COLLABORATION

- University of California at Los Angeles
  Dr. Marie-Francoise Chesselet
- University of Texas Health Science Center at San Antonio
  Dr. Marty Meltz
  Dr. Bijoy Nayak
- University of Wisconsin
  Dr. Susan Hageness
- Old Dominion University
  Dr, Karl H. Schoenbach
- Naval Health Research Center Detachment
  Dr. John Ziriax
- Air Force Research Laboratory, Mathematical Products Division
  Dr. Richard Albanese
- U.S. Army Communications Electronics Command, Directorate for Safety
  Dr. John M. Tobias
- Walter Reed Army Institute of Research, Division of Neurosciences
  Dr. Jitendra Dave
- Air Force Research Laboratory, Division of Veterinary Science
  Dr. Jeffrey Egger
- Air Force Research Laboratory, Radio Frequency Radiation Branch
  Mr. William Hurt

McKESSON
Empowering Healthcare
USAMRD - WRAIR, BROOKS CITY-BASE, TX, U.S.A.

PUBLICATIONS

U.S. ARMY MEDICAL RESEARCH DETACHMENT
MICROWAVE BIOEFFECTS BRANCH
PUBLICATION STATISTICS



McKESSON
Empowering Healthcare
USAMRD - WRAIR, BROOKS CITY-BASE, TX, U.S.A.

Radio Frequency Specific Effects Potential Medical Application

Presentation to the USAMRMC Medical Technology Review Panel F

By

Shin-Tsu Lu, BVM, Ph.D., Project Manager
McKesson BioServices / USAMRD Microwave Bioeffects Branch
Brooks City-Base, TX 78235-5323

October 20 – 22, 2003

McKESSON
Empowering Healthcare

USAMRD - WRAIR, BROOKS CITY-BASE, TX, U.S.A.



MISSION

- The mission of the U.S. Army Medical Research Detachment, Microwave Bioeffects Branch is to develop radio frequency (RF) bioeffects criteria and predictive models for safe exposure standards of the electromagnetic radiation to assure the health and welfare of warfighters.
- The Directorate of Operational Medicine of the U.S. Army Medical Research and Materiel Command, Fort Detrick, Maryland is responsible for the radio frequency bioeffects mission through contracts with McKesson BioServices Corporation and is being performed at Brooks City-Base, Texas.

McKESSON Empowering Healthcare — USAMRD - WRAIR, BROOKS CITY-BASE, TX, U.S.A.

RF IN MILITARY OPERATIONAL ENVIRONMENT

- The military operational environment is heavily and increasingly dependent on radio frequency devices for command, control and communication, and intelligence.

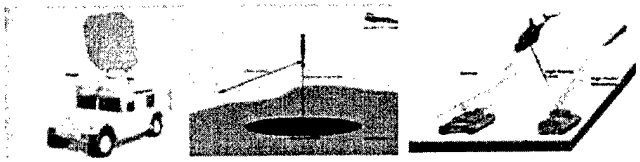


- Military RF devices radiate higher average power and/or higher peak power than similar devices do in civilian sectors if they exist.

McKESSON Empowering Healthcare — USAMRD - WRAIR, BROOKS CITY-BASE, TX, U.S.A.

RF EXPOSURES IN MILITARY ENVIRONMENT

- Intentional exposure: targets of opposing force's devices, e.g., RF non-lethal weapon, EMP (electromagnetic impulse) bomb, Jamming devices, and directed energy devices, etc. Depending on devices, exposure levels range from low to high. Unavoidable.



- Unintentional exposure: operators and personnel in the vicinity of RF devices. Exposure levels are usually low if precautions are exercised.
- Accidental exposure: errors in operating the RF devices or during repair, calibration and testing. Exposure level can be high if high power RF device is under consideration.

McKESSON Empowering Healthcare — USAMRD - WRAIR, BROOKS CITY-BASE, TX, U.S.A.

MYTH OF RF BIOLOGICAL EFFECTS

Comment on SPY radar on board of Aegis-class cruiser: "The solid-state components could combine to blast six *megawatts* of RF power down a one-degree line of bearing, enough to make a helicopter pilot, for example, produce what cruel physicians called FLKs: funny-looking kids." (Tom Clancy, The Bear and The Dragon, Berkley Books, 741)



New Cell Phone Link To Brain Cancer Found
By Beezy Marsh
Daily Mail - UK
3-17-3

Cell Phone Cancer Scare: Are You At Risk?
PR Newswire
October 20, 1999

New research shows cell phone usage may cause cancer

Cell phones linked to eye cancer
By Graeme Wearden
ZDNet (UK)
January 15, 2001, 4:00 PM PT

McKESSON Empowering Healthcare — USAMRD - WRAIR, BROOKS CITY-BASE, TX, U.S.A.

BIOPHYSICAL MECHANISMS OF RF BIOEFFECTS[1]

- Thermal Mechanism: Specific Absorption Rate (SAR), 30 V/m can produce 1 W/kg at 1 GHz and 1 W/kg, ≈ human basal metabolic rate, can potentially induce 1.7×10^{-2} °C increase per min.
  - Bulk temperature increase:
    - warmth sensation at 0.07 °C in 3 s = 293 J/kg or 98 W/kg for 3 s
  - Rate of temperature increase:
    - Thermoelastic expansion and microwave hearing: 10 mJ/kg or 2.4×10^{-6} °C in 1-30 μs ≈ 1 °C/s, 350 W/kg peak SAR in 70-500 μs pulse
    - Thermally induced membrane depolarization:
      - Cessation in firing rate of Aplasia pacemaker at peak SAR 40,000 W/kg in 0.1 s or 4,000 J/kg ≈ 1 °C or 10 °C/s
      - Microwave-induced whole-body movements required 1.2 °C in 1 s or less ≈ 5,000 J/kg or 5,000 W/kg.

BIOPHYSICAL MECHANISMS OF RF BIOEFFECTS[2]

- Membrane excitation and breakdown:
  - Electroporation: 50,000 V/m for more than 0.15 μs
  - Cell destruction: 6,000,000 V/m in tens of ns to tens of μs
- Direct electrical forces on cells or cell constituents
  - Field-charge interactions: ≈ 10^{-4} m/s per 1,000 V/m for small electrolyte ions, 8 to 9 orders of magnitude below velocity of Brownian motion
  - Field-permanent dipole interactions: alignment of DNA molecule >10,000 V/m
  - Electric field-induced dipole interactions: pearl chain effect > 1,000 V/m
  - Electrode effects: electrochemical reactions by current passing through electrode at electrode-tissue interface, artifact by some

Foster KR. Thermal and nonthermal mechanisms of interaction of radio-frequency energy with biological systems. IEEE Trans Plasma Sci. 28: 15-23, 2000

TISSUE DAMAGE MECHANISMS OF ULTRASHORT PULSES

- Molecular conformation changes, e.g., strand unwinding in polynucleotides (2,000 kV/m, 10 μs), confirmation changes in phage DNA during pulsed electrophoresis (350 V/m, 10 min)
- Alteration in chemical reaction rates (1 % change in equilibrium constant per kV/m)
- Membrane effects (e.g., electroporation, 400 - 600 kV/m)
- Thermal damage through molecular heating resulted from rate of energy removal slower than absorption of electromagnetic energy

These proposed tissue damage mechanisms were not concurred by others.

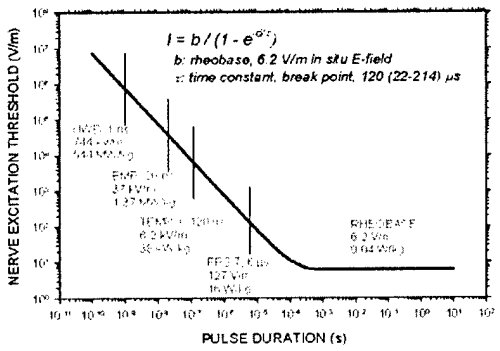
Altamirano R, Blasak J, Medina R and Perrin J. Ultrashort electromagnetic signal: biophysical questions, safety issues and medical opportunity. Aviat Space Environ Med 65: A116-A120, 1994.
Merritt JH, Kiel JL and Hurt WD. Considerations of human exposure standards for fast rise time, high-peak-power electromagnetic pulses. Aviat Space Environ Med 66: 586-590, 1995.
Adair RK. Ultrashort microwave signals: a didactic discussion. Aviat Space Environ Med 66: 702-704, 1995.

SPECIAL CONSIDERATIONS PERTAINING TO PULSED RF BIOEFFECTS

- Lack of adequate and appropriate biological database for pulsed RF radiation prevents a rationalized promulgation of personnel protection guidelines against pulsed RF [INCIRP 1998].
- Peak power limits were arbitrary selected and varied among guidelines/standards promulgated by different organizations.
- An arbitrary peak intensity electric field limit of 100 kV/m (≈26.5 MW/m^2 or 2.65 kW/cm^2) can produce at resonance, a whole-body average specific absorption rate (SAR) of 0.66 – 1.06 MW/kg equivalent to temperature increase at 150 – 250 °C per second.
- Special considerations pertaining to pulsed RF of equal SAR are:
  - Pulse specific effects (effect occurs only with pulse modulation)
  - Pulse synergistic effects (positive, negative or none in comparison to CW)

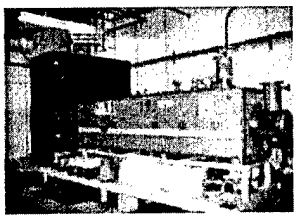
LAW OF NERVE EXCITATION (BLAIR EQUATION)

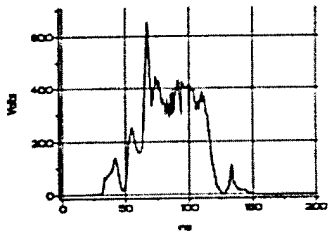
- A mathematical equation based on known resistive and capacitive properties of cell membranes.
- Appears to hold true for pulse duration down to 1 μs range.



- Long pulse has higher probability to cause nerve excitation. For tissue conductivity of 1 S/m, Blair equation predicts that nerve excitation can occur below current standards and it is impossible for UWB pulse to cause nerve excitation.

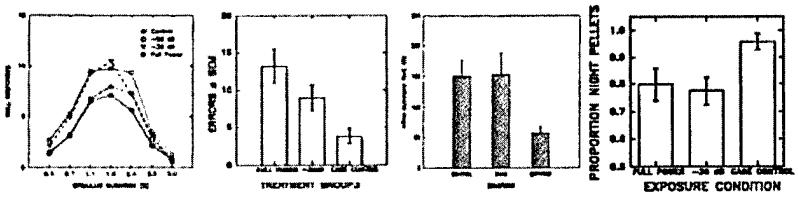
TRANSFORMER ENERGIZED MEGAVOLT PULSE OUTPUT (TEMPO) SYSTEM





- Virtual cathode oscillator
- Longitudinally slotted waveguide
- 60° dual corner reflector
- 3 GHz carrier frequency
- 500-700 MW peak power, 200 MW square wave equivalent peak power
- 120 ns pulse duration
- 20 ns rise time
- 0.125 Hz pulse repetition rate
- 10^{-8} duty factor, 2 W average
- 7.2 MW/kg peak SAR, 0.072 W/kg average SAR and 0.86 J/kg pulse SA (2-3 orders of magnitude higher than the auditory threshold)

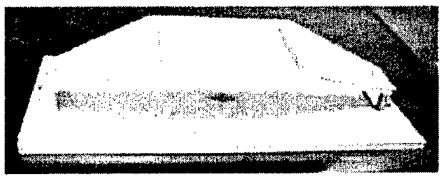
EFFECTS OF 200 TEMPO PULSES

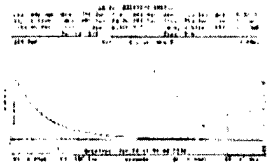


- Increased session time and null response in a time perception and discrimination task after exposure at 0.072 W/kg and 0.000072 W/kg (decision making process)
- Made more errors in a y-maze task after exposure at 0.072 W/kg and 0.000072 W/kg (memory consolidation)
- Decreased run time in a treadmill performance test at 0.072 W/kg (endurance)
- Consumed more food during light period at FR1 but not other FRs (15, 45, 90, 180 and 360) after exposure at 0.072 and 0.000072 W/kg (circadian rhythm)
- No effect on immobility time in a Porsolt's behavior despair test after exposure at 0.072 W/kg (depression/despair)

McKESSON *Empowering Healthcare* USAMRD - WRAIR, BROOKS CITY-BASE, TX, U.S.A.

EFFECTS OF ELECTROMAGNETIC PULSES (EMP)

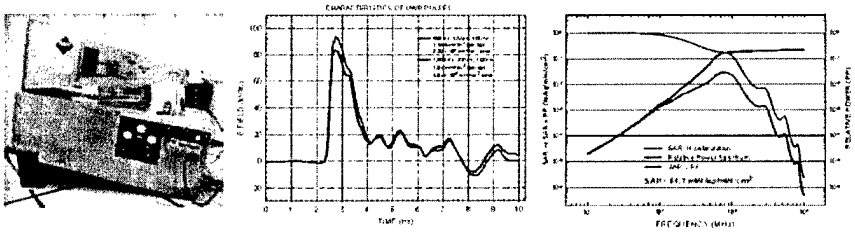




- Parallel plate simulator, 12 kV peak voltage, 67 kV/m peak electric field, 8 ns rise time, 15 μs pulse duration, 6 pulses per s, 20-30 minutes.
- 0.8 A, 7 ns rise time, 20 ns pulse duration short circuit current in rats (≈ 12 mA per kV/m, 2 orders of magnitude lower than in man, 1.7 A per kV/m)
- Rats appeared to prefer the EMP-field site than the no EMP-field site of the shuttle tube in a simple preference test.
- Rats displayed ear "twitch" with EMP pulses from noise of EMP generator.
- No EMP effects on memory consolidation (Y-maze) or behavior despair (Porsolt's swin test) were noted in rats.

McKESSON *Empowering Healthcare* USAMRD - WRAIR, BROOKS CITY-BASE, TX, U.S.A.

EXPOSURE SYSTEM FOR ULTRA-WIDE-BAND PULSES



- Spark-gap generator, GTEM cell, impulse, carrierless
- Peak electric field intensity: 85 – 100 kV/m or 19.1 – 26.5 MW/m^2
- Pulse duration: 1 ns; pulse rise time: 160 ps
- Maximum pulse repetition rate: 1,000 Hz; Duty factor: < 10^{-6}
- Whole-body average SAR for medium rats: 6.17 mW/kg per W/m^2, 112 mW/kg at 1,000 Hz
- Whole-body average SAR for mice: 37 mW/kg at 600 Hz
- Thermal equivalency of WBA-SAR is low (40 J/kg, ≈ 0.01 °C) for 6 min at 1,000 Hz in rats and for 30 min at 600 Hz (67 J/kg, ≈ 0.016 °C) in mice.

McKESSON Empowering Healthcare — USAMRD - WRAIR, BROOKS CITY-BASE, TX, U.S.A.

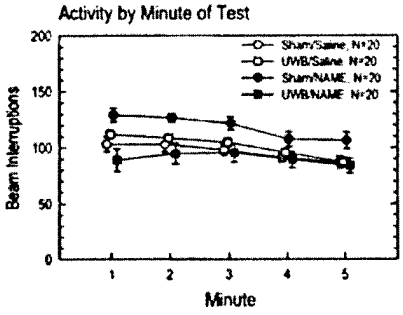
BIOLOGICAL EFFECTS OF ULTRA-WIDE-BAND PULSES[1]

- No effects of 30 min exposure at 16 Hz (104 kV/m peak, 1 ns pulse duration, 165 ps rise time) and 60 Hz (102 kV/m, 1 ns pulse duration, 165 ps rise time) UWB pulses on yeast cell suspensions (Saccharomyces cerevisiae, strain D7) with or without ultraviolet (100 J/m^2) pre-treatment. Endpoints included colony forming ability, frequencies of segregation, mutations to isoleucine independence, and gene recombination such as mitotic cross-over and conversion to tryptophan independence.
- 90 min (30 on 30 off × 3) exposure to UWB pulses (100 kV/m, 1 ns pulse duration, 150 – 250 ps rise time, 250 pps) did not alter cell cycle distribution, transcription of p53 tumor suppressor gene (cell growth arrest and apoptosis), or the p53 target genes p21, gadd45, PCNA and bax in 244B human lymphoblastoid cell line, human MM6 monocyte cell line, and the human HL-60 myeloid leukemic cell line.
- 90 min (30 on 30 off × 3) exposure to UWB pulses (100 kV/m, 1 ns pulse duration, 150 – 250 ps rise time, 250 pps) induced a marked increase in the NF-κB DNA binding activity (one of cell signaling mediators) in MM6 cells at 24 h post exposure but not at 10 min, 0.5 h, 4 h, 8 h and 48 h.

McKESSON Empowering Healthcare — USAMRD - WRAIR, BROOKS CITY-BASE, TX, U.S.A.

BIOLOGICAL EFFECTS OF ULTRA-WIDE-BAND PULSES[2]

- No effects of 30 min exposure to UWB pulses (60 and 600 Hz, 99 – 105 kV/m peak, 0.97 – 1.03 ns pulse duration, 155 – 174 ps rise time) on morphine-induced analgesia in CF-1 mice or morphine-induced hyperactivity in C57-BL/6 mice.
- Exposure to 30 min of UWB pulses at 600 Hz (102 kV/m peak, 0.9 ns pulse duration, 160 ps rise time) reversed the hyperactivity induced by N^G-nitro-L-arginine methyl ester HCl (L-NAME, 50 mg/kg, i.p., a nitric oxide synthase inhibitor) but not the L-NAME induced analgesia in CF-1/Plus mice.



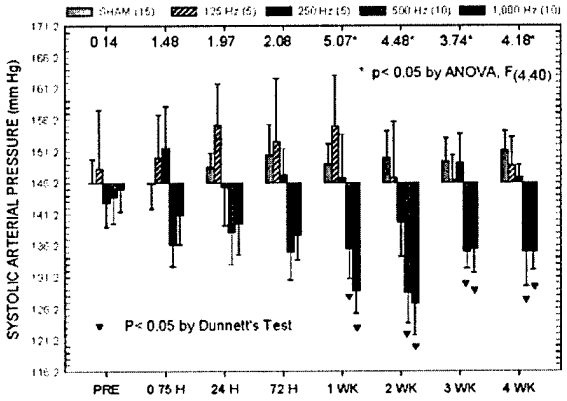
- Exposure to UWB pulses enhanced the nitric oxide produced in stimulated (potassium nitrate) murine macrophages, RAW 264.7 (600 Hz, 72 – 95 kV/m peak, 1.02 – 1.07 ns pulse duration, 198 – 218 ps rise time).

BIOLOGICAL EFFECTS OF ULTRA-WIDE-BAND PULSES[3]

- Two min exposure to UWB pulses at 50, 500 and 1,000 Hz (87 – 104 kV/m peak, 0.97 – 0.99 ns pulse duration, 174 – 218 ps rise time) did not alter the heart rate or mean arterial blood pressure significantly in Sprague-Dawley rats during or immediately after exposure.
- Exposure to UWB pulses at 1,000 Hz (106 kV/m. 0.79 ns pulse duration, 186 ps rise time for 10 s) starting at ECG R-wave or T-wave did not alter the R-R (inverse of heart rate) or P-R (sinoatrial conduction) intervals during exposure or after exposure in Sprague-Dawley rats.
- A delayed hypotension in Wistar-Kyoto rats was observed in rats 2 – 4 weeks after 6 min to UWB pulses at 1 ns pulse duration, 89 – 95 kV/m peak (118 – 148 MW/kg peak SAR; 0.12 – 0.15 mJ/kg per pulse) at 1,000 and 500 Hz but not at 250 or 125 Hz. The heating potential from UWB pulses was less than 0.012 °C. Hypotensive effect was replicated in an abbreviated double blind experiment at 500 Hz. This delayed hypotension appeared to be a change in basal tonicity of cardiovascular system since response to a 47° head-up tilt was not altered at 2 weeks after exposure.

BIOLOGICAL EFFECTS OF ULTRA-WIDE-BAND PULSES[4]

DOSE-RESPONSE CHARACTERISTICS OF UWB-INDUCED HYPOTENSION

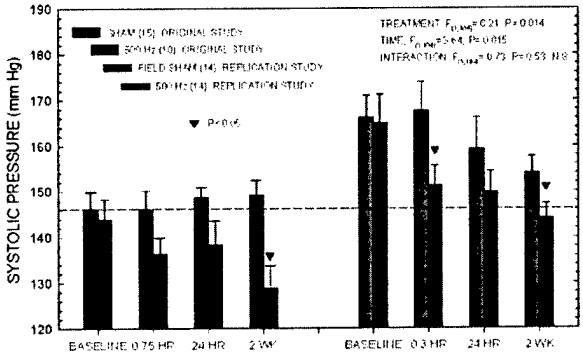


Results of ANOVA indicated that significant difference among groups appeared at 1, 2, 3 and 4 weeks after exposure. Hypotension was noted in the 500 and 1,000 Hz groups but not 125 and 250 Hz groups. Maximum changes in magnitude occurred at 2 weeks after exposure. Recovery was evident but incomplete at 4 weeks after exposure.

McKESSON Empowering Healthcare — USAMRD - WRAIR, BROOKS CITY-BASE, TX, U.S.A.

BIOLOGICAL EFFECTS OF ULTRA-WIDE-BAND PULSES[5]

UWB-INDUCED HYPOTENSION ABBREVIATED STUDY 500 Hz

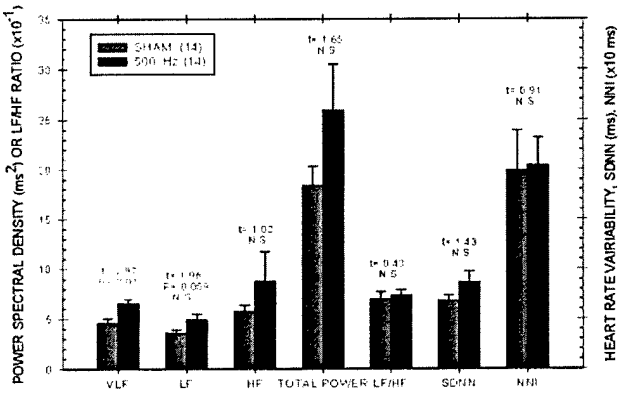


Data on left panel were from sham and 500 Hz groups in the dose-response study. Data on the right panel were from a double-blind replication study. Higher base-line systolic pressure and subsequent decline in sham-exposed rats could be resulted from inadequate acclimation and/or inadequate equilibration. Nevertheless, significant decreases in systolic pressure were noted at 0.3 hour and 2 weeks after exposure.

McKESSON Empowering Healthcare — USAMRD - WRAIR, BROOKS CITY-BASE, TX, U.S.A.

BIOLOGICAL EFFECTS OF ULTRA-WIDE-BAND PULSES[6]

EFFECTS OF UWB EXPOSURE ON HEART RATE VARIABILITY IN FREQUENCY- AND TIME-DOMAIN

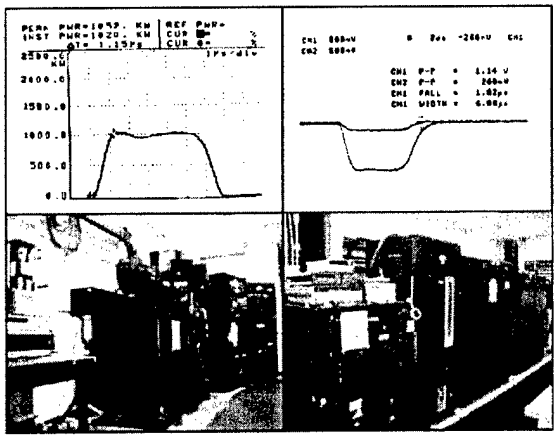


Majority of measurements of heart rate variability in time- and frequency-domain were not changed by UWB exposure in rats. Exceptions are a significant change in VLF PSD and a marginal change in LF PSD. Physiological significance of VLF change is not known. Changes in VLF and LF PSD in absence of alteration in beat-to-beat interval (NNI) and its standard deviation (SDNN) may still point to a low-grade disturbance in autonomic control of heart rate.

McKESSON *Empowering Healthcare* USAMRD - WRAIR, BROOKS CITY-BASE, TX, U.S.A.

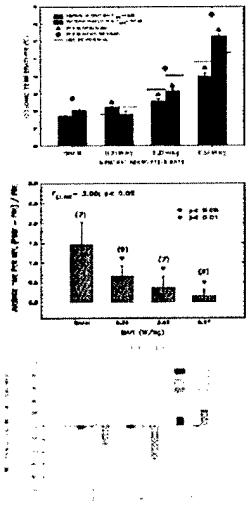
FPS-7B L-BAND EXPOSURE SYSTEM (1.25 GHz)

- Replacement transmitter for original 1 MW peak power Cober transmitter
- Carrier frequency: 1.25 – 1.30 GHz
- Peak output power: 10 MW rated, varies with pulse repetition rate, 7.5 MW at 21 Hz
- Pulse duration: 6μs fixed
- Pulse repetition rate: 1 – 244 Hz
- Duty factor: < 1.02×10^{-4}, 204 W average
- SAR: 0.4 W/kg per mW/cm² or 1.12 W/kg per W output at 7.6 cm from open-ended WR650 waveguide



McKESSON *Empowering Healthcare* USAMRD - WRAIR, BROOKS CITY-BASE, TX, U.S.A.

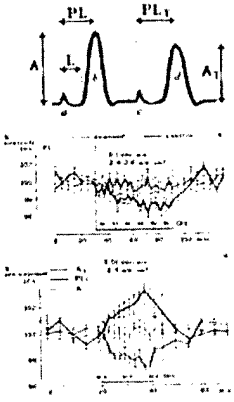
HIGH POWER EFFECTS *IN VIVO*



- Water restriction enhanced 30 min core body temperature responses significantly and could reach a heat stroke level at 6.59 W/kg whole-body average SAR (WBA-SAR).
- 24 hours after RF exposure, rats did not make more errors than sham exposed rats did in a Y-maze test (memory) but time spent in each arm decreased reliable with WBA-SAR and as low as 0.4 W/kg (foraging behavior, decision making?).
- Behavior effects of 10 μs, 0.21 MW/kg peak, and 2.1 J/kg pulses for 10 min
  - 0.4, 1.2, 3.6 and 10.8 Hz; 0.84, 2.5, 7.6 and 23.0 W/kg WBA-SAR
  - Immediately after exposure at 23.0 W/kg (2.5 °C) only, work stoppage occurred in all three schedules, performance resumed 13 min after exposure (1.1 °C) at reduced rate in FR 20, VI 30s but not DRL 30s.

McKESSON *Empowering Healthcare* USAMRD - WRAIR, BROOKS CITY-BASE, TX, U.S.A.

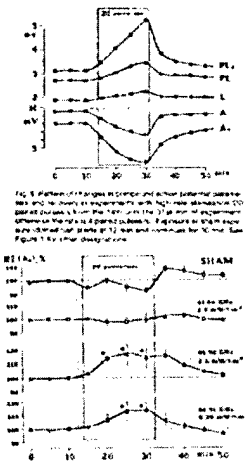
FREQUENCY-SPECIFIC mm-WAVES ON ISOLATED NERVE FUNCTION[1] (LOW RATE STIMULATION)



- Isolated nerve preparation (n. ischiadicus + n. peroneus), conditioning and test compound action potentials (CAP) produced by pairs of supra-maximal stimulation (0.2 ms width, 2 – 3 V, 9 ms interval) at low rate (4 pairs per s) or high rate (20 pairs per s), 40 – 52 GHz CW, 0.24 – 3.0 mW/cm², stepwise frequency change at 0.01 or 0.1 GHz per min
- mm Wave irradiation at 0.24 – 1.5 mW/cm² for 10 – 60 min did not alter amplitude, latency and peak latency of CAPs by low rate stimulation.
- Similar to conventional heating, mm wave irradiation at 2.4 – 2.8 mW/cm² increased amplitude of test CAP, no effect on conditioning CAP amplitude, decreased latency and decreased peak latency of conditioning CAP and peak latency of test CAP. Changes were also equal to 0.3 – 0.4 °C measured.

McKESSON *Empowering Healthcare* USAMRD - WRAIR, BROOKS CITY-BASE, TX, U.S.A.

FREQUENCY-SPECIFIC mm-WAVES ON ISOLATED NERVE FUNCTION[2] (HIGH RATE STIMULATION)



- With high rate stimulation (20 pairs /s), the interval between pairs of stimuli is not long enough for complete recovery after conduction of the preceding CAPs, thus leading to nerve fatigue with gradual decreases of CAPs' amplitude and conduction velocity.
- mm wave irradiation could attenuate the amplitude decrease of test CAPs due to high rate stimulation. This attenuation effect was frequency dependent. Minimal changes were found at 42.04 and 41.42 GHz at 2.4 – 2.7 mW/cm^2. Effective irradiations occurred at 45.9 GHz at 2.6 mW/cm^2, 51.41 GHz at 2 mW/cm^2, and 41.22 and 50.91 GHz at 0.24 – 0.28 mW/cm^2.

McKESSON Empowering Healthcare — USAMRD - WRAIR, BROOKS CITY-BASE, TX, U.S.A.

FREQUENCY-INTENSITY-SPECIFIC mm-WAVES ON ISOLATED NERVE FUNCTION[3] (HIGH RATE STIMULATION)

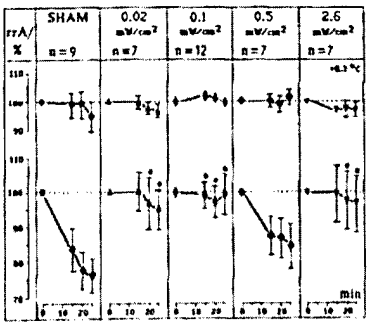


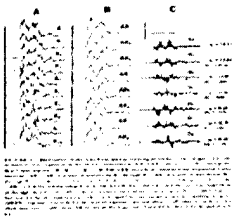
Fig. 2. Effect of millimeter waves (41.34 GHz) at different field intensities on isolated nerve ability to sustain a high-rate stimulation (HRS). Horizontal axes: time into the second HRS trial. In all groups, irradiation began at 2 min, and the HRS began at 4 min; both continued till the end of the experiment. Vertical axes: relative amplitude ratio values (rrA; mean ± SE) for the conditioning and test compound action potentials (top and bottom graphs, respectively). The field intensity (in mW cm^{-2}) and the number of independent experiments in each group (n) are indicated above the graphs. Asterisks show statistically significant differences from the sham exposure ($p < 0.05$, t-test with Dunnett's correction). See text for more details on the rrA calculation.

- Irradiation was also performed at 41.34 at various power densities (0.02, 0.1, 0.5 and 2.6 mW/cm^2) for 20 min.
- No effect on the amplitude of the conditioning CAPs (upper panel)
- Attenuation of the effect of high rate stimulation on test CAPs were dependent on power density, i.e., significant attenuation at 0.02, 0.1 and 2.6 mW/cm^2 but without effect at 0.5 mW/cm^2.
- This is an example of frequency-intensity specific effect that occurs at exposure intensity below current guidelines in controlled environment (occupational MPL).

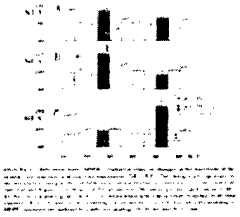
McKESSON Empowering Healthcare — USAMRD - WRAIR, BROOKS CITY-BASE, TX, U.S.A.

EFFECTS OF mm-WAVES ON SYNAPTIC TRANSMISSION

- Isolated hemi-sectioned spinal cord of bullfrog, poly-synaptic conduction recorded at ventral root evoked by dorsal root supra-maximal electrical stimuli, 20 – 30 V, 0.6 ms pulse width, 1 pulse per 30 s



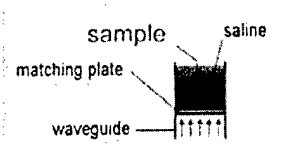
- Typical ventral root responses were polyphasic wave with 8 – 15 ms latency, 0.5 – 3 mV peak amplitude and 30 – 70 ms duration
- Two identical 5 min 41.34 GHz exposures at 2.8 mW/cm^2 during 6th (25 – 30 min) and 10th (50 – 55 min)

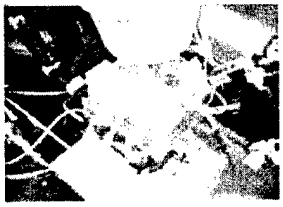


- Nine of 13 preparations showed response to the first but not the second exposure, 4 preparations failed to show response during the first exposure but they responded to the second exposure.
- Without consistent changes in amplitude, latency or area of potentials, the effect was considered as a mild modulation of reflex conduction rather than inhibition or facilitation

EXTREMELY HIGH PEAK POWER (EHPP) *IN VITRO*[1]

"While there is very little likelihood that the microwave auditory effect at threshold incident power can constitute a hazard, exposures at levels that are significantly higher than threshold **will undoubtedly be very harmful to cell membranes, cytoplasm, and whole organisms**." (*Lin 1989*) "However, there are few experimental data available to support this conjecture..." (*Pakhomov et al. 2000*).





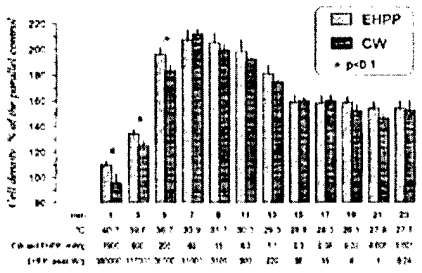
- Are EHPP effects differed from "regular" microwave effects?
- Are they differed from "heating" effects?
- What is the threshold if EHPP effect differed?

A 9.2 GHz waveguide (WR90, 22.86 × 10.16 mm) exposure system was used to produce a peak absorption rate of hundreds of MW/kg into a small specimen.

EXTREMELY HIGH PEAK POWER (EHPP) *IN VITRO*[2]

COMPARISON BETWEEN EHPP AND CW ON YEAST CELLS

- An ingenious method of exposure that provided continuous average SAR from 1.9 kW/kg to 1 W/kg for CW and peak SAR 0.38 MW/kg to 0.24 kW/kg with a constant duty factor of 5×10^{-6} (0.5 μs width and 10 pps)



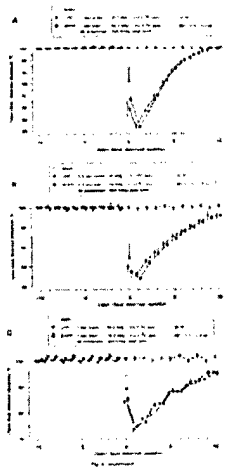
- 9.3 GHz CW (1.3 W) or pulsed (260-270 kW peak) for 6 hours
- 4.5 ml of yeast cells (Saccharomyces cerevisiae, BY4741), 2×10^6 cells/ml in YPD medium gelled with agarose in 4.5 ml rectangular cuvettes.
- Cell density determined by optical density in 12 2-mm slices.

- Cell density was temperature dependent and borderline significant difference was found in slices that exposed at 100 W/kg or higher.

McKESSON Empowering Healthcare — USAMRD - WRAIR, BROOKS CITY-BASE, TX, U.S.A.

EXTREMELY HIGH PEAK POWER (EHPP) *IN VITRO*[3]

COMPARISON BETWEEN EHPP AND CW ON CARDIAC PACEMAKER



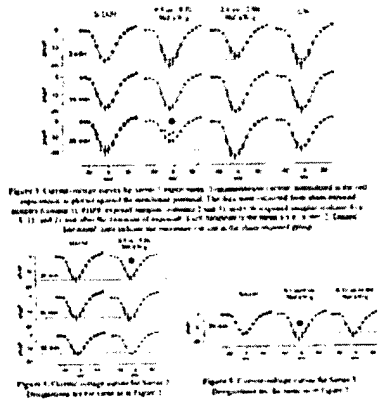
- Isolated sinoatrial area of the bullfrog heart
- 9.2 GHz, 1 or 0.5 μs width, 260 – 316 MW/kg peak, 50 pps for 1 s, 3.16 – 26.4 kW/kg average SAR, $2.5 - 5 \times 10^{-5}$ duty factor and gated CW of equal average SAR for 1 s
- A single EHPP pulse train or gated CW immediately decreased the inter-beat interval, i.e., increased pacemaker pacemaker beating rate (tachycardia). Arrest could occur if overheated.
- The tachycardia effect was proportional to heating, fully reversible, easily reproducible, and of equal magnitude between EHPP and gated CW.
- No signs of adaptation, sensitization, long-lasting functional alteration or damage
- Entirely thermal and no EHPP specific effect

McKESSON Empowering Healthcare — USAMRD - WRAIR, BROOKS CITY-BASE, TX, U.S.A.

EXTREMELY HIGH PEAK POWER (EHPP) *IN VITRO*[4]

COMPARISON BETWEEN EHPP AND CW ON CALCIUM CHANNELS

- GH_3 rat pituitary tumor cells, whole-cell patch clamp technique at 5- to 45-min after a 10-min 10.6 GHz at 3.8 kW/kg either CW or pulsed (960 MW/kg peak, 0.25 μs width at 16 pps, 0.5 μs width at 8 pps or 2 μs width at 2 pps)



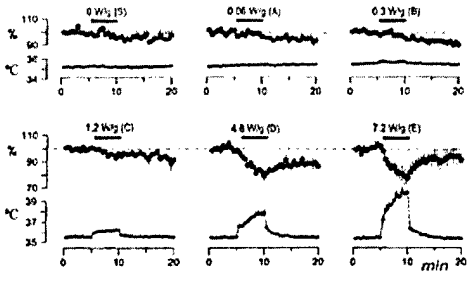
- Peak transmembrane current carried by Ba^{21} during 200-ms steps from holding potential (–80 mV or –40 mV) to different test potentials from –70 to +70 mV with 10 mV increments
- Initial observation of a pulse-specific effect (decreased inward current) at 25-min after a pulsed exposure (960 MW/kg, 0.5 μs width, 8 pps) was not confirmed.

McKESSON Empowering Healthcare — USAMRD - WRAIR, BROOKS CITY-BASE, TX, U.S.A.

EXTREMELY HIGH PEAK POWER (EHPP) *IN VITRO*[5]

COMPARISON BETWEEN EHPP AND CW ON POPULATION SPIKES IN RAT HIPPOCAMPAL SLICES[1]

- 350 μm hippocampal slices from 4 – 6 weeks old Sprague-Dawley rats, stimulated at Stratum radiatum area at 30-s intervals and extracellular population spikes recorded at CA1 area

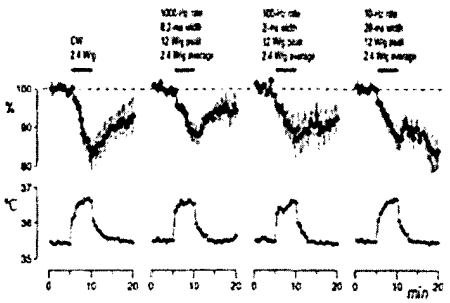


- 9.2 GHz, fixed repetition rate (16 Hz), 0.06 – 7.2 kW/kg average SAR, 2.4 – 14.4 kW/kg peak SAR, and 1.55 to 31 ms pulse duration for 5 min
- Pulsed microwave irradiation had no effects on population spikes if temperature did not increase by >1 °C or exceeded 36.5 °C (from ≈ 35 °C)

McKESSON Empowering Healthcare — USAMRD - WRAIR, BROOKS CITY-BASE, TX, U.S.A.

EXTREMELY HIGH PEAK POWER (EHPP) *IN VITRO*[6]

COMPARISON BETWEEN EHPP AND CW ON POPULATION SPIKES IN RAT HIPPOCAMPAL SLICES[2]

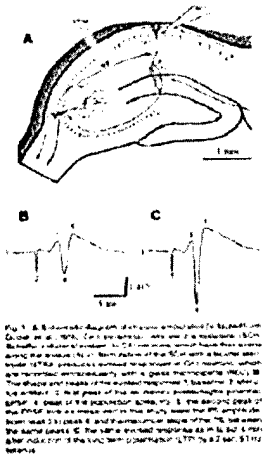


- 9.2 GHz, fixed average SAR (2.4 kW/kg), fixed peak SAR (12 kW/kg), fixed duty cycle (0.2) and variable pulse repetition rates (10, 100 and 1,000 Hz) for 5 min
- Above threshold, population spikes decreased in proportion to average SAR and heating
- No pulse specific effect

McKESSON Empowering Healthcare — USAMRD - WRAIR, BROOKS CITY-BASE, TX, U.S.A.

EXTREMELY HIGH PEAK POWER (EHPP) *IN VITRO*[7]

COMPARISON BETWEEN EHPP AND CW ON LONG TERM POTENTIATION IN RAT HIPPOCAMPAL SLICES[1]



- 350 μm hippocampal slices from 4 – 8 weeks old Sprague-Dawley rats, stimulated at Schaffer collateral pathway at 30-s intervals and extracellular population spikes (PS) recorded at CA1 area
- Stimuli intensity adjusted to produce PS amplitude of 1.5 – 3 mV
- A brief tetanus (2 s at 50 Hz) to induce Long Term Potentiation (LTP), a model of memory consolidation
- 9.3 GHz EHPP and CW irradiation applied before, after and during tetanus

McKESSON Empowering Healthcare — USAMRD - WRAIR, BROOKS CITY-BASE, TX, U.S.A.

EXTREMELY HIGH PEAK POWER (EHPP) *IN VITRO*[8]

COMPARISON BETWEEN EHPP AND CW ON LONG TERM POTENTIATION IN RAT HIPPOCAMPAL SLICES[2]

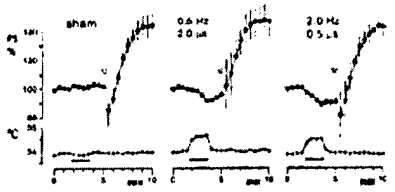


Fig 2. Effect of EHPP exposures on the ability of neurons to develop LTP. The amplitude of the PS (% to the average pre-exposure value) and temperature (°C) are plotted against the time into the experiment (minutes). All the data, including temperature, are mean ± SE, n=8–9, however, the error bars are often smaller than the central symbol and therefore not visible. Sham and EHPP exposures are shown by horizontal bars. Triangles indicate the time of tetanus (2 sec at 50 Hz). The peak SAR is 330 MW/kg, the time average SAR is 0.33 kW/kg; the pulse width and repetition rate are shown next to the graphs.

- Tetanus applied 1.5 min after 2 min EHPP exposures (350 MW/kg peak, 330 W/kg average, 2 µs width at 0.5 pps or 0.5 µs at 2 pps) sufficient to cause 0.5 – 0.6 °C increase in temperature
- EHPP applied before tetanus caused a transient decrease PS but did not alter the ability of hipocampal slice to develop LTP

EXTREMELY HIGH PEAK POWER (EHPP) *IN VITRO*[9]

COMPARISON BETWEEN EHPP AND CW ON LONG TERM POTENTIATION IN RAT HIPPOCAMPAL SLICES[3]

- Tetanus applied 2.5 min into experiment and LTP reached maximum in 3 – 4 min.

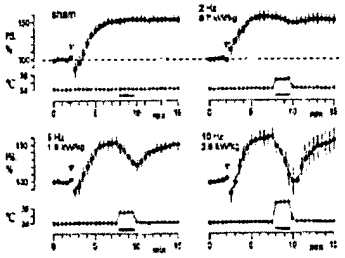


Fig 3. Effect of EHPP exposure at different time average SAR on retainment of the LTP state by hippocampal neurons. The time average SAR and pulse repetition rates are shown on the graphs. The peak SAR is 360 MW/kg and the pulse width is 1 µs in all the groups. Each group includes 13–14 independent experiments. Note different temperature scales for the upper and lower graphs. Other designations are the same as in Figure 2.

- 2 min of EHPP (1 µs width, 360 MW/kg peak, 2, 5 or 10 pps for 0.7, 1.8 and 3.6 kW/kg average) applied after tetanus at 7 min 45 s into experiment
- 1.4, 3.0 and 5.8 °C increases in temperature in EHPP exposed slices
- Potentiated PS decreased during EHPP exposure, recovered completely after exposure
- "Memory record" could be temporarily unavailable by EHPP heating but was not erased or altered.

EXTREMELY HIGH PEAK POWER (EHPP) *IN VITRO*[10]

COMPARISON BETWEEN EHPP AND CW ON LONG TERM POTENTIATION IN RAT HIPPOCAMPAL SLICES[4]

- LTP induced by tetanus at 4 min into the experiment
- 7 min of CW (0.25 or 1 kW/kg) or EHPP (500 MW/kg peak, 0.5 or 2 μs at 1 pps, 0.25 or 1 kW/kg average) applied 1 min 45 s into the experiment resulted in 0.3 – 0.4 and 1.5 – 1.6 °C temperature increases in CW and EHPP exposed slices

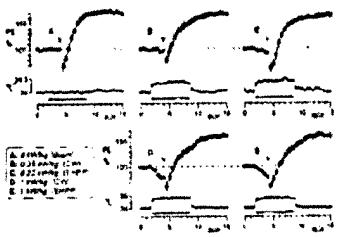
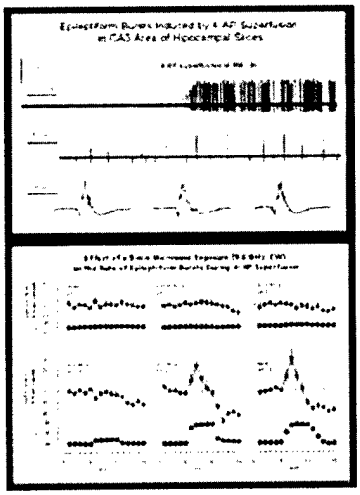


Fig. 4. Comparative effect of EHPP and CW exposures at equal SAR on the development of LTP. EHPP exposures were performed at 500 MW/kg peak SAR and 1 Hz pulse repetition rate; the pulse width is 0.5 μs (C) or 2 μs (E). Each group includes experiments in 11–18 brain slices, one experiment per slice. Note different temperature scales for the upper and lower graphs. Other designations are the same as in Figure 2.

- Exposure covered the transitional period to potentiated state representing memorizing process or memory consolidation
- Slower course of transition dependent on average SAR but potentiated PS stabilized at the same level after cessation of exposures

EXTREMELY HIGH PEAK POWER (EHPP) *IN VITRO*[11]

COMPARISON BETWEEN EHPP AND CW EPILEPTIFORM ACTIVITY CAUSED BY 4-AMINOPYRIDINE IN RAT HIPPOCAMPAL SLICES



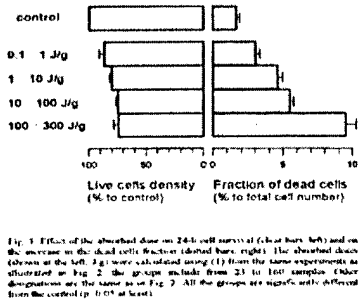
- Epileptiform activity induced by 4-aminopyridine (4-AP, non-specific K^+ channels blocker, 100 μM) in 350 μm hippocampal slices recorded at CA3 area
- 9.6 GHz CW at 0, 0.024, 0.12, 0.6, 3 kW/kg for 5 min
- 3 kW/kg caused 4 °C increase and a biphasic changes in spontaneous epileptiform activity caused by 4-AP which was replicated by conventional heating.
- Pulsed exposures are in progress.

CYTOTOXICITY OF NANOSECOND ELECTRIC PULSES[1]



- 10 ns electrical pulses produced by a Blumlein line generator and 1- or 2-mm gap electroporation cuvettes
- U937 human histiocytic lymphoma cells
- Cytotoxicity determined 24 hr after treatment (≈ 1 cell cycle)

- No effect on cell density by single electrical pulse at 300 kV/cm
- Cytotoxicity from 1 – 20 pulses of 40 – 380 kV/m at 0.1 Hz depended on absorbed dose.



McKESSON Empowering Healthcare — USAMRD - WRAIR, BROOKS CITY-BASE, TX, U.S.A.

CYTOTOXICITY OF NANOSECOND ELECTRIC PULSES[2]

- Cell survival depended on number of pulses and electrical field intensity; significant shoulder (sublethal) was noted in the survival curve

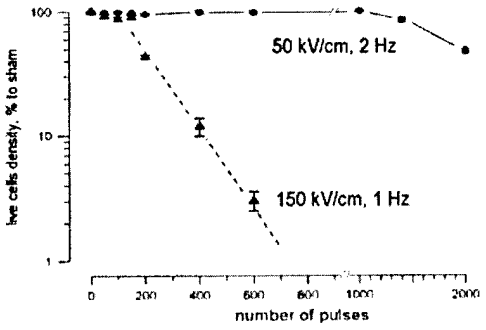


Fig. 5. Effect of the number of pulses applied at 150 or 50 kV/cm on 24-h cells survival. Each datapoint is the mean ± s.e., 12 to 40 samples per measurement (error bars may be not visible if smaller than the central symbol). Dashed line is the best fit approximation of the cells survival decline using exponential function

- Lethally exposed cells did not display specific cleavage of poly(ADP-ribose) polymerase, an hallmark of activation of caspases in apoptosis
- Change in temperature from the highest dose (≈ 31 °C from room temperature, ≈ 9 °C increase) was below known threshold for thermal lethality of cells

McKESSON Empowering Healthcare — USAMRD - WRAIR, BROOKS CITY-BASE, TX, U.S.A.

SUMMARY

- Current personnel protection guidelines are adequate to prevent injuries defined as degenerative changes caused by radio frequency radiation.
- Neural, behavioral and cardiovascular endpoints appear to be susceptible to perturbation by radio frequency radiation.
- Long-term and/or delay effects have not been adequately studied.
- Modulation specific effects have not been observed if the effect is primarily dependent on temperature increases.
- Neural, behavioral and cardiovascular functions can be perturbed by radio frequency radiation at intensities below current guidelines. This is especially apparent in studies on biological effects of mm waves, TEMPO pulses and UWB pulses. In addition, effects caused by exposure to TEMPO and UWB pulses occurred without any potential increase in body temperature at a magnitude less than 0.1 °C.
- Representative studies at narrow-band SAR similar to TEMPO and UWB pulses are needed to elucidate their uniqueness and thermal independency.

McKESSON Empowering Healthcare — USAMRD - WRAIR, BROOKS CITY-BASE, TX, U.S.A.

FULTURE RESEARCH PLANS[1]

- Continue research on radio frequency radiation and rotenone on nigrostriatal neurodegeneration.
- Continue research on effect of extremely high peak power radio frequency radiation on hippocampal slices.
- Continue research on cytotoxic effects of ns electrical pulses.
- Continue provide technical expertise and dosimetric evaluation of body borne antennas for compliance.
- Initiate research on delayed cardiovascular effects by low intensity narrow band radio frequency with SAR in the range used in the previous UWB studies for specificity of UWB pulses.
- Initiate the proposed neurological and psychological studies for characterization of radio frequency radiation induced "neurasthenia".
- Initiate studies on biological effects of localized RF exposure, especially in the area of skin electrical impedance spectrometry and "neurasthenia" endpoints.

McKESSON Empowering Healthcare — USAMRD - WRAIR, BROOKS CITY-BASE, TX, U.S.A.

FULTURE RESEARCH PLANS[2]

- Explore the therapeutic application of UWB pulses in spontaneously hypertensive rats.
- Explore the potential medical applications of ns electrical pulses.
- Explore the potential medical applications of pulsed magnitude fields and mm waves on neural regeneration using crashed nerve and/or spinal hemisection models.
- Explore the potential medical applications of transcutaneous and/or transsclera drug delivery by electrophoresis.



Effects of Microwave Radiation on Nigrostriatal Neurodegeneration in the Rat



USAMRD-WRAIR
Brooks City-Base TX

Ronald L. Seaman, Ph.D., McKesson BioServices, P.I.
Presented by Cheryl D. DiCarlo, D.V.M., Ph.D.,
Diplomate ACLAM; LTC, VC, USA
Deputy Director, USAMRD, WRAIR

US Army Medical Research Detachment
Walter Reed Army Institute of Research
Brooks City-Base TX 78235-5108



Overview

- Research Team
- Background & Animal Model
- Animal Model Refinement
- Microwave Exposure of Model
- Behavioral Testing
- Neuropathology & Pathology of non-CNS Tissues
- Publications
- Collaborative Research with WRAIR
- Future Directions



Research Team

- USAMRD/Microwave Branch McKesson BioServices
  - Dr. Ronald Seaman, Principal Investigator
  - Dr. Satnam Mathur
  - Dr. Shin-Tsu Lu, Co-Investigator
  - Mr. Tommy Garza
  - Mr. Juan Morin
  - Mr. John Ashmore
- USAMRD/Laser Branch
  - LTC Cheryl DiCarlo, Co-Investigator
  - SPC Andres Grado
- University of California at Los Angeles (UCLA)
  - Dr. Marie-Francoise Chesselet, UCLA Principal Investigator
  - Dr. Sheila Fleming
  - Dr. Chunni Zhu
  - Mr. Arpesh Mehta

USAMRD-WRAIR Brooks City-Base TX

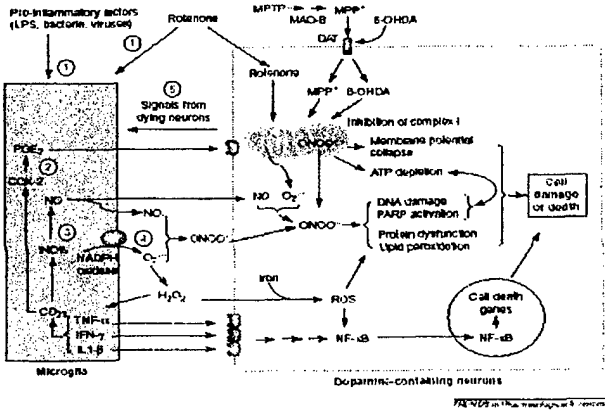
Background and Animal Model

- Pesticides and microwaves are widely used in military environments
- Emory animal model of neurodegeneration
  - Chronic intravenous (IV) administration of rotenone
  - Male Lewis rats
  - Mitochondrial toxin reduces production of ATP
- Model shows features of Parkinson's disease
  - Postural "hunching" and reduced locomotor activity
  - Decreased tyrosine hydroxylase in substantia nigra and striatum
  - Lewy bodies in neurons of substantia nigra

USAMRD-WRAIR Brooks City-Base TX

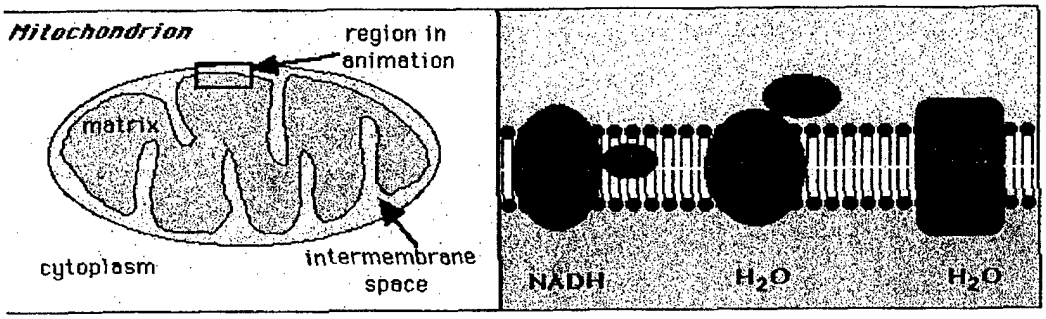
Background

- Pesticides and microwaves are widely used in military environment
- Rotenone, administered intravenously (IV), can produce Parkinsonian-like disease in Lewis rats (Emory University)



USAMRD-WRAIR Brooks City-Base TX

Background - Mechanism

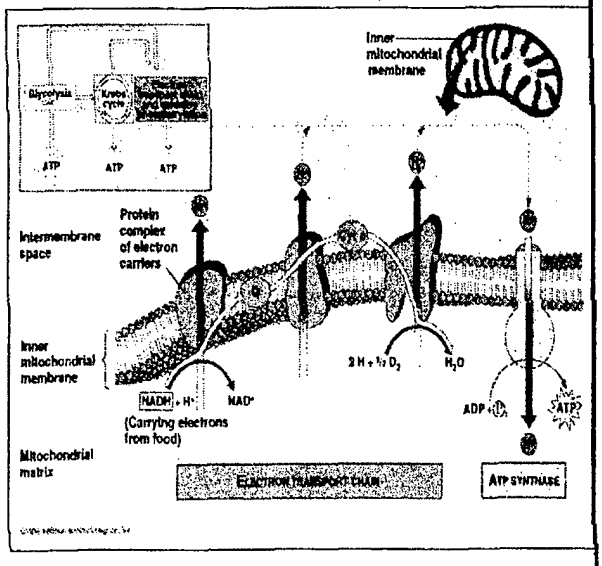


- Rotenone impairs the Mitochondrial cytochrome oxidase system
- Cytochrome oxidase system is an ATP producing system

USAMRD-WRAIR Brooks City-Base TX

Background - Mechanism

- Hydrogen atoms are removed from food in pairs and are ionized with NAD^+
- Electrons removed from the Hydrogen atoms enter the electron transport chain of electron acceptors
- Cytochrome oxidase complex has inner mitochondrial membrane spanning units, 4 protons pumped out for each reactive oxygen molecule
- Pathway for oxygen reduction at the bi-metallic center



Bioelectromagnetics 24:174–181 (2003)

Effects of High Power Microwave Pulses on Synaptic Transmission and Long Term Potentiation in Hippocampus

Andrei G. Pakhomov,[1,3]* Joanne Doyle,[1] Bruce E. Stuck,[2] and Michael R. Murphy[3]

[1]*McKesson BioServices Corporation, Brooks Air Force Base, San Antonio, Texas*
[2]*US Army Medical Research Detachment of the Walter Reed Army Institute of Research, Brooks Air Force Base, San Antonio, Texas*
[3]*Directed Energy Bioeffects Division, Human Effectiveness Directorate, Air Force Research Laboratory, Brooks Air Force Base, San Antonio, Texas*

Effects of short, extremely high power microwave pulses (EHPP) on neuronal network function were explored by electrophysiological techniques in the isolated rat hippocampal slice model. Population spikes (PS) in the CA1 area were evoked by repeated stimulation (1 per 30 s) of the Schaffer collateral pathway. A brief tetanus (2 s at 50 Hz) was used to induce long term potentiation (LTP) of synaptic transmission. In three different series of experiments with a total of 160 brain slices, the EHPP irradiation was performed before, during, or after the tetanus. The EHPP carrier frequency was 9.3 GHz, the pulse width and repetition rate were from 0.5 to 2 μs and from 0.5 to 10 Hz, respectively, and the peak specific absorption rate (SAR) in brain slices reached up to 500 MW/kg. Microwave heating of the preparation ranged from 0.5 °C (at 0.3 kW/kg time average SAR) to 6 °C (at 3.6 kW/kg). The experiments established that the only effect caused by EHPP exposure within the studied range of parameters was a transient and fully reversible decrease in the PS amplitude. Recovery took no more than a few minutes after the cessation of exposure and return to the initial temperature. This effect's features were characteristic of an ordinary thermal response: it was proportional to the temperature rise but not to any specific parameter of EHPP, and it could also be induced by a continuous wave (CW) irradiation or conventional heating. Irradiation did not affect the ability of neurons to develop LTP in response to tetanus or to retain the potentiated state that was induced before irradiation. No lasting or delayed effects of EHPP were observed. The results are consistent with the thermal mechanism of EHPP action and thus far provided no indication of EHPP-specific effects on neuronal function. Bioelectromagnetics 24:174–181, 2003. Published 2003 Wiley-Liss, Inc.[†]

Key words: high power microwave pulses; specific effects; hippocampal slices; LTP

INTRODUCTION

Recent advances in pulsed power technologies have resulted in increased availability and wider use of microwave transmitters that can emit nano- and microsecond pulses at peak powers of hundreds of megawatts or even gigawatts. One can reasonably expect that high peak, low average power radiation from such transmitters may cause biological reactions that are qualitatively different from known microwave effects and cannot be explained by ordinary heating. Extremely high power microwave pulses (EHPP) represent a new, unknown, and potentially hazardous environmental factor. This concern dictates the need to identify EHPP-specific bioeffects, if any, and to explore underlying physical and biological mechanisms.

Current knowledge of EHPP biological effects is very limited. The few studies that have explored peak SAR levels of 0.1–60 MW/kg in animals and in vitro, have produced isolated, sometimes contradictory, and generally inconclusive data [see for review Lu and DeLorge, 2000; Pakhomov et al., 2000b]. The data on EHPP bioeffects at still higher peak SAR (100 MW/kg and higher) are even more scarce: aside from our

Grant sponsor: US Army Medical Research and Material Command (AMRMC); Grant sponsor: US Air Force Research Laboratory (AFOSR) (to McKesson BioServices Corporation) (by US AMRMC); Grant number: DAMD17-94-C-4069.

*Correspondence to: Dr. Andrei G. Pakhomov, McKesson BioServices, 8308 Hawks Road, Building 1168, Brooks Air Force Base, San Antonio, TX 78235-5324.
E-mail: andrei.pakhomov@brooks.af.mil

Received for review 5 June 2002; Final revision received 26 July 2002

DOI 10.1002/bem.10079
Published online in Wiley InterScience (www.interscience.wiley.com).

Published 2003 Wiley-Liss, Inc.
[†]This article is a US government work, and, as such, is in the public domain of the United States of America.

previous work, only three studies have been reported. These studies claimed profound EHPP-specific (nonthermal) effects, including changes in the growth rate and metabolism of alga cultures [Tambiev et al., 1989]; stimulation of the immune system, suppression of tumor growth in vivo and in vitro [Deviatkov et al., 1994, 1998]; and inhibition of a fungus *Fusarium* growth, induction of developmental aberrations, imago death, and infertility in *Drosophila* flies [Bolshakov et al., 2000a,b]. These studies, however, could have suffered various flaws, both in biological experiment protocols and dosimetry [Pakhomov and Murphy, 2000], thus requiring confirmation for the findings.

Our previous studies explored EHPP effects in isolated, spontaneously beating frog heart slices [Pakhomov et al., 1999, 2000b] and in gel suspended yeast cells [Pakhomov et al., 2002]. All observed effects were consistent with the thermal paradigm and provided no proof of EHPP-specific effects.

One possible explanation for these negative findings is that the employed biological models and endpoints are relatively simple. One could speculate that EHPP-specific bioeffects could be more readily observed in higher organized systems and using more sophisticated tests. This possibility motivated us to further examine EHPP effects using an isolated mammalian brain slice model and long term potentiation (LTP) as a functional test. We selected rat hippocampal slices, a well studied and widely used model that offers wide opportunities for electrophysiological and pharmacological analyses. LTP is one of the best studied but still intriguing phenomena of synaptic plasticity, and it is commonly implied as one of the likely cellular mechanisms of memory [Bliss and Lynch, 1988; Martinez and Derrick, 1996]. An additional important reason for choosing isolated hippocampal slices were recent data presented by Tattersall et al. [2001] that this preparation manifests sensitivity to low intensity radiofrequency radiation.

MATERIALS AND METHODS

Male Sprague-Dawley rats (4–8 weeks old) were anesthetized with sodium pentobarbital (50 mg/kg i.p.) and decapitated. The brain was quickly removed and 350 μm thick parasagittal slices were cut with a Vibratome device (WPI, FL). Typically, 3–5 brain slices from the same animal could be used for different experiments during the same day. The slices were stored at room temperature in a holding chamber filled with artificial cerebrospinal fluid (ACSF) that was continually gassed with 95% O_2 and 5% CO_2 mixture. The ACSF was composed of: (mM): glucose, 11; NaCl, 125; KCl, 3; $MgCl_2$, 1; NaH_2PO_4, 1.25; $NaHCO_3$, 26, $CaCl_2$, 2; pH 7.2–7.4. For brain slicing procedure only, NaCl was substituted with an equimolar amount of sucrose and ACSF was chilled to about 0 °C.

One slice at a time was transferred into an exposure chamber and set at its bottom. The exposure chamber design was principally the same as described before [Pakhomov and Doyle, 2000; Pakhomov et al., 2000b], with modifications that enabled adequate life support for brain slices and stable electrophysiological recording. The chamber was mounted atop a waveguide flange; the waveguide opening was sealed with a sapphire matching plate, flush with the flange. Both the flange and the sapphire plate were covered with 0.5 mm Plexiglas, which served as a bottom of the exposure chamber; it insulated the waveguide flange from ACSF and prevented ACSF leakage between the sapphire and waveguide walls. To minimize microwave radiation leakage from the chamber and interference with electrophysiological and other equipment, the depth of ACSF in the chamber had to be kept at about 20 mm.

A brain slice was centered in a small frame (also made of 0.5 mm Plexiglas), which was affixed to the chamber bottom and aligned with the waveguide axis. Preventing the slice from floating away without damaging the slice or distorting the field while maintaining a continuous but laminar flow of fresh ACSF to the slice was a technical challenge, which was resolved in two different ways. The first way relied on a jet flow of ASCF from a nozzle above the slice, which forcefully pushed the slice to the bottom. The second solution used suction of ACSF through tiny grooves in the holding frame around the slice, which pulled the slice down. Both these techniques provided sufficient mechanical stability for extracellular microelectrode recording and adequate supply of fresh oxygenated ACSF to the slice.

The ACSF temperature was maintained at 34 °C and continually monitored with a Reflex fiber optic thermometer (Nortech Fibronic, Canada). An artifact-free PMDE-type temperature sensor (0.5 mm height, 0.55 mm diameter) was situated on the bottom of the chamber, 1–2 mm away from the brain slice. It is important to note that the temperature stabilization system did not (and was not intended to) compensate for microwave heating.

The area of Schaffer collateral of hippocampus (Fig. 1) was stimulated with a bipolar electrode assembled of two tungsten microelectrodes (0.25 mm shank diameter, type LF01G, Micro Probe, Inc., MD). The electrodes were coated with 3 μm thick parylene-C for electrical insulation, except 0.25 mm long tip tapering to 3–4 μm. The presence of a metal electrode in the chamber during microwave exposure could, at least theoretically, cause artifacts, so we employed a

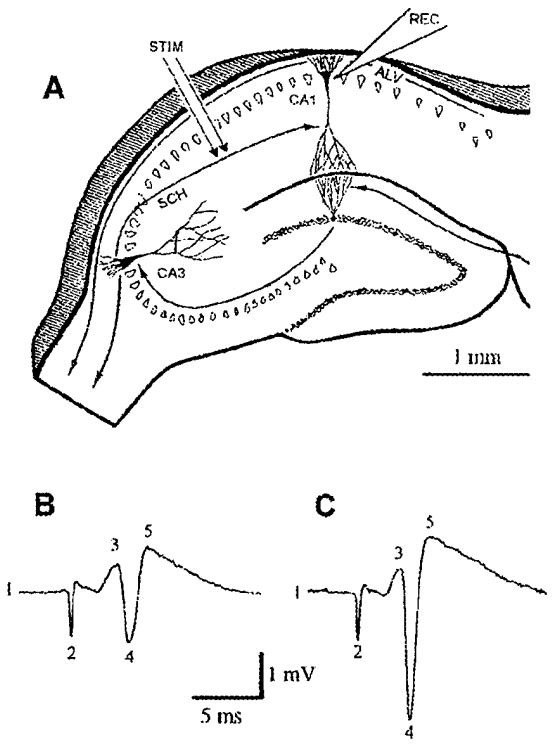


Fig. 1. **A**: Schematic diagram of a hippocampal slice [adapted from Dudek et al., 1976]. CA3 pyramidal cells send a collateral (SCH, Schaffer collateral system) to CA1 neurons, which have their axons along the alveus (ALV). Stimulation of the SCH with a bipolar electrode (STIM) produces evoked responses in CA1 neurons, which are recorded extracellularly with a glass micropipette (REC). **B**: The shape and peaks of the evoked response: 1, baseline; 2, stimulus artifact; 3, first peak of the excitatory postsynaptic potential, EPSP; 4, peak of the population spike, PS; 5, the second peak of the EPSP. Indices measured in this study were the PS amplitude, from peak 3 to peak 4, and the maximum slope of the PS, between the same peaks. **C**: the same evoked response as in B, but 4 min after induction of the long term potentiation (LTP) by a 2 sec, 50 Hz tetanus.

system that enabled withdrawing an electrode for the duration of exposure, subsequently returning it precisely into its original position. This feature was accomplished by driving the electrode with an MX831 motorized micromanipulator equipped with an MC1100e targeting motion controller (Siskiyou Design Instruments, OR). However, no artifacts were detected in any of the experiments, and this feature proved unnecessary.

A glass micropipette filled with 2 M NaCl (2–10 Mohm resistance) was used to record the stimulation evoked extracellular field potential of pyramidal neurons in the CA1 area (socalled population spike, PS, Fig. 1B). This signal was passed through a Duo 773 Amplifier (WPI), then digitized at 20 kHz and recorded using an MP100 data acquisition system (Biopac Systems, Inc., CA). Measured PS parameters were peak-to-peak amplitude and maximum slope; they correlated closely in all experiments, so only the amplitude data are depicted in the graphs in this article.

Generation of PS is a complex process that may be affected by events not directly related to LTP, such as polysynaptic inhibition and neuronal excitability changes. The excitatory postsynaptic potential (EPSP) would be a more selective measure of LTP, but PS is far more sensitive. It is routinely seen in brain slice experiments that alterations in electrical stimulation, temperature, oxygenation, etc. which cause a profound (e.g., twofold) change of the PS, have little or no measurable effect on the EPSP. Thus, the use of more sensitive PS measurements better served the goal of revealing possible bioeffects of EHPP.

Experiments usually began after a 30–120 min stabilization of the preparation activity in the exposure chamber. Stimulus intensity was adjusted to produce PS amplitude of 1.5–3 mV, which was typically 30–50% of the amplitude at the supramaximal stimulation. Afterwards, the stimuli were repeatedly delivered once every 30 s. LTP was induced by a 2 s, 50 Hz tetanus (these parameters were chosen in preliminary experiments), either before, after, or during microwave irradiation (series 1, 2, and 3, respectively). The LTP was manifested as a profound and stable increase in the PS amplitude and slope (Fig. 1C).

To facilitate comparison of experiments with different initial PS amplitude, this parameter was normalized in each individual experiment to the mean value of the first four or five datapoints, which were recorded before tetanus or exposure. Each brain slice was used in a single experiment and then discarded. The average data for exposed groups and sham exposed controls were compared by Student's paired *t*-test.

Microwave exposures were performed essentially the same way as described before [Pakhomov et al., 2002]. EHPP were generated by a model 337X magnetron transmitter (Applied Systems Engineering, Inc.) with the peak output of 230–260 kW. The pulse duration could be varied between 0.5 and 2 μs, at any pulse repetition rate less than 300 Hz. The peak E field in the waveguide (WR90, 22.86 mm × 10.16 mm) reached 1.57 MV/m. CW radiation was produced into the same waveguide by means of an HP 8690A sweep oscillator and Hughes 8020H amplifier. Both the transmitters were tuned to 9.3 GHz using an HP 8566B spectrum analyzer. Incident and reflected powers in the waveguide were measured via directional couplers by an HP 438A power meter with HP 8481A power

sensors. Reflection from the exposure chamber into the waveguide was less than 3%. EHPP shape was nearly rectangular, as monitored via an HP 432 detector on a TEK 2430A digital oscilloscope.

Local SAR values were measured in the ACSF using a microthermocouple technique [Pakhomov et al., 2000a,b, 2002]. For field mapping at the location of the brain slice, the MTC was driven in precision 0.2 or 0.5 mm steps in three orthogonal directions in ACSF by means of a micromanipulator. An analytical approach proposed by Alekseev and Ziskin [2000] was employed to account for differences in dielectric properties of the brain tissue and ACSF. The measurements established that the presence of the plastic bottom cover and the brain slice holding frame in the exposure chamber decreased local SAR by 50–60%, probably due to greater field scattering. However, both these structures were necessary for physiological stability of the slice, and the decreased SAR was an unwelcome but acceptable compromise. At the same time, the field uniformity noticeably improved, and variations of local SAR at the brain slice location did not exceed ± 20% of the SAR value at its geometrical center.

RESULTS

This article summarizes the data collected from over 160 brain slices in three independent series of experiments. In series 1, 2, and 3, respectively, tetanic stimulation that induced LTP was performed after, before, and during microwave exposure. If we follow the somewhat equivocal parallel between LTP and memory, these experiments would correspond to studying EHPP effect on the ability of neurons to form a memory record after the exposure (series 1), on the ability to maintain an already created memory record (series 2), and on the process of formation of the memory record (series 3). These series also differed in the exposure duration and exposure regimens tested. Within each series, different exposure regimens and sham exposures were alternated in a random manner.

In series 1, EHPP exposure lasted for 2 min, and tetanus was applied 1.5 min after the exposure. Two EHPP pulsing regimens were tested: 2 μs pulses at 0.5 Hz repetition rate, and 0.5 μs pulses at 2 Hz. The peak and time average SAR for these two regimens were the same (330 MW/kg and 0.33 kW/kg), producing identical heating of the preparation, by 0.5–0.6 °C (Fig. 2). In both the exposed groups, EHPP caused transient decrease in the EHPP amplitude by 8–10% ($P < 0.05$). However, the exposures did not alter the preparations' ability to develop LTP: in all three groups, tetanization caused PS to increase to

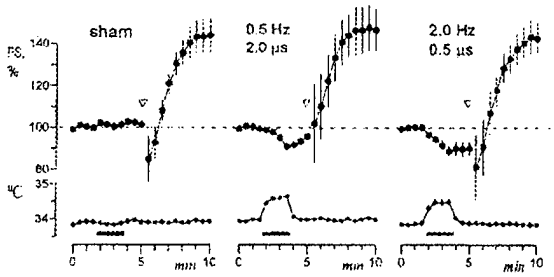


Fig. 2. Effect of EHPP exposures on the ability of neurons to develop LTP. The amplitude of the PS (% to the average pre-exposure value) and temperature (°C) are plotted against the time into the experiment (minutes). All the data, including temperature, are mean ± SE, n=8–9; however, the error bars are often smaller than the central symbol and therefore not visible. Sham and EHPP exposures are shown by horizontal bars. Triangles indicate the time of tetanus (2 sec at 50 Hz). The peak SAR is 330 MW/kg, the time average SAR is 0.33 kW/kg; the pulse width and repetition rate are shown next to the graphs.

140–150% of the initial value. The time course of LTP development showed no significant differences either.

In all groups of the series 2, LTP was induced by tetanization at 2.5 min into the experiment and reached its maximum (about 150%) in 3–4 min. Then, a 2 min EHPP exposure was applied at 7 min 45 s. The pulse duration and peak SAR were chosen to be the same in all the groups (1 μs and 360 MW/kg), whereas the pulse repetition rates and average SAR levels were set different: the rates of 2, 5, and 10 Hz resulted in SAR of 0.7, 1.8, and 3.6 kW/kg, and preparation heating of 1.4, 3.0, and 5.8 °C, respectively (Fig. 3). The potentiated PS decreased during EHPP irradiation, but recovered shortly and completely after cessation of the exposure and return of the temperature to the initial level. The magnitude of the PS suppression was proportional to the average SAR and temperature rise during the exposure. These data may be interpreted in a way that the intense irradiation and heating made the "memory record" temporarily unavailable, but did not erase or alter it.

Out of five groups of the series 3, two were exposed to EHPP, and the other two to CW radiation at the same wavelength and time average SAR (0.25 or 1 kW/kg). For EHPP irradiation at these SARs, 0.5 or 2 μs wide pulses were delivered at a rate of 1 Hz; the peak SAR was 500 MW/kg. Exposures began at 1 min 45 s into the experiment, and continued for 7 min. Microwave heating was 0.3–0.4 °C at the lower SAR and 1.5–1.6 °C at the higher one. Tetanus was applied at 4 min; thus, the exposure "covered" several minutes immediately prior to LTP induction and the period of transition to the potentiated state immediately after the

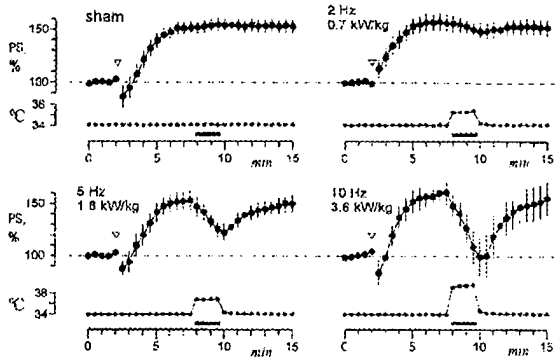


Fig. 3. Effect of EHPP exposure at different time average SAR on retainment of the LTP state by hippocampal neurons. The time average SAR and pulse repetition rates are shown on the graphs. The peak SAR is 360 MW/kg and the pulse width is 1 μs in all the groups. Each group includes 10–14 independent experiments. Note different temperature scales for the upper and lower graphs. Other designations are the same as in Figure 2.

tetanus. The transition state can be likened to a memorizing process or to consolidation of a memory record, and supposedly is the most vulnerable.

Indeed, all tested exposure regimens clearly affected the course of the transition: it became more gradual, and the difference from sham exposure reached maximum at 4–5 min after the tetanus (Fig. 4). For example, at 4 min (i.e., at 8 min into the experiment), the PS amplitude grew to 162 ± 5% of the initial value in sham-exposed controls, but only to 146 ± 5% and

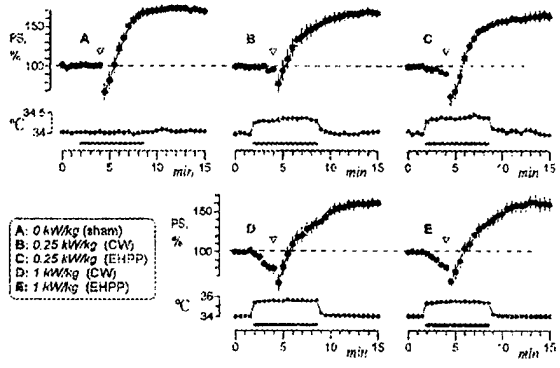


Fig. 4. Comparative effect of EHPP and CW exposures at equal SAR on the development of LTP. EHPP exposures were performed at 500 MW/kg peak SAR and 1 Hz pulse repetition rate; the pulse width is 0.5 μs (**C**) or 2 μs (**E**). Each group includes experiments in 11–15 brain slices, one experiment per slice. Note different temperature scales for the upper and lower graphs. Other designations are the same as in Figure 2.

132 ± 8% under EHPP exposure at 0.25 and 1 kW/kg, respectively ($P < 0.05$). However, CW exposures caused practically identical departure from the sham control values, to 146 ± 9% and 131 ± 8%.

At 1 kW/kg, both CW and EHPP exposures decreased the PS amplitude prior to tetanus by 20–30%. Interestingly, even this substantial inhibition did not change the efficacy of LTP induction, and the amplitude of potentiated PS after cessation of exposures stabilized at the same level as in the other groups, at 160–170%.

DISCUSSION

The only microwave effect established in our experiments was a transient PS suppression during irradiation. This suppression, which occurs uniformly in potentiated and non-potentiated PS, reflects the effect of radiation on the PS itself, rather than on the LTP. The LTP magnitude can be judged better from the potentiated PS amplitude when the transient suppression is already over, i.e., in several minutes after the exposure. As shown in Figures 2–4, the amplitude of the potentiated PS stabilized after the exposure at the same level in exposed and control groups in each series of experiments. This sameness suggests that all tested types of EHPP exposure, regardless of their specific parameters (different pulse widths and repetition rates, peak and average SAR, different exposure duration and timing with respect to tetanus) did not alter the ability of hippocampal neurons to develop LTP or to maintain the potentiated state. Thus, to the extent to which the LTP is implied to be involved in memory, one can expect that EHPP within the studied range of parameters will not affect the memory function either.

The magnitude of the transient PS suppression was proportional to the time average SAR and temperature rise during exposure, whereas other details of the exposure regimen, e.g., various combinations of pulse rate and pulse width, appeared to play no role. Moreover, EHPP and CW exposures at equal time average intensity (hence, producing equal temperature rise) produced identical biological effects. The reversible PS suppression was also observed under a "regular," i.e., non-EHPP, pulsed microwave exposure at sufficient intensities [Pakhomov and Doyle, 2000] and in numerous studies that explored the effect of conventional heat in brain slices [Fujii and Ibata, 1982; Schiff and Somjen, 1985; Masino and Dunwiddie, 1999; Masino et al., 2001]. The most likely physiological mechanism for this PS suppression is a reversible decrease of the resting input resistance of neurones [Thompson et al., 1985]; an additional mechanism may be a heat induced activation of presynaptic A_1-adenosine receptors, which inhibits the excitatory

transmitter release from the Schaffer collateral terminals to CA1 neurons [Masino and Dunwiddie, 1999; Masino et al., 2001].

While all the evidence points to the fact that the transient PS suppression under EHPP exposure was just a result of general heating, it may be difficult or impossible to prove this thesis incontrovertibly. Such proof would require a quantitative comparison with the effect of conventional heating, identical in the magnitude, temporal and spatial dynamics to EHPP heating; however, technical difficulties may prevent such experiment from ever being done. At this point, we can only state that the thermal mechanism adequately explains all observed effects and dependences, and that our experiments provided no indication for EHPP-specific effects on the synaptic transmission, evoked potentials, or LTP in isolated hippocampal slices.

This conclusion is consistent with our previous studies in isolated frog heart slices and yeast cells [Pakhomov et al., 1999, 2000b, 2002], but contrasts positive findings of other authors [Deviatkov et al., 1994, 1998; Tambiev et al., 1989; Bolshakov et al., 2000a,b]. Coincidentally, all these "positive effect" studies tested the same carrier frequency and the same pulse duration (10 GHz and 10 ns). This frequency happened to be very close to 9.2, 9.3, and 9.5 GHz in our "negative effect" studies, but the pulse duration was very different indeed (10 ns vs. 0.5–2 μs). Thus, the frequency was not responsible for differences in biological findings, but the shorter pulse duration could be. Other factors that should be accounted for are the differences in biological endpoints and peak intensity of the microwave pulses.

The lack of adequate dosimetry in the cited "positive effect" studies makes any comparison questionable at best; but, as far as we could estimate, peak SAR could reach even several GW/kg [Deviatkov et al., 1998], which is an order of magnitude higher than in our work, and 2–3 orders of magnitude higher than in any other EHPP studies of which we are aware [Akyel et al., 1991; Raslear et al., 1993; Jauchem and Frei, 1995]. One may conjecture that induction of EHPP-specific effects would require higher peak SAR combined with much shorter pulses than tried in our study. This hypothesis has yet to be experimentally tested, under strict experimental conditions that will exclude flaws and uncertainties of the reported "positive effect" studies.

Many institutions in the United States and elsewhere follow the human exposure standard developed by the IEEE [IEEE std C95.1, 1999]. One feature of this standard is the recommendation that the peak incident E field from any exposure should not exceed 100 kV/m. In the current set of experiments, as well as our previous work, we could find no effects associated with peak E field, per se, including incident exposures up to 1570 kV/m, even when the exposures were directed to sensitive electrically excitable tissues (heart and brain). All effects were related to temperature increase associated with SAR induced by the cumulative exposures. Our results suggest that an exposure limit to the body surface of 100 kV/m may be unnecessarily low or that a limit based on peak E field may be unnecessary altogether.

Aside from the above conclusions related to EHPP effects, it may be important to compare our findings with those of a recent study by Tattersall et al. [2001]. These authors employed the same in vitro model (rat hippocampal slices) to identify possible nonthermal effects of a brief (5–15 min) exposure to 700 MHz CW microwaves. The electric field intensity was kept under 71 V/m, which produced too little absorption for any appreciable heating: the respective SAR, by different estimates, was between 1.6 and 4.4 mW/kg. Nonetheless, these exposures strongly decreased or increased PS amplitude, thus significantly increasing the variance of this index, and inhibited epileptiform activity induced by 4-aminopyridine. Our study was not designed to replicate or verify these results, but if our exposures had the same effect on the PS, it would have readily been noticed. As of today, we tested exposure effects in more than a dozen series of experiments with over 400 brain slices, using various stimulation protocols and measurements which were precise enough to reveal less than 10% effects (e.g., Fig. 2 at 4 min). However, any effects could only be established when microwave heating exceeded a certain threshold (about 0.5 °C).

It is tempting to explain the nonthermal effects of Tattersall's group by higher effectiveness of their irradiation modality, i.e., to conclude that 700 MHz at 1–4 mW/kg is biologically effective, whereas 9–10 GHz in the range from 60 W/kg to 3–4 kW/kg is not. We feel, however, that other differences should be considered first, particularly, those in the exposure setup. In our design, the ACSF in the exposure chamber attenuated microwaves some 2^{20} times, thereby minimizing field pickup and any potential artifacts, even when working with EHPP. In contrast, parallel plate waveguide devices, like the one used for 700 MHz exposure, may be more "leaky" and more prone to producing interference. Whereas in the experience of one of the authors (A.P.) experimental artifacts due to interference are uncommon, their possibility cannot be neglected. Any connections to stimulating and recording electrodes, to the bead thermistor downstream from the brain slice, as well as the electrodes and the thermistor themselves, and even ground wires could potentially be a source of artifacts. It is encouraging that, as shown in the experiments with 4-aminopyridine,

nonthermal effects could still be elicited in the absence of a stimulation electrode, but the other potential sources of artifacts still have to be thoroughly checked. If the reported nonthermal effects are unambiguously replicated under artifact free conditions, this finding could have a major impact on modern microwave biology and RF exposure safety guidelines.

DISCLAIMER

The animals involved in this study were procured, maintained, and used in accordance with Federal Animal Welfare Act and the "Guide for the Care and Use of laboratory Animals," prepared by the Institute of Laboratory Animal Resources—National Research Council. The views expressed are those of the authors and should not be construed as reflecting the official policy or position of the Department of the Army, Department of the Air Force, or the United States Government.

REFERENCES

Akyel Y, Hunt EL, Gambrill C, Vargas C Jr. 1991. Immediate post-exposure effects of high-peak-power microwave pulses on operant behavior of Wistar rats. Bioelectromagnetics 12: 183–195.

Alekseev SI, Ziskin MC. 2000. Reflection and absorption of millimeter waves by thin absorbing films. Bioelectromagnetics 21:264–271.

Bliss TVP, Lynch MA. 1988. Long-term potentiation in the hippocampus: Properties and mechanisms. In: Landfield P, Deadwyler SA, editors. LTP: From biophysics to behavior. New York: Liss. pp 3–72.

Bolshakov MA, Bugaev SP, Elchaninov AA, Evdokimov EV, Goncharik AO, Gunin AV, Klimov AI, Knyazeva IR, Korovin SD, Kutenkov OP, Pegel IV, Rostov VV. 2000a. Effect of repetitive HPM pulses on some biological objects. In: Radiation physics and chemistry of condensed matter, high current electronics, and modification of materials with particle beams and plasma flows. Vol 2. Tomsk, Russia: Proc. 1st International Congress. pp 514–518.

Bolshakov MA, Bugaev SP, Goncharik AO, Gunin AV, Evdokimov EV, Klimov AI, Korovin SD, Pegel IV, Rostov VV. 2000b. Effects of intense microwave radiation of nanosecond pulse duration on some biological objects. Dokladi Academii Nauk 371:691–695. (Rus.)

Deviatkov ND, Pletnev SD, Chernov ZS, Faikin VV, Bernashevskii GA, Shchitkov KG. 1994. Effect of low-energy pulses of EHF and SHF-radiation of nanosecond duration with a high peak intensity on biological structures (malignant neoplasms). Dokladi Academii Nauk 336:826–828. (Rus.)

Deviatkov ND, Betskii OV, Kabisov RK, Morozova NB, Pletnev SD, Faikin VV, Chernov ZS. 1998. Effect of low-energy pulsed EHF and microwave radiation with nanosecond pulse duration and high peak power on biological structures (malignant neoplasms). Biomedicinskaya Radioelectronica 1:56–62. (Rus.)

Dudek FE, Deadwyler SA, Cotman CW, Lynch G. 1976. Intracellular responses from granule cell layer in slices of rat hippocampus: Perforant path synapse. J Neurophysiol 39:384–393.

Fujii T, Ibata Y. 1982. Effects of heating on electrical activities of guinea pig olfactory cortical slices. Pflugers Archiv 392: 257–260.

IEEE Std C95.1. 1999. IEEE standard for safety levels with respect to human exposure to radio frequency electromagnetic fields, 3 kHz To 300 GHz. 1999 edition. New York: Inst. of Electrical and Electronics Engineers, Inc. 73 p.

Jauchem JR, Frei MR. 1995. High-peak-power microwave pulses: Effects on heart rate and blood pressure in unanesthetized rats. Aviat Space Environ Med 66:992–997.

Lu ST, DeLorge JO. 2000. Biological effects of high peak power radiofrequency pulses. In: Lin JC, editor. Advances in electromagnetic fields in living systems. Vol 3. New York: Kluwer Academic/Plenum Publishers. pp 207–264.

Martinez JL, Derrick BE. 1996. Long-term potentiation and learning. Annual Rev Psychol 47:173–203.

Masino SA, Dunwiddie TV. 1999. Temperature-dependent modulation of the synaptic transmission in hippocampal slices is mediated by extracellular adenosine. J Neurosci 19:1932–1939.

Masino SA, Latini S, Bordoni F, Pedata F, Dunwiddie TV. 2001. Changes in hippocampal adenosine efflux, ATP levels, and synaptic transmission induced by increased temperature. Synapse 41:58–64.

Pakhomov AG, Doyle J. 2000. Effect of pulsed microwaves on the population spike in rat hippocampal slices. In: Kostarakis P, Stavroulakis P, editors. Biological effects of EMFs. Proc millennium international workshop on biological effects of electromagnetic fields. Heraklio, Crete, Greece. pp 480–485.

Pakhomov AG, Murphy MR. 2000. A comprehensive review of the research on biological effects of pulsed radiofrequency radiation in Russia and the former Soviet Union. In: Lin JC, editor. Advances in electromagnetic fields in living systems. Vol 3. New York: Kluwer Academic/Plenum Publishers. pp 265–290.

Pakhomov AG, Mathur SP, Belt M, Murphy MR. 1999. Dose dependencies in bioeffects of extremely high peak power microwave pulses. In: Repacholi MH, Rubtsova NB, Muc AM, editors. Electromagnetic fields: Biological effects and hygienic standardization. Geneva, Switzerland: World Health Organization. pp 325–334.

Pakhomov AG, Mathur SP, Akyel Y, Kiel JL, Murphy MR. 2000a. High-resolution microwave dosimetry in lossy media. In: Klauenberg BJ, Miklavcic D, editors. Radio frequency radiation dosimetry. Netherlands: Kluwer Academic Publishers. pp 187–197.

Pakhomov AG, Mathur SP, Doyle J, Stuck BE, Kiel JL, Murphy MR. 2000b. Comparative effects of extremely high power microwave pulses and a brief CW irradiation on pacemaker function in isolated frog heart slices. Bioelectromagnetics 21:245–254.

Pakhomov AG, Gajšek P, Allen L, Stuck BE, Murphy MR. 2002. Comparison of dose dependences for bioeffects of continuous-wave and high-peak power microwave emissions using gel-suspended cell cultures. Bioelectromagnetics 23:158–167.

Raslear TG, Akyel Y, Bates F, Belt M, Lu ST. 1993. Temporal bisection in rats: The effects of high-peak-power pulsed microwave irradiation. Bioelectromagnetics 14:459–478.

Schiff SJ, Somjen GG. 1985. The effect of temperature on synaptic transmission in hippocampal tissue slices. Brain Res 345: 279–284.

Tambiev AKh, Kirikova NN, Lapshin OM, Betzkii OV, Novskova TA, Nechaev VM, Petrov IYu. 1989. The combined effect of

exposure to EMF of millimeter and centimeter wavelength ranges on productivity of microalgae. In: Devyatkov ND, editor. Millimeter waves in medicine and biology. Moscow: Radioelectronica. pp 183–188. (Rus.)

Tattersall JEH, Scott LR, Wood SJ, Nettell JJ, Bevir MK, Wang Z, Somasin NP, Chen X. 2001. Effects of low intensity radiofrequency electromagnetic fields on electrical activity in rat hippocampal slices. Brain Res 904:43–53.

Thompson SM, Masukawa LM, Prince DA. 1985. Temperature dependence of the intrinsic membrane properties and synaptic potentials in hippocampal CA1 neurons in vitro. J Neurosci 5:817–824.

3rd International EMF Seminar in China:

Electromagnetic Fields and Biological Effects

Guilin, China

October 13-17, 2003



Session 7-2

IN VITRO MODEL RESEARCH INTO BIOEFFECTS OF EXTREMELY HIGH POWER MICROWAVE PULSES

Andrei G. Pakhomov[1,3], Bruce E. Stuck,[2] and Michael R. Murphy[3]
[1]McKesson BioServices Corporation, Brooks City-Base, San Antonio, Texas USA
[2]US Army Medical Research Detachment of the Walter Reed Army Institute of Research, Brooks City-Base, San Antonio, Texas USA
[3]Directed Energy Bioeffects Division, Human Effectiveness Directorate, Air Force Research Laboratory, Brooks City-Base, San Antonio, Texas, 78235-5324, USA.
Tel: 210 536-5599. Fax: 210 536 5382. E-mail: andrei.pakhomov@brooks.af.mil

Recent advances in pulsed power technologies have resulted in increased availability and wider use of microwave transmitters that can emit nano- and microsecond pulses at peak powers of hundreds of megawatts and even gigawatts. High-peak, low-average power radiation from such transmitters may cause biological reactions that are qualitatively different from known microwave effects, thereby representing a new, unknown, and potentially hazardous environmental factor. However, current knowledge of bioeffects of extremely high power microwave pulses (EHPP) remains very limited. The few studies that have explored peak specific absorption rate (SAR) levels of 0.1-20 kW/g have produced isolated and generally inconclusive data (see [1, 2] for review). EHPP bioeffects at still higher peak SAR (> 100 kW/g) remain mostly "uncharted territory" for biologists and safety specialists.

However, EHPP studies in animals are very costly, because they require gigawatt-output transmitters and custom-made exposure facilities, such as specialized anechoic chambers. Alternatively, many key aspects of EHPP biological action can be studied *in vitro* in cell and tissue models. Concentrating radiated energy in a small sample (e.g., 0.1-1 ml) can produce very high peak SAR (up to 1 MW/g) at relatively low transmitter output power (e.g., 250 kW). Other advantages of the *in vitro* approach are the possibilities for precise control of temperature and SAR in the exposed sample, greater flexibility of pulsing regimens, and safety of the exposure system for personnel and laboratory equipment.

In 1998, a one-of-a-kind EHPP exposure system designed specifically for in vitro biological research was assembled and put in operation at Brooks AFB Tri-Service Directed Energy Bioeffects Facility in San Antonio, TX, USA. In its current configuration (after several upgrades), this system is based on a model 337X magnetron transmitter (Applied Systems Engineering, Inc.) with the peak output of 230-260 kW at carrier frequencies from 9 to 10.5 GHz. The pulse duration can be varied between 0.5 and 2 μs, at any pulse repetition rate less than 300 Hz. The peak E-field in the waveguide (WR90, 22.86 x 10.16 mm) reaches 1.57 MV/m. For comparison of biological effects, the system can also be energized from a "regular" microwave source (HP 8690A sweep oscillator and Hughes 8020H amplifier) in CW or pulsed regimens, at the same carrier frequency and time-average power as the EHPP transmitter.

The chamber for exposure of biological specimens is made atop a vertical end section of the waveguide. The waveguide is sealed with a sapphire matching plate flush with the flange, and the chamber is filled with an appropriate electrolyte solution (e.g., a culture medium or a Ringer solution). Local SAR in solution above the matching plate was calculated theoretically (by an analytical technique and by a finite difference time domain modeling), and was measured using a novel method of precision high-resolution dosimetry [3]. The latter technique was particularly useful, including such tasks as SAR mapping within the exposed volume and local SAR measurements inside biological samples. It was established that our EHPP system is capable of producing peak SAR of up to 1 MW/g, which is about 20 times higher than ever reported by other investigators.

So far, EHPP effects have been explored is several biological models using various endpoints, including changes in the pacemaker rate in isolated, spontaneously beating frog heart slices [4]; the growth rate of gel-suspended yeast cells [5]; function of voltage-gated calcium channels in the membrane of cultured mammalian cells [6]; synaptic transmission and long-term potentiation in isolated rat hippocampal slices [7]. Exposure duration varied from less than a second to several hours, at pulse repetition rates from 0.1 Hz (practically no heating) up to 10-50 Hz (up to 20 °C temperature rise). Details of these studies, specific research techniques, objectives, and findings will be reviewed during the presentation. Overall,

EHPP exposures produced no biological effect if the temperature rise during exposure was negligible. On the contrary, when the temperature rise exceeded some 0.2-0.5 °C (depending on test sensitivity), EHPP produced same effects as CW irradiation at equal SAR or conventional heating of the same intensity. Within studied limits, no EHPP-specific bioeffects could be observed. One can speculate that all the tested biological objects just happened to be insensitive to EHPP; however, there is no guidance or indications that any other objects or processes might be more vulnerable. As of the up-to-date knowledge, EHPP appear to be a no more dangerous modality than CW emissions, and the safety standards based on general microwave heating of tissues should be just as applicable to EHPP as to "regular" microwave radiations. To test this implication, future studies should explore effects of still shorter pulses and at different carrier frequencies; also, special attention should be given to the possibility of delayed biological effects of EHPP exposure.

References:

1. Pakhomov A.G and Murphy M.R. A comprehensive review of the research on biological effects of pulsed radiofrequency radiation in Russia and the former Soviet Union. *In: Advances in Electromagnetic Fields in Living Systems, V. 3 (J. C. Lin, ed.), Kluwer Academic /Plenum Publishers, New York, 2000, 265-290.*
2. Lu S.-T and DeLorge J.O. 2000. Biological effects of high peak power radiofrequency pulses. Ibid., 207-264.
3. Pakhomov A.G, Mathur S.P., Akyel Y., Kiel J.L., and Murphy M.R. High-resolution microwave dosimetry in lossy media. *In: Radio Frequency Radiation Dosimetry (B. J. Klauenberg and D. Miklavcic, eds.), Kluwer: Netherlands, 2000, 187-197.*
4. Pakhomov A.G, Mathur S.P., Doyle J., Stuck B.E., Kiel J. L., and Murphy M.R. Comparative effects of extremely high power microwave pulses and a brief CW irradiation on pacemaker function in isolated frog heart slices. *Bioelectromagnetics, 2000, 21(4), 245-254.*
5. Pakhomov A.G, Gajšek P., Allen L., Stuck B.E., and Murphy M.R. Comparison of dose dependences for bioeffects of continuous-wave and high-peak power microwave emissions using gel-suspended cell cultures. *Bioelectromagnetics, 2002, 23(2), 158-167.*
6. Pakhomov A.G, Du, X., Doyle J., Ashmore J., and Murphy M.R. Patch-clamp analysis of the effect of high-peak power and CW microwaves on calcium channels. In: Biological Effects of EMFs. (P. Kostarakis, ed.). 2002, V. 1, p. 281-288.
7. Pakhomov A.G, Doyle J., Stuck B.E., and Murphy M.R. Effects of high-power microwave pulses on synaptic transmission and long-term potentiation in hippocampus. *Bioelectromagnetics, 2003 (in press).*

Acknowledgements: *The work was supported by the U.S. Army Medical Research and Materiel Command and the U.S. Air Force Research Laboratory (AFOSR) under U.S. Army contract DAMD17-94-C-4069 awarded to McKesson BioServices Corporation. The views expressed are those of the authors and should not be construed as reflecting the official policy or position of the Department of the Army, Department of the Air Force, or the United States Government.*

Session 7-3

9.37GHz microwave irradiation alter NMDA mRNA expression in the hippocampus of rats

Yu Zheng-ping, Zhang Yan-wen, Zhong Min, Zhou Zhou, and Zhang Guang-bin
PLA Center of Microwave bioeffects Research, Third Military Medical University
Chong Qing 400038, China

The nervous system is very sensitive to electromagnetic irradiation and hence is one of the major targets of microwave bioeffects. Disturbance to nervous system leads to behavioral changes. Dysfunction of learned behaviors is the prominent effect of microwave irradiation in experimental animals. However, the exact mechanisms of microwave irradiation induced behavioral disorders remain to be elucidated. In the past several years, we have been focused on exploring the possible role of NMDA receptors in functional changes of learned behaviors following exposure to 9.37GHz microwave.

Expressions of different NMDA receptor (NR1, NR2A, NR2B, NR2C, NR2D) subunit mRNA and formation of NMDA-dependent long term potential (LTP) were determined by RT-PCR , Western blotting and patch clamp technique in Wistar rats with 9.37 GHz microwave irradiation. It was found that: ①

Available online at www.sciencedirect.com
SCIENCE DIRECT®
Experimental Neurology 187 (2004) 418–429
Experimental Neurology
www.elsevier.com/locate/yexnr

Behavioral and immunohistochemical effects of chronic intravenous and subcutaneous infusions of varying doses of rotenone

Sheila M. Fleming,[a] Chunni Zhu,[a] Pierre-Olivier Fernagut,[a] Arpesh Mehta,[a] Cheryl D. DiCarlo,[b] Ronald L. Seaman,[c] and Marie-Françoise Chesselet[a,*]

[a] *Departments of Neurology and Neurobiology, The David Geffen School of Medicine at UCLA, Los Angeles, CA 90095-1769, USA*
[b] *U.S. Army Medical Research Detachment, Brooks City-Base, TX 78235, USA*
[c] *McKesson BioServices at USAMRD, Brooks City-Base, TX 78235, USA*

Received 28 August 2003; revised 23 January 2004; accepted 29 January 2004

Available online 24 March 2004

Abstract

Mitochondrial toxins such as the complex 1 inhibitor rotenone are widely used as pesticides and may be present in military environments. Administration of rotenone can induce biochemical and histological alterations similar to those of Parkinson's disease in rats. However, only a subset of animals show these effects and it is unclear whether more subtle alterations are caused by chronic administration of rotenone in those animals that appear resistant to its toxic effects on dopaminergic nerve terminals. To address this question, vehicle or rotenone (2.0, 2.5, or 3.5 mg/kg/day) was administered intravenously or subcutaneously for 21 days to adult rats, and rotenone effects on survival, motor behavior, and striatal tyrosine hydroxylase immunoreactivity (TH-IR) were examined. Both intravenous and subcutaneous rotenone induced a dose-dependent decrease in survival rates. Surviving animals showed a decrease in spontaneous rearing. Locomotor activity and movement initiation time were also altered in some of the experimental groups. Confirming previous results, TH-IR in the striatum was markedly decreased in rats that fell ill early in the study and in a few of the surviving rats with high rotenone doses. However, none of the surviving rats receiving 2.0 mg/kg/day showed TH-IR loss reminiscent of Parkinson's disease, and loss of striatal TH-IR across doses was not correlated with motor behavior in individual rats. Thus, chronic administration of low doses of rotenone induces motor anomalies even in animals that do not develop histological signs of Parkinson's disease, indicating a pervasive neurological effect of moderate mitochondrial dysfunction in vivo.
© 2004 Elsevier Inc. All rights reserved.

Keywords: Mitochondria complex 1; Rotenone; Microglia; Motor function; Tyrosine hydroxylase

Introduction

Many mitochondrial toxins are present in the environment because of their use as pesticides and herbicides in agricultural areas across the country. Intermittent or chronic exposure to these toxins may have deleterious affects on humans and animals. Indeed, epidemiological studies show a correlation between exposure to pesticides and herbicides and an increased risk of developing Parkinson's disease (Checkoway and Nelson, 1999; Gorell et al., 1998; Hertzman et al., 1994; Ritz and Yu, 2000; Semchuk et al., 1992). In view of the environmental risk to the general population and the presence of such agents in military applications, the study of animal models of mitochondrial dysfunction has become increasingly important.

Depending on the severity, mitochondrial inhibition in neurons can result in reduced ATP synthesis, excitotoxicity, and increased mitochondrial free radical generation (Murphy et al., 1999). Furthermore, it can potentiate dopamine and NMDA toxicity (Greene et al., 1998; McLaughlin et al., 1998a,b). Mitochondrial dysfunction has been implicated in several neurodegenerative disorders including Parkinson's disease (Haas et al., 1995; Mizuno et al., 1989; Parker et al., 1989; Schapira et al., 1989), Alzheimer's disease (Chandrasekaran et al., 1994; Kish et al., 1992), amyotrophic lateral sclerosis (Fiskum et al., 1999), and Huntington's disease (Panov et al., 2002). Even partial mitochondrial inhibition

* Corresponding author. Departments of Neurology and Neurobiology, The David Geffen School of Medicine at UCLA, 710 Westwood Plaza, Los Angeles, CA 90095-1769. Fax: +1-310-267-1786.
E-mail address: MChesselet@mednet.ucla.edu (M.-F. Chesselet).

0014-4886/$ - see front matter © 2004 Elsevier Inc. All rights reserved.

may trigger a cascade of events that ultimately leads to cell death (Betarbet et al., 2000; Sherer et al., 2003b).

Mitochondrial inhibitors have been used to generate animal models of neurodegenerative disorders. Administration of the complex 2 inhibitors 3-nitropropionic acid and malonate produces anatomical and clinical features consistent with Huntington's disease (Beal et al., 1993; Brouillet et al., 1995). In contrast, complex 1 inhibitors such as 1-methyl-4-phenyl-1-1,2,3,6-tetrahydropyridine (MPTP), paraquat, maneb, and rotenone can induce the death of nigrostriatal dopaminergic neurons, a hallmark of Parkinson's disease (Betarbet et al., 2000; Burns et al., 1983; Heikkila et al., 1984; McCormack et al., 2002; Sherer et al., 2003b; Tawara et al., 1996; Zhang et al., 2003).

The mitochondrial toxin rotenone is particularly interesting because it is widely used as an herbicide and to kill fish in reservoirs. A majority of studies of rotenone have focused on the ability of this toxin to induce neuropathological effects reminiscent of those seen in Parkinson's disease: loss of dopaminergic terminals in striatum and the formation of Lewy body-like inclusions in the substantia nigra (Alam and Schmidt, 2002; Betarbet et al., 2000; Sherer et al., 2003b). Others have shown that rotenone can also affect striatal neurons and other basal ganglia structures (Ferrante et al., 1997; Höglinger et al., 2003). It has been well documented that rotenone effects on nigrostriatal neurons are variable among animals, and major neuronal loss is more frequently observed in a subset of animals that become severely ill and must be euthanized early during treatment. Environmental exposure to mitochondrial toxins rarely leads to acute Parkinson's disease. It could, however, cause more subtle neurological impairments.

Our goal in the present study was to determine whether rotenone exerts any behavioral effects in the surviving animals and in those with little or no loss of dopaminergic terminals in the striatum. To this end, we have compared intravenous and subcutaneous administration routes of rotenone at varying doses on survival rates and established a behavioral profile of sensorimotor function following chronic infusion of rotenone for 3 weeks in animals that survive this regimen. Behavioral measures sensitive to varying degrees of sensorimotor dysfunction (locomotor activity, rearing, movement initiation, and adjusting steps) were used (Schallert and Tillerson, 2000; Schallert et al., 2000). In addition, the presence of tyrosine hydroxylase-containing axons and microglial activation were analyzed in the striatum with immunohistochemistry.

Materials and methods

Animals

A total of 108 adult male Lewis rats (240–327 g, from Charles River Labs, Michigan) were used in the study. Animals were housed in cages under controlled conditions of humidity (40–70%), lighting (12 h light/dark cycle), and temperature (20–22 °C), with free access to food and water. All experiments were performed in accordance with the National Research Council Guide for the Care and Use of Laboratory Animals and were approved by the U.S. Air Force Research Laboratory (AFRL)-Brooks Institutional Animal Care and Use Committee.

Treatment

Animals were randomly divided into three groups, intravenous infusion group (iv, rotenone = 45, vehicle control = 8), subcutaneous infusion group (sc, rotenone = 37, vehicle control = 12), and an unoperated cage control group ($n = 6$). A 2ML4 Alzet osmotic minipump (Durect Corp., Cupertino, CA) was prefilled 1–2 days before implantation with rotenone (Sigma, St Louis, MO) in equal amounts of dimethylsulfoxide (DMSO) and polyethylene glycol (PEG) using aseptic technique. A length of autoclaved Teflon micro tubing (0.013 in diameter, BB311-30, SCI, Lake Havasu City, AZ) was used as the flow moderator. The filled minipumps were placed into sterile 0.9% saline until implantation. Animals in infusion groups were anesthetized under 2.5% isoflurane in 100% oxygen for implantation surgery. Minipumps were placed into subcutaneous burrows on the dorsal surface for subcutaneous infusion. The Teflon micro tubing from the minipump was connected to a jugular vein cannula for intravenous infusion. Animals were continuously infused with rotenone at a rate of 2 (iv, $n = 15$; sc, $n = 12$), 2.5 (iv, $n = 16$; sc, $n = 11$), 3.5 (iv, $n = 14$; sc, $n = 11$), or 5 mg/kg/day (sc, $n = 3$) or with DMSO/PEG vehicle only (iv, $n = 8$; sc, $n = 12$) for 21 days after surgery. The use of 5 mg/kg/day dose was discontinued because the three animals tested did not survive. At the end of the experiment, animals were deeply anesthetized with injections of ketamine HCl (100 mg/kg, ip) and xylazine (10 mg/kg) and intracardially perfused with saline, followed by 10% formalin in PBS (pH 7.4). Brains were removed, postfixed in the same fixative for 2–4 h, and then transferred to PBS until being cryoprotected in 30% sucrose and stored at −80 °C.

Behavioral tests

A battery of behavioral tests sensitive to varying degrees of dopamine loss in the striatum and substantia nigra were used in this study to assess motor function. Animals with intravenous and subcutaneous drug treatments were evaluated for rearing activity, initiation of movement, and postural stability in three different tests. In addition, intravenous animals were tested for locomotor activity in automated chambers. For rearing and movement initiation, animals were videotaped and later scored by an experimenter blind to the condition of the animal. Animals were tested for locomotor activity, rearing, and postural stability at four time points: before pump implantation (baseline) and 1, 2, and 3 weeks after implantation.

Movement initiation was measured at three time points: 1, 2, and 3 weeks after pump implantation. Only animals that completed all 3 weeks of the experiment were included in statistical analyses.

Locomotor activity

Locomotor activity was measured by detecting animal movements in a 40.8 by 40.8 cm square arena of an AccuScan activity monitor (AccuScan, Columbus, OH). Interruptions of infrared beams at 3.6 and 14.7 cm above the arena floor were automatically detected during a 10-min test session in the dark. The arena was cleaned after each session. Beam interruption information was processed on-line with DigiScan software (AccuScan) to provide indices of horizontal and vertical movements and total distance traveled.

Rearing activity

To measure rearing activity, animals were placed in a clear Plexiglas cylinder (17.6 m inside diameter, 34 cm height). All animals were tested and videotaped under red light. While in the cylinder, animals typically rear and engage in exploratory behavior by placing their forelimbs along the wall of the cylinder (Schallert and Tillerson, 2000). Because rotenone affects motor behavior bilaterally, activity was measured by counting the number of rears made by each animal in a 5-min period without recording specific limb use. Videotapes were rated and analyzed by an experimenter blind to experimental condition.

Movement initiation

To test movement initiation, stepping movements made by each forelimb were assessed with an isolated forelimb test (Lindner et al., 1995; Olsson et al., 1995; Schallert and Tillerson, 2000; Schallert et al., 1992; Tillerson et al., 2001, 2002). The rat was held by its torso with its hindlimbs and one forelimb lifted above the surface of a table so that the weight of the animal's body was supported by one forelimb alone. Bedding from the animal's homecage was placed on the table near the animal to encourage movement. Animals with nigrostriatal damage typically take longer to initiate a movement compared to control animals (Schallert et al., 1992). The time to initiate one step was recorded for each forelimb. Due to the bilateral effect of rotenone, initiation times for both forelimbs were averaged together to create one score.

Step test

The step test was used to measure postural stability (Chang et al., 1999; Schallert and Tillerson, 2000). In this test, animals were held in the same manner as in the movement initiation test where one forelimb bore the weight of the animal. The animal was then moved laterally across a distance of 80 cm on a tabletop. The number of adjusting steps made as the animal was moved across a table was recorded for each forelimb. The average number of steps in three trials for each forelimb was used for analysis. Animals with nigrostriatal damage typically drag their forelimb across the tabletop instead of making adjusting steps (Schallert et al., 1979).

Immunocytochemistry

Coronal brain sections (40 μm) were cut on a Leica CM 1800 cryostat (Deerfield, IL) and processed for tyrosine hydroxylase (TH) and OX-42 immunostaining. OX-42 is a mouse monoclonal antibody against the type 3 complement receptor (CR3) that is expressed by activated macrophages and microglial cells. Sections were processed in batches that included tissue from groups of animals that were balanced across all experimental treatments. Sections were washed in phosphate-buffered saline (PBS) and then incubated in 0.3% H_2O_2/0.3% goat serum/PBS for 30 min to block endogenous peroxidase. After washing in PBS, sections were incubated in 10% goat serum/0.3% Triton X 100/PBS for 1 h. Sections were then incubated in the primary antibodies, mouse anti-tyrosine hydroxylase (1:20000; i.e., 0.2 μg/ml, Sigma) or OX-42 (1:100; i.e., 10 μg/ml, Serotec, England) at 4°C overnight. Sections were washed in PBS and then incubated in the secondary antibody, biotinylated goat anti-mouse IgG $F(ab)_2$ (1:500, ICN Biomedicals, Costa Mesa, CA) for 1 h. The avidin–biotin complex method was used to detect the secondary antibody (ABC elite kit, Vector laboratories, Burlingame, CA) and the reaction product was visualized by 3,3′-diaminobenzidine tetrachloride (DAB, Sigma). Control sections for TH were incubated with mouse IgG_1 (0.2 μg/ml, Sigma). Control sections for OX-42 were incubated with mouse IgG_{2a} (10 μg/ml, Sigma). Sections were dehydrated and cleared with xylene, mounted with Eukit mounting medium (Calibrated Instruments, Hawthorne, NY), and examined under bright-field illumination with a Zeiss Axioskop microscope (Thornwood, NY). Digital images were captured by a Spot digital camera (Sterling Heights, MI).

Optical density of tyrosine hydroxylase immunoreactivity in the striatum

Optical density (OD) measurements of tyrosine hydroxylase immunoreactivity (TH-IR) were determined with a computer-assisted image analysis system (Sony DKC-CM30 camera with 55 mm micro Nikkor lens f/2.8, Scion Image beta 4.0.2). Images were acquired after calibration of the system to eliminate saturation of gray levels for an accurate determination of OD. Regions of interest (striatum and adjacent cortex) were determined as follows: the outer border of the striatum was defined by the lateral ventricle medially, the corpus callosum dorsally and laterally, and

ventrally by a line drawn between the two anterior commissures, while the adjacent cortex was defined ventrally by the corpus callosum. Anatomical landmarks (aspect, size, and position of the anterior commissures, corpus callosum, septum, lateral ventricles, striatum, nucleus accumbens) were used to ensure that TH-IR levels were analyzed in similar regions within and between groups.

Striatal sections processed without primary antibody were used to determine the level of nonspecific staining for the entire experiment. After subtraction of the nonspecific staining, the TH-IR OD was measured in the dorsal striatum and the adjacent sensorimotor cortex. Because TH-IR fibers are very sparse in rat cortex, the value in cortex was considered a "blank" and was used to normalize staining levels for each section. Accordingly, reported TH-OD values in striatum represent the difference between TH-OD measured in striatum and cortex. Measures were performed on the left and right side and averaged for each section. In addition, TH-IR was visually rated for level of staining in sections throughout the striatum by an experimenter blind to condition as strong (+++), reduced (++), markedly reduced (+), almost absent (±), or absent (−) TH-IR. Similarly, OX-42 staining was rated for resting, partial activation, and full activation by an experimenter blind to condition.

Statistics

Intravenous and subcutaneous rotenone groups were analyzed using a mixed design (repeated and between measures) ANOVA. For locomotor activity, rearing activity and the step test, scores were calculated as percent of preimplantation scores (baseline). For movement initiation, no preimplantation testing was performed; therefore, the scores were presented as time to initiate movement. Mean percent baseline scores or mean movement initiation times were compared using a two-factor ANOVA for rotenone dose (between measure) and time tested (repeated measure). Post hoc analysis was done using Fisher's LSD. Mean TH-IR OD measurements were analyzed using a one-way ANOVA comparing rotenone and vehicle-treated groups for both intravenous and subcutaneous administration routes. For correlation analysis, TH-IR ratings were transformed into numerical values and compared with rearing and movement initiations scores from the 3 weeks time point. All analyses were conducted using GB-STAT software (Dynamic Microsystems, Inc. 2000) for Macintosh. The level of significance was set at $P < 0.05$.

Results

Survival analysis

Any animal that showed severe signs of illness during the experiment was prematurely euthanized. A dose-dependent survival rate was observed in animals chronically infused with rotenone. For intravenous infusion, there was no mortality in vehicle-infused animals ($n = 8$). At 2.0 mg/kg/day of rotenone, 7 out of 15 animals survived, resulting in a survival rate of 47%. At the 2.5 dose, 44% of the animals survived (7 of 16), and at the 3.5 dose, only 29% survived (4 of 14). A similar pattern of survival was observed in the subcutaneous group. There was no mortality in the vehicle-infused group ($n = 12$), 67% survived in the 2.0 group (8 of 12), 36% in the 2.5 group (4 of 11), 9% in the 3.5 group (1 of 11), and 0% survived in the 5.0 group (0 of 3). All cage control animals survived the length of the experiment ($n = 6$).

Locomotor activity

Locomotor activity counts were collected only for the intravenous group. A group of cage control animals were

Table 1
Locomotor activity

Rotenone dose (mg/kg/day)					
Activity	CC ($n = 6$)	0.0 ($n = 8$)	2.0 ($n = 7$)	2.5 ($n = 7$)	3.5 ($n = 4$)
V.1	45.72 ± 4.15	113.0 ± 27.2	28.9 ± 7.0	42.3 ± 14.4	30.9 ± 6.4
V.2	62.70 ± 4.35	72.7 ± 17.6	46.7 ± 16.1	82.2 ± 28.6	50.3 ± 22.5
V.3	54.26 ± 7.57	87.9 ± 30.5	59.8 ± 13.4	68.7 ± 16.0	28.1 ± 10.8
H.1	59.42 ± 4.95	120.4 ± 20.3††	55.5 ± 9.3**	54.6 ± 11.2**	51.8 ± 7.0**
H.2	76.82 ± 7.47	84.9 ± 11.1	61.8 ± 12.8	86.7 ± 14.8	65.9 ± 14.8
H.3	60.38 ± 6.59	93.4 ± 21.6†	75.9 ± 12.0	82.8 ± 11.9	46.6 ± 4.7*
D.1	55.62 ± 4.35	122.1 ± 25.0††	45.4 ± 10.3**	55.2 ± 12.0**	46.4 ± 6.7**
D.2	75.89 ± 6.58	84.2 ± 13.7	56.0 ± 15.0	88.3 ± 19.5	60.7 ± 17.6
D.3	60.56 ± 6.50	92.8 ± 25.4†	77.5 ± 13.9	84.5 ± 17.5	41.5 ± 5.2*

Locomotor activity scores (percent of baseline) for the intravenous group across 3 weeks are expressed as mean ± standard error. Cage control (CC), vehicle-infused controls (0.0), 2.0 mg/kg/day rotenone (2.0), 2.5 mg/kg/day rotenone (2.5), and 3.5 mg/kg/day rotenone (3.5) are shown. Animals were measured for vertical activity (V.1, V.2, V.3), horizontal activity (H.1, H.2, H.3), and distance traveled (D.1, D.2, D.3) at 1, 2, and 3 weeks after pump implantation.

* Represents $P < 0.05$ compared to vehicle-infused animals.

** Represents $P < 0.01$ compared to vehicle-infused animals.

† Represents $P < 0.05$ compared to cage control animals.

†† Represents $P < 0.01$ compared to cage control animals.

included in this analysis. Horizontal and vertical activity (respective numbers of beam interruptions) and total distance traveled in centimeters were measured for cage control, vehicle-infused, 2.0, 2.5, and 3.5 mg/kg/day rotenone groups. Separate analyses of horizontal activity, vertical activity, and distance using a 5 × 3 mixed design ANOVA revealed no effect of dose or time but did show a significant dose × time interaction for horizontal activity and total distance traveled, $F(8,54) = 2.59$, $P < 0.05$ and $F(8,54) = 2.18$, $P < 0.05$, respectively. Post hoc tests revealed significant reductions in horizontal activity and distance traveled at week 1 for 2.0, 2.5, and 3.5 mg/kg/day rotenone compared to vehicle-infused controls, $P < 0.05$. At week 3, only the 3.5 mg/kg/day rotenone group showed significant reductions in horizontal activity and distance traveled compared to vehicle-infused animals, $P < 0.05$ (Table 1). In addition, scores were significantly higher for the vehicle-infused animals compared to cage control at 1 ($P < 0.01$) and 3 ($P < 0.05$) weeks for horizontal activity and distance traveled. It is possible that the increase in activity may be due to stress from the minipump and constant infusion of vehicle solution that contained a combination of DMSO, PEG, and saline. It has been shown that physical and emotional stress can increase locomotor activity in rats (Pijlman et al., 2003). Therefore, further analyses for the intravenous-treated animals were performed using a 4 × 3 mixed design ANOVA that included only vehicle-infused animals as controls.

Rearing activity

The number of spontaneous rears made during 5 min in the cylinder was measured for each animal. For the intravenous rotenone infusion group, a mixed design 4 × 3 ANOVA indicated a significant effect of dose $F(3,22) = 5.40$, $P < 0.01$ and time $F(2,44) = 6.90$, $P < 0.01$. There was no significant dose × time interaction. Animals receiving the 2.0 and 3.5 mg/kg/day dose consistently reared significantly less compared to vehicle-infused animals at 1, 2, and 3 weeks following pump implantation ($P < 0.01$ for the 2.0 dose at each time point and the 3.5 dose at week 1; $P < 0.05$ for the 3.5 dose at weeks 2 and 3). At week one, animals in the 2.5 mg/kg/day dose also reared significantly less than vehicle-infused controls ($P < 0.01$).

Due to the high mortality rate, the numbers of surviving animals in the sc 3.5 and 5.0 mg/kg/day rotenone groups were not sufficient to perform statistical analyses. Therefore, a 3 × 3 mixed design ANOVA was performed on subcutaneous animals receiving vehicle, 2.0 and 2.5 mg/kg/day rotenone at each time point (weeks 1, 2, and 3) on the behavioral tests. For the subcutaneous rotenone infusion group, there was a significant effect of dose $F(2,18) = 4.68$, $P < 0.05$. There was no significant effect of time and no dose × time interaction. Animals receiving both the 2.0 and 2.5 doses of subcutaneous rotenone reared significantly less compared to vehicle-infused animals at 1, 2, and 3 weeks after pump implantation ($P < 0.01$ except for the 2.5 mg/kg/day dose at week 3 where $P < 0.05$, Fig. 1).

Movement initiation

Time to initiate a step was recorded for both forelimbs of each animal and then averaged. In the intravenous infusion group, ANOVA indicated no significant effect of dose or time and no significant dose × time interaction. For the subcutaneous infusion group, ANOVA showed a significant effect of time $F(2,42) = 4.43$, $P < 0.05$. Initiation times for

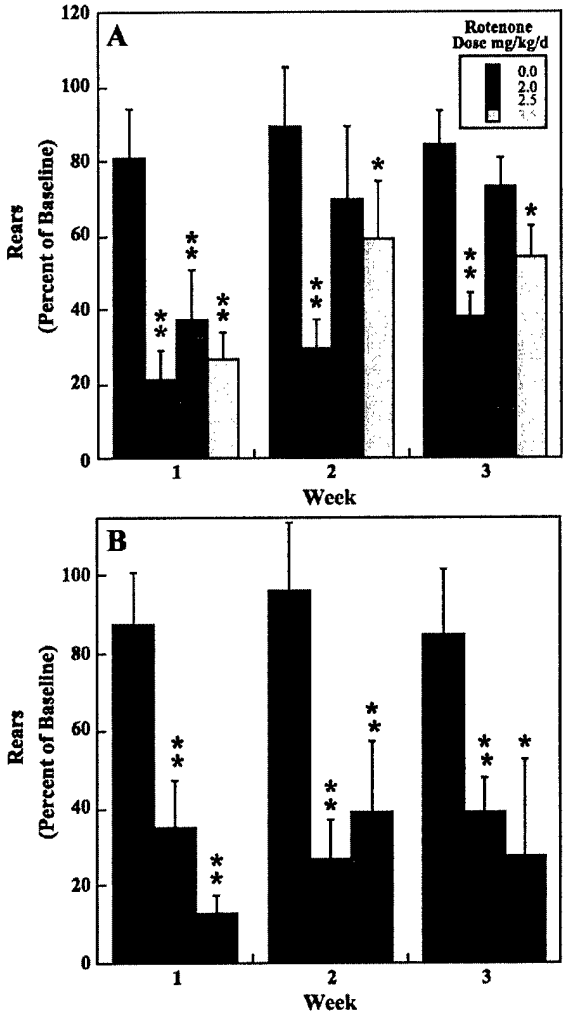


Fig. 1. Spontaneous rearing scores (percent of baseline) for animals treated with vehicle, 2.0, 2.5, and 3.5 mg/kg/day of rotenone and tested at 1, 2, and 3 weeks during chronic intravenous (A) or subcutaneous (B) administration. Only scores from animals that survived 3 weeks were included. Baseline rearing scores for intravenous and subcutaneous groups were 21.94 ± 1.13 and 21.52 ± 1.35, respectively. There were between 4 and 10 animals per group (two vehicle rats were excluded for technical reasons). Values are expressed as mean ± standard error of the mean. *Represents $P < 0.05$ and **represents $P < 0.01$ compared to vehicle-infused animals in the same week.

the 2.0 mg/kg/day subcutaneous rotenone dose were significantly longer at 2 weeks ($P < 0.05$) and initiation times for the 2.5 dose were significantly longer at 3 weeks after pump implantation ($P < 0.05$, Fig. 2).

Step test

Postural stability was measured by calculating the number of adjusting steps an animal made in response to experimenter-induced lateral movement. For the intravenous rotenone group, ANOVA revealed a small but significant effect of time $F(2,44) = 4.00$, $P < 0.05$. Post hoc analysis revealed a significant increase in the number of steps made

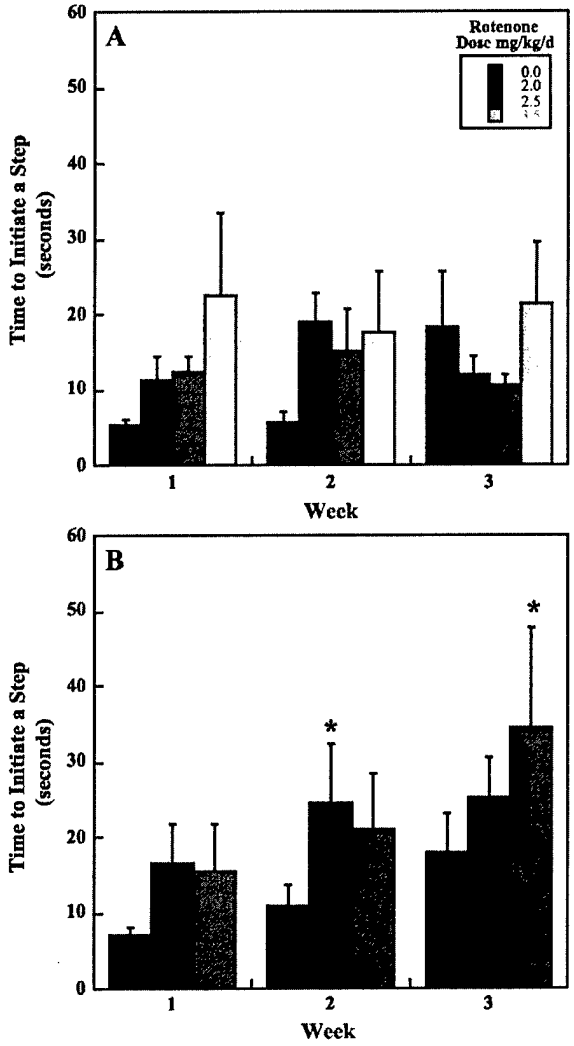


Fig. 2. Movement initiation times for animals treated with vehicle, 2.0, 2.5, and 3.5 mg/kg/day rotenone and tested at 1, 2, and 3 weeks during chronic intravenous (A) or subcutaneous (B) administration. Only scores from animals that survived 3 weeks were included ($n = 4-12$ per group). Values are expressed as mean ± standard error of the mean. *Represents $P < 0.05$ compared to vehicle-infused animals in the same week.

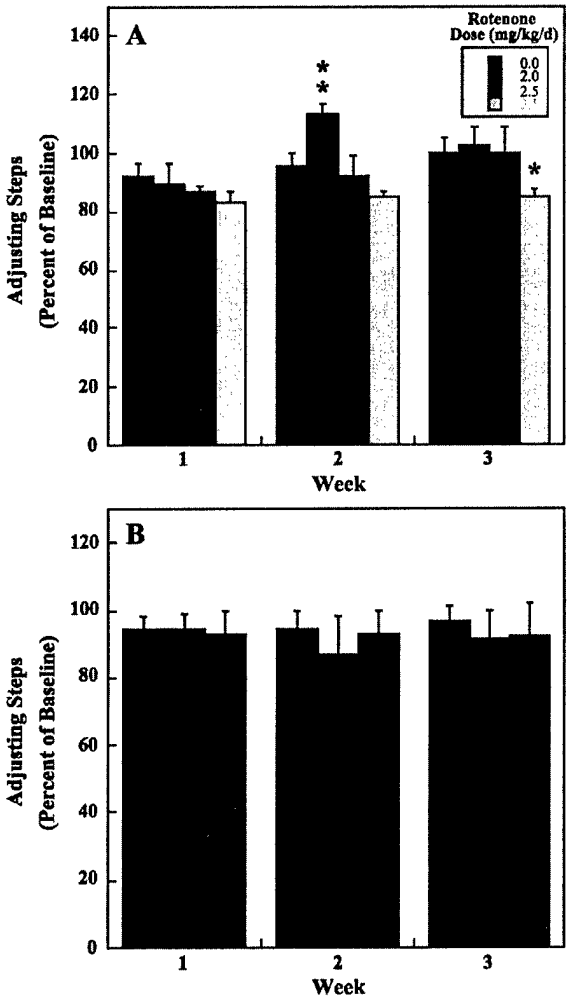


Fig. 3. Adjusting step scores (percent of baseline) for animals treated with vehicle, 2.0, 2.5, and 3.5 mg/kg/day rotenone and tested at 1, 2, and 3 weeks during chronic intravenous (A) or subcutaneous (B) administration. Only scores from animals surviving 3 weeks were included ($n = 4-12$ per group). Baseline stepping scores for intravenous and subcutaneous groups were 19.32 ± 0.45 and 19.62 ± 0.39, respectively. Values are expressed as mean ± standard error of the mean. *Represents $P < 0.05$ and **represents $P < 0.01$ compared to vehicle-infused animals in the same week.

in the 2.0 mg/kg/day group at week 2 ($P < 0.01$ compared to vehicle control animals), and a significant decrease in adjusting steps for the 3.5 mg/kg/day dose at week 3 ($P < 0.05$). There was no significant effect of dose and no dose × time interaction. For the subcutaneous experiment, ANOVA showed no significant effects of dose or time, and no dose × time interaction (Fig. 3).

Tyrosine hydroxylase immunoreactivity in the striatum

TH-IR optical density measurements in the striatum were calculated for both intravenous and subcutaneous infusion groups. Several animals in both the intravenous and subcu-

Table 2
TH-IR optical density measurements

Dose (mg/kg/day)	Intravenous	*n* size	Subcutaneous	*n* size
Vehicle	0.20 ± 0.04	7	0.12 ± 0.02	8
2.0	0.18 ± 0.03	6	0.17 ± 0.02	7
2.5	0.12 ± 0.04	6	0.11 ± 0.07	4
3.5	0.08 ± 0.04	4	0.002	1

Relative TH-IR optical density measurements in the striatum were calculated for animals receiving chronic intravenous or subcutaneous rotenone. Only scores from animals that survived 3 weeks were included.

taneous infusion groups showed obvious reductions in TH-IR; however, due to the variable response to rotenone, ANOVA revealed no significant effect of dose on TH-IR ($P > 0.05$; Table 2). Therefore, in addition to TH-IR optical density measurements, a qualitative visual inspection and rating of TH-IR staining in the striatum was performed. Fig. 4 shows examples of strong (+++: Fig. 4A), markedly reduced (+: Fig. 4C), or absence (−; Fig. 4D) of TH-IR and a rare case where TH-IR was absent from the central striatum (Fig. 4B), as previously reported (Betarbet et al., 2000). Based on visual ratings, a loss of TH-IR was observed in the striatum of a subset of animals with intravenous rotenone. In surviving animals, there was no reduction in TH-IR at the 2 mg/kg/day. At the 2.5 mg/kg/day, 33% (two of six rats) showed reduced or complete loss of TH-IR in the striatum. At 3.5 mg/kg/day, 50% (two of four rats) of the animals showed reduced TH-IR in the striatum. Loss of TH-IR in the striatum was also observed with the subcutaneous infusion group. Survivors showed no reduction in TH-IR at 2 mg/kg/day. At 2.5 mg/kg/day, 50% (2 of 4) of the animals showed reduced or profound loss of TH-IR in striatum and the one animal in the 3.5 dose group showed profound loss of TH-IR. The heterogeneity of TH-IR loss and the lack of a dose effect of rotenone are consistent with previous studies (Betarbet et al., 2000; Sherer et al., 2003b), indicating that some animals are more susceptible to the toxic effects of rotenone treatment compared to others.

In both intravenous and subcutaneous groups, the non-survivors (animals that were euthanized prematurely) showed reduced or profound loss of TH-IR in the striatum, 70% (7/10) for the intravenous group and 83% (10/12) for the subcutaneous group. Most of these animals did not undergo behavioral testing because they died within the first week of the experiment.

TH-IR and behavior

Correlations between TH-IR levels in the striatum and behavioral outcome measures were calculated for both intravenous and subcutaneous groups. Analyses were done using behavioral data collected at 3 weeks and pooled across dose according to TH-IR. Therefore, only animals that survived the entire experiment were included in the correlation analyses. TH-IR ratings were transformed into numerical values. Strong TH-IR was given a score of 3 and reduced TH-IR was given a score of 2. Markedly reduced, almost absent and absent scores were all given a score of 1. Rearing and movement initiation scores were not signifi-

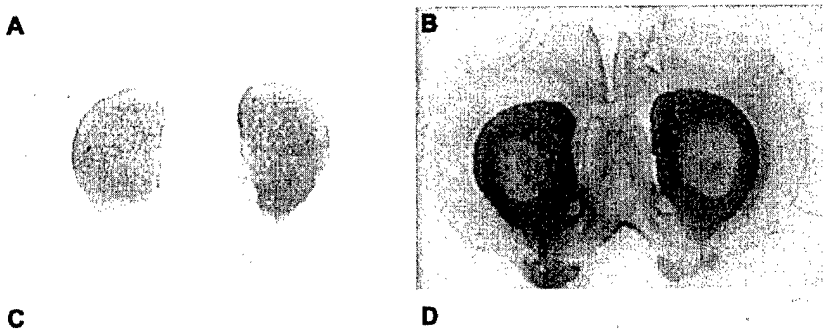


Fig. 4. Pattern of TH-IR reduction in the striatum after rotenone administration. Coronal brain sections from vehicle control animal (A) and rotenone-treated animals (B–D) were immunostained for TH. The control brain showed strong immunoreactivity in the striatum (rated +++). After rotenone infusion, one animal (nonsurvivor) receiving the sc 2.0 mg/kg/day dose showed circumscribed loss of TH-IR in the striatum (B). Some animals showed more diffuse (C, rated as +) or complete loss of TH-IR (D, rated as −).

Table 3
TH-IR ratings and behavior

	Number of animals	TH-IR rating	Step initiation time (s)	Percent cylinder rears
Intravenous infusion	19	+++	12.3 ± 1.9	67.17 ± 7.76
	7	++	21.6 ± 7.8	69.5 ± 17.3
	6	+± –	14.5 ± 4.8	81.5 ± 13.4
Subcutaneous infusion	8	+++	30.5 ± 7.2	57.7 ± 6.8
	9	++	20.6 ± 5.1	60.81 ± 16.6
	7	+± –	19.4 ± 7.2	47.08 ± 30.85

Step initiation time and rearing in the cylinder (percent of baseline) are expressed as mean ± standard error and were collapsed across all experimental groups (cage control, vehicle-infused controls, 2.0, 2.5, and 3.5 mg/kg/day rotenone) according to their TH-IR ratings.

cantly correlated with TH-IR ratings within the striatum for either the intravenous ($r = -0.01$ and 0.23, $P > 0.05$, respectively) or subcutaneous ($r = 0.13$ and 0.14, $P > 0.05$, respectively) groups (Table 3).

Microglia activation

Activated microglia are characterized by dramatic changes in morphology and increased expression of surface molecules such as the complement CR3 receptor, which is detected by the OX-42 antibody. Immunostaining for OX-42 was performed in a subset of animals ($n = 11$; Fig. 5). Within this subset, animals that received the low dose of subcutaneous rotenone (2.0 mg/kg/day) and did not show a loss of TH-IR in the striatum showed no microglial activation. However, rotenone-treated animals that did show TH-IR loss also showed significant microglial activation, indicating that failure to detect microglial activation was not technical.

Discussion

In the present study, chronic exposure to rotenone administered intravenously or subcutaneously resulted in a dose-dependent decrease in survival rates as well as robust behavioral impairments in rearing activity. Impairments in locomotor activity, movement initiation, and a modest impairment in postural stability were also observed but were inconsistent across groups and/or time tested. The subcutaneous method produced more consistent behavioral results in rearing compared to the intravenous administration. Although TH-IR was affected by the higher doses of rotenone, it was not correlated with behavioral impairment. These findings indicate that even when they do not markedly alter TH-IR in the striatum, low doses of rotenone have a significant effect on some aspects of motor behavior.

Survival analysis and TH immunoreactivity

Survival analysis revealed a low survival rate (under 50%) for doses 2.5 mg/kg/day and higher for both administration routes. Animals receiving 2.0 mg/kg/day of rote-

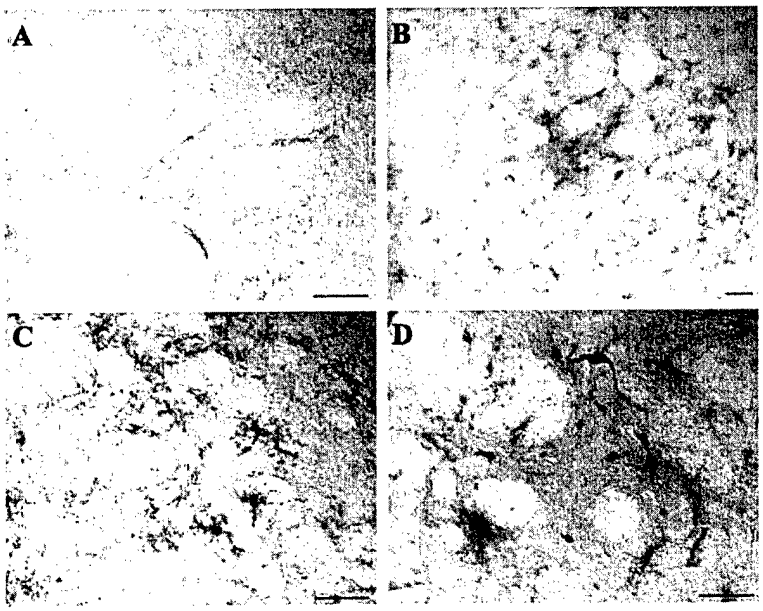


Fig. 5. Microglial activation in the striatum after rotenone infusion. Coronal brain sections from vehicle control animal (A) and a rotenone-treated animal (B–D) were stained for OX-42. Microglia in the control brain were ramified and lightly stained for OX-42 (A). A rotenone-infused animal with the circumscribed TH-IR loss is shown at lower magnification to illustrate the extensive microglial activation in this area of the striatum (B). In the same animal, microglia were activated to different stages, from partial activation showing bushy processes (C) to more advanced activation showing amoeboid cell bodies (D). Scale bar, 100 μm.

none maintained the highest survival rates, particularly in the subcutaneous group (67% survival). It has been shown that after systemic administration (2–3 mg/kg/day), the concentration of free rotenone in the brain is approximately 20–30 nM (Talpade et al., 2000), which results in only partial inhibition of complex I (Betarbet et al., 2000; Sherer et al., 2003b). This suggests that inhibition of complex I in brain may not account for the adverse effects seen in most animals. Peripheral mitochondrial inhibition is likely to play a critical role in the poor survival rate.

Of the rotenone-treated animals that survived the experiment, 24% (4/17) showed a reduction in TH-IR in the striatum for the intravenous group and 23% (3/13) showed reduced TH-IR in the subcutaneous group indicating a loss or dysfunction of dopaminergic terminals. These findings are similar to previous studies of animals chronically infused with rotenone (2–3 mg/kg/day; Sherer et al., 2003a). Evidence from several studies including the present study demonstrates a highly variable loss of TH-IR in response to rotenone suggesting a differential vulnerability between animals to the toxin while Lewis rats, an inbred strain, were used (Betarbet et al., 2000; Höglinger et al., 2003; Sherer et al., 2003b). At the 2.0 mg/kg/day, no changes in TH-IR were observed in the striatum in both intravenous and subcutaneous groups in surviving animals. However, more animals did show a decrease in TH-IR as the dose of rotenone increased. Additionally, of the subset of animals that became severely ill soon after rotenone treatment (nonsurvivors), 70% in the intravenous group and 83% in the subcutaneous group showed significantly reduced or profound loss of TH-IR in the striatum. Thus, TH-IR loss was much more frequent in nonsurvivors than in survivors.

Microglial activation

Rats chronically treated with rotenone have been shown to exhibit microglial activation in the striatum with or without nigrostriatal damage (Sherer et al., 2003a). However, in our study, microglial activation was not observed in rats with no loss of TH-IR. Varying levels of microglial activation were observed in the striatum of animals with TH-IR loss: some microglia were highly activated with an ameboid shape, others remained partially activated or in a resting status. Although microglial activation could be a consequence of rotenone-induced damage to dopaminergic terminals, it could also contribute to the pathology. Microglia, the immune cells in the brain, are involved in immune surveillance and control and have been considered to be a sensor for pathological changes in the brain (Kreutzberg, 1996). Activated microglia secrete cytotoxic factors and proinflammatory cytokines such as nitric oxide, superoxide, tumor necrosis factor-α (TNF-α), and interleukin-1β that may further contribute to brain injury (Liu and Hong, 2003) and in particular, to the loss of dopaminergic neurons (Gao et al., 2002, 2003).

Motor function

Most nonsurvivors rapidly showed signs of extreme sickness and had to be euthanized within the first week of rotenone exposure. Their status would have precluded meaningful behavioral analysis. Therefore, behavioral testing was only performed on animals that survived at least 1 week or longer. To permit a time-course analysis of the data without including more affected animals at the early than later time points, the few animals that died between 1 and 3 days were not included in the statistical analyses presented. Accordingly, the results of the sensorimotor tests are reflective of animals that withstood the rotenone treatment (survivors) and not the more vulnerable animals (nonsurvivors). However, analyses including the few animals tested at week 1 that did not survive 3 weeks did not differ significantly from these.

Behaviorally, animals treated with subcutaneous rotenone showed a more consistent dose-dependent decrease in rearing across the 3 weeks, compared with animals in the intravenous group. The variable behavioral response in the intravenous group may be due to problems with catheter patency. The subcutaneous route of administration is not only methodologically more efficient, but it also produces more consistent rearing deficits throughout the experiment.

Locomotor activity was only examined in animals with intravenous rotenone administration. These animals displayed significant impairments in horizontal activity and distance traveled in automated chambers at 1 week, and for the highest dose (3.5 mg/kg/day), at 3 weeks after pump implantation. However, impairment in vertical activity was not statistically significant by ANOVA in this test. This is in contrast to rearing in the cylinder, which may be a more sensitive measure of vertical activity. Indeed, the number of vertical beam interruptions during a rear was dependent on horizontal motion of the animal's body through two different planes and was more of a vertical index than an actual rear, whereas in the cylinder, rearing was determined visually by an experimenter and did not depend on horizontal movement of the animal.

The transient effect of the 2 and 2.5 mg/kg/day doses of rotenone on horizontal activity and distance traveled suggests that the behavioral deficits observed were not solely due to a systemic effect of complex 1 inhibition. In previous studies, animals with systemic toxicity did not survive the entire experiment and usually died within 3 days after pump implantation (Höglinger et al., 2003; Sherer et al., 2003b). The marked loss of TH-IR in the nonsurvivors and in a subset of surviving rats that received the higher doses of rotenone confirms that the mitochondrial toxin does affect the nigrostriatal dopamine system, and the robust decrease in rearing activity is compatible with alterations in dopamine function (Hofele et al., 2001; Sedelis et al., 2001). However, of all the behavioral measures, rearing was the only test consistently affected by rotenone. Alterations in locomotor activity, movement initiation, and postural sta-

bility were also observed but only at some time points. It is unclear why these were not sustained, but in the absence of severe neuronal loss, it is possible that compensatory mechanisms overcame these more subtle deficits.

It is well established that in nigrostriatal injury induced by 6-OHDA in rats, substantial compensation occurs within the DA system. Residual DA terminals in the striatum can maintain normal extracellular DA levels even with an 80% loss of DA input in the substantia nigra (Castaneda et al., 1990; Zigmond et al., 1984). This can be due to increases in DA synthesis and release, tyrosine hydroxylase production, and/or sprouting of residual terminals (Castaneda et al., 1990; Finkelstein et al., 2000; Robinson et al., 1990; Song and Haber, 2000; Zigmond et al., 1984). Although only 23–24% of rotenone-treated animals that completed the study showed a reduction in TH-IR, compensatory mechanisms within the nigrostriatal system may have prevented detection of dopaminergic changes by using only TH-IR as a measure of the integrity of the nigrostriatal system. For example, TH protein, activity, and mRNA levels have been shown to be regulated by the dopamine transporter. In mice lacking the dopamine transporter, TH protein level in the striatum was decreased by 90%; however, the rate of DA synthesis was doubled indicating increased TH activity by residual neurons (Gainetdinov et al., 2001; Jaber et al., 1999; Jones et al., 1998). It is possible that chronic infusion of rotenone may also affect dopamine transporter activity and influence the expression and activity of striatal TH. Therefore, it is possible that the motor abnormalities observed following rotenone treatment were caused by alterations in the nigrostriatal dopaminergic system but were not detected by TH-IR alone.

The inconsistent effect of rotenone on locomotor activity, movement initiation, and postural stability and the lack of a correlation between the behavioral anomalies and TH-IR in the striatum also suggests that other systems may be affected. It has been shown that nondopaminergic striatal neurons and the globus pallidus can be damaged by rotenone administration (Ferrante et al., 1997; Höglinger et al., 2003). Alterations to other neurotransmitter systems and damage to basal ganglia structures may contribute to the observed motor impairments.

In conclusion, the survival and histochemical analyses presented here confirm the toxicity of rotenone for dopaminergic nigrostriatal neurons in a subset of animals, and reveals marked survival differences within a narrow dose range following various doses and routes of administration for chronic rotenone exposure. The profile of behavioral deficits induced by rotenone reveals that even the lowest dose used (2 mg/kg/day) affectively disrupts motor behavior. Furthermore, behavioral anomalies occurred in the absence of the histological hallmark of Parkinson's disease, namely a massive loss of dopaminergic nerve terminals in the striatum. Thus, moderate chronic mitochondrial inhibition in the rat significantly affects the central nervous system. This is of particular importance in view of the current widespread use of this and other mitochondrial toxins in civilian and military environments.

Acknowledgments

This work is supported by the U.S. Army Medical Research and Materiel Command under contract DAMD17-94-C-4069 awarded to McKesson BioServices Corporation.

The views, opinions, and/or findings contained in this report are those of the authors and should not be construed as an official Department of the Army position, policy, or decision.

In conducting this research, the investigator(s) adhered to the *Guide for the Care and Use of Laboratory Animals* prepared by the NRC Institute of Laboratory Animal Resources.

For support in various technical areas of this work, we thank F. Wood, S. Adam, and A. Grado, U.S. Army Medical Research Detachment (USAMRD); A. Phinney and A. Garcia, McKesson BioServices; and S. Savoie and J. Toner, AFRL Veterinary Services at Brooks City-Base. We also thank Mr. Bruce Stuck, USAMRD Director, and Dr. Shin-Tsu Lu, McKesson BioServices, for their continued support and oversight of the work.

References

Alam, M., Schmidt, W.J., 2002. Rotenone destroys dopaminergic neurons and induces parkinsonian symptoms in rats. Behav. Brain Res. 136, 317–324.

Beal, M.F., Brouillet, E., Jenkins, B.G., Ferrante, R.J., Kowall, N.W., Miller, J.M., Storey, E., Srivastava, R., Rosen, B.R., Hyman, B.T., 1993. Neurochemical and histologic characterization of striatal excitotoxic lesions produced by the mitochondrial toxin 3-nitropropionic acid. J. Neurosci. 13, 4181–4192.

Betarbet, R., Sherer, T.B., MacKenzie, G., Garcia-Osuna, M., Panov, A.V., Greenamyre, J.T., 2000. Chronic systemic pesticide exposure reproduces features of Parkinson's disease. Nat. Neurosci. 3, 1301–1306.

Brouillet, E., Hantraye, P., Ferrante, R.J., Dolan, R., Leroy-Willig, A., Kowall, N.W., Beal, M.F., 1995. Chronic mitochondrial energy impairment produces selective striatal degeneration and abnormal choreiform movements in primates. Proc. Natl. Acad. Sci. U. S. A. 92, 7105–7109.

Burns, R.S., Chiueh, C.C., Markey, S.P., Ebert, M.H., Jacobowitz, D.M., Kopin, I.J., 1983. A primate model of parkinsonism: selective destruction of dopaminergic neurons in the pars compacta of the substantia nigra by *N*-methyl-4-phenyl-1,2,3,6-tetrahydropyridine. Proc. Natl. Acad. Sci. U. S. A. 80, 4546–4550.

Castaneda, E., Whishaw, I.Q., Robinson, T.E., 1990. Changes in striatal dopamine neurotransmission assessed with microdialysis following recovery from a bilateral 6-OHDA lesion: variation as a function of lesion size. J. Neurosci. 10, 1847–1854.

Chandrasekaran, K., Giordano, T., Brady, D.R., Stoll, J., Martin, L.J., Rapoport, S.I., 1994. Impairment in mitochondrial cytochrome oxidase gene expression in Alzheimer disease. Brain Res. Mol. Brain Res. 24, 336–340.

Chang, J.W., Wachtel, S.R., Young, D., Kang, U.J., 1999. Biochemical and anatomical characterization of forepaw adjusting steps in rat models of Parkinson's disease: studies on medial forebrain bundle and striatal lesions. Neuroscience 88, 617–628.

Checkoway, H., Nelson, L.M., 1999. Epidemiologic approaches to the study of Parkinson's disease etiology. Epidemiology 10, 327–336.

Ferrante, R.J., Schulz, J.B., Kowall, N.W., Beal, M.F., 1997. Systemic administration of rotenone produces selective damage in the striatum and globus pallidus, but not in the substantia nigra. Brain Res. 753, 157–162.

Finkelstein, D.I., Stanic, D., Parish, C.L., Tomas, D., Dickson, K., Horne, M.K., 2000. Axonal sprouting following lesions of the rat substantia nigra. Neuroscience 97 (1), 99–112.

Fiskum, G., Murphy, A.N., Beal, M.F., 1999. Mitochondria in neurodegeneration: acute ischemia and chronic neurodegenerative diseases. J. Cereb. Blood Flow Metab. 19, 351–369.

Gainetdinov, R.R., Mohn, A.R., Bohn, L.M., Caron, M.G., 2001. Glutamatergic modulation of hyperactivity in mice lacking the dopamine transporter. Proc. Natl. Acad. Sci. U. S. A. 98, 11047–11054.

Gao, H.M., Hong, J.S., Zhang, W., Liu, B., 2002. Distinct role for microglia in rotenone-induced degeneration of dopaminergic neurons. J. Neurosci. 22, 782–790.

Gao, H.M., Hong, J.S., Zhang, W., Liu, B., 2003. Synergistic dopaminergic neurotoxicity of the pesticide rotenone and inflammogen lipopolysaccharide: relevance to the etiology of Parkinson's disease. J. Neurosci. 23, 1228–1236.

Gorell, J.M., Johnson, C.C., Rybicki, B.A., Peterson, E.L., Richardson, R.J., 1998. The risk of Parkinson's disease with exposure to pesticides, farming, well water, and rural living. Neurology 50, 1346–1350.

Greene, J.G., Sheu, S.S., Gross, R.A., Greenamyre, J.T., 1998. 3-Nitropropionic acid exacerbates *N*-methyl-D-aspartate toxicity in striatal culture by multiple mechanisms. Neuroscience 84, 503–510.

Haas, R.H., Nasirian, F., Nakano, K., Ward, D., Pay, M., Hill, R., Shults, C.W., 1995. Low platelet mitochondrial complex I and complex II/III activity in early untreated Parkinson's disease. Ann. Neurol. 37, 714–722.

Heikkila, R.E., Hess, A., Duvoisin, R.C., 1984. Dopaminergic neurotoxicity of 1-methyl-4-phenyl-1,2,5,6-tetrahydropyridine in mice. Science 224, 1451–1453.

Hertzman, C., Wiens, M., Snow, B., Kelly, S., Calne, D., 1994. A case-control study of Parkinson's disease in a horticultural region of British Columbia. Mov. Discord. 9, 69–75.

Hofele, K., Sedelis, M., Auburger, G.W., Morgan, S., Huston, J.P., Schwarting, R.K., 2001. Evidence for a dissociation between MPTP toxicity and tyrosinase activity based on congenic mouse strain susceptibility. Exp. Neurol. 168, 116–122.

Höglinger, G.U., Feger, J., Prigent, A., Michel, P.P., Parain, K., Champy, P., Ruberg, M., Oertel, W.H., Hirsch, E.C., 2003. Chronic systemic complex I inhibition induces a hypokinetic multisystem degeneration in rats. J. Neurochem. 84, 491–502.

Jaber, M., Dumartin, B., Sagne, C., Haycock, J.W., Roubert, C., Giros, B., Bloch, B., Caron, M.G., 1999. Differential regulation of tyrosine hydroxylase in the basal ganglia of mice lacking the dopamine transporter. Eur. J. Neurosci. 11, 3499–3511.

Jones, S.R., Gainetdinov, R.R., Jaber, M., Giros, B., Wightman, R.M., Caron, M.G., 1998. Profound neuronal plasticity in response to inactivation of the dopamine transporter. Proc. Natl. Acad. Sci. U. S. A. 95, 4029–4034.

Kish, S.J., Bergeron, C., Rajput, A., Dozic, S., Mastrogiacomo, F., Chang, L.J., Wilson, J.M., DiStefano, L.M., Nobrega, J.N., 1992. Brain cytochrome oxidase in Alzheimer's disease. J. Neurochem. 59, 776–779.

Kreutzberg, G.W., 1996. Microglia: a sensor for pathological events in the CNS. Trends Neurosci. 19, 312–318.

Lindner, M.D., Winn, S.R., Baetge, E.E., Hammang, J.P., Gentile, F.T., Doherty, E., McDermott, P.E., Frydel, B., Ullman, M.D., Schallert, T., et al., 1995. Implantation of encapsulated catecholamine and GDNF-producing cells in rats with unilateral dopamine depletions and parkinsonian symptoms. Exp. Neurol. 132, 62–76.

Liu, B., Hong, J.S., 2003. Role of microglia in inflammation-mediated neurodegenerative diseases: mechanisms and strategies for therapeutic intervention. J. Pharmacol. Exp. Ther. 304, 1–7.

McCormack, A.L., Thiruchelvam, M., Manning-Bog, A.B., Thiffault, C., Langston, J.W., Cory-Slechta, D.A., Di Monte, D.A., 2002. Environmental risk factors and Parkinson's disease: selective degeneration of nigral dopaminergic neurons caused by the herbicide paraquat. Neurobiol. Dis. 10, 119–127.

McLaughlin, B.A., Nelson, D., Erecinska, M., Chesselet, M.F., 1998a. Toxicity of dopamine to striatal neurons in vitro and potentiation of cell death by a mitochondrial inhibitor. J. Neurochem. 70, 2406–2415.

McLaughlin, B.A., Nelson, D., Silver, I.A., Erecinska, M., Chesselet, M.F., 1998b. Methylmalonate toxicity in primary neuronal cultures. Neuroscience 86, 279–290.

Mizuno, Y., Ohta, S., Tanaka, M., Takamiya, S., Suzuki, K., Sato, T., Oya, H., Ozawa, T., Kagawa, Y., 1989. Deficiencies in complex I subunits of the respiratory chain in Parkinson's disease. Biochem. Biophys. Res. Commun. 163, 1450–1455.

Murphy, A.N., Fiskum, G., Beal, M.F., 1999. Mitochondria in neurodegeneration: bioenergetic function in cell life and death. J. Cereb. Blood Flow Metab. 19, 231–245.

Olsson, M., Nikkhah, G., Bentlage, C., Bjorklund, A., 1995. Forelimb akinesia in the rat Parkinson model: differential effects of dopamine agonists and nigral transplants as assessed by a new stepping test. J. Neurosci. 15, 3863–3875.

Panov, A.V., Gutekunst, C.A., Leavitt, B.R., Hayden, M.R., Burke, J.R., Strittmatter, W.J., Greenamyre, J.T., 2002. Early mitochondrial calcium defects in Huntington's disease are a direct effect of polyglutamines. Nat. Neurosci. 5, 731–736.

Parker Jr., W.D., Boyson, S.J., Parks, J.K., 1989. Abnormalities of the electron transport chain in idiopathic Parkinson's disease. Ann. Neurol. 26, 719–723.

Pijlman, F.T.A., Herremans, A.H.J., van de Kieft, J., Kruse, C.G., van Ree, J.M., 2003. Behavioural changes after different stress paradigms: prepulse inhibition increased after physical, but not emotional stress. Eur. Neuropsychopharmacol. 13, 369–380.

Ritz, B., Yu, F., 2000. Parkinson's disease mortality and pesticide exposure in California 1984–1994. Int. J. Epidemiol. 29, 323–329.

Robinson, T.E., Castaneda, E., Whishaw, I.Q., 1990. Compensatory changes in striatal dopamine neurons following recovery from injury induced by 6-OHDA or methamphetamine: a review of evidence from microdialysis studies. Can. J. Psychol. 44 (2), 253–275.

Schallert, T., Tillerson, J.L., 2000. Intervention strategies for degeneration of DA neurons in parkinsonism: optimizing behavioral assessment of outcome. In: Emerich, D.F., Dean III, R.L., Sandberg, P.R. (Eds.), Central Nervous System Diseases. Humana Press, Torowa, NJ.

Schallert, T., De Ryck, M., Whishaw, I.Q., Ramirez, V.D., Teitelbaum, P., 1979. Excessive bracing reactions and their control by atropine and L-DOPA in an animal analog of Parkinsonism. Exp. Neurol. 64, 33–43.

Schallert, T., Norton, D., Jones, T.A., 1992. A clinically relevant unilateral rat model of parkinsonian akinesia. J. Neural Transplant. Plast. 3, 332–333.

Schallert, T., Fleming, S.M., Leasure, J.L., Tillerson, J.L., Bland, S.T., 2000. CNS plasticity and assessment of forelimb sensorimotor outcome in unilateral rat models of stroke, cortical ablation, parkinsonism and spinal cord injury. Neuropharmacology 39, 777–787.

Schapira, A.H., Cooper, J.M., Dexter, D., Jenner, P., Clark, J.B., Marsden, C.D., 1989. Mitochondrial complex I deficiency in Parkinson's disease. Lancet 1, 1269.

Sedelis, M., Schwarting, R.K., Huston, J.P., 2001. Behavioral phenotyping of the MPTP mouse model of Parkinson's disease. Behav. Brain Res. 125, 109–125.

Semchuk, K.M., Love, E.J., Lee, R.G., 1992. Parkinson's disease and exposure to agricultural work and pesticide chemicals. Neurology 42, 1328–1335.

Sherer, T.B., Betarbet, R., Kim, J.H., Greenamyre, J.T., 2003a. Selective microglial activation in the rat rotenone model of Parkinson's disease. Neurosci. Lett. 341, 87–90.

Sherer, T.B., Kim, J.H., Betarbet, R., Greenamyre, J.T., 2003b. Subcutaneous rotenone exposure causes highly selective dopaminergic degeneration and alpha-synuclein aggregation. Exp. Neurol. 179, 9–16.

Song, D.D., Haber, S.N., 2000. Striatal responses to partial dopaminergic lesion: evidence for compensatory sprouting. J. Neurosci. 20 (13), 5102–5114.

Talpade, D.J., Greene, J.G., Higgins Jr., D.S., Greenamyre, J.T., 2000. In vivo labeling of mitochondrial complex I (NADH:ubiquinone oxidoreductase) in rat brain using [(3)H]dihydrorotenone. J. Neurochem. 75, 2611–2621.

Tawara, T., Fukushima, T., Hojo, N., Isobe, A., Shiwaku, K., Setogawa, T., Yamane, Y., 1996. Effects of paraquat on mitochondrial electron transport system and catecholamine contents in rat brain. Arch. Toxicol. 70, 585–589.

Tillerson, J.L., Cohen, A.D., Philhower, J., Miller, G.W., Zigmond, M.J., Schallert, T., 2001. Forced limb-use effects on the behavioral and neurochemical effects of 6-hydroxydopamine. J. Neurosci. 21, 4427–4435.

Tillerson, J.L., Cohen, A.D., Caudle, W.M., Zigmond, M.J., Schallert, T., Miller, G.W., 2002. Forced nonuse in unilateral parkinsonian rats exacerbates injury. J. Neurosci. 22, 6790–6799.

Zhang, J., Fitsanakis, V.A., Gu, G., Jing, D., Ao, M., Amarnath, V., Montine, T.J., 2003. Manganese ethylene-bis-dithiocarbamate and selective dopaminergic neurodegeneration in rat: a link through mitochondrial dysfunction. J. Neurochem. 84, 336–346.

Zigmond, M.J., Acheson, A.L., Stachowiak, M.K., Stricker, E.M., 1984. Neurochemical compensation after nigrostriatal bundle injury in an animal model of preclinical parkinsonism. Arch. Neurol. 41, 856–861.

EFFECTS OF AMBIENT TEMPERATURE ON MICROWAVE-INDUCED "STRESS" RESPONSES

SHIN-TSU LU
MCKESSON BIOSERVICES CORPORATION
U.S. ARMY MEDICAL RESEARCH DETACHMENT
8355 HAWKS ROAD, BUILDING 1168
BROOKS CITY-BASE, TEXAS 78235
U.S.A.

Abstract

"Stress" can be defined as non-specific responses of an organism to a threat or challenge to the integrity and survival of the organism, to any demand made upon it, or any threat or disturbance of homeostasis. The stress system coordinates the adaptive responses of organism to stressors through corticotrophin-releasing hormone (CRH) and locus ceruleus-norepinephrine-autonomic systems and their effectors. CRH stimulates the pituitary secretiona of adrenocorticotropic hormone (ACTH) that in tern stimulates species-dependent secretion of cortisol or corticosterone (CS) from adrenal cortex. CRH plays an important role in inhibiting gonadotropin releasing hormone by direct and by indirect actions through catecholaminergic and opiates systems, and in inhibiting growth hormone (GH) secretion through somatostatin. Somatostatin, in term, inhibits the secretion of throtropin releasing hormone (TRH) and subsequently, the thyroid-stimulating hormone (TSH, thyrotropin). Prolactin (PRL) secretion is enhanced through the reduction in its inhibitor, TRH. Manifestation of "stress" stereotype changes in endocrine functions has been demonstrated in rats exposed to microwaves. They were stimulation of CS and PRL secretions, and inhibition of GH and TSH secretions in conjunction with increases in colonic temperature. It was hypothesized that elevated ambient temperature may exaggerate the microwave-induced "stress" responses through enhanced hyperthermic responses. Colonic temperature, tail skin temperature, CS, TSH and PRL concentrations were evaluated in rats exposed to graded microwaves at 0.21 to 10.5 W/kg for two hours under two ambient temperatures, 24 and 28 °C. Results indicated that the higher ambient temperature reduced the threshold and also exaggerated the magnitude of responses of all endpoints above the threshold. Correlation between body temperatures and hormonal endpoints indicated that microwave-induced hormonal changes were highly dependent on changes in body temperatures irrespective of ambient conditions. The CS concentration was dependent on changes in colonic temperature alone and tail skin temperature made a negligible contribution. Both colonic (core) and tail skin (surface) temperatures affected TSH and PRL concentrations significantly. Magnitude of "stress" can be represented by CS concentration. A rat model was constructed from to portraits the inter-relationship among CS, SAR and ambient temperature. It can be concluded that microwave radiation and ambient temperature above a critical temperature can compound each other to induce a higher degree of "stress". The critical ambient temperature in rats was 28.5 °C at the lower limit of thermal neutral temperature for this species of animal.

Introduction

"Stress" is a tern seems to be understood by everyone in the western world. But even as of now, a concise and stringent definition that stress researchers can agree upon does not exist. "Stress" is originally defined by Hans Selye [1] as "...the non-specific response of the body to any demand made upon it." At all levels of biological organization, adverse environment elicits a complex array of nervous, endocrine, neurohumoral, and motor reactions to adjust body fluid balance, energy metabolism, and behavior to the needs concomitant with survival in a changed environment. Life exists by maintaining a complex dynamic equilibrium or *homeostasis* that is constantly challenged by intrinsic or extrinsic adverse forces, the *stressors* [2]. Therefore, in addition to physiologic responses of the body, behavioral, psychological as well as physical consequences should also be included in the general concept of "stress". Operationally, "stress" can be subdivided into three major components, *input*, *processing systems*, and *output*. Input is the stress stimulus or stressor that includes physical, chemical, physiological, psychological and psychosocial stimuli. The processing systems are

mesocortical/mesolimbic system, amygdale/hippocampus complex, and hypothalamus and brain stem. Sawchenko [3] reviewed the final common path, the paraventricular nucleus of the hypothalamus, of stress response. Visceral sensory inputs reach PVH via direct projections from nucleus of solitary tract that receives vagal and glosso-pharyngeal afferents, or via projection through C1 adrenergic cell group of the parabrachial nucleus. Other ascending sensory modalities may gain access via relays in midbrain and pons, including peduncuopontine and laterodorsal tegmental nuclei (somatosensory), the central gray, the peripeducular and posterior intralaminar nuclei (auditory), and the intergeniculate leaflet (visual). Nearly all recognized hypothalamic cell groups project to PVH. Prominent inputs also arise from subfornical organ (thirst and cardiovascular responses, reproduction and fever regulation). The bed neuleus of the stria terminals provide a potential conduit for influence of several limbic system cell groups (olfactory: smell, amygdale: fear, hippocampus: memory). The output can involve up to more than 1,400 various physiochemical, behavioral and psychological changes through activation of autonomic nerve and neuroendocrine systems [4]. The main components of the stress system are corticotropin releasing hormone (CRH) and locus ceruleus-norepinephrine (LC/NE)-autonomic systems and their peripheral effectors, the pituitary-adrenal axis, and the limb of the autonomic system. Activation of the stress system leads to behavioral and peripheral changes that improve the ability of the organism to adjust homeostasis and increase its chances for survival. The CRH and LC/NE systems stimulate arousal and attention, as well as the mesocorticolimbic dopaminergic system, which is involved in anticipatory and reward phenomena, and the hypothalamic β-endorphin system, which suppresses pain sensation and, hence increases analgesia. CRH inhibits appetite and activates thermogenesis via the catecholaminergic system. CRH also acts on other neuroendocrine systems to coordinates additional adaptive responses of the organism to stressors of any kind.

CRH plays a primordial role in a cascade of neuroendocrine events resulted from the action of stressor. Stressor acts on CRH-rich paraventricular nuclei for releasing CRH into portal system then transported to anterior pituitary gland to stimulate the secretion of adrenocorticotropic hormone (ACTH) and β-endorphin simultaneously [5, 6]. Arginine-vasopressin is also release from paraventricular nuclei by the stressor's action. ACTH in turn stimulates adrenal cortex to increase species-dependent glucocorticoid secretion, cortisol in human, primates and dogs, and corticosterone (CS) in rodents. CRH plays an important role in directly inhibiting and indirectly inhibiting the release of gonadotropin releasing hormone (GnRH) through the actions of the catecholamines, glucocorticoids and opiates. Thus stressor inhibits gonad function through a reduction of GnRH and its subsequent reduction in luteinizing hormone (LH) secretion from the anterior pituitary gland. CRH also stimulates somatostatin (growth hormone inhibiting hormone) to reduce the secretion of growth hormone from the anterior pituitary gland. Somatostatin also inhibits throtropin releasing hormone (TRH). TRH acts on thyrotropes of the anterior pituitary gland to secrete thyrotropin (TSH) that in turn stimulate the thyroid gland to enhance the release and synthesis of thyroid hormones, thyroxine (T_4) and triiodothyronine (T_3). Due to reduction of TRH, stressor can inhibit thyroid functions. In addition, TRH inhibits prolactin secretion at the anterior pituitary gland. Due to somatostatin inhibition of TRH, stressor is stimulatory for the prolactin (PRL) secretion through a reduction in inhibition. In short, stressor can result in stimulation of adrenocortical axis, inhibition of sex steroids synthesis and secretion in the gonads, inhibition of the thyroid axis, reduction in circulating growth hormone concentration, and enhancing PRL secretion. A myriad of physiochemical changes are the end results of these alterations in circulating hormone levels.

Heat is a well-known stressor. The most investigated and document effect of microwaves/radiofrequency energy on biological tissue is the transformation of energy into kinetic energy of the absorbing molecules, which produces a general heating in the absorbing body. Therefore, it is not surprising to find investigators studying the role of microwave radiation as a stressor. In 1980, Lu *et al.* [7] introduced the concept of stress in describing the microwave-induced neuroendocrine effects. Confirmed microwave-induced acute neuroendocrine changes include stimulation of CS [7-10] and PRL [11] secretions, and inhibition of GH [9] and TSH secretion [9-11]. LH was not altered in rats 6.5 to 52 days after exposure at 9 W/kg for 8 hours [12]. Due to long delay time and limited information available, the participation of LH in microwave-induced stress responses is not clear.

It has been demonstrated in rats that hyperthermic (increased core body temperature) effect of the microwave radiation depended on ambient temperature [13]. Therefore, microwave and ambient heating can potentially enhance each other in inducing a higher degree of "stress". However, majority of *in* vivo experiments were performed under laboratory condition, i.e., ambient temperature between 20-25 °C. Combined effects of ambient temperature and microwave radiation on stress responses have not been evaluated. Therefore, it is the purpose of this study to evaluate the co-stressing effect of microwave radiation and ambient heating in rats from euthermia to lethal hyperthermia level. Colonic and tail skin temperatures, and serum CS, TSH and PRL

concentrations were studied in rats exposed to 2.45 GHz microwaves at 0.21 to 10.5 W/kg at 24 and 28 °C ambient temperature.

Materials and Method

One hundred and twelve 64 to 65 day-old male Long-Evans hooded rats from a commercial source (Charles River Breeding Laboratories, Inc., Wilmington, MA) were used. They were obtained at 35 days of age and acclimated and gentled for 2 weeks according to procedures described previously [9-11]. These animals were maintained at 24 ± 1 °C on a 12-h light-dark cycle (light on: 0800 to 2000 h). Feed and water were available *ad libitum*. They were randomly divided into groups of 8 rats subjected to microwave exposure at 24 or 28 °C in foamed polystyrene cages (20 x 20 x 30 cm) with polystyrene grid bottom and fiberglass screen tops. They were unanesthetized and unrestrained during the exposure. Rats were subjected to microwave exposure four at a time in an anechoic chamber (1.2 x 1.2 m) that was housed in a customized environmental chamber (1.8 x 3.0 x 1.8 m). The average air velocity inside these cages was 1.6 m/s. The microwave exposures were 2.45 GHz, 120 amplitude-modulated waves at 1, 10, 20, 30, 40 and 50 mW/cm^2 in the far-field region of a standard gain horn for 2 hours. The whole-body average specific absorption rates (SAR), determined by calorimetric method, were 0.21 W/kg per mW/cm^2 corresponding to 0.21, 2.1, 4.2, 6.3, 8.4 and 10.5 W/kg. Sham-exposed animals at 24 and 28 °C were also done in a similar way except the high voltage circuit of the microwave transmitter was not energized. The animal was equilibrated at 24 °C for 2.5 h and remained undisturbed for additional 0.5 h. Switching to a new ambient temperature occurred during the last 0.5 h of the 3 h equilibration period. After exposure, rats were quickly decapitated at 1400 h. Blood was collected to provide serum samples for hormonal assays. Colonic temperature (Tco, 5 cm into the rectal orifice, YSI 423) and tail skin temperature (Tsk, 0.5 cm from the base of the tail, YSI 427) were measured immediately after the decapitation. Serum was frozen until the time of assay for CS concentration by a competitive protein-binding method, and for TSH and PRL concentrations by homologous radioimmunoassay. Body masses of the animals on the day of experiment were 305 ± 1.7 g (S.E., n= 56) and 308 ± 1.5 g (S.E., n= 56) for the 24 and 28 °C groups respectively. Two way analysis of variance were used. Main factors under evaluation were ambient temperature, microwave exposure and the interaction between the two. Studen-Newman-Keuls method was used for *post hoc* analysis for difference between groups. Multiple regression was used to evaluate the dependence of hormone concentration (CS, TSH, PRL) on body temperatures (colonic temperature and tail skin temperature). Null hypothesis was rejected at 0.05.

Result

Results of Tco, Tsk, CS, TSH and PRL are shown in figures 1 through 5. The solid symbol indicated that endpoint in the exposed animals was significantly different from corresponding sham exposed animals. It is clearly evident that microwave exposure and ambient temperature had significant effects on endpoints under study. Results of two way analysis of variance are included in each figure. The interactions between microwave exposures and ambient temperatures were also statistically significant indicating that the effect of microwave exposure depended on the ambient temperature. Microwave radiation was clearly thermogenic, which increased both colonic temperature and tail skin temperature (Fig. 1, 2).

Increasing ambient temperature from 24 to 28 °C had no effect on baseline colonic temperature (Fig. 1) but the 4 °C increase in ambient temperature was adequate to elevate the baseline tail skin temperature (Fig. 2) in sham exposed animals. The constant colonic temperature but variable skin temperature under various ambient condition is typical profile of euthermia of an endotherm. In this series of experiment, the threshold for microwave-induced colonic temperature elevation was lowered from 6.3 to 4.2 W/kg as ambient temperature increased from 24 to 28 °C. Microwave-induced colonic temperature elevation was greatly exaggerated by the increase in ambient temperature at SARs somewhere between 2.1 and 4.2 W/kg, and any SAR higher than 4.2 W/kg. In addition, thermal intolerance, 50% lethality, occurred in rats exposed at 10.5 W/kg at 28 °C. The magnitude of ambient induced tail skin temperature elevation preserved fairly well independent of microwave exposure intensities. In relation to respective sham-exposure control, the threshold for microwave-induced tail skin temperature elevation was lowed from 4.2 W/kg to 2.1 W/kg.

Corticosterone secretion could be enhanced by microwave exposure (Fig. 3). The effect of increased ambient temperature was similar to that on colonic temperature elevation, i.e., no effect on baseline CS concentrations, decreased threshold from 6.3 W/kg to 4.2 W/kg as ambient temperature increased, and exaggerated microwave-induced secretion from 4.2 to 10.5 W/kg due to increased ambient temperature. The exaggerated CS response

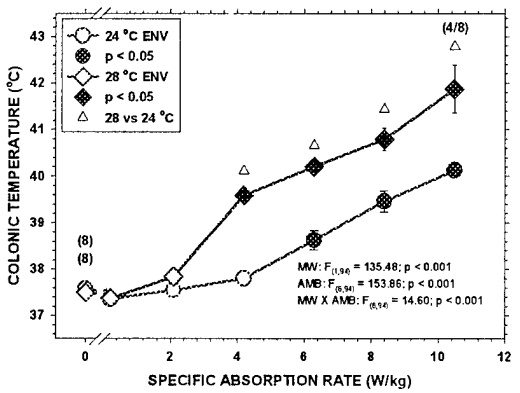


Figure 1. Effect of microwave exposure on colonic temperature under two ambient temperatures

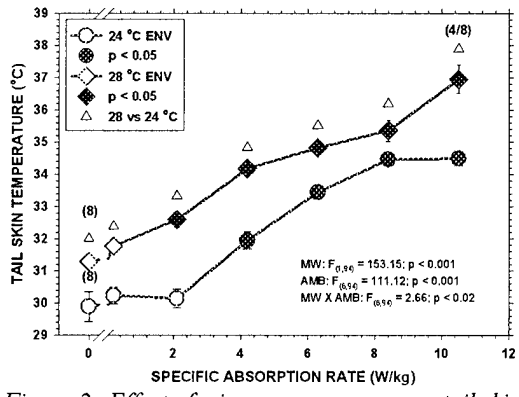


Figure 2. Effect of microwave exposure on tail skin temperature under two ambient temperatures

might have occurred at SAR between 2.1 and 4.2 W/kg also. Serum CS concentration reached a plateau at 6.3 W/kg at 28 °C. The CS concentration at the plateau (60 to 70 μg/dl) was about level can be maintained by male rats under maximum activation.

Microwave radiation could decrease the serum TSH concentration (Fig. 4). Increased ambient temperature did not affect the baseline concentration. Thyrotroin secretion appeared to be more sensitive than Tco, Tsk or TSH to the interaction of ambient temperature. The threshold for TSH depression decreased from 6.3 to 2.1 W/kg when ambient temperature increased from 24 to 28 °C. Thyrotropin depression appeared to reach a plateau at 6.3 W/kg irrespective of ambient temperature. Due to this response plateau, the exaggerated microwave-induced inhibition in TSH secretion could only be observed at 2.1 and 4.2 W/kg when ambient temperature increased from 24 to 28 °C. An equivocal TSH depression occurred in rats exposed at 0.21 W/kg at 24 °C while no change in TSH concentration at 28 °C. The difference in TSH concentrations in these two groups of rats was significant.

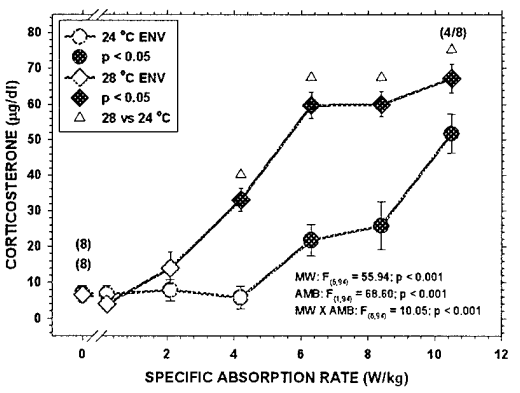


Figure 3. Effect of microwave exposure on serum corticosterone concentration under two ambient temperatures

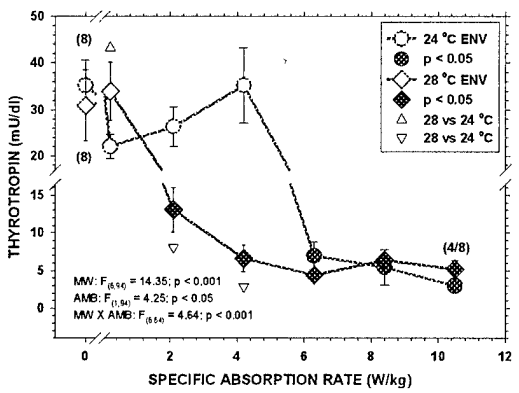


Figure 4. Effect of microwave exposure on serum thyrotropin concentration under two ambient temperatures

In this series of animals, baseline PRL concentrations were higher than those noted previously in three different strains of rats [11]. Due to this drift in baseline, significant elevation in PRL concentrations of rats exposed to microwaves at 24 °C was not found (Fig. 5). At 28 °C, significant elevation in PRL concentrations were found in rats exposed to microwaves from 4.1 W/kg to 10.5 W/kg. These PRL concentrations were not only higher than that in sham-exposed rats at 24 °C but also higher than the corresponding values in rats exposed at similar SAR at 24 °C. Response plateau was also noted in rats exposed to microwaves at 8.4 and 10.5 W/kg at 28 °C.

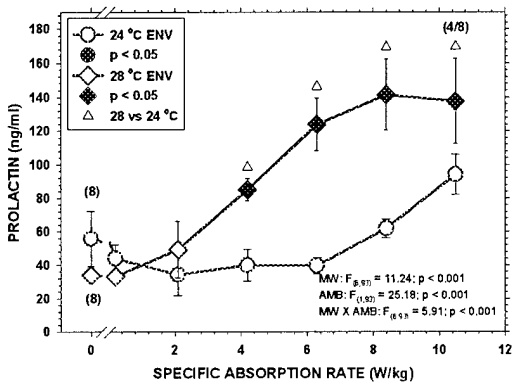


Fig. 5. Effect of microwave exposure on serum prolactin concentration under two ambient temperatures

The relative roles of body temperatures as "stressors" were evaluated by multiple regression. Results indicated that CS was highly correlated to colonic temperature in a linear fashion (Fig. 6). Due to high degree of correlation to colonic temperature, the effect of tail skin temperature appeared to be inconsequential on the CS concentration. For TSH and PRL, Tco was more potent of the two body temperatures. Nevertheless, Tsk had a significant effect on TSH (Fig. 7) and PRL concentrations (Fig. 8). The TSH concentration depended on body temperatures in a logarithmic fashion, most likely due to saturation of the depression effect at more than 2 °C (> 38.8 °C) elevation or more from the offset temperature (36.8 °C) used for evaluation. Saturation of stimulatory effect in CS and PRL concentrations

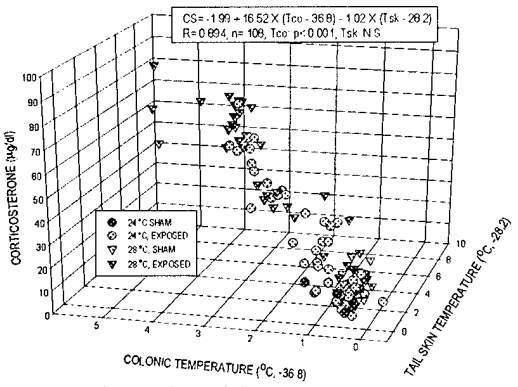


Fig. 6. Relationship of the serum corticosterone concentration and colonic and tail skin temperatures

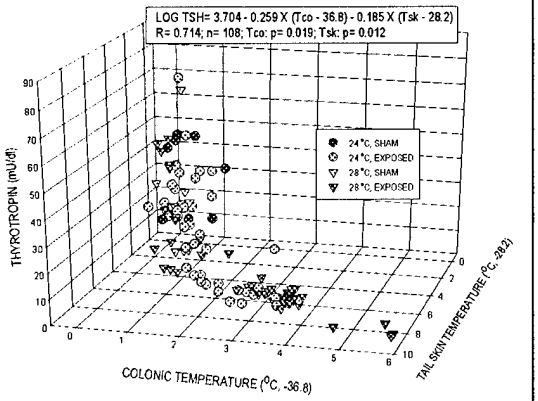


Fig. 7. Relationship of the serum thyrotropin concentration and colonic and tail skin temperatures

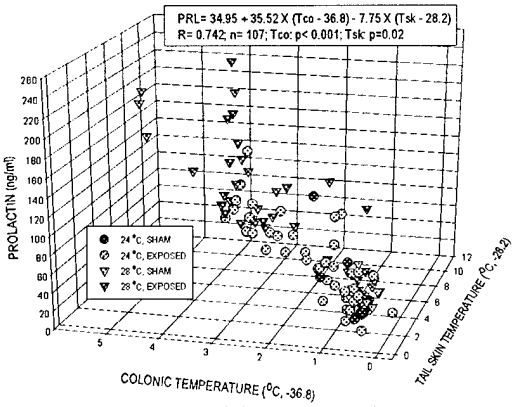


Fig. 8. Relationship of the serum prolactin concentration and colonic and tail skin temperatures

appeared to occur at 5 °C elevation (41.8 °C) or higher. Saturated responses in CS and PRL occurred in the same three rats exposed to microwaves at 28 °C, two of the four survivors at 10.5 W/kg, and one out of eight at 8.4 W/kg.

Discussion

It has been repetitively demonstrated that microwave exposure can influence neuroendocrine functions [7-17]. Abundant data on acute responses of animal, such as TSH, GH, PRL, CS, T_3, T_4, Free T_3 and Free T_4 to microwave-induced "stress" are available. Due to large reserve capacity (thyroglobulin), individual variation, long half lives (16-18 hours) of thyroid hormones (T_3, T_4, Free T_3 and Free T_4), depression of their stimulator - TSH to "stress", and localized stimulatory effect from increase in thyroidal temperature, results in microwave experiments could be quite variable [16]. Effects of microwave-induced "stress" on LH and gonadal hormones (estrogens and androgens) were scarce and equivocal. Testosterone concentration was reported to increase at 3 days but not at 10 min, 8 days or 15 days after 24-h exposure to an unspecified 2.45 GHz microwaves [18]. Results of this report do not fit the general outline of the anticipated acute "stress" responses pattern. Significant higher LH but no changes in FSH or GH contents in pooled pituitary glands were found in rats exposed to 2.86 GHz microwave at 10

mW/cm^2 (2 W/kg), 6 h daily, 6 days per week for 6 weeks [19]. No changes in plasma follicle-stimulating hormone (FSH) and LH were found in male rats 6.5, 13, 26 and 52 days after exposure to 1.3 GHz microwaves at 6.3 and 9 W/kg for 8 h [20, 21]. Decreased estradiol and progesterone was noted in pregnant rats exposed to a 915 MHz microwaves at 2 W/kg for 90 min but not at 0.4 W/kg [22]. Caution should be exercised in interpreting this report because of the unusual hyperthermic responses of pregnant rats, i.e., 0.97 °C (37.67 °C) at 0.4 W/kg and 3.48 °C (40.03 °C) at 2 W/kg. Common physiological conditions such as pregnancy, elderly, young children respiratory and cardiovascular disorders, dehydration, etc. should deserve special attention because of limited thermoregulatory capacity or compromised thermoregulation. Example of the locus ceruleus-norepinephrine-autonomic system in microwave-induced "stress" was a decrease in adrenal epinephrine and an increase in adrenal phenylethanolamine-N-methyltransferase (PNMT) concentrations in absence of any effects on plasma and adrenal CS concentrations in rats exposed to 2.45 GHz microwaves at 2 W/kg for 16 hours [23]. The author considered these adrenal epinephrine depletion and increase in PNMT activity as indicatives of sympathetic-adrenomedullary activation. Therefore, all neuroendocrine axes have been explored, albeit at various details consistencies.

Of available knowledge in microwave-induced "stress", CS provided the most consistent and replicable endpoint to quantify the degree of acute microwave-induced "stress" through its serum or plasma concentration. The dependency of microwave-induced CS response on pituitary ACTH secretion was initially demonstrated indirectly by absence of increased CS concentration in hypophysecomized rats exposed to microwaves and in normal rats received dexamathasone and microwave exposures at supra-threshold intensities [24]. More recent studies indicated a concomitant increase of CS and ACTH in pregnant rats exposed to 2.45 GHz microwave at 2 W/kg for 90 min [25] and in rats exposed to 1.439 GHz microwave at 0.68-0.45 W/kg, 90 min per day, 5 days per week for 6 weeks [26]. In rats, threshold for CRH, ACTH and 11-oxycorticosteroid increases was reported as a 30 min exposure to 2.6 GHz microwaves at 0.1 mW/cm^2 (0.02 W/kg) and the effects peaked at 1 mW/cm^2 (0.2 W/kg) [27]. Microwave-induced activation of the hypothalamus-hypophysis-adrenal cortex axis was also demonstrated in organisms other than rats, e.g., rhesus monkey [28], rabbits [29], dogs [30], and human beings [31]. In chronic exposures, threshold was reported to be as low as 2 or 10 $\mu W/cm^2$ (0.0004 or 0.002 W/kg) of 2.5 GHz microwaves, 10-12 h per day for 180 days [29]. This extremely low threshold has not been verified in rats chronically exposed to higher SARs such as 2.45 GHz microwaves at 0.15-0.4 W/kg [32], 435 MHz microwaves at 0.35 W/kg [33] or 2.45 GHz microwaves at 0.14 W/kg, 7 h per day, 7 days per weeks for 9 weeks [34] or at 0.7 W/kg 7 h per day 7 days per week for 14 weeks [35]. In addition, the results of 435 MHz chronic experiments did not find any changes in PRL concentration either [33].

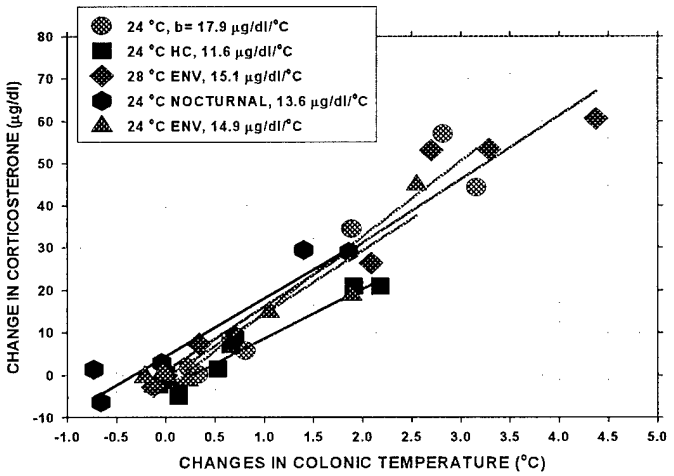


Fig. 9. Relationships between corticosterone concentration and colonic temperature in rats under various experimental conditions. 24 ℃ and 24 ℃ HC were experiments done in an anechoic chamber. HC indicated facilitated heat loss by hair clipped from the torso and extremities of rats under barbiturate anesthesia. Three remaining experiment protocols were performed with animals in the same anechoic chamber enclosed in an environmental chamber to controlling ambient temperature at 24 or 28 ±0.1 ℃ and relative humility between 45 and 50 %. Nocturnal indicated that exposure was carried out during mid-dark cycle in contrast to mid-light cycle in all other experiment protocols. (Data extracted from reference 36)

In addition to responding to intrinsic and extrinsic stimuli, neuroendocrine functions were also known to vary according to commercial source, strain and species of animals [11, 16], and circadian rhythms [9]. To limit the baseline variation, extensive acclimation to experimental procedures other than the intended microwave exposure, maintaining a constant environment and allowance of an equilibration period after transferring animals to the exposure facility should be incorporated into the experimental designs. All these factors had been taken into considerations to assess quantitatively and reliably the microwave-induced "stress".

Endpoints should also be allowed to reach equilibrium or a steady-state. A series of experiments on CS response to 2-hour exposure in Long-Evans rats from a commercial supplier meets these requirements [36]. Graded whole-body average SARs were used at 1.9 to 2.1 W/kg intervals. These data are shown in Fig. 9. The following discussion based on the quantitative responses in rats at 24 °C exposed at mid-light period of the light-dark cycle. Facilitated heat loss by hair clipping increased the threshold SAR from 2.1 to 6.3 W/kg in Tco and 4.2 to 6.3 W/kg in CS. Baseline CS and Tco were higher at mid-dark than at mid-light periods. Tco decreased in rats exposed at 2.1 and 4.2 W/kg and CS decreased insignificantly at 2.1 W/kg for the mid-dark exposures. When exposures changed from mid-light to mid-dark periods, threshold SAR increased from 2.1 W/kg to 6.3 W/kg for increases in Tco and from 6.3 to 8.4 W/kg for increases in CS. Exaggeration of the Tco and CS by increasing ambient temperature has already shown in the result section. With an exception of hair-clipped animals, the CS-Tco relationships were surprisingly constant if changes in CS concentration and Tco from those in respective sham exposed animals were used. Due to possible residual effect of sodium pentobarbital, the slope of CS-Tco relationship in hair clipped animals (11.6 μg/dl/°C) was significantly smaller than that in 24 °C animals (17.9 μg/dl/°C). Excluding the slope from hair clipped animals, averaged slope of the CS-Tco relationships was 15.4 μg/dl/°C ranging from 13.6 to 17.9 μg/dl/°C. Correlation coefficients for each of these CS-Tco relationships were better than 0.95.

Apparently, Tsk plays a minor role in microwave-induced alteration in CS (Fig. 6). However, Tsk appeared to be an important index of thermal stress that depended on ambient temperature and heal load, even if the heat load was generated by microwave radiation [13]. Figure 10 compared the Tco and Tsk responses at graded

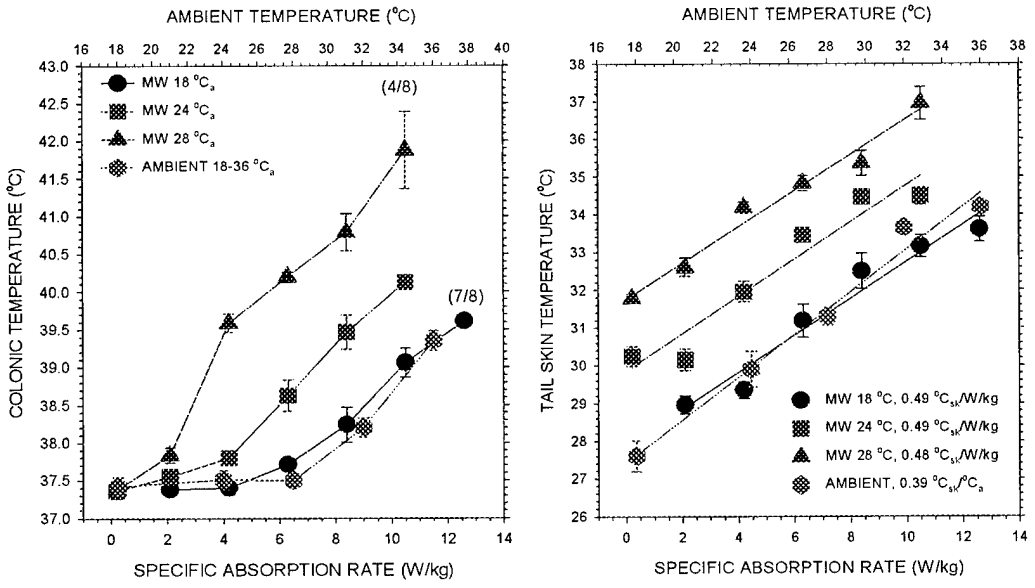


Figure 10. Responses of colonic and tail skin temperatures from graded microwave exposures under various ambient temperatures and conventional heating in warm environments (adapted from data in reference 13).

SARs under various ambient conditions and conventional heating from warm environments. While changes in Tco were curvilinear, Tsk increased linearly with SARs independent of ambient temperature and the slopes were constant at 0.48-0.49 °C/W/kg. Changes in ambient temperature also alter the Tsk in a linear fashion with a slope of 0.39 °C Tsk per °C increase in ambient temperature. The operational characteristics in controlling Tco and Tsk appeared to follow the classical example of euthermia (constant core body temperature within a narrow range but variable surface temperature in various ambient conditions) and hyperthermia stages (both core and surface temperatures increased simultaneously) (Fig. 11) [13]. The sources of heating, either ambient or microwave radiation, were virtually indistinguishable. Euthermia indicated the ability to maintain core body temperature within a narrow range irrespective of changing ambient conditions or heat load from either metabolic or radiant in nature. The euthermia was shown as relatively constant Tco and variable Tsk at the left side of figure 11. Hyperthermia was defined by a an increase in core body temperature above normal, and in this case, both Tco and Tsk increased concomitantly as shown at the right side of figure 11. Limiting factor appeared to be the skin temperature. The transition from euthermia to hyperthermia occurred at 31.8 °C Tsk or

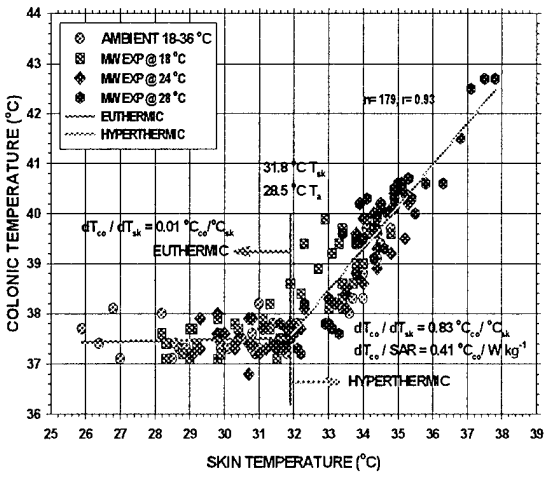


Figure 11. Relationship between colonic and tail skin temperatures in rats from ambient heating or microwave radiation under various ambient temperatures.

28.5 °C ambient temperature that was at the lower end of thermal neutral temperature (28-30 °C). Below the transition, Tco increased negligibly at 0.01 °C for every °C increase in Tsk. Above the transition, Tco increased at slower rate than Tsk at 83 % or 0.41 °C/W/kg.

The magnitude of microwave-induced "stress" in various ambient conditions can be derived from operational characteristics at equilibrium as shown in figure 9, 10 and 11. Several operational constants were independent of transition temperature: d(CS)/d(Tco)= 15 μg $dl^{-1}/°C_{Tco}$, d(Tsk)/d(Ta)= 0.39 $°C_{Tsk}/°C_{Ta}$, and d(Tsk)/SAR= 0.49 °C/W kg^{-1}. Transition temperature was a critical point in thermoregulation predicting probability and magnitude of increases in core body temperature. At ambient temperature (Ta) below the transition ambient temperature, 28.5 °C, microwave exposure could only increase Tsk. Once the critical Tsk was reached, the increase in Tco was d(Tco)/SAR= 0.41 $°C_{Tco}$ / Wkg^{-1} and d(Tco)/d(Tsk)= 0.83 $°C_{Tco}/°C_{Tsk}$. At ambient temperature below 28.5 °C, portion of SAR was ineffective in raising Tco, therefore, effective SAR (SAR_e) was dependent the deviation of ambient temperature, d(Ta)= Ta – 28.5. SARe can be calculated.

For Ta < 28.5 °C:

$$SAR_e = SAR + \left[d(T_a) \times \frac{d(T_{sk})}{d(T_a)} \times \frac{SAR}{d(T_{sk})} \right]$$

and

$$d(CS) = \frac{d(CS)}{d(T_{co})} \times \frac{d(T_{co})}{SAR} \times SAR_e \qquad \text{therefore,} \qquad d(CS)= 6.15 \times [SAR + 0.80 \times d(Ta)] \qquad (1)$$

At ambient temperature above the transition temperature, both Ta and microwave could work in concert to increase Tco and CS. Thus,

For Ta > 28.5 °C:

$$d(CS) = \frac{d(CS)}{d(T_{co})} \times \left[SAR \times \frac{d(T_{co})}{SAR} + d(T_a) \times \frac{d(T_{sk})}{d(T_a)} \times \frac{d(T_{co})}{d(T_{sk})} \right] \qquad \text{and} \qquad d(CS)= 6.15 \times [SAR + 0.79 \times d(Ta)] \qquad (2)$$

The difference between equations 1 and 2 could be a rounding error. Either equation can be use to describe the inter-relationship among d(CS), SAR and Ta as shown (Fig. 12). At ambient temperature higher than 28.5 °C, ambient and microwave heating was additive in rats in magnitude of "stress".

Summary: Threshold for microwave-induced "stress" response depended on ambient temperature. Increasing ambient temperature from 24 to 28 °C reduced the "stress" threshold by at least 2 W/kg. Additional study on the effect of ambient temperature higher than 28 °C on the threshold of microwave-induced biological effects

should be performed to evaluate the combined effects of ambient and microwave heating. Changes in corticosterone concentration can be used to quantify the magnitude of microwave-induced "stress" at equilibrium. Model based on operational characteristics of CS regulation and thermoregulation indicated that ambient and microwave heating on magnitude of "stress" was additive in rats at ambient temperature higher than 28.5 °C.

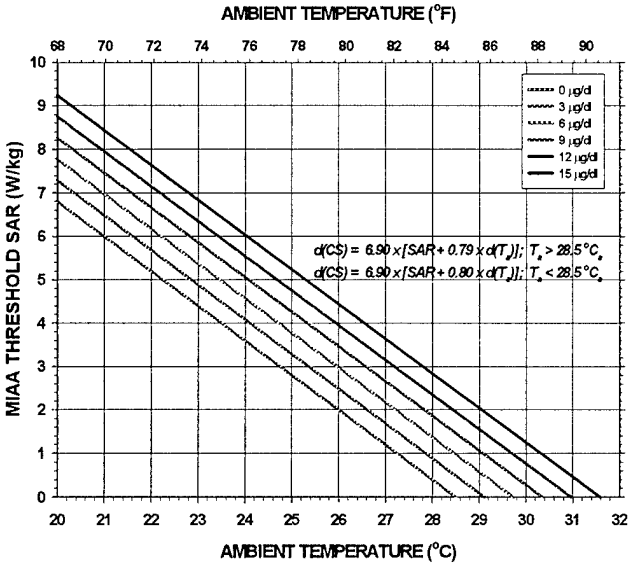


Figure 12. Inter-relationship among ambient temperature, microwave absorbption and changes in corticosterone concentration

Acknowledgement: This work is supported by U.S. Army Medical Research and Materiel Command under contract DAMD17-94-4069 with McKesson BioServices and PHS Grant ES 03330. Technical assistances by S. Pettit and S.-J. Lu are acknowledged. Use of laboratory animals adhered to the "Guide for the Care and Use of Laboratory Animnals". The views, opinions and/or findings are those of author and should not be construed as an official Department of the Army position, policy, or decision unless so designated by other documentation. This work is a US Government work and, as such, is in the public domain in the United States of America.

Reference

[1]. Selye H. The evolution of the stress concept. Am Scientist 61: 692-699, 1970

[2]. Chrousos GP, and Gold PW. The concepts of stress system disorders: overview of behavioral and physical homeostasis. JAMA 267: 1244-1252, 1990.

[3]. Sawchenko PE. The final common path: issues concerning the organization of central mechanisms controlling corticotropin secretion. In: "Stress, Neurobiology and Neuroendocrinology", Brown, MR, Koob GF and Rivier C ed., New York: Marcel Dekker, Inc., 1991, pp. 55-71.

[4]. Asterita MF. The stress response. In: "The Physiology of Stress, with Special Reference to the Neuroendocrine System", New York: Human Sciences Press, Inc., 1985, pp. 35-45.

[5]. Rivier C. Neuroendocrine mechanisms of anterior pituitary regulation in the rat exposed to stress. In: "Stress, Neurobiology and Neuroendocrinology", Brown, MR, Koob GF and Rivier C ed., New York: Marcel Dekker, Inc., 1991, pp. 119-136.

[6]. Tsigos C, and Chrousos GP. Hypothalamic-pituitary-adrenal axis, neuroendocrine factors and stress. J. Psychosomatic Res. 53: 865-871, 2002.

[7]. Lu S-T, Lotz, WG, and Michaelson, SM. Advances in microwave-induced neuroendocrine effects: the concept of stress. Proc. IEEE 68: 73-77.

[8]. Lotz WG and Michaelson SM. Temperature and corticosterone relationship in microwave-exposed rats. J. Appl. Physiol.: Respiratory, Environmental, and Exercise Physiol. 44: 438-445, 1978.

[9]. Lu S-T, Lebda N, Pettit S, and Michaelson SM. Delineating acute neuroendocrine responses in microwave-exposed rats. J. Appl. Physiol.: Respiratory, Environmental, and Exercise Physiol. 48: 927-932, 1980.

[10]. Lu S-T, Lebda N, Pettit S., and Michaelson SM. Microwave induced temperature, corticosterone, and thyrotropin interrelationships. J. Appl. Physiol.: Respiratory, Environmental, and Exercise Physiol. 50: 399-405, 1981.

[11]. Lu S-T, Lebda NA, Lu S-J, Pettit S, and Michaelson SM. Effects of microwaves on three different strains of rats. Radiat. Res. 110: 173-191, 1987.

[12]. Lebovitz RM, and Johnson L. Acute, whole-body microwave exposure and testicular function of rats. Bioelectromagnetics 8: 37-43, 1987.

[13]. Lu S-T. Effect of interaction between ambient temperature and SAR on microwave-induced hyperthermia in rats. In: "Electricity and Magnetism in Biology and Medicine", Blank M ed., San Francisco: San Francisco Press, Inc., 1993, pp. 679-682.
[14]. Michaelson SM, Houk, WM, Lebda NJA, Lu S.-T, and Magin RL. Biochemical and neuroendocrine aspects of exposure to microwaves. Ann. N.Y. Acad. Sci. 247: 21-45.
[15]. Lu S-T, Lebda N, Pettit S, and Michaelson SM. Microwave-induced temperature, corticosterone and thyrotropin interrelationships. J. Appl. Physiol. 50: 399-405, 1981.
[16]. Lu S.-T, Lebda NA, Michaelson SM, and Pettit S. Serum thyroxine levels in microwave-exposed rats. Radiat. Res. 101: 413-423, 1985.
[17]. Lu S-T, Lebda NA, Pettit S, and Michaelson SM. The relationship of decreased serum thyrotropin and increased colonic temperature in rats exposed to microwaves. Radiat. Res. 104: 365-386, 1985.
[18]. Deschaux P, and Pelissier J-P. Effect of microwaves on steroids plasma levels in male rats. J. Microwave Power 12: 46-47, 1977.
[19]. Mikolajczyk H. Microwave-induced shifts of gonadotropic activity in anterior pituitary gland of rats. In: " Biological Effects of Electromagnetic Waves, Volume I', Johnson CC and Shore ML, eds., Rockville: Bureau of Radiological Health, HEW Publication (FDA) 77-8010, 1977, pp. 377-383.
[20]. Johnson L, Lebovitz RM, and Samson WK. Germ cell degeneration in normal and microwave-irradiated rats: potential sperm production rates at different development steps in spermatogenesis. Anat. Rec. 209: 501-507, 1984.
[21]. Lebovitz RM and Johnson L. Acute, whole-body microwave exposure and testicular function of rats. Bioelectromagnetics 8: 37-43, 1987.
[22]. Nakamura H, Matsuzaki I, Hatta K, Nobukuni Y, Kambayashi Y, and Ogino K. Nonthermal effects of mobile-phone frequency microwaves on uteroplacental functions in pregnant rats. Reprod. Tox. 17: 321-326, 2003.
[23]. Parker LN. Thyroid suppression and adrenomedullary activation by low-intensity microwave radiation. Am. J. Physiol. 224: 1388-1390, 1973.
[24]. Lotz WG and Michaelson SM. Effects of hypophysectomy and dexamathasone on rat adrenal response to microwave exposure. J. Appl. Physiol. 47: 1284-1288, 1979.
[25]. Nakamura H, Seto T, Nagase H, Yoshida M, Dan S, and Ogino K. Effects of exposure to microwaves on cellular immunity and placental steroids in pregnant rats. Occup. Environ. Med. 54: 676-680, 1997.
[26]. Imaida K, Take M, Wanatabe S, Kaminura Y, Ito T, Yamaguchi T, Ito N, and Shirai T. The 1.5 GHz electromagnetic near-field used for cellular phones does not promote rat liver carcinogenesis in a medium-term liver bioassay. Jpn. J. Cancer Res. 89: 995-1002, 1998.
[27]. Novitskii AA, Murashov BF, Krasnobaev PE and Markozova NF. The functional condition of the system hypothalamus-hypophysis-adrenal cortex as a criterion in establishing the permissible levels of superhigh frequency electromagnetic emission. Voen. Med. Zh. 8: 53-56, 1977.
[28]. Lotz WG and Podgorski RP. Temperature and adrenocortical responses in rhesus monkeys exposed to microwaves. J. Appl. Physiol. 53: 1565-1571, 1982.
[29]. Dumansky YuD and Shandala MG. The biological action and hygienic significance of electromagnetic fields of superhigh and ultrahigh frequencies in densely populated area. In:" Biological Effects and Health Hazards of Microwave Radiation", Czerski P, Ostrowski K, Silverman C, Shore ML, Suess MJ and Waldeskog eds., Warsaw: Polish Medical Publishers, 1974, pp 289-293.
[30]. Petrov IR and Syngayevskaya VA. Endocrine glands. In: "Influence of Microwave Radiation on the Organism of Man and Animals", Petrov IR ed., Leningrad: Meditsina Press, 1970, pp. 31-41.
[31]. Schliephake E. Endocrine influence on bleeding and coagulation time. Zbl. Chir. 85: 1063-1066, 1960.
[32]. Chou C-K, Guy AW, Kunz LL, Johnson RB, Crowley JJ, Krupp JH. Long-term low-level microwave irradiation of rats. Bioelectromagnetics 13: 469-496, 1992.
[33]. Toler J, Popovic V, Bonasera S, Popovic P, Honeycutt C, Sgoutas D. Long-term study of 435 MHz radio-frequency radiation on blood-borne end points in cannulated rats. Part II: methods, results, and summary. J. Microwave Power Electromagnetic Energy 23: 105-136, 1988.
[34]. D'Andrea JA, DeWitt JR, Gandhi OP, Stensaas S, Lords JL and Neilson HC. Behavioral and physiological effects of chronic 2,450-MHz microwave irradiation of the rat at 0.5 mW/cm^2. Bioelectromagnetics 7: 45-56, 1986.
[35]. D'Andrea JA, DeWitt JR, Emmerson RY, Bailey C, Stensaas S and Gandhi OP. Intermittent exposure of rats to 2450 MHz microwaves at 2.5 mW/cm^2: behavioral and physiological effects. Bioelectromagnetics 7: 315-328, 1986.
[36]. Lu S-T. Microwave-induced responses of colonic temperature and serum corticosterone concentration in rats are susceptible to changing environmental conditions. In: "Abstracts of the 25th Annual Meeting of the Bioelectromagnetics Society, Wailea, Maui, Hawaii, June 22-27, 2003, pp. 107-108.

Determination of p53 Protein Stabilization and Transactivation of its Target Genes in Response to Ultrawideband Electromagnetic Radiation Exposure in Human Hematopoietic Cells

Bijaya K. Nayak[1*], Mohan Natarajan [1], Cynthia Galindo [1], Satnam P. Mathur [2], and Martin L. Meltz[1]

[1] Department of Radiation Oncology, University of Texas Health Science Center at San Antonio, 7703 Floyd Curl Drive, San Antonio, TX 78229, USA.

[2] McKesson BioServices, US Army Medical Research Detachment, Brooks Air Force Base, 8355 Hawks Road, Building 1168, San Antonio, TX 78235, USA.

Number of Copies Submitted: Original and 4 copies

Number of Figures: 4

Running Head: Effect of UWB EMR exposure on p53 gene response

***Corresponding author**

Bijaya K. Nayak, Ph.D.

Department of Radiation Oncology
University of Texas Health Science Center at San Antonio
7703 Floyd Curl Drive
San Antonio, TX-78229, USA.

Email: nayak@uthscsa.edu
Tel: 210-567-8033
Fax: 210-567-8051

Nayak, B. K., Natarajan M., Galindo C., Mathur S. P. and Meltz M. L. Determination of p53 Protein Stabilization and Transactivation of its Target Genes in Response to Ultrawideband Electromagnetic Radiation Exposure in Human Hematopoietic Cells. Radiat. Res.

ABSTRACT

Since ultrawideband (UWB) technology is finding its way into commercial applications, it is important to investigate the possibility of biological responses to this type of electromagnetic radiation (EMR). The present study was undertaken to address this question by examining the impact of pulsed UWB EMR on p53 gene response in three human hematopoietic cell lines that are different in their p53 gene competencies. The cell lines included 244B normal lymphoblastoid cells (p53 competent), MM-6 monocyte leukemic cells (p53 compromised), and HL-60 myeloid leukemic cells (p53 null). The UWB EMR pulses used in this study had an average peak amplitude of 102.17 $\pm$ 5.00 kV/m, an average pulse width of 0.80 $\pm$ 0.02 ns, and an average rise time of 229.46 $\pm$ 25.56 ps. The total exposure time was 90 min, at 250 pulses/sec. The frequency range was from D.C. to approximately 2 GHz. Stabilization of the p53 protein was analyzed by Western blot analysis. Transcription of the p53 gene and its target genes was examined using the RNase protection assay. The p53 protein was not stabilized after the UWB EMR exposure in 244B and MM-6 cells. There was no evidence of transcriptional induction of p53, or the p53 target genes p21, gadd45, PCNA, and Bax in 244B cells, and no transactivation of p53 responsive genes in MM-6 and HL-60 cells.

INTRODUCTION

The use of ultrawideband electromagnetic radiation (UWB EMR) systems is of current interest to the U.S. Air Force (1), and is in expanding use in telecommunications, industry, and health care (2-4). In our laboratory, we have initiated a broad series of investigations to determine the possible biological responses associated with ultrawideband electromagnetic radiation exposures. These pulsed signals range from DC through the extremely low frequency range to the microwave region of the radiofrequency range; we have therefore represented the pulses as UWB EMR. The unusual properties of pulsed UWB electromagnetic radiation, including very high peak powers, very short pulse widths, and extremely fast rise times, suggested the hypothesis that unique bioeffects might result from such exposures. While a large number of studies reporting the presence or absence of effects of narrowband radiofrequency (RF) field exposures have been performed at the cellular, cytogenetic and organism levels (for reviews, 5), there are only a limited number of studies carried out on the biological effects of UWB EMR. The majority of these studies were focused on behavioral and physiological effects after exposure of animal models (6-12). Almost no information is available on whether or not molecular responses occur after ultrawideband electromagnetic radiation exposures.

The p53 tumor suppressor gene is activated in response to a variety of stress signals, including DNA damaging compounds, chemotherapeutic drugs, ultraviolet radiation, ionizing radiation, and non-genotoxic stressors such as heat shock and ribonucleotide depletion (Fig. 1). The active p53 in turn transactivates

a number of target genes, including those that can elicit growth arrest and/or apoptosis (13-17). The p53 gene is mutated in a large percentage of cancers. Some of the p53 mutants exhibit a gain of function, and can modulate tumor cell phenotype by increasing clonogenic potential, tumorigenicity, and invasiveness (18-20). There is no report available on the effect of UWB EMR exposure on p53 gene response. The present study was undertaken to examine the effect of pulsed ultrawideband radiofrequency radiation exposure on transcription of the p53 gene, and on stabilization of the p53 protein. In addition, the effects of UWB EMR exposures on transcription of p53-dependent and p53-independent growth arrest and apoptotic genes were investigated in p53-wild-type, p53-compromised, and p53-null hematopoietic cells.

MATERIALS AND METHODS

Cell Line Selection

Cell lines with different p53 gene status were selected to address the p53-dependent and p53-independent effects of pulsed UWB EMR exposures on different genes involved in DNA damage repair, cell growth arrest, and apoptosis. The 244B human lymphoblastoid cells have a wild-type p53 gene activity (p53 competent), the MM-6 human monocyte cells have a compromised p53 gene activity, and the HL-60 human myeloid leukemic cells used are p53-null.

Cell Line Maintenance

The MM-6 cells were maintained in 20 ml of RPMI-1640 medium (Cellgro, Hendron, VA) supplemented with 10% FBS (Hyclone, Logan, UT), 10 mM

HEPES (Cellgro), 2mM L-Glutamine (Cellgro), 200U penicillin/200 µg/ml streptomycin (Cellgro), 2mM non-essential amino acids (NEAA) (Invitrogen, Carlsbad, CA), and 1 vial of OPI (0.15g oxaloacetate, 0,05g pyruvate, and 0.0082g bovine insulin (Sigma, St Louis, MO) per liter of medium. The 244B and HL-60 cells were maintained in 20 ml of RPMI-1640 medium supplemented with 10% heat inactivated FBS, 10 mM HEPES, 2mM L-Glutamine, and 50 µg/ml gentamicin (Sigma, St Louis, MO). All of the cells were maintained in disposable T-75 tissue culture flasks with filter caps in a humidified 5% CO_2/95% air atmosphere at 37°C.

Ionizing Radiation Exposure

Cells were exposed to a 2 Gy dose of ^{137}Cs gamma rays (Atomic Energy of Canada/Nordion). The dose rate over the course of the experiments ranged from 127.9 cGy/min to 127.2 cGy/min. The cells were exposed at room temperature in T-25 flasks with 10 ml of medium, immediately after removal of the flasks from the 37°C incubator. The flasks were returned to the incubator in the adjoining laboratory immediately after the exposure. The sham controls were carried to and from the irradiation room at the same time.

UWB EMR Exposure System

The UWB electromagnetic radiation exposures were performed in a custom-built giga-transverse electromagnetic (GTEM) cell originally constructed by Sandia National Laboratories (Albuquerque, NM). The GTEM cell, a tapered two-conductor transmission line with a square cross-section, was positioned so that one ground plane wall was horizontal (8). A modified RG-220 coaxial cable

connected the center conductor of the GTEM cell to a source of high voltage. Ionization of nitrogen in a center-conductor gap in the cable generated UWB pulses in the GTEM cell, with the electric field vector directed from the center conductor to the ground conductor. A EG&G ACD(A) D-dot probe mounted in the wall of the GTEM cell was used to detect UWB pulses during the cell exposures. The signal from the probe was sampled with 0.01-ns resolution by a Tektronix SCD 5000 Transient Digitizer. Each digitized wave-form, representing the average of 200 individual pulses, was stored and later processed using a correction algorithm (21) to give the corrected average peak pulse electric field, rise time, and pulse width. The pulses were triggered by an external pulse generator at 250 pulses/s. The mean pulse duration was 0.80 $\pm$ 0.02 ns. The average peak E-field was 102.17 $\pm$ 5.00 kV/m. The frequencies ranged from D.C. to approximately 2 GHz. The average rise time was 229.46 $\pm$ 25.56 ps.

Temperature Measurement and Control

Prior to initiating the UWB EMR experiments, the temperature distribution was determined at the bottom of vertically oriented T-25 flasks positioned in a custom built foam "air incubator" box (described below). The temperature was measured using a Luxtron 3000 Data Acquisition Program. The assessment indicated an average of 37.0$\pm$ 0.3°C at the bottom of the flask in the two center position flasks, in the foam incubator box where the temperature distribution was most uniform. Only these two positions were used for the experimental studies; two dummy flasks filled with 10 ml of RPMI medium were always placed in the two outer positions of the holder. To verify that the temperature remained close

to 37°C during and between the intermittent exposures, the temperature in the sham and UWB-exposed flasks were monitored continuously for 5 minutes before, during and for 5 min after the pulsed UWB EMR exposures (using the Luxtron System). To accomplish this, a Luxtron probe was inserted vertically downward through holes in the foam incubator box and in the caps of each of the two center flasks, to the bottom of the column of the medium in those flasks. The mean temperature during each of the three 30 min UWB exposure periods, and also in the two 30 min EMR off interim periods, was 36.96 $\pm$ 0.06°C. Two sham exposure flasks were handled in exactly the same manner. These flasks were placed in a second foam holder (with two flasks with medium in the outer positions in the holder) in a Faraday Cage in the anechoic chamber alongside the GTEM cell. The temperature in all the flasks was maintained by computer controlled (Luxtron probe feed back) warm-air flow into the incubator boxes.

Cell Handling for UWB EMR Exposure

The cells were seeded at 500,000 cells/ml in 10 ml complete growth medium in T-25 flasks with vent caps (Corning) on the day prior to exposure. The cell density was determined by haemocytometer count. Viability was checked using the trypan blue dye exclusion method. The flasks were incubated at 37°C in a humidified 5% CO_2/95% air atmosphere for up to 1 hr, before being transported in a warmed styrofoam container (with water packs) to a similar incubator in the UWB exposure facility at Brooks City-Base. The flasks were then incubated overnight at 37°C. After checking the performance of the UWB source (pre-exposure check), and 30 min prior to the UWB EMR exposure, two

of the T-25 flasks with cells were placed vertically in the two center positions of the two custom designed 4-flask foam holders (for exposure and sham exposure). The foam holders served as incubators, allowing the temperature of the medium in the flasks to be maintained at 37°C throughout the exposure period. The cells were allowed to settle to the bottom of the flask during this 30 min. The exposure holder was positioned at a distance of 72.7 cm from the opening of the GTEM cell, into which the UWB pulses were emitted. The cells were exposed to UWB pulses intermittently for a total period of 90 minutes (30 min on and 30 min off, repeated three times) at a pulse repetition rate of 250 pulses per second.

Cell Handling Post-Exposure

After the last of the three 30 min UWB EMR exposures, the flasks were allowed to remain in position in the holder to collect 5 min of post-exposure temperature data. The flasks were then removed from the exposure system and the plug-seal caps were replaced with vented caps. The flasks were placed in the incubator until transported at near 37°C to the incubator at UTHSCSA. The cells were incubated for the different times indicated below.

Western Blot Analysis

The stabilization of p53 protein and the change in expression of the p53 target gene p21 were examined by Western blot analysis. Cells were lysed directly in 2X sample buffer {0.125M Tris-Cl, pH 6.8; 4% SDS (Sigma, St Louis, MO); 0.2M DTT (Sigma) and 0.02% bromphenol blue (Sigma)}, boiled at 100^{0}C for 10 minutes and centrifuged at 12,000 rpm in a microcentrifuge for 5 minutes to pellet

the chromatin. The protein concentration in the supernatant of the whole cell lysate was estimated using the Non-Interfering Protein Assay Kit (Geno Technology, Inc., St. Louis, MO). A 50 µg sample of the cell lysate was electrophoresed on a 10% SDS-polyacrylamide gel for ~3 hours and transferred to a nitrocellulose membrane. The membrane was blocked in TBS-T (10 mM tris-HCl, pH 8; 150 mM NaCl; 0.01% Tween 20) containing 5% blocking agent (Amersham Pharmacia, UK), and was then probed with the primary antibody (p53, p21, and actin). After washing, the membrane was incubated with horseradish peroxidase-conjugated secondary antibody and was developed with an enhanced chemiluminescence (ECL) kit (Amersham Pharmacia Biotech, UK). The same membrane was used for all antibodies (p53, p21, and actin) after stripping in strip buffer (125 mM Tris-HCl, pH 6.8; 2% SDS; 0.68% 2-mercaptoethanol).

RNase Protection Assay (RPA)

Total RNA was isolated at 2, 6, and 24 hr post-exposure using Trizol reagent (Invitrogen, CA). Transcription of p53 and its target genes was examined using the RNase Protection Assay (RPA). A human multi-probe template set consisting of p53, p21, PCNA, gadd45, Bax, bcl_2, Bcl-xL, c-fos, and the house keeping genes L32 and GAPDH was used (BDPharmingen, California). The housekeeping genes L32 and GAPDH served as internal controls. The probe set was labeled with T7 RNA polymerase in the presence of α^{32}P-UTP, and was used for RPA as per BDPharmingen's protocol. Briefly, 10 µg of RNA was hybridized with riboprobe ($1x10^6$ cpm) in 20 µl of hybridization buffer (40 mM

PIPES, pH 6.7; 0.4 M NaCl, 1mM EDTA, and 80% v/v formamide) at 56°C for 12 to 16 hours. Samples were digested with RNase (RNase A and RNase T1 mix) at 30°C for 45 minutes. After proteinase K (Sigma) digestion and phenol-chloroform extraction, the RNA samples were dissolved in 5 μl of loading buffer (80% formamide, 0.1% bromphenol blue, 0.1% xylene cyanol). Samples were electrophoresed for ~1 hour on a 5% denaturing polyacrylamide gel at 50 W in 0.5X TBE. The gels were fixed, dried, and autoradiographed.

RESULTS

p53 and p53 target gene transcription

Transcription of the p53 and the p53 target genes involved in DNA damage repair (PCNA, and gadd45), cell cycle arrest (p21, gadd45), and apoptosis (bcl_2, bcl-xL, and Bax) was examined in all the three cell lines after UWB EMR and 5 Gy ionizing radiation exposures using the RNase protection assay. Representative results for the three cell lines, selected from three independent experiments for each cell line, are shown in Figures 2 (244B cells), 3 (MM-6 cells), and 4 (HL-60 cells). After the UWB EMR exposures, there was no evidence of transcriptional induction of p53 or the p53 responsive genes p21, gadd45, PCNA, and Bax in 244B (Fig. 2A) or MM-6 (Fig. 3A) cells. In the p53 null HL-60 cells, a change in expression of p21, gadd45, Bax, and PCNA was also not observed in response to UWB EMR exposure (Fig. 4). In the 244B cells exposed to ionizing radiation (as a positive control), an induction of the p53 target genes p21 and Bax was observed, indicating that cell cycle arrest and apoptosis

after this type of irradiation could be expected. In the MM-6 (p53 compromised) and HL-60 (p53 null) cells, no change in expression of the p21, gadd45, Bax, bcl_2, bcl-xL, and PCNA genes was observed after exposure to ionizing radiation (Fig. 3 and Fig. 4), as would be expected for p53 compromised or p53 null cells.

p53 protein stabilization

The stabilization of p53 protein was examined by Western blot analysis. A representative set of results for 244B and MM-6 cells, out of three independent experiments for each cell line, is shown in Figures 2 and 3. The p53 protein was not stabilized after the UWB EMR exposure of 244B cells i.e., there was no increase in the p53 protein level as compared to the sham and incubator control (Fig. 2B). There was also no change in the p53 regulated p21 protein in UWB EMR exposed 244B cells (Fig. 2B). Increases in p53 and p21 protein levels, and therefore stabilization, were evident at 6 and 24 hours after 5 Gy ionizing radiation exposures (Fig. 2B). In the p53 compromised MM-6 cells, the p53 protein was also not stabilized in response to UWB EMR exposure (Fig. 3B). The p53 protein level relative to the actin housekeeping gene in both the 244B cells and the MM-6 cells was the same for control, sham-exposed, and UWB EMR-exposed cells (Fig. 2B and Fig. 3B).

In the p53 compromised MM-6 cells, in contrast to the 244B cells, there was no evidence of stabilization of p53 after the 5 Gy ionizing radiation exposures (Fig. 3B). The p21 protein could not be detected in MM-6 cells by western blot analysis, indicating a compromised p53 function in these cells.

DISCUSSION

There is a great deal of public concern regarding the bioeffects of radiofrequency radiation exposure. The weight of evidence appears to support the absence of genotoxic damage(s). This does not preclude the possibility that other types of molecular alterations occur in cells after radiofrequency exposures. Several studies at the molecular level have reported an effect of narrowband radiofrequency exposures on mammalian cells (22-24). Goswami *et al.* (22) reported an increase in fos proto-oncogene in C3H 10T 1/2 murine embryonic fibroblasts, when cells in transit to the plateau phase or in plateau-phase were exposed to 835.62 MHz frequency-modulated continuous wave (FMCW) or 847.74 MHz code division multiple-access (CDMA) RF. Natarajan *et al.* (23) reported an increase in NF-κB DNA binding activity in MM-6 human monocytes after a high peak power pulsed RF (8.2 GHz) exposure. Leszczynski *et al.* (24) reported a transient increase in phosphorylation of hsp27 in EA.hy926 human endothelial cells after exposure to 900 MHz mobile phone microwave radiation. In the present study, we have examined transcriptional induction of p53, p53 protein stabilization, and the transactivation of p53 responsive genes as indicators of a general stress response after UWB EMR exposures.

Recent studies indicating that p53 mRNA is induced in different physiological conditions suggest a transcriptional activation of p53 (25, 26). It has been reported that p53 is required for maintaining and establishing quiescence growth arrest in human cells (25). Tang *et al.* (26) have shown that basal level of p21 protein is regulated by p53 in cells without any DNA damage.

Transcriptional deregulation of p53 may play a role in the genesis of some tumors (27, 28). There are reports showing an altered p53 mRNA expression in a number of myeloid leukemic cell lines (29, 30) and in human breast tumors (31, 32). A stage and tissue specific p53 regulation at the level of p53 mRNA expression has also been proposed (33). The p53 mRNA level was examined in the present study to address the possible effect of pulsed UWB EMR exposure on transcriptional regulation of the p53 gene. In this investigation, p53 mRNA induction was not observed in either p53 competent 244B lymhphoblastoid or p53 compromised MM-6 monocyte cells after exposure to pulsed UWB EMR (Fig. 2A and Fig. 3A).

The p53 protein is activated by post-translational modification and stabilized in response to different stress agents, including ionizing radiation (Fig. 1). The stabilized p53 activates or represses its target genes, which can lead to cell cycle arrest and/or apoptosis (14-17). In the present study, p53 protein stabilization was not observed in response to pulsed UWB EMR exposure in 244B lymphoblastoid and MM-6 monocyte cells (Fig. 2B and Fig. 3B). Consistent with our observations, Li *et al.* (34) have reported that the p53 protein levels remain unchanged in normal human fibroblasts in response to 837 MHz RF exposure. A recent study has reported that whole body exposure of rats to microwaves emitted from a cell phone (890-925 MHz) did not affect the p53 immunostaining in sections of the testes, suggesting that no p53 protein accumulation occurred after this type of exposures (35). There is no evidence, therefore, for an increase in the expression of the p53 responsive genes after

narrowband RF radiation exposure. In this study cells were exposed to pulsed UWB EMR, with frequencies extending from D.C. to approximately 2 GHz. There was again no evidence of activation of the p53 gene, and also no indication of transactivation of p53 responsive genes known to be involved in cell cycle arrest (p21, gadd45), DNA damage repair (gadd45, PCNA), and apoptosis (Bax, bcl_2, bcl-xL) in cells with different p53 capabilities.

In the study reported here, the pulsed UWB EMR exposures were to a very high average peak electric field amplitude (102.17 $\pm$ 5.10 kV/m), a very rapid rise time (229.46 $\pm$ 25.56 ps), a very small pulse width (0.80 $\pm$ 0.02 ns), and a reasonable experimental exposure duration (a total of 90 minutes pulsed UWB EMR exposure). This study demonstrates for the first time that pulsed UWB electromagnetic radiation exposure does not induce p53 mRNA expression, does not effect p53 protein stabilization, and has no effect on the transcription of its target genes. Lack of induction of p53 protein stabilization and no transcriptional activation of p53 target genes in response to pulsed UWB radiofrequency radiation exposure suggest that UWB EMR exposure does not induce DNA damage, and that this type of radiation might not be a stress factor to the cells.

ACKNOWLEDGMENTS

The authors thank Mr. John Ashmore of Brooks Air Force Base, San Antonio for his assistance in conducting the UWB exposures. This work was supported by the United States Air Force Office of Scientific Research Grant No. F49620-01-1-0349. This work was also supported in part by the U.S. Army Medical Research and Material Command under contract DAMD-17-94-4069 awarded to McKesson BioServices.

REFERENCES

1. J. R. Goldsmith, Epidemiologic evidence of radiofrequency radiation (microwave) effects on health in military, broadcasting, and occupational studies. Int. J. Occup. Environ. Health 1, 47-57 (1995).

2. E. Jerby, V. Dikhtyar, O. Aktushev , U. Grosglick, The microwave drill. Science 298, 587-589 (2002).

3. S. Gupta, Z. Hadzibabic, M. W. Zwierlein, C. A. Stan, K. Dieckmann, C. H. Schunck, E. G. M. van Kempen, B. J. Verhaar and W. Ketterle, Radio-frequency spectroscopy of ultracold fermions. Science 300, 1723-1726 (2003).

4. F. J. Agee, C. E. Baum, W. D. Prather, J. M. Lehr, J. P. O'Loughlin, J. W. Burger, J. S. H. Schoenberg, D. W. Scholfield, R. J. Torres and J. A. Gaudet, Ultra- wideband transmitter research. IEEE Trans. Plasma Sci. 26, 860-873 (1998).

5. Reviews of the effects of RF fields on various aspects of human health. Bioelectromagnetics Supp. 6, S1-S213 (2003).

6. C. J. Sherry, D. W. Blick, T. J. Walters, G. C. Brown and M. R. Murphy, Lack of behavioral effect in non-human primates after exposure to ultrawideband electromagnetic radiation in the microwave frequency range. Radiat. Res. 143, 93-97 (1995).

7. T. J. Walters, P. A. Mason, C. J. Sherry, C. Steffen and J. H. Merritt, No detectable bioeffects following acute exposure to high peak power ultra-wide band electromagnetic radiation in rats. Aviat. Space Environ. Med. 66, 562-567 (1995).

8. J. R. Jauchem, R. L. Seaman, H. M. Lehnert, S. P. Mathur, K. L. Ryan, M. R. Frei and W. D. Hurt, Ultra-wideband electromagnetic pulses: Lack of effects on heart rate and blood pressure during two minute exposures of rats. Bioelectromagnetics 19, 330-333 (1998).

9. R. L. Seaman, J. E. Parker, J. L. Kiel, S. P. Mathur, T. R. Grubbs and H. K. Prol, Ultra-wideband pulses increase nitric oxide production by RAW 264.7 macrophages incubated in nitrate. Bioelectromagnetics 23, 83-87 (2002).

10. S-T. Lu, S. P. Mathur, Y. Akyel and J. C. Lee, Ultra-wideband electromagnetic pulses induced hypotension in rats. Physiol. Behav. 65, 753-761 (1999).

11. R. L. Seaman, M. L. Belt, J. M. Doyle and S. P. Mathur, Hyperactivity caused by a nitric oxide synthase inhibitor is countered by ultra-wideband pulses. Bioelectromagnetics 20, 431-439 (1999).

12. B. L. Cobb, J. R. Jauchem, P. A. Mason, M. P. Dooley, S. A. Miller, J. M. Ziriax and Murphy MR, Neural and behavioral teratological evaluation of rats exposed to ultra-wideband electromagnetic fields. Bioelectromagnetics 21, 524-537 (2000).

13. A. J. Levine, p53, the cellular gatekeeper for growth and division. Cell 88, 323-331 (1997).

14. B. Vogelstein, D. Lane and A.Levine, Surfing the p53 network. Nature (London) 408, 307-310 (2000).

15. B. K. Nayak and G. M. Das, Stabilization of p53 and transactivation of its target genes in response to replication blockade. Oncogene 21, 7226-7229 (2002).

16. K. H. Vousden, Activation of the p53 tumor suppressor protein. Biochem. Biophys. Acta. 1602, 47-59 (2002).

17. A. Mirza, Q. Wu, L. Wang, T. McClanahan, W. R. Bishop, F. Gheyas, W. Ding, B. Hutchins, T. Hockenberry and S. Liu, Global transcriptional program of p53 target genes during the process of apoptosis and cell cycle progression. Oncogene 22, 3645-3654 (2003).

18. M. Hsiao, J. Low, E. Dorn, D. Ku, P. Pattengale, J. Yeargin and M. Hass, Gain-of-function mutations of the p53 gene induce lymphohematopietic metastatic potential and tissue invasiveness. Am. J. Pathol. 145, 702-714 (1994).

19. K. V. Gurova, O. W. Rokhlin, A. V. Budanov, L. G. Burdelya, P. M. Chumakov, M. B. Cohen and A. V. Gudkov, Cooperation of two mutant p53 alleles contributes to Fas resistance of prostate carcinoma cells. Cancer Res. 63, 2905-2912 (2003).

20. A. Zalcenstein, P. Stambolsky, L. Weisz, M. Muller, D. Wallach, T. M. Goncharov, P. H. Krammer, V. Rotter and M. Oren, Mutant p53 gain of function: repression of CD95 (Fas/APO-1) gene expression by tumor-associated p53 mutants. Oncogene 22, 5667-5676 (2003).

21. J. Z. Bao, Picosecond domain electromagnetic pulse measurements in an exposure facility: an error compensation routine using deconvolution technique. Rev. Sci. Instrum. 68, 2221-2227 (1997).

22. P. C. Goswami, L. D. Albee, A. J. Parsian, J. D. Baty, E. G. Moros, W. F. Pickard, J. L. Roti Roti and C. R. Hunt, Proto-oncogene mRNA levels and activities of multiple transcription factors in C3H 10T 1/2 murine embryonic fibroblasts exposed to 835.62 and 847.74 MHz cellular phone communication frequency radiation. Radiat. Res. 151, 300-309 (1999).

23. M. Natarajan, Vijayalaxmi, M. Szilagyi, F. N. Roldan and M. L. Meltz, NF-kB DNA-binding activity after high peak power pulsed microwave (8.2 GHz) exposure of normal human monocytes. Bioelectromagnetics 23, 271-277 (2002).

24. D. Leszczynski, S. Joenvaara, J. Reivinen and R. Kuokka, Non-thermal activation of the hsp27/p38MAPK stress pathway by mobile phone radiation in human endothelial cells: Molecular mechanism for cancer- and blood-brain barrier-related effects. Differentiation 70, 120-129 (2002).

25. K. Itahana, G. P. Dimri, E. Hara, Y. Itahana, Y. Zou, P-Y. Desprez and J. Campisi, A role for p53 in maintaining and establishing the quiescence growth arrest in human cells. J. Biol. Chem. 277, 18206-18214 (2002).

26. H-Y. Tang, K. Zhao, J. F. Pizzolato, M. Fonarev, J. C. Langer and J. J. Manfredi, Constitutive expression of the cyclin-dependent kinase inhibitor p21 is transcriptionally regulated by the tumor suppressor protein p53. J. Biol. Chem. 273, 29156-29163 (1998).

27. A. Rogel, M. Popliker, C. G. Webb and M. Oren, p53 cellular tumor antigen: analysis of mRNA levels in normal adult tissues, embryos, and tumors. Mol. Cell. Biol. 5, 2851-2855 (1985).

28. M. Oren, Regulation of the p53 tumor suppressor protein. J. Biol. Chem. 274, 36031-36034 (1999).

29. H. P. Koeffler, C. Miller, M. A. Nicolson, J. Ranyard and R. A. Bosselman, Increased expression of p53 protein in human leukemic cells. Proc. Natl. Acad. Sci. USA 83, 4035-4039 (1986).

30. E. Baliant and D. Reisman, Increased rate of transcription contributes to elevated expression of the mutant p53 gene in Burkitt's lymphoma cells. Cancer Res. 56, 1648-1653 (1996).

31. B. K. Nayak, S. Patnaik and B. R. Das, Reaarangement of the p53 gene in human breast tumors. Biochem. Biophys. Res. Commun. 245, 388-391 (1998).

32. B. K. Nayak and B. R. Das, Differential binding of NF1 transcription factor to p53 gene promoter and its depletion in human breast tumors. Mol. Biol. Rep. 26, 223-230 (1999).

33. E. Gottlieb, R. Haffner, A. King, G. Asher, P. Gruss, P. Lonai and Oren M, Transgenic mouse model for studying the transcriptional activity of the p53 gene: age and tissue-dependent changes in radiation-induced activation during embryogenesis. EMBO J. 16, 1381-1390 (1997).

34. J. R. Li, C. K. Chou, J. A. McDougall, G. Dasgupta, H-H. Wu, R. L. Ren, A. Lee, J. Han and J. Momand, TP53 tumor suppressor protein in normal human fibroblasts does not respond to 837 MHz microwave exposure. Radiat. Res. 151, 710-716 (1999).

35. S. Dasdag, M. Z. Akdag, F. Aksen, F. Yilmaz, M. Bashan, M. M. Dasdag and M. S. Celik, Whole body exposure of rats to microwaves emitted from a cell phone does not affect the testes. Bioelectromagnetics 24, 182-188 (2003).

FIGURE LEGENDS

Fig 1: Activation and stabilization of the p53 protein in response to different stress agents that can result in cell cycle arrest and apoptosis. ELF – Extremely Low Frequency Field Exposure, RF – Narrowband Radiofrequency Field Exposure, UWB EMF – Ultrawideband Electromagnetic Field Exposure

Figure 2: Stabilization of the p53 protein and transcription of p53 responsive genes in response to pulsed ultrawideband electromagnetic radiation (UWB EMR) in human lymphoblastoid 244B cells. A- RNase protection assay (RPA) showing transcription of the p53 and its target genes at 2, 6, and 24 hours post-exposure. B- Western blot analysis showing stabilization of the p53 and p21 protein at 6, and 24 hours post-exposure. Control-incubator control, Sham-sham exposed, UWB-UWB EMR exposed, IR-5-Gy-ionizing radiation exposed.

Figure 3: Stabilization of the p53 protein and transcription of p53 responsive genes in response to pulsed ultrawideband electromagnetic radiation (UWB EMR) in human monocyte MM-6 cells. A- RNase protection assay (RPA) showing transcription of the p53 and its target genes at 2, 6, and 24 hours post-exposure. B- Western blot analysis showing stabilization of the p53 protein at 6, and 24 hours post-exposure. Control-incubator control, Sham-sham exposed, UWB-UWB EMR exposed, IR-5-Gy-ionizing radiation exposed.

Figure 4: Transcription of p53 target genes in response to pulsed ultrawideband electromagnetic radiation (UWB EMR) in human myeloid HL-60 cells. RNase protection assay (RPA) showing transcription of p53 target genes at 2, 6, and 24 hours post-exposure. Control-incubator control, Sham-sham exposed, UWB-UWB EMR exposed, IR-5-Gy-ionizing radiation exposed.

Fig. 1

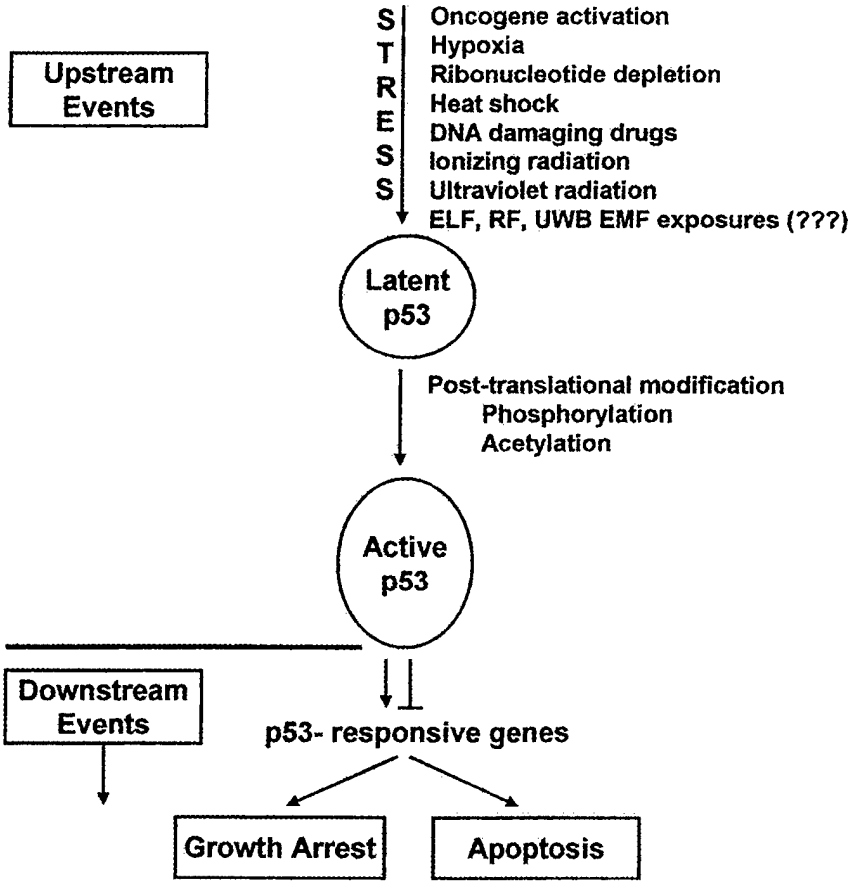

Upstream Events
STRESS
Oncogene activation
Hypoxia
Ribonucleotide depletion
Heat shock
DNA damaging drugs
Ionizing radiation
Ultraviolet radiation
ELF, RF, UWB EMF exposures (???)
Latent p53
Post-translational modification
Phosphorylation
Acetylation
Active p53
Downstream Events
p53- responsive genes
Growth Arrest
Apoptosis

Fig. 2

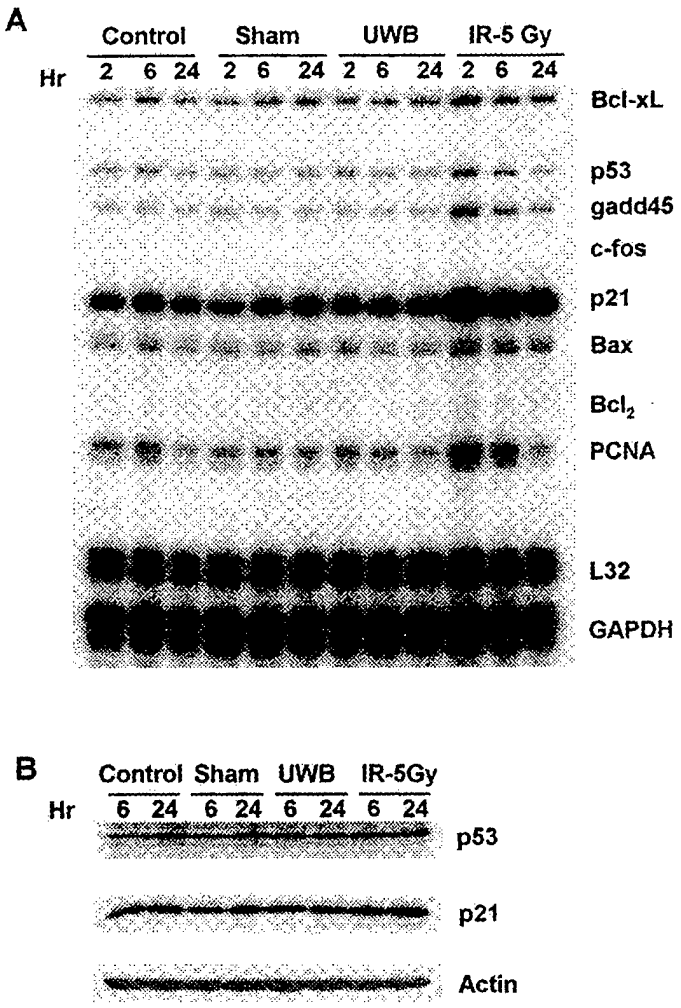

A
Control
Sham
UWB
IR-5 Gy
Hr
2 6 24 2 6 24 2 6 24 2 6 24
Bcl-xL
p53
gadd45
c-fos
p21
Bax
Bcl2
PCNA
L32
GAPDH
B
Control Sham UWB IR-5Gy
Hr
6 24 6 24 6 24 6 24
p53
p21
Actin

Fig. 3

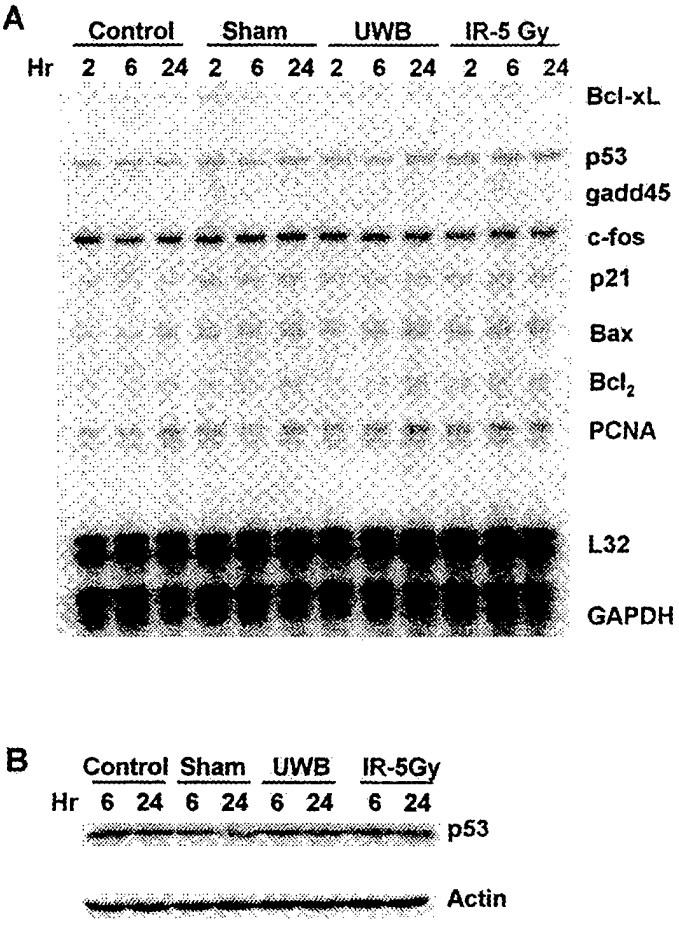
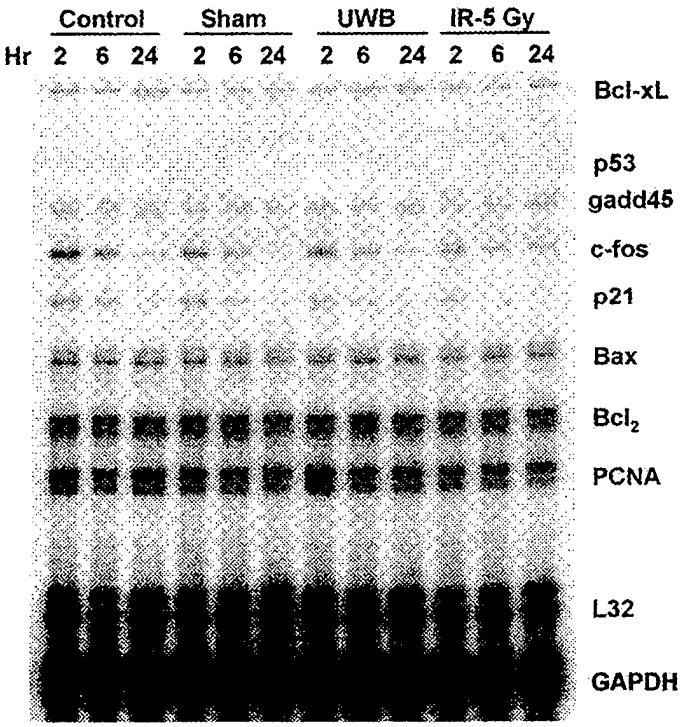

A
Control
Sham
UWB
IR-5 Gy
Hr 2 6 24 2 6 24 2 6 24 2 6 24
Bcl-xL
p53
gadd45
c-fos
p21
Bax
Bcl2
PCNA
L32
GAPDH
B
Control Sham UWB IR-5Gy
Hr 6 24 6 24 6 24 6 24
p53
Actin

Fig. 4


Control
Sham
UWB
IR-5 Gy
Hr 2 6 24 2 6 24 2 6 24 2 6 24
Bcl-xL
p53
gadd45
c-fos
p21
Bax
Bcl2
PCNA
L32
GAPDH

Effect of Ultrawideband Electromagnetic Radiation on Cell Cycle Progression in Human Hematopoietic Cells

Bijaya K. Nayak[1*], Mohan Natarajan [1], Cynthia Galindo [1], Satnam P. Mathur [2], and Martin L. Meltz[1]

[1] Department of Radiation Oncology, University of Texas Health Science Center at San Antonio, 7703 Floyd Curl Drive, San Antonio, TX 78229, USA.

[2] McKesson BioServices, US Army Medical Research Detachment, Brooks Air Force Base, 8355 Hawks Road, Building 1168, San Antonio, TX 78235, USA.

Running Title: Cell Cycle Progression after UWB EMR Exposure

*Corresponding author

Bijaya K. Nayak, Ph.D.

Department of Radiation Oncology
University of Texas Health Science Center at San Antonio
7703 Floyd Curl Drive
San Antonio, TX-78229, USA.

Email: nayak@uthscsa.edu
Tel: 210-567-8033
Fax: 210-567-8051

Funding: This work was supported by the United States Air Force Office of Scientific Research Grant No. F49620-01-1-0349.

ABSTRACT

There are many published studies examining the possible effects of narrow band (single frequency) radiofrequency radiation (RF) exposure on mammalian cells. When cell proliferation has been examined, increases, decreases and the absence of any effect have been reported. Similar studies on mammalian cell proliferation in response to pulsed ultrawideband electromagnetic radiation (UWB EMR) exposures have not previously been reported. Since ultrawideband technologies are finding their way into commercial applications, it is important to investigate the possible biological responses resulting from exposure to this type of electromagnetic field(s). The present study was undertaken to begin addressing this question by examining the impact of pulsed UWB EMR on cell cycle progression in three continuously proliferating human hematopoietic cell lines, which are different in their p53 gene competencies. To do this, the distribution of the cells in different stages of the cell cycle was determined by flow cytometry at different times within the first cell cycle time after the exposure. The human cell lines included 244B lymphoblastoid cells, MM6 monocytes, and HL-60 myeloid leukemic cells. The UWB pulses used in this study had an average peak amplitude of 102 $\pm$ 6.13 kV/m, an average pulse width of 0.79 $\pm$ 0.03 ns, and an average rise time of 206.80 $\pm$ 22.10 ps. The frequency range was up to approximately 2 GHz. No effect of the UWB EMR exposure on the cell cycle distribution, and therefore on cell cycle progression, was observed in any of the three cell lines examined. There was therefore no evidence for either an early increase or decrease in cell proliferation. This is the first report showing no alteration in mammalian cell cycle progression in response to pulsed UWB electromagnetic field exposures.

Key words: pulsed ultrawideband electromagnetic radiation, pulsed radiofrequency radiation, cell cycle progression, human cells, proliferation, p53 gene

INTRODUCTION

Radiofrequency (RF) generating devices are finding expanding use in tele-communications, industry, and health care [Goldsmith, 1995; Jerby *et al.*, 2002]. Because of this increase in use, and the advent of cellular phones and other wireless devices, there has been ever-growing attention by the public to concerns about possible health effects of both extremely low frequency and radiofrequency fields. This has led to a number of reports from agencies and governments around the world, drawing sometimes very different conclusions, about the possible health effects of electromagnetic fields. Some argue that there is no reproducible scientific evidence for biological effects, even before considering adverse health effects; others may be less demanding of the data and methodologies used to obtain it, and strongly suggest that there is biological evidence for adverse health effects. This study extends the information base beyond that of narrowband investigations (studies at specific frequencies), into the much less well investigated area of pulsed ultrawideband electromagnetic radiation (UWB EMR) exposures.

The use of UWB EMR systems is of current interest to the U.S. Air Force for use in radar, as well as a means to suppress electronically vulnerable targets [Agee *et al.*, 1998]. It also has commercial applications, including (but not limited to) communications. Pulsed UWB fields are generated as short high-peak-power electromagnetic pulses with an extremely fast-rise-time, with most of the energy in each pulse being in the frequency range of D.C. to approximately 2 GHz. The unusual properties of pulsed UWB electromagnetic radiation suggest the possibility that such exposures might lead to bioeffects not established for narrow band exposures.

There are only a limited number of studies carried out on the biological effects of pulsed UWB electromagnetic radiation, with the majority being focused on behavioral and physiological effects after exposure of animal models [Sherry *et al.*, 1995; Walters *et al.*, 1995; Jauchem *et al.*, 1998; Seaman *et al.*, 2002]. While most of these studies have reported no biological effect in response to the exposures, some have reported the presence of an effect. It has been reported that UWB pulses induced hypotension in rats [Lu *et al.*, 1999]. Further, it has been reported that UWB pulses countered the hyperactivity caused by a nitric oxide synthase inhibitor [Seaman *et al.*, 1999]. Cobb *et al.* [2000] reported a teratologic effect in rats exposed to UWB electromagnetic fields. With respect to the mechanism of the latter, it could be hypothesized that the teratogenic outcome was due to an effect of the UWB EMR on cell proliferation in the developing embryo or fetus. There is no report available addressing this question with regard to mammalian cells. If an exposure of a mammalian cell to an agent increased the rate of proliferation, a shortening of the cell cycle would be expected, and a change in the percentage of cells in different stages of the cell cycle would occur. The same would be expected if there was an inhibition of cell proliferation. This study was therefore undertaken to determine if there is any evidence for an alteration in cell cycle progression after a 90 min exposure to pulsed high peak power UWB EMR.

METHODS

Cell Line Selection

The role of the p53 tumor suppressor gene in mediating growth arrest in the G1 (at the G1/S border), in the S, and in the G2/M phases of the cell cycle in response to different stress signals has been well documented [Bunz *et al.*, 1998; Vogelstein *et al.*, 2000; Nayak and Das, 2002]. Therefore, cell lines with different p53 gene status were selected to examine the possible effects of pulsed UWB EMR exposure on cell cycle progression. The 244B human lymphoblastoid cells have a wild-type p53 gene activity (they are p53 competent), the MM-6 human monocyte cells have a compromised p53 gene activity (the p53 cannot be induced), and the HL-60 human myeloid leukemic cells used are p53-null (they have no p53 gene).

Cell Line Maintenance

The 244B and HL-60 cells were maintained in RPMI-1640 medium (Cellgro, Herndon, VA) supplemented with 10% FBS (Hyclone, Logan, UT), 10 mM HEPES (Cellgro, Herndon, VA), 2mM L-Glutamine (Cellgro, Herndon, VA), and 50 µg/ml gentamicin (Sigma, St Louis, MO). The MM-6 cells were maintained in RPMI-1640 medium supplemented with 10% FBS, 10 mM HEPES, 2mM L-Glutamine, 200U penicillin/200 µg/ml streptomycin (Cellgro, Herndon, VA), 2mM non-essential amino acids (NEAA) (Invitrogen, Carlsbad, CA), and 1 vial of OPI (0.15g oxaloacetate, 0,05g pyruvate, and 0.0082g bovine insulin) per liter of medium (Sigma, St Louis, MO). The cells were maintained in disposable tissue culture flasks with filter caps in a humidified 5% CO_2/95% air atmosphere at 37°C.

Ionizing Radiation Exposure

Cells were exposed to a 2 Gy dose of ^{137}Cs gamma rays (Atomic Energy of Canada/Nordion). The dose rate over the course of the experiments ranged from 127.9 cGy/min to 125.3 cGy/min. The cells were exposed at room temperature in T-25 flasks with 10 ml of medium, immediately after removal of the flasks from the 37°C incubator. The flasks were returned to the incubator in the adjoining laboratory immediately after the exposure. The sham controls were carried to and from the irradiation room at the same time.

UWB EMR Exposure System

The UWB electromagnetic radiation exposures were performed in a custom-built giga-transverse electromagnetic (GTEM) cell originally constructed by Sandia National Laboratories (Albuquerque, NM). The GTEM cell, a tapered two-conductor transmission line with a square cross-section, was positioned so that one ground plane wall was horizontal. A modified RG-220 coaxial cable connected the center conductor of the GTEM cell to a source of high voltage. Ionization of nitrogen in a center-conductor gap in the cable generated UWB pulses in the GTEM cell, with electric field vector directed from center conductor to ground conductor. A EG&G ACD(A) D-dot probe mounted in the wall of the GTEM cell was used to detect UWB pulses during cell exposures. The signal from the probe was sampled with 0.01-ns resolution by a Tektronix SCD 5000 Transient Digitizer. Each digitized wave-form, representing the average of 200 *individual pulses was stored and later processed using a correction algorithm* [Bao, 1997] to give the corrected average peak pulse electric field, rise time, and pulse width. The pulses were triggered by an external pulse generator at 250 pulses/s. The mean pulse

duration was 0.79 ± 0.03 ns. The average peak E-field was 102.03 ± 6.13 kV/m. The frequencies ranged from 1 Hz to approximately 2 GHz. The rise time was 206.80 ± 22.10 ps. The exposure system has been previously described (Jauchem *et al.*, 1998).

Temperature Measurement and Control

Prior to initiating the UWB EMR experiments, the temperature distribution was determined at the bottom of the T-25 flasks positioned in a custom built foam "air incubator" box (described below). The temperature was measured using a Luxtron 3000 Data Acquisition Program. The assessment indicated an average of 37.0± 0.3°C at the bottom of the flask in the two center position flasks in the foam incubator box, where the temperature distribution around the bottom of the flask was most uniform. Only these two positions were used for the experimental studies; two dummy flasks filled with 10 ml of RPMI medium were always placed in the two outer positions of the holder. To verify that the temperature remained close to 37°C during and between the intermittent exposures, the temperatures in the sham and UWB-exposed flasks were monitored continuously for 5 minutes before, during and for 5 min after the pulsed UWB EMR exposures (using the Luxtron System). To accomplish this, a Luxtron probe was inserted vertically downward through holes in the foam incubator box and in the caps of each of the two center flasks, to the bottom of the column of the medium in those flasks. The mean temperature during each of the three 30 min UWB exposure periods, and also in the two 30 min EMR off interim periods, was 36.96 ± 0.06°C. Two sham exposure flasks were handled in exactly the same manner. These flasks were placed in a second foam holder (with two flasks with medium in the outer positions in the holder) in a Faraday Cage in the anechoic chamber alongside the GTEM cell. The temperature in all the

flasks was maintained by computer controlled (Luxtron probe feed back) warm-air flow into the incubator boxes.

Cell Handling for UWB EMR Exposure

The cells were seeded at 500,000 cells/ml in 10 ml complete growth medium in T-25 flasks with vent caps (Corning) on the day prior to exposure. The cell density was determined by haemocytometer count. Viability was checked using the trypan blue dye exclusion method. The flasks were incubated at 37°C in a humidified 5% CO_2/95% air atmosphere for up to 1 hr, before being transported in a warmed styrofoam container (with water packs) to a similar incubator in the UWB exposure facility at Brooks City-Base. The flasks were then incubated overnight at 37°C. After checking the performance of the UWB source (pre-exposure check), and 30 min prior to the UWB EMR exposure, two of the T-25 flasks with cells were placed vertically in the two center positions of the two custom designed 4-flask foam holders (for exposure and sham exposure). The foam holders served as incubators, allowing the temperature of the medium in the flasks to be maintained at 37°C throughout the exposure period. The cells were allowed to settle to the bottom of the flask during this 30 min. The exposure holder was positioned at a distance of 72.7 cm from the opening of the GTEM cell, into which the UWB pulses were emitted. Prior exposure distribution information at the selected exposure parameters (stated above) is being separately reported (Satnam *et al.*, in preparation).

Cell Handling Post-Exposure

After the last of the three 30 min UWB EMR exposures, the flasks were allowed to remain in position in the holder to collect 5 min of post-exposure temperature data. The flasks were then removed from the exposure system and the plug-seal caps were

replaced with vented caps. The flasks were placed in the incubator until transported at near 37°C to the incubator at UTHSCSA. The cells were incubated for the different times indicated below.

Cell Cycle Analysis

The cell cycle analysis was carried out at 6, 10, and 24 h post-exposure following a standard protocol. Briefly, the cells were harvested, washed with phosphate buffered saline (PBS) and fixed in 70% ethanol. The fixed cells were resuspended in PBS containing propidium iodide (50 µg/ml), RNase A (500 µg/ml), and Triton X-100 (0.5%), and incubated in the dark for 1 hour. The cell cycle analysis was performed by flow cytometry in a Becton Dickinson FACSCalibur Flow Cytometer. The results were determined using ModFit software and reported as percentage G0/G1, percentage S, and percentage G2/M cells.

RESULTS

The results of the experiments are presented separately for 244B cells (Figure 1, Table 1), MM6 cells (Figure 2, Table 2), and HL-60 cells (Figure 3, Table 3).
Figure 1 shows a representative flow cytometry pattern for the 244B (p53 competent) cells: the results from 4 independent experimental exposures performed on different days are averaged in Table 1. The sham exposed distributions are consistent with the incubator controls, indicating little if any handling effect being observed at the 6, 10 or 24 hr time points. After the 2 Gy ionizing radiation exposure, a decrease in G0/G1, an increase in S and an increase in G2/M cells was observed at 6 hr. The G0/G1 decrease extended out to 24 hr. The percentage S phase cells at 10 hr had declined to the control value, and

continued to decline to a still lower value at 24 hr. The percentage of cells in G2/M increased further at 10 hr, and remained elevated with a further increase at 24 hr. There was no difference in the percentage of the UWB EMR exposed cells and the sham exposed cells in the different cell cycle stages over the 24 hr observation period.

Figure 2 shows a representative flow cytometry pattern for the MM-6 (p53 compromised) cells; the results from 4 independent experimental exposures performed on different days are averaged in Table 2. Again, the sham exposed distributions are consistent with the incubator controls, indicating little if any handling effect being observed at the 6, 10 or 24 hr time points. After the 2 Gy ionizing radiation exposure, a decrease in G0/G1, an increase in S and an increase in G2/M stage cells was observed at 6 hrs (similar to the 244B cells). A small additional decrease in G0/G1 stage cells was observed at 10 hrs post-exposure, with this increasing back to the 6 hr level at 24 hr. The percentage S phase cells increased further at 10 hr, but decreased back to the 6 hr level at 24 hrs. The percentage of cells in the G2/M stage remained elevated at 10 and 24 hrs. There was no difference in the percentage of the UWB EMR exposed cells and the sham exposed cells in the different cell cycle stages over the 24 hr observation period.

Figure 3 shows a representative flow cytometry pattern for the HL-60 (p53 null) cells; the results from 4 independent experimental exposures performed on different days are averaged in Table 3. The sham exposed distributions are consistent with the incubator controls, indicating little if any handling effect being observed at the 6, 10 or 24 hr time points. After the 2 Gy exposure, there is a considerable decrease in the G0/G1 stage cells, at most a minimal increase in the S phase cells, and an increase in the G2/M stage cells at 6 hr. At 10 hr, there is a large additional decrease in G0/G1 stage cells, with the low

level still being present at 24 hrs post-exposure. An increase in the S phase cells is present at 10 hr, but a large decrease is present at 24 hrs. Again, there was no difference in the percentage of the UWB EMR exposed cells and the sham exposed cells in the different cell cycle stages over the 24 hr observation period. Figure 4 is a graphical summary of the results.

DISCUSSION

The debate over whether or not there are measurable biological responses to exposure of mammalian cells to radiofrequency (RF) radiation, where heating is not involved, has been ongoing (Meltz, 2003). Studies have reported a change in cell proliferation in response to narrowband RF radiation at 27 MHz and at 2450 MHz in human lymphocytes [Cleary *et al.*, 1990a] and in dividing glioma cells [Cleary *et al.*, 1990b] several days after the RF exposures. The assay was not a measurement of an increase in cell number over time, but rather the relative uptake of the radioactive DNA precursor ^{3}H-thymidine in exposed compared to control cells. The rate of DNA synthesis measured using the radioactive labeling method is a surrogate and not a direct measure of cell proliferation. Stagg *et al.* [1997] also reported that there was an increase in proliferation after a narrowband RF exposure (cell phone frequency of 836.55 MHz) using radioactive thymidine uptake as the measure. However, when actual cell counts were performed as a direct measure of cell proliferation in the same experiments, no difference was observed between the exposed and control cultures. The use of the ratio method and radioactive labeling for assessing proliferation several days after exposure is therefore questionable. If the rate of cell proliferation during an RF exposure was altered

by that RF exposure, the outcome would be expected to be an altered increase in cell number over time. Meltz *et al.* [1989] examined whether or not RF exposure at 2450 MHz altered the rate of ^{3}H-thymidine incorporation into DNA during a 1 hour RF exposure and labeling period. No effect on the rate of DNA synthesis was observed. In a paper by Byus *et al.* [1988], an increase in the activity of the enzyme ornithine decarboxylase (ODC) was reported after an RF exposure at 450 MHz, with modulation at 16 Hz. The suggestion has been made that the increase in ODC observed immediately after the exposure implies that cell proliferation would increase, since DNA synthesis was supposedly being turned on. However, when the investigators (in the same study) looked for an increase in the rate of DNA synthesis 16 hours after the exposure, no increase was observed. French *et al.* [1997] reported that electromagnetic radiation at 835 MHz inhibited cell proliferation of the human U-87 MG astrocytoma cell line. The same group also reported that the rate of DNA synthesis and cell replication was increased in the rat RBL-2H3 mast cell line after exposure to electromagnetic radiation at 835 MHz [Donnellan *et al.*, 1997]. It is therefore not clear whether exposure to RF radiation can induce, increase, or inhibit cell proliferation, and if so, whether there is a cell-type-specific response to radiofrequency electromagnetic fields. In contrast to the reports of effects, several studies have reported no effect of RF exposure on cell proliferation. These studies included exposure of rat glioma and primary glial cells to 836.55 MHz RF [Stagg *et al.*, 1997], mouse C3H 10T1/2 fibroblasts and human U87MG glioma cells to 835.62 and 847.74 MHz RF [Higashikubo *et al.*, 2001], and Chinese hamster ovary (CHO) cells exposed to 2450 MHz RF [Ciaravino *et al.*, 1991].

An alternative method to examine the effect of EMR on cell proliferation is to look at the impact of the exposure on cell cycle progression. Normally, upon cell division, proliferating cells move from their mitotic or M phase into G1, progress from G1 into S phase (the DNA synthetic phase) if no DNA damage has occurred (in p53 competent cells), and on into G2 stage and the subsequent M stage. For untreated cells growing exponentially *in vitro*, the distribution of the cells in the G0/G1, S, and G2/M stages will be consistent over time. If the DNA in p53 competent cells is damaged by RF or any other agent, the times that the cells take to progress through the different stages of the cell cycle would be altered, and the overall cell cycle time would be increased. This would be reflected by a change in the numbers of cells in the different stages of the cell cycle, i.e. a change in % G0/G1, % S, and/or % G2/M cells. Cao *et al.* [1995] and Cleary *et al.* [1996] reported alterations in the cell cycle in Chinese hamster ovary (CHO) cells after narrowband RF exposures of 27 and 2450 MHz. There were technical problems in both their interpretation of the data, and the statistical approach used. They stated that a small change in the shape of the G2/M peak was an indication of an effect, although the G2/M peak represents one DNA content. Each of the channels used in the flow cytometer assessment is not a different DNA content, as was stated in one of the papers. In addition, the authors did not report the percentages of cells in each of the compartments resulting from the flow cytometry analysis. They instead described a unique method of statistical analysis never used before, and to our knowledge, never used since. In the paper by Higashikubo *et al.* [2001], where the measurement of the effects of 835.62 and 847.74 MHz RF on cell cycle distribution were made, no alterations were observed. Based on the above observations, it appears that there is no substantiated

evidence that narrowband RF exposures, where no measurable increase in the temperature of the culture medium above 37°C has been reported to occur, can alter cell cycle progression. This is consistent with the reports showing the absence of effects of narrowband RF exposures on the kinetics of cell progression (cells in first and second cell divisions after RF exposure) by Ciaravino *et al.* [1991], Vijayalaxmi *et al.* [1997], and Stagg *et al.* [1997]. In the study reported here, we have expanded the investigations of cell cycle progression effects into the area of ultrawideband electromagnetic radiation exposures. The exposures were to a very high average peak electric field (102.03 $\pm$ 6.13 kV/m), a very rapid rise time (206.80 $\pm$ 22.10 ps), a very small pulse width (0.79 $\pm$ 0.03 ns), and a reasonable experimental exposure duration (a total of 90 minutes UWB EMR exposure). Our study in human hematopoietic cells clearly demonstrates for the first time that UWB electromagnetic radiation exposure does not effect cell cycle distribution in cells with different p53 competencies, and therefore does not effect the cell cycle progression within the first cell cycle post-exposure. Further, it suggests that this UWB EMR exposure is unlikely to induce DNA strand breakage, since activation of the p53 gene that would be expected after such damage would lead to a cell cycle alteration. Direct measures of both DNA single strand breakage and p53 gene activation are currently underway.

ACKNOWLEDGMENTS

The authors thank Mr. Charles Thomas of the San Antonio Cancer Institute (SACI) Institutional Flow Cytometry Core Facility for the cell cycle analysis. We also thank Mr. John Ashmore of Brooks Air Force Base, San Antonio for his assistance in developing the temperature control system, and assisting with the UWB EMR exposures.

REFERENCES

Agee FJ, Baum CE, Prather WD, Lehr JM, O'Loughlin JP, Burger JW, Schoenberg JSH, Scholfield DW, Torres RJ, Hull JP, Gaudet JA. 1998. Ultra-wideband transmitter research. IEEE Trans Plasma Sci 26:860-873.

Bao JZ. 1997. Picosecond domain electromagnetic pulse measurements in an exposure facility: an error compensation routine using deconvolution technique. Rev Sci Instrum 68:2221-2227.

Bunz F, Dutriaux A, Lengauer C, Waldman T, Zhou S, Brown JP, Sedivy JM, Kinzler KW, Vogelstein B. 1998. Requirement for p53 and p21 to sustain G2 arrest after DNA damage. Science 282:1497-1501.

Byus CV, Kartun K, Pieper S, Adey WR. 1988. Increased ornithine decarboxylase activity in cultured cells exposed to low energy modulated microwave fields and phorbol ester tumor promoters. Cancer Res 48:4222-4226.

Cao G, Liu L-M, Cleary SF. 1995. Cell cycle alterations induced by isothermal 27 MHz radio-frequency radiation exposure. Bioelectrochem Bioenerget 37:131-140.

Ciaravino V, Meltz ML, Erwin DN. 1991. Absence of synergistic effect between moderate-power radio-frequency electromagnetic radiation and adriamycin on cell cycle progression and sister-chromatid exchange. Bioelectromagnetics 12:289-298.

Cleary SF, Li-Ming L, Merchant RE. 1990a. In vitro lymphocyte proliferation induced by radio-frequency electromagnetic radiation under isothermal conditions. Bioelectromagnetics 11:47-56.

Cleary SF, Li-Ming L, Merchant RE. 1990b. Glioma proliferation modulated *in vitro* by isothermal radiofrequency radiation exposure. Radiat Res 121:38-45.

Cleary SF, Cao G, Liu L-M. 1996. Effects of isothermal 2.45 GHz microwave radiation on the mammalian cell cycle: comparison with effects of isothermal 27 MHz radiofrequency radiation exposure. Bioelectrochem Bioenerget 39:167-173.

Cobb BL, Jauchem JR, Mason PA, Dooley MP, Miller SA, Ziriax JM, Murphy MR. 2000. Neural and behavioral teratological evaluation of rats exposed to ultra-wideband electromagnetic fields. Bioelectromagnetics 21:524-537.

Donnellan M, McKenzie DR, French PW. 1997. Effects of exposure to electromagnetic radiation at 835 MHz on growth, morphology and secretory characteristics of a mast cell analogue, RBL-2H3. Cell Biol International 21:427-439.

French PW, Donnellan M, McKenzie DR. 1997. Electromagnetic radiation at 835 MHz changes the morphology and inhibits proliferation of a human astrocytoma cell line. Bioelectrochem Bioenerget 43:13-18.

Goldsmith JR. 1995. Epidemiologic evidence of radiofrequency radiation (microwave) effects on health in military, broadcasting, and occupational studies. Int J Occup Environ Health 1:47-57.

Higashikubo R, Ragouzis M, Moros EG, Straube WL, Roti Roti JL. 2001. Radiofrequency electromagnetic fields do not alter the cell cycle progression of C3H 10T1/2 and U87MG cells. Radiat Res 156:786-795.

Jauchem JR, Seaman RL, Lehnert HM, Mathur SP, Ryan KL, Frei MR, Hurt WD. 1998. Ultra-wideband electromagnetic pulses: Lack of effects on heart rate and blood pressure during two minute exposures of rats. Bioelectromagnetics 19:330-333.

Jerby E, Dikhtyar V, Aktushev O, Grosglick U. 2002. The microwave drill. Science 298:587-589.

Lu S-T, Mathur SP, Akyel Y, Lee JC. 1999. Ultra-wideband electromagnetic pulses induced hypotension in rats. Physiol Behav 65:753-761.

Meltz ML, Eagan P, Erwin DN. 1989. Absence of mutagenic interaction between microwaves and mitomycin C in mammalian cells. Environ Mol Mutagen 13:294-303.

Meltz ML. 2003. Radiofrequency exposure and mammalian cell toxicity, genotoxicity, and transformation. Bioelectromagnetics Supplement 6:S196-S213.

Nayak BK, Das GM. 2002. Stabilization of p53 and transactivation of its target genes in response to replication blockade. Oncogene 21:7226-7229.

Seaman RL, Belt ML, Doyle JM, Mathur SP. 1999. Hyperactivity caused by a nitric oxide synthase inhibitor is countered by ultra-wideband pulses. Bioelectromagnetics 20:431-439.

Seaman RL, Parker JE, Kiel JL, Mathur SP, Grubbs TR, Prol HK. 2002. Ultra-wideband pulses increase nitric oxide production by RAW 264.7 macrophages incubated in nitrate. Bioelectromagnetics 23:83-87.

Sherry CJ, Blick DW, Walters TJ, Brown GC, Murphy MR. 1995. Lack of behavioral effect in non-human primates after exposure to ultrawideband electromagnetic radiation in the microwave frequency range. Radiat Res 143:93-97.

Stagg RB, Thomas WJ, Jones RA, Adey WR. 1997. DNA synthesis and cell proliferation in C_6 glioma and primary glial cells exposed to a 836.55 MHz modulated radiofrequency field. Bioelectromagnetics 18:230-236.

Vijayalaxmi, Mohan N, Meltz ML, Wittler MA. 1997. Proliferation and cytogenetic studies in human blood lymphocytes exposed *in vitro* to 2450 MHz radiofrequency radiation. Int J Radiat Biol 72:751-757.

Vogelstein B, Lane D, Levine A. 2000. Surfing the p53 network. Nature (London) 408:307-310.

Walters TJ, Mason PA, Sherry CJ, Steffen C, Merritt JH. 1995. No detectable bioeffects following acute exposure to high peak power ultra-wide band electromagnetic radiation in rats. Aviat Space Environ Med 66:562-567.

244B

	6h			10h			24h		
	G0/G1	S	G2/M	G0/G1	S	G2/M	G0/G1	S	G2/M
Control									
Mean	71.8	16.3	11.8	72.8	16.3	11.0	75.0	14.0	11.8
STD	1.3	2.6	1.5	0.5	1.5	1.4	1.6	1.8	1.0
Sham									
Mean	74.0	17.0	9.0	74.5	15.0	10.5	74.3	14.8	11.0
STD	0.8	2.2	2.2	1.3	2.2	1.7	1.3	2.1	0.8
UWBEMR									
Mean	73.8	15.8	10.8	73.5	15.5	11.3	74.8	15.0	10.3
STD	1.0	1.7	1.7	1.3	0.6	2.1	1.0	1.2	1.3
IR (2 Gy)									
Mean	64.5	18.5	17.0	62.5	15.3	22.0	64.8	10.8	24.5
STD	2.1	3.9	2.6	3.7	5.1	1.4	2.8	2.1	1.3

Table 1: Cell cycle distribution in human lymphoblastoid 244B cells after UWB EMR exposure. Mean values of % of cells in G0/G1, S, and G2/M phases of the cell cycle and standard deviation in control, sham, and IR-exposed (2 Gy) cells from 4 independent experiments is presented.

MM-6

	6h			10h			24h		
	G0/G1	S	G2/M	G0/G1	S	G2/M	G0/G1	S	G2/M
Control									
Mean	68.3	20.8	11.0	64.5	24.0	11.8	62.0	26.0	11.8
STD	1.3	1.0	0.8	2.6	2.2	1.0	0.8	1.4	0.5
Sham									
Mean	70.5	19.0	10.5	66.3	26.0	7.8	64.0	25.3	10.8
STD	1.7	0.8	1.0	1.7	1.2	1.0	0.8	1.0	1.5
UWBEMR									
Mean	69.5	20.3	10.3	69.0	23.5	7.5	62.0	26.8	11.3
STD	1.0	0.5	0.5	2.2	1.7	0.6	1.8	1.7	1.3
IR (2 Gy)									
Mean	60.3	24.5	15.3	54.0	29.5	16.5	60.8	23.5	15.8
STD	1.7	1.3	0.5	1.8	2.9	1.3	1.5	0.6	1.3

Table 2: Cell cycle distribution in human monocyte MM-6 cells after UWB EMR exposure. Mean values of % of cells in G0/G1, S, and G2/M phases of the cell cycle and standard deviation in control, sham, and IR-exposed (2 Gy) cells from 4 independent experiments is presented.

HL-60

	6h			10h			24h		
	G0/G1	S	G2/M	G0/G1	S	G2/M	G0/G1	S	G2/M
Control									
Mean	52.0	36.0	12.0	49.8	37.3	12.8	54.8	32.5	12.5
STD	1.8	2.4	0.8	1.0	1.0	1.0	1.3	0.6	1.0
Sham									
Mean	49.8	37.3	13.0	50.3	37.5	12.3	52.8	35.3	12.0
STD	5.1	3.3	2.2	1.3	1.7	1.9	1.5	1.9	0.8
UWBEMR									
Mean	50.5	37.5	12.0	46.3	38.0	15.8	55.0	32.3	12.8
STD	1.3	1.9	0.8	1.0	2.3	1.5	1.4	1.9	0.5
IR (2 Gy)									
Mean	42.0	39.5	18.5	28.3	43.8	28.0	32.5	26.8	40.8
STD	1.4	2.4	1.0	1.5	1.7	1.4	2.9	2.1	2.1

Table 3: Cell cycle distribution in human myeloid leukemic HL-60 cells after UWB EMR exposure. Mean values of % of cells in G0/G1, S, and G2/M phases of the cell cycle and standard deviation in control, sham, and IR-exposed (2 Gy) cells from 4 independent experiments is presented.

FIGURE LEGENDS

Figure 1: Effect of ultrawideband electromagnetic radiation (UWB EMR) exposure on cell cycle distribution of human lymphoblastoid 244B cells (p53 competent). A-Incubator control: A1 (at 6 hour), A2 (at 10 hour), A3 (at 24 hour). B-Sham-exposed: B1 (at 6 hour), B2 (at 10 hour), B3 (at 24 hour). C-UWB EMR-exposed: C1 (at 6 hour), C2 (at 10 hour), C3 (at 24 hour). D: Ionizing radiation (IR)-exposed (2 Gy): D1 (at 6 hour), D2 (at 10 hour), and D3 (at 24 hour).

Figure 2: Effect of ultrawideband electromagnetic radiation (UWB EMR) exposure on cell cycle distribution of human monocyte MM-6 cells (p53 compromised). A-Incubator control: A1 (at 6 hour), A2 (at 10 hour), A3 (at 24 hour). B-Sham-exposed: B1 (at 6 hour), B2 (at 10 hour), B3 (at 24 hour). C-UWB EMR-exposed: C1 (at 6 hour), C2 (at 10 hour), C3 (at 24 hour). D: Ionizing radiation (IR)-exposed (2 Gy): D1 (at 6 hour), D2 (at 10 hour), and D3 (at 24 hour).

Figure 3: Effect of ultrawideband electromagnetic radiation (UWB EMR) exposure on cell cycle distribution of human myeloid leukemic HL-60 cells (p53 null). A-Incubator control: A1 (at 6 hour), A2 (at 10 hour), A3 (at 24 hour). B-Sham-exposed: B1 (at 6 hour), B2 (at 10 hour), B3 (at 24 hour). C-UWB EMR-exposed: C1 (at 6 hour), C2 (at 10 hour), C3 (at 24 hour). D: Ionizing radiation (IR)-exposed (2 Gy): D1 (at 6 hour), D2 (at 10 hour), and D3 (at 24 hour).

Figure 4: Effect of ultrawideband electromagnetic radiation (UWB EMR) exposure on cell cycle distribution. Mean values of % of cells in G0/G1, S and G2/M phases of the cell cycle in sham and UWB EMR exposed cells from 4 independent exposures is presented. A-244B, B-MM-6, and C-HL-60 cells.

Fig. 1

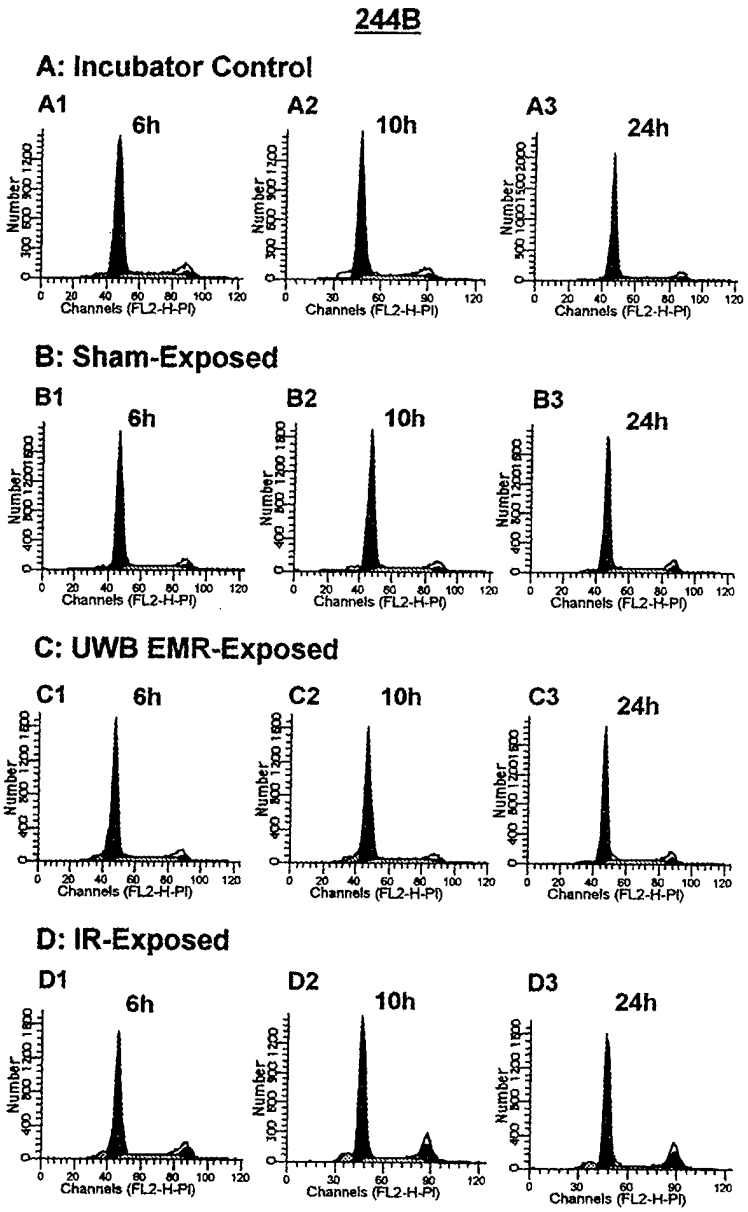

244B
A: Incubator Control
A1
6h
A2
10h
A3
24h
B: Sham-Exposed
B1
6h
B2
10h
B3
24h
C: UWB EMR-Exposed
C1
6h
C2
10h
C3
24h
D: IR-Exposed
D1
6h
D2
10h
D3
24h
Number
Channels (FL2-H-PI)

Fig. 2

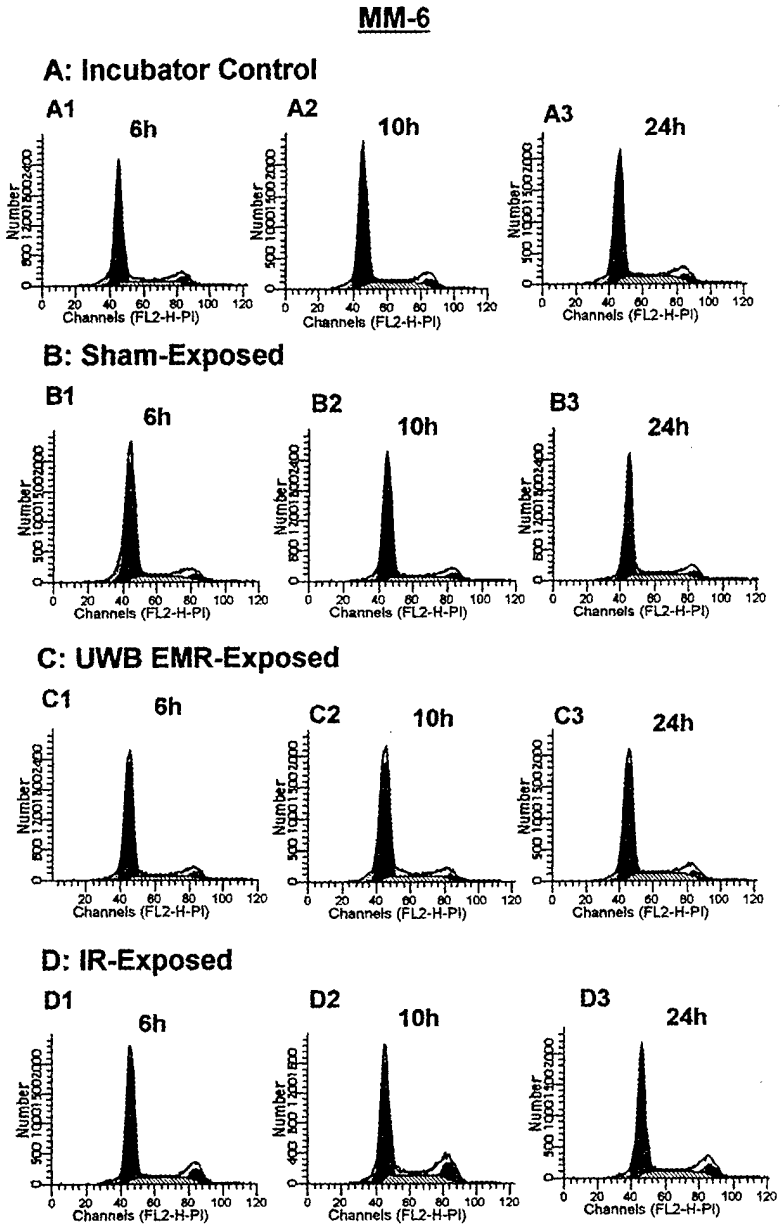

MM-6
A: Incubator Control
A1
6h
A2
10h
A3
24h
B: Sham-Exposed
B1
6h
B2
10h
B3
24h
C: UWB EMR-Exposed
C1
6h
C2
10h
C3
24h
D: IR-Exposed
D1
6h
D2
10h
D3
24h
Number
Channels (FL2-H-PI)

Fig. 3

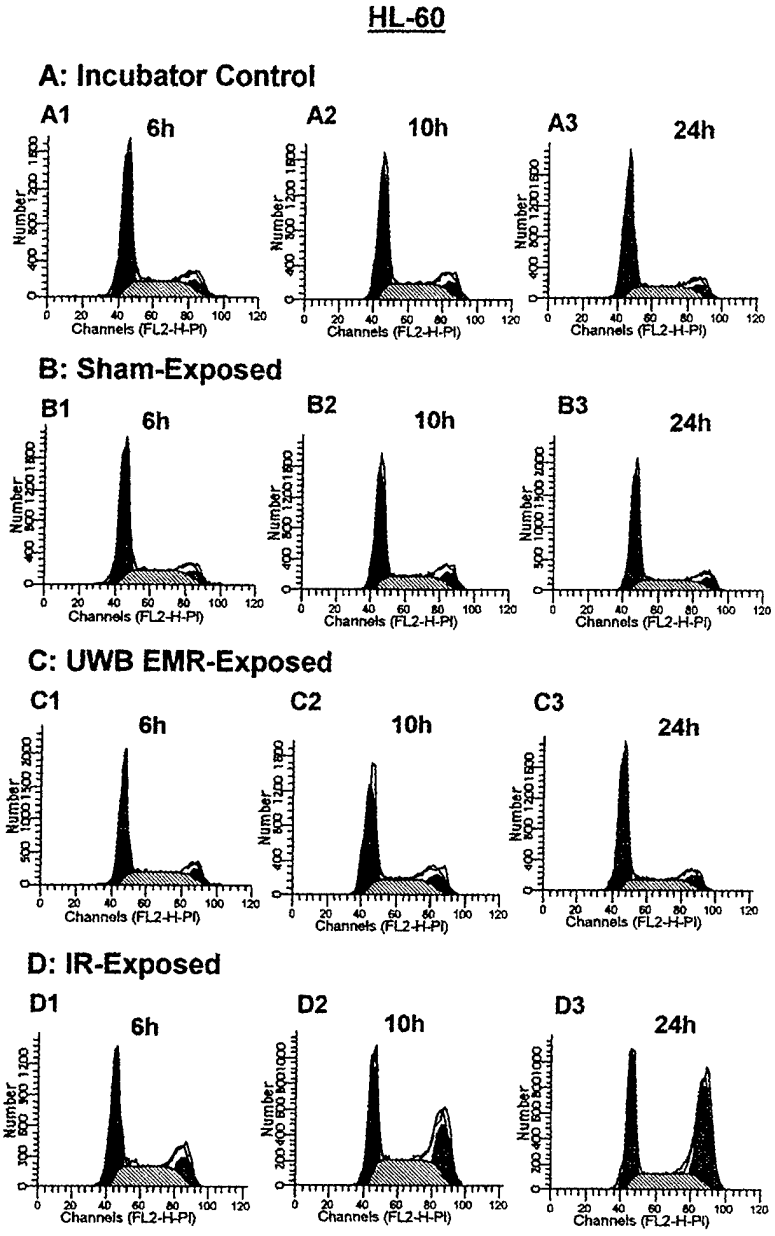
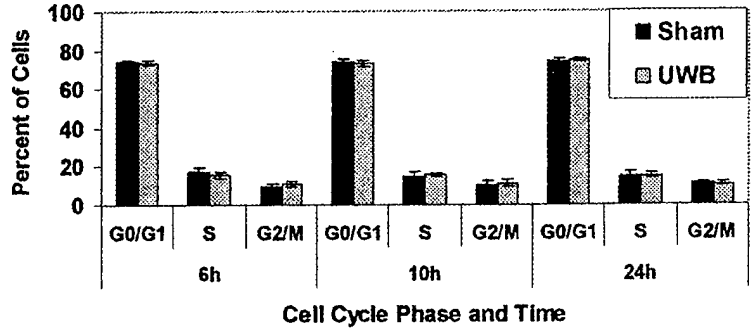
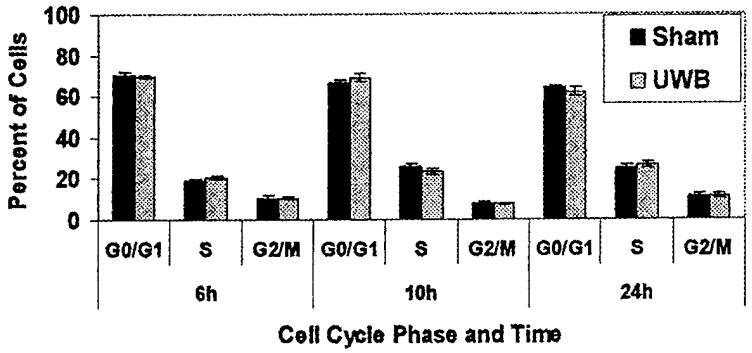

HL-60
A: Incubator Control
A1
6h
A2
10h
A3
24h
B: Sham-Exposed
B1
6h
B2
10h
B3
24h
C: UWB EMR-Exposed
C1
6h
C2
10h
C3
24h
D: IR-Exposed
D1
6h
D2
10h
D3
24h
Number
Channels (FL2-H-PI)

Fig. 4

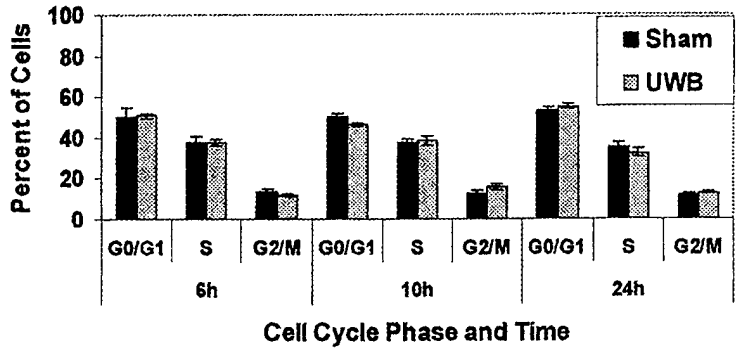
A: 244B



B: MM-6



C: HL-60



Some Characteristics of the Cytotoxic Effect of Nanosecond Duration, High-Intensity Electrical Pulses

Andrei G. Pakhomov, Amy Phinney, John Ashmore, Kerfoot Walker III, Juergen Kolb, Susumu Kono, Karl H. Schoenbach, *Fellow, IEEE,* and Michael R. Murphy, *Associate Member, IEEE*

***Abstract*— Cytotoxic effects of 10-ns electrical pulses (EP, 50 to 380 kV/cm) were analyzed in cultured U937 cells (human lymphoma). Densities of live and dead cells were compared in over 500 samples at intervals from 0.5 to 48 hours post exposure. EP trains of 1 to 20 pulses caused a minor, if any, decrease in cell survival: 24 h post exposure, the live cells density typically dropped just 10-20% compared with unexposed parallel control. Within studied limits, this effect did not significantly depend on the EP number, voltage, or repetition rate. However, much longer EP trains could cause a sharp survival decline. The transition from plateau to profound cell killing occurred at about 150 pulses at 150 kV/cm, and at over 1000 pulses at 50 kV/cm. Artifact-free thermometry using a fiber optic microprobe established unequivocally that cell killing by extra-long EP trains was not a result of sample heating and has to be explained by other mechanisms. Lethally exposed cells did not display specific cleavage of poly(ADP-ribose) polymerase, which is an established hallmark of activation of caspases in apoptotic cells. Overall, 10-ns EP caused far weaker cytotoxic effect than it was reported earlier from experiments in other cell lines and mostly with longer pulses (60 and 300 ns). The survival curve shape, i.e., the shoulder followed by exponential decline, is also characteristic for other cytotoxic factors, such as low-LET ionizing radiation, thereby possibly pointing to common mechanisms or targets.**

***Index Terms*— Apoptosis, cytotoxicity, nanosecond electrical pulses.**

Manuscript received September 29, 2003. The work was supported by the U.S. Army Medical Research and Materiel Command and the U.S. Air Force Research Laboratory under U.S. Army contract DAMD17-94-C-4069 awarded to McKesson BioServices Corporation, and by an AFOSR/DOD MURI grant on Subcellular Responses to Narrowband and Wideband Radiofrequency Radiation, administered through Old Dominion University.

A. G. Pakhomov is with McKesson BioServices Corporation, U.S. Army Medical Research Detachment, and Air Force Research Laboratory, Human Effectiveness Directorate, Directed Energy Bioeffects Division, at Brooks City-Base, San Antonio, TX 78235 USA (phone: 210-536-5599; fax: 210-536-5382; e-mail: andrei.pakhomov@brooks.af.mil).

A. Phinney, J. Ashmore, and K. Walker III are with McKesson BioServices Corporation, US Army Medical Research Detachment, at Brooks City-Base, San Antonio, TX, USA.

J. Kolb and K. H. Schoenbach are with the Center for Bioelectrics, Old Dominion Univ., Norfolk, VA, USA (jkolb@odu.edu; kschoenb@odu.edu)

S. Kono was with the Center for Bioelectrics, Old Dominion Univ., Norfolk, VA, USA, and currently is with the Ariake College of Technology, Japan.

M. R. Murphy is with Air Force Research Laboratory, Human Effectiveness Directorate, Directed Energy Bioeffects Division, at Brooks City-Base, San Antonio, TX 78235 USA (e-mail: michael.murphy@brooks.af.mil).

I. Introduction

ELECTROSTIMULATION of excitable tissues and electroporation of cell plasma membrane are the best known and widely used bioeffects of electrical pulses (EP). Electrostimulation can be achieved by changing the natural transmembrane potential by 10-20 mV, and electroporation (dielectric breakdown) occurs when transmembrane voltage reaches 0.2-1 V [1]. Typical duration of EP for these applications lays in a rather comprehensively studied range, from microseconds to milliseconds [1]-[8]. On the contrary, cellular effects of shorter, namely, nanosecond-range electrical pulses (nsEP) have only scarcely been explored. One reason for this deficiency is that devices capable of producing high-voltage nsEP and delivering them to low-impedance biological samples have not been engineered until recently [9], [10].

Although difficult to study, nsEP may prove to be a promising means to deliberately manipulate cell physiology. Equivalent electrical circuit modeling of a cell suggested that a reduction in EP duration concurrently with increasing its voltage may result in more efficient charging and faster breakdown of cell internal membranes than of the plasma membrane [11], [12]. Consequently, it may be possible to disrupt organelles' membranes by nsEP without damage to the outer cell membrane, giving rise to some unique and, perhaps, previously unknown biological effects. Moreover, with the instant electric fields as extreme as 200-300 kV/cm, 2-3 ns rise time, and energy absorption rates of the order of a gigawatt per gram, it is plausible to expect bioeffects due to other specific mechanisms, such as electrolysis and electrodissociation of some compounds, cell electrodeformation [13], and mechanical stress due to thermoelastic expansion [14], [15]. Indeed, first experimental studies with nsEP reported bioeffects that were qualitatively different from what is known as common consequences of plasma membrane electroporation. Among such effects were permeabilization of intracellular granules in eosinophiles and shrinkage of these cells [16], efficient induction of apoptosis in mammalian cells in culture [12], [17], [18], and tumor

growth inhibition [17].

The potency of nsEP to control cell growth and induce apoptosis is of particular interest and may find applications in research, medicine, and biotechnology. However, the exact mechanism how nsEP cause cells to die has not been understood, and even the dependence of nsEP cytotoxic effect on exposure parameters has not been studied yet. The goal of the present work was to characterize the cell killing effect of 10-ns EP as a function of some exposure metrics (the number of delivered pulses, their intensity and repetition rate), and to check if lethally exposed cells express any hallmarks of the apoptotic process, namely, specific cleavage of poly(ADP-ribose) polymerase (PARP) into 89-kDa fragment [19]-[21]. The experiments were performed in cultured human lymphoma cells U937, which is an established model to study mechanisms of mammalian cell death [22]-[25], and is also characterized by high sensitivity to many standard apoptotic stimuli, e.g., heat [26].

II. Matherials and Methods

A. Cell Culture Procedures

U937 human histiocytic lymphoma cells were obtained from American Type Culture Collection (ATCC, Manassas, VA) and cultured according to their recommendations. The cells were grown in ATCC-modified RPMI 1640 medium supplemented with 10% fetal bovine serum (both acquired from ATCC), at 37 °C with 5% CO_2 in air. The cell density was maintained at 0.2-0.8 x 10^6 cells/ml, either by dilution of the growing cell suspension, or by pelleting cells by gentle centrifugation (5 min at 300 g) and re-suspending in a fresh medium. The cell cultures showed same properties over a wide range of passage numbers, except for a slightly higher percentage of dead cells in "younger" populations (3-6% dead cells for passages 1-5, and 0.5-3% later on)

B. Cytotoxicity and Apoptosis Assays

Cell culture growth and survival were assessed directly, by counting live and dead cells in eight fields of a hemocytometer, adhering to guidelines outlined in [27]. Live cells were identified by exclusion of Trypan blue, which was added to cell suspension at 25% v/v, 1-2 min prior to cell counting. In isolated experiments, cell growth was additionally assessed indirectly, from conversion of an MTS tetrazolium compound into a soluble formazan product by actively metabolizing cells (CellTiter 96 AQ Assay, #G3580, Promega, Madison, WI). The indirect and direct assays produced similar results, so only hemocytometer data are reported below.

For apoptosis detection by PARP cleavage, some 5-10 x 10^6 cells were collected and lysed using a Mammalian Cell Lysis Kit (MCL-1, Sigma, St. Louis, MO). The lysates were stored at –70 °C until analyzed by immunoblotting. Proteins were separated in a tris-glycine gel and transferred onto a nitrocellulose membrane. The membrane was incubated overnight on cold with mouse anti-PARP monoclonal antibodies (BD PharMingen, CA). Intact and cleaved PARP (116 and 89 kDa, respectively) was detected using ProteoQwest Colorimetric Western Blotting Kit with TMB substrate (Sigma) as of manufacturer's recommendations. Extracts of induced and uninduced HL-60 cells (Calbiochem, San Diego, CA) were used as standards for detection of cleaved and uncleaved PARP. For additional positive control, we induced apoptosis in U937 cells by a moderate heat shock, 44 °C for 40 min [24]-[26].

C. Nanosecond Pulse Generator and Exposure Control

Nearly rectangular pulses of about 10-ns width were produced by a Blumlein line generator manufactured at the Old Dominion University, Norfolk, VA. The design of the generator is described in detail elsewhere [10], [18]. In short, it represented a stripline designed for load impedance of 10 Ohm and operated in self-breakdown mode. To energize the stripline, a spark gap in a pressurized switch chamber was charged from a high-voltage DC power supply (HR-100, American High Voltage, Elko, NV). A breakdown occurred once the voltage across the spark gap exceeded a critical value, which, in turn, was determined by the composition and pressure of the gas medium in the switch chamber. When filled with air at the atmospheric pressure, the breakdown occurred at about 10 kV. To increase the breakdown voltage (and, consequentially, the voltage delivered to the biological sample), the switch chamber was filled with SF_6 gas. In most experiments, the gas pressure was set at various levels between 70 and 200 kPa, corresponding to discharge voltages of up to 30-35 kV. For exposures to multiple nsEP, the interpulse interval and the total number of pulses in a train were controlled automatically by a PC, using a specialized program written in LabVIEW (National Instruments, Austin, TX) and an interface device to detect nsEP and to engage/disengage the high voltage power supply. The shape and voltage of nsEP delivered to the sample were continuously monitored on a 500-MHz digital oscilloscope (TDS3052B, Tektronix, Wilsonville, OR) via a custom-made high-voltage probe. Due to the load capacitance, recorded nsEP were somewhat distorted by additional peaks, and the peak voltage usually measured 10-20% higher than the "plateau" voltage corresponding to precisely rectangular pulse shape. The E-field values reported in this paper are the peak values, obtained by dividing the peak pulse voltage by the gap distance in electroporation cuvettes.

D. Exposure Procedures and Protocols

Cell samples were exposed to nsEP in the complete growth medium, using 1- or 2-mm gap GenePulser electroporation cuvettes (Bio-Rad Laboratories, Hercules, CA). For cytotoxicity assays, cells were diluted to approximately 0.2 x 10^6 cells/ml, and dispensed uniformly into several cuvettes (up to 16 cuvettes per set). Regardless of the protocol for any

specific experiment, one cuvette was designated as a control, which underwent all the same treatments except for nsEP exposure itself. The cuvettes were capped and remained together at room temperature until all exposures were completed. As a rule, cuvettes in each set underwent different exposures in a random sequence. Aliquots of exposed and control samples (typically, 100 µl) were stored in the incubator until analysis. Cell counts were performed mostly in 24 h after exposure, which is approximately the duration of one cell cycle; in isolated experiments, cell counts were also performed at intervals from 0.5 to 48 h. Cell count data were analyzed both as "raw" and as percentage to the respective parallel control. Student's paired t-test was used for statistical analysis.

Exposures of cells for PARP cleavage assay were performed somewhat differently, because much greater amounts of cells were required. Cells were concentrated by a mild centrifugation (5 min at 300-400 g) to densities of up to 40 x 10^6 cells/ml and dispensed into electroporation cuvettes for nsEP treatment. After exposure, samples were diluted to less than 10^6 cells/ml and moved to the incubator until lysis (from 1 to 24 h after exposure). Live and dead cells were counted in hemocytometer both prior to exposures and prior to lysis. Within the accuracy of the employed assays, concentration/dilution procedures per se had no effect on cells' growth rate or viability.

E. Dosimetry and Thermometry

In this study, the absorbed dose (AD, J/g) in the sample was calculated as:

$$AD = (E^2 \times W \times n)/(d^2 \times R \times M), \quad (1)$$

where E is the E-field in the sample (V/m), W is the pulse width (10^{-8} s), n is the number of nsEP delivered, d is the gap in the cuvette (2 x 10^{-3} or 10^{-3} m), R is the resistance of the cuvette with medium (8-9 Ohm), and M is the mass of the medium (about 0.125 and 0.45 g for 1- and 2-mm gap cuvettes, respectively).

Maximum temperature rise (ΔT, °C) in the exposed medium could be calculated from the assumption that the entire delivered energy is spent on heating:

$$\Delta T = AD/C, \quad (2)$$

where C is the specific heat of the medium (assumed as 4.2 J/(g x °C)).

Physical measurements of temperature rise during exposure to individual nsEP and nsEP trains were performed with a help of a miniature fiber optic probe, FOT-HERO (FISO Technologies, Quebec City, Canada). The sensitive element of this probe is just a 5-µm thick film of SiH on top of a tiny glass plate, which forms a Fabry-Pérot interferometer chamber. This sensor is connected to a VELOCE signal conditioner (FISO) via a 100-µm diameter fiber optic cable. The probe is completely immune to the electric field, features negligible heat capacity, exceptionally fast and linear response to temperature changes, and fits well even into 1-mm gap electroporation cuvettes. The output signal of the conditioner was digitized with an MP100 data acquisition system (BIOPAC Systems, Goleta, CA) and monitored on a PC. Prior to measurements, the entire setup was calibrated against a mercury thermometer.

III. Results

A. Effects of a Single nsEP and Brief nsEP Trains

In preliminary experiments, we tested the effect of a single pulse on the growth of U937 cell culture. Cell density was measured at intervals of 0.15, 0.5, 1, 2, 4, 8, 24, 35, and 48 h after exposure. Little or no exposure effect was observed, even at the maximum E-field tested (300 kV/cm, Fig.1).

The next series of experiments was focused primarily on the effect of brief pulse trains. Cell samples were exposed to 1, 5, 10, 15, or 20 pulses, delivered at 0.1 pulses/s. The E-field was varied from 40 to 380 kV/cm. Live and dead cells were counted in 24 h post exposure, which is approximately the doubling time in U937 cells. Findings from over 350 processed samples are summarized in Fig. 2.

All tested exposure regimens except two (1 and 5 pulses at the lowest voltage) caused a small (20-30%), but significant ($p<0.05$ at least) decrease in the live cells density. Surprisingly, this effect stayed practically the same across the entire range of E-field intensities and train lengths, so its dependence on the absorbed dose was essentially flat (Fig. 3).

It is important to note that the live cells density at the time of measurement (24 h post exposure) in all samples was higher than the density at the time of exposure (the density at the time of exposure would be at about 45% on the scale used in Fig. 2). Therefore, even after the most intense nsEP treatment, most cells did not go to death by either apoptosis or necrosis, but continued propagation as usual. Moreover, in many experiments the total number of cells (live + dead) was 5-15% higher than in parallel controls, indicating possible stimulation of cell division by nsEP (data not shown).

Concurrently, all studied exposures increased the fraction of dead cells, from the average of about 2% in controls up to 14% after the most intense nsEP treatment (Fig. 2). This effect was proportional to both the number of pulses per train and their amplitude (albeit the increase was rather gradual); consequentially, this effect increased with increasing the absorbed dose (Fig. 3). One may speculate that the reduction of cell population by cell death could have been offset by enhanced cell division, resulting in seemingly flat dependence of live cells density on the intensity of exposure.

In several sets of experiments, cells were additionally counted in 48 h after exposure. In both control and exposed

samples, the live cells doubled at 48 h compared with the 24-h timepoint, thus providing no indication of delayed cell death (data not shown).

B. Effects of nsEP repetition rate

One may reasonably expect that cytotoxic effect of nsEP trains could be augmented by shortening the interpulse interval, i.e., by applying the next pulse before cells recover after the previous one. Therefore, we compared cell survival after exposures to nsEP at 0.1, 0.25, and 1 Hz (20 pulses/train, 160-200 or 330-360 kV/cm). Live and dead cells were counted 24 h post exposure in 64 samples. The experiments established no statistically significant increase in cell killing at shorter interpulse intervals (data not shown). Furthermore, later modifications to the stripline increased the maximum pulsing rate to over 2 Hz, and the rate of 2 Hz was then routinely employed in most experiments. These changes had no apparent effect on the cytotoxic efficiency of nsEP.

C. Sample Heating by nsEP

Using (1) and (2), it is easy to calculate that maximum sample heating by a single nsEP could exceed 3 °C. Since exposures are performed at room temperature (22-24 °C), a temperature rise of 3 °C is not expected to damage cells which are normally cultured at 37 °C. However, trains of 10-20 nsEP may deliver enough energy to samples to kill all cells by heating, unless this energy is dissipated fast into environment.

Theoretical modeling of the heat dissipation from the exposed medium would be rather complicated, because of the shape of electroporation cuvette and different materials it is made of. Therefore, the best choice was direct measurement of temperature changes in the medium, which was accomplished using an FOT-HERO sensor (see "Methods"). As of our knowledge, this was the first successful recording of temperature in a liquid medium in a pulsed electric field of tens of kV/cm.

The measurements were performed with 1-Hz pulse repetition rate, at 150 kV/cm in 0.45 ml of medium in a 2-mm gap cuvette, and at 360 kV/cm in 0.125 ml of medium in a 1-mm gap cuvette (Fig. 4). In both these settings, heat dissipation proved to be very efficient, and the temperature only reached 30 °C after 200 pulses at 360 kV/cm and after 400 pulses at 150 kV/cm. Extrapolation of the heating curves showed that the normal physiological temperature (37 °C) will only be achieved after 1400 and 3300 pulses at the respective voltages; and heating to a potentially damaging temperature (e.g., 42 °C) would take as many as 5000 and 14000 pulses.

These measurements showed incontrovertibly that trivial heating by nsEP was not the cause of cell death in the biological experiments described above. Moreover, these data proved that heat inactivation of cells is not a concern even with much longer nsEP trains, thereby opening the road for new research. If such extra-long pulse trains are proven to cause profound cell death, this effect will need to be explained by mechanisms other than mere heating.

D. Enhanced Cytotoxic Effect of Extra-Long nsEP Trains

Cell survival as a function of nsEP train length was studied at 150 kV/cm (1 Hz) and at 50 kV/cm (2 Hz). Cell counts were performed 24 h after exposure in over 200 samples. In agreement with the findings described above in section *III, A,* both survival curves started essentially flat (Fig. 5). At 150 kV/cm, once the train exceeded 150 pulses, the initial plateau ("shoulder") was abruptly replaced by a steep exponential decline. The 24-h survival dropped to 40% after 200 EP and to just 3% after 600 EP. At 50 kV/cm, the shoulder continued to as many as 1000 pulses, and the subsequent survival decline was far less steep. For both tested voltages, the increase in the dead cells fraction due to nsEP exposure was essentially a mirror reflection of the survival curves (data not shown).

E. PARP Cleavage Assay

Immunoblotting for intact and cleaved forms of PARP was performed in 28 samples, 21 of which were exposed to nsEP. In different experiments, E-field was varied from 90 to 330 kV/cm; the number of pulses per exposure was from 20 to 2000; cells were lysed at intervals from 0.5 to 24 hours after the exposure; and cell survival by the time of lysis ranged from almost 100% to zero.

A typical result of Western analysis is shown in Fig. 6. Lanes 1 and 2, respectively, were loaded with apoptotic and non-apoptotic HL-60 standards, to identify the position of uncleaved 116 kDa PARP and of the 89 kDa PARP fragment. A sham-exposed sample on lane 3 displays a strong signal for PARP and no signal for the 89 kDa fragment. The next lane was for heat-shocked cells, lysed 5 h after 40 min at 44 °C. This treatment effectively induced apoptosis, and most detected PARP was in the cleaved form. Note that the fraction of dead cells in this sample (counted by Trypan blue exclusion) was almost the same as in the control: indeed, PARP cleavage normally is a much earlier event in apoptosis than plasma membrane disintegration and permeabilization to the dye. Later on (22 h after the same heat shock, lane 5), the fraction of dead cells was increased 6-fold, and by that time even the 89 kDa fragment was almost eliminated by further cleavage.

Lanes 6 and 7 were loaded with nsEP-exposed samples, lysed 4 h after 50 and 100 pulses at 330 kV/cm. Both lanes display a strong signal of intact PARP, but none of the cleaved form. Note that the fraction of dead cells after 100 nsEP increased almost 5-fold; if it were a "typical" apoptosis (compare to lane 5), one would expect most of PARP to be already cleaved into 89 kDa and smaller fragments. However, it was not the case.

Out of 21 nsEP-exposed samples, a faint lane at 89-kDa level was detected in only one (lysed 1 h after 400 pulses at 100 kV/cm), but the intact PARP signal in the same sample

was incomparably stronger. Also, samples lysed 1 h after 200 and 600 nsEP at 100 kV/cm showed no trace of cleaved PARP. Overall, the absence of 89-kDa PARP fragment after nsEP exposures indicated that the cell death proceeded in a caspase-independent manner.

IV. Discussion

The study presented here is essentially the first that was focused specifically on bioeffects of 10-ns EP. Earlier studies [13], [17], [18] dealt predominantly with 60- and 300-ns pulses; some of them touched upon isolated findings with 10-ns pulses, but no systematic research has been reported yet.

To a degree they may be compared, our data appear strikingly different from previous observations of nsEP cytotoxic effects. For example, a train of only three 60-ns pulses at 60 kV/cm killed 85-90% of Jurkat cells in 18-24 h [18], and three 300-ns pulses at 60 kV/cm caused a 6-fold increase in the number of apoptotic cells in a fibrosarcoma tumor exposed *ex vivo* [17]. Pulses of 10-ns duration were considerably less effective in all tests performed, even though the E-field was appropriately increased to deliver the same energy density as with the longer pulses [18]. Albeit being less effective, a single 10-ns pulse or a train of 3-5 pulses at 150-300 kV/cm caused small but detectable poration of plasma membrane [13, 18], activated caspases, increased Annexin-V-FITC binding to intact cells, initiated the release of cytochrome C from mitochondria into cytosol [18], and induced apoptotic DNA fragmentation [17]. On the contrary, in our experiments only extra-long nsEP trains caused significant cell killing effect, and lethally exposed cells did not display apoptosis-specific PARP cleavage.

In our opinion, this difference may have resulted from one or more of the following conditions:

(1) In the previous studies, cells were exposed in Hank's balanced salt solution (HBSS) without Ca^{2+} or Mg^{2+} [17], [18]. We exposed cells in a full growth medium (RPMI 1640 + 10% FBS), which is a closer imitation of treatment conditions for tissues or tumors exposed *in situ*. One may speculate that HBSS did not supply certain substances or ions, which were essential for cells' survival after nsEP treatment.

(2) Our experiments employed U937 human histiocytic lymphoma cells, which is different from mammalian cells tested before: Jurkat (human T-cell leukemia), HL-60 (human promyelocytic leukemia), 3T3-L1 (murine fibroblasts), and B10.2 (murine fibrosarcoma). Among these cell types, U937 has probably the highest sensitivity to the apoptotic effect of a heat shock treatment [25], but is much less vulnerable to the cytotoxic effect of diethyldithiocarbamate (DDTC) than either Jurkat or HL-60 [23]. No doubt that sensitivity to nsEP may vary between different cell lines, but the contrast in our findings and previous studies appears too profound to be explained solely by cell physiology.

(3) Once again, most observations of efficient apoptosis induction and cell killing were done with 60- and 300-ns pulses, and the findings, to a large extent, were just extrapolated to still shorter 10-ns pulses. However, it has not been adequately explained why 10-ns pulses, even at much higher voltage and equal energy delivered to the sample, were far less effective than 60- or 300-ns pulses [18]. These data indicate that the 10-ns duration is probably marginal, just above the threshold for induction of apoptosis by electroporation of cell internal membranes. This threshold in certain cell lines may be slightly higher, thus rendering 10-ns pulses almost ineffective. In other words, strikingly low cytotoxicity of brief nsEP trains in our study could be a combined effect of using short 10-ns pulses and a more resistant cell line.

It is premature to discuss which exact mechanisms determined nsEP-induced cell death in our study, but some possibilities and parallels can be outlined. The minor decrease in cell survival after individual 10-ns pulses and brief pulse trains may be explained by the presence of a sensitive cell subpopulation (such as cells in the process of mitosis, for example). Once these cells are eliminated, the effect essentially reaches saturation, forming the initial plateau (shoulder) of the survival curve, such as in Fig. 5. Further increase in the number of pulses eventually exhausts the repair capabilities of "nsEP-resistant" cells, causing sharp decline in survival. Alternatively, one may hypothesize that long trains of pulses could trigger some different and unexplored mechanisms of cell damage.

Noteworthy, the shoulder followed by an exponential decline is a well-known, "classical" shape of survival curve after exposure to other cytotoxic factors, such as low-LET ionizing radiation (x-rays or electrons) [28], [29]. In bioelectromagnetics area, it is taken as basics that the electric field is a non-ionizing factor; however, this is not wholly true for extreme voltages like those used in our study: 300 kV/cm is tenfold (!) higher than ionization and conventional breakdown (spark) voltage in air. We have not observed nsEP-induced sparking in the exposed liquid medium with cells; nonetheless, the possibility of ionization and/or water dissociation could not be entirely ruled out. If ions and electrons are accelerated during nsEP to sufficient energies, their collision with water and other molecules may produce H, OH, H_2O_2, and other reactive species (similar to water radiolysis [30]). These radicals would damage cell DNA, just as with ionizing radiation exposure, and the mechanisms regulating cell death and survival will also be similar.

At present, we were unable to identify any studies that confirm or reject the possibility of free radicals formation by nsEP exposure, or estimate their yield. This mechanism remains only hypothetical and should be tested both by physical modeling and in specific biological experiments. As a first step, it would be feasible to check how nsEP cytotoxicity is modified by free radical scavengers, such as DMSO [31], and whether nsEP cytotoxicity, like cytotoxicity of ionizing radiation, is attenuated in an oxygen-depleted

medium [28], [29].

ACKNOWLEDGMENT

The authors are thankful to Drs. V. Gabai (Dept. Biochemistry, Boston Univ. School of Medicine, Boston, MA), O. Pakhomova (Univ. Texas Health Sci. Center., San Antonio, TX), and V. Moiseenko (Lawson Regional Cancer Center, London, Ontario, Canada) for valuable advice and discussions during this project.

REFERENCES

[1] J. C. Weaver, "Electroporation of cells and tissues," *IEEE Trans. Plasma Sci.*, vol. 28(1), pp. 24–33, February 2000.

[2] E. Neumann, A. E. Sowers, and C. A. Jordan, Eds., Electroporation and Electrofusion in Cell Biology. New York: Plenum, 1989.

[3] U. Zimmeramann, Ed., The Effect of High Intensity Electric Field Pulses on Eukaryotic Cell Membranes: Fundamentals and Applications. Boca Raton, FL: CRC, 1996.

[4] B. Katz, Nerve, Muscle, and Synapse. New York: McGraw-Hill, 1966.

[5] J. G. Nicholls, A. R. Martin, and B. G. Wallace. From Neuron to Brain (3rd edition). Sunderland, MA: Sinauer Associates, 1992.

[6] J. P. Reilly, Applied Bioelectricity: From Electrical Stimulation to Electropathology. New York: Springer-Verlag New York Inc., 1998.

[7] B. I. Khodorov, The Problem of Excitability. Electrical Excitability and Ionic Permeability of the Nerve Membrane. New York: Plenum, 1974.

[8] B. Hille, Ionic Channels of Excitable Membranes (2nd edition), Sunderland, MA: Sinauer Associates, 1992.

[9] J. Mankowski and M. Kristiansen, "A review of short pulse generator technology," *IEEE Trans. Plasma Sci. vol. 28(1), pp. 102-108, February 2000.*

[10] J. Deng, R. H. Stark, and K. H. Schoenbach, "A nanosecond pulse generator for intracellular electromanipulation," in *Conf. Record, 2000 Twenty-Fourth Intern. Power Modulator Symp.*, Norfolk, VA, pp. 47-50, 2000.

[11] K. H. Schoenbach, R. H. Stark, J. Deng, and R. E.-S. Aly, "Biological/medical pulsed electric field treatments," in *Conf. Record, 2000 Twenty-Fourth Intern. Power Modulator Symp.*, Norfolk, VA, pp. 42-46, 2000.

[12] K. H. Schoenbach, S. Katsuki, R. H. Stark, E. S. Buesher, and S. J. Beebe, "Bioelectrics – new applications for pulsed power technology," *IEEE Trans. Plasma Sci.*, vol. 30(1), pp. 293–300, February 2002.

[13] K. J. Muller, V. L. Sukhorukov, and U. Zimmermann, "Reversible electropermeabilization of mammalian cells by high-intensity, ultra-short pulses of submicrosecond duration," *J. Membrane Biol.*, vol. 184, pp. 161-170, 2001.

[14] J. C. Lin, Ed. Microwave auditory effects and applications. Springfield: Charles C. Thomas, 1978.

[15] C-K. Chou, A. W., Guy, and R. Galambos, "Auditory perception of radio-frequency electromagnetic fields," *J. Acoust. Soc. Am.*, vol. 71(6), pp. 1321-1334, 1982.

[16] K. H. Schoenbach, S. J. Beebe, and E. S. Buesher, "Intracellular effect of ultrashort electrical pulses," *Bioelectromagnetics*, vol. 22, pp. 440-448, 2001.

[17] S. J. Beebe, P. M. Fox, L. J., Rec, K. Somers, R. H. Stark, and K. H. Schoenbach, "Nanosecond pulsed electric field (nsPEF) effects on cells and tissues: apoptosis induction and tumor growth inhibition," *IEEE Trans. Plasma Sci.*, vol. 30(1), pp. 286–292, February 2002.

[18] S. J. Beebe, P. M. Fox, L. J., Rec, L. K. Willis, and K. H. Schoenbach, "Nanosecond, high-intensity pulsed electric fields induce apoptosis in human cells," FASEB J. Express article 10.1096/fj.02-0859fje. Published online June 17, 2003. Available: http://www.fasebj.org/cgi/reprint/02-0859fjev1.pdf

[19] S. H. Kaufmann, S. Desnoyers, Y. Ottaviano, N. E. Davidson, G. G. Poirier, "Specific proteolytic cleavage of poly(ADP-ribose) polymerase: an early marker of chemotherapy-induced apoptosis," *Cancer Res.*, vol. 53(17), pp. 3976-3985, 1993.

[20] C. A. Casiano, R. L. Ochs, and E. M. Tan, "Distinct cleavage products of nuclear proteins in apoptosis and necrosis revealed by autoantibody probes," *Cell Death and Differentiation*, vol. 5, pp. 183-190, 1998.

[21] S. A. Proskuryakov, A. G. Konoplyannikov, and V. L. Gabai, "Necrosis: a specific form of programmed cell death?", *Experim. Cell Research*, vol. 283, pp. 1-16, 2003.

[22] A. Troyano, C. Fernandez, P. Sancho, E. de Blas, and P. Aller, "Effect of gluthatione depletion on antitumor drug toxicity (apoptosis and necrosis) in U937 human promonocytic cells: the role of intracellular oxidation," *J. Biol. Chem.*, vol. 276(50), pp. 47107-47115, 2001.

[23] S. Kanno, E. Matsukawa, A. Miura, A. Shouji, K. Asou, and M. Ishikawa, "Diethyldithiocarbamate-induced cytotoxicity and apoptosis in leukemia cell lines," *Biol. Pharm. Bull.*, vol. 26(7), pp. 964-968, 2003.

[24] C.-Y. Li, J.-S. Lee, Y.-G. Ko, J.-Il Kim, and J.-S. Seo, "Heat shock protein 70 inhibits apoptosis downstream of cytochrome C release and upstream of caspase-3 activation," *J. Biol. Chem.*, vol. 275(33), pp. 25665-25671, 2000.

[25] V. L. Gabai, A. B. Meriin, D. D. Mosser, A. W. Caron, S. Ritz, V. I. Shifrin, and M. Y. Sherman, "HSP70 prevents activation of stress kinases. A novel pathway of cellular thermotolerance," *J. Biol. Chem.*, vol. 272(29), pp. 18033-18037, 1997.

[26] V. L. Gabai, Dept. Biochemistry, Boston Univ. School of Medicine, Boston, MA, private communication, December 2002.

[27] A. Richardson and S. Fedorof, "Quantification of cells in culture," in Protocols for Neural Cell Culture, 3rd ed., A. Richardson and S. Fedorof, Eds. Totowa, NJ: Humana Press, 2001, pp. 333-339.

[28] E. J. Hall, *Radiobiology for the Radiologist, 4th ed.* Philadelphia: Lippincott, 1994.

[29] A. H. W. Nias, *An Introduction to Radiobiology, 2nd ed.* Chichester: Wiley, 1998.

[30] I. G. Draganic and Z. D. Draganic. *The Radiation Chemistry of Water.* New York: Academic, 1971.

[31] L. G. Littlefield, E. E. Loiner, S. P. Coyler, A. M. Sayer, and E. L. Frome, "Modulation of radiation-induced chromosome aberrations by DMSO, an OH radical scavenger. 1: Dose-response studies in human lymphocytes exposed to 220 kV X-rays," *Int. J. Radiat. Biol.*, vol. 53, pp. 875-890, 1988.

First A. Author (M'76–SM'81–F'87) and the other authors may include biographies at the end of regular papers. Biographies are often not included in conference-related papers. This author became a Member (M) of IEEE in 1976, a Senior Member (SM) in 1981, and a Fellow (F) in 1987. The first paragraph may contain a place and/or date of birth (list place, then date). Next, the author's educational background is listed. The degrees should be listed with type of degree in what field, which institution, city, state or country, and year degree was earned. The author's major field of study should be lower-cased.

The second paragraph uses the pronoun of the person (he or she) and not the author's last name. It lists military and work experience, including summer and fellowship jobs. Job titles are capitalized. The current job must have a location; previous positions may be listed without one. Information concerning previous publications may be included. Try not to list more than three books or published articles. The format for listing publishers of a book within the biography is: title of book (city, state: publisher name, year) similar to a reference. Current and previous research interests ends the paragraph.

The third paragraph begins with the author's title and last name (e.g., Dr. Smith, Prof. Jones, Mr. Kajor, Ms. Hunter). List any memberships in professional societies other than the IEEE. Finally, list any awards and work for IEEE committees and publications. If a photograph is provided, the biography will be indented around it. The photograph is placed at the top left of the biography. Personal hobbies will be deleted from the biography.

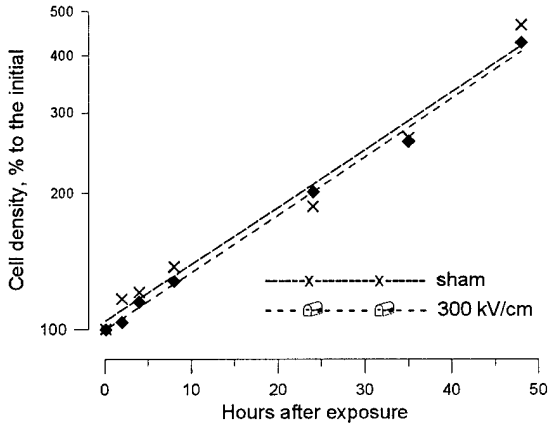


Fig. 1. Lack of the effect of a single 10-ns, 300 kV/cm electrical pulse on the growth of U937 cell population. Data from one typical experiment. The cell density at the time of exposure (2 x10^5 cells/ml) was taken as 100%. Lines are the best fit data approximations using exponential function.

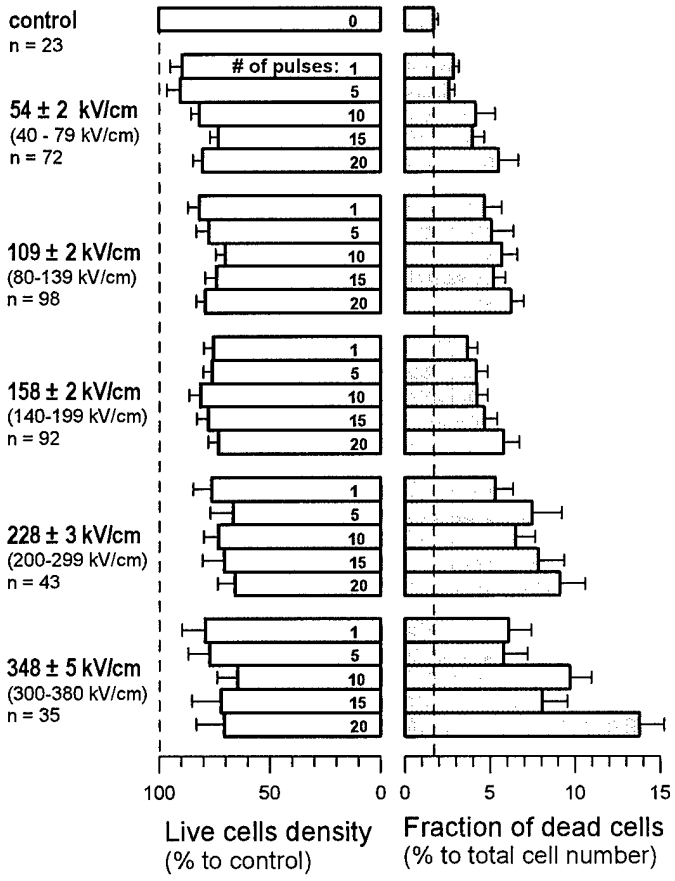


Fig. 2. Effect of brief nsEP trains on 24-h cell survival (clear bars, left) and on the increase in the dead cells fraction (dotted bars, right). Numbers at the left indicate the mean E-field (± s.e.) in each group, the full range of E-field values included in that group, and the number of exposed samples. The number of pulses per train (from 1 to 20) is given within the clear bars. All data are shown as the mean ± s.e. See text for more explanation.

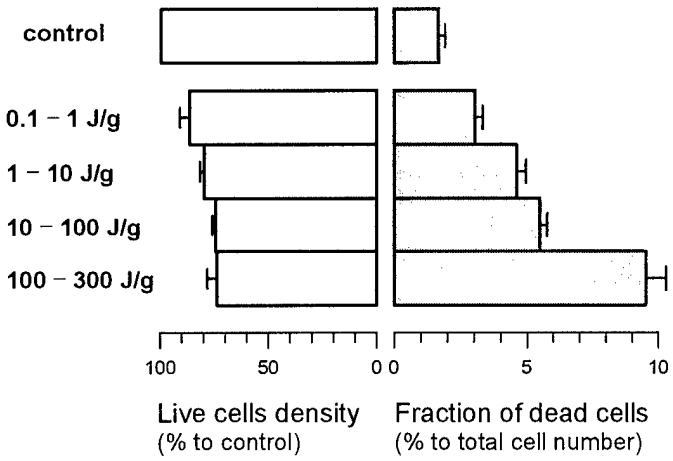


Fig. 3. Effect of the absorbed dose on 24-h cell survival (clear bars, left) and on the increase in the dead cells fraction (dotted bars, right). The absorbed doses (shown at the left, J/g) were calculated using (1) from the same experiments as illustrated in Fig. 2; the groups include from 23 to 160 samples. Other designations are the same as in Fig. 2. All the groups are significantly different from the control ($p < 0.05$ at least).

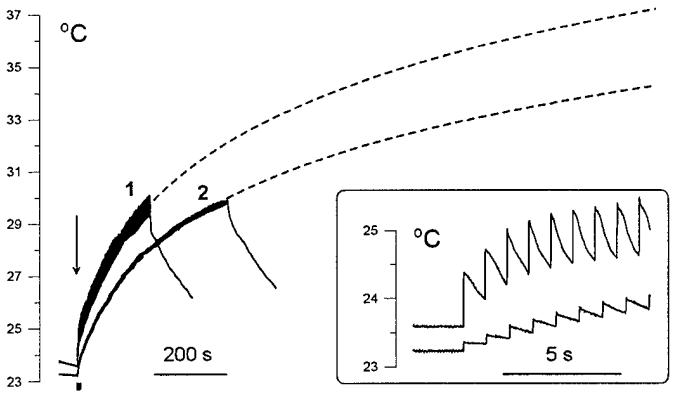


Fig.4. Heating of the medium in an electroporation cuvette by a train of 200 pulses at 360 kV/cm (1) or 400 pulses at 150 kV/cm (2). The pulse repetition rate was 1 Hz in both measurements. Arrow indicates the onset of exposure. Dashed lines are the best-fit approximations of heating dynamics. The portion of the graph identified by a small rectangle under the curves is expanded in the inset, to show heating and cooling by individual nsEPs in the train.

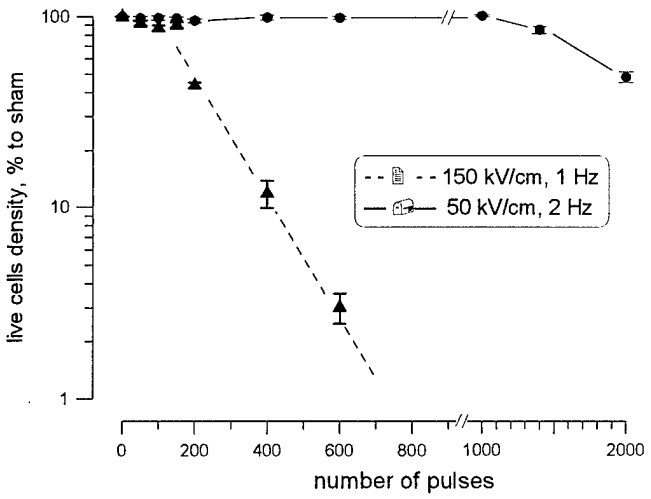


Fig. 5. Effect of the number of pulses applied at 150 or 50 kV/cm on 24-h cells survival. Each datapoint is the mean ± s.e., 12 to 40 samples per measurement (error bars may be not visible if smaller than the central symbol). Dashed line is the best fit approximation of the cells survival decline using exponential function.

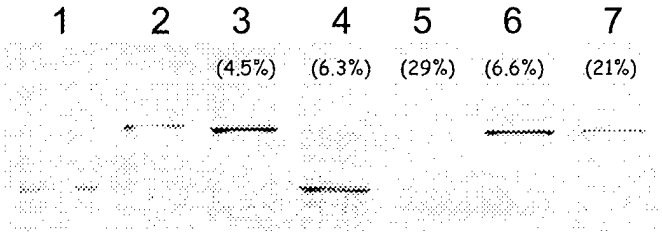


Fig. 6. Detection of apoptotic cleavage of poly(ADP-ribose) polymerase by Western analysis. Lanes **1** and **2**: standards for 89 kDa PARP fragment (lysate of induced HL-60 cells) and for 116 kDa intact PARP (uninduced HL-60 cells). Lanes **3**-**7**, lysates of U937 cells: **3**, control; **4**, 5 h after a moderate heat shock (44 °C for 40 min); **5**, 22 h after the same heat shock; **6**, 4 h after exposure to a train of 50 nsEP at 330 kV/cm, 1 Hz; **7**, same as 6, but a train of 100 pulses. Numbers in parentheses indicate the fraction of dead cells (% to the total cell density) immediately before lysis. See text for more detail.

PUBLICATION 22
(In Preparation, Abstract Only)

EXTREMELY-HIGH POWER MICROWAVE PULSES (EHPP) ALTER 4-AMINOPYRIDINE-INDUCED BURSTS IN ISOLATED HIPPOCAMPAL SLICES

Andrei Pakhomov[1], Joan Doyle[1], Juan Morin[1], Michael Murphy[2]. 1McKesson BioServices / U.S. Army Medical Research Detachment, Brooks City-Base, Texas 78235; 2Air Force Research Laboratory, Brooks City-Base, Texas 78235, U.S.A.

Epileptiform-type bursts in isolated rat hippocampal slices were induced by superfusion with 4-aminopyridine (100 or 150 μM) and recorded extracellularly from CA3 neuronal area. The slices were exposed to EHPP (250 ns, 600 kW/g peak SAR, 9.6-GHz) for 5 min at the pulse repetition rates of 0 (sham control), 1, 2, 4, or 8 Hz. The maximum heating during exposure was 0, 0.25, 0.4, 0.9 and 1.5 °C, respectively. The data from 38 experiments (6 to 9 per group) were rendered acceptable and used for statistical analysis. EHPP exposure caused the following effects: (1) Up to 6-fold increase in the dispersion of durations of inter-burst intervals during and/or after exposure. This effect was often seen with just the minimum microwave heating. (2) On- and off-responses, which usually appeared as a temporary cessation of bursts; they were most profound in the 8-Hz group, but occasionally were seen at the lower intensities as well. (3) In the 8-Hz group only, the average bursting rate during exposure increased by 15-20%. The latter effect was apparently caused by heating, whereas the origin and mechanism of the effects (1) and (2) have yet to be analyzed. Additional experiments demonstrated that on-off responses similar to (2) could also be evoked by continuous-wave irradiation.

Rat Electrocardiogram During Acute Exposure to Synchronized Bursts of Ultra Wideband Pulses

Ronald L. Seaman, *Senior Member, IEEE*, and James R. Jauchem

***Abstract*—Rats under ketamine anesthesia were exposed to bursts of ultra-wideband (UWB) electromagnetic pulses at two different times during the electrocardiogram (ECG) to investigate possible changes in the ECG immediately after start of exposure. Animals were exposed to UWB pulses in a giga transverse electromagnetic cell (GTEM) with the body axis parallel to the direction of UWB propagation (k-polarization) or the magnetic field vector (H-polarization) in separate experiments. In both experiments, UWB pulses at animal thorax had 106 kV/m peak amplitude, 0.78-0.79 ns duration, and 170-186 ps rise time (mean values) and were applied in 25-ms bursts at 1 kHz repetition frequency. The bursts were synchronized to the artifact-free ECG and occurred either during the R-wave or the T-wave of the ECG. Time intervals measured and analyzed in the ECG were PR, the time between start of P-wave and start of R-wave; RT, the time between start of R-wave and apex of the T-wave; and QT, the time between start of R-wave and end of T-wave. The time between successive R-waves, RR, was also determined. No change attributable to UWB exposure was seen in any of these intervals within 5 cardiac cycles of the start of exposure. We conclude that UWB pulses applied during the R-wave or the T-wave do not acutely change timing of events in the cardiac cycle of the anesthetized rat**

***Index Terms*—UWB pulses, ECG, respiratory rate, R-wave, T-wave, R-R interval, GTEM, peak-to-peak amplitude, ketamine, Sprague-Dawley.**

Manuscript received November 29, 2003. This work was supported by the U.S. Army Medical Research and Materiel Command under contract DAMD17-94-C-4069 awarded to McKesson BioServices Corporation.

R. L. Seaman is with McKesson BioServices, Brooks City-Base, TX 78235 USA at the U.S. Army Medical Research Detachment (USAMRD) of the Walter Reed Army Institute of Research (WRAIR) (phone: 210-536-5595; fax: 210-536-5382; e-mail: ronald.seaman@brooks.af.mil).

J. R. Jauchem is with the U.S. Air Force Research Laboratory, Directed Energy Bioeffects Division, Radiofrequency Radiation Branch, Brooks City-Base, TX 78235 USA (e-mail: james.jauchem@brooks.af.mil).

The views, opinions and/or findings contained in this report are those of the authors and should not be construed as an official Department of the Army or Department of the Air Force position, policy or decision. In conducting this research, the investigator(s) adhered to the "Guide for the Care and Use of Laboratory Animals," prepared by the Institute of Laboratory Animal Resources, National Research Council. The Institutional Animal Care and Use Committee of the Air Force Research Laboratory, Brooks City-Base, Texas, had approved all animal procedures.

I. Introduction

Developments in electromagnetic technology have resulted in exposure sources capable of generating high intensity pulses with extremely short pulse widths. These sources produce pulses having nanosecond (ns) durations with sub-ns rise times. The pulses can be represented in the frequency domain by ultra-wideband (UWB) frequency content that include microwaves [1]. Devices utilizing UWB pulses find many applications in civilian and military systems for communication and detection [2], [3]. High-intensity UWB pulses may also be used as a countermeasure against vulnerable military electronic systems [4], [5].

No acute reaction of the cardiovascular system has been observed in studies conducted with UWB pulses in which measured variables were averaged over 30-s periods [6], [7]. However, delayed effects on blood pressure by 6-min UWB exposures have been observed [8]. Previous studies have established that effectiveness of more traditional stimuli to disrupt acutely the regular beating rhythm of the heart depends on the timing of the stimulus [9]. The heart is most vulnerable to an applied pulse of electric or magnetic field during the T-wave of the electrocardiogram (ECG), when ventricular repolarization is occurring [10] - [12]. We might also expect that heart activity, especially heart rate, would be most susceptible to UWB pulses when they are applied during the T-wave. However, UWB pulses in previous investigations have not been delivered specifically during the T-wave or in any other way synchronized with the ECG.

An increase in heart rate is a common result of exposure to microwaves at high enough power levels to raise body temperature, e.g., [13] - [15]. Effects of low-level exposures such as those expected for pulse-modulated microwaves and UWB pulses, however, are equivocal. Although tachycardia or arrhythmia was reported as a direct, non-thermal action of pulsed microwaves on isolated frog hearts [16], this was not confirmed by other investigators [17], [18]. Human cardiovascular effects of exposure to extremely-low-frequency electromagnetic fields and microwaves follow the same body-temperature rule [19].

We report two experiments performed on the anesthetized

rat to determine whether changes in the timing of events in the cardiac cycle occurred at the onset of exposure to UWB pulses applied during the ECG T-wave. We selected the rat as the animal model for this cardiovascular study for a number of reasons that included the ability to place this animal in different orientations within the volume of the available UWB exposure system. Regulation of cardiac output in laboratory rats is qualitatively and quantitatively very similar to that in humans [20]. For example, ligation of the coronary artery of the Sprague-Dawley rat results in a model for human myocardial infarction and chronic heart failure [21]. Although the hearts of some small animals such as the mouse and rabbit are less vulnerable to some types of arrhythmias than larger animals such as the pig and dog, this is not the case for the rat [22]. This report focuses on the timing of events in the ECG recorded from animals exposed to well-characterized UWB pulses applied in bursts that occurred before the T-wave peak or during the T-wave peak. This plan recognized that the time of the T-wave peak was a period of vulnerability to other types of stimuli [9] – [12]. Emphasis was placed on changes immediately after onset of exposure that might not appear in data averaged over time. Results were expressed in terms of time intervals between electrical events in the ECG during contraction of the heart and the time interval between contractions.

II. MATERIALS AND METHODS

A. Animals

Data were obtained from 20 Sprague-Dawley male rats (330-440 g): 10 for each of the two animal orientations described below. Anesthesia was induced with intramuscular (IM) ketamine HCl (100 mg/kg) in a hind limb. Supplemental ketamine was given IM in the opposite hind limb as needed during experimental procedures to maintain an acceptable level of anesthesia. The carotid artery was cannulated with PE-50 tubing terminated with a closed stopcock. The cannula was secured by 00 suture to chest-wall muscle for mechanical stability.

B. UWB Exposures

Animals were exposed to UWB pulses in a giga transverse electromagnetic cell (GTEM) that has previously been described [6], [8]. Briefly, the GTEM is a two-conductor transmission line with a ground conductor of square cross section surrounding a flat center conductor. The GTEM is tapered with its narrow end connected to RG-220 coaxial cable, which carries a high-voltage pulse, and its wide end appropriately terminated internally to minimize pulse reflection. The GTEM, supported such that one side of the ground conductor was horizontal, and UWB pulse circuitry were located in an electrically shielded room. Instruments to generate the signal for triggering UWB pulses and to record signals from the animal and from an electric-field probe were located outside the room.

For exposure, an animal was placed ventral recumbent on a solid dielectric sheet 21 mm thick on the GTEM horizontal ground conductor. The animal was arranged in one of two orientations with its thorax at a central location where UWB pulses had been carefully characterized. In the k-polarization orientation, the body axis was in the direction of UWB pulse propagation with the head toward source end of the GTEM. For animal k-polarization, the tail extended toward the termination end of the GTEM and thus the tail was also in k-polarization. In H-polarization orientation, the body axis was orthogonal to the propagation direction and parallel to the magnetic field vector of the propagating pulse. For animal H-polarization, the tail curved with its tip at about the midpoint of the body on the GTEM termination side of the animal. In this position, the tail was in k- and H-polarization.

The applied UWB pulses were characterized by sampling the propagating electric field with an EG&G ACD(A) D-dot probe mounted on the GTEM wall at the mirror-image site of the animal thorax. Signals from the D-dot probe were captured and averaged by a Textronix SCD 5000 Transient Digitizer and later used to derive pulse parameters [23]. For the k-polarization experiment, pulse parameters computed from 18 waveforms, each the average of 10-15 pulses, were (mean±SD) 106±5 kV/m amplitude, 0.79±0.02 ns duration, and 186±17 ps rise time. Parameters derived in the same manner for the H-polarization experiment were 106±9 kV/m amplitude, 0.78±0.02 ns duration, and 170±6 ps rise time.

C. Procedure

After placement of the animal in the GTEM, the carotid cannula and stopcock were carefully threaded through a small hole in the GTEM wall and connected to a pressure transducer (Model 700-0500, International Biomedical) in an electrically shielded box mounted on the exterior wall of the GTEM. Carbon-loaded Teflon conductors were secured subcutaneously on each limb of the animal near the body. The conductors passed through the same wall hole as the cannula into the shielded box where they connected to a standard shielded ECG cable. The ECG cable and leads from the pressure transducer were connected to Gould ECG/Biotach (Model 20-4615-65) and Pressure Processor (Model 20-4615-52) units, respectively, outside the shielded room. Artifact-free recording of Lead II ECG (right fore limb to left hind limb) and blood pressure were obtained by passing the ECG cable and transducer leads through solid copper tubing (13 mm ID) that was electrically connected to the shielded box on the GTEM. The solid copper tubing and coaxial cables carrying UWB-trigger and D-dot-probe signals were passed separately through the wall of the shielded room. Signals from the two Gould units as well as the UWB trigger signal were recorded using a BioPac MP100 system (BIOPAC

Systems, Inc., Goleta, CA). The sampling rate of 4 kHz, used in order to detect the pulsed trigger signal reliably, gave a time resolution of 0.25 ms for each of the three recorded signals.

The UWB pulses were delivered at 1 kHz, the maximum repetition frequency of the UWB system, in 25-ms bursts, i.e., 25 pulses per burst (Fig. 1). Using the R-wave signal output of the Gould ECG/Biotach unit, bursts were timed to start during the R-wave or 25 ms after the R-wave. A burst delayed by 25 ms was found in pilot studies to occur during the T-wave peak while a burst triggered without delay ended before the peak. By being triggered by the R-wave detection signal, the bursts of each delay, 0 or 25 ms, were delivered synchronously at the same respective part of the ECG in successive cardiac cycles . A 10-s exposure period was used because it was shorter than exposure and analysis periods used in earlier UWB studies but long enough to detect short-term, transient changes. The exposure duration was, of course, arbitrary, but because multiple exposures were to be delivered to each animal, the duration was not made longer in order to minimize the possibility of any carryover effect and to complete an experimental session while a stable preparation could be expected.

A total of nine 10-s exposures were applied in random sequence to each animal: three control exposures with no pulses (sham); three exposures with bursts of UWB pulses starting at each R-wave (0 ms); and three exposures with bursts of UWB pulses starting 25 ms after each R-wave (25 ms), and occurring during the T-wave. Because we expected no change in measured variables for sham exposures and exposures with bursts starting at 0 ms, these exposures served as controls for comparison. Except for the first exposure of a particular animal, the start of an exposure was approximately 20 s after the end of the previous exposure.

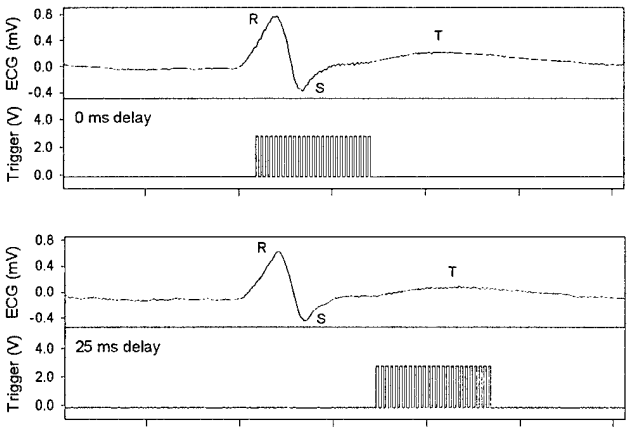


Fig. 1. Representative ECG and trigger pulses synchronized to the ECG. Intervals on the horizontal axis are 20 ms. The letters R, S, and T designate respective ECG waves. One UWB pulse was triggered by each of the 25 trigger pulses in each burst. Trigger pulses were 1 ms apart in a burst. Top: burst of pulses starts with no delay (0 ms) from R-wave detection signal (not shown). Bottom: burst of pulses starts with 25-ms delay from R-wave detection signal (not shown).

After an animal was placed in the GTEM and connected to instrumentation, a period of 5-10 min was used to establish stable recording. The nine exposures were then delivered over the next 5-6 min

Because of the ability of UWB pulses to affect electronic instruments, the ECG was displayed on a Hewlett Packard 54501A digitizing oscilloscope during experimental runs and visually examined for artifacts that might be caused by UWB pulses or the pulsed trigger signal. The blood pressure signal and trigger signal were also displayed on the oscilloscope. Artifacts seen in the ECG were found to be due to coupling of signals from inside the shielded room to instrumentation outside the room, and not through ECG leads. With the door of the shielded room completely closed the extraneous signals were eliminated or reduced to levels that would not interfere with ECG interpretation. The ECG was also examined during data extraction to avoid any artifact that might have been recorded by error. The blood pressure signal showed no change during the period to be examined for transient changes and so was not analyzed.

D. Data Analysis

Time intervals in the ECG waveform were measured from data files using AcqKnowledge software (v.3.5.7, BIOPAC Systems). Only the ECG channel was present in coded files used for measurement so that the experimental condition was not known when measurements were made. Absence of the Q-wave or a Q-wave of small amplitude and lack of an ST interval seen here in Lead II (Fig. 2) have been previously noted in the rat ECG [24], [25]. Three intervals were measured for each ECG cycle: PR, the time between start of P-wave and start of R-wave; RT, the time between start of R-wave and peak of T-wave; and QT, the time between start of R-wave and end of T-wave (Fig. 2). Intervals PR and QT followed common terminology. We found that onset of a subsequent P-wave did not have to be used as the end of QT, as done in some rat studies [25]. Interval RT corresponded to intervals RαT and QTa used in some reports, with 'α' and 'a' referring to the apex, or peak, of the T-wave [24], [26].

AcqKnowledge recorded three values automatically for each ECG interval measured: interval length, in milliseconds; time at the end of the interval from start of the data file, in seconds; and peak-to-peak ECG amplitude within the interval, in millivolts. The peak-to-peak amplitude

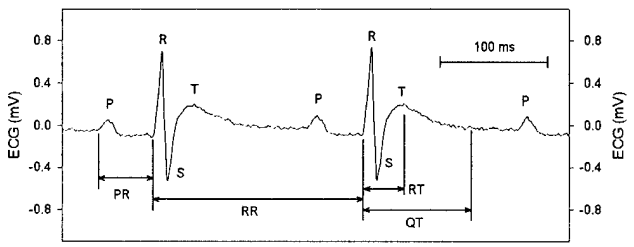


Fig. 2. Time intervals measured in the ECG and described in the text. The letters P, R, S, and T designate the respective waves.

during RT and QT intervals, referred to here as PP, was the difference in potential between R-wave peak and S-wave peak (Fig. 2). Intervals were measured over the 10-s period starting 5 s before the start of exposure and ending 5 s after the start of exposure. Because analysis of RR and PR for k-polarization over the 20-s period from 10 s before start of exposure through 10 s of exposure showed no change with UWB exposure [27], the shorter, 10-s period used here was deemed appropriate for efficient analysis of all intervals in both polarizations.

Data extracted using AcqKnowledge were recorded in ASCII text files and processed in QuattroPro spreadsheets and by programs written in the R language (version 1.7.1, The R Development Core Team). The RR interval, or RR, in milliseconds, was calculated as the difference in times recorded for two successive R-wave onsets. Values of each variable were determined at 100-ms intervals by cubic interpolation using the splinefun() function in R in order to average values across exposures of the same type. Data were aligned in time using the start of exposure as time 0. Five variables – RR, PR, RT, QT, and PP – were plotted and analyzed at the 100-ms time intervals. Values for each variable for sham, 0-ms, and 25-ms exposures for an animal were represented by the average for its three exposures of each type.

Data were plotted as mean values. Because variability around the mean of each variable was quite similar for different exposure types and time points, a representative value of the standard error of the mean (s.e.m.) was used to illustrate variability for each variable. Analysis of variance (ANOVA) was performed with GB-STAT (Version 5.2, Dynamic Microsystems). Two-way ANOVA was performed on each variable with exposure type (sham, 0 ms, 25 ms) and time as factors and with repeated measures on time. The time factor had 10 levels consisting of five values immediately before and five values immediately after the start of exposure at time 0. For interpolated values occurring at regular time intervals, this corresponded to time points -0.5, -0.4, -0.3, -0.2, -0.1, +0.1, +0.2, +0.3, +0.4, and +0.5 s. The *F*-value and *p*-value were examined for main effect of exposure type, main effect of time, and exposure type-time interaction effect in each ANOVA. A *p*-value less than 0.05 was used to reject a null hypothesis of equal means or no interaction.

III. RESULTS

A. RR Interval

Because of indications in the literature of changes in heart rate due to external stimuli applied during the T-wave, RR, the inverse of heart rate, was examined first. The RR interval is shown in the top of Fig. 3 for k-polarization (10 animals) and in the top of Fig. 4 for H-polarization (10 animals). Values interpolated for the regular 100-ms intervals are plotted in these and subsequent figures as well as used for ANOVA unless otherwise indicated. The rather large variability in RR indicated by the representative s.e.m. in both

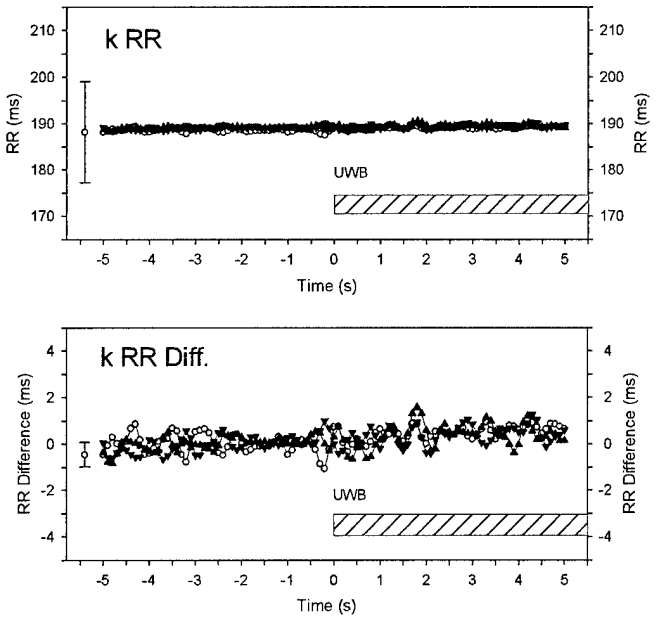


Fig. 3. Time interval RR and RR difference for k-polarization exposure. O, sham exposure; ▲, UWB pulses with 0 ms delay; ▼, UWB pulses with 25 ms delay. Data from 10 animals. The symbol at the far left of each panel is the first mean value for sham exposures with error bars (±s.e.m.) representative of variation of data in the panel.

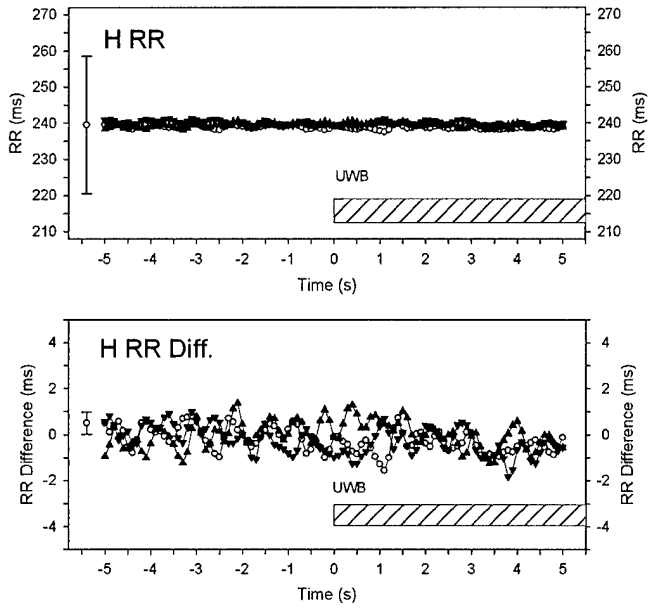


Fig. 4. Time interval RR and RR difference for H-polarization exposure. O, sham exposure; ▲, UWB pulses with 0 ms delay; ▼, UWB pulses with 25 ms delay. Data from 10 animals. The symbol at the far left of each panel is the first mean value for sham exposures with error bars (±s.e.m.) representative of variation of data in the panel.

figures can be attributed to differences in RR between individual animals. Mean RR across animals in the 5 s preceding exposure ranged from 145 to 248 ms for

k-polarization and from 153 to 328 ms for H-polarization. Because any change due to UWB exposure would be a difference from pre-exposure RR, difference from the respective average value for the 5 s before exposure was also examined (bottoms of Figs. 3 and 4). Note that differences in RR ranged within roughly ±2 ms, which was only ±0.7-3% of the pre-exposure average RR. An oscillatory pattern having a period of 0.5-1 s was evident in RR difference for both polarizations.

In ANOVA of RR, the main effects of exposure type and time were not significant for either k- or H-polarization. The exposure type-time interaction was likewise not significant for H-polarization but was significant (F=2.58, p<0.001) for k-polarization. Results of ANOVA of RR difference were quite similar to results for the respective RR, which can be expected with use of repeated measures on time. Upon examination of RR difference for k-polarization, the interaction effect was seen to be due to a relatively large deviation in sham RR before start of exposure, and possibly to differences in the phases of RR oscillation among types of exposure. Thus, the statistically significant interaction did not reflect changes due to different types of UWB exposure.

B. PR Interval

The PR interval is shown in Figs. 5 and 6 for k-polarization and H-polarization, respectively. Difference in PR from the respective pre-exposure average value is also shown for the two polarizations. The oscillatory pattern seen in RR was also apparent in PR. ANOVA showed that the main effect of exposure type, the main effect of time, and the exposure type-time interaction were not significant for either polarization.

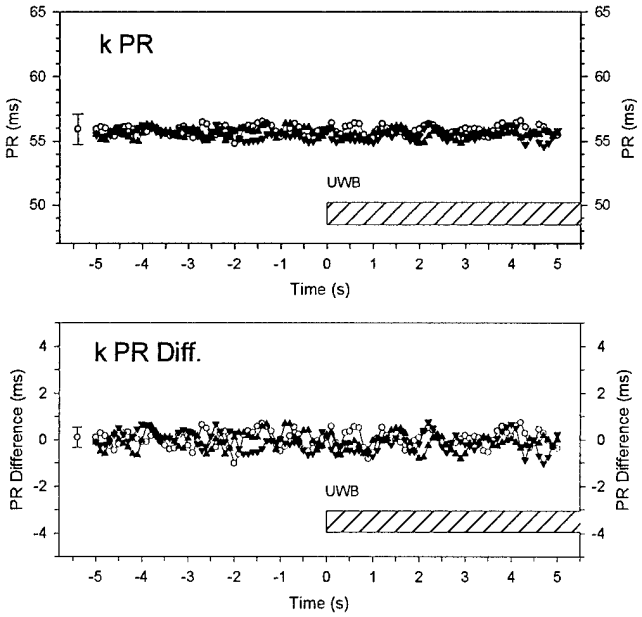


Fig. 5. Time interval PR and PR difference for k-polarization exposure. O, sham exposure; ▲, UWB pulses with 0 ms delay; ▼, UWB pulses with 25 ms delay. Data from 10 animals. The symbol at the far left of each panel is the first mean value for sham exposures with error bars (±s.e.m.) representative of variation of data in the panel.

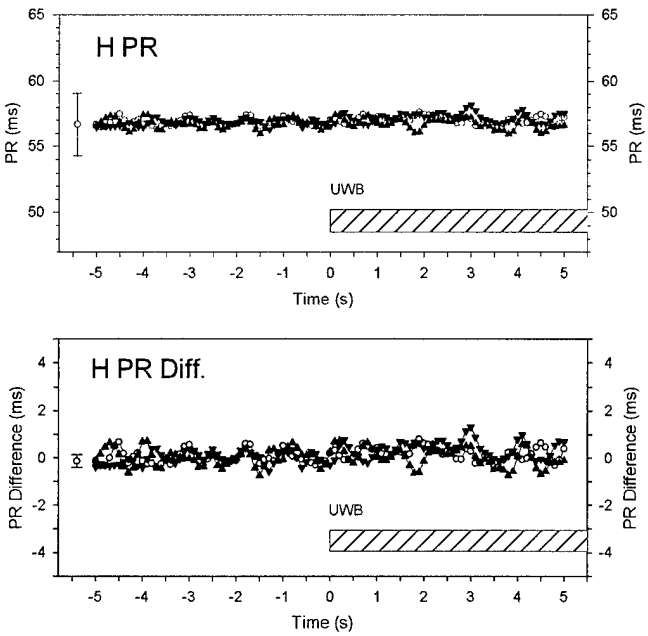


Fig. 6 Time interval PR and PR difference for H-polarization exposure. O, sham exposure; ▲, UWB pulses with 0 ms delay; ▼, UWB pulses with 25 ms delay. Data from 10 animals. The symbol at the far left of each panel is the first mean value for sham exposures with error bars (±s.e.m.) representative of variation of data in the panel.

C. RT and QT Intervals

The RT interval is shown in Figs. 7 and 8 for k-polarization and H-polarization, respectively, and the QT interval is shown in Figs. 9 and 10 for k-polarization and H-polarization, respectively. The respective differences in RT and QT from respective pre-exposure average values are shown in the same figures. The oscillatory pattern with a period of 0.5-1 s was again present in both RT and QT. Although onset of the R-wave was well defined in the ECG as the start of these two intervals, the ends of the intervals were more difficult to determine. For RT, the time of the T-wave peak was not always a single value, i.e., there was a double peak, and the peak was often relatively flat, and sometimes not apparent because of bumps of unknown origin in the wave. For QT, the end of the T-wave, defined as the return to isopotential (unchanging potential), was difficult to determine due to absence of the isopotential or to gradual tapering of the T-wave into an isopotential. The T-wave rarely overlapped the next P-wave in our data. For both RT and QT intervals, using a consistent definition of terminating feature for each animal minimized measurement variation. This provided valid data because we were interested in changes with UWB exposure, not differences between animals. Even with these precautions, variability was quite large for both intervals, but QT had greater variability most likely because of the greater difficulty in measuring it.

Respective ANOVAs of RT and QT showed that the main effect of exposure type, the main effect of time, and the

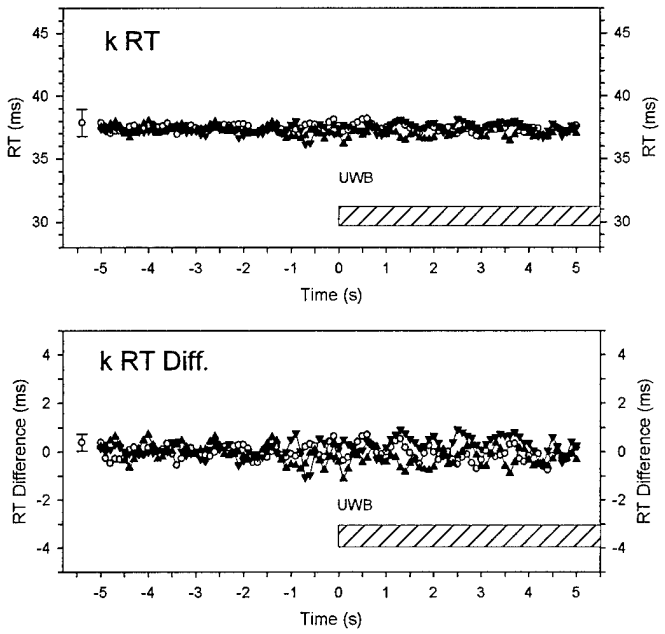


Fig. 7. Time interval RT and RT difference for k-polarization exposure. O, sham exposure; ▲, UWB pulses with 0 ms delay; ▼, UWB pulses with 25 ms delay. Data from 10 animals. The symbol at the far left of each panel is the first mean value for sham exposures with error bars (±s.e.m.) representative of variation of data in the panel.

exposure type-time interaction were not significant for k-polarization. This was also the case for ANOVA of QT for H-polarization. ANOVA of RT for H-polarization (Fig. 8) showed that the main effects of exposure type and time were not significant but that the exposure type-time interaction was significant (F=2.96, p<0.001). Examination of RT and RT

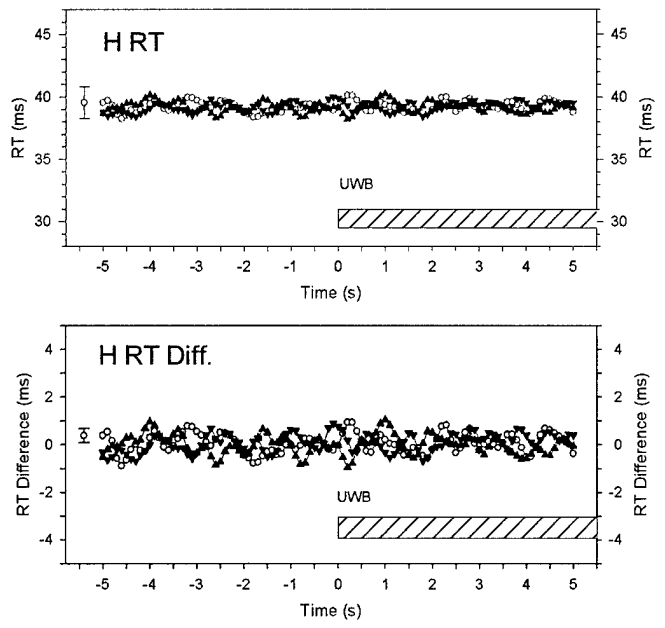


Fig. 8 Time interval RT and RT difference for H-polarization exposure. O, sham exposure; ▲, UWB pulses with 0 ms delay; ▼, UWB pulses with 25 ms delay. Data from 10 animals. The symbol at the far left of each panel is the first mean value for sham exposures with error bars (±s.e.m.) representative of variation of data in the panel.

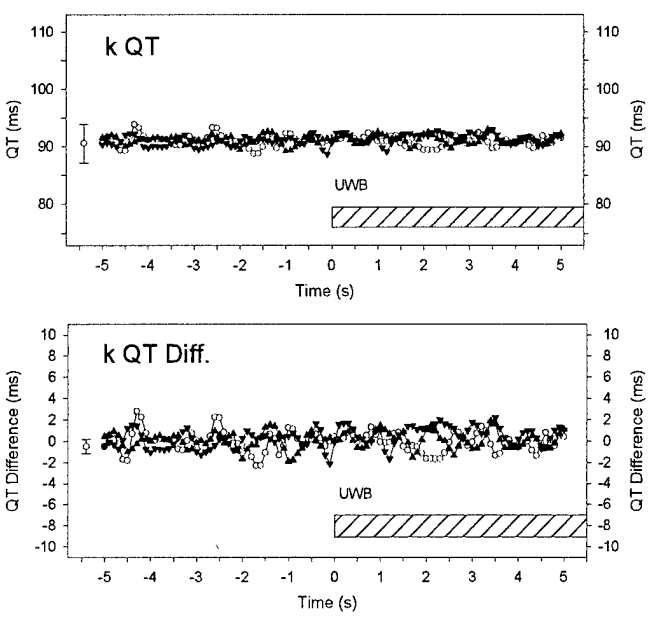


Fig. 9. Time interval QT and QT difference for k-polarization exposure. O, sham exposure; ▲, UWB pulses with 0 ms delay; ▼, UWB pulses with 25 ms delay. Data from 10 animals. The symbol at the far left of each panel is the first mean value for sham exposures with error bars (±s.e.m.) representative of variation of data in the panel.

difference for H-polarization in Fig. 8 revealed that this interaction was due to oscillations in sham, 0-ms, and 25-ms RT data having different phases at the start of exposure rather than to an effect of type of exposure.

D. Peak-to-Peak Amplitude

The peak-to-peak amplitude PP is shown in Figs. 11 and 12 for k-polarization and H-polarization, respectively,

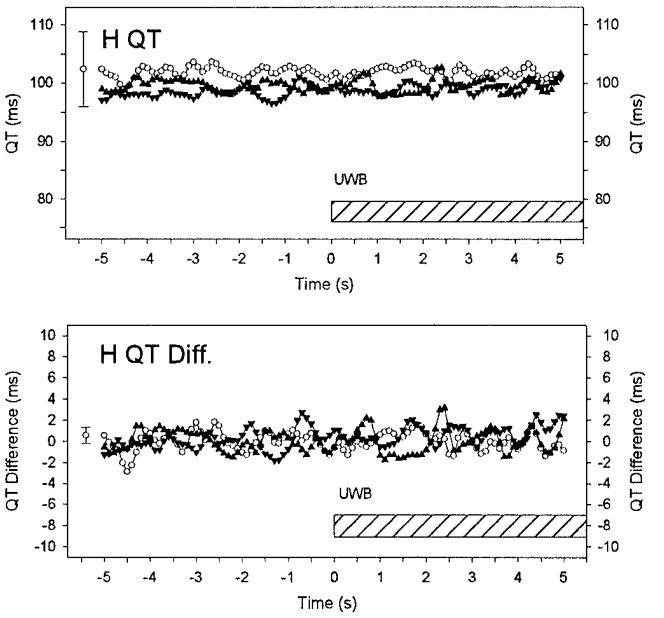


Fig. 10 Time interval QT and QT difference for H-polarization exposure. O, sham exposure; ▲, UWB pulses with 0 ms delay; ▼, UWB pulses with 25 ms delay. Data from 10 animals. The symbol at the far left of each panel is the first mean value for sham exposures with error bars (±s.e.m.) representative of variation of data in the panel.

along with differences from the respective pre-exposure average value. Variation in PP before and during exposure was very small, being on the order of ±20 μV for mean values of 0.9-1.0 mV. ANOVA of PP showed that the main effect of exposure type and the main effect of time were not significant for either polarization. Exposure type-time interaction for H-polarization was also not significant. However, ANOVA of PP for k-polarization (Fig. 11) showed a significant exposure type-time interaction (F=2.02, p=0.009). But, as was the case for the significant exposure type-time interaction for RT, this interaction was seen to be due to the oscillations in PP having different phases at the start of sham, 0-ms, and 25-ms exposures rather than to an effect of type of exposure (Fig. 11).

E. Analysis of Uninterpolated Data

Analyses of variance were also performed on the measured values of each variable for each polarization rather than the interpolated values at 100-ms intervals. The results of these ANOVAs were the same as for the interpolated values described above in detail. No main effect of exposure type or of time was found to be significant. Occasional significant exposure type-time interactions were attributable to chance variations in the particular variable at the start of exposure. We concluded that no significant effect of UWB exposure was present in unprocessed interval or amplitude data. The agreement in the two sets of analyses, one using interpolated values at regular intervals and one using unmodified measured values, reassured us that our results were not due to manipulation of data during analysis.

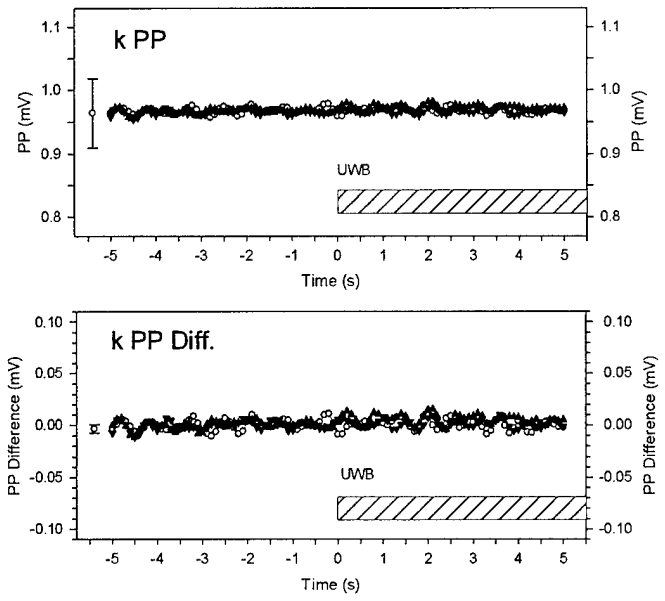


Fig. 11. Peak-to-peak amplitude PP and PP difference for k-polarization exposure. O, sham exposure; ▲, UWB pulses with 0 ms delay; ▼, UWB pulses with 25 ms delay. Data from 10 animals. The symbol at the far left of each panel is the first mean value for sham exposures with error bars (±s.e.m.) representative of variation of data in the panel.

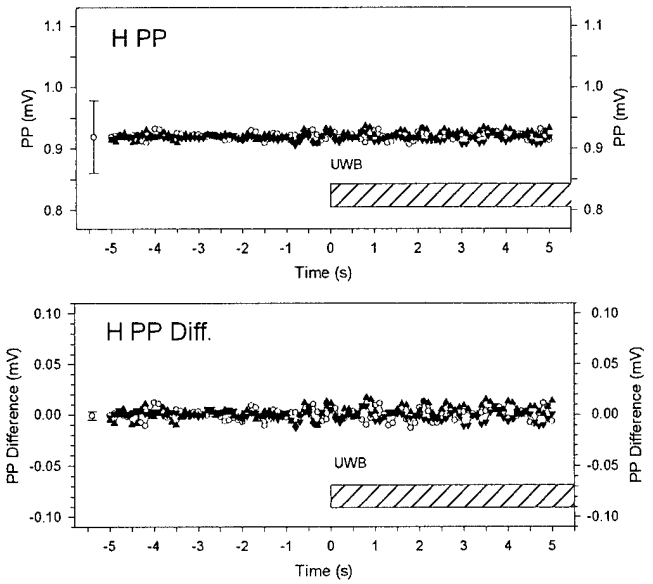


Fig. 12. Peak-to-peak amplitude PP and PP difference for H-polarization xposure. O, sham exposure; ▲, UWB pulses with 0 ms delay; ▼, UWB ulses with 25 ms delay. Data from 10 animals. The symbol at the far left f each panel is the first mean value for sham exposures with error bars ±s.e.m.) representative of variation of data in the panel.

IV. DISCUSSION

The duration of less than 1 ns and the rise time of less than 200 ps of the UWB pulse used in this study were typical of UWB pulses produced by other systems [1]. The frequency spectrum of the pulse had components from 0 Hz up to at least 2 GHz [8]. The relatively large contribution of components at low frequencies was due to the unipolar nature of the pulse produced by a spark gap in the coaxial cable feeding the GTEM. Because of the representative nature of the pulses used here, we can expect that our findings extend to exposures with other UWB pulses. Bursts of UWB pulses synchronized to the R-wave or the T-wave in this study are not likely to be experienced outside of the laboratory. However, because of the vulnerability of the heart to stimuli during the T-wave [9] – [12], the burst of UWB pulses during the T-wave peak used here can be expected to have provided a sensitive test of UWB pulses to change ECG time intervals. The burst parameters used here were based on having pulses occur reliably during the T-wave peak and at the maximum repetition frequency of the laboratory UWB system. Because of the acute nature of the experiments here and use of anesthetized animals, the results do not provide information on long-term cardiovascular effects such as those reported for other UWB experiments [8].

An oscillatory variation with time was seen in the measured cardiac variables in the present experiments, most prominently in the RR difference. The oscillation had a period of 0.5-1 s or, equivalently, a frequency of 1-2 Hz in each variable. Heart rate variability is known to have a rather strong spectral peak at the respiratory rate, the frequency of

which, of course, is specific to individuals [28]. In rats under anesthesia with 100-150 mg/kg ketamine, the respiratory rate is 80-100 breaths/min, or 1.3-1.7/s [14], [15], which falls within the range of the observed oscillations. In conscious rats, the respiratory spectral peak in RR is at 1-1.8 Hz, thought to be vagally mediated, and, to some extent, a reflection of intrathoracic pressure variations during respiration [29], [30]. Thus, the oscillatory variation in measured variables at 1-2 Hz was almost certainly due to respiration or the parasympathetic (vagal) nerve activity fluctuating in phase with respiration.

Lack of effect on heart activity and the nerves that influence the heart was indicated in this study by the lack of effect on the studied intervals, which can be related to cardiac events [31]. The RR interval, the period of rhythmic electrical activity of the heart, is the reciprocal of heart rate. The rhythmic pacemaker of the sinoatrial node is principally responsible for the regular beating of the heart, but the pacemaker action potential, which occurs near the start of the P-wave, is too small to be seen in the ECG. The PR interval represents the time for conduction of electrical activity from atria to ventricles, the P-wave and Q- or R-wave of the ECG indicating the onset of cardiac-cell depolarizations in atria and ventricles, respectively. The QT interval is an index of the duration of the ventricular action potential, with the T-wave indicating ventricular repolarization. The UWB pulses did not significantly affect the electrical activity of cardiac tissue where these events originated. We can also make a similar statement regarding the sympathetic and parasympathetic nerves that modulate the activity [31].

Based on results of previous studies of rats exposed to radiofrequency/microwave-frequency radiation, differential absorption of energy or increased body temperature in the UWB-exposed animals was not expected to affect our results. The previous results are relevant because energy at these frequencies are present in the frequency spectrum of the UWB pulse. Energy absorption by the tail can be much higher than at other locations in the body when it is parallel to the propagating electric field [32], [33]. However, when the tail is placed close to the body or parallel to either the magnetic field or the direction of propagation, the absorption is similar to that in other parts of the body [32] - [34]. Because the tail was always in k- or H-polarization in our exposure configurations, no peak absorption was expected at or near the tail, and certainly not absorption intense enough to have an effect on the measured cardiovascular variables. In addition, the effect of any but an extreme differential absorption would be difficult to imagine in the anesthetized rat.

We can also reasonably exclude any effect due to an increase in body temperature based on previous microwave experiments. The whole-body specific absorption rate (SAR) of rats exposed to the UWB pulses at 1 kHz repetition frequency has been estimated to be 114-121 mW/kg [6], [8]. Whole-body averaged SAR of 6 W/kg does not change heart rate in this animal preparation exposed to continuous or pulsed microwave radiation at 5.6 GHz while SAR of 12 W/kg is effective [35]. Thus, because the SAR during UWB exposures was many times smaller than the SAR required to change heart rate through change in body temperature, such an effect in our experiments was unlikely. This was especially the case because the cumulative exposure time of each animal was only 60 s during 180-200 s of data collection.

The lack of knowledge of the biological effects of UWB pulses is understandable when we consider that only recently has technology been developed to produce reliably large amplitude electromagnetic pulses with nanosecond and shorter durations. One can expect that the biological cells most sensitive to UWB pulses are the electrically excitable cells of the nervous system and the heart. Traditional understanding of the stimulation of these cells by electrical pulses is represented by the so-called strength-duration curve [9]. The curve illustrates the relationship between amplitude (strength) and duration of an applied stimulating electrical pulse just sufficient to elicit a response in the form of an action potential. At small pulse durations, a constant energy proportional to the product of pulse amplitude and duration describes the relationship. Combinations of amplitude and duration above threshold stimulation defined by the strength-duration curve are also able to elicit the response. Until the availability of pulses with UWB characteristics, the shortest durations of applied pulses were typically 10 μs-1 ms, e.g., [9], [36]. Recent research shows that voltage pulses of ~1 ns duration, or at least 10 000 times shorter than those previously studied, can stimulate excitable tissue when applied with sufficient amplitude directly to the tissue preparation [37]. However, the lack of change in ECG intervals here indicated that energy coupled to tissue from the propagating UWB pulses was not capable of stimulating nerve cells or heart cells in a way that would cause a change in measured endpoints. Thus, in spite of the relatively high electric field of the incident 1-ns UWB pulse, the energy coupled to the body appeared to be smaller than that needed for stimulation.

V. CONCLUSION

We showed that by following certain precautions the ECG can be recorded during exposure to UWB pulses without artifact due to the pulses. No difference was seen in any ECG interval that was attributable to exposure to UWB pulses under our experimental conditions. Therefore, we conclude that no acute effect of UWB exposure on timing of events in the cardiac cycle occurred. Any undetected effect that might have occurred would have been smaller than the fluctuations that normally occur in the cardiac events measured, e.g., with respiration as seen in our study. Thus, results here are consistent with previous findings of no effect over longer

periods of analysis [6], [7].

ACKNOWLEDGMENT

We are grateful to A. Phinney for handling and preparation of animals; J. Ashmore for instrumentation and operation of the UWB system; and Dr. S. P. Mathur for determination of UWB-pulse characteristics. A. Phinney, A. Garcia, and J. Morin performed a large majority of interval measurements in the recorded ECGs. We thank Dr. S.-T. Lu, McKesson BioServices, and Mr. B. Stuck, USAMRD, for their support and review of the study.

REFERENCES

[1] F.J. Agee, C.E. Baum, W.D. Prather, J.M. Lehr, J.P. O'Loughlin, J.W. Burger, J.S.H. Schoenberg, D.W. Scholfield, R.J. Torres, J.P Hull, and J.A. Gaudet, "Ultra-wideband transmitter research," *IEEE Trans. Plasma Sci.* vol. 26, pp. 860-873, June 1998.

[2] G. Micolau, M. Saillard, and P. Borderies, "DORT method as applied to ultrawideband signals for detection of buried objects," *IEEE Trans. Geosci. Remote Sensing*, vol. 41, pp. 1813-1820, Aug. 2003.

[3] D.M. Pozar, "Waveform optimizations for ultrawideband radio systems," *IEEE Trans. Antennas Propagation*, vol. 51, pp. 2335-2345, Sept. 2003.

[4] J.A. Brunderman, "High power radio frequency weapons: A potential counter to U.S. stealth and cruise missile technology," Air War College, Air University, Maxwell Air Force Base, AL, Unnumbered Tech. Rep., Dec. 1999.

[5] J.R. Jauchem, K.L. Ryan, M.R. Frei, S.J. Dusch, H.M. Lehnert, and R.M. Kovatch, "Repeated exposure of mammary C3H/HeJ mice to ultra-wideband electromagnetic pulses: Lack of effects on mammary tumors," *Radiat. Res.*, vol. 155, pp. 369-377, Feb. 2001.

[6] J.R. Jauchem, R.L. Seaman, H.M. Lehnert, S.P. Mathur, K.L. Ryan, M.R. Frei, and W.D. Hurt, "Ultra-wideband electromagnetic pulses: Lack of effects on heart rate and blood pressure during two-minute exposures of rats," *Bioelectromagnetics*, vol. 19, pp. 330-333, 1998.

[7] J.R. Jauchem, M.R. Frei, K.L. Ryan, J.H. Merritt, and M.R. Murphy, "Lack of effects on heart rate and blood pressure in ketamine-anesthetized rats briefly exposed to ultra-wideband electromagnetic pulses," *IEEE Trans. Biomed. Eng.*, vol. 46, pp. 117-120, Jan. 1999.

[8] S.T. Lu, S.P. Mathur, Y. Akyel, and J.C. Lee, "Ultrawide-band electromagnetic pulses induced hypotension in rats," *Physiol. Behav.*, vol. 65, pp. 753-761, Sept. 1999.

[9] L.A. Geddes, *Handbook of Electrical Hazards and Accidents.* Boca Raton: CRC, 1995, ch. 2.

[10] L.P. Ferris, B.G. King, P.W. Spence, and H.B. Williams, "Effect of electric shock on the heart," *Electr. Eng.*, vol. 55, pp. 498-515, May 1936.

[11] W.H. Olson, "Electrical safety," ch. 14, in *Medical Instrumentation: Application and Design.* J.G. Webster, Ed. Boston: Houghton Mifflin,1992, pp. 751-792.

[12] M. Yamaguchi, T. Andoh, T. Goto, A. Hosono, T. Kawakami, F. Okumura, T. Takenaka, and I. Yamamoto, "Effects of strong pulsed magnetic fields on the cardiac activity of an open chest dog," *IEEE Trans. Biomed. Eng.*, vol. 41, pp. 1188-1191, Dec. 1994.

[13] J.R. Jauchem, K.L. Ryan, J.D. Lovelace, and M.R. Frei, "Effects of esmolol on 35-GHz microwave-induced lethal heat stress," *J. Auton. Pharmacol.*, vol. 17, pp. 165-174, June 1997.

[14] M. Frei, J. Jauchem, and F. Heinmets, "Physiological effects of 2.8 GHz radio-frequency radiation: A comparison of pulsed and continuous-wave radiation," *J. Microw. Power Electromagn. Energy.*, vol. 23, pp. 85-93, 1988.

[15] J.R. Jauchem and M.R. Frei, "Cardiorespiratory changes during microwave-induced lethal heat stress and β-adrenergic blockade, *J. Appl. Physiol.*, vol. 77, pp. 434-440, July 1994.

[16] A.H. Frey and E. Seifert, "Pulse modulated UHF energy illumination of the heart with change in heart rate," *Life Sci.*, vol. 7, Part II, pp. 505-512, 1968.

[17] R.M. Clapman and C.A. Cain, "Absence of heart-rate effects in isolated frog heart with pulse modulated microwave energy," *J. Microw. Power*, vol. 10, pp. 411-419, Dec. 1975.

[18] L.M. Liu, F.J. Rosenbaum, and W.F. Pickard, "The insensitivity of frog heart rate to pulse modulated microwave energy," *J. Microw. Power*, vol. 11, pp. 225-232, Sept. 1976.

[19] J.R. Jauchem, "Exposure to extremely-low-frequency electromagnetic fields and radiofrequency radiation: Cardiovascular effects in humans," *Int. Arch. Occup. Environ. Health*, vol. 70, pp. 9-21, June 1997.

[20] A.C. Guyton. *Circulatory Physiology: Cardiac Output and Its Regulation*, 2nd ed. Philadelphia: Saunders, 1973, ch. 1.

[21] T. Kobayashi, T. Miyauchi, S. Sakai, M. Kobayashi, I. Yamaguchi, K. Goto, and Y. Sugishita, "Expression of endothelin-1, ET_A and ET_B receptors, and ECE and distribution of endothelin-1 in failing rat heart," *Am. J. Physiol.*, vol. 276, pp. H1197-H1206, April 1999.

[22] D.J. Hearse and F.J. Sutherland, "Experimental models for the study of cardiovascular function and disease," *Pharmacol. Res.*, vol. 41, pp. 597-603, June 2000.

[23] J.Z. Bao, "Picosecond domain electromagnetic pulse measurements in an exposure facility: An error compensation routine using deconvolution techniques," *Rev. Sci. Instrum.*, vol. 68, pp. 2221-2227, May 1997.

[24] D.K. Detweiler, "The use of electrocardiography in toxicological studies with rats," in *The Rat Electrocardiogram in Pharmacology and Toxicology*, R. Budden, D.K. Detweiler, and G. Zbinden, Eds. Oxford: Pergamon, 1981, pp. 83-115.

[25] P. Driscoll, "The normal rat electrocardiogram (ECG)," in *The Rat Electrocardiogram in Pharmacology and Toxicology*, R. Budden, D.K. Detweiler, and G. Zbinden, Eds. Oxford: Pergamon, 1981, pp. 1-14.

[26] R. Budden, G. Buschmann, and U.G. Kühl, "The rat ECG in acute pharmacology and toxicology," in *The Rat Electrocardiogram in Pharmacology and Toxicology*, R. Budden, D.K. Detweiler, and G. Zbinden, Eds. Oxford: Pergamon, 1981, pp. 41-81.

[27] R.L. Seaman, J.R. Jauchem, S.P. Mathur, A.M. Phinney, and J.L Ashmore, "Lack of change in temporal characteristics of the rat ECG during exposure to ultra-wideband pulses," in *Symp. Rec. Abstr. Electromed 2003*, pp. 123-124.

[28] H. Cammann and J. Michel, "How to avoid misinterpretation of heart rate variability power spectra?" *Comput. Methods Programs Biomed.*, vol. 68, pp. 15-23, April 2002.

[29] N. Japundzic, M.-L. Grichois, P. Zitoun, D. Laude, and J.-L. Elghozi, "Spectral analysis of blood pressure and heart rate in conscious rats: Effects of autonomic blockers," *J. Auton. Nerv. Syst.*, vol. 30, pp. 91-100, June 1990.

[30] C. Cerutti, M.P. Gustin, C.Z. Paultre, M. Lo, C. Julien, M. Vincent, and J. Sassard, "Autonomic nervous system and cardiovascular variability in rats: A spectral analysis approach," *Am. J. Physiol.*, vol. 261, pp. H1292-H1299, Oct. 1991.

[31] A.M. Katz, *Physiology of the Heart*, 2nd ed. New York: Raven, 1992, ch. 20.

[32] J.A. D'Andrea, R.Y. Emmerson, C.M. Bailey, R.G. Olsen, and O.P. Gandhi, "Microwave radiation absorption in the rat: Frequency-dependent SAR distribution in body and tail," *Bioelectromagnetics*, vol. 6, no. 2, pp. 199-206, 1985.

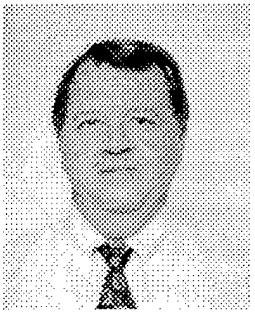
[33] C.K. Chou, A.W. Guy, J.A. McDougall, and H. Lai, "Specific absorption rate in rats exposed to 2,450 MHz microwaves under seven exposure conditions," *Bioelectromagnetics*, vol. 6, no. 1, pp. 73-88, 1985.

[34] A.W. Guy, J. Wallace, and J.A. McDougall, "Circularly polarized 2450-MHz waveguide system for chronic exposure of small animals to microwaves," *Radio Sci.*, vol. 14, no. 6S, pp. 63-74, 1979.

[35] J.R. Jauchem, M.R. Frei, and F. Heinmets, "Heart rate changes due to 5.6-GHz radiofrequency radiation: Relation to average power density," *Proc. Soc. Exp. Biol. Med.*, vol. 177, pp. 383-387, Dec. 1984.

[36] A. Vinet, D.R. Chialvo, D.C. Michaels, and J. Jalife, "Nonlinear dynamics of rate-dependent activation in models of single cardiac cells," *Circ. Res.*, vol. 67, pp. 1510-1524, Dec. 1990.

[37] W.R. Rogers, J.H. Merritt, J.A. Comeaux Jr, C.T. Kuhnel, D.F. Moreland, D.G. Teltschik, J.H. Lucas, and M.R. Murphy, "Strength-duration curve for an electrically excitable tissue extended down to near 1 nanosecond," *IEEE Trans. Plasma Sci.*, submitted for publication.



Ronald L. Seaman ((S'68-M'75-SM'83) was born in Seaman, Ohio. He received a B.S. in electrical engineering from the University of Cincinnati, Cincinnati, Ohio (1970); a Ph.D. in biomedical engineering from Duke University, Durham, North Carolina (1975), and an M.S. in management from the Georgia Institute of Technology, Atlanta, Georgia (1986).

He was an instructor at the University of Texas Health Science Center at Dallas before joining the Georgia Tech Research Institute in 1979. From 1986 to 1994, he was an Associate Professor of Biomedical Engineering at Louisiana Tech University and served as Coordinator of Research in the Center for Rehabilitation Science and Biomedical Engineering. Joining McKesson BioServices in 1994, Dr. Seaman is a Senior Biomedical Research Scientist in the Microwave Bioeffects Branch of the US Army Medical Research Detachment at Brooks AFB.

Dr. Seaman's research interests are the effects of electromagnetic fields on biological systems at organism, system, and cell levels. He has authored or co-authored a number of reports and published articles on effects of ultra-wideband pulses and pulsed L-band radiation on animal physiology and behavior. Earlier work included development of unique exposure devices and research on effects of microwave radiation on individual excitable cells. In addition to being a senior member of IEEE, he is a member of Eta Kappa Nu, Tau Beta Pi, American Association for the Advancement of Science, Society for Neuroscience, Bioelectromagnetics Society, New York Academy of Sciences, The American Physiological Society, and American Statistical Association.



James R. Jauchem was born in 1951 in Washington, DC. He received a BS in biology from Heidelberg College, Tiffin, Ohio (1973) and a PhD in physiology from Baylor College of Medicine, Houston, Texas (1977).

He developed an *in vitro* blood vessel preparation during a postdoctoral position with the Microcirculatory Systems Research Group at the University of Missouri. At the Department of Pathology, University of Texas Health Science Center at San Antonio, he was the first to discover white-blood-cell chemotactic activity in arteries. Subsequently, at the National Aeronautics & Space Administration's Johnson Space Center and at the US Air Force's School of Aerospace Medicine, he studied blood factor changes in humans during altitude decompression sickness. For the last 20 years, his research emphasis has been biological effects of microwave exposure.

Dr Jauchem has been the author of over 190 research publications, abstracts, and technical reports, including 85 peer-reviewed journal articles (first author of 65). He has served as a reviewer for 10 peer-review journals, and has been a member of: American Physiological Society (since 1985), Bioelectromagnetics Society, IEEE Committee on Man & Radiation, Society for Experimental Biology & Medicine, Aerospace Medical Association, Undersea & Hyperbaric Medical Society, and Divers Alert Network. He has also reviewed grant proposals for the Cardiovascular and Renal Study Section of the National Institutes of Health.

Acute Effects of Pulsed Microwaves and 3-Nitropropionic Acid on Neuronal Ultrastructure in the Rat Caudate-Putamen

Ronald L. Seaman[1*] and Clyde F. Phelix[2]

[1]McKesson BioServices Corporation and Microwave Bioeffects Branch,
U.S. Army Medical Research Detachment, Brooks City-Base, Texas 78235
[2]Department of Biology,
University of Texas at San Antonio, San Antonio, Texas 78249

Running title: Microwaves and neuronal ultrastructure

*Correspondence: Dr. Ronald L. Seaman
McKesson BioServices
8355 Hawks Road, Bldg. 1168
Brooks City-Base, TX 78235

Telephone: (210) 536-5595

FAX: (210) 536-5382

Internet: ronald.seaman@brooks.af.mil

This work is supported by U.S. Army Medical Research and Materiel Command contract DAMD17-94-C-4069 awarded to McKesson BioServices. [Note to editor: This statement is required by the contract cited. If it cannot be printed, please provide a written explanation.]

Notes:
1. The authors request that you please restrict circulation of this manuscript to the following persons at this time: authors, internal reviewers, journal editor, journal reviewers, and, if warranted, journal office for publication processing.
2. This manuscript is formatted for Bioelectromagnetics

PUBLICATION 24 (continued)

ABSTRACT

Ultrastructure of the medium-sized "spiny" neuron in rat dorsal-lateral caudate-putamen was assessed after administration of 3-nitropropionic acid (3-NP) and exposure to pulsed microwaves. Sprague-Dawley male rats were given two daily intraperitoneal doses of 0 or 10 mg/kg 3-NP and at 1.5 h after each dose exposed to microwave radiation at whole-body averaged specific absorption rate (SAR) of 0 (sham exposure), 0.6, or 6 W/kg for 30 min. Microwave exposure consisted of 1.25-GHz radiation delivered as 5.9-μs pulses at repetition frequency 10 Hz. Tissue samples taken 2-3 h after the second sham or microwave exposure examined with light-microscope methods showed no injury. Blinded qualitative assessment of ultrastructure of randomly selected neurons from the same samples did reveal differences. Subsequent detailed, quantitative measurements showed that, when followed by sham exposure, administration of 3-NP significantly increased endoplasmic reticulum (ER) intracisternal width, ER area density, and nuclear envelope thickness. Microwave exposure at 6 W/kg alone also significantly increased these measures. Exposure of 3-NP-treated animals at 6 W/kg significantly increased effects of 3-NP on ultrastructure. Although exposure at 0.6 W/kg alone did not affect ultrastructure measures, exposure of 3-NP-treated animals at 0.6 W/kg reduced the effects of 3-NP. We concluded that 3-NP changed neuronal ultrastructure and that the microwave exposures used here changed neuronal ultrastructure in ways that depended on microwave SAR and neuron metabolic status. The apparent cancellation of 3-NP-induced changes by exposure to pulsed microwaves at 0.6 W/kg indicated the possibility that such exposure can protect against the effects of mitochondrial toxins on the nervous system.

Key Words:

Sprague-Dawley rats	chemical hypoxia	stereology
endoplasmic reticulum	nuclear envelope	mitochondria
striatum	electron microscopy	

PUBLICATION 24 (continued)

INTRODUCTION

Because electromagnetic fields at microwave frequencies are used in military operations for communication, detection, and countermeasure purposes [DeFrank et al., 1993; Williamson, 1997; Streetly, 2001], they constitute an environmental factor for military personnel. The potential of these fields to cause neuronal injury is supported by reports of neuropathology and changes in neuronal ultrastructure found in animals exposed to microwaves [Baranski, 1972; Tolgskaya & Gordon, 1973; Albert & DeSantis, 1975; Michaelson, 1986; Albert & Sherif, 1988; Hansson, 1988; Lai, 1994; Somosy, 2000; Salford et al., 2003]. Although some of the findings can be attributed to elevated tissue temperature resulting from sufficiently high specific absorption rate (SAR) and/or sufficiently long exposure, heating by absorption of microwave energy does not fully explain all findings. Reports indicating that exposure to microwaves can lead to oxidative stress and free radical production in biological systems [Phelan et al., 1992; Philippova et al., 1994; Kalns et al., 2000] and altered brain energy metabolism [Sanders et al., 1985; Lai, 1994] support the idea that microwaves can act through or on normal mechanisms of cell injury, possibly in ways that do not depend on gross heating of tissue.

Military personnel can be subjected to a variety of environmental factors of different types in the performance of duties [Deeter & Gaydos, 1993; Sidell et al., 1997; Joellenbeck et al., 1999; Eldridge, 2001]. These factors include toxic chemical compounds used as pesticides, herbicides, or nerve agents that can lead to nervous system injury. Because more than one of these environmental factors may be encountered, the effect of factors acting in combination must be considered [NAS, 1996; Joellenbeck et al., 1999]. In addition, neuronal injury can be caused or enhanced by tissue hypoxia resulting from chemical exposure, hypoxic conditions, physical exertion, and blood loss. Susceptibility of neurons to injury can also be increased by psychological stress and physical trauma. The ever-present microwave

PUBLICATION 24 (continued)

electromagnetic fields could possibly interact with effects of the various factors and their modifiers.

An established model for investigating effects of environmental factors on the central nervous system is the mammalian striatum, a part of the basal ganglia, which is sensitive to compromised energy metabolism due to ischemia, hypoxia, hypoglycemia, and neurotoxins [Petito & Pulsinelli, 1984; Beal, 1992; Alexi et al., 1998b; Albin, 2000; Calabresi et al., 2000]. Most sensitive to insult are the medium-sized spiny neurons of the striatum, so called because of their densely packed dendritic spines, that account for more than 90% of striatal neurons [Calabresi et al., 2000; Pollack, 2001] and transmit neural signals to other parts of the brain using the neurotransmitter GABA (γ-aminobutyric acid) [Beal et al., 1993b; Calabresi et al., 1998; Mitchell et al., 1999]. The human striatum is known to be susceptible to injury, as seen in global ischemia, neurotoxicity, and Huntington's disease [Brouillet et al., 1999; Mitchell et al., 1999; Calabresi et al., 2000; Albin, 2000] and, possibly, factors experienced during certain military service [Haley et al., 2000]. Regardless of the particular initial cause or causes of injury, a number of mechanisms are common in neuronal injury [Alexi et al., 1998b; Budd, 1998; McIntosh et al., 1998; Vécsei et al., 1998; Heales et al., 1999]. These mechanisms include oxidative stress, free radical production, nitric oxide production, increased intracellular calcium, and N-methyl-D-aspartate (NMDA) receptor activation.

In the study reported here, we used 3-nitropropionic acid (3-NP) in a rat model of striatal neurodegeneration [Brouillet et al., 1999] to investigate possible combined effects of 3-NP-induced chemical hypoxia and microwave exposure in the rat caudate-putamen. This mitochondrial toxin irreversibly inhibits succinate dehydrogenase (SDH) in the brain [Gould & Gustine, 1982; Gould et al., 1985; Alexi et al., 1998a,b; Brouillet et al., 1998; Wiegand et al., 1999; Dautry et al., 2000; Garcia et al., 2002; Bizat et al., 2003]. This reduces production of adenosine triphosphate (ATP) [Beal et al., 1993b; Matthews et al., 1998] and the resulting

PUBLICATION 24 (continued)

interruption in energy metabolism can trigger oxidative stress, nitric oxide production, and NMDA receptor activation and consequently lead to neuronal cell death [Beal et al., 1993a, 1995; Wüllner et al., 1994; Schulz et al., 1995, 1996; Alexi et al., 1998b; Brouillet et al., 1999; Wiegand et al., 1999; La Fontaine et al., 2000]. The caudate-putamen has been found to be the most susceptible site for 3-NP injury in rats [Hamilton & Gould, 1987; Beal et al., 1993a; Borlongan et al., 1995a,b; Guyot et al., 1997; Alexi et al., 1998a,b; Garcia et al., 2002], primates [Brouillet et al., 1995, 1999; Dautry et al., 2000], and humans [Ludolph et al., 1991; Brouillet et al., 1999]. We studied the dorsolateral caudate-putamen because of its known greater susceptibility to 3-NP [Guyot et al., 1997; Sugino et al., 1997; Vis et al., 1999; Dautry et al., 2000; Ouary et al., 2000; Blum et al., 2002; Garcia et al., 2002] by examining ultrastructure of the medium-sized spiny neurons in this part of the striatum that, as for other types of injury, are the most susceptible to 3-NP [Beal et al., 1993a,b; Brouillet et al., 1993, 1995; Vis et al., 1999].

We used 30-min microwave exposures with SARs of 0.6 W/kg, which does not elevate body temperature, and 6 W/kg, which elevates body temperature [Lotz & Michaelson, 1978; Gordon et al., 1986; D'Andrea & de Lorge, 1990]. Exposure at SAR of 6 W/kg also disrupts ongoing behavior of animals [D'Andrea & de Lorge, 1990]. Effects of the experimental protocol on spontaneous motor activity, acoustic startle, and histology of the caudate-putamen at the light microscope level have been previously described [Seaman et al., 2004]. Here, we report on the ultrastructure of caudate-putamen neurons from a subset of animals used in that study. Neuronal ultrastructure was initially assessed qualitatively. Findings using this approach motivated quantitative measurements of dimensions of somatic mitochondria, endoplasmic reticulum (ER), and nuclear envelope (NE), which are known to reflect cell injury and its progress [Söderfeldt et al., 1981; Petito & Pulsinelli, 1984; Kalimo et al., 1985; Trump & Berezesky, 1998; Lin et al., 1999; Schmechel, 1999; Martin et al., 2000]. We report findings

PUBLICATION 24 (continued)

here from more animals than in our preliminary reports[1]. In addition, the ER has been further characterized by unbiased two-dimensional stereology.

Because cellular injury had been reported to result from both microwave exposure and 3-NP administration, we expected to find that effects of microwave exposure combined with 3-NP administration were greater than effects of the exposure or 3-NP alone. We found that this was the case for exposure at 6 W/kg but that exposure at 0.6 W/kg counteracted effects of 3-NP on the measured endpoints.

---

[1] (1) Seaman RL, Phelix CF. 2001. Changes in ultrastructure of rat caudate-putamen neurons with a neurotoxin and exposure to pulsed microwaves. Abstracts of European Bioelectromagnetics Association (EBEA) 2001: 420-421. (2) Seaman RL, Phelix CF. 2001. Acute changes in rat caudate-putamen neuronal ultrastructure due to 3-nitropropionic acid and microwave exposure are not reflected in behavior. Abstracts of Society for Neuroscience Annual Meeting 31: 892.

PUBLICATION 24 (continued)

MATERIALS AND METHODS

Animals

The 20 male Sprague-Dawley rats (Charles River Labs, Portage, Michigan) used for ultrastructure were 16-24 weeks of age and weighed 580±45 g (mean±SD) at the start of experimental procedures. They were a subset of animals for which behavior was measured after treatments. After delivery from the vendor and 10-day quarantine, animals were housed individually in polycarbonate shoebox cages in a room having 22±1°C temperature, 50±5% relative humidity, 10-15 hourly air exchanges, and a 12/12 light/dark cycle with lights-on either from 0500 to 1700 or from 0600 to 1800. Purina rodent chow and tap water were provided *ad libitum*. Intraperitoneal (IP) injections of 10 mg/kg 3-nitropropionic acid (Sigma-Aldrich, St. Louis, USA) or sterile 0.9% saline (0 mg/kg) were given. The 3-NP solutions were prepared in sterile distilled water with pH adjusted to 7.4 with 1 N NaOH and used within two weeks.

In conducting this research, the investigator(s) adhered to the "Guide for the Care and Use of Laboratory Animals," prepared by the Institute of Laboratory Animal Resources, National Research Council (Washington, DC: National Academy Press, 1996). The U.S. Air Force Research Laboratory (AFRL) at Brooks City-Base is fully accredited by the Association for Assessment and Accreditation of Laboratory Animal Care, International (AAALAC). The AFRL-Brooks Institutional Animal Care and Use Committee had approved all animal procedures.

Microwave exposure and dosimetry

Microwave exposure and dosimetry were carefully characterized [Seaman et al., 2004]. For exposure to microwave radiation, animals were put in a well-ventilated clear plastic holder that minimally restricted animal movement. As diagrammed in Fig. 1, the holder was placed in front of the open end of a WR-650 waveguide used as an antenna inside a microwave anechoic chamber, where the air temperature was 23.0±0.7°C (mean±SD). A table made of

PUBLICATION 24 (continued)

STYROFOAM® supported the holder at one of the two positions shown in Fig. 1. The center of the holder was at the same height as the center of the waveguide in both positions. The waveguide antenna was connected to a General Electric FPS-7B radar transmitter that generated 5.9-μs pulses at microwave frequency 1.25-GHz, both parameters being fixed by permanent transmitter components. Pulse repetition frequency was selected after balancing trade-offs among applying pulses at a low, physiologically relevant frequency, utilizing a higher repetition frequency in the range of normal transmitter operation, having low pulse-to-pulse variability, and delivering desired SARs to animals. The selected repetition frequency of 10 Hz allowed stable transmitter performance while being within the range of electroencephalograph (EEG) frequency spectra of awake rats [e.g., Mandile et al., 2003; Vorobyov et al., 2003].

Whole-body averaged SAR was set to 0.6 or 6 W/kg by placing the holder with its center at 85 or 30 cm, respectively, from the antenna and setting average net microwave power to the antenna by adjusting pulse peak power at the transmitter. The SAR measured in carcasses and anesthetized animals exposed to continuous wave (CW) microwaves [Seaman et al., 2004] was in agreement with SAR calculated for rats of the size used [Durney et al., 1986]. Peak power and duration of microwave pulses were checked ten times during each exposure. Procedures were the same for sham-control exposures except that microwave pulses were not generated and the SAR was 0 W/kg,

Procedure

Animals in the behavioral study, among which were the 20 animals here, were assigned in sequence to one of six 3-NP-microwave (mg/kg-W/kg) conditions: 0-0, 0-0.6, 0-6, 10-0, 10-0.6, and 10-6, each consisting of injections on two consecutive days and microwave exposure after each injection [Seaman et al., 2004]. Conditions were delivered in random sequence within each series of six animals and all conditions were completed for a series before starting the next series. On the day before its first treatment described below, an

PUBLICATION 24 (continued)

animal was familiarized with procedures by being placed in the animal holder in the anechoic chamber for 20-30 min and having its colonic temperature measured with a YSI 423 temperature probe. Also on this day, an animal was tested for acceptable motor activity and placed in the holder used for acoustic startle testing for 10-20 min.

On the first day of treatment, an animal was injected with saline or 10 mg/kg 3-NP 3-5.5 h after the lights turned on in the light/dark cycle of the animal room. One hour after injection, colonic temperature was measured, the animal was placed into the animal holder, and the holder was placed in front of the open-ended waveguide at one of the two positions shown in Fig. 1. After 30 min, exposure at 0, 0.6, or 6 W/kg SAR was started, with 1.5 h elapsed since injection. When exposure was terminated 30 min later, the animal was removed from the animal holder and colonic temperature was again measured.

On the second day of treatment, the procedure of the first day was repeated with the same 3-NP dose and microwave SAR for a given animal. In addition, the animal was tested for motor activity and acoustic startle starting 1.5-2.5 h after exposure, or 3.5-4.5 h after the second injection. Results reported here were obtained from 20 animals that were perfused 2-3 h after exposure to microwaves (4-5 h after injection) on the second day of treatment with 3, 3, 3, 3, 4, and 4 animals for conditions 0-0, 0-0.6, 0-6, 10-0, 10-0.6, and 10-6, respectively.

Histology

Tissues for histological evaluation were taken from animals perfused under deep anesthesia induced with IP injection of ketamine and xylazine. After the descending aorta was clamped, the animal was perfused transcardially with 100 ml of 4% paraformaldehyde in sodium acetate buffer at pH 6.5. This was followed by 500 ml of 4% paraformaldehyde and 0.05% glutaraldehyde in sodium bicarbonate/carbonate buffer at pH 10.0. A coronal slab 0.9 mm thick was cut from the brain between approximate anterior-posterior stereotaxic coordinates of bregma +0.4 to +1.7 mm [Paxinos & Watson, 1986]. A unilateral sample of

PUBLICATION 24 (continued)

dorsolateral caudate-putamen was obtained by punching a 5-mm annulus through the slab, leaving the contralateral caudate-putamen in the slab intact for examination by light microscope. The circular brain sample obtained from the punch was placed in the glutaraldehyde fixative for later analysis by electron microscopy. The remainder of the brain and samples of heart, lung, and liver tissues were placed in 10% buffered formalin for evaluation by light microscopy [Seaman et al., 2004]. Only animal number identified samples so that persons assessing tissue did not know experimental conditions.

Coded samples for electron microscopy were embedded in generic Epon812 plastic. Full block face sections were cut at 1 □m and evaluated after staining with toluidine blue. Ultrathin sections were collected on formvar-coated nickel grids and counter stained with lead citrate and uranyl acetate. Digitized images of random fields of view were captured at 4,000X or 7,000X magnification using a Philips 208 S transmission electron microscope. The fields were chosen such that they included cell bodies (somata) of medium-sized spiny neurons identified by their somata of 10-20 μm, nuclei without indentation, and large ratio of nuclear area to soma area [Chang & Kitai, 1982; Kita & Kitai, 1988; Calabresi et al., 2000]. Affected medium-sized spiny neurons were often found in clusters that did not seem to depend on distance between somata boundaries in the electron microscope images. Although not included in our study, somata identified as belonging to large, aspiny neurons on the basis of their large size and small, indented nuclei [Chang & Kitai, 1982; Kita & Kitai, 1988] were occasionally observed. Ultrastructure of these large neurons always appeared normal. Using these procedures, we recorded images of 2-11 medium-sized spiny neurons per animal, as listed by experimental condition in Table 1.

Evaluation of neurons proceeded from initial qualitative assessment of ultrastructural appearance of membranes and subcellular organelles to quantitative morphometric measures. Qualitative assessment was made by examination of printed copies of the digitized images.

PUBLICATION 24 (continued)

Neurons were assigned to two categories of appearance: affected or not affected. Neurons were categorized as affected if one or more of the following criteria were met: cistern of ER profiles distinctively evident; ER profiles with erratic distribution (e.g., elongation); NE margin with irregular delineation; and cytoplasm showing dispersion or disappearance of ribosomes and polyribosomes, i.e., dissolution of Nissl substance. Because not every image included Golgi apparatus, likely due in part to its poor development in medium-sized spiny neurons [Chang & Kitai, 1982], its change in structure could not be used in every case. The affected category was further subdivided into mild and severe depending on the degree of alteration from known normal ultrastructural appearance of striatal medium-sized spiny neurons.

Quantitative measurements of selected features were made on digitized 7,000X images by using Image Tool software (University of Texas Health Science Center at San Antonio) calibrated using standard calibration bars from the Philips 208 S. Measurements were made to assess intralumenal width of ER, short-axis diameter of mitochondria, and thickness of NE. From randomly selected areas of interest within the soma of each neuron, ER segments with the most obvious cisternae were measured first. Intracisternal width of rough endoplasmic reticulum (RER) was measured from membrane to membrane, excluding ribosomes to avoid bias due to absence of ribosomes on the ER membrane in some affected cells. New areas of interest were used until five ER profiles had been measured for a neuron. The smallest diameters of mitochondria in the same or nearby areas as measured ER were then determined. Thickness of the NE was measured at five separate locations as the perinuclear space, the distance between the two lipid layers separating the nucleus from cytoplasm and normal to the layers. In this way, five measurements were made of each dimension in each neuron to give 10-55 measurements of each dimension per animal. As a result, 535 individual measurements were made across experimental conditions for each dimension (Table 1).

PUBLICATION 24 (continued)

Unbiased stereological assessment of ER area density was performed on the digitized 7,000X images using standard techniques [Gundersen et al. 1988; Russ & Dehoff, 2001]. A grid of regularly spaced cross hairs was superimposed on the entire neuron image. The total number of cross hair intersections that fell within the cytoplasm, exclusive of the nucleus, was counted manually using Image Tool. The number of cross hair intersections that fell on ER profiles was similarly counted. Area density was calculated as the ratio of ER counts to cytoplasm counts.

Data analysis

Experimental conditions were designated by 3-NP dose and microwave SAR as described above. Chi-square tests for independence were used on a contingency table and its subdivisions to test for differences in proportions of affected neurons. The table had 2 rows (affected and unaffected) and 6 columns (3-NP-microwave conditions). Organelle dimensions and area density were averaged over neurons so as to obtain a value of each variable for each animal to provide equal weighting of data from each animal in statistical testing. Mean and median for dimension and density variables were tabled by 3-NP-microwave condition. A rank-sum Kruskal-Wallis test (a nonparametric one-way analysis of variance, or ANOVA), was used on each variable to test for a significant difference among experimental conditions. Nonparametric Newman-Keuls multiple comparisons followed Kruskal-Wallis ANOVAs that indicated presence of a significant difference. Statistical testing was done with GB-STAT software (v5.4, Dynamic Microsystems, Silver Spring, MD) with a (two-tailed) significance level of 0.05 in all tests.

PUBLICATION 24 (continued)

RESULTS

Change in colonic temperature resulting from sham or microwave exposure was computed as the post-exposure temperature minus the pre-exposure temperature. For exposures at 0 (sham) and 0.6 W/kg, the mean change ranged from –0.7 to +0.5°C. For exposures at 6 W/kg, the change ranged from +2.8 to +3.9°C, with colonic temperature of 38.2-40.9°C after exposure. The ranges corresponded respectively to –0.58 to –0.15°C and +2.43 to +3.05°C observed in the behavioral study with 11 animals in each experimental group from which the animals here were drawn [Seaman et al., 2004]. Statistical testing of the larger dataset of temperature changes from all animals was done across the six 3-NP-microwave conditions with Friedman ANOVA followed by Newman-Keuls multiple pair-wise comparisons. The testing showed that temperatures changes at 0 and 0.6 W/kg were not different from each other for different 3-NP doses, SARs, or treatment days, and were not different from zero. The testing also showed that all temperature changes at 6 W/kg were greater than zero but were not different from each other for different 3-NP doses and treatment days. At 0 and 0.6 W/kg, the sleeping, resting, grooming, and/or exploring by the animal indicated lack of thermal stress during exposure. At 6 W/kg, animals were obviously heat stressed, becoming progressively more active and grooming more frequently during exposure. Stress during exposure at 6 W/kg was also indicated by greater urination and defecation than during exposure at 0 or 0.6 W/kg [Seaman et al., 2004].

Light microscopic examination of the dorsolateral caudate-putamen contralateral to the circular punch was performed on paraffin-embedded sections of the 0.9-mm brain slab stained with hematoxylin and eosin (H&E). Plastic-embedded sections of the circular punch stained with toluidine blue were also examined by light microscopy. In general, results were unremarkable across experimental conditions, with all neurons appearing normal at this level of examination, which was consistent with earlier observations [Seaman et al., 2004].

PUBLICATION 24 (continued)

Qualitative analysis of ultrastructure

Examination of electron micrographs of striatal medium-sized spiny neurons revealed structural differences at the subcellular level not evident with the light microscope. Representative images for the six experimental conditions are shown in Figs. 2-7. The most prominent ultrastructural distinctions, collectively identified as peripheral washout of cytoplasm, seen in Figs. 4 and 7 were observed only in the two groups of animals exposed at 6 W/kg. Equally remarkable was a greater incidence of discontinuous (Fig. 3) and continuous (Fig. 6) segments of ER, these figures representing neurons from animals exposed at 0.6 W/kg. Because these ER segments were outlined with numerous ribosomes and had slightly dilated lumina this was considered as proliferation of RER. The degree of ER dilation was gradated beyond this recognizable extent to an extreme state as seen in Figs. 4 and 7 and an intermediate state seen in Fig. 5. Extreme dilation was typically accompanied by degranulation wherein the ribosomes were dissociated from the ER membrane [Somosy, 2000]. Dilations of the NE perinuclear space [Somosy, 2000] were observed in several neurons (e.g., Figs. 4 & 7).

The general appearance of the cytoplasm showed a remarkable change in polysome (Nissl substance) that was noted on a gradated scale: numerous (Fig. 2), zones of sparsity (Figs. 3, 5, and 6), and considerable to extensive dissolution resulting in translucency (Figs. 4 and 7). This latter condition was seen predominantly with the peripheral washout state. Overt differences or abnormalities in mitochondria and plasma membrane were rarely observed.

The fraction of affected neurons for each treatment group was determined by using the qualitative ultrastructural assessment. That is, each neuron was rated as being normal, showing mild affect, or showing severe affect based on integrity of cytoplasm, mitochondria, ER, nucleus, and membranes. The numbers and fractions of neurons judged to display mild or severe affect are listed by experimental condition in Table 2. For the 0 mg/kg 3-NP conditions 0-0, 0-0.6, and 0-6, the fraction of affected neurons progressively increased with microwave

PUBLICATION 24 (continued)

SAR: 15, 43, and 71%, respectively. Neurons rated as affected for conditions 0-0 and 0-0.6 were all in the mild-affect category. For the 10 mg/kg 3-NP conditions 10-0 and 10-6, the fraction of affected neurons was larger than for the 0 mg/kg 3-NP conditions, with all neurons (100%) exhibiting affect for condition 10-6. However, the fraction for 10 mg/kg 3-NP at 0.6 W/kg (condition 10-0.6) was smaller than for conditions 10-0 and 10-6, being about one-third of these values and falling between values for conditions 0-0 and 0-0.6. A chi-square test for independence of all conditions indicated a significant difference among them ($p<.0001$). Separate chi-square tests of the respective three conditions for 0 mg/kg 3-NP and 10 mg/kg indicated a significant difference with microwave SAR for each 3-NP dose ($p=.0048$ and $p<.0001$, respectively). Subsequent chi-square tests on pairs of conditions gave the significant differences indicated in Table 2. Note that the fraction for condition 10-0.6 was significantly smaller than fractions for conditions 10-0, 10-6, and 0-6 but not different from fractions for conditions 0-0 and 0-0.6.

Quantitative analysis and morphometrics of ultrastructure

Measured dimensions of mitochondria, ER, and NE appearing in micrographs gave the morphometrics in Table 3. The representative neuron for condition 0-0 in Fig. 2 was considered normal in appearance. The cytoplasm contained numerous mitochondria that were elongated or oval with a mean short axis diameter of approximately 400 nm; a few short segments of ER were present and outlined with ribosomes; and numerous rosettes of polyribosomes, Nissl substance, were present throughout the cytoplasm. The lumen or cistern of the ER segments was barely distinguishable at mean intracisternal width of 38 nm, as was the NE perinuclear space with mean of 28 nm. The NE was intact and continuous and nuclear pores were occasionally observed. The chromatin was dispersed throughout the nucleus with typical euchromatin and heterochromatin arrangements. Aberrations, such as ER with more

PUBLICATION 24 (continued)

prominent lumina, were rare for condition 0-0, as reflected in the small fraction of affected cells for this condition (Table 2).

Representative electron micrograph images of neurons for conditions 0-0.6 and 10-0.6 are shown in Figs. 3 and 6, respectively. Neurons in these two groups were quite similar in the degree of change, which was considered mild affect because of the more evident ER lumina. Although a tendency for increased ER intracisternal width relative to condition 0-0 was apparent in the two conditions, these widths were not significantly different from the 0-0 width. A second characteristic difference in appearance of the ER in neurons from these two groups was the greater prevalence of ER segments. However, area density of ER in neurons from the 0-0.6 group exhibiting discontinuous ER segments (Fig. 3) and in neurons from the 10-0.6 group exhibiting more, but continuous, ER segments (Fig. 6) were both not significantly different from the 0-0 area density. Both intracisternal width and area density of ER in the 10-0.6 group were significantly smaller than for 3-NP and microwave exposure at 6 W/kg (condition 10-6). Mitochondria diameter and NE thickness for conditions 0-0.6 and 10-0.6 were not significantly different from the respective 0-0 dimension.

Representative electron micrograph images of neurons for conditions 0-6, 10-0, and 10-6 are shown in Figs. 4, 5, and 7, respectively. In general, neurons from the 3-NP-only group (condition 10-0), showed robust changes in ER intracisternal width from the normal condition 0-0, more than doubling on average: 89 nm vs. 38 nm. In our study, this larger ER was taken to indicate mild affect, between the slight dilation in the 0-0.6 group and the more extensive dilation in the 0-6 and 10-6 groups. However, unlike changes seen in conditions 0-0.6 and 10-0.6, there was no apparent change in the presence of ER segments in the 10-0 group (Fig. 5). Two-thirds of neurons in the 0-6 group appeared similar to those in the 10-0 group; whereas, the other one-third in the 0-6 group showed significant peripheral washout. This pattern was reversed in the 10-6 treatment group in which two-thirds of the neurons

PUBLICATION 24 (continued)

showed peripheral washout. In those neurons in the 0-6 and 10-6 groups with moderate ER dilation, i.e., without washout, the number of ER segments also increased. In neurons with peripheral washout, ER was extensively dilated with maximum intracisternal widths of 500-700 nm and, even within the perinuclear rim of less disrupted cytoplasm, vesiculated (Figs. 4 & 7). The other major effect of exposure at 6 W/kg with or without 3-NP (conditions 0-6 and 10-6) was the greater NE thickness, which was approximately double the NE thickness for the 0-0 group but similar to that for the 10-0 group. This effect on perinuclear space is evident in Figs. 4 & 7. Otherwise, neurons in the 0-6 and 10-6 groups showed the most prominent degranulation of ER and dispersion of polysomes. Disruption of inner mitochondrial membrane and cristae was seen most often in neurons with peripheral washout in the 0-6 and 10-6 groups, but the size of visible mitochondria was similar to that for other experimental conditions.

Measured dimensions are summarized in Table 3 for all experimental conditions. Mitochondria for microwave exposure-only conditions 0-0.6 and 0-6, were smaller than for control condition 0-0 by 6-14%. Mitochondria for conditions 10-0, 10-0.6, and 10-6 with 3-NP tended to be even smaller: 12-30% less than for the control condition. However, these differences were not significant ($\chi^2(5)=4.07$, $p=.54$).

The ER intracisternal width was different for the different 3-NP-microwave conditions. The widths and corresponding ER area densities had a similar pattern across conditions. The width for microwave-only condition 0-0.6 was slighter larger than the width for control condition 0-0 while the width for microwave-only condition 0-6 was 2.5-3.5 times larger. The width for 3-NP-only condition 10-0 was about 2.5 times the width for condition 0-0. With the addition of microwave exposure at 6 W/kg in condition 10-6 the width was even larger, larger than for any other condition. But with the addition of exposure at 0.6 W/kg to 3-NP administration in condition 10-0.6 the width was less than 2 times the control width. A significant difference

PUBLICATION 24 (continued)

between conditions was indicated ($\chi^2(5)=15.65$, $p=.008$). Multiple comparisons indicated the significant differences shown in Table 3. Note that the three smallest widths, those for conditions 0-0, 0-0.6, and 10-0.6, were not different from each other. This was also the case for the three largest widths, those for conditions 0-6,10-0, and 10-6, each of which was also larger than the width for control condition 0-0. A significant difference was also indicated for the ER area density ($\chi^2(5)=17.19$, $p=.004$). The differences in ER area density between conditions indicated in Table 3 followed a pattern quite similar to that seen for ER intracisternal width, with the exception that densities for conditions 0-0.6 and 0-6 were not different.

The NE thickness for microwave-only condition 0-0.6 was only about 10% larger than the thickness for control condition 0-0 while the thickness for microwave-only condition 0-6 was about 2 times larger. Thicknesses for 3-NP-only condition 10-0 and 3-NP-microwave condition 10-6 were also about 2 times the thickness for control condition 0-0. Thickness for 3-NP-microwave condition 10-0.6 was about 1.5 times that of the control condition. A significant difference in thickness between conditions was indicated ($\chi^2(5)=14.13$, $p=.015$). Multiple comparisons indicated the significant differences in Table 3, which showed a pattern across 3-NP-microwave conditions similar to that for ER intracisternal width and area density. As was the case for the ER variables, NE thicknesses for conditions 0-0, 0-0.6, and 10-0.6 were not different from each other and thicknesses for conditions 0-6, 10-0, and 10-6 were not different from each other. Somewhat different from the ER-variable pattern was the significantly larger NE thickness for the 3-NP-only condition 10-0 relative to the microwave-only condition 0-0.6, as well as to control condition 0-0.

PUBLICATION 24 (continued)

DISCUSSION

Microwave results

Results of this study indicated that whole-body exposure to microwave radiation delivered as 5.9-μs pulses at repetition frequency 10 Hz and at sufficient SAR for 30 min can change the ultrastructure of neurons in the rat caudate-putamen. The changes, seen 2-3 h after the second of two exposures at whole-body averaged SAR of 6 W/kg, consisted of alterations in appearance of neuronal somata in transmission electron micrographs. Measured ER intracisternal width, ER area density, and NE thickness increased with exposure at this SAR while measured size of mitochondria did not change significantly. Peripheral washout of cytoplasm was observed in the most affected neurons after exposures at 6 W/kg. The elevated body temperature and thermal stress experienced by animals exposed for 30 min at 6 W/kg might well have been factors in producing the observed changes in ultrastructure. No statistically significant change in ultrastructure from the control condition was detected after two microwave exposures at 0.6 W/kg, during which colonic temperature did not increase.

Comparison of microwave results here with results of previous studies is made difficult by the differences in brain regions examined, time sequence of microwave exposures, and the many microwave parameters themselves. In addition, information for comparison at the electron microscope level is limited and qualitative in nature. Lesions have been detected in brains of experimental animals by gross and light-microscope examination after exposures that raised body temperature [Tolskaya & Gordon, 1973; Michaelson, 1986; Hansson, 1988]. The clearing of peripheral cytoplasm along with dilation of ER and disappearance of ribosomes seen here after exposures at 6 W/kg was likely similar to the dissolution of ER and polyribosomes reported for some of these exposures. The peripheral cytoplasmic clearing might also be similar to the cytoplasmic swelling with appearance of vacuoles in rat basal

PUBLICATION 24 (continued)

ganglia and hypothalamus after chronic exposures that did not raise temperature [Tolskaya & Gordon, 1973].

Comparison of our findings with neuronal ultrastructure changes in microwave-exposed animals, although limited, shows some interesting consistencies. Vacuoles in cytoplasm, re-arrangement of ER, and paucity of ribosomes observed in neurons of the hypothalamus of Chinese hamsters exposed at 25 mW/cm² (14 h/day, 22 days, 2.45 GHz CW; whole-body averaged SAR of 5 W/kg by our estimate) [Albert & DeSantis, 1975] are qualitatively similar to changes seen here. With the exception of increased thickness of the nuclear membrane in our material, the undisturbed nuclei reported for the hypothalamic neurons are consistent with our observations. The disorderly arrays of rough ER in cerebellar Purkinje cells of neonatal rats exposed at 10 mW/cm² (7 h/day, 5 days, 2.45 GHz CW; whole-body averaged SAR of 2 W/kg by our estimate) [Albert & Sherif, 1988] are also qualitatively similar. Swelling of ER and vacuoles in cytoplasm have also been observed in snail neurons exposed *in vitro* at 12.9 W/kg (1 h, 2450 MHz CW) held at 21°C [Arber et al., 1986]. The common finding of slightly swollen ER among these previous studies of neurons is similar to our finding of discontinuous and continuous segments of ER noted for conditions 0-0.6 and 10-0.6 (Figs. 3 and 6, respectively). The presence of cytoplasmic vacuoles also seems to be a common finding, although the prominence of vacuoles varies among studies and exposure conditions.

Our methods and analyses differed considerably from those employed in a recently reported study [Salford et al., 2003]. Fischer 344 rats were exposed in a transverse electromagnetic transmission (TEM) cell for 2 h to signals from a GSM (Global System for Mobile Communications) mobile phone. With presumed operating frequency near 900 MHz, their highest whole-body SAR, 0.2 W/kg, was not that different than our lowest SAR of 0.6 W/kg. Tissue samples were taken 50 days after the exposure and brain sections were stained with cresyl violet. Several instances of neuronal damage were observed in the form of

PUBLICATION 24 (continued)

"dark" neurons throughout the brain. We did not see such damage in our material taken on the same day as the last microwave exposure and processed similarly except for the use of H&E staining. Because of the many differences between this earlier study and the study here, identifying the cause or causes of the seemingly different results is difficult.

We can reasonably expect that microwave electromagnetic fields inside the animal during exposure, including those in the caudate-putamen, were not in any fixed pattern that would lead to differences in affect of the medium-sized spiny neurons studied. The fields in an exposed animal are strongly dependent on animal size and orientation [Guy et al., 1979; Chou et al., 1985] so that movement, especially movement of the head, would have changed the fields in the head during exposure. Although, as reflected in the fractions in Table 2, medium-sized spiny neurons were not all affected to the same degree by treatment. Because these differences in affect were seen for conditions with and without microwave exposure, they cannot readily be ascribed to differences in microwave field pattern. The normal somata of large aspiny neurons could possibly be thought of as delineating regions of injury, but the lack of effect on these neurons is readily explained by the much greater susceptibility of medium-sized spiny neurons to injury, as described in the introduction. Although the clusters of injured neurons observed in our material might initially be interpreted as reflecting a novel pattern, clustering of injured neurons in rat caudate-putamen has also been noted in studies without microwave exposure [Mitchell et al., 1999; Keene et al., 2001]. The clustering of affected neurons could well be due to clustering of spiny neuron subtypes with different properties [Kawaguchi, 1997; Calabresi et al., 1998, 2000; Pollack, 2001]. For these various reasons, we attributed the clustering of affected neurons here to intrinsic characteristics of the animal model itself and not to patterns of absorbed microwave energy.

The changes in ultrastructure seen here are similar in some respects to changes seen in rats that develop heat stress symptoms as a result of being exposed to 38°C ambient

temperature for 4 h [Sharma et al., 1998]. Neuronal ultrastructure was studied in a number of brain regions after the induced heat stress but not in the caudate-putamen. The animals had a mean rise in colonic temperature of 3.64°C, similar to the change during exposure to 6 W/kg for 30 min here. The common finding of vacuoles in the cytoplasm of neurons in the heat-stressed animals is qualitatively similar to our findings of changes in ER and clearing of cytoplasm after 10 mg/kg 3-NP, microwave exposure at 6 W/kg, and their combination. Irregular folding of the nuclear membrane, degenerating nucleolus, and dark material in cytoplasm and nucleus observed in heat-stressed animals were not seen in our material. These more extreme responses could be due to the longer duration of elevated body temperature during the 4-h exposure to heat or, less likely, to the different brain regions studied.

3-NP results

Our results indicated that two injections of 10 mg/kg 3-NP were capable of changing ultrastructure in rat caudate-putamen neurons sampled at 4-5 h after the second injection. The increased ER intracisternal width and area density seen here is consistent with increased cytoplasmic lucency, dissolution of ribosomes, and dilatation of ER seen in caudate-putamen neurons mildly affected by LD_{50} doses of 140 mg/kg 3-NP in mice [Gould & Gustine, 1982] and in early stages of animal recumbency after 30 or 40 mg/kg 3-NP in rats [Hamilton & Gould, 1987]. Swollen mitochondria were seen in the more severely affected neurons in the mice and in rats during later stages of recumbency in these studies. Repeated daily injection of 10 mg/kg 3-NP in rats over 28 days also results in "markedly swollen striatal mitochondria", with abnormal structure [Keene et al., 2001]. The enlarged mitochondria seen in each of these previous studies were not seen here. The small, and statistically not significant, decrease in mitochondrial size observed here contrasts with the previous observations and was likely due to the smaller amount of 3-NP administered and/or the shorter time until tissue sampling.

PUBLICATION 24 (continued)

Neuronal damage and potential recovery

The changes in neuronal subcellular structure observed here would certainly be expected to compromise function of each affected organelle to some degree. Because of the significant change in ER ultrastructure for experimental conditions with 3-NP at 10 mg/kg, microwave exposure at 6 W/kg, or their combination, we expect disturbances in ER function for those conditions. Response of the ER in various cell types, including neurons, to other types of cell injury includes release of stored calcium, incorrect processing of proteins, and activation of proapoptotic and antiapoptotic factors [Paschen & Doutheil, 1999; Paschen & Frandsen, 2001; Verkhratsky & Petersen, 2002; Breckenridge et al., 2003]. The frequently observed dispersion of cytosolic ribosomes and polyribosomes in our material, another indication of disturbed protein synthesis, has been linked to depletion of the ER calcium store [Paschen & Doutheil, 1999]. However, the changes in ultrastructure revealed through the sensitive electron microscope methods used here were not necessarily severe enough to change nervous system information processing, or lead to permanent change or cell death.

Because the medium-sized spiny neurons of the caudate-putamen studied here are among neurons that are the most susceptible to different types of injury [Calabresi et al., 1998; Mitchell et al., 1999], they can be expected to respond to injury at low levels of insult. These features of the neurons studied and the method used to study them provided a useful test for action of microwaves, 3-NP, and their combination at the cellular level. But changes detected using this approach do not directly indicate dysfunction. Indeed, motor activity and inhibition of acoustic startle, two behaviors that involve the caudate-putamen, were largely unchanged by the two 10 mg/kg 3-NP doses with or without microwave exposures at 0.6 and 6 W/kg SAR [Seaman et al., 2004]. The lack of change in startle inhibition at this 3-NP dose was consistent with results of previous studies [Kodsi & Swerdlow, 1997; Seaman, 2000]. No change seen in ultrastructure here was judged to be irreversible. This is consistent with previous microwave

studies in which all but the most severe lesions were reversed in the sense that lesions were not found if enough time had elapsed after exposure to microwaves [Tolskaya & Gordon, 1973; Albert & Sherif, 1988]. This is also consistent with the 3-NP dose used here being smaller in individual and cumulative doses than those used to induce brain lesions and changes in animal locomotion [Wüllner et al., 1994; Borlongan et al., 1995a,b; Schulz et al., 1995; Guyot et al., 1997; Brouillet et al., 1998; Ouary et al., 2000; Blum et al., 2002; Bizat et al., 2003].

A separate indicator of potential recovery of neurons with the ultrastructural changes observed here was the absence of damage to the outer cell membrane. Rupture and distortion of the cell membrane is an early hallmark of lethal cell injury [Trump & Berezesky, 1998]. Even in the most severely affected neurons here (e.g., Figs. 4 & 7) no break in the cell membrane was detected that could not be attributed to variation in tissue preparation. Likewise, no damage was seen that might have resulted from a ruptured cell membrane such as caused by a large calcium influx.

Mitochondria with unchanged or smaller size have been seen in cortex and caudate-putamen of ischemic and hypoglycemic animals [Kalimo et al., 1977, 1985] and are known to occur in early stages of cell response to injury [Trump & Berezesky, 1998; Schmechel, 1999]. The somewhat smaller mitochondria observed here after 3-NP treatment were consistent with early cell response to injury or response to a mild stressor. Thus, the finding of smaller mitochondria was compatible with the idea of reversibility of the changes in neuronal ultrastructure.

Microwave-3-NP results

One might initially attribute the apparent opposing action of microwave exposure at 0.6 W/kg on the effects of 3-NP on ultrastructure to accelerated metabolism or detoxification of 3-NP possibly occurring outside the brain. However, because inhibition of SDH has reached a

plateau or peak 1-3 h after 3-NP injection [Brouillet et al., 1998; Nony et al., 1999; Wiegand et al., 1999; Bizat et al., 2003] and because plasma 3-NP level drops substantially after 2 h [Schulz et al., 1996], alteration of detoxification processes by the microwave exposures, which occurred 1.5-2 h after injection, was unlikely. That the cancellation of 3-NP effect occurred after microwave exposure at 0.6 W/kg, which did not raise body temperature can be used to argue for an opposing action that is not dependent on raised temperature due to heat production. The cancellation of 3-NP effect by 0.6 W/kg might instead represent opposing actions on the same energy-metabolism or cell-injury pathways by 3-NP and microwave exposure at this SAR level.

The seemingly synergistic effect of 3-NP and microwave exposure at 6 W/kg was suggestive of similar action on organelles. The action of 3-NP is to disrupt ATP production through inhibition of SDH, as reflected by lower levels of SDH activity [Alexi et al., 1998b; Brouillet et al., 1998; Nony et al., 1999]. We would expect that an action that enhances the inhibition of SDH by 3-NP or that reduces ATP production by other means would be synergistic with 3-NP action. Exposure to microwaves has been observed to cause such an effect. Reduced SDH activity has been observed in guinea pig brain after a single 3-h exposure to pulsed or CW microwaves that did not cause an increase in body temperature (whole-body averaged SAR of 0.7 W/kg by our estimate) [Baranski, 1972]. Reduced ATP has been observed in rat brain during 5-min microwave exposure at brain SAR of 2.5 W/kg with the change being similar in magnitude to the reduction seen during hypoxia (2% ambient oxygen) [Sanders & Joines, 1984; Sanders et al., 1985]. Although the whole-body averaged SAR of 6 W/kg here was greater than SARs used in these earlier studies showing reduced energy production, we cannot entirely rule out such a reduction by exposures at this level. If microwave exposure at 0.6 W/kg here was acting to reduce energy production as in these earlier studies, effects of the exposure and 3-NP on ultrastructure might also be expected to

be synergistic. This expectation was not supported by our findings because changes due to 3-NP were not seen after subsequent microwave exposure at 0.6 W/kg. At least two explanations can account for this lack of synergistic effect by microwave exposure at 0.6 W/kg: (1) some action of 3-NP changed an effect of microwave exposure that occurred after 3-NP administration and (2) microwaves acted differently for our exposure parameters. Further investigation will be needed to clarify the interesting action of exposure at 0.6 W/kg on cellular effects of 3-NP.

For the microwave exposures here to have an effect on changes in the caudate-putamen caused by 3-NP injection, we might suspect a microwave action on cellular processes occurring at the time of exposure, i.e., at 1.5-2 h and 25.5-26 h after respective injections. Increased number of NMDA receptors [Wüllner et al., 1994], oxidative stress [Binienda & Kim, 1997], and nitric oxide production [Matthews et al., 1998] as well as changing striatal metabolites [Chyi & Chang, 1999; Lee et al., 2000] have been detected in the rat striatum at 1-3 h post-injection. These are in addition to the reduced SDH activity at this time, summarized above, that remains low for up to 7 days [Alexi et al., 1998a; Nony et al., 1999; Wiegand et al., 1999]. Although these previous studies used somewhat higher 3-NP doses than the 10 mg/kg used here and different strains of rats, we can expect the effects to be similar. In fact, SDH activity is reduced by a single injection of 10 or 15 mg/kg 3-NP or two injections of 7.5 mg/kg 3-NP separated by 12 h when the activity is measured at 24 h after single injection or the first of two injections [Brouillet et al., 1998; Ouary et al., 2000] but recovers from a single 10-20 mg/kg dose by day 7 post-injection [Alexi et al., 1998a]. In these low-dose experiments that suggest 3-NP effects were occurring at the times of our microwave exposures, no striatal lesion was found and no change in gross behavior was noted, as was also the case in the study here.

In addition to the above changes, apoptosis-like changes have been seen in the

caudate-putamen after 3-NP administration. Bcl-2, a protein that is a key regulator of apoptosis, is increased by two injections of 10 mg/kg separated by 12 h at 24 h after the first injection [Sugino et al., 1997]. Activity has been detected in both proapoptotic and antiapoptotic molecular pathways at 12 and 24 h after a single 3-NP injection and two closely spaced 3-NP injections [Sugino et al., 1997; Brambrink et al., 2000; Duan et al., 2000; Antonawich et al., 2002; Bizat et al., 2003] and in cultured rat striatal neurons [Galas et al., 2004]. This activity includes release of cytochrome-c from mitochondria, an increase in Bcl-2, increased levels of one or more activated cysteine-dependent, aspartate-specific proteases, caspase-9, caspase-8, and caspase-3, and increased level of calpain. These molecular changes might be useful in the future to monitor cell response to microwave-mitochondrial toxin combinations. Another possible indicator for future use is poly(ADP-ribose) polymerase, which is increased after 3-NP injection [Sugino et al., 1997] and reported to decrease in whole brain after long-term microwave exposure of rats 1 mW/cm² (60 days, 2.45 GHz; whole-body averaged SAR on the order of 0.2 W/kg by our estimate) [Singh et al., 1994].

Previous 3-NP results from other laboratories described above indicate that due to the first 3-NP injection of 10 mg/kg used here SDH activity was reaching or at a reduced level during the first microwave exposure and that excitotoxicity, involving NMDA receptor activation, and oxidative stress were underway at this time. The SDH activity had reached a lower, stable level by 24 h after the first injection, the time of the second exposure, although further inhibition of SDH might have resulted from the second injection of 10 mg/kg 3-NP. Activation of apoptotic pathways was also well underway at the time of the second microwave exposure. Because we have previously seen no change in ER ultrastructure at 4.5 h but dilation of ER at 24 h after a single injection of 10 mg/kg 3-NP in the same animal model (Brewer et al., unpublished), the second injection here probably did not contribute much to the ER dilation seen in our material, which was taken 27.5 h after the first injection.

PUBLICATION 24 (continued)

The actions and interactions of 3-NP and microwave exposure could have well occurred within the medium-sized neurons examined. As discussed above, the observed changes in ER ultrastructure indicated the strong possibility of altered ER function. That this was due to direct effects of 3-NP and microwaves on the ER itself was not tested in this study. The well-established action of 3-NP on SDH within mitochondria, e.g., [Alexi et al., 1998b; Brouillet et al., 1999], releases cytochrome c [Antonawich et al., 2002; Galas et al., 2004], which can be expected to enhance ER calcium release and modulate processes associated with apoptosis, many of which also involve the ER [Antonawich et al., 2002; Boehning et al., 2003; Breckenridge et al., 2003; Galas et al, 2004]. Because electromagnetic fields at microwave frequencies penetrate biological cells [Foster & Schwan, 1986, pp 83-87], effects of microwave exposure on mitochondria, the ER, other organelles, or interactions among organelles to modify their normal function or response to 3-NP cannot be ruled out.

In addition to 3-NP-microwave interaction within the medium-sized spiny neurons themselves, interaction with combinations of neurons was also possible. Soma-somatic and soma-dendritric contact between cell membranes of neurons in the rat caudate-putamen has been reported [Paskevich et al., 1991; Pickel & Chan, 1991]. Cell-to-cell coupling by means of gap junctions between medium-sized spiny neurons has also been identified and found to be enhanced by loss of dopamine terminals in the caudate-putamen [Cepeda et al., 1989; Onn & Grace, 1994, 1999]. Because five days of 3-NP infusion at 56 mg/kg/day is necessary before loss of dopamine terminals in Lewis rats [Blum et al., 2004], we can expect that despite the strain difference only the sparse interneuronal connections by direct contact or gap junctions that are typical of untreated rats were present in the work here using two 10 mg/kg 3-NP doses. That any of these connections influenced our results is not known.

Involvement of other cells types in the rat caudate-putamen can also be considered for our results. The astrocyte, a type of glial cell, is known to respond to 3-NP *in vivo* and in

PUBLICATION 24 (continued)

culture [Nishino et al., 1997; Tsai et al., 1997; Fukuda et al., 1998; Pubill et al., 2001]. Glutamate released from such activated astrocytes [Parpura et al., 1994; Parpura & Haydon, 2000] would be expected to contribute to excitotoxicity seen with 3-NP treatment [Beal et al., 1993a,b; Wüllner et al., 1994; Alexi et al., 1998b; Brouillet et al., 1999]. Release of ATP from activated astrocytes [Cotrina et al., 2000; Stout et al., 2002] would also be expected to enhance processes involved in neurodegeneration [Le Feuvre et al., 2002; Ryu et al., 2002]. Glial activation by chronic and repeated 3-NP administrations is indicated by detection of glial fibrillary acidic protein (GFAP) in the caudate-putamen [Wüllner et al., 1994; Nishino et al., 1995; Guyot et al., 1997; Vis et al., 1999]. However, for chronic dosing at 12 mg/kg/day [Wüllner et al., 1994] and single doses of 10-20 mg/kg [Alexi et al., 1998a], GFAP is not detected. The lack of GFAP activation along with the absence of cell pathology in light microscopy here and in another studies with 3-NP doses similar to the 10 mg/kg used here [Kodsi & Swerdlow, 1997; Nishino et al., 1997] suggests that glial cells were not activated in our experiment. The lack of lesion and presumed lack of glial activation at our sampling time on the second day of injection are also consistent with the multiple 3-NP injections [Nishino et al., 1995, 1997; Guyot et al., 1997] and the 5 days of chronic 3-NP infusion [Dautry et al., 2000; Ouary et al., 2000; Blum et al., 2002; Bizat et al, 2003] required before a lesion can be detected. Although rat strains and doses in much of this previous work differs from those used here, in male Sprague-Dawley rats, 12 or 14 mg/kg/day for 5 days results in only 31 or 54%, respectively, of animals having lesions [Ouary et al., 2000]. If, because of the low 3-NP dose and/or short time to sampling, astrocytes were indeed not activated in our study, a 3-NP-microwave interaction with astrocyte activation is difficult to propose. Regardless of astrocyte activation, whether microwave electromagnetic fields acted on astrocytes in the caudate-putamen is not known.

PUBLICATION 24 (continued)

Treatment by 3-NP has also been shown to affect microglia [Pubill et al., 2001; Ryu et al., 2003] and endothelial cells [Hamilton & Gould, 1987; Mogami et al., 2002], which are also possible sites of microwave action and interaction in our study. In addition, isolated neurons are affected by exposure to 3-NP [Lee et al., 2002; Nasr et al., 2003]. Because of these effects on multiple cell types that are present in the caudate-putamen, we cannot state with certainty what cell type was most affected by 3-NP or microwave exposure in our study. Further, we cannot rule out the possibility that some or all types of cells acted together, as seen in other systems [Le Feuvre et al., 2002; Hansson & Rönnbäck, 2003].

In addition to neuropathology and neuronal ultrastructure results described above for microwave studies, some work with microwave exposures has been done that can be related to non-neuronal cells in the brain. Compromise of the blood-brain barrier by unknown mechanisms in rats after microwave exposure has been reported [Salford et al., 1994, 2003]. The cell-stress pathways activated in human endothelial cells in culture when exposed to GSM signals [Leszczynski et al., 2002] might provide an explanation for these *in vivo* findings. The reported breakdown in the blood-brain barrier caused by microwave exposure could involve mechanisms similar to those in breakdown of the barrier with 3-NP intoxication [Nishino et al., 1995, 1997], for which effects on endothelial cells, as well as on astrocytes, could be responsible.

In another microwave study, exposure of the heads of rats that resulted in brain SAR of 7.5 W/kg for CW 900 MHz or 0.3 or 1.5 W/kg for GSM signals at a similar frequency failed to activate astrocytes and microglia anywhere in the brain [Fritze et al., 1997]. This supports the idea that our microwave exposures with whole-body averaged SAR of 0.6 and 6 W/kg were not likely to have activated these cell types.

Taken together, information from the various studies above point toward weak changes occurring for both the 3-NP doses and the microwave SARs used in this study. Because 3-NP

PUBLICATION 24 (continued)

doses and microwave SARs needed to activate astrocytes and microglia in the studies are higher than those used here, action of 3-NP and microwave radiation, as well as interaction between them, to change neuronal ultrastructure most likely occurred within the neurons.

We have speculated above on sites of microwave action responsible for changes in ultrastructure observed after exposure. Changes after microwave exposure at 6 W/kg resembled changes produced by the mitochondrial toxin 3-NP and the exposure also increased 3-NP-induced changes. Increased body temperature seen after exposure at 6 W/kg most likely contributed to these effects. On the other hand, the effect of microwave exposure at 0.6 W/kg to reduce 3-NP-induced changes occurred without increased body temperature while exposure at 0.6 W/kg itself did not change ultrastructure significantly. This indicated that some effect of this exposure that caused no change, or a change too subtle to detect, in ER ultrastructure was able to affect the ER response to 3-NP in this animal model. Overall, the different effects on neuronal ultrastructure by 0.6 and 6 W/kg indicated the real possibility that exposures at the two SARs acted in different ways to change the measured indicators of cell injury used here. Because microwave exposures enhanced (6 W/kg) or suppressed (0.6 W/kg) the changes in ultrastructure after 3-NP administration, we can reasonably hypothesize that the pulsed microwave radiation directly or indirectly acted on the same processes triggered by 3-NP.

Summary

The results of this study indicated that pulsed microwave radiation is capable of interacting with processes of injury to neurons of the rat caudate-putamen and, possibly, processes involved in their repair. This raises the intriguing possibility that pulsed microwave radiation can be used therapeutically to alter the progression of tissue injury to neuronal cell death in brain injury and neurodegenerative disease. Because the types of interaction here depended on microwave SAR, intensity of microwave radiation might be a useful parameter to

PUBLICATION 24 (continued)

vary. Of course, pulse characteristics and repetition frequency could also be factors in the observed effects. The medium-sized spiny neuron of the caudate-putamen may provide a cellular crucible for the study of microwave radiation interaction with cellular processes of cell death and its prevention at the molecular level.

PUBLICATION 24 (continued)

ACKNOWLEDGMENTS

The continued interest and support of B. Stuck, Director of USAMRD, is greatly appreciated. We are grateful to M. Gonzalez, A. Phinney, L. Mery, and E. Wood who provided valuable technical support at various times; S. Mathur and N. Harris for operation of radar equipment and microwave instruments; and S. Mathur for SAR calculations. We also thank S.-T. Lu and E. Brouillet for their readings of the manuscript and E. Brouillet for helpful insight into the actions of 3-NP. The FPS-7B radar transmitter was used through an agreement with the U.S. Naval Health Research Center Detachment at Brooks City-Base, Texas.

OTHER INFORMATION

The views, opinions and/or findings contained in this report are those of the author(s) and should not be construed as an official Department of the Army position, policy or decision unless so designated by other documentation.

[Note to editor: The above statement and information in paragraph 2 under "animals" in MATERIALS AND METHODS are required by the contract cited on the title page. If these statements cannot be printed, please provide a written explanation.]

Notes to the typesetter:

μ is small Greek letter mu

χ^2 is small Greek letter chi with superscript 2

PUBLICATION 24 (continued)

REFERENCES

Albert EN, DeSantis M. 1975. Do microwaves alter nervous system structure? Ann New York Acad Sci 247:87-106.

Albert EN, Sherif M. 1988. Morphological changes in cerebellum of neonatal rats exposed to 2.45 GHz microwaves. Prog Clin Biol Res 257:135-151.

Albin RL. 2000. Basal ganglia neurotoxins. Neurol Clin 18:665-680.

Alexi T, Hughes PE, Knusel B, Tobin AJ. 1998a. Metabolic compromise with systemic 3-nitropropionic acid produces striatal apoptosis in Sprague-Dawley rats but not in BALB/c ByJ mice. Exp Neurol 153:74-93.

Alexi T, Hughes PE, Faull RLM, Williams CE. 1998b. 3-nitropropionic acid's lethal triplet: Cooperative pathways of neurodegeneration. Neuroreport 9:R57-R64.

Antonawich FJ, Fiore-Marasa SM, Parker CP. 2002. Modulation of apoptotic regulatory proteins and early activation of cytochrome C following systemic 3-nitropropionic acid administration. Brain Res Bull 57:647-649.

Arber SL, Neilly JP, Lin JC, Kriho V. 1986. The effect of 2450 MHz microwave radiation on the ultrastructure of snail neurons. Physiol Chem Phys Med NMR 18:243-249.

Baranski S. 1972. Histological and histochemical effect of microwave irradiation on the central nervous system of rabbits and guinea pigs. Am J Phys Med 51:182-191.

Beal MF. 1992. Does impairment of energy metabolism result in excitotoxic neuronal death in neurodegenerative illnesses? Ann Neurol 31:119-130.

Beal MF, Brouillet E, Jenkins BG, Ferrante RJ, Kowall NW, Miller JM, Storey E, Srivastava R, Rosen BR, Hyman BT. 1993a. Neurochemical and histologic characterization of striatal excitotoxic lesions produced by the mitochondrial toxin 3-nitropropionic acid. J Neurosci 13:4181-4192.

Beal MF, Brouillet E, Jenkins B, Henshaw R, Rosen B, Hyman BT. 1993b. Age-dependent striatal excitotoxic lesions produced by the endogenous mitochondrial inhibitor malonate. J Neurochem 61:1147-1150.

Beal MF, Ferrante RJ, Henshaw R, Matthews RT, Chan PH, Kowall NW, Epstein CJ, Schulz JB. 1995. 3-nitropropionic acid neurotoxicity is attenuated in copper/zinc superoxide dismutase transgenic mice. J Neurochem 65:919-922.

Binienda Z, Kim CS. 1997. Increase in levels of total free fatty acids in rat brain regions following 3-nitropropionic acid administration. Neurosci Lett 230:199-201.

PUBLICATION 24 (continued)

Bizat N, Hermel JM, Boyer F, Jacquard C, Créminion C, Ouary S, Escartin C, Hantraye P, Krajewski S, Brouillet E. 2003. Calpain is a major cell death effector in selective striatal degeneration induced *in vivo* by 3-nitropropionate: Implications for Huntington's disease. J Neurosci 23:5020-5030.

Blum D, Galas MC, Gall D, Cuvelier L, Schiffmann SN. 2002. Striatal and cortical neurochemical changes induced by chronic metabolic compromise in the 3-nitropropionic model of Huntington's disease. Neurobiol Dis 10:410-426.

Blum D, Galas MC, Cuvelier L, Schiffmann SN. 2004. Chronic intoxication with 3-nitropropionic acid in rats induces the loss of striatal dopamine terminals without affecting nigral cell viability. Neurosci Lett 354:234-238.

Boehning D, Patterson RL, Sedaghat L, Glebova NO, Kurosaki T, Snyder SH. 2003. Cytochrome c binds to inositol (1,4,5) triphosphate receptors, amplifying calcium-dependent apoptosis. Nat Cell Biol 5:1051-1060.

Borlongan CV, Koutouzis TK, Freeman TB, Cahill DW, Sanberg PR. 1995a. Behavioral pathology induced by repeated systemic injections of 3-nitropropionic acid mimics the motoric symptoms of Huntington's disease. Brain Res 697:254-257.

Borlongan CV, Koutouzis TK, Randall TS, Freeman TB, Cahill DW, Sanberg PR. 1995b. Systemic 3-nitropropionic acid: Behavioral deficits and striatal damage in adult rats. Brain Res Bull 36:549-556.

Brambrink AM, Schneider A, Noga H, Astheimer A, Götz B, Körner I, Heimann A, Welschof M, Kempski O. 2000. Tolerance-inducing dose of 3-nitropropionic acid modulates bcl-2 and bax balance in the rat brain: A potential mechanism of chemical preconditioning. J Cereb Blood Flow Metab 20:1425-1436.

Breckenridge DG, Germain M, Mathai JP, Nguyen M, Shore GC. 2003. Regulation of apoptosis by endoplasmic reticulum pathways. Oncogene 22:8608-8618.

Brouillet E, Jenkins BG, Hyman BT, Ferrante RJ, Kowall NW, Srivastava R, Roy DS, Rosen BR, Beal MF. 1993. Age-dependent vulnerability of the striatum to the mitochondrial toxin 3-nitropropionic acid. J Neurochem 60:356-359.

Brouillet E, Hantraye P, Ferrante RJ, Dolan R, Leroy-Willig A, Kowall NW, Beal MF. 1995. Chronic mitochondrial energy impairment produces selective striatal degeneration and abnormal choreiform movements in primates. Proc Natl Acad Sci USA 92:7105-7109.

PUBLICATION 24 (continued)

Brouillet E, Guyot MC, Mittoux V, Altairac S, Condé F, Palfi S, Hantraye P. 1998. Partial inhibition of brain succinate dehydrogenase by 3-nitropropionic acid is sufficient to initiate striatal degeneration in rat. J Neurochem 70:794-805.

Brouillet E, Condé F, Beal MF, Hantraye P. 1999. Replicating Huntington's disease phenotype in experimental animals. Prog Neurobiol 59:427-468.

Budd SL. 1998. Mechanisms of neuronal damage in brain hypoxia/ischemia: Focus on the role of mitochondrial calcium accumulation. Pharmacol Ther 80:203-229.

Calabresi P, Centonze D, Pisani A, Sancesario G, Gubellini P, Marfia GA, Bernardi G. 1998. Striatal spiny neurons and cholinergic interneurons express differential ionotropic glutamatergic responses and vulnerability: Implication for ischemia and Huntington's disease. Ann Neurol 43:586-597.

Calabresi P, Centonze D, Gubellini P, Marfia GA, Pisani A, Sancesario G, Bernardi G. 2000. Synaptic transmission in the striatum: From plasticity to neurodegeneration. Prog Neurobiol 61:231-265.

Cepeda C, Walsh JP, Hull CD, Howard SG, Buchwald NA, Levine MS. 1989. Dye-coupling in the neostriatum of the rat: I. Modulation by dopamine-depleting lesions. Synapse 4:229-237.

Chang HT, Kitai ST. 1982. Large neostriatal neurons in the rat: An electron microscopic study of gold-toned Golgi-stained cells. Brain Res Bull 8:631-643.

Chou CK, Guy AW, McDougall JA, Lai H. 1985. Specific absorption rate in rats exposed to 2,450 MHz microwaves under seven exposure conditions. Bioelectromagnetics 6:73-88.

Chyi T, Chang C. 1999. Temporal evolution of 3-nitropropionic acid-induced neurodegeneration in the rat brain by T_2-weighted, diffusion-weighted, and perfusion magnetic resonance imaging. Neuroscience 92:1035-1041.

Cotrina JL, Lin JHC, Alves-Rodrigues A, Liu S, Li J, Azmi-Ghadimi H, Kang J, Naus CCG, Nedergaard M. 1998. Connexins regulate calcium signaling by controlling ATP release. Proc Natl Acad Sci USA 95:15735-15740.

D'Andrea JA, de Lorge JO. 1990. Behavioral effects of electromagnetic fields. In Gandhi OP (ed): *Biological Effects and Medical Applications of Electromagnetic Energy*. Englewood Cliffs, NJ: Prentice Hall. p 319-338.

Dautry C, Vaufrey F, Brouillet E, Bizat N, Henry PG, Condé F, Bloch G, Hantraye P. 2000. Early N-acetylaspartate depletion is a marker of neuronal dysfunction in rats and primates chronically treated with the mitochondrial toxin 3-nitropropionic acid. J Cereb Blood Flow Metab 20:789-799.

PUBLICATION 24 (continued)

Deeter DP, Gaydos JC (eds). 1993. *Occupational Health: The Soldier and the Industrial Base.* Washington DC: Office of the Surgeon General, U.S. Department of the Army. 643 p.

DeFrank JJ, Bryan PK, Hicks CW, Jr., Sliney DH. 1993. Ch. 15, Nonionizing radiation. In: *Textbook of Military Medicine*, Part III, Vol. 2. Washington DC: Office of the Surgeon General, U.S. Department of the Army. p 539-580.

Duan W, Guo Z, Mattson MP. 2000. Participation of Par-4 in the degeneration of striatal neurons induced by metabolic compromise with 3-nitropropionic acid. Exp Neurol 165:1-11.

Durney CH, Massoudi H, Iskander MF. 1986. *Radiofrequency Radiation Dosimetry Handbook*, Fourth Edition. Technical Report USAFSAM-TR-85-73. Brooks Air Force Base: USAF School of Aerospace Medicine.

Eldridge J (ed). 2001. *Jane's Nuclear, Biological and Chemical Defence.* Alexandria, Virginia: Jane's Information Group Inc. 386 p.

Foster KR, Schwan HP. 1986. Dielectric properties of tissues. In Polk C, Postow E (eds): *CRC Handbook of Biological Effects of Electromagnetic Fields.* Boca Raton: CRC Press, pp 27-96.

Fritze K, Wiessner C, Kuster N, Sommer C, Gass P, Hermann DM, Kiessling M, Hossmann KA. 1997. Effect of global system for mobile communication microwave exposure on the genomic response of the rat brain. Neuroscience 81:627-639.

Fukuda A, Deshpande SB, Shimano Y, Nishino H. 1998. Astrocytes are more vulnerable than neurons to cellular Ca^{2+} overload induced by a mitochondrial toxin, 3-nitropropionic acid. Neuroscience 87:497-507.

Galas MC, Bizat N, Cuvelier L, Bantubungi K, Brouillet E, Schiffmann SN, Blum D. 2004. Death of cortical and striatal neurons induced by mitochondrial defect involves differential molecular mechanisms. Neurobiol Dis 15:152-159.

Garcia M, Vanhoutte P, Pages C, Besson MJ, Brouillet E, Caboche J. 2002. The mitochondrial toxin 3-nitropropionic acid induces striatal neurodegeneration via a c-Jun N-terminal kinase/c-Jun module. J Neurosci 22:2174-2184.

Gordon CJ, Long MD, Fehlner KS, Stead AG. 1986. Body temperature in the mouse, hamster, and rat exposed to radiofrequency radiation: An interspecies comparison. J Therm Biol 11:59-65.

Gould DH, Gustine DL. 1982. Basal ganglia degeneration, myelin alterations, and enzyme inhibition induced in mice by the plant toxin 3-nitropropanoic acid. Neuropathol Appl Neurobiol 8:377-393.

PUBLICATION 24 (continued)

Gould DH, Wilson MP, Hamar DW. 1985. Brain enzyme and clinical alterations induced in rats and mice by nitroaliphatic toxicants. Toxicol Lett 27:83-89.

Gundersen HJG, Bendtsen TF, Korbo L, Marcussen N, Møller A, Nielsen K, Nyengaard JR, Pakkenberg B, Sørensen FB, Vesterby A, West MJ. 1988. Some new, simple and efficient stereological methods and their use in pathological research and diagnosis. APMIS 96:379-394.

Guy AW, Wallace J, McDougall JA. 1979. Circularly polarized 2450-MHz waveguide system for chronic exposure of small animals to microwaves. Radio Sci 14:63-74.

Guyot MC, Hantraye P, Dolan R, Palfi S, Maziére M, Brouillet E. 1997. Quantifiable bradykinesia, gait abnormalities and Huntington's disease-like striatal lesions in rats chronically treated with 3-nitropropionic acid. Neuroscience 79:45-56.

Haley RW, Fleckenstein JL, Marshall WW, McDonald GG, Kramer GL, Petty F. 2000. Effect of basal ganglia injury on central dopamine activity in Gulf War syndrome. Arch Neurol 57:1280-1285.

Hamilton BF, Gould DH. 1987. Nature and distribution of brain lesions in rats intoxicated with 3-nitropropionic acid: A type of hypoxic (energy deficient) brain damage. Acta Neuropathol (Berl) 72:286-297.

Hansson E, Rönnbäck L. 2003. Glial neuronal signaling in the central nervous system. FASEB J 17:341-348.

Hansson HA. 1988. Effects on the nervous system by exposure to electromagnetic fields: Experimental and clinical studies. Prog Clin Biol Res 257:119-134.

Heales SJR, Bolaños JP, Stewart VC, Brookes PS, Land JM, Clark JB. 1999. Nitric oxide, mitochondria and neurological disease. Biochim Biophys Acta 1410:215-228.

Joellenbeck LM, Russell PK, Guze SB, editors. 1999. *Strategies to Protect the Health of Deployed U.S. Forces: Medical Surveillance, Record Keeping, and Risk Reduction*. Washington DC: National Academy Press. 282 p.

Kalimo H, Garcia JH, Kamijyo Y, Tanaka J, Trump BF. 1977. The ultrastructure of "brain death". I. Electron microscopy of feline cerebral cortex after complete ischemia. Virchows Arch B Cell Pathol 25:207-220.

Kalimo H, Auer RN, Siesjö BK. 1985. The temporal evolution of hypoglycemic brain damage. III. Light- and electron-microscopic findings in the rat caudoputamen. Acta Neuropathol (Berl) 67:37-50.

Kalns J, Ryan KL, Mason PA, Bruno JG, Gooden R, Kiel JL. 2000. Oxidative stress precedes circulatory failure induced by 35-GHz microwave heating. Shock 13:52-59.

PUBLICATION 24 (continued)

Kawaguchi Y. 1997. Neostriatal cell subtypes and their functional roles. Neurosci Res 27:1-8

Keene CD, Rodrigues CMP, Eich T, Linehan-Stieers C, Abt A, Kren BT, Steer CJ, Low WC. 2001. A bile acid protects against motor and cognitive deficits and reduces striatal degeneration in the 3-nitropropionic acid model of Huntington's disease. Exp Neurol 171:351-360.

Kita H, Kitai ST. 1988. Glutamate decarboxylase immunoreactive neurons in rat neostriatum: Their morphological types and populations. Brain Res 447:346-352.

Kodsi MH, Swerdlow NR. 1997. Mitochondrial toxin 3-nitropropionic acid produces startle reflex abnormalities and striatal damage in rats that model some features of Huntington's disease. Neurosci Lett 231:103-107.

La Fontaine MA, Geddes JW, Banks A, Butterfield DA. 2000. 3-nitropropionic acid induced *in vivo* protein oxidation in striatal and cortical synaptosomes: Insights into Huntington's disease. Brain Res 858:356-362.

Lai H. 1994. Neurological effects of radiofrequency electromagnetic radiation. In Lin JC (ed): *Advances in Electromagnetic Fields in Living Systems*. Vol. 1. New York: Plenum. p 27-80.

Lee WT, Lee CS, Pan YL, Chang C. 2000. Temporal changes of cerebral metabolites and striatal lesions in acute 3-nitropropionic acid intoxication in the rat. Mag Res Med 44:29-34.

Lee WT, Yin HS, Shen YZ. 2002. The mechanisms of neuronal death produced by mitochondrial toxin 3-nitropropionic acid: The roles of N-methyl-D-aspartate glutamate receptors and mitochondrial calcium overload. Neuroscience 112:707-716.

Le Feuvre R, Brough D, Rothwell N. 2002. Extracellular ATP and P2X7 receptors in neurodegeneration. Eur J Pharmacol 447:261-269.

Leszczynski D, Joenvaara S, Reivinen J, Kuokka R. 2002. Non-thermal activation of the hsp27/p38MAPK stress pathway by mobile phone radiation in human endothelial cells: Molecular mechanism for cancer- and blood-brain barrier-related effects. Differentiation 70:120-129.

Lin TY, Wang SM, Fu WM, Chen YH, Yin HS. 1999. Toxicity of tunicamycin to cultured brain neurons: Ultrastructure of the degenerating neurons. J Cell Biochem 74:638-647.

Lotz WG, Michaelson SM. 1978. Temperature and corticosterone relationships in microwave-exposed rats. J Appl Physiol 44:438-445.

Ludolph AC, He F, Spencer PS, Hammerstad J, Sabri M. 1991. 3-Nitropropionic acid – exogenous animal neurotoxin and possible human striatal toxin. Can J Neurol Sci 18:492-498.

PUBLICATION 24 (continued)

Mandile P, Giuditta A, Romano F, Montagnese P, Piscopo S, Cotugno M, Vescia S. 2003. Waking EEG power spectra in the rat: Correlations with training performance. Cogn Brain Res 17:94-105.

Martin LJ, Brambrink AM, Price AC, Kaiser A, Agnew DM, Ichord RN, Traystman RJ. 2000. Neuronal death in newborn striatum after hypoxia-ischemia is necrosis and evolves with oxidative stress. Neurobiol Dis 7:169-191.

Matthews RT, Yang L, Jenkins BG, Ferrante RJ, Rosen BR, Kaddurah-Daouk R, Beal MF. 1998. Neuroprotective effects of creatine and cyclocreatine in animal models of Huntington's disease. J Neurosci 18:156-163.

McIntosh TK, Saatman KE, Raghupathi R, Graham DI, Smith DH, Lee VM, Trojanowski JQ. 1998. The molecular and cellular sequelae of experimental traumatic brain injury: Pathogenetic mechanisms. Neuropathol Appl Neurobiol 24:251-267.

Michaelson SM. 1986. Interaction of nonmodulated radio frequency fields with living matter: Experimental results. In Polk C, Postow E (eds): *CRC Handbook of Biological Effects of Electromagnetic Fields.* Boca Raton: CRC Press. pp 339-423.

Mitchell IJ, Cooper AJ, Griffiths MR. 1999. The selective vulnerabilibty of striatopallidal neurons. Prog Neurobiol 59:691-719.

Mogami M, Hida H, Hayashi Y, Kohri K, Kodama Y, Gyun Jung C, Nishino H. 2002. Estrogen blocks 3-nitropropionic acid-induced $Ca^{2+}{}_i$ increase and cell damage in cultured rat cerebral endothelial cells. Brain Res 956:116-125.

NAS (National Academy of Science, Committee to review the health consequences of service during the Persian Gulf War). 1996. Ch. 3, Environment and exposures. In *Health Consequences of Service During The Persian Gulf War: Recommendations For Research and Information Systems.* Washington DC: National Academy Press. p 36-66.

Nasr P, Gursahani HI, Pang Z, Bondada V, Lee J, Hadley RW, Geddes JW. 2003. Influence of cytosolic and mitochondrial Ca^{2+}, ATP, mitochondrial membrane potential, and calpain activity on the mechanism of neuron death induced by 3-nitropropionic acid. Neurochem Int 43:89-99.

Nishino H, Shimano Y, Kumazaki M, Sakurai T. 1995. Chronically administered 3-nitropropionic acid induces striatal lesions attributed to dysfunction of the blood-brain barrier. Neurosci Lett 186:161-164.

Nishino H, Kumazaki M, Fukuda A, Fujimoto I, Shimano Y, Hida H, Sakurai T, Deshpande SB, Shimizu H, Morikawa S, Inubushi T. 1997. Acute 3-nitropropionic acid intoxication induces striatal astrocytic

PUBLICATION 24 (continued)

cell death and dysfunction of the blood-brain barrier: Involvement of dopamine toxicity. Neurosci Res 27:343-355.

Nony PA, Scallet AC, Rountree RL, Ye X, Binienda Z. 1999. 3-nitropropionic acid (3-NPA) produces hypothermia and inhibits histochemical labeling of succinate dehydrogenase (SDH) in rat brain. Metabolic Brain Dis 14:83-94.

Onn SP, Grace AA. 1994. Dye coupling between rat striatal neurons recorded in vivo: Compartmental organization and modulation by dopamine. J Neurophysiol 71:1917-1934.

Onn SP, Grace AA. 1999. Alterations in electrophysiological activity and dye coupling of striatal spiny and aspiny neurons in dopamine-denervated rat striatum recorded in vivo. Synapse 33:1-15.

Ouary S, Bizat N, Altairac S, Ménétrat H, Mittoux V, Condé F, Hantraye P, Brouillet E. 2000. Major strain differences in response to chronic systemic administration of the mitochondrial toxin 3-nitropropionic acid in rats: Implications for neuroprotection studies. Neuroscience 97:521-530.

Parpura V, Basarsky TA, Liu F, Jeftinija K, Jeftinija S, Haydon PG. 1994. Glutamate-mediated astrocyte-neuron signalling. Nature 369:744-747.

Parpura V, Haydon PG. 2000. Physiological astrocytic calcium levels stimulate glutamate release to modulate adjacent neurons. Proc Natl Acad Sci USA 97:8629-8634.

Paschen W, Doutheil J. 1999. Disturbances of the functioning of endoplasmic reticulum: A key mechanism underlying neuronal cell injury? J Cereb Blood Flow Metab 19:1-18.

Paschen W, Frandsen A. 2001. Endoplasmic reticulum dysfunction – a common denominator for cell injury in acute and degenerative diseases of the brain? J Neurochem 79:719-725.

Paskevich PA, Evans HK, Domesick VB. 1991. Morphological assessment of neuronal aggregates in the striatum of the rat. J Comp Neurol 305:361-369.

Paxinos G, Watson C. 1986. *The Rat Brain In Stereotaxic Coordinates*, Second Edition. San Diego: Academic Press.

Petito CK, Pulsinelli WA. 1984. Sequential development of reversible and irreversible neuronal damage following cerebral ischemia. J Neuropathol Exp Neurol 43:141-153.

Phelan AM, Lange DG, Kues HA, Lutty GA. 1992. Modification of membrane fluidity in melanin-containing cells by low-level microwave radiation. Bioelectromagnetics 13:131-146.

Philippova TM, Novoselov VI, Alekseev SI. 1994. Influence of microwaves on different types of receptors and the role of peroxidation of lipids on receptor-protein shedding. Bioelectromagnetics 15:183-192.

PUBLICATION 24 (continued)

Pickel VM, Chan J. 1991. Plasmalemmal appositions between cholinergic and non-cholinergic neurons in rat caudate-putamen nuclei. Neuroscience 41:459-472.

Pollack AE. 2001. Anatomy, physiology, and pharmacology of the basal ganglia. Neurol Clin 19:523-534.

Pubill D, Verdaguer E, Canudas AM, Sureda FX, Escubedo E, Camaras J, Pallas M, Camins A. 2001. Orphenadrine prevents 3-nitropropionic acid-induced neurotoxicity in vitro and in vivo. Br J Pharmacol 132:693-702.

Russ JC, Dehoff RT. 2001. *Practical Stereology*, Second Edition. New York: Plenum Press. 382 p.

Ryu JK, Kim J, Choi SH, Oh YJ, Lee YB, Kim SU, Jin BK. 2002. ATP-induced in vivo neurotoxicity in the rat striatum via P2 receptors. Neuroreport 13:1611-1615.

Ryu JK, Nagai A, Kim J, Lee MC, McLarnon JG, Kim SU. 2003. Microglial activation and cell death induced by the mitochondrial toxin 3-nitropropionic acid: In vitro and in vivo studies. Neurobiol Dis 12:121-132.

Salford LG, Brun A, Sturesson K, Eberhardt JL, Persson BR. 1994. Permeability of the blood-brain barrier induced by 915 MHz electromagnetic radiation, continuous wave and modulated at 8, 16, 50, and 200 Hz. Microsc Res Tech 27:535-542.

Salford LG, Brun AE, Eberhardt JL, Malmgren L, Persson BRR. 2003. Nerve cell damage in mammalian brain after exposure to microwaves from GSM mobile phones. Environ Health Perspect 111:881-883.

Sanders AP, Joines WT. 1984. The effects of hyperthermia and hyperthermia plus microwaves on rat brain energy metabolism. Bioelectromagnetics 5:63-70.

Sanders AP, Joines WT, Allis JW. 1985. Effects of continuous-wave, pulsed, and sinusoidal-amplitude-modulated microwaves on brain energy metabolism. Bioelectromagnetics 6:89-97.

Schmechel DE. 1999. Assessment of ultrastructural changes associated with apoptosis. In Hannun YA, Boustany RM (eds): *Apoptosis in Neurobiology.* Boca Raton FL: CRC Press. p 153-181.

Schulz JB, Matthews RT, Jenkin BG, Ferrante RJ, Siwek D, Henshaw DR, Cipolloni PB, Mecocci P, Kowall NW, Rosen BR, Beal MF. 1995. Blockade of neuronal nitric oxide synthase protects against excitotoxicity *in vivo*. J Neurosci 15:8419-8429.

Schulz JB, Henshaw DR, MacGarvey U, Beal MF. 1996. Involvement of oxidative stress in 3-nitropropionic acid neurotoxicity. Neurochem Int 29:167-171.

Seaman RL. 2000. Effects of acute systemic 3-nitropropionic acid administration on rat activity and acoustic startle. Neurosci Lett 280:183-186.

PUBLICATION 24 (continued)

Seaman RL, Mathur SP, Dick EJ Jr. 2004. Effects of pulsed microwaves and 3-nitropropionic acid on rat motor activity, acoustic startle, and brain histology. WRAIR/USAMRD Technical Report.

Sharma HS, Westman J, Nyberg F. 1998. Pathophysiology of brain edema and cell changes following hyperthermic brain injury. Prog Brain Res 115:351-412.

Sidell FR, Takafuji ET, Franz DR (eds). 1997. *Medical Aspects of Chemical and Biological Warfare*. Washington DC: Office of the Surgeon General, U.S. Department of the Army. 721 p.

Singh N, Rudra N, Bansal P, Mathur R, Behari J, Nayar U. 1994. Poly ADP ribosylation as a possible mechanism of microwave-biointeraction. Indian J Physiol Pharmacol 38:181-184.

Söderfeldt B, Kalimo H, Olsson Y, Siesjö BK. 1981. Pathogenesis of brain lesions caused by experimental epilepsy. Light- and electron-microscopic changes in the rat cerebral cortex following bicuculline-induced status epilepticus. Acta Neuropathol (Berl) 54:219-231.

Somosy Z. 2000. Radiation response of cell organelles. Micron 31:165-181.

Stout CE, Costantin JL, Naus CCG, Charles AC. 2002. Intercellular calcium signaling in astrocytes via ATP release through connexin hemichannels. J Biol Chem 277:10482-10488.

Streetly M (ed). 2001. *Jane's Radar and Electronic Warfare Systems*. Alexandria, Virginia: Jane's Information Group Inc. 651 p.

Sugino T, Nozaki K, Tokime T, Hashimoto N, Kikuchi H. 1997. 3-nitropropionic acid induces poly(ADP-ribosyl)ation and apoptosis related gene expression in the striatum in vivo. Neurosci Lett 237:121-124.

Tolgskaya MS, Gordon ZV. 1973. *Pathological Effects of Radio Waves*. New York: Consultants Bureau. 146 p.

Trump BF, Berezesky IK. 1998. The reactions of cells to lethal injury: Oncosis and necrosis – The role of calcium. In Lockshin RA, Zakeri Z, Tilly JL (eds): *When Cells Die.* New York: Wiley-Liss. p 57-96.

Tsai MJ, Goh CC, Wan YL, Chang C. 1997. Metabolic alterations produced by 3-nitropropionic acid in rat striata and cultured astrocytes: Quantitative *in vitro* ^{1}H nuclear magnetic resonance spectroscopy and biochemical characterization. Neuroscience 79:819-826.

Vécsei L, Dibó G, Kiss C. 1998. Neurotoxins and neurodegenerative disorders. Neurotoxicology 19:511-514.

Verkhratsky A, Petersen OH. 2002. The endoplasmic reticulum as an integrating signaling organelle: From neuronal signaling to neuronal death. Eur J Pharmacol 447:141-154.

PUBLICATION 24 (continued)

Vis JC, Verbeek MM, de Waal RMW, ten Donkelaar HJ, Kremer HPH. 1999. 3-Nitropropionic acid induces a spectrum of Huntington's disease-like neuropathology in rat striatum. Neuropathol Appl Neurobiol 25:513-521.

Vorobyov VV, Schibaev NV, Morelli M, Carta AR. 2003. EEG modifications in the cortex and striatum after dopaminergic priming in the 6-hydroxydopamine rat model of Parkinson's disease. Brain Res 972:177-185.

Wiegand F, Liao W, Busch C, Castell S, Knapp F, Lindauer U, Megow D, Meisel A, Redetzky A, Ruscher K, Trendelenburg G, Victorov I, Riepe M, Diener HC, Dirnagl U. 1999. Respiratory chain inhibition induces tolerance to focal cerebral ischemia. J Cereb Blood Flow Metab 19:1229-1237.

Williamson J (ed). 1997. *Jane's Military Communications*. Alexandria, Virginia: Jane's Information Group Inc. 845 p.

Wüllner U, Young AB, Penney JB, Beal MF. 1994. 3-nitropropionic acid toxicity in the striatum. J Neurochem 63:1772-1781.

PUBLICATION 24 (continued)

Table 1. Numbers of animals, neurons, and measurements.

Experimental Condition (mg/kg-W/kg)	0-0	0-0.6	0-6	10-0	10-0.6	10-6	Total
Animals	3	3	3	3	4	4	20
Neurons/Animal	4-5	3-7	6-11	4-6	5-7	2-7	—
Measurements/Dimension /Neuron	5	5	5	5	5	5	—
Measurements/Dimension	65	70	120	75	120	85	535
Neurons	13	14	24	15	24	17	107

Table 2. Number and fraction of affected neurons.

Experimental Condition (mg/kg-W/kg)	0-0	0-0.6	0-6	10-0	10-0.6	10-6
Number Affected	2	6	17	14	8	17
Number Unaffected	11	8	7	1	16	0
Total Number	13	14	24	15	24	17
Fraction Affected	15%	43%	71% §§	93% §§ ¶¶	33% ♥♥‡‡	100% §§ ¶¶ ‡

§§, $p<.01$ different from condition 0-0
¶¶, $p<.01$ different from condition 0-0.6
‡, $p<.05$ different from condition 0-6
‡‡, $p<.01$ different from condition 0-6
♥♥, $p<.01$ different from both condition 10-0 and condition 10-6

PUBLICATION 24 (continued)

Table 3. Measured ultrastructure dimensions (mean and median).

Experimental Condition (mg/kg-W/kg)		0-0	0-0.6	0-6	10-0	10-0.6	10-6
Mitochondrial Diameter (nm)	Mean	402	376	372	353	323	312
	Median	433	393	374	348	300	306
ER Intracisternal Width (nm)	Mean	38	43	100	89	54	176
	Median	32	42	113 § ¶	80 §	53	181 §§ ¶¶ †
ER Area Density	Mean	0.190	0.266	0.357	0.352	0.215	0.443
	Median	0.186	0.266	0.370 §§	0.350 §§	0.212	0.432 §§ ¶ ††
Nuclear Envelope Thickness (nm)	Mean	28	31	58	53	42	56
	Median	28	32	54 §§ ¶¶	49 §§ ¶	44	53 §§ ¶

§, $p<.05$ different from condition 0-0
§§, $p<.01$ different from condition 0-0
¶, $p<.05$ different from condition 0-0.6
¶¶, $p<.01$ different from condition 0-0.6
†, $p<.05$ different from condition 10-0.6
††, $p<.01$ different from condition 10-0.6

PUBLICATION 24 (continued)

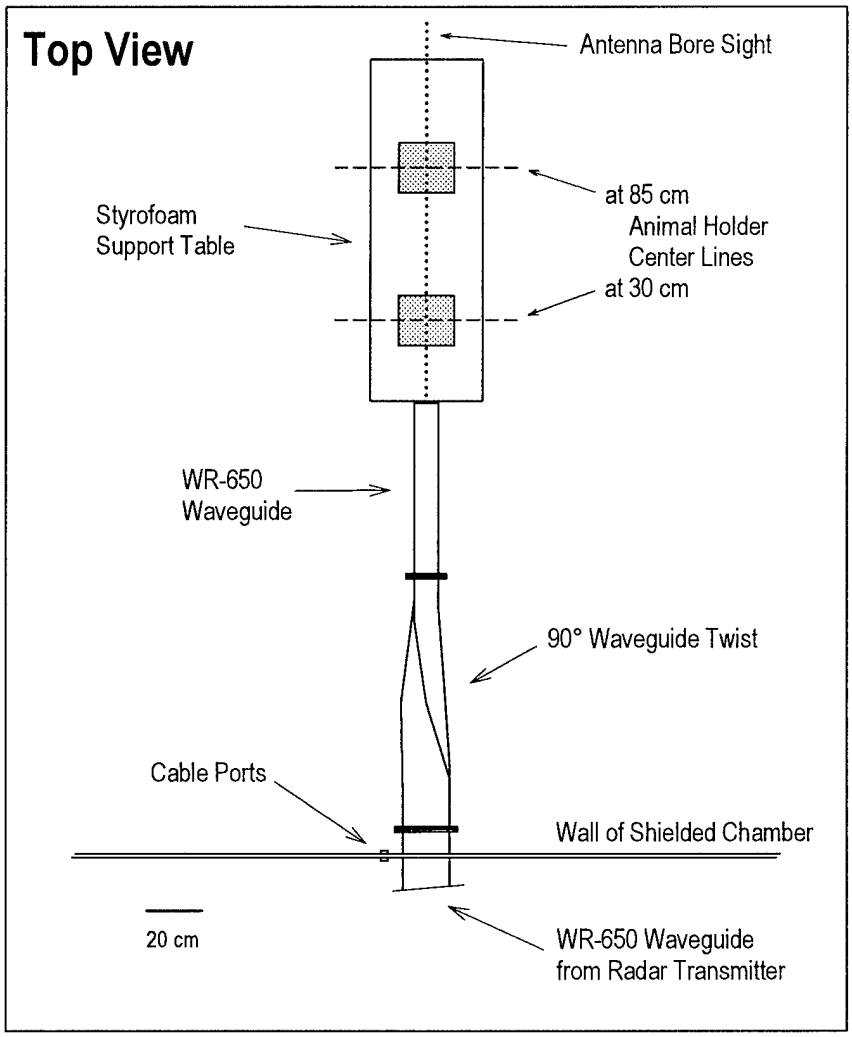


Fig. 1. Schematic diagram of the microwave exposure set-up. The waveguide twist was used to have a horizontal electric field. In either animal holder location, the center of the holder was on the boresight of the waveguide antenna. Only one location of the animal holder was used during an exposure.

PUBLICATION 24 (continued)

MICROGRAPH CAPTIONS

Fig. 2. TEM image of neuron for condition 0-0, 0 mg/kg 3-NP and 0 W/kg (sham exposure). m, mitochondrion; N, nucleus; small arrows, nuclear envelope; large arrows, endoplasmic reticulum.

Fig. 3. TEM image of neuron for condition 0-0.6, 0 mg/kg 3-NP and 0.6 W/kg microwave exposure. m, mitochondrion; N, nucleus; small arrows, nuclear envelope; large arrows, endoplasmic reticulum.

Fig. 4. TEM image of neuron for condition 0-6, 0 mg/kg 3-NP and 6 W/kg microwave exposure. m, mitochondrion; N, nucleus; small arrows, nuclear envelope; large arrows, endoplasmic reticulum.

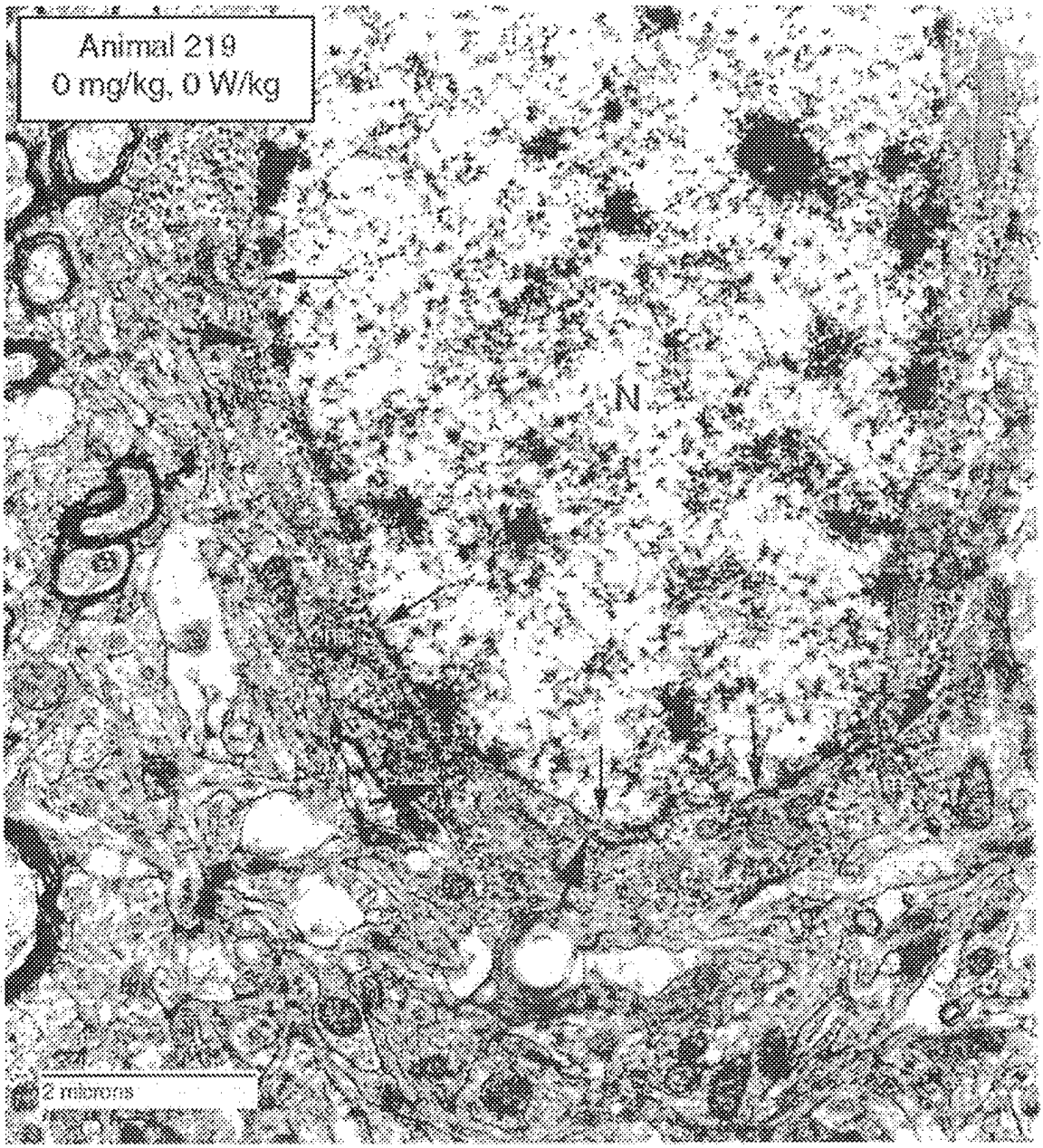
Fig. 5. TEM image of neuron for condition 10-0, 10 mg/kg 3-NP and 0 W/kg (sham exposure). m, mitochondrion; N, nucleus; small arrows, nuclear envelope; large arrows, endoplasmic reticulum.

Fig. 6. TEM image of neuron for condition 10-0.6, 10 mg/kg 3-NP and 0.6 W/kg microwave exposure. m, mitochondrion; N, nucleus; small arrows, nuclear envelope; large arrows, endoplasmic reticulum.

Fig. 7. TEM image of neuron for condition 10-6, 10 mg/kg 3-NP and 6 W/kg microwave exposure. d, dendrite; m, mitochondrion; N, nucleus; small arrows, nuclear envelope; large arrows, endoplasmic reticulum.

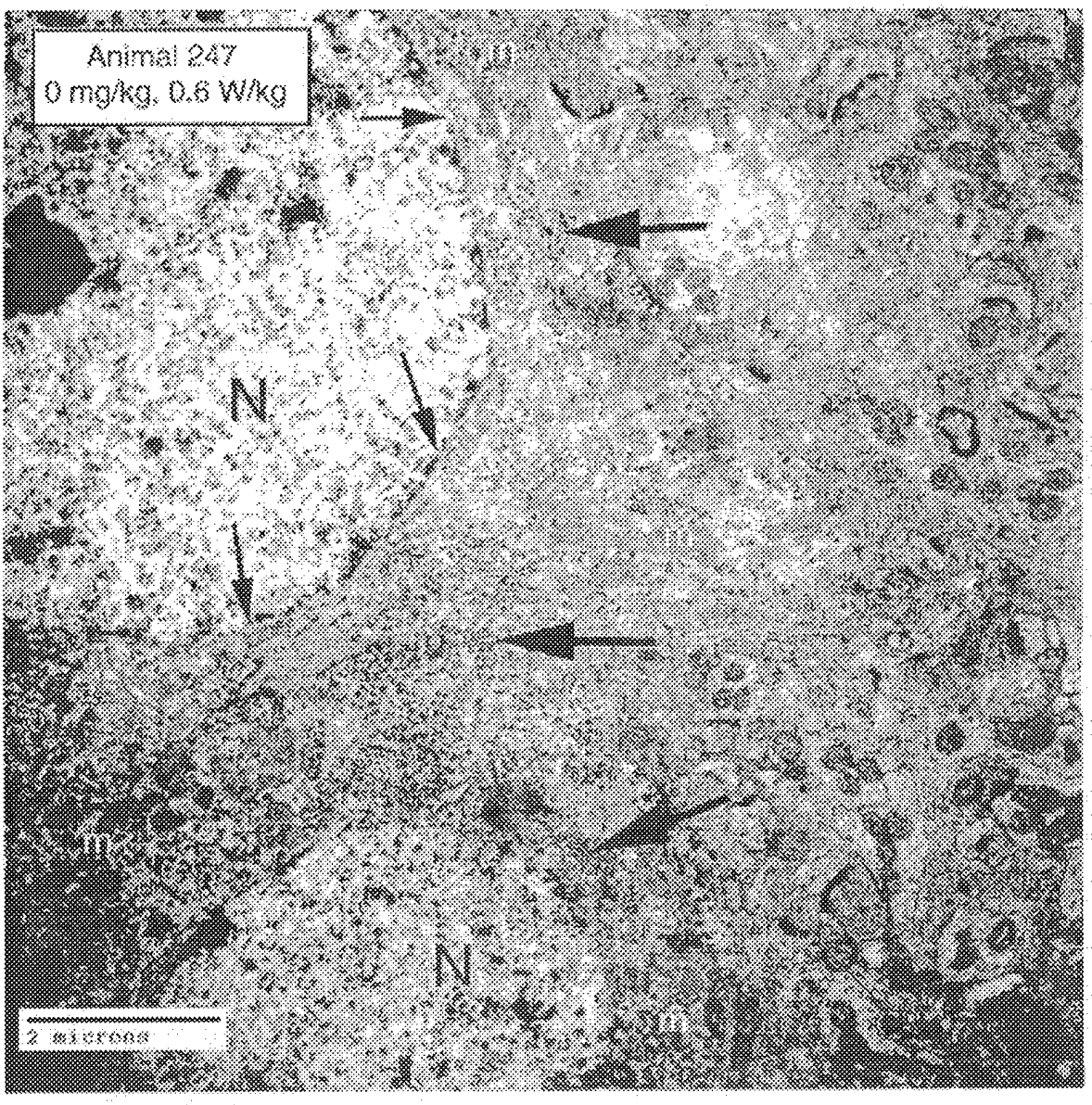
PUBLICATION 24 (continued)

Seaman & Phelix
"Acute Effects ... "
Figure 2



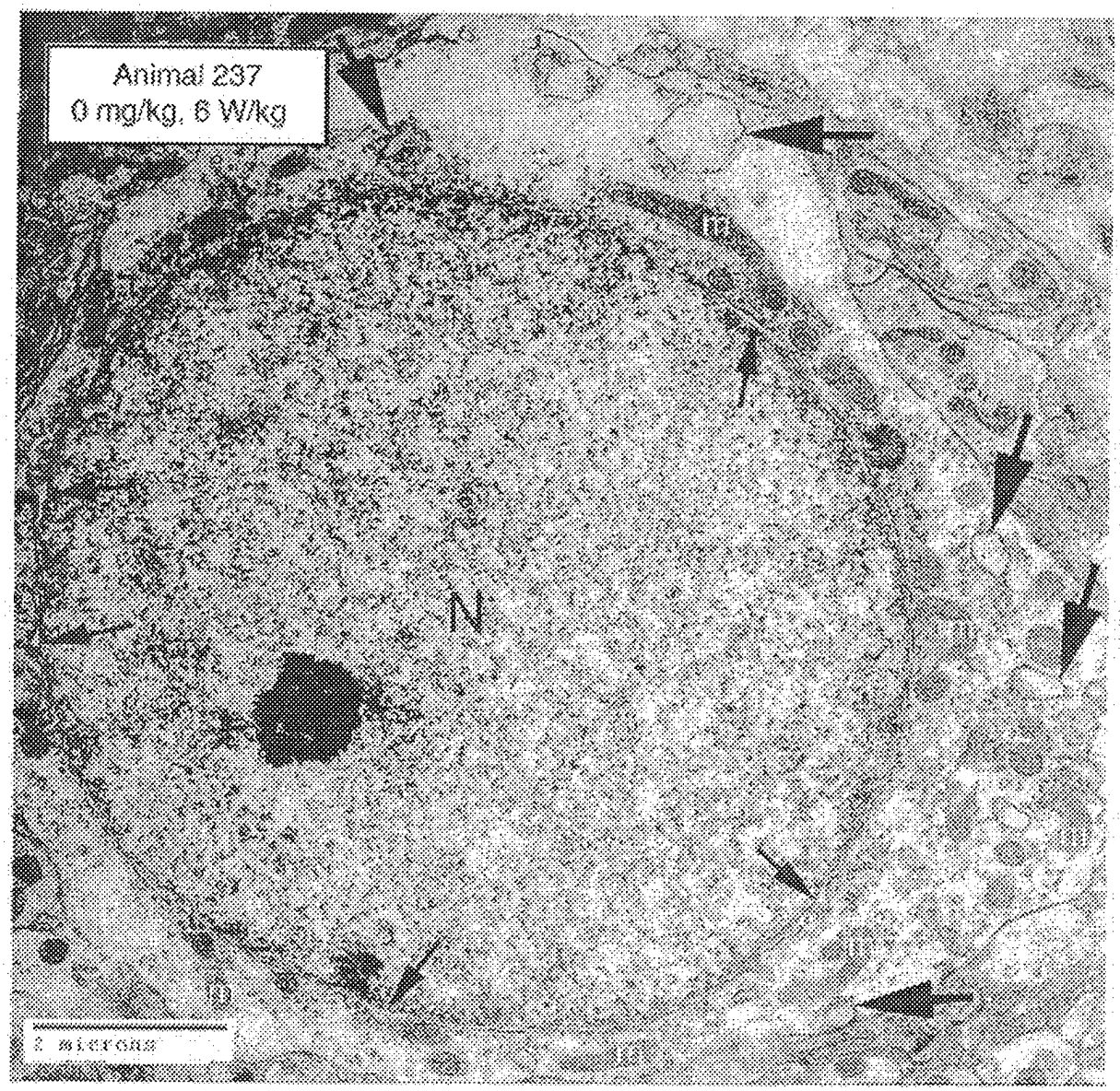
PUBLICATION 24 (continued)

Seaman & Phelix
"Acute Effects . . "
Figure 3



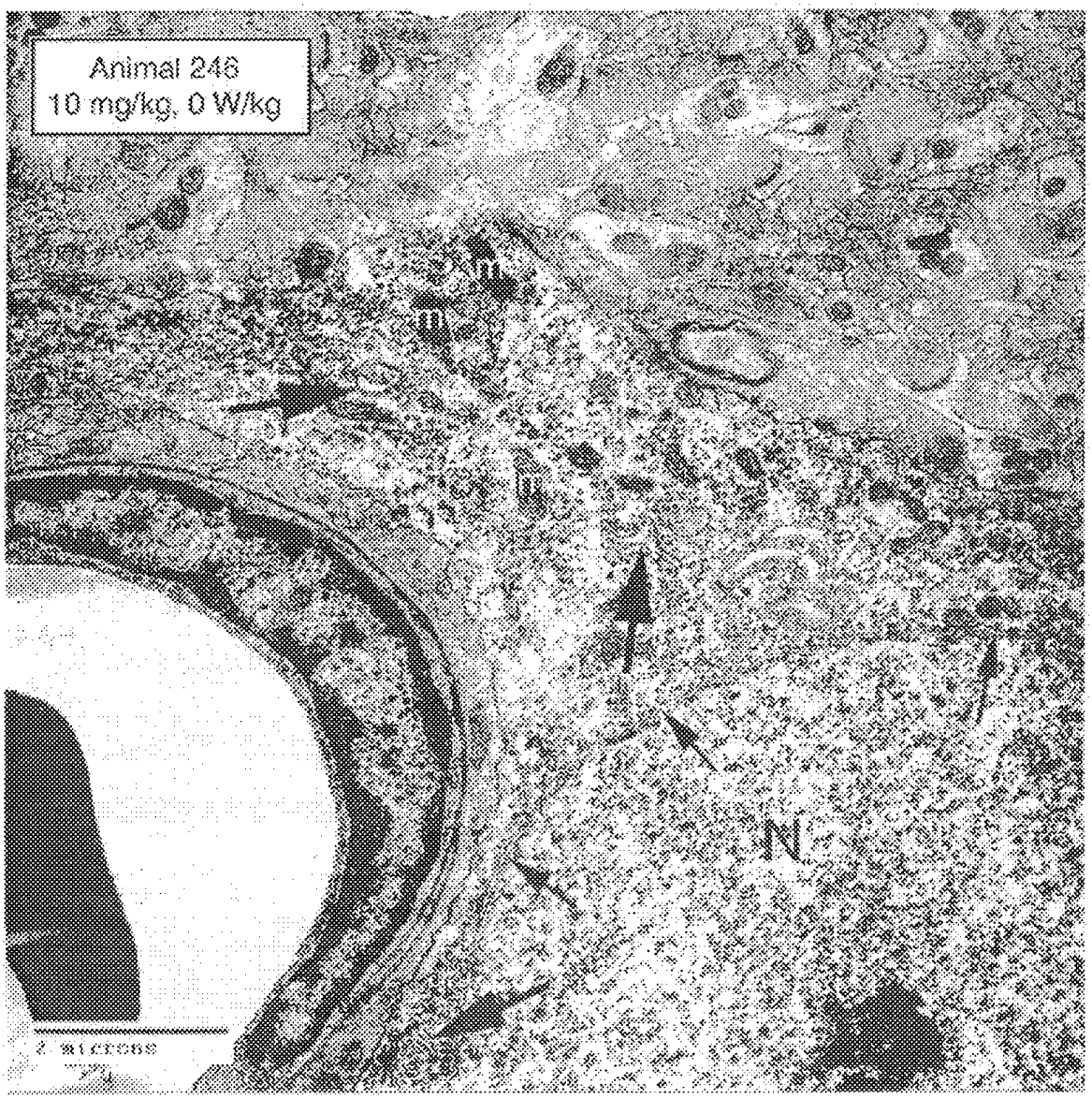
PUBLICATION 24 (continued)

Seaman & Phelix
"Acute Effects ..."
Figure 4



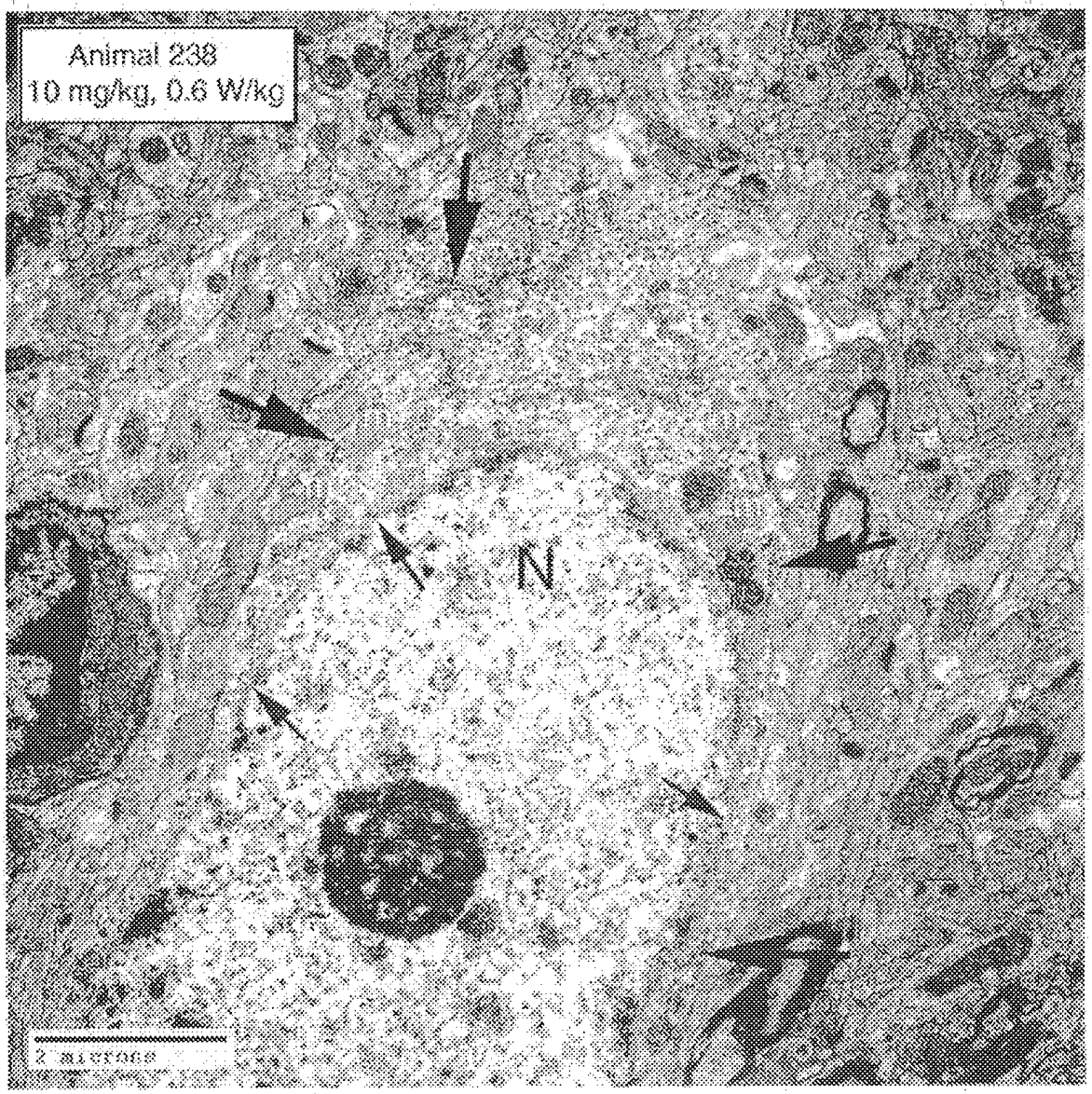
PUBLICATION 24 (continued)

Seaman & Phelix
"Acute Effects ..."
Figure 5



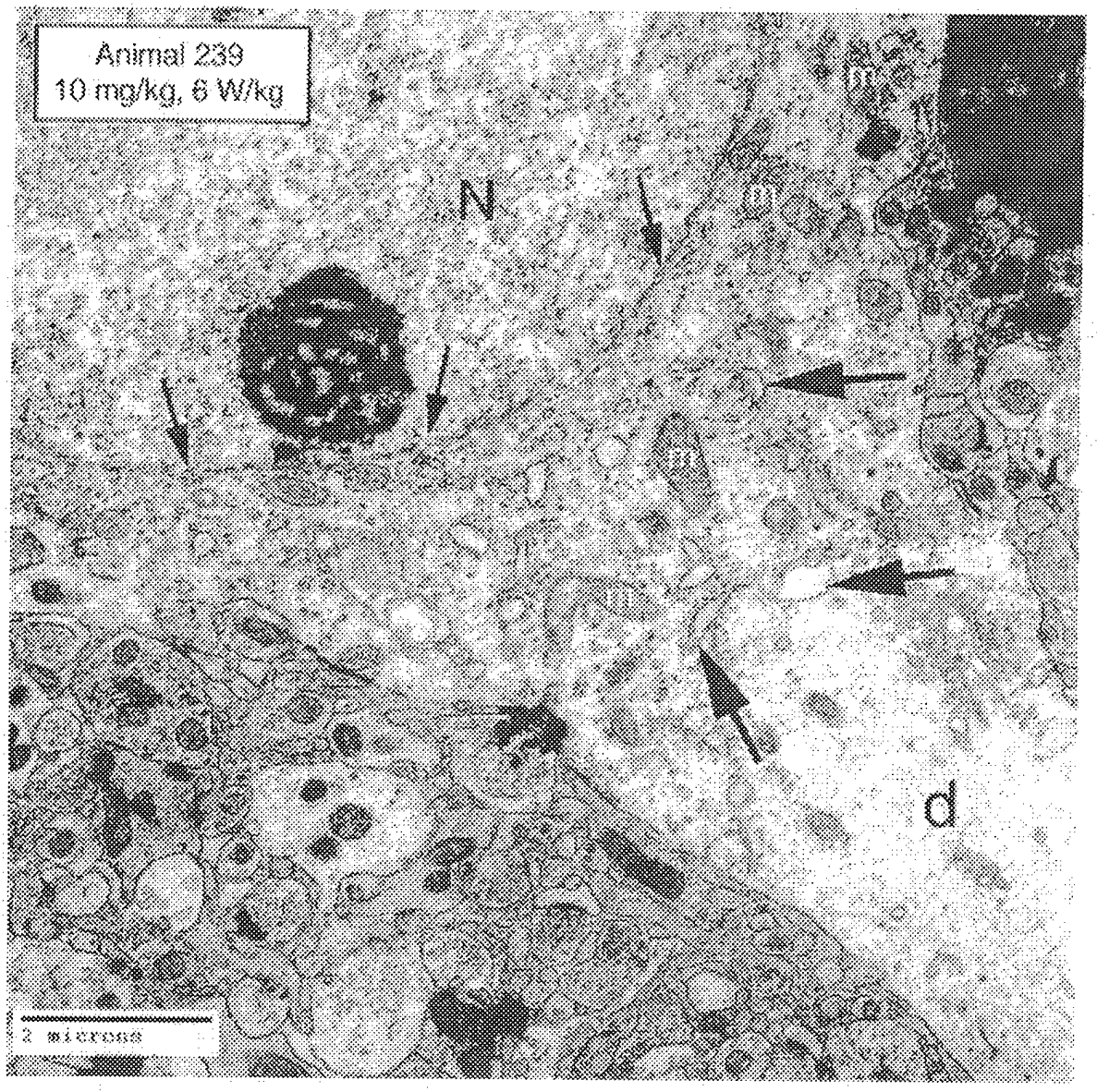
PUBLICATION 24 (continued)

Seaman & Phelix
"Acute Effects ..."
Figure 6



PUBLICATION 24 (continued)

Seaman & Phelix
"Acute Effects ... "
Figure 7



PUBLICATION 25
(In Preparation, Abstract Only)

Sensorimotor function in rotenone-treated rats after acute exposure to 1.25 -GHz microwave pulses in circular waveguide at 0.4 W/kg

Ronald L. Seaman[1], Marie-Francoise Chesselet[2], Satnam P. Mathur[1], Cheryl D. DiCarlo[3], Sheila M. Fleming[2], John L. Ashmore[1], Thomas H. Garza[1], Andres M. Grado[3]. [1]McKesson BioServices at WRAIR US Army Medical Research Detachment, Brooks City-Base, Texas 78235; [2]Dept. of Neurology, UCLA School of Medicine, Los Angeles, CA 90095; [3]US Army Medical Research Detachment, Brooks City-Base, Texas 78235.

Male Lewis rats (247 -289 g) were used in an experiment to test effects of radar-like 6 -μs pulses of 1.25-GHz microwave radiation at 10 pps on rotenone-induced changes in sensorimotor function. Animals were assessed by (1) a timed movement-initiation (MI) test and (2) counting vertical rears made in 5 min in a plastic cylinder. On the following day, animals were implanted subcutaneously with 2ML4 Alzet® osmotic minipumps fitted with nonmetallic flow modulators. The minipumps delivered 0 or 2 mg/kg/day rotenone in a dimethylsulfoxide/polyethylene glycol vehicle. On post-op days 4 and 5, animals were placed in a nonrestrictive holder and exposed at specific absorption rate (SAR) 0.4 W/kg for 6 min in a circular waveguide (N=10 and 17 for 0 and 2 mg/kg/day rotenone, respectively). Sham exposures (0 W/kg SAR) were done at the same time (N=10 and 18, respectively). On post-op day 6, MI time and cylinder rears were again assessed. Data were tested using ANOVA with rotenone and microwaves as factors. For cylinder rears, in the absence of significant interaction, rotenone had a strong main effect to decrease the number of rears after treatment ($p<0.0001$) while the microwave main effect was not significant. For MI time, the main effects of rotenone and microwave exposure and their interaction were not significant ($p>0.2$). We concluded that the microwave exposures alone or in combination with rotenone did not alter sensorimotor function in this animal model.

Supported by US Army MRMC contract DAMD17-94-C-4069. Investigator(s) adhered to the "Guide for the Care and Use of Laboratory Animals". The views, opinions and/or findings contained in this report are those of the author(s) and should not be construed as an official Department of the Army position, policy or decision.

REPORT 1

Technical Report

Short-Term Motor Activity and Acoustic Startle after Microwave Exposure and Toxin-Induced Hypoxia

By

Ronald L. Seaman, Satnam P. Mathur
McKesson BioServices Corporation at USAMRD
Brooks City-Base, Texas 78235

And

Edward J. Dick, Jr.
Veterinary Sciences Branch,
U.S. Air Force Research Laboratory, Brooks City-Base, Texas 78235

For

Walter Reed Army Institute of Research
U.S. Army Medical Research Detachment
Brooks City-Base, Texas 78235

Under

U.S. Army Medical Research and Materiel Command
Fort Detrick, Maryland 21702
Contract DAMD17-94-C-4069

April 2003

SUMMARY

Interaction of pulsed microwave radiation and tissue hypoxia was tested using behavioral and histological endpoints in an animal model using male Sprague-Dawley rats. Experimental treatments represented possible military occupational conditions of chemical hypoxia, induced in the model by intraperitoneal administration of 3-nitropropionic acid (3-NP), and microwave exposure, consisting of 5.9-μs pulses of 1.25 GHz radiation at 10 Hz for 30 min. The treatments consisted of two daily doses of 0 mg/kg or 10 mg/kg 3-NP administered 1.5 h before microwave exposure at specific absorption rate (SAR) of 0, 0.6, or 6 W/kg. The behavioral endpoints, spontaneous motor activity and acoustic startle, were tested 1.5-2.5 h after the second microwave exposure, to assess short-term effects of the 3-NP-microwave treatments.

Short-term motor activity was significantly reduced about 12% by 3-NP administration but not by microwave exposure at either SAR. No evidence was found for a short-term difference in amplitude or within-session habituation of startle due to 3-NP-microwave treatments. Short-term startle prepulse inhibition (PPI) was in large part unaffected by 3-NP-microwave treatments with no statistically significant difference among the treatments. Only small differences for 3-dBA prepulses suggested a microwave effect and possible 3-NP-microwave interaction.

Long-term results obtained from a subset of animals as a pilot study at 1, 2, and 3 weeks after 3-NP-microwave treatments are presented in an appendix. In this subset of animals, some evidence was found for 1) reduction of activity over time after microwave exposure at 0.6 W/kg without 3-NP administration, 2) reduction in startle PPI on the second day of microwave exposure at 0.6 W/kg after 3-NP administration, and 3) lack of 3-NP-induced reduction in PPI at 3 weeks after microwave exposure at 0.6 or 6 W/kg.

Brain, liver, heart, and lung tissues were sampled 2-3 h (short-term) and 4-5 weeks (long-term) after the second microwave exposure. Histologic examination by light microscopy showed no pathology linked to microwave exposure or 3-NP administration at either time point.

In summary, short-term results indicated very little to no change in measured endpoints due to microwave exposure, 3-NP administration, or their combination. Long-term results indicated some changes in the endpoints in a subset of tested animals. Together, results indicated the possible presence of small effects on these endpoints, which would be evidence for an effect on the central nervous system. Recommendations for further testing of this animal model include using more sensitive testing apparatus and increasing the 3-NP dose.

KEY WORDS

Sprague-Dawley rats	3-nitropropionic acid	chemical hypoxia
microwave pulses	heat stress	histopathology
acoustic startle	prepulse inhibition	within-session habituation
thermal strain	thermal stress	

TABLE OF CONTENTS

Section	Page
Acknowledgments	v
I. Background and Introduction	1
II. Materials and Methods	5
A. Animals	5
B. Activity and startle testing	5
C. Microwave exposure and dosimetry	7
D. Exposure of animals to microwaves	12
E. Histology	15
F. Procedure	16
G. Data analysis	17
III. Results	18
IV. Discussion, Conclusions, and Recommendations	26
A. Discussion	26
B. Conclusions	31
C. Recommendations	32
V. References	33
Appendix. Long-term assessment results	A1

LIST OF TABLES

Table	Page
1. Change in colonic temperature during 30-min exposure to pulsed microwaves.	19

LIST OF FIGURES

Figure — Page

1. Power density along antenna boresight. 9
2. Relative power density in vertical x-y plane at 30 cm. 10
3. Photograph of the microwave exposure set-up. 13
4. Diagram of the microwave exposure set-up. 14
5. Spontaneous motor activity. 20
6. Acoustic startle amplitude. 21
7. Within-session ratio of acoustic startle amplitude. 22
8. Prepulse inhibition of acoustic startle. 24

A1. Motor activity in first activity monitor for long-term animals, weeks 0-3. .... A4

A2. Acoustic startle amplitude for long-term animals, weeks 0-3. .... A5

A3. Within-session ratio of acoustic startle amplitude for long-term animals, weeks 0-3. .... A6

A4. Prepulse inhibition of acoustic startle for long-term animals, week 0. .... A9

A5. Prepulse inhibition of acoustic startle for long-term animals, week 1. .... A10

A6. Prepulse inhibition of acoustic startle for long-term animals, week 2. .... A11

A7. Prepulse inhibition of acoustic startle for long-term animals, week 3. .... A12

A8. Measures of horizontal activity from two-level IR activity monitor for long-term animals, weeks 0-3. .... A14

A9. Measures of vertical activity from two-level IR activity monitor for long-term animals, weeks 0-3. .... A15

A10. Measures of stereotypical activity from two-level IR activity monitor for long-term animals, weeks 0-3. .... A16

ACKNOWLEDGMENTS

This work is supported by U.S. Army Medical Research and Materiel Command contract DAMD17-94-C-4069 awarded to McKesson BioServices. Dr. Ronald L. Seaman served as Principal Investigator for this project. Dr. Satnam Mathur and Dr. Edward Dick, Jr. (LTC, Army) were Co-Investigators who contributed to this report. The experimental work reported here was performed for the US Army Medical Research Detachment (USAMRD), Mr. Bruce Stuck, Director. Dr. John DeLorge and Dr. Shin-Tsu Lu held the position of Facilities Manager of the USAMRD Microwave Branch at different times during the performance of this work. Drs. Seaman, Mathur, DeLorge, and Lu were employees of McKesson BioServices. This research was performed at the USAMRD at Brooks Air Force Base, Texas, from August 1999 through October 2000 under AFRL-Brooks animal protocol ARMY 98-03.

The project was a multidisciplinary effort drawing on the talents of a number of individuals. Dr. Mathur performed characterization of microwave exposure parameters with measurement assistance from Dr. Lu and Mr. Norm Harris, McKesson BioServices. LTC Dick, US Air Force Research Laboratory, Human Effectiveness Directorate, Veterinary Sciences Division (AFRL/HEDV), read and interpreted histology results on material prepared by Mr. Andrey Barshay (TSgt, Air Force) and Mr. Jason Brown (A1C, Air Force), AFRL/HEDV. Bryan Wohlfeld, Monica Gonzalez, and Amy Phinney, McKesson BioServices, carried out animal handling, testing, and tissue collection in this project. Mr. Fremont Wood, USAMRD, provided valuable technical advice in various early aspects of this study. Dr. Clyde Phelix, UTSA Division of Life Sciences, served as a Co-Investigator on the protocol and provided

advice on using the 3-NP animal model. Preceding the work reported here Mr. Wohlfeld tested different doses of toxin and different behavioral measures to determine those most suitable for use.

The FPS-7B radar transmitter was used through an agreement with the US Naval Health Research Center Detachment, Brooks AFB. Dr. Mathur and Mr. Harris maintained and operated the transmitter during the project.

In conducting this research, the investigator(s) adhered to the "Guide for the Care and Use of Laboratory Animals," prepared by the Institute of Laboratory Animal Resources, National Research Council (Washington, DC: National Academy Press, 1996). The AFRL at Brooks Air Force Base was fully accredited by the Association for Assessment and Accreditation of Laboratory Animal Care, International (AAALAC) during the performance of this project and continues to be at the time of this report. The AFRL-Brooks Institutional Animal Care and Use Committee (IACUC) had approved all procedures involving animals.

The views, opinions and/or findings contained in this report are those of the author(s) and should not be construed as an official Department of the Army position, policy or decision unless so designated by other documentation.

This report was prepared as a Word document using Microsoft Word 2000 software. The name of the corresponding computer file contained the character string MW&3NPTR. We thank Mr. Stuck and Dr. Lu for reading drafts of this report.

I. BACKGROUND AND INTRODUCTION

Neurons in the brain can be injured by a number of different causes. These causes include ischemia, hypoxia, trauma, neurodegenerative diseases, and actions of some toxins [Alexi et al., 1998b; Budd, 1998; McIntosh et al., 1998; Vécsei et al., 1998; Heales et al., 1999]. Mechanisms common to neuronal injury regardless of cause include oxidative stress and production of free radicals and nitric oxide. Altered calcium metabolism, NMDA glutamate receptor activation (excitotoxicity), and depolarized cell membrane potential are also implicated. These mechanisms interact with one another so that cell injury from one cause can be enhanced by action of another cause. Through these interactions, an environmental factor that triggers cell injury mechanisms or alters cellular response to injury can be expected to modify effects of another injurious environmental factor when they occur together.

Military personnel can be subjected to a variety of concurrent adverse environmental factors in the performance of duties, including potentially toxic pesticides, herbicides, and nerve agents [Deeter & Gaydos, 1993; Sidell et al., 1997; Joellenbeck et al., 1999]. In addition, tissue hypoxia can result from chemical exposure, hypoxic conditions, physical exertion, and loss of blood. Military communication, detection, and countermeasure systems use microwave and radiofrequency electromagnetic fields that are a common factor in military environments. Because more than one of these environmental factors may be encountered at a time, the effect of factors acting in combination, as well as singly, must be considered [Joellenbeck et al., 1999].

Evidence for neuronal injury from exposure to microwave radiation comes from various reports of neuropathology and changes in neuronal ultrastructure in animals exposed to microwaves [Baranski, 1972; Tolgskaya & Gordon, 1973; Albert et al., 1981; Albert & Sherif, 1988; Hansson, 1988; Lai, 1994; Mickley, 1995]. Although a number of these findings can be attributed to elevated temperature due to sufficiently high specific absorption rate (SAR) and/or sufficiently long exposure, heating does not fully explain results in some cases. That microwaves can act through normal cell injury mechanisms is supported by reports of oxidative stress and free radical production by microwave exposure [Phelan et al., 1992; Philippova et al., 1994; Kalns et al., 2000]. Direct effects of microwave exposure on brain energy metabolism that could enhance injury have also been reported [Lai, 1994].

Many of the brain pathologies reported to result from microwave exposure can be expected to change animal behavior. We wanted to see whether histologic findings in the brain of experimental animals after exposure to microwave radiation could be produced in our hands and whether any change in the nervous system corresponded to changes in measured behavior.

We used 3-nitropropionic acid (3-NP) in this project as an agent to cause tissue hypoxia. This mitochondrial toxin interferes with metabolic energy production by inhibiting succinate dehydrogenase (SDH) [Brouillet et al., 1998; Nony et al., 1999] and this inhibition can trigger neurodegeneration through neuronal injury processes of oxidative stress, nitric oxide production, and excitotoxicity [Alexi et al., 1998b; Schulz et al., 1995; Wüllner et al., 1994]. In rats treated chronically with 3-NP, the induced

tissue hypoxia is followed by formation of brain lesions that are located primarily in the caudate-putamen [Alexi et al., 1998a,b; Borlongan et al., 1995a,b; Guyot et al., 1997].

We used SARs of 0.6 and 6 W/kg as averaged over the entire animal (whole-body SAR) in 30-min exposures to have one SAR that did not elevate body temperature or disrupt ongoing behavior (0.6 W/kg) and one that did (6 W/kg) [Lotz & Michaelson, 1978; Gordon et al., 1986; D'Andrea & de Lorge, 1990]. This is based on whole-body SAR greater than about 4 W/kg having been shown to increase core body temperature by at least 1°C and to disrupt operant behaviors by different types of laboratory animals [D'Andrea & de Lorge, 1990; IEEE, 1999]. With a safety factor of 10 to give 0.4 W/kg, this SAR is represented in various standards, guidelines, and regulations for human exposure to microwave radiation [Department of the Army, 1999; Department of Defense, 1999; IEEE, 1999]. The underlying basis for a threshold of 4 W/kg for biological effect is based primarily on evaluation of reported data for subhuman species, e.g., the disruption of lever pressing, and consideration of thermal loading [Elder, 1994; IEEE, 1999]. The SAR of 6 W/kg used here was thus expected to cause thermal strain[1] in exposed animals; the SAR of 0.6 W/kg was not expected to cause thermal strain. Exposure at the lower SAR might also be expected to alter behavior [Lai, 1994; Lai et al., 1994; Wang & Lai, 2000].

---

[1] The term "thermal strain" is used to mean the deviation of body temperature or the activation of thermoeffector activity brought about by "thermal stress", a change in thermal relation between a temperature regulator and its environment that, if uncompensated, would result here in hyperthermia. This usage is consistent with published terminology preferences: IUPS Thermal Commission. 1987. Glossary of terms for thermal physiology. Second edition. Revised by The Commission for Thermal Physiology of the International Union of Physiological Sciences. Pflugers Arch 410:567-87.

Based on information from the literature, different doses of 3-NP and schedules for 3-NP administration were investigated in a preliminary study [e.g., Seaman, 2000]. The two days of treatment and the 3-NP dose of 10 mg/kg were selected for use in the project based on a measurable change in spontaneous motor activity and a high survival rate.

We studied spontaneous motor activity and modification of acoustic startle as behavioral endpoints because of involvement of striatal neural circuits in these behaviors [Koch & Schnitzler, 1997; Hauber, 1998; Swerdlow & Geyer, 1999]. The caudate-putamen of the rat striatum was expected to be the most affected by 3-NP as outlined above and thus the most likely site of any microwave interaction with 3-NP. We also performed histology on selected brain regions and organs. Results from these aspects of the project are reported here, while results from electron microscopy of neuronal ultrastructure in the caudate-putamen are being reported separately [Seaman & Phelix, 2003].

Section II of this report describes the materials and methods used in this project, including information on animals, apparatus, and procedures. Section III summarizes experimental results. Section IV is a discussion that relates results to published studies. Section V presents conclusions based on the results and lists recommendations for future experiments. The appendix contains results from a subset of animals studied over three weeks that included use of an additional activity monitor.

II. MATERIALS AND METHODS

A. Animals

Male Sprague-Dawley rats weighing 569±52 g (mean±SD) and 15-23 weeks of age were used. Animals were purchased from Charles River Labs, Portage, Michigan, through AFRL/HEDV at Brooks AFB. Animals of this age were used because the toxin used in the project was known to have a more consistent effect in Sprague-Dawley rats older than about 4 months [Bossi et al., 1993; Tsai et al., 1997]. After a 10-day quarantine upon delivery, animals were housed individually in polycarbonate shoe box cages in a room having 22±1°C temperature, 50±5% relative humidity, 10-15 hourly air exchanges, and a 12/12 light/dark cycle. Purina rodent chow and tap water were provided *ad libitum*. AFRL/HEDV and its contractors provided animal housing and feeding services.

For the experiment, animals were injected intraperitoneally (IP) with 10 mg/kg 3-nitropropionic acid (Sigma-Aldrich, St. Louis, USA) or sterile 0.9% saline (0 mg/kg). The 3-NP solutions were prepared in sterile distilled water with pH adjusted to 7.4 with 1 N NaOH and used within two weeks.

B. Activity and startle testing

For testing of spontaneous motor activity, an animal was placed into a 38.5 x 38.5 cm square arena with 24-cm walls of clear plastic that was part of an activity monitor. The floor and walls of the arena were cleaned with diluted Simple Green cleaning solution (1 volume Simple Green in 40 volumes water) before each activity test. Room lights were off during the activity test, which lasted 5 min. Animal movement interrupted ten horizontal light beams, five in each orthogonal direction, and

the number of beam interruptions was counted under computer control. Animals with more than 700 beam interruptions in a similar test lasting 10 min on the day before the first treatment were used in the experiment.

Amplitude of acoustic startle was measured as the peak of the whole-body response to startling acoustic stimuli [Koch, 1999] after each post-treatment test of activity. For testing, an animal was put into a clean cylindrical holder (8.9 cm diameter x 18 cm long inside) with its axis horizontal. The holder, mildly constraining for larger animals, was placed within a sound-attenuating chamber (San Diego Instruments) with light and fan on. The 21-min test session began with a 5-min acclimation period during which 70-dBA broadband noise was presented. This noise continued throughout the session as the background noise level. After the acclimation period, three startle trials, each consisting of a 40-ms, 120-dBA startling noise burst, were presented. Subsequent startle trials consisted of a 40-ms, 120-dBA startling noise burst presented with or without a prepulse. Each prepulse was a 20-ms noise burst delivered 100 ms before a startling noise burst. Nine iterations of four types of trials were presented: trials with prepulses 3, 6, or 12 dBA above the 70-dBA background noise level and trials with no prepulse. Trial type was randomized within each iteration and inter-trial intervals were randomized over all 39 trials with a mean of 25.4 s. Peak amplitude of the startle response was recorded in a computer data file by the San Diego Instruments computer software controlling the startle test.

Analysis of the startle data file was done with QuattroPro spreadsheet software. Three startle variables were derived for each test session: amplitude, prepulse inhibition (PPI), and within-session amplitude ratio. Average amplitude was computed

for the initial three responses in the session and for the subsequent nine responses to each of the four prepulse conditions. Average amplitude of responses to the no-prepulse condition during the nine iterations was taken as response amplitude for the session. The PPI was calculated for each prepulse intensity by subtracting its average amplitude from the no-prepulse average amplitude, dividing the difference by the no-prepulse average amplitude, and expressing the resulting fraction as a percentage. Thus, PPI was expressed as a percentage of the no-prepulse average amplitude. Within-session habituation, a form of short-term habituation, was indexed using the within-session amplitude ratio, which was calculated by dividing session response amplitude by the average amplitude of the initial three responses. Smaller ratios indicated greater habituation.

C. Microwave source and dosimetry

Microwave exposure of animals was accomplished with an antenna consisting of the open end of a WR-650 rectangular waveguide, fed by a 90-degree waveguide twist, which provided a horizontal electric field within a microwave anechoic chamber. The waveguide was connected to a General Electric FPS-7B radar transmitter that produced 5.9-μs, 1.25-GHz (L-band) pulses at 10 Hz pulse repetition frequency. The transmitter high voltage was switched on and off to begin and end, respectively, microwave exposures used for SAR measurements and experimental microwave exposures. Forward and reflected pulse powers were sampled with crystal detectors at calibrated waveguide couplers and displayed on a Tektronix Model 2430A digital oscilloscope. Sampled forward power was also measured with a General Microwave Corporation Model 478A peak power meter.

The pattern of microwave electromagnetic fields in front of the waveguide antenna was characterized with continuous-wave (CW) microwaves generated by an HP signal generator Model 8657B. The low power output of the signal generator was amplified by a CMT traveling wave tube amplifier Model 88-0127 to feed the antenna through the waveguide. The fields were measured as equivalent plane-wave power density with a Narda electromagnetic survey meter Model No. 8718 and Narda omnidirectional electric field probe Model No. 8721. Measurements were taken at 1-cm intervals with the axis of the field probe parallel to the antenna boresight.

The distribution of power density along the boresight line and in the space occupied by the animal holder is shown in Figs. 1 and 2, respectively. The measured power density was 0.25 mW/cm^2 per watt of net average power to the antenna on the antenna boresight 30 cm from the antenna aperture. This was the planned location in the far-field region of the antenna for the center of an animal. Within the space to be occupied by the animal holder the power density relative to the value at the center was within ±31% along the boresight and declined less than 22% to the side of and 11% above the boresight.

Normalized whole-body SAR derived for a prolate spheroid model of a large rat (520 g, 24-cm major axis, 6.44-cm minor axis) irradiated in **E** polarization by a plane wave has been computed to be 0.24 W/kg/mW/cm^2 at 1.25 GHz [Durney et al., 1986]. This was confirmed experimentally for this project by measuring temperature changes at various locations in a fresh 525-g carcass exposed 30 cm from the antenna. Temperature was measured during exposure using two Model 3000 Luxtron Fluoroptic thermometers and two MAM-05 fiber optic probes, each of which has four sensors

spaced 5 mm apart. Eight different probe locations were studied giving temperature profiles at a total of 32 locations. Temperatures were averaged over four microwave exposures with a probe at a particular location. Normalized SARs were derived from rises in temperature during exposure as adjusted by measured pre-exposure and post-exposure temperature changes [Gambrill et al., 1993]. Ignoring extreme values on surfaces facing toward and away from the antenna, the local SARs ranged from 0.29 to 3.8 times the normalized whole-body SAR based on the prolate spheroid model. This range of SARs was consistent with previous results from thermography in rats [Guy & Chou, 1976; Chou et al., 1985].

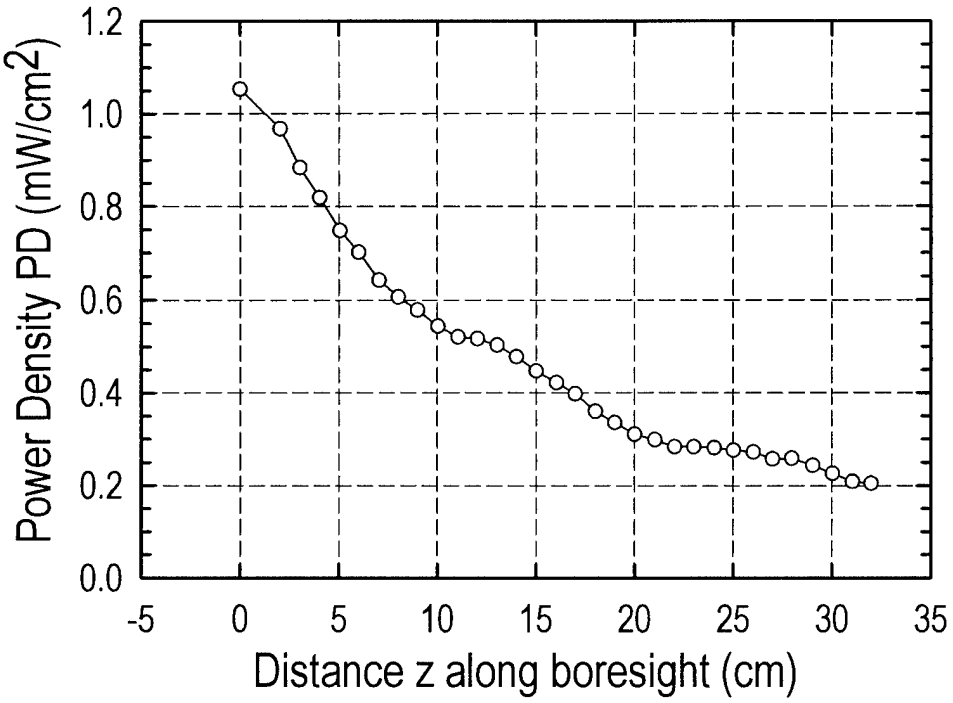
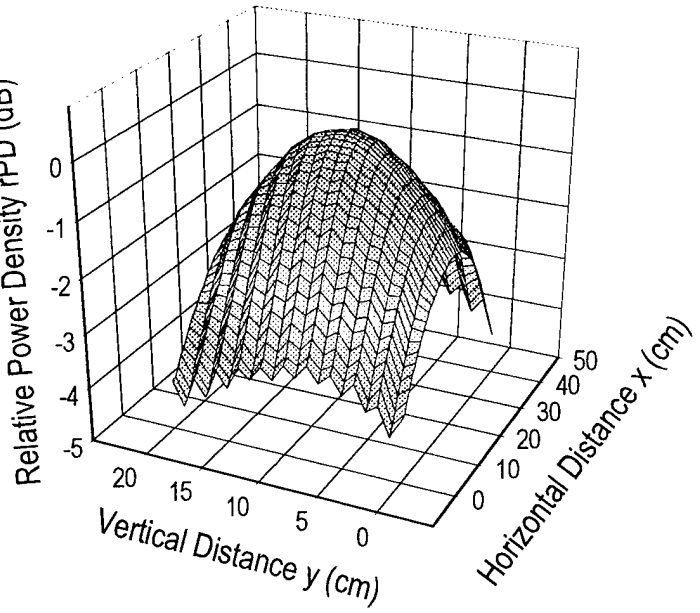


Figure 1. Power density (PD, mW/cm^2) along antenna boresight. The center of the animal holder was at z=0, which was 30 cm from the antenna. Net power to the antenna was 4.2 W.

A.



B.

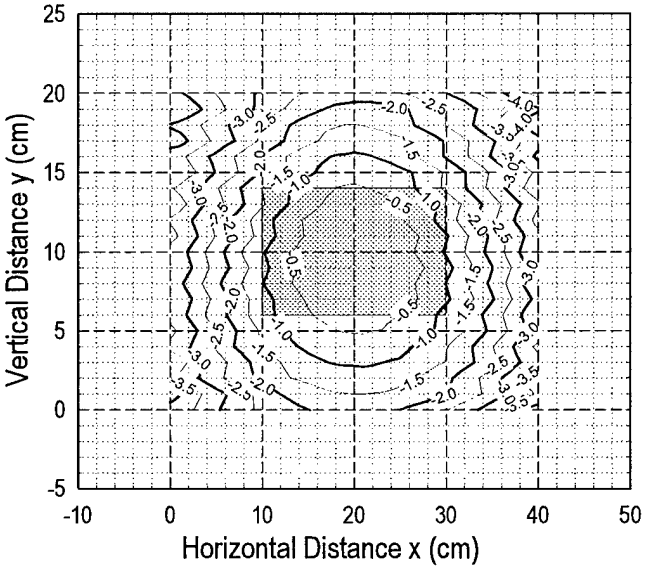


Figure 2. Relative power density (rPD, dB referenced to maximum PD) in vertical x-y plane at 30 cm. The rPD is shown as 3-D surface plot (**A**) and as contour plot showing rPD labeled with dB values (**B**). Gray rectangle in **B** is area occupied by the holder. Center of holder is at x=20, y=10.

Whole-body SAR was also determined from colonic temperatures measured during microwave exposure with the Luxtron system in anesthetized rats. An animal was placed 30 cm from the antenna and enclosed in a Styrofoam box to minimize heat loss. Circulating blood provided natural thermal mixing within the body so that the SAR obtained was representative of whole-body average SAR. Pre-exposure and post-exposure temperature changes were again taken into account [Gambrill et al., 1993]. The average normalized whole-body SAR derived from these measurements was 0.066 W/kg per watt of net average power, or 0.264 W/kg/mW/cm^2. This latter value agreed well with the model-based value as well as with the range of local SARs measured in an animal carcass.

The whole-body SAR was expected to be different for different body configurations assumed by an animal that is awake during microwave exposure. Two prolate spheroidal shapes were used to estimate this difference in SAR. A prolate spheroid for a curled rat with the same volume as the 520-g rat model described above had major and minor axes of 10 and 9.96 cm, respectively. Measurements of a live curled rat with a mass similar to that used for the model gave major and minor axes of 10 and 7.5 cm, respectively. Based on a semiempirical formula for a prolate spheroid [Durney et al., 1986], whole-body SAR for the equal-volume and measured prolate spheroid models of a curled large rat exposed to a plane wave in **E** polarization was calculated to be 51 and 88%, respectively, of whole-body SAR of the original prolate spheroid model in **E** polarization. A value of 70%, approximately midway between these values, was used for subsequent estimates. For different body configurations, different possible positions of the animal in the holder, and distribution of power

density in the holder, calculated whole-body SAR ranged from 0.55 to 1.12 times the whole-body SAR for an animal in **E** polarization at the holder center. During a 30-min microwave exposure the whole-body SAR would thus likely average to a value somewhat smaller than, but not less than 70% of, the value for a continuously centered, sitting animal. Because this estimated time-averaged SAR is quite similar to the target **E**-polarization value, we use the **E**-polarization SAR to designate exposure level in this study.

D. Exposure of animals to microwaves

For microwave exposure, an animal was placed in a nonrestricting holder consisting of a hollow clear plastic cylinder 19.5 cm long with 17.1-cm inside diameter, 0.32-cm thick walls, closed ends, and a 19.5x14.7 cm floor made of plastic rods. At the center of the holder vertical clearance was 12.9 cm between the floor and the inside top of the holder. Holes with 1-cm diameters arranged in 11 rows of 6 holes each allowed air exchange. Animal holders are shown in two positions in Fig. 3.

The SAR was set to 6 or 0.6 W/kg in part by placing the animal holder so that its center was 30 or 85 cm, respectively, from the antenna for the respective predetermined net average power to the antenna. The axis of the holder, which was horizontal as well as orthogonal to antenna boresight, was parallel to the propagating electric field **E**. The configuration of apparatus for animal exposure is shown in the photograph of Fig. 3 and in the schematic diagram (plan view) of Fig. 4. An animal in the center of the holder was on the antenna boresight and its body axis tended to be aligned with the holder axis and thus oriented in the direction of the electric field (**E** polarization). This orientation was the one most adopted by an animal because full

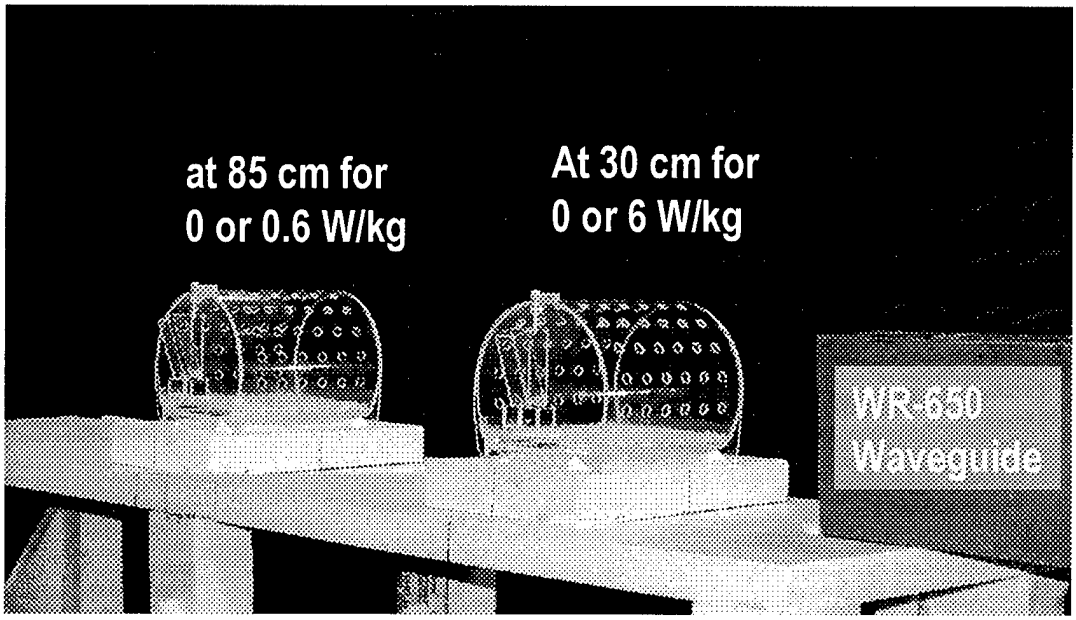


Figure 3. Photograph of the microwave exposure set-up. Two animal holders on the waveguide boresight are shown with centers at 85 cm and 30 cm from the waveguide antenna. Only one animal holder was used during each exposure.

vertical movement (rearing) was not possible and the narrower dimension of the cylinder and the orientation of floor rods along the boresight discouraged orientation of the animal parallel to the boresight.

To start a microwave exposure the transmitter high voltage was switched on and quickly adjusted manually to attain the pulse peak power necessary for the required net average power to the antenna. The high voltage was switched off to terminate the exposure. If necessary, peak power was adjusted during exposure to maintain the average power required for desired SAR. At the beginning and the end of a 0 W/kg (sham) exposure the high voltage switch was momentarily moved from stand-by to off.

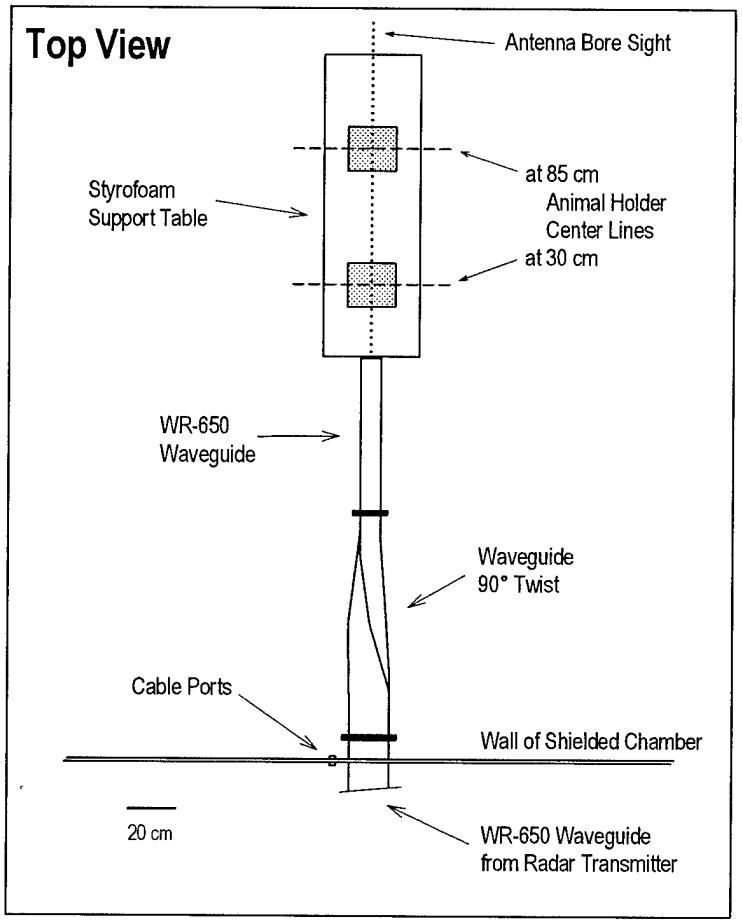


Figure 4. Diagram of the microwave exposure set-up. The waveguide twist was used to have a horizontal electric field. The animal holder (shaded) was supported by a nonmetallic table so that the center of the holder was at the same height as the open end of the waveguide. Only one location of the animal holder was used at a time.

Peak power and duration of the microwave pulses were measured ten times during each exposure and used to calculate average power to the antenna. Average net power, and thus average power density and whole-body SAR, had coefficients of variation of 1.95% and 4.43% (100xSD/mean) over all exposures at 6 and 0.6 W/kg, respectively. Repeated measures ANOVA showed that respective average powers

used for animal exposures did not differ significantly between doses of 3-NP or between days of exposure. .

Controlled air temperature inside the anechoic chamber, monitored using a YSI 401 temperature probe placed behind the antenna, was 23.03±0.43°C (mean±SD). Repeated measures analysis of variance (ANOVA) showed that chamber ambient air temperature did not differ significantly between 3-NP-microwave conditions, between pre-exposure and exposure periods, or between days of exposure. Air temperature within the animal holder was measured with the Luxtron system while a fresh carcass in **E** polarization was exposed at 6 W/kg for 30 min. The maximum temperature increase was about 1.2°C. Because other body positions would decrease SAR, we estimated that temperature in the holder during animal exposures was less than 1°C higher than chamber temperature

E. Histology

Tissues for histological evaluation were taken from selected animals in each 3-NP-microwave condition. For tissue collection, deep anesthesia was first induced with IP ketamine (80 mg/kg) and xylazine (5 mg/kg) with supplements as needed. After the descending aorta was clamped, the animal was perfused transcardially with 100 ml of 4% paraformaldehyde in sodium acetate buffer at pH 6.5 followed by 500 ml of 4% paraformaldehyde and 0.05% glutaraldehyde in sodium bicarbonate/carbonate buffer at pH 10.0. These solutions were used in anticipation of the electron microscopy of brain tissue [Seaman & Phelix, 2003]. The brain and samples of heart, lung, and liver were collected and immersed in 10% neutral buffered formalin. Before immersion of the brain, two coronal slabs 0.9 mm thick were formed: one containing

caudate-putamen and one containing deep nuclei of the cerebellum, reported sites of 3-NP- and/or microwave-induced lesions [Albert et al., 1981; Albert & Sherif, 1988; Wüllner et al., 1994; Borlongan et al., 1995a,b; Schulz et al., 1995; Guyot et al., 1997; Schmued & Slikker, 1999]. Brain slabs and other tissue samples were embedded in paraffin, sectioned at 5 μm, stained with hematoxylin and eosin, and evaluated by light microscopy.

F. Procedure

Animals were assigned in sequence to one of six 3-NP-microwave conditions (mg/kg-W/kg): 0-0, 0-0.6, 0-6, 10-0, 10-0.6, and 10-6, each consisting of injections on two consecutive days with a 30-min sham or microwave exposure after each injection. Conditions were applied in 11 sequential groups of animals with each condition in random sequence within a group. All conditions in a group were completed before the next group was started. On the day before its first injection and exposure, an animal was familiarized with procedures by being in the animal holder in the anechoic chamber for 30 min and having its colonic temperature measured with a YSI 423 temperature probe. Also on this day, an animal was tested for acceptable motor activity and also placed in the holder used for startle testing for 10-20 min.

Procedures for 3-NP injections and microwave exposures were the same on each of the two days of treatment. On the first day, an animal was injected IP with saline or 10 mg/kg 3-NP 3-5.5 h after the lights turned on in the animal room light/dark cycle. One hour after injection, colonic temperature was measured, the animal was placed into the animal holder, and the holder was placed in front of the open-ended waveguide at 30 or 85 cm, depending on desired SAR. After 30 min, exposure at 0,

0.6, or 6 W/kg SAR was started. When exposure was terminated 30 min later, the animal was removed from the animal holder and the presence of urine and number of fecal boli were noted. Colonic temperature was measured and the animal was returned to its home cage.

On the second day of treatment of an animal, the above procedure was repeated with the same 3-NP dose and microwave SAR. In addition, the animal was tested for motor activity and acoustic startle starting 1.5-2.5 h after exposure, which was 3.5-4.5 h (3.51±0.26 h, mean±SD) after injection. Microwave exposures occurred between 4.5-8 h after lights on; activity and startle testing, 6-9 h after lights on. After testing, animals from the first 3 groups were perfused 2-3 h after exposure (4-5 h after injection) for histology.

G. Data analysis

Experimental conditions were designated by 3-NP dose and microwave SAR as described above. The Shapiro-Wilk test was used to test normality of data. Parametric tests used when data were accepted as normally distributed were analysis of variance (ANOVA) [$F(df_1,df_2)$] and Newman-Keuls pair-wise tests. Nonparametric tests used were chi-square test for independence [$\chi^2(df)$], Kruskal-Wallis one-way ANOVA [*KW*(cases,df)], Friedman two-way ANOVA by ranks [*Fr*(cases,df)], and Newman-Keuls pair-wise multiple comparisons. Statistical testing was done with GB-STAT software (v5.4, Dynamic Microsystems, Silver Spring, MD) with a (two-tailed) significance level of 0.05 in all tests. Values of individual statistics are reported here as they were calculated and presented by GB-STAT. Bar graphs were constructed using SigmaPlot 2001 for Windows software (Version 7.0, SPSS, Inc.).

III. RESULTS

The study involved a total of 77 animals. Three animals were excluded because of low pre-treatment activity level. Data from eight animals for which technical difficulties occurred were not included in analysis of results. Activity and startle data were obtained from the remaining 66 animals, 11 per 3-NP-microwave condition.

During the 30-min pre-exposure period in the animal holder, animals moved about slowly, explored the animal holder interior, and groomed. Most animals were resting or sleeping at the end of the pre-exposure period and animals exposed at 0 and 0.6 W/kg continued resting or sleeping during exposure. Animals exposed at 6 W/kg continued to exhibit these behaviors for the first 10-15 min of exposure but then started grooming more frequently and became progressively more active.

The difference between colonic temperatures measured before and after microwave exposure is listed in Table 1. Colonic temperature decreased slightly for exposure at 0 and 0.6 W/kg regardless of 3-NP dose or day of exposure. On the other hand, the temperature increased 2.4-3.1 C° for exposure at 6 W/kg regardless of 3-NP dose or day of exposure, corresponding to post-exposure colonic temperature of 38.9-41.0°C. Friedman ANOVA indicated a significant difference in colonic temperature changes ($Fr(11,11)=85.0699$, $p<.0001$). Multiple comparisons showed that the four changes at 6 W/kg were each significantly different from individual changes at 0 and 0.6 W/kg, but that they were not different from each other. The eight changes at 0 and 0.6 W/kg were not different from one another. Thus, exposure at 6 W/kg increased colonic temperature, but exposure at 0 or 0.6 W/kg did not.

Table 1. Change in colonic temperature during 30-min exposure to pulsed microwaves (°C, mean±s.e.m.). The change is the difference between temperatures taken before and after the microwave exposure. N=11 per condition.

3-NP (mg/kg)	SAR (W/kg)	Day 1 $T_{after} - T_{before}$	Day 2 $T_{after} - T_{before}$
0	0	–0.39±0.17	–0.15±0.24
0	0.6	–0.21±0.16	–0.43±0.16
0	6	+3.05±0.20	+2.87±0.23
10	0	–0.31±0.17	–0.58±0.14
10	0.6	–0.22±0.14	–0.33±0.11
10	6	+2.43±0.14	+2.91±0.51

Presence of urine and number of boli were respectively similar for both days of exposure for each 3-NP-microwave condition (individual data not shown). For the four conditions with 0 or 0.6 W/kg, urine was present for 0-3 animals per condition and fecal boli numbered 0-4 per animal per condition. For the two conditions with 6 W/kg, urine was present for 7-11 animals per condition and fecal boli numbered 0-11 per animal per condition. A chi-square test performed on frequency of occurrence of urine in a contingency table indicated a significant difference ($\chi^2(5)=60.5854$, $p<.0001$). Subsequent tests on partitions of the table showed that frequencies for the two conditions with 6 W/kg were greater than frequencies for other conditions, but that they were not different from each other. In addition, frequencies for the conditions with 0 or 0.6 W/kg were not different from one another. Friedman ANOVA indicated a significant difference in number of boli between 3-NP-microwave conditions ($Fr(9,11)=25.0769$, $p=.0089$). Multiple comparison analysis showed that the pattern of

differences in number of boli among conditions was nearly the same as for presence of urine. Thus, urination and defecation were both significantly more pronounced during exposure at 6 W/kg than during exposure at 0 or 0.6 W/kg for both 0 mg/kg 3-NP and 10 mg/kg 3-NP.

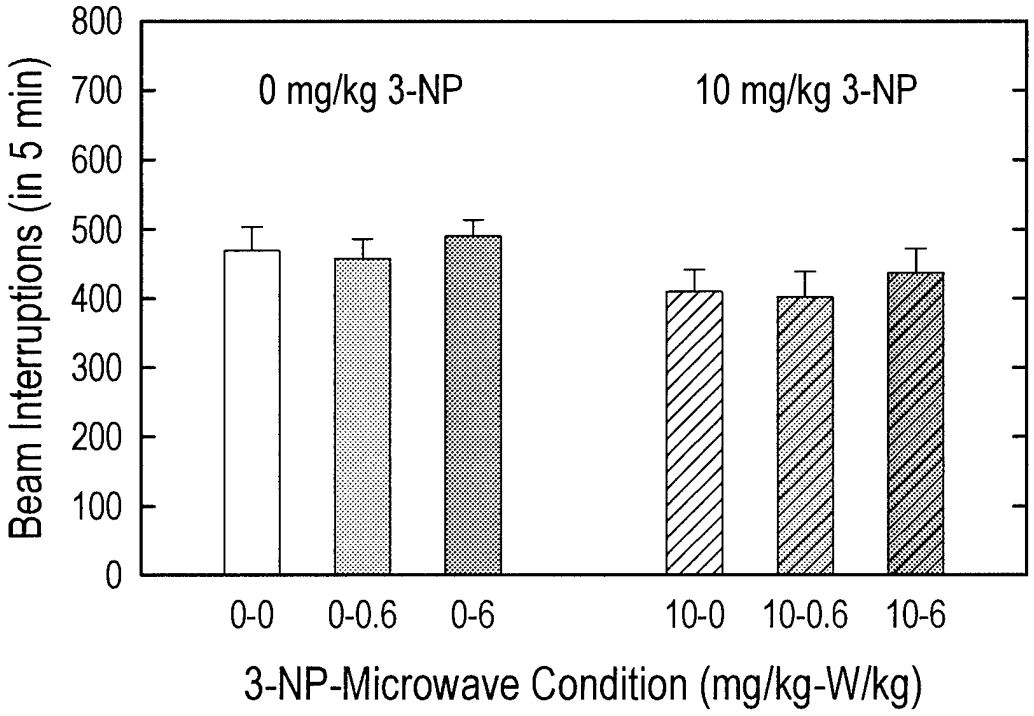


Figure 5. Spontaneous motor activity (mean and s.e.m. beam interruptions). N=11 per condition.

Motor activity, shown in Fig. 5, was less for conditions with 10 mg/kg 3-NP than for conditions with 0 mg/kg 3-NP. In ANOVA, 3-NP dose had a significant main effect ($F(1,60)=4.6055$, $p=.0359$), but the main effect of microwave SAR, as well as the interaction between dose and SAR, was not significant ($F(2,60)<1$). No pair of conditions had a significant difference in mean number of beam interruptions in Newman-Keuls testing. Thus, the reduction of about 12% between the average numbers of beam interruptions for conditions with 0 mg/kg 3-NP and for conditions

with 10 mg/kg 3-NP was supported. No interaction was detected between 3-NP and microwave exposure.

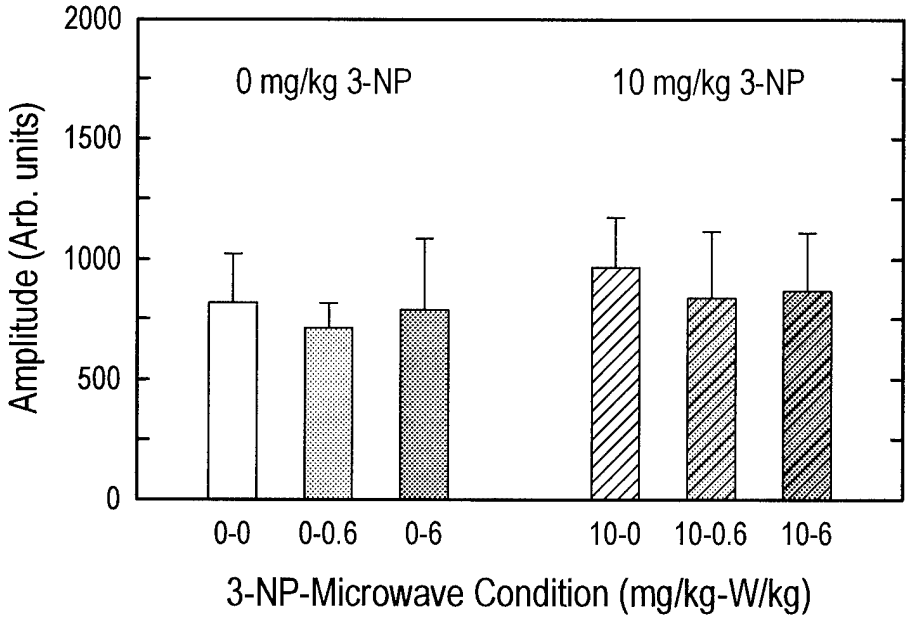


Figure 6. Acoustic startle amplitude (mean and s.e.m.). N=11 per condition.

The peak amplitude of the acoustic startle response is shown in Fig. 6. For each 3-NP-microwave condition, the amplitude spanned a large range of values as evident from the rather large variation in amplitude for each condition. The amplitude did not differ significantly between 3-NP-microwave conditions ($KW(11,5)=1.9271$, $p=.8591$). Thus, any difference in startle amplitude between 3-NP-microwave conditions is much smaller than the observed variations for individual conditions.

The amplitude of acoustic startle decreased during test sessions, i.e., exhibited within-session habituation, for each 3-NP-microwave condition. Mean within-session

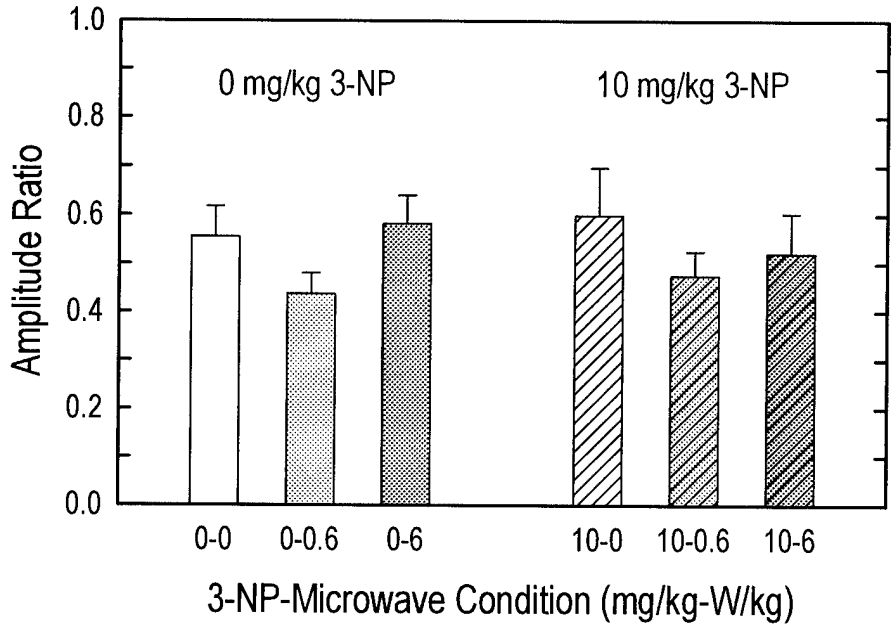


Figure 7. Within-session ratio of acoustic startle amplitude (mean and s.e.m.). A smaller value indicates a greater within-session habituation of startle. N=11 per condition.

amplitude ratios were between 0.4 and 0.6, as shown in Fig. 7. ANOVA showed that the main effects of 3-NP dose ($F(1,60)<1$) and microwave SAR ($F(2,60)=1.76413$, $p=.1801$) as well as the interaction between dose and SAR ($F(2,60)<1$) were not significant. Thus, no difference in within-session habituation occurred between 3-NP-microwave conditions, and no 3-NP-microwave interaction was detected.

Prepulse inhibition (PPI) is shown in Fig. 8 in two formats. Fig. 8A presents PPIs for the three prepulse intensities in a group for each 3-NP-microwave condition. Comparisons among the prepulses of 3, 6, and 12 dBA above background are straightforward in this format. Fig. 8B presents PPIs for the three microwave SARs in a group for each prepulse intensity making comparisons among SARs of 0, 0.6, and

6 W/kg straightforward. Evaluations between 3-NP doses can be made by comparing PPIs in the left half of either graph with those in its right half.

The PPI increased with higher prepulse intensity for each 3-NP-microwave condition, as evident in Fig. 8A. PPI for 10 mg/kg 3-NP was similar or somewhat smaller than PPI for 0 mg/kg 3-NP for respective prepulse-microwave conditions, as seen in both panels of Fig. 8. Two differences seemed to occur for the 3-dBA prepulse. The 3-dBA PPI for 0 mg/kg 3-NP progressively increased with SAR, with values of approximately 9, 24, and 41% for 0, 0.6, and 6 W/kg, respectively. This difference with SAR did not occur in 3-dBA PPI for 10 mg/kg 3-NP. A difference in PPI between conditions was indicated by Friedman ANOVA ($Fr(11,17)=91.4482$, $p<.0001$). In multiple comparisons, a number of significant differences in PPI were found between prepulse intensities for a given 3-NP-microwave condition, as indicated by asterisks in Fig. 8. However, for a given prepulse intensity no difference in PPI between pairs of conditions for the same microwave SAR or the same 3-NP dose was significant in multiple comparisons. This indicated a lack of effect on startle PPI by 3-NP and microwave exposure.

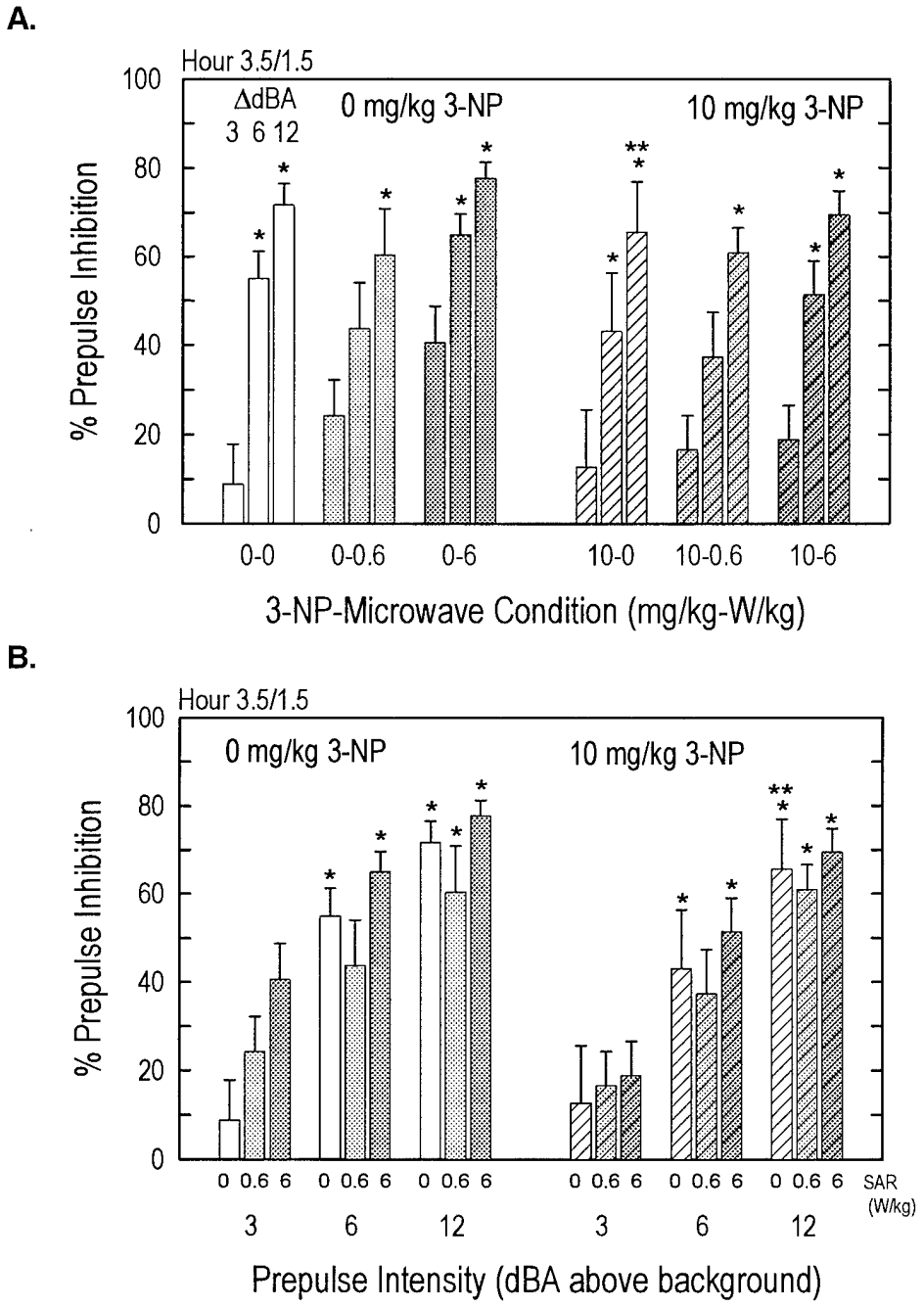


Figure 8. Prepulse inhibition (PPI) of acoustic startle (mean and s.e.m. percent PPI). PPI grouped for same 3-NP-microwave condition (**A**) and for same prepulse intensity (**B**). **N**=11 per condition. *, $p<.05$ compared to PPI by the 3-dBA prepulse for the same 3-NP-microwave condition. **, $p<.05$ compared to PPI by the 6-dBA prepulse for the same 3-NP-microwave condition.

Material for histology was available for the following numbers of animals: 3 each for conditions 0-0, 0-0.6, 0-6, and 10-0; 2 for condition 10-0.6; and 4 for condition 10-6. Histologic examination revealed minor lesions in heart and lung but not in liver. Lesions were distributed across 3-NP-microwave conditions and consistent with incidental findings historically observed in rats. Lesions attributable to 3-NP-microwave conditions were also not seen in brain, with two possible exceptions. One animal (condition 10-0) had a minimal, bilaterally symmetrical accumulation of pigmented cells in the frontoparietal cortex dorsal to the caudate-putamen and corpus callosum. The linear arrangement of the cells, which were morphologically consistent with macrophages and stained positively for iron, suggested proximity to a capillary. One animal (condition 10-6) had mild multifocal spongiosis of white matter in cerebellum and brainstem.

IV. DISCUSSION, CONCLUSIONS, AND RECOMMENDATIONS

A. Discussion

In terms of 3-NP effect, changes in activity and startle after the two relatively low doses of 3-NP here were similar to those seen in other studies. The decrease in motor activity on the second day of 3-NP-microwave treatment (Fig. 5) is consistent with decreases seen after multiple administrations of 10 or 15 mg/kg 3-NP [Borlongan et al., 1995a,b; Guyot et al., 1997]. Absence of effect of 3-NP on acoustic startle amplitude (Fig. 6) has been noted after one and two 10 or 15 mg/kg doses [Kodsi & Swerdlow, 1997; Seaman, 2000]. The testing in this project was done 27.5 and 3.5 h after the first and second 3-NP administrations, respectively. At this time, SDH levels in the brain, as well as throughout the body, are reduced for 3-NP doses similar to and larger than that used here [Alexi et al., 1998a,b; Brouillet et al., 1998; Nony et al., 1999; Ouary et al., 2000]. As a result of the induced chemical hypoxia, cell injury processes have begun [Wüllner et al., 1994; Binienda & Kim, 1997; Alexi et al., 1998a, Chyi & Chang, 1999; Lee WT et al., 2000]. Reduction in motor activity in animals receiving 3-NP here was most likely due to altered mitochondrial function in the brain and, possibly, initial neurodegeneration processes. Of course, SDH inhibition in brainstem, spinal cord, and skeletal muscle might have also contributed.

As indicated by greater restlessness and more pronounced urination and defecation, animals experienced greater stress when exposed at 6 W/kg than when exposed at 0 or 0.6 W/kg regardless of 3-NP dose. The 2.4-3.1°C elevation in colonic temperature at 6 W/kg indicated thermal strain [Gordon, 1993; Sharma et al., 1998] that likely activated the hypothalamic-pituitary-adrenal axis [Lotz & Michaelson, 1978;

Mickley, 1995] and prompted the observed increase in grooming and locomotion during exposure [Roberts, 1988; Gordon, 1993; Caputa et al., 1998; Sharma et al., 1998]. When tested in the rat within 30 min after other types of acute stress, motor activity increases [Katz et al., 1981; Galina et al., 1983; Harris et al., 1998] and startle amplitude and PPI increase [Acri, 1994; Faraday et al., 1999]. The stress during exposure at 6 W/kg, therefore, might have been expected to increase activity as well as increase startle amplitude and PPI. The only change consistent with these known effects of stress, however, was weakly suggested by the not significant increase in PPI at 3 dBA for 6 W/kg and 0 mg/kg 3-NP.

The probable decline in efficacy of such stress during the 1.5 h between end of microwave exposure and start of testing could have well resulted in elimination or decrement of an effect. Declining stress in the rat after microwave exposure is indicated by return of elevated colonic temperature and plasma corticosterone to pre-exposure levels within 30 min after termination of exposure [Michaelson et al., 1975; Guillett et al., 1975]. The relevance of colonic temperature to post-exposure behavioral measures has been demonstrated for rats exposed for 10 min to high-peak-power microwave pulses at 23 W/kg with mean colonic temperature elevated 2.5°C at the end of exposure [Akyel et al., 1991]. The animals did not respond in operant behavior tests until their colonic temperature fell to within 1.1°C of pre-exposure temperature. Other animals in the same study that were exposed at SAR of 7.6 W/kg and less had colonic temperature elevated by less than 1°C and responded immediately after exposure in testing. The lack of change in activity and startle seen here at 1.5 h after the second microwave exposure is consistent with these previous

observations that relate change of behavior to declining temperature and stress after microwave exposure. Another possible explanation for the apparent absence of effect is that animals experienced less thermal strain on the second day of exposure at 6 W/kg than on the first day of exposure, as has been observed in an operant endpoint with repeated exposures [Lebovitz, 1981]. Yet another possibility is that some combination of less thermal strain with decreased post-exposure temperature and stress could have occurred.

In thermal stress, rodent brain temperature is normally lower than core temperature because of selective cooling mechanisms [Gordon, 1993; Caputa et al., 1998], but sufficiently high SAR in the head might overcome this. In this project, measurements in an animal carcass in **E** polarization showed that SAR in the brain was 1-3 times larger than the whole-body SAR, depending on location in the brain. This was consistent with previous findings [Guy & Chou, 1976; Chou et al., 1985; Walters et al., 1998]. The colonic temperature of 38.9-41.0°C at the end of microwave exposure at 6 W/kg was a typical core temperature in rodents under thermal stress [Gordon, 1993; Caputa et al., 1998].

Thermal damage to tissue gauged by necrosis occurs at temperatures above 41°C [Matsumi et al., 1994; van der Vusse et al., 1998; Lee SY et al., 2000] and at temperatures of 40-41°C maintained for 30-60 min [Skibba et al., 1991; Lee SY et al., 2000]. Thus, direct tissue damage by elevated temperature causing cell death would not be expected here with a colonic temperature of 41°C or lower during a 30-min exposure. Because colonic temperature was likely representative of temperatures throughout the body due to time-averaging of SAR by changes in animal position and

to thermal mixing by internal heat conduction and convection [Walters et al., 1998], necrosis would not be expected anywhere in the animal. This was supported by the lack of lesions in brain, heart, lung, and liver.

Two difficulties with accurate measurement of the behaviors studied should be noted. First, the activity monitor used here detected movement based on counting light beam interruptions. The monitor was constructed in-house at WRAIR for measurement of locomotor activity. However, beam interruptions from any type of movement were accumulated into a single measure. Movements associated with non-locomotor activities such as grooming, head bobbing, jaw motion, vertical rearing, and tail motion that interrupted light beams were grouped into the measure. This reduced the sensitivity of the monitor for measurement of locomotor activity.

The second difficulty with measurement of behavior concerns the startle apparatus. The plastic cylinder used to hold animals for startle testing did not accommodate the larger animals in this project well. This resulted in a high level of variability and possibly low sensitivity of the apparatus to whole-body startle amplitude, on which all startle variables depended. Substantial variability can be readily seen in Figs. 6, 7, and 8 for amplitude, within-session habituation, and prepulse inhibition of startle, respectively. A larger cylinder was not available from the manufacturer of the startle apparatus used in this project. A larger cylinder was not fabricated in-house because its incorporation in the apparatus would have entailed irreversible structural modifications to the unit that was on loan from another military unit at Brooks Air Force Base. In any case, animal rolling and lateral recumbence,

which were the most likely sources of variability, were not expected to be affected by use of a cylinder that would fit into the sound isolation box of the startle system.

B. Conclusions

The only statistically significant effect observed in rat behavior here after 3-NP dosing and microwave exposure was the small reduction of about 12% in spontaneous motor activity with two IP doses of 10 mg/kg 3-NP. Somewhat surprisingly, the general lack of effect held even for animals that experienced thermal strain, as indicated by increased levels of urination and defecation, during microwave exposure at 6 W/kg. Lack of effect of the stress on behavior might have been due to the delay between treatment and testing.

Pathology was not observed in any organ assessed by light microscope. This included a lack of necrosis in the brain at this level of examination. In contrast, changes in neuronal ultrastructure have been observed for animals exposed at 6 W/kg, animals receiving 10 mg/kg 3-NP, and animals having both these treatments [Seaman & Phelix, 2003].

The lack of short-term effect of microwave exposure at both SAR levels – 0.6 W/kg and 6 W/kg –is consistent with data used to formulate guidelines for human exposure to microwave radiation. The rationale behind these guidelines was summarized in Section I. That is, if whole-body SAR does not exceed 4 W/kg or core temperature does not increase more than 1°C, one does not observe a change in behavior. Although the higher SAR applied here during exposure at 1.25 GHz for two 30-min periods exceeded 4 W/kg, it did not cause a detectable change in behavior or in tissue histology assessed after the second exposure. This suggests that, based on thermal considerations, lower SARs would also not change the behaviors. As pointed

out above in discussion, these findings are consistent with results of previous research on effects of microwave-induced heating.

This animal model can still be used productively in the study of effects of microwave exposure on the mammalian central nervous system. It can be used for both normal and compromised metabolic states and to study interaction of effects with a number of agents.

C. Recommendations

In order to pursue possible effects of 3-NP and microwave exposure on the central nervous system more effectively in an animal model, the following recommendations are made:

- Use a more sensitive activity monitor to assess spontaneous motor activity. One such monitor is described in the appendix.
- Use startle apparatus that easily accommodates larger animals.
- Determine SDH levels in the brain, especially in the caudate-putamen, to confirm 3-NP effectiveness.
- Use a higher dose of 3-NP if animals can tolerate it. Examine endpoints after a single injection of 3-NP with and without subsequent microwave exposure.
- Use another rat strain, such as the Lewis rat, with more consistent sensitivity to 3-NP [Ouary et al., 2000]. The smaller size of the Lewis rat is also more suitable for the existing startle apparatus.
- Consider use of chronic infusion of 3-NP by means of an implanted osmotic minipump instead of administration by injection.

V. REFERENCES

Acri JB. 1994. Nicotine modulates effects of stress on acoustic startle reflexes in rats: Dependence on dose, stressor and initial reactivity. Psychopharmacology 116:255-265.

Akyel Y, Hunt EL, Gambrill C, Vargas C Jr. 1991. Immediate post-exposure effects of high-peak-power microwave pulses on operant behavior of Wistar rats. Bioelectromagnetics 12:183-195.

Albert EN, Sherif M. 1988. Morphological changes in cerebellum of neonatal rats exposed to 2.45 GHz microwaves. Prog Clin Biol Res 257:135-151.

Albert EN, Sherif MF, Papadopoulos, Slaby FJ, Monahan J. 1981. Effect of nonionizing radiation on the Purkinje cells of the rat cerebellum. Bioelectromagnetics 2:247-257.

Alexi T, Hughes PE, Knusel B, Tobin AJ. 1998a. Metabolic compromise with systemic 3-nitropropionic acid produces striatal apoptosis in Sprague-Dawley rats but not in BALB/c ByJ mice. Exp Neurol 153:74-93.

Alexi T, Hughes PE, Faull RLM, Williams CE. 1998b. 3-nitropropionic acid's lethal triplet: Cooperative pathways of neurodegeneration. Neuroreport 9:R57-R64.

Baranski S. 1972. Histological and histochemical effect of microwave irradiation on the central nervous system of rabbits and guinea pigs. Am J Phys Med 51:182-191.

Binienda Z, Kim CS. 1997. Increase in levels of total free fatty acids in rat brain regions following 3-nitropropionic acid administration. Neurosci Lett 230:199-201.

Borlongan CV, Koutouzis TK, Freeman TB, Cahill DW, Sanberg PR. 1995a. Behavioral pathology induced by repeated systemic injections of 3-nitropropionic acid mimics the motoric symptoms of Huntington's disease. Brain Res 697:254-257.

Borlongan CV, Koutouzis TK, Randall TS, Freeman TB, Cahill DW, Sanberg PR. 1995b. Systemic 3-nitropropionic acid: Behavioral deficits and striatal damage in adult rats. Brain Res Bull 36:549-556.

Bossi SR, Simpson JR, Isacson O. 1993. Age dependence of striatal neuronal death caused by mitochondrial dysfunction. Neuroreport 4:73-76.

Brouillet E, Guyot MC, Mittoux V, Altairac S, Condé F, Palfi S, Hantraye P. 1998. Partial inhibition of brain succinate dehydrogenase by 3-nitropropionic acid is sufficient to initiate striatal degeneration in rat. J Neurochem 70:794-805.

Budd SL. 1998. Mechanisms of neuronal damage in brain hypoxia/ischemia: Focus on the role of mitochondrial calcium accumulation. Pharmacol Ther 80:203-229.

Caputa M, Dokladny K, Kurowicka B. 1998. Behavioral approach to the study of the upper limit of temperature tolerance in rats. Physiol Behav 65:183-189.

Chou CK, Guy AW, McDougall JA, Lai H. 1985. Specific absorption rate in rats exposed to 2,450-MHz microwaves under seven exposure conditions. Bioelectromagnetics 6:73-88.

Chyi T, Chang C. 1999. Temporal evolution of 3-nitropropionic acid-induced neurodegeneration in the rat brain by T_2-weighted, diffusion-weighted, and perfusion magnetic resonance imaging. Neuroscience 92:1035-1041.

D'Andrea JA, de Lorge JO. 1990. Behavioral effects of electromagnetic fields. In: Gandhi OP, editor. Biological effects and medical applications of electromagnetic energy. Englewood Cliffs, NJ: Prentice Hall. p 319-338.

Department of the Army. 1999. Army Regulation 11-9 "The Army Radiation Safety Program". Washington, DC: Department of the Army. 29 June 1999.

Department of Defense. 1999. DoD Instruction 6055.11 "Protection of DoD Personnel from Exposure to Radio Frequency Radiation". December 4, 1999. Also predecessor instruction with same title, February 21, 1995. Washington, DC: Department of Defense.

Deeter DP, Gaydos JC, editors. 1993. Occupational Health: The Soldier and the Industrial Base. Washington DC: Office of the Surgeon General, U.S. Department of the Army. 643 p.

Durney CH, Massoudi H, Iskander MF. 1986. Radiofrequency radiation dosimetry handbook, Fourth Edition. Technical Report USAFSAM-TR-85-73. Brooks Air Force Base: USAF School of Aerospace Medicine.

Elder JA. 1994. Thermal, cumulative, and life span effects and cancer in mammals exposed to radiofrequency radiation. In: Carpenter DO, Ayrapetyan S, editors.

Biological effects of electric and magnetic fields, beneficial and harmful effects, volume 2. San Diego: Academic Press. p 279-295.

Faraday MM, O'Donoghue VA, Grunberg NE. 1999. Effects of nicotine and stress on startle amplitude and sensory gating depend on rat strain and sex. Pharmacol Biochem Behav 62:273-284.

Gambrill CS, DeAmgelis ML, Lu ST. 1993. Error analysis of a thermometric microwave-dosimetry procedure. In: Blank M, editor. Electricity and magnetism in biology and medicine. San Francisco CA: San Francisco Press. p 593-595.

Guillet R, Lotz WG, Michaelson SM. 1975. Time-course of adrenal response in microwave-exposed rats. Abstracts of 1975 Annual Meeting of USNC/URSI. p 316.

Galina ZH, Sutherland CJ, Amit Z. 1983. Effects of heat-stress on behavior and the pituitary adrenal axis in rats. Pharmacol Biochem Behav 19:251-256.

Gordon CJ. 1993. Temperature regulation in laboratory rodents. Cambridge: University Press. 267 p.

Gordon CJ, Long MD, Fehlner KS, Stead AG. 1986. Body temperature in the mouse, hamster, and rat exposed to radiofrequency radiation: An interspecies comparison. J Therm Biol 11:59-65.

Guy AW, Chou CK. 1976. System for quantitative chronic exposure of a population of rodents to UHF fields. In: Johnson CC, Shore ML, editors. Biological effects of electromagnetic waves. HEW Publication (FDA) 77-8011. Rockville MD: Bureau of Radiological Health. p 389-410.

Guyot MC, Hantraye P, Dolan R, Palfi S, Maziére M, Brouillet E. 1997. Quantifiable bradykinesia, gait abnormalities and Huntington's disease-like striatal lesions in rats chronically treated with 3-nitropropionic acid. Neuroscience 79:45-56.

Hansson HA. 1988. Effects on the nervous system by exposure to electromagnetic fields: Experimental and clinical studies. Prog Clin Biol Res 257:119-134.

Harris RBS, Zhou J, Youngblood BD, Smagin GN, Ryan DH. 1998. Failure to change exploration or saccharin preference in rats exposed to chronic mild stress. Physiol Behav 63:91-100.

Hauber W. 1998. Involvement of basal ganglia transmitter systems in movement initiation. Prog Neurobiol 56:507-540.

Heales SJR, Bolaños JP, Stewart VC, Brookes PS, Land JM, Clark JB. 1999. Nitric oxide, mitochondria and neurological disease. Biochim Biophys Acta 1410:215-228.

IEEE. 1999. IEEE Std C95.1. IEEE Standard for Safety Levels with Respect to Human Exposure to Radio Frequency Electromagnetic Fields, 3 kHz to 300 GHz. New York: Institute of Electrical and Electronics Engineers, Inc. 73 p.

Joellenbeck LM, Russell PK, Guze SB, editors. 1999. Strategies to Protect the Health of Deployed U.S. Forces: Medical Surveillance, Record Keeping, and Risk Reduction. Washington DC: National Academy Press. 282 p.

Kalns J, Ryan KL, Mason PA, Bruno JG, Gooden R, Kiel JL. 2000. Oxidative stress precedes circulatory failure induced by 35-GHz microwave heating. Shock 13:52-59.

Katz RJ, Roth KA, Carroll BJ. 1981. Acute and chronic stress effects on open field activity in the rat: Implications for a model of depression. Neurosci Biobehav Rev 5:247-251.

Koch M. 1999. The neurobiology of startle. Prog Neurobiol 59:107-128.

Koch M, Schnitzler HU. 1997. The acoustic startle response in rats: Circuits mediating evocation, inhibition and potentiation. Behav Brain Res 89:35-49.

Kodsi MH, Swerdlow NR. 1997. Mitochondrial toxin 3-nitropropionic acid produces startle reflex abnormalities and striatal damage in rats that model some features of Huntington's disease. Neurosci Lett 231:103-107.

Lai H. 1994. Neurological effects of radiofrequency electromagnetic radiation. In: Lin JC, editor. Advances in Electromagnetic Fields in Living Systems. Vol. 1. New York: Plenum. p 27-80.

Lai H, Horita A, Guy AW. 1994. Microwave irradiation affects radial-arm maze performance in the rat. Bioelectromagnetics 15:95-104.

Lebovitz RM. 1981. Prolonged microwave irradiation of rats: effects on concurrent operant behavior. Bioelectromagnetics 2:169-185.

Lee SY, Lee SH, Akuta K, Uda M, Song CW. 2000. Acute histological effects of interstitial hyperthermia on normal rat brain. Int J Hyperthermia 16:73-83.

Lee WT, Lee CS, Pan YL, Chang C. 2000. Temporal changes of cerebral metabolites and striatal lesions in acute 3-nitropropionic acid intoxication in the rat. Mag Res Med 44:29-34.

Lotz WG, Michaelson SM. 1978. Temperature and corticosterone relationships in microwave-exposed rats. J Appl Physiol 44:438-445.

Matsumi N, Matsumoto K, Mishima N, Moriyama E, Furuta T, Nishimoto A, Taguchi K. 1994. Thermal damage threshold of brain tissue: Histological study of heated normal monkey brains. Neurol Med Chir (Tokyo) 34:209-215.

McIntosh TK, Saatman KE, Raghupathi R, Graham DI, Smith DH, Lee VM, Trojanowski JQ. 1998. The molecular and cellular sequelae of experimental traumatic brain injury: Pathogenetic mechanisms. Neuropathol Appl Neurobiol 24:251-267.

Michaelson SM, Houk WM, Lebda NJ, Lu ST, Magin RL. 1975. Biochemical and neuroendocrine aspects of exposure to microwaves. Ann N Y Acad Sci 247:21-45.

Mickley GA. 1995. Effects of radiofrequency radiation (RFR) on neurophysiological stress indicators. In: Klauenberg BJ, Grandolfo M, Erwin DN, editors. Radiofrequency radiation standards: Biological effects, dosimetry, epidemiology, and public health policy. New York: Plenum Press. p 223-234.

Nony PA, Scallet AC, Rountree RL, Ye X, Binienda Z. 1999. 3-nitropropionic acid (3-NPA) produces hypothermia and inhibits histochemical labeling of succinate dehydrogenase (SDH) in rat brain. Metabolic Brain Dis 14:83-94.

Ouary S, Bizat N, Altairac S, Ménétrat H, Mittoux V, Condé F, Hantraye P, Brouillet E. 2000. Major strain differences in response to chronic systemic administration of the mitochondrial toxin 3-nitropropionic acid in rats: Implications for neuroprotection studies. Neuroscience 97:521-530.

Phelan AM, Lange DG, Kues HA, Lutty GA. 1992. Modification of membrane fluidity in melanin-containing cells by low-level microwave radiation. Bioelectromagnetics 13:131-146.

Philippova TM, Novoselov VI, Alekseev SI. 1994. Influence of microwaves on different types of receptors and the role of peroxidation of lipids on receptor-protein shedding. Bioelectromagnetics 15:183-192.

Roberts WW. 1988. Differential thermosensor control of thermoregulatory grooming, locomotion, and relaxed postural extension. Ann NY Acad Sci 525:363-374.

Schulz JB, Matthews RT, Jenkin BG, Ferrante RJ, Siwek D, Henshaw DR, Cipolloni PB, Mecocci P, Kowall NW, Rosen BR, Beal MF. 1995. Blockade of neuronal nitric oxide synthase protects against excitotoxicity *in vivo*. J Neurosci 15:8419-8429.

Schmued L, Slikker W Jr. 1999. Black-Gold: A simple, high-resolution histochemical label for normal and pathological myelin in brain tissue sections. Brain Res 837:289-297.

Seaman RL. 2000. Effects of acute systemic 3-nitropropionic acid administration on rat activity and acoustic startle. Neurosci Lett 280:183-186.

Seaman RL, Phelix CF. 2003. Acute effects of pulsed microwaves and 3-nitropropionic acid on neuronal ultrastructure in the rat caudate-putamen. In preparation.

Sharma HS, Westman J, Nyberg F. 1998. Pathophysiology of brain edema and cell changes following hyperthermic brain injury. Prog Brain Res 115:351-412.

Sidell FR, Takafuji ET, Franz DR, editors. 1997. Medical Aspects of Chemical and Biological Warfare. Washington DC: Office of the Surgeon General, U.S. Department of the Army. 721 p.

Skibba JL, Powers RH, Stadnicka A, Cullinane DW, Almagro UA, Kalbfleisch JH. 1991. Oxidative stress as a precursor to the irreversible hepatocellular injury caused by hyperthermia. Int J Hyperthermia 7:749-761.

Swerdlow NR, Geyer MA. 1999. Neurophysiology and neuropharmacology of short lead interval startle modification. In: Dawson ME, Schell AM, Böhmelt AH, editors. Startle modification: Implications for neuroscience, cognitive science, and clinical science. Cambridge: University Press. p 114-133.

Tolgskaya MS, Gordon ZV. 1973. Pathological effects of radio waves. New York: Consultants Bureau. 146 p.

Tsai MJ, Goh CC, Wan YL, Chang C. 1997. Metabolic alterations produced by 3-nitropropionic acid in rat striata and cultured astrocytes: Quantitative *in vitro* ^{1}H nuclear magnetic resonance spectroscopy and biochemical characterization. Neuroscience 79:819-826.

van der Vusse GJ, Cornelussen RN, Roemen TH, Snoeckx LH. 1998. Heat stress pretreatment mitigates postischemic arachidonic acid accumulation in rat heart. Mol Cell Biochem 185:205-211.

Vécsei L, Dibó G, Kiss C. 1998. Neurotoxins and neurodegenerative disorders. Neurotoxicology 19:511-514.

Walters TJ, Ryan KL, Belcher JC, Doyle JM, Tehrany MR, Mason PA. 1998. Regional brain heating during microwave exposure (2.06 GHz), warm-water immersion, environmental heating and exercise. Bioelectromagnetics 19:341-353.

Wang B, Lai H. 2000. Acute exposure to pulsed 2450-MHz microwaves affects water-maze performance of rats. Bioelectromagnetics 21:52-56.

Wüllner U, Young AB, Penney JB, Beal MF. 1994. 3-nitropropionic acid toxicity in the striatum. J Neurochem 63:1772-1781.

APPENDIX

LONG-TERM ASSESSMENT RESULTS

Introduction and Methods

Approximately halfway through efforts described in the main body of this report a decision was made to follow animals for a longer period of time after 3-NP-microwave treatment. This was based on the expectation that any deleterious effect on the nervous system triggered by 3-NP-microwave treatments would manifest itself over a period of time and affect endpoints to a greater degree than on the second day of treatment. Consequently, animals in the last five groups of animals studied, called long-term animals here, were retested for motor activity and acoustic startle at 1, 2, and 3 weeks after the second day of treatment. The second day of treatment was renamed week 0 for long-term animals. The 3-NP-microwave treatments as well as tests of activity and startle that were experienced by the first six groups of animals were done exactly the same for long-term animals. Data obtained at week 0 from long-term animals are also included in the short-term results described in the main body of this report. Instead of being perfused for histology on the second day of treatment or euthanized, long-term animals were returned to housing in the animal room. These animals were then tested at weekly intervals at the same time of day as on the second day of treatment, i.e., 6-9 h after lights on.

At 4-5 weeks after 3-NP-microwave treatment, long-term animals were submitted to AFRL/HEDV for necropsy and histology. Animals were euthanized with CO_2 and brain and samples of heart, lung, and liver were collected and placed in 10% neutral buffered formalin for fixation. The two brain slabs described in Section II.D

were obtained after this fixation. Tissue samples were embedded in paraffin, sectioned at 5 μm, stained with hematoxylin and eosin, and evaluated by light microscopy.

Also at about halfway through the project, a new activity monitor became available. This was an AccuScan activity monitor with DigiScan software (AccuScan, Columbus, Ohio). This activity monitor system had infrared (IR) beams at 3.6 cm and 14.7 cm above the floor that were detected under software control. It is thus referred to in this report as a two-level IR activity monitor. Information on interruptions of the beams was processed by the software to derive measures of horizontal, vertical (rearing), and stereotypical animal movements. The software defined stereotypical movements as animal movements causing repetitive interruptions of the same horizontal beam within 1 s.

Testing with the two-level IR activity monitor supplemented the tests described for short-term results to obtain information on spontaneous activity of long-term animals. Testing of a particular animal with this monitor was done just after activity and startle testing described in Section II.B of the animal. Although the testing sequence might have influenced measurement of activity with the newer monitor, the importance of having all animals in the overall project tested the same way outweighed this concern. Due to a number of factors, the number of animals reliably assessed with the new monitor was not the same for each 3-NP-microwave condition. Because of the sequence of testing and the small and unequal numbers, the results obtained with the monitor are provided here for information purposes only.

Spontaneous motor activity was tested in the two-level IR activity monitor by placing an animal in the square arena (40.8x40.8 cm with 30.5 cm walls) for 5 min with

room lights off. The arena was cleaned between animals with diluted Simple Green (Section II.B). Nine activity measures derived by software during the test session were recorded as activity data that were later processed with QuattroPro spreadsheet software. Derived measures of horizontal movement were number of lower-level, horizontal sensor beam interruptions (HACTV), distance moved in cm (TOTDIST), and number of horizontal-movement episodes (MOVNO). Derived measures of vertical movement were number of upper-level, vertical sensor beam interruptions (VACTV), number of vertical-movement episodes, or rears, (VMOVNO), and time spent in vertical movement, or rearing time (VTIME). Derived measures of stereotypy were number of repetitive rapid beam interruptions (STRCNT), number of stereotypy episodes (STRNO), and time spent in stereotypy (STRTIME).

Results in this appendix are first given for activity measured in long-term animals using the original activity monitor that was used throughout the project. Results for each startle variable are then presented. These activity and startle measures are the same ones described in the main body of this report. Results from the two-level IR activity monitor are reported next. Histology results are then summarized.

Spontaneous Activity Results

Motor activity measured by the original activity monitor on 1, 2, and 3 weeks after 3-NP-microwave treatment is shown in Fig. A1. Motor activity at week 0, the second day of treatment, is included for long-term animals. For each 3-NP-microwave condition, activity at weeks 1, 2, and 3 was lower than at week 0. Friedman ANOVA indicated the presence of a significant difference ($Fr(5,23)=44.718$, $p=.0043$). In multiple comparisons, only four differences were found significant. These were all decreases in activity with time and are indicated in Fig. A1. The number of beam interruptions for weeks 1-3 in condition 0-0.6 were similar to levels in other conditions. The significant decreases revealed for condition 0-0.6 might be due in part to the slightly higher level for week 0. For this activity measure, no significant difference was

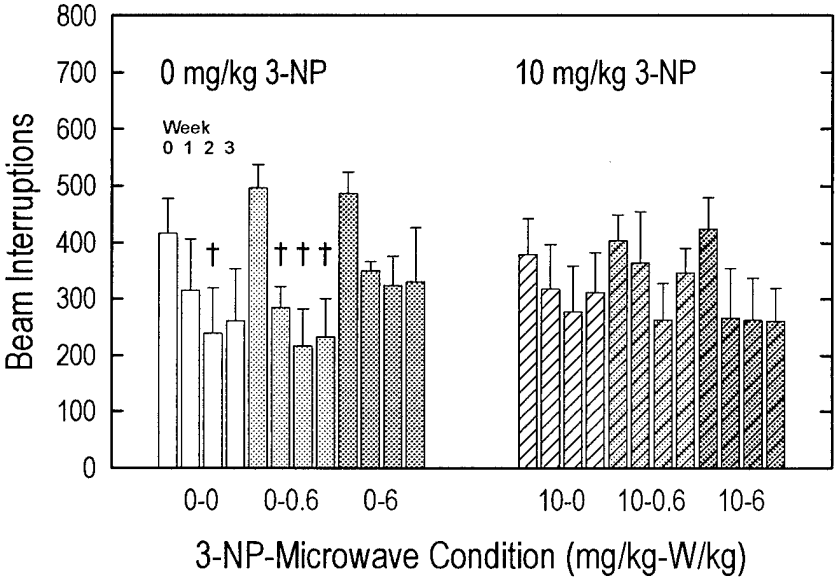


Figure A1. Motor activity in original activity monitor (mean and s.e.m. beam interruptions) for long-term animals, weeks 0-3. N=5 for each 3-NP-microwave condition. †, $p<.05$ compared to motor activity at week 0 for the same 3-NP-microwave condition.

found between 3-NP-microwave conditions for any one-week.

In this subset of animals, the number of beam interruptions did not decrease significantly with 3-NP in week 0. This is different than what was found for results obtained from all animals at that time (Section III, Fig. 5) and may be due to smaller sample size or variations in animals.

Acoustic Startle – Startle Amplitude Results

Amplitude of the acoustic startle response from tests on weeks 0, 1, 2, and 3 after 3-NP-microwave treatment is shown in Fig. A2. The amplitude was quite variable over the 4 weeks of testing. The largest variability was seen for the 10-0 condition, which on average was larger than for other conditions. Possibly due to the large variability in amplitude, no significant difference was indicated for this measure ($Fr(5,23)=32.992$, $p=.0812$).

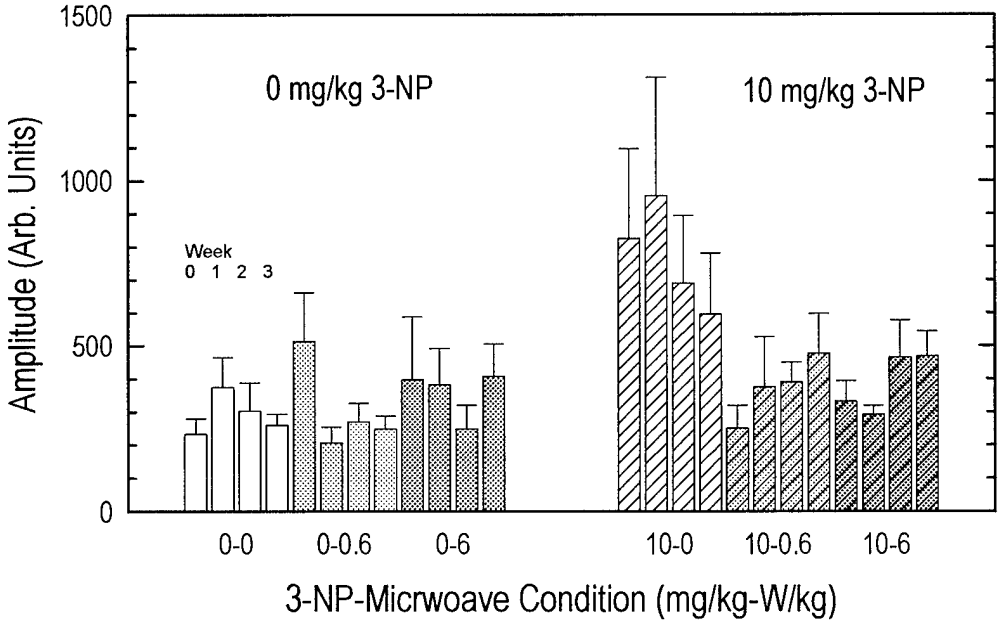


Figure A2. Acoustic startle amplitude (mean and s.e.m.) for long-term animals, weeks 0-3. N=5 for each 3-NP-microwave condition.

Acoustic Startle – Within-Session Habituation Results

The within-session amplitude ratio for acoustic startle tests on weeks 0, 1, 2, and 3 after 3-NP-microwave treatment is shown in Fig. A3. Smaller values of the amplitude ratio correspond to greater within-session habituation. The within-session amplitude ratio tended to increase somewhat over time for some 3-NP-microwave conditions. However, no significant difference was indicated for this measure ($Fr(5,23)=30.988$, $p=.1231$).

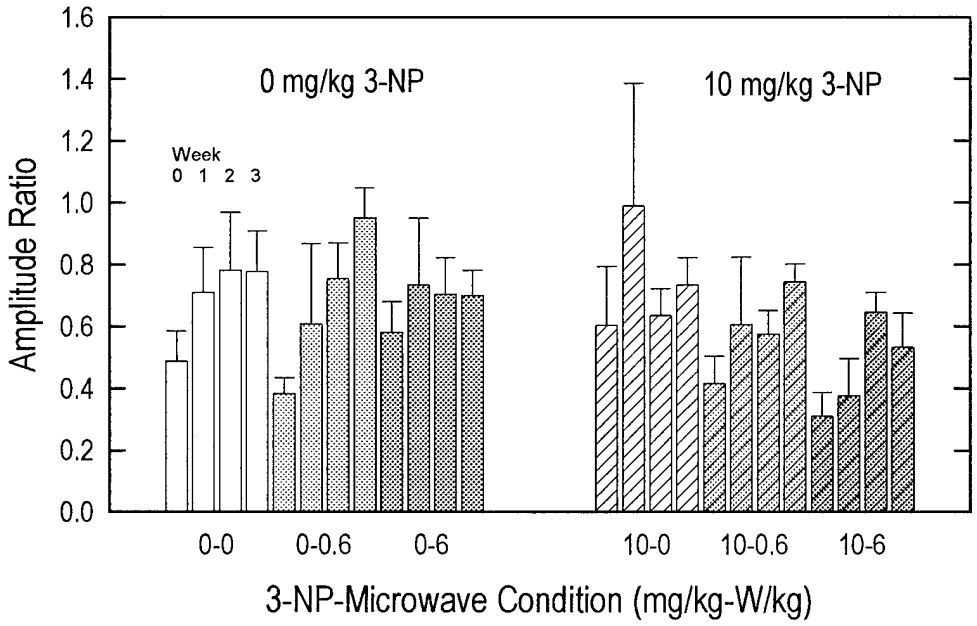


Figure A3. Within-session ratio of acoustic startle amplitude (mean and s.e.m.) for long-term animals, weeks 0-3. N=5 for each 3-NP-microwave condition.

Acoustic Startle – Prepulse Inhibition Results

Prepulse inhibition in startle tests at weeks 0, 1, 2, and 3 after 3-NP-microwave treatment is shown in Figs. A4-A7. Because of the number of data, PPI is presented for each week separately and two formats in each figure, as done in the main body of this report.

In each week, PPI generally increased with higher prepulse intensity for each 3-NP-microwave condition, as expected. This is most easily seen in part A of each figure. Differences were found for PPI in long-term animals in weeks 0, 1, and 3 of testing: $Fr(5,17)=55.6947$, $p<.0001$; $Fr(5,17)=39.9193$, $p=.0013$; $Fr(5,17)=25.6667$, $p=.0808$; and $Fr(5,17)=47.4702$, $p=.0001$ for weeks 0, 1, 2, and 3, respectively. In respective multiple comparisons, a number of significant differences in PPI were found for each week. Most of these differences were between prepulse intensities for a given 3-NP-microwave condition, which are indicated by asterisks in Figs. A4, A5, and A7.

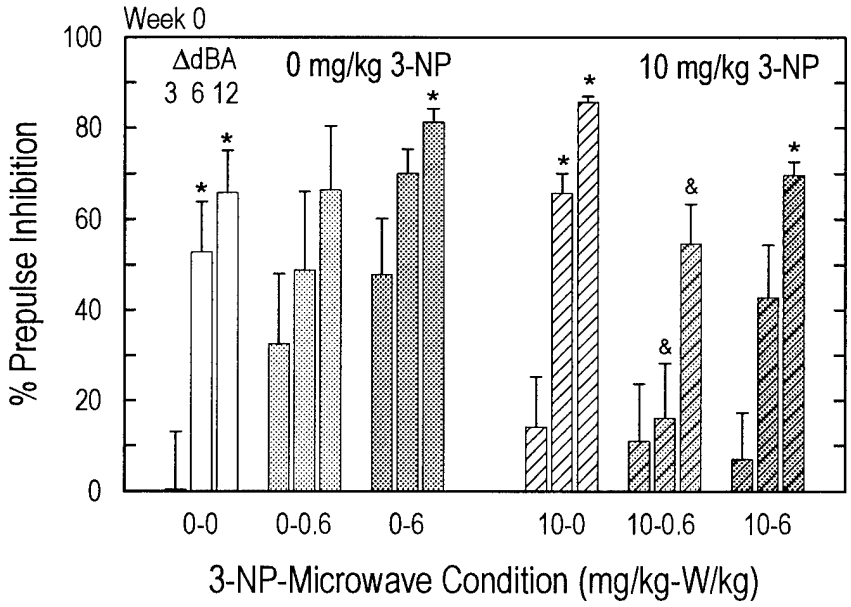
Two significant differences were found in multiple comparisons for microwave SAR in week 0. As indicated by "&" in Fig. A4, PPI by both 6- and 12-dBA prepulses was significantly smaller for condition 10-0.6 than for condition 10-0. That is, animals having 10 mg/kg had significantly smaller prepulse inhibition after microwave exposure at 0.6 W/kg than did animals that had the same 3-NP dose but were sham-exposed. The overall significance of these differences is clouded by the fact that they were not found when all 11 groups of animals were considered (Section III, Fig. 8).

Two significant differences were found in multiple comparisons for 3-NP dose in week 3. Indicated by "#" in Fig. A7, PPI by the 6-dBA prepulse was smaller for condition 10-0 than for condition 0-0. This was also the case for the 12-dBA prepulse

between the two conditions. That is, in week 3, animals not exposed to microwaves (sham-exposed) after administration of 10 mg/kg 3-NP (condition 10-0) had PPI smaller than in control animals (condition 0-0), presumably a long-term effect of the 3-NP. However, animals exposed to microwaves at either 0.6 or 6 W/kg after 10 mg/kg 3-NP had PPI similar to control animals, i.e., no decrease in PPI. This lack of decrease indicated a possible cancellation of the 3-NP-induced effect by the microwave exposures.

The differences in PPI noted above for weeks 1 and 3 were the only significant differences found between 3-NP-microwave conditions. No other difference in PPI was found to be significant in any week for the same prepulse.

A.



B.

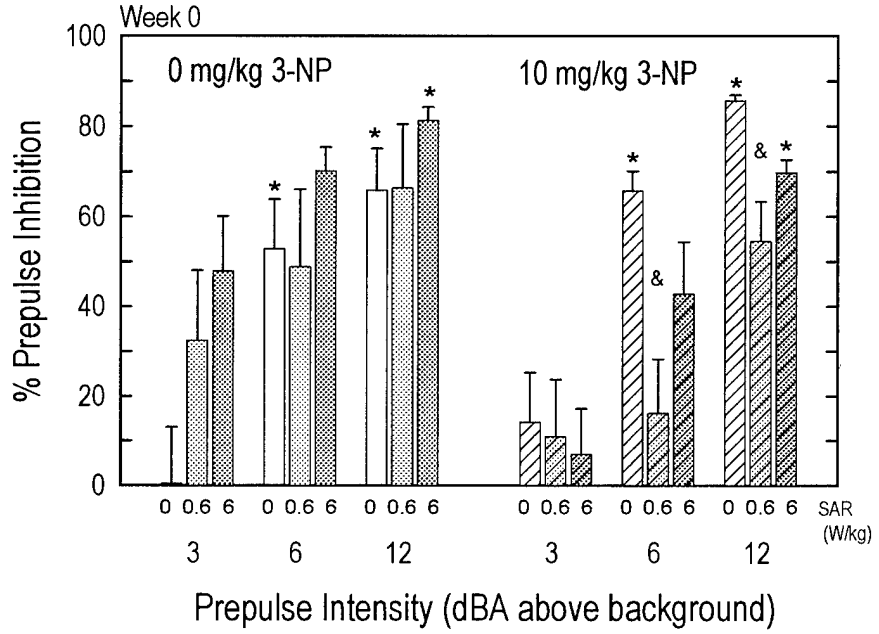
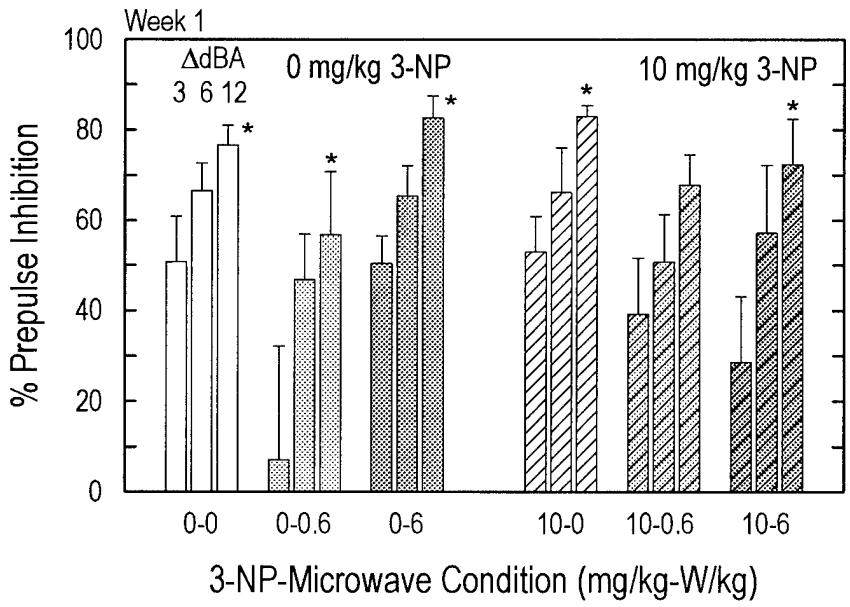


Figure A4. Prepulse inhibition (PPI) of acoustic startle (mean and s.e.m. percent PPI) for long-term animals, week 0. PPI grouped by 3-NP-microwave condition (**A**) and by prepulse (PP) intensity (**B**). N=5 for each condition. *, $p<.05$ compared to PPI by 3-dBA prepulse for same 3-NP-microwave condition. **, $p<.05$ compared to PPI by 6-dBA prepulse for same 3-NP-microwave condition. &, $p<.05$ compared to same prepulse intensity for condition 10-0.

A.



B.

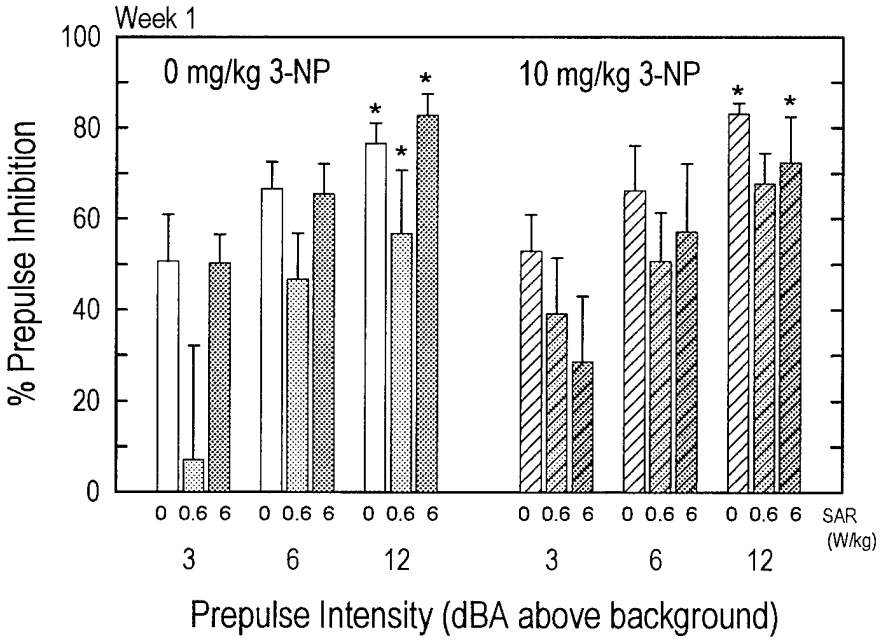
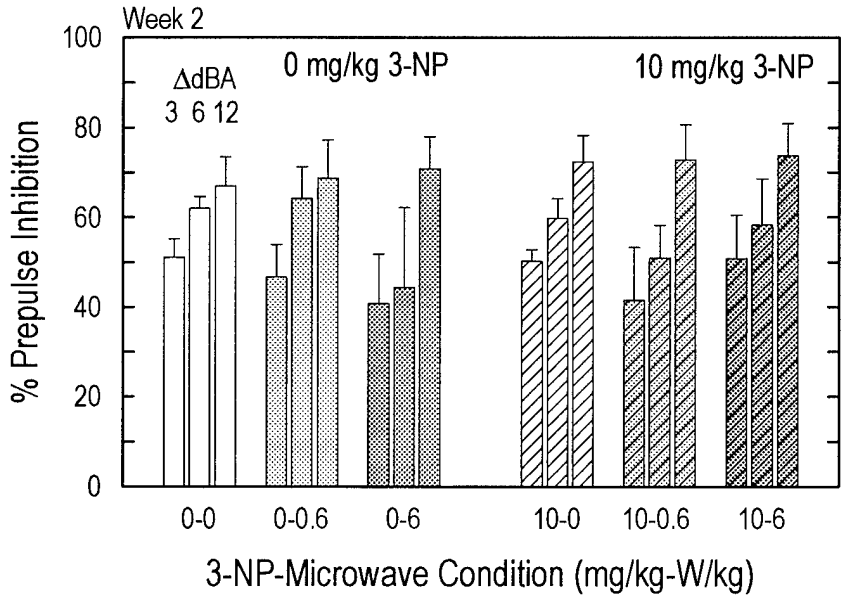


Figure A5. Prepulse inhibition (PPI) of acoustic startle (mean and s.e.m. percent PPI) for long-term animals, week 1. PPI grouped by 3-NP-microwave condition (**A**) and by prepulse intensity (**B**). N=5 for each 3-NP-microwave condition. *, $p<.05$ compared to PPI by 3-dBA prepulse for same 3-NP-microwave condition.

A.



B.

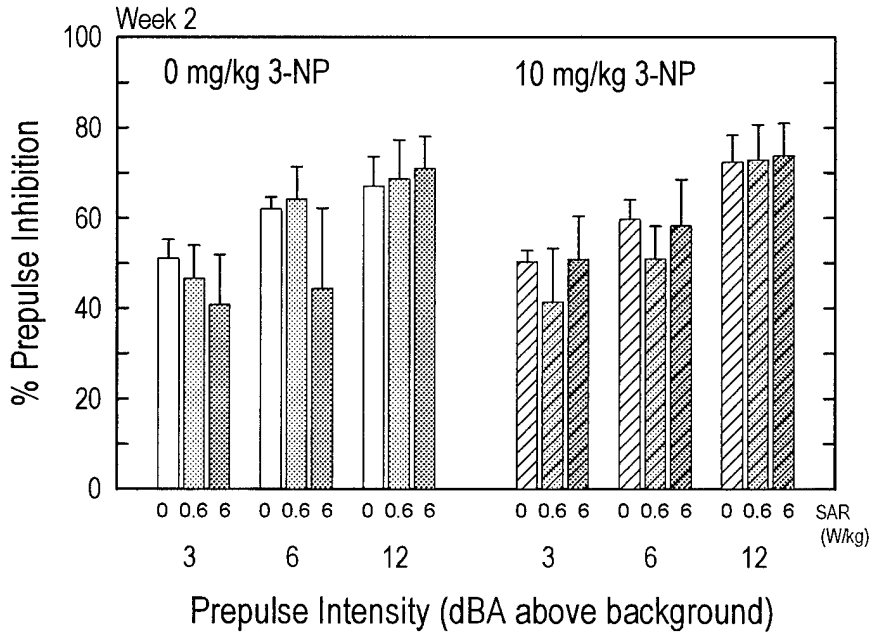
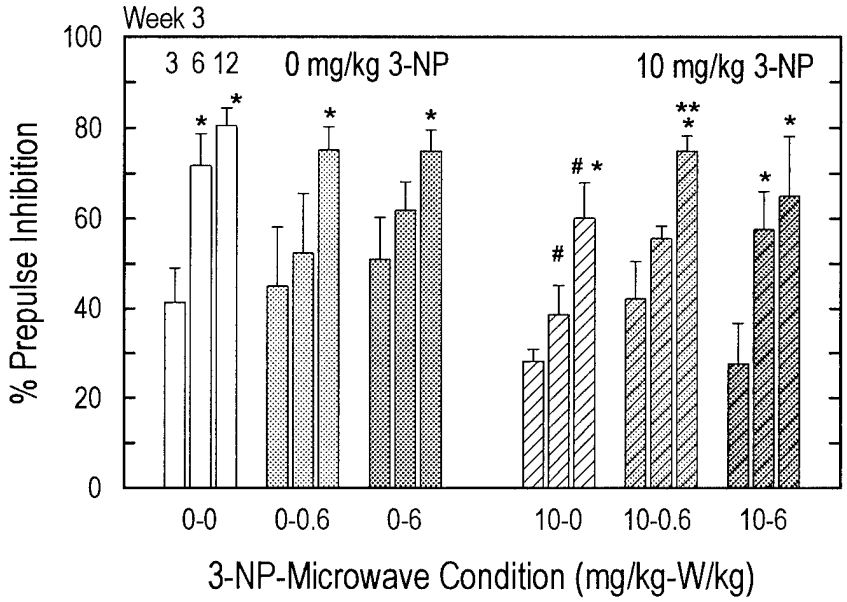


Figure A6. Prepulse inhibition (PPI) of acoustic startle (mean and s.e.m. percent PPI) for long-term animals, week 2. PPI grouped by 3-NP-microwave condition (**A**) and by prepulse intensity (**B**). N=5 for each 3-NP-microwave condition.

A.



B.

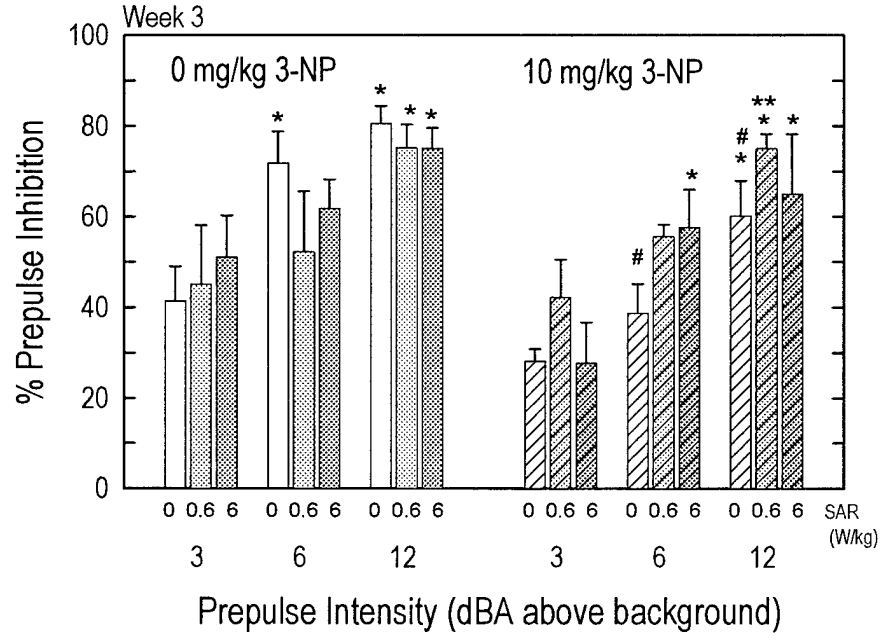


Figure A7. Prepulse inhibition (PPI) of acoustic startle (mean and s.e.m. percent PPI) for long-term animals, week 3. PPI grouped by 3-NP-microwave condition (**A**) and by prepulse intensity (**B**). N=5 for each 3-NP-microwave condition. *, $p<.05$ compared to PPI by 3-dBA prepulse for same 3-NP-microwave condition. #, $p<.05$ compared to the same prepulse intensity for condition 0-0.

Two-Level IR Activity Monitor Results

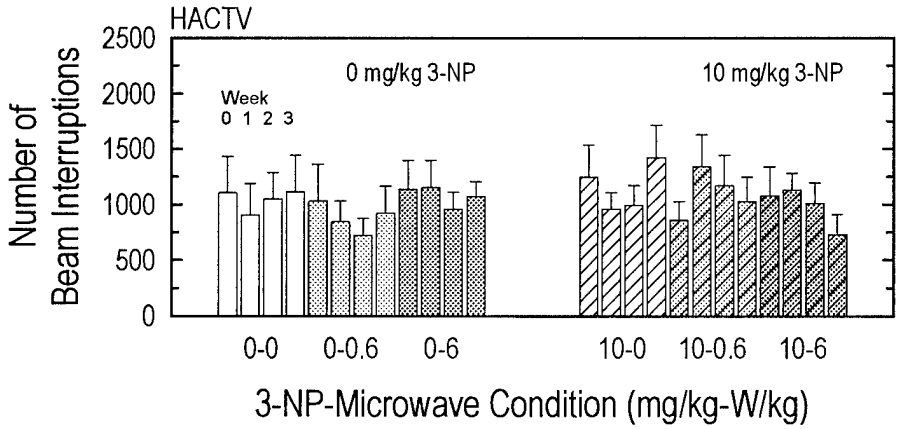
Measurements made with the two-level IR activity monitor 0, 1, 2, and 3 weeks after 3-NP-microwave treatment are shown in Figs. A8, A9, and A10 for horizontal, vertical, and stereotypical movements, respectively. All weeks are represented in each figure. Although the number of animals for each condition was small (4-6) and variability consequently large, a few trends in activity over time were qualitatively noted in some measures and differences between 3-NP-microwave conditions were suggested by the measurements. Because of the reasons given above, statistical tests were not done on these activity data.

Comparisons between results from the two-level IR activity monitor and results from the original activity monitor (Fig. A1) are difficult. This is because information from the original apparatus 1) was based on one level of visible light beams and 2) did not discriminate between types of beam interruptions. Comparisons between monitors are not attempted here.

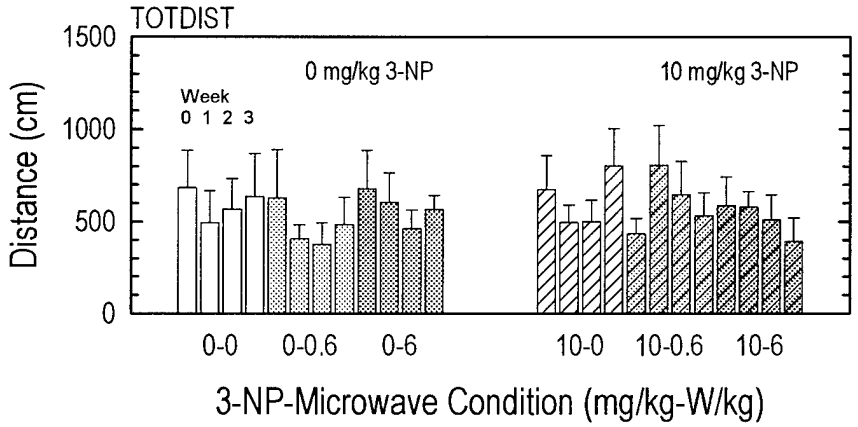
Histology Results

Histology results were available for the following numbers of animals at 4-5 weeks after 3-NP-microwave treatments: 2 each for conditions 0-0 and 10-0; 3 each for conditions 0-0.6, 10-0.6, and 10-6; and 5 for condition 0-6. Histologic examination found minor lesions in heart but not in brain, lung, or liver. Lesions were consistent with incidental findings historically observed in rats and could not be attributed to any 3-NP-microwave condition. This lack of pathology was also found for short-term animals (Section III).

A.



B.



C.

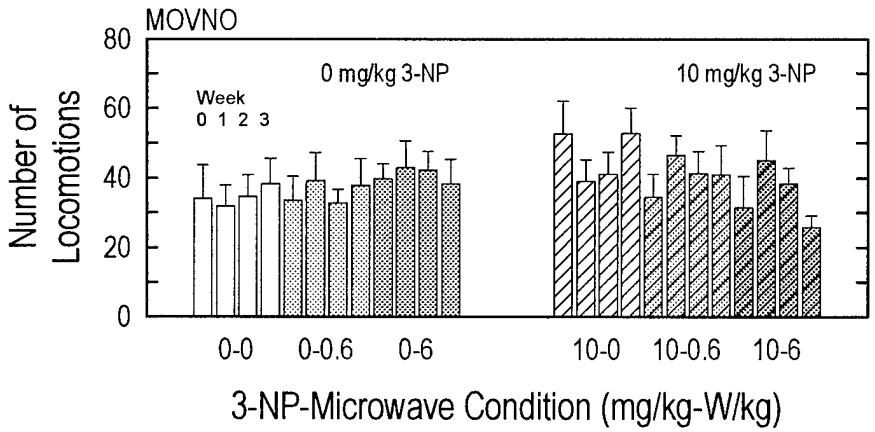
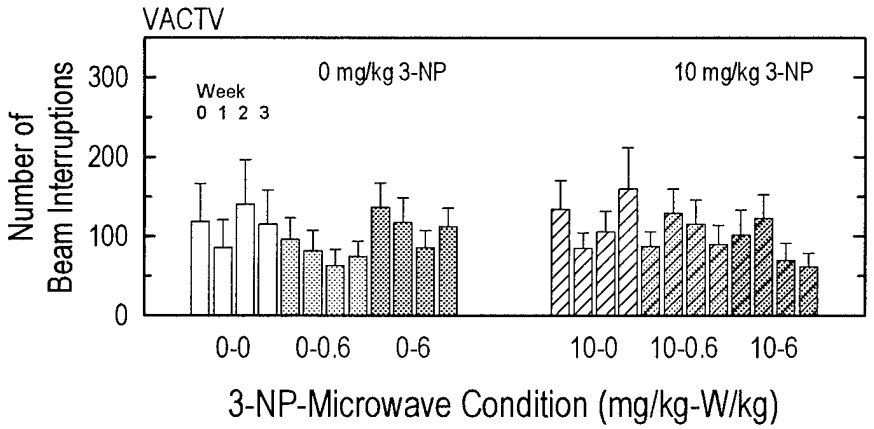
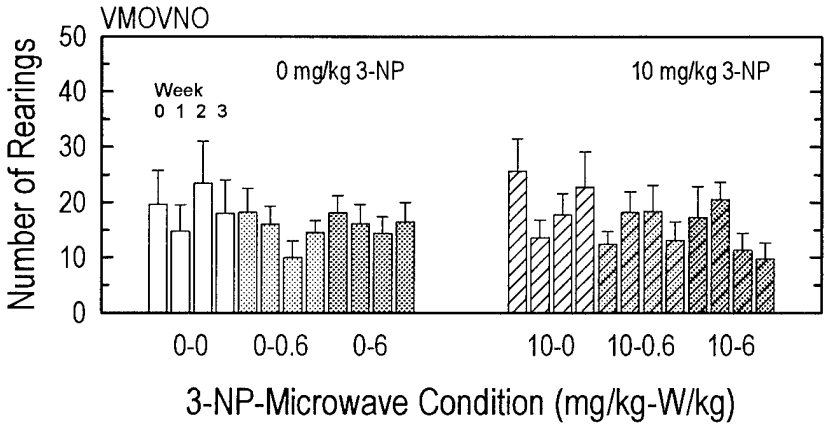


Figure A8. Measures of horizontal activity from two-level IR activity monitor (mean and s.e.m.) for long-term animals, weeks 0-3. N=4-6 for each 3-NP-microwave condition.

A.



B.



C.

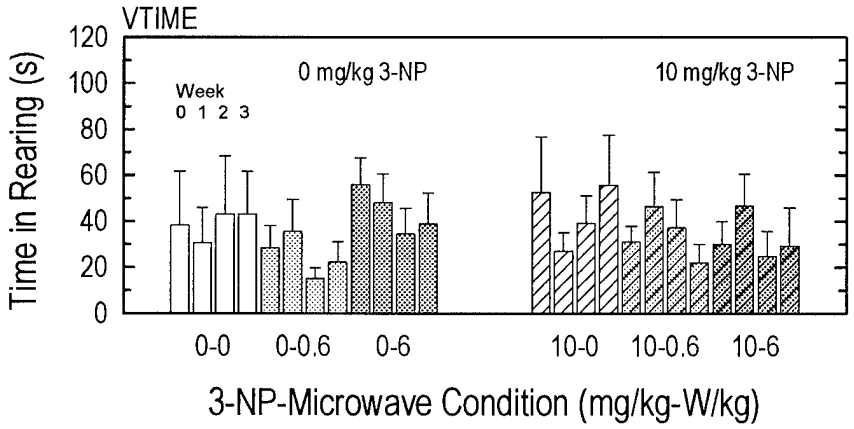
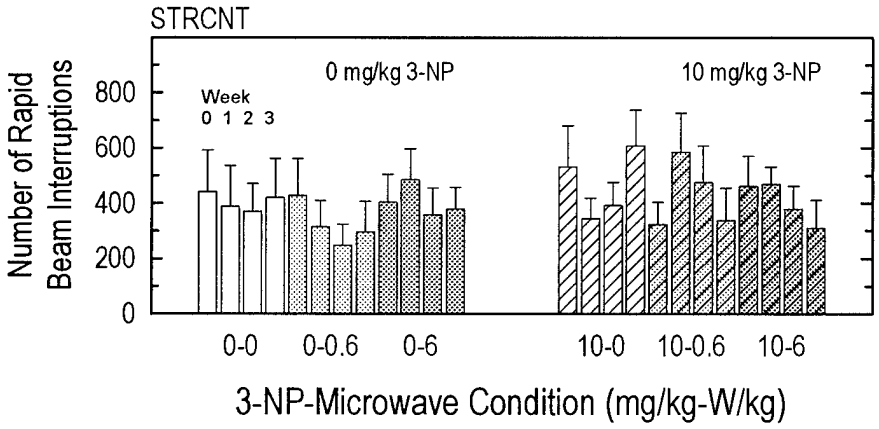
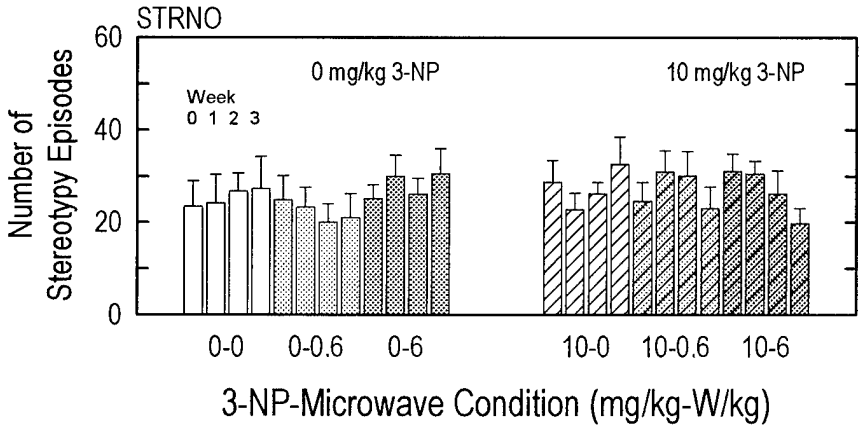


Figure A9. Measures of vertical activity from two-level IR activity monitor (mean and s.e.m.) for long-term animals, weeks 0-3. N=4-6 for each 3-NP-microwave condition.

A.



B.



C.

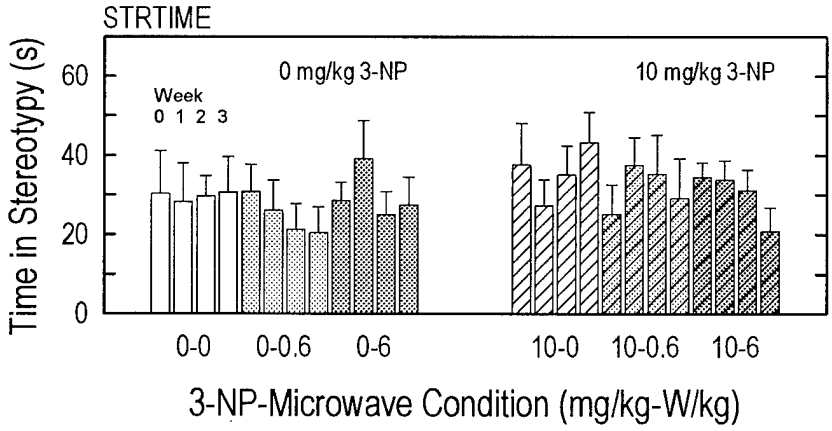


Figure A10. Measures of stereotypical activity from two-level IR activity monitor (mean and s.e.m.) for long-term animals, weeks 0-3. N=4-6 for each 3-NP-microwave condition.